(2)

SAN-1570-2/2

OCEAN THERMAL ENERGY CONVERSION (OTEC) POWER SYSTEM DEVELOPMENT

Preliminary Design Report—Appendices—Part 1 (Final)

December 4, 1978

Work Performed Under Contract No. EG-77-C-03-1570

TRW Systems and Energy
Redondo Beach, California

U.S. Department of Energy

Solar Energy

DISCLAIMER

DISCLAIMER

Available from the National Technical Information Service, U. S. Department of Commerce, Springfield, Virginia 22161.

Price: Paper Copy $38.00
Microfiche $3.50

SAN-1570-2/2
Distribution Category UC-64

OCEAN THERMAL ENERGY CONVERSION (OTEC) POWER SYSTEM DEVELOPMENT

Preliminary Design Report—Appendices—Part 1 (Final)

December 4, 1978

Contract No. EG-77-C-03-1570

TRW Systems and Energy
Redondo Beach, California

THIS PAGE

WAS INTENTIONALLY

LEFT BLANK

APPENDICES

CONTENTS

		Page
Part I		
A.	DEVELOPED COMPUTER MODELS	A–1
A.1	SYSTEM DESIGN AND OPTIMIZATION MODEL UPDATE	A–3
A.2	SYSTEM PERFORMANCE MODEL	A–37
A.3	HYDRAULIC TRANSIENT MODEL	A–89
B.	WATER SYSTEM DYNAMICS STUDIES	B–1
B.1	SUMMARY	B–2
B.1.1	Introduction	B–4
B.1.2	Conduit Distribution Systems	B–5
B.1.3	Dynamics of Flow in the Open Trough System	B–8
B.2	COMPLETELY CLOSED CONDUIT SYSTEM	B–13
B.2.1	Basic Features and Simplified Representation	B–14
B.2.2	Startup	B–18
B.2.3	Vertical Hull Motion	B–27
B.3	DECOUPLED CLOSED CONDUIT SYSTEM	B–37
B.3.1	Basic Features	B–38
B.3.2	Dynamics of Flow	B–38
B.4	OPEN TROUGH SYSTEM	B–41
B.4.1	Basic Features	B–42
B.4.2	Pump Startup	B–42
B.4.3	Standing Waves in the Trough	B–45
B.4.4	Vertical Motion of Water Surface	B–46
C.	MISCELLANEOUS PERFORMANCE ANALYSIS	C–1
C.1	VARIABILITY OF AMMONIA LOOP PARAMETERS	C–3
C.2	OPTIMUM DESIGN ΔT	C–15
D.	MATERIALS AND PROCESSES	D–1
D.1	TUBE MANUFACTURING	D–3
D.2	EROSION AND CORROSION CONTROL	D–47
D.3	MATERIALS COMPATIBILITY, RECOMMENDED MATERIALS	D–69

APPENDICES

CONTENTS (Continued)

		Page
E.	DETAILED EQUIPMENT LISTS	E–1
	E.1 SYSTEM EQUIPMENT LISTS	E–3
	E.2 SPECIAL SUPPORT EQUIPMENT LIST	E–13
	E.3 MACHINERY, TOOLS, AND SPARE PARTS LIST 10 MWe	E–17
	E.4 LONG LEAD TIME PROCUREMENT LIST, 200 kWe and 10 MWe	E–19
F.	TURBINE DESIGN STUDIES	F–1
	F.1 TURBINE PRELIMINARY DESIGN ANALYSIS	F–3
	F.2 ELLIOTT'S TURBINE STUDY	F–15
G.	TUBE CLEANER DESIGN	G–1
	G.1 HYDRAULIC TUBE CLEANER ANALYSIS	G–3
	G.2 OTHER DESIGN CONSIDERATIONS WITH RESPECT TO THE HYDRAULIC TUBE CLEANER	G–13
	G.3 MAINTENANCE AND OPERATING PLAN INPUTS FOR THE 10 MWe AND THE 0.2 MWe TUBE CLEANERS	G–27
	G.4 TUBE CLEANER MEASUREMENTS AND CONTROLS	G–33
H.	AMMONIA LEAK DETECTION	H–1
	H.1 OTEC AMMONIA LEAK DETECTION SYSTEM	H–3
	H.2 OTEC PSD–1, EFFECTS OF SEAWATER LEAKAGE INTO AMMONIA SYSTEM	H–37
I.	HEAT EXCHANGER DESIGN SUPPORTING DATA	I–1
	I.1 THERMAL/HYDRAULIC ANALYSIS	I–3
	I.1.1 Tube Side Equations – Heat Transfer and Pressure Drop	I–4
	I.1.2 Evaporation Heat Transfer Coefficient	I–5
	I.1.3 Condensing Heat Transfer Coefficient	I–7
	I.1.4 Metal Resistance	I–8
	I.1.5 Shell Side Pressure Drop	I–10
	I.1.6 Evaporator and Condenser Dimensions	I–12
	I.1.7 Non-Condensibles	I–12
	I.2 STRESS ANALYSIS	I–133
	I.2.1 10 MWe Heat Exchanger	I–137
	I.2.2 0.2 MWe Test Articles	I–201
	I.2.3 Heat Exchangers Support	I–213
	I.3 TUBE SELECTION/DESIGN DATA	I–231
	I.4 0.2 MWe TEST ARTICLE LOOP	I–275

APPENDIX A
DEVELOPED COMPUTER MODELS

THIS PAGE

WAS INTENTIONALLY

LEFT BLANK

APPENDIX A.1

SYSTEM DESIGN AND OPTIMIZATION MODEL UPDATE

TRW
DEFENSE AND SPACE SYSTEMS GROUP
ONE SPACE PARK • REDONDO BEACH • CALIFORNIA 90278

INTEROFFICE CORRESPONDENCE

PSD-I-322
78.6852.4.7-05

TO: Paul Bakstad

CC: Distribution
P. Fukunaga P.C.F.
R. Pearson

DATE: 2 June 1978

H.D.L.

SUBJECT: OTEC System Optimization Program Update

FROM: Gregory S. Gibson
BLDG 81 MAIL STA. 1569 EXT. 63374

The OTEC-I system optimization computer model is described in reference 3, pages E-1 to E-37. The OTEC-II system optimization computer model has greater capabilities than the OTEC-I model. The areas of modification include:

- o Heat transfer coefficients
- o Programming inputs
- o Gross power iteration
- o Cost equations
- o Printout

These modifications were developed by myself and P. Bakstad. G. Kikin developed the enclosed heat exchanger cost equations. J. Kaellis developed the thermal thickness evaluation technique.

PROGRAM INPUTS

The OTEC-II optimization computer program has more flexibility and capability than the OTEC-I model. Inputs listed in Table 1 allow the programmer to change tube geometry and tube material with each computer run. Tube geometry of each heat exchanger is inputted by choosing the appropriate values of DO, D, Dw, Ar and Thick. Tube material is inputted by choosing the appropriate value of CON, the tube thermal conductivity. Tube cost parameters depend on both the tube geometry and tube material.

Table 1
OTEC OPTIMIZATION COMPUTER
PROGRAM INPUTS

C_1, C_2 and B_1, B_2	Tube Cost Parameters, $/FT (see Tables 3 and 4)
DO_C, D_C, D_{WC}, Thick $_C$ and DO_B, D_B, D_{WB}, Thick $_B$	Tube Geometry, Inches (see Figure 1)
A_r	Water Side Area Ratio
CON	Tube Wall Thermal Conductivity, BTU/HR/FT/°F
Subscript C	Symbolizes Condenser
B	Symbolizes Boiler

Figure 1

Fluted Tube Geometry

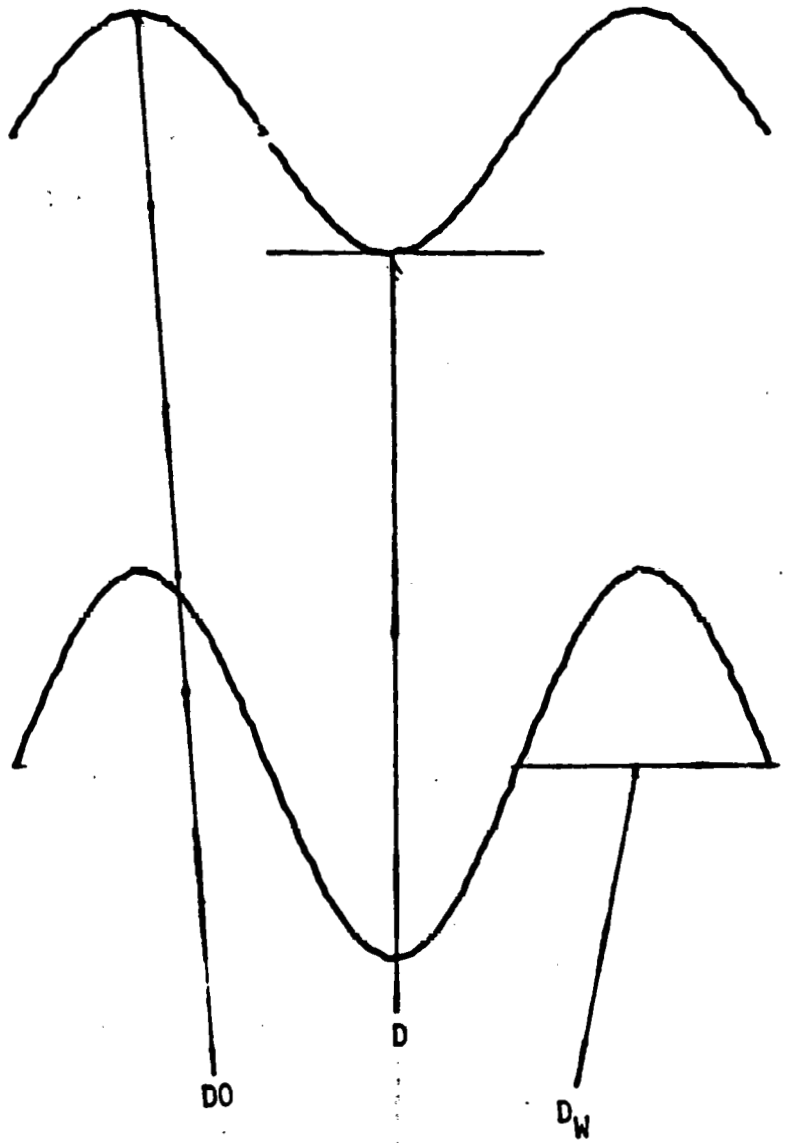

The input parameter "Thick" is not the tube thickness. It is the tube thermal thickness. The thermal thickness is used to compute the wall heat transfer resistance using the following equation:

$$R = (Thick)\ (D)/(CON(D-Thick))$$

The thermal thickness is computed for each tube geometry using an isotherm analysis technique.

COST EQUATIONS

Our customer requested an itemized list of heat exchanger cost. Evaporator and condenser cost equations are listed in Tables 2 and 3. Heat exchanger cost depends on the number of tubes N, the tube total length, L, in feet and the tube outside diameter, D, in inches (this D is equal to the DO in Table 1). In the evaporator the total tube length is greater than the tube heat transfer length by 3.5 feet. In the condenser, the difference is one foot. A clad or unclad tubesheet cost option is included. Input cost parameter B_1, B_2, C_1, and C_2 appear in the tube material cost equations.

The cost of space (cost of heat exchanger size) is no longer a part of the total system cost. Thus the penalty for large heat exchangers has been removed.

Figure 2 shows the insensitivity of evaporator length and hot water exit temperature with total system cost. Seawater entrance temperature is 80°F. The optimum length and exit temperatures are 34 feet, 73.8°F. At 26 feet, 74.7°F, the total system cost increases by $0.15 million which is 0.93%. The differences between 40 feet, 73.2°F and 26 feet, 74.4°F is only 0.56%.

Table 2
EVAPORATOR Cost Equations

TUBES	MATERIAL	LABOR
	$N(B_1L+B_2)$	$28.1D^{0.7}N$
Tubesheets Clad Unclad	 $1.24D^{2.30}N^{1.15}$ $0.105D^{2.5}N^{1.27}$	 $0.457N^{1.34}D^{0.68}(D-0.5) + 329(DN^{1/2}-148)^{1.5}$ * $0.307N^{1.33}D^{0.66}(D-0.5) + 221(DN^{1/2}-148)^{1.5}$ *
Tube Support Plates	$9.22(10^{-4})D^{3.046}N^{1.523}$	$0.124N^{1.295}D^{0.591}(D-0.5)$
Shell	$.012D^{2.29}N^{1.145}L$	$3.16D^{1.654}N^{0.827}L^{0.7}$
Water Boxes	$0.175D^{2.1}N^{1.05}$	$172.5D^{1.32}N^{0.66}$
Nozzles	$79.6D^{0.908}N^{0.454}$	$62.3D^{1.34}N^{0.67}$
Ammonia Distribution (Evaporator only)	$0.024D^{2.592}N^{1.296}$	$0.0962N^{1.38}D^{0.756}(D-0.5)$
Bustle (Evaporator only)	$0.0104D^{2.69}N^{1.345}$	$147.4D^{1.35}N^{0.675}$
Water Inlets	$12.0D^{1.28}N^{0.64}$	$92.3D^{1.27}N^{0.635}$
Supports	$0.053D^{2.090}N^{1.045}$	$27.1D^{1.33}N^{0.665}$

*If $(DN^{1/2}-148)$ is less than zero set $(DN^{1/2}-148)$ to zero.

B_1 and B_2 are tube cost inputs

Table 3
CONDENSER Cost Equations

	MATERIAL	LABOR
TUBES	$N(C_1L+C_2)$	$28.1D^{0.7}N$
Tubesheets Clad Unclad	 $1.24D^{2.30}N^{1.15}$ $0.105D^{2.5}N^{1.27}$	 $0.457N^{1.34}D^{0.68}(D-0.5) + 329(DN^{1/2}-148)^{1.5}$ * $0.307N^{1.33}D^{0.66}(D-0.5) + 221(DN^{1/2}-148)^{1.5}$ *
Tube Support Plates	$9.22(10^{-4})D^{3.046}N^{1.523}$	$0.124N^{1.295}D^{0.591}(D-0.5)$
Shell	$.012D^{2.29}N^{1.145}L$	$3.16D^{1.654}N^{0.827}L^{0.7}$
Water Boxes	$0.175D^{2.1}N^{1.05}$	$172.5D^{1.32}N^{0.66}$
Nozzles	$79.6D^{0.908}N^{0.454}$	$62.3D^{1.34}N^{0.67}$
Ammonia Distribution (Evaporator only)	Zero	Zero
Bustle (Evaporator only)	Zero	Zero
Water Inlets	$12.0D^{1.28}N^{0.64}$	$92.3D^{1.27}N^{0.635}$
Supports	$0.053D^{2.090}N^{1.045}$	$27.1D^{1.33}N^{0.665}$

*If $(DN^{1/2}-148)$ is less than zero set $(DN^{1/2}-148)$ to zero.

C_1 and C_2 are tube cost inputs

Figure 2

SENSITIVITY OF PROTOTYPE MODULE COST TO EVAPORATOR LENGTH (BTL) AND TO CHANGE IN WARM WATER TEMPERATURE (DTH). OTHER PROGRAM PARAMETERS ARE FIXED (CONDENSER LENGTH 35 FT. CHANGE IN COLD WATER TEMPERATURE 6.2°F).

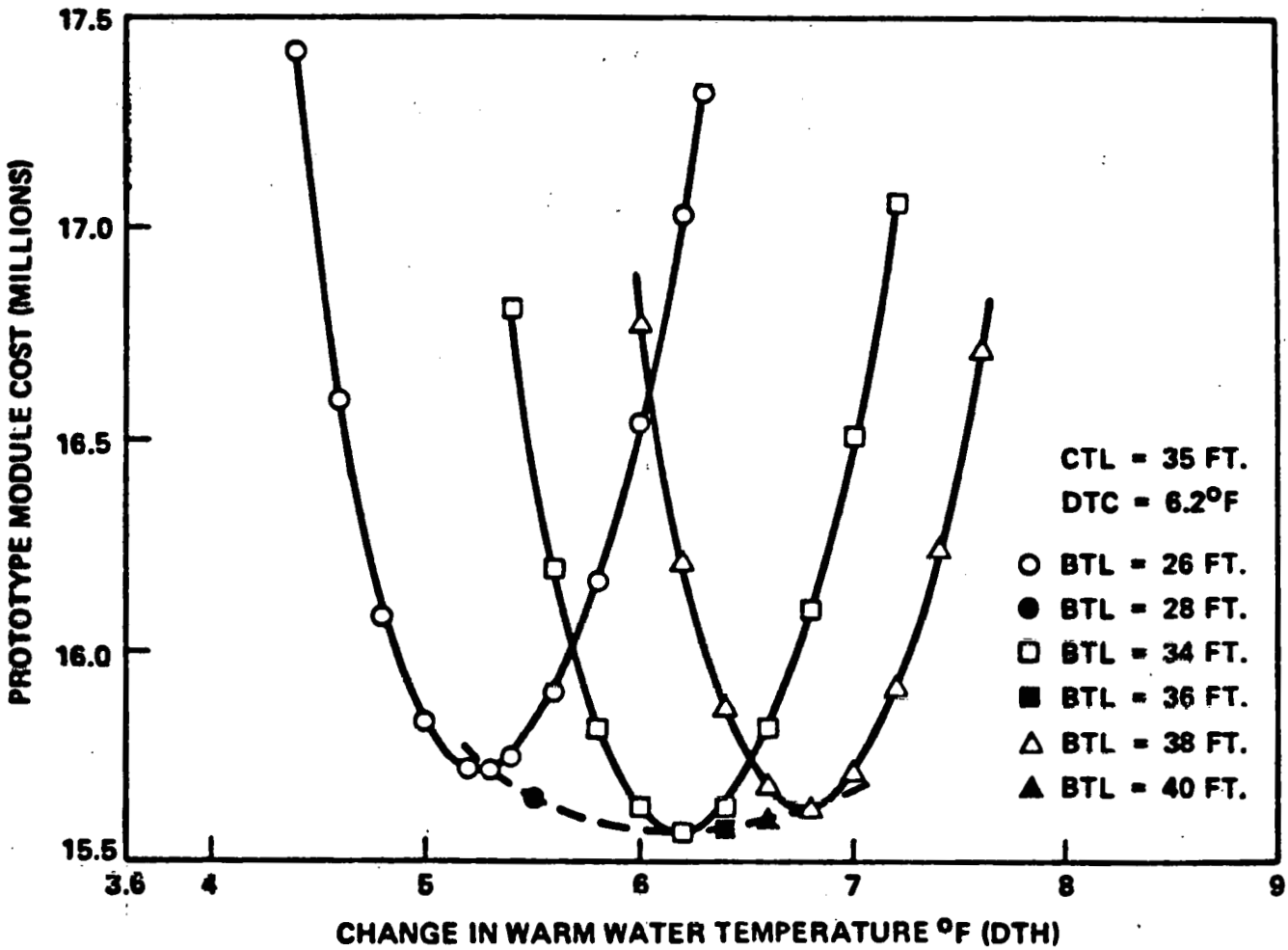

Figure 2 also illustrates the computer sequential search optimization method described in reference 3, page E-2. Starting at BTL = 40 feet, DTH is varied in the direction of decreasing cost until a local minimum is reached at DTH = 6.8°F. The process is repeated with a new value of BTL, until a global minimum is found.

GROSS POWER ITERATION

Table 4 illustrates the updated gross power iteration method used in OTEC-II. This iteration finds the value of P_G (gross power) which solves

$$P_G = P_P + P_N$$

P_p (total parasitic power loss) is a function of P_G. P_N (net power, i.e. 10.5 MWe) is constant. The iteration usually requires 2 or 3 steps because the initial guess is very good. This method is much simpler, more accurate, and more reliable than the method in OTEC-I.

PRINTOUT

Table 5 shows the OTEC-II printout.

Table 4

Gross Power Iteration

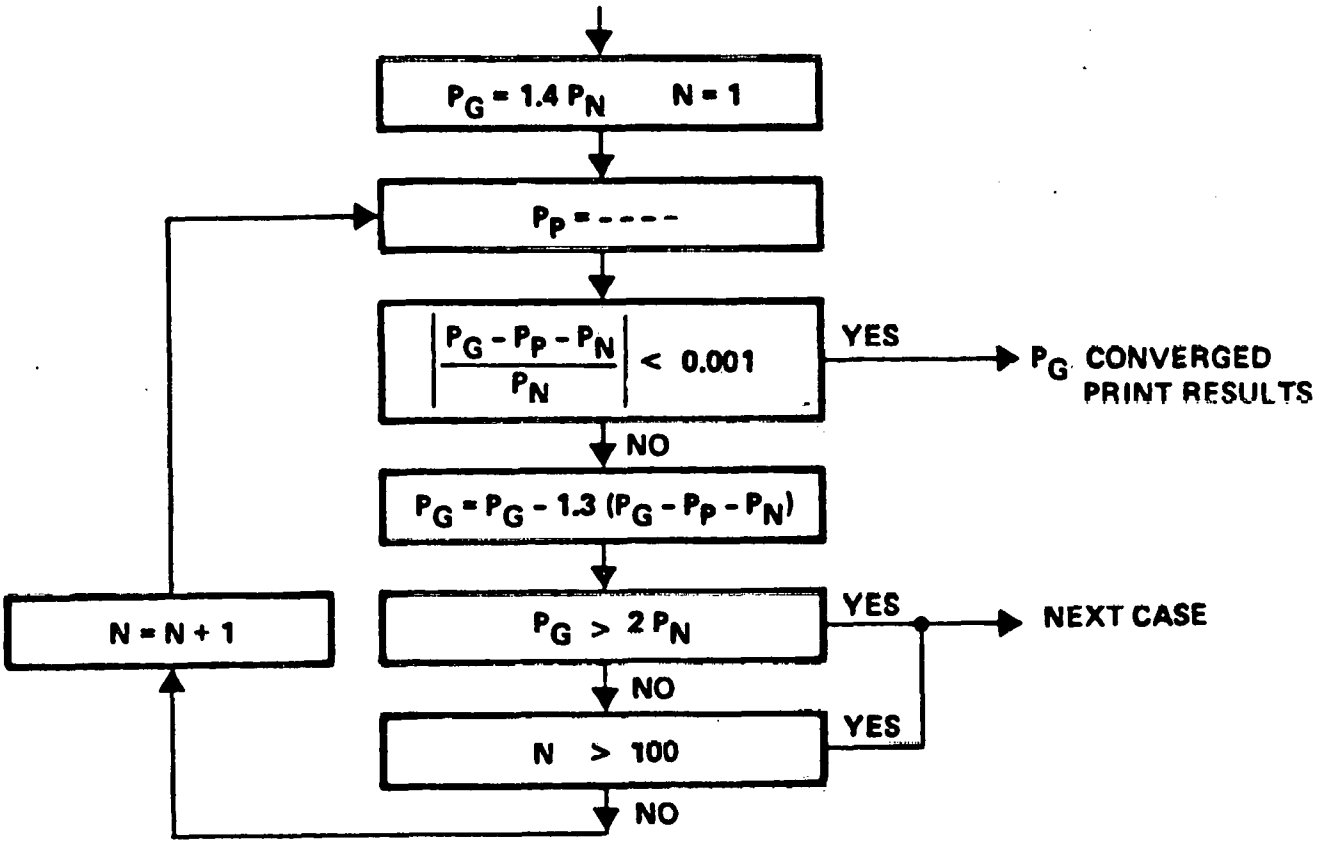

P_G = Gross Power

P_N = Net Power

P_P = Total Parasitic Power

CASE NO 17

	W WATER PIPE	C WATER PIPE
LENGTH FEET	300	2900.0000
DIAMETER FT	15.8975	15.2525
NUMBER OF PIPES	1	1
H2O VEL FT/S	6.0000	6.0000
WATER FLOW LB/HR	2.7348E+08	2.5262E+08
PRESSURE DROP PSI	.5577	3.0504
	EVAPORATOR	CONDENSER
BOTTOM REYNOLDS NUM	2.0403E+03	2.7510E+03
TOP REYNOLDS NUM	5.2243E+03	0.0
HEAT TRAN LENGTH FT	26.5000	29.0000
TOTAL LENGTH FT	30.0000	30.0000
SHELL DIAM FT	24.9483	25.2422
TUBE DIAMETER IN	.9900	.9900
NUMBER TUBES	42667	43678
TUBE MAT COST $/FOOT	1.6500	1.3100
WATER TUBE VEL FT/SEC	6.6140	5.8228
NH3 ENT FLOW CFS		2.5943E+03
NH3 EXIT FLOW CFS	1.8666E+03	2.0691E+01
HEAT TRAN AREA SQ. FT.	2.6039E+05	2.9481E+05
HEAT TRANSFERED	1.5431E+09	1.4950E+09
OVERALL BTU/HR/F/FT**2	895.5240	796.0179
NH3 HTC BTU/HR/F/FT**2	11915.3145	15421.6060
WALL HTC BTU/HR/F/FT**2	2302.5576	2774.5603
WATER HTC BTU/HR/F/FT**2	1939.0474	1349.8842
H2O AREA RATIO	1.4600	1.4600
FOULING (FT**2 HR F/BTU)	1.0000E-04	1.0000E-04
H2O ENTRANCE TEMP F	80.0000	40.0000
CHANGE IN WATER TEMP	5.9000	6.2000
PRESSURE DROP PSID	4.1150	3.6098
NH3 OUTLET TEMP F	70.0000	50.0000
NH3 OUTLET PRES PSIA	128.7997	89.1924

CYCLE DATA

GROSS POWER MW	1.4032E+01	NET POWER MW	1.0500E+01
WW PUMPS MW	1.3514E+00	CW PUMPS MW	1.7731E+00
NH3 PUMPS MW	4.0766E-01	EVAPOR LB/SEC	8.0715E+02
TUR ENTHAL BTU	1.6813E+01	TUR EX QUALITY	2.4553E-02
PLANT EFF	2.3217E-02		

COST BREAKDOWN ($)

EVAP HE COST	4.8252E+06	CON HE COST	4.1391E+06
WW PUMP COST	4.5070E+05	CW PUMP COST	4.1885E+05
NH3 R PUMP	1.0394E+05	NH3 F PUMP	8.0886E+04
GEN COST	6.2274E+05	TURBINE COST	8.2473E+05
CW PIPE	1.4591E+06	MISCEL	1.5000E+06
TOTAL SYSTEM	1.4425E+07	TOTAL BOTH HE	8.9643E+06

	EVAPORATOR		CONDENSER	
PART	MATERIAL	LABOR	MATERIAL	LABOR
TUBES	2.1120E+06	1.1905E+06	1.7165E+06	1.2187E+06
CLAD	0.	0.	0.	0.
UNCLAD	7.7713E+04	3.0886E+05	8.0059E+04	3.2173E+05
PLATES	1.0071E+04	5.9842E+04	1.0437E+04	6.1685E+04
SHELL	7.0431E+04	2.2675E+05	7.2345E+04	2.3118E+05
BOXES	1.2459E+04	1.9359E+05	1.2769E+04	1.9661E+05
NOZZLES	9.9773E+03	7.7768E+04	1.0084E+04	7.8998E+04
DIST	2.3415E+04	1.1471E+05	0.	0.
BUSTLE	1.7091E+04	1.9405E+05	0.	0.
INLETS	1.0886E+04	7.9390E+04	1.1050E+04	8.0580E+04
SUPPORT	3.5777E+03	3.2076E+04	3.6663E+03	3.2579E+04
EACH TOTAL	2.3476E+06	2.4776E+06	1.9170E+06	2.2221E+06

HEAT TRANSFER COEFFICIENTS

Correlations for the ammonia side heat transfer coefficients are usually given on a per tube basis. It was therefore decided to improve the OTEC computer model so that it could accept heat transfer correlations that are given on a per tube basis.

The overall heat transfer coefficient is given by:

$$\frac{1}{U} = \frac{D_w}{D\, H^c_{wf}} + \frac{1}{H_{sw}} + F\, F_{sw} \qquad (1)$$

The sea water heat transfer coefficient is given by:

$$H_{sw} = C_2 V^{0.8}$$

$$\text{Where } C_2 = 0.027\, K\, Pr^{1/3} \frac{Ar}{D_w}\left[\frac{D_w \rho}{\mu}\right]^{0.8} \qquad (2)$$

The working fluid (ammonia) heat transfer coefficient (H^c_{wf}) is a composite heat transfer coefficient. It is computed in the OTEC computer model in subroutine NH3 HTC as a function of the number of tubes.

$$H^c_{wf} = H^c_{wf}(N) \qquad (3)$$

The seawater side fouling factor ($F\, F_{sw}$) is input to the program.

$$F\, F_{sw} = 0.0001 \text{ hr ft}^2 \text{ °F/BTU} \qquad (4)$$

The seawater velocity V is given by the volumetric flow per tube ($\frac{Q}{N}$) divided by the cross sectional area. This gives another equation for H_{sw}.

$$H_{sw} = C_2 \left(\frac{4Q}{D_w^2 \pi}\right)^{0.8} N^{-0.8} \qquad (5)$$

Substitution of equation (5) into (1) and rearranging gives

$$U = \left[\frac{D_w}{DH^c_{wf}} + \frac{N^{0.8}}{C_2 X_2} + F\, F_{sw}\right]^{-1} \qquad (6)$$

$$\text{Where } X_2 = \left(\frac{4Q}{D_w^2 \pi}\right)^{0.8}$$

The total seawater side heat transfer area is given by

$$A = \pi D_w L N \qquad (7)$$

Multiplying equations (6) by A and rearranging gives

$$N - X_3 N^{0.8} - \frac{X_4}{H^c_{wf}} - X_5 = 0 \qquad (8)$$

Where $X_1 = \pi D_w L$

$$X_3 = \frac{(UA)}{X_1 X_2 C_2}$$

$$X_4 = \frac{D_w (UA)}{D X_1}$$

$$X_5 = \frac{(UA) F F_{sw}}{X_1}$$

Equation (8) can be solved by Newton-Raphson iteration for N. This iteration also requires knowledge of H^c_{wf} and $\frac{\partial H^c_{wf}}{\partial N}$ which are computed for each heat exchanger in subroutine NH3 HTC. Equations (9), (10) and (11) demonstrate the Newton-Raphson method.

$$F = N - X_3 N^{0.8} - \frac{X_4}{H^c_{wf}} - X_5 \qquad (9)$$

$$\frac{\partial F}{\partial N} = 1 - 0.8 X_3 N^{-0.2} + \frac{X_4}{(H^c_{wf})^2} \frac{\partial H^c_{wf}}{\partial N} \qquad (10)$$

$$N_{New} = N_{old} - \frac{F}{\left(\frac{\partial F}{\partial N}\right)} \qquad (11)$$

EVAPORATOR

The evaporator heat transfer coefficient model is taken from Carnegie-Mellon data (see reference 1 and Figure 3). Since these coefficients are believed to be high, they were reduced by 20%. Equation (12) is the reduced correlation.

$$H^C = \frac{(2.939\ Re_T^{.4151} - 63.217)\ 8 \times 10^5 - 5.633\ Re_B^{1.8452}}{Re_T - Re_B} \qquad (12)$$

This is a composite correlation for fluted tubes. We estimated the experimental wall resistance in this correlation to be Ro. Therefore the ammonia heat transfer coefficient (H_{wfb}) is:

$$H_{wfb} = 1/(\frac{1}{H^C} - Ro) \qquad (13)$$

We estimated the wall resistance in our system to be R. Therefore the composite coefficient for our system is:

$$H^C_{wf} = 1/(\frac{1}{H_{wfB}} + R) \qquad (14)$$

The value of H^C_{wf} used in the Newton-Raphson iteration on the number of tubes is computed from equations (14), (13) and (12). The reynolds number at the top (Re_T) and the reynolds number at the bottom (Re_B) of the evaporator are computed separately as explained later.

The derivative of equations (14), (13) and (12) with respect to the number of tubes gives the value of $\frac{\partial Hwf}{\partial N}$ used in the Newton-Raphson iteration on the number of tubes (equations (8), (9), (10) and (11)).

$$\frac{\partial H^C_{wf}}{\partial N} = \frac{1}{(1 + RH_{wfB})^2} \frac{\partial H_{wfB}}{\partial N} \qquad (15)$$

$$\frac{\partial H_{wfB}}{\partial N} = \frac{1}{(1-R_o H^C)^2} \frac{\partial H^C}{\partial N} \qquad (16)$$

$$\frac{\partial H^C}{\partial N} = \frac{F_2 \frac{\partial F_1}{\partial N} - F_1 \frac{\partial F_2}{\partial N}}{F_2^2} \qquad (17)$$

Where

$$H^c = F_1/F_2$$

$$F_1 = (2.939\ Re_T^{0.4151} - 63.217)8 \times 10^5 - 5.633\ Re_B^{1.8452}$$

$$\frac{\partial F_1}{\partial N} = (-2.939)(0.415)8 \times 10^5\left(\frac{Re_T^{0.4151}}{N}\right) + 5.633(1.8452)\frac{Re_B^{1.8452}}{N}$$

$$F_2 = Re_T - Re_B$$

$$\frac{\partial F_2}{\partial N} = \frac{-Re_T}{N} + \frac{Re_B}{N}$$

With these values of H^c_{Wf} and $\frac{\partial H^c_{Wf}}{\partial N}$ the Newton-Raphson iterations can now be used to find the number of tubes. The reynolds number at the top (Re_T) and at the bottom (Re_B) of the evaporator are computed using:

$$Re_T = \frac{3.17508\ X10^8}{Re_B^{1.44537}} \qquad (18)$$

$$WWF_T = WWF_B + WWF_e \qquad (19)$$

$$Re_i = \frac{4\ WWF_i}{\mu\pi DN} \qquad (20)$$

Equation (18) is the relationship that gives the optimum recirculation ratio. WWF_e is known. Equations (18), (19) and (20) imply:

$$Re_B + C - \frac{A}{(Re_B)^B} = 0 \qquad (21)$$

Where

$$C = \frac{4\ WWF_e}{\pi\mu DN} = 3.546628\ \frac{WWF_e}{DN}$$

$$A = 3.17508X10^8$$

$$B = 1.44537$$

Equations (21) can be used to find Re_B by Newton-Raphson iteration.

This Newton-Raphson iteration goes as follows:

$$X = Re_B$$

$$F = X + C - AX^{-B}$$

$$\frac{\partial F}{\partial X} = 1 + BAX^{-B-1}$$

$$X_{new} = X_{old} \frac{F}{(\frac{\partial F}{\partial X})}$$

Figure 3

EVAPORATOR AMMONIA HEAT TRANSFER MODEL

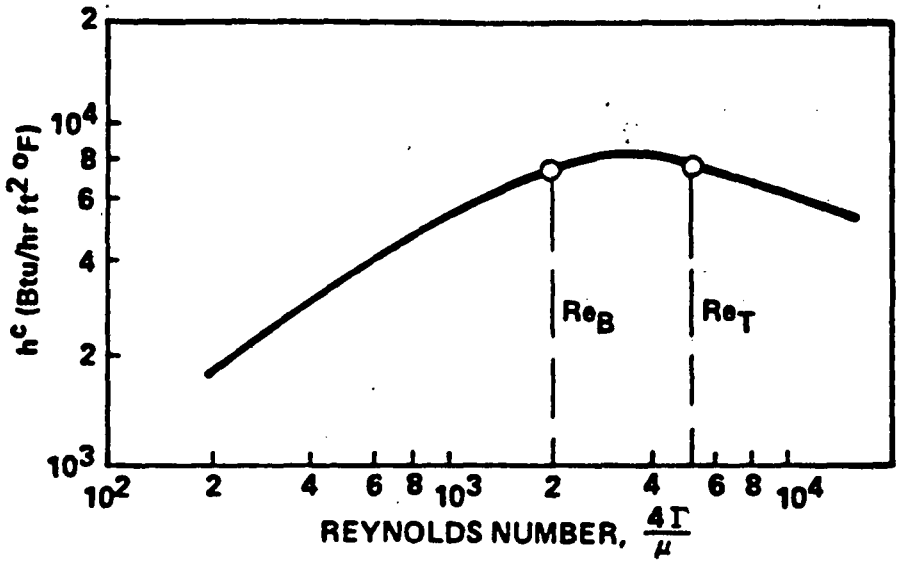

BASIS:

EXPERIMENTAL DATA ON FLUTED TUBES OBTAINED BY CMU. EQUIVALENT SMOOTH AREA BASED ON RILL-TO-RILL DIAMETER IS THE REFERENCE AREA.

CORRELATION RELATING Re_T AND Re_B:

$$Re_T = \frac{3.1751 \times 10^8}{Re_B^{1.4454}}$$

COMPOSITE COEFFICIENT:

$$h^c = \frac{[2.939\, Re_T^{0.4151} - 63.22]\, 0.8 \times 10^6 - 5.633\, Re_B^{1.8452}}{Re_T - Re_B}$$

SINCE h^c INCLUDES EFFECT OF 65 MILS WALL (ALUMINUM, k = 116):

$$\frac{1}{h}_{NH3} = \frac{1}{h^c} - \left(\frac{\Delta X}{k}\right)_{Al}$$

CONDENSER

The condenser heat transfer coefficient model is computed from a curve fit of Oak Ridge data for fluted tubes (see reference 2 and figure 4). Equation (22) is the composite Oak Ridge coefficient (h^c_{OR}) curve fit.

$$h^c_{OR} = K_1 + \frac{K_2}{\frac{Q}{A_{OR}} + K_3} \qquad (22)$$

$$= K_1 + \frac{K_2 \frac{P_{OR}}{P_{TRW}}}{\frac{Q}{A_{OR}} \frac{P_{OR}}{P_{TRW}} + K_3 \frac{P_{OR}}{P_{TRW}}} \qquad (23)$$

Equation (22) was multiplied by the ratio P_{OR}/P_{TRW} to convert the Oak Ridge reference area to the TRW reference area. Equation (24) gives the relationship between the Oak Ridge coefficient and the TRW coefficient. Equation (25) is the condenser coefficient relation used in the OTEC computer model.

$$h^c_{TRW} = h^c_{OR} \frac{P_{OR}}{P_{TRW}} \qquad (24)$$

$$h^c_{TRW} = C_1 + \frac{C_2}{\left(\frac{Q}{A}\right)_{TRW} + C_3} \qquad (25)$$

Where K_1, K_2, K_3 are curve fit constants

P_{OR} = Oak Ridge outside tube perimeter for Tube E = 0.41667 FT.

P_{TRW} = TRW reference perimeter for Tube E = (.078125) = 0.2454

$\frac{Q}{A_{OR}}$ = Oak Ridge Heat Flux (Figure 2)

$$\frac{Q}{A_{TRW}} = \frac{Q}{A_{OR}} \frac{P_{OR}}{P_{TRW}}$$

$$C_1 = K_1 \frac{P_{OR}}{P_{TRW}} = -3231.62$$

$$C_2 = K_2 \left(\frac{P_{OR}}{P_{TRW}}\right)^2 = 3.684X10^8$$

$$C_3 = K_3 \left(\frac{P_{OR}}{P_{TRW}}\right) = 20129.28$$

$$A = \pi DLN$$

To find the number of tubes in the condenser using Newton-Raphson iteration (equation (8), (9), (10) and (11)), h^c_{wf} and $\frac{\partial h^c_{wf}}{\partial N}$ must be known. As in the evaporator, the resistance R_0 and R in the condenser give the corresponding equations (13), (14), (15) and (16) for the condenser. The final equation is equation 17 which for the condenser comes from equation (25).

$$\frac{\partial h^c_{TRW}}{\partial N} = \frac{C_2 A}{NQ\left(1 + \frac{C_3 A}{Q}\right)^2} \qquad (26)$$

Figure 4

CONDENSER HEAT TRANSFER MODEL

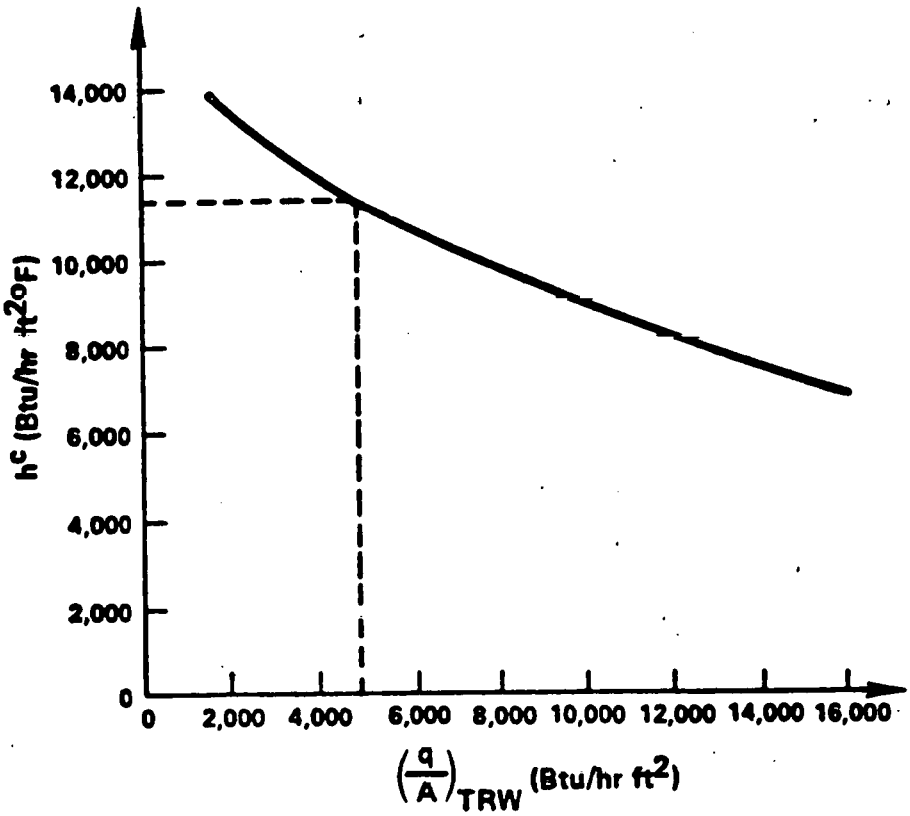

BASIS:

EXPERIMENTAL DATA ON FLUTED TUBES OBTAINED BY ORNL (TUBE "E"). EQUIVALENT SMOOTH AREA BASED ON RILL-TO-RILL DIAMETER IS THE REFERENCE AREA.

$$h^c_{TRW} = -3231.62 + \frac{3.684 \times 10^8}{\left(\frac{q}{A}\right)_{TRW} + 20{,}129.3}$$

THIS COMPOSITE h INCLUDES THE EFFECT OF THE ALUMINUM WALL IN THE OAK RIDGE EXPERIMENT, THEREFORE ($\Delta X \approx 0.031$", $k = 116$)

$$\left(\frac{1}{h}\right)_{NH_3} = \frac{1}{h^c} - \left(\frac{\Delta X}{k}\right)_{Al}$$

LIST OF SYMBOLS

Ar	Seawater side area ratio.
D	Ammonia side diameter measured to the flute root, FT
Dw	Seawater side (inside) diameter, FT
K	Thermal conductivity, BTU/HR/FT/°F
L	Tube length, FT
N	Number of tubes.
PG	Gross power, MWe
Pr	Prandtl number.
Re_B	Bottom reynolds number.
Re_T	Top reynolds number.
WWF_B	Mass flow rate of ammonia at the bottom of the evaporator, LB/HR
WWFe	Mass flow rate of ammonia evaporated, LB/HR
WWF_T	Mass flow rate of ammonia at the top of the evaporator, LB/HR
ρ	Density of ammonia, LB/FT^3
μ	Viscosity of ammonia, LB/HR/FT

REFERENCES

1. Sallie Ann Ward, "Analytical Models for Vertical Fluted Tube Heat Exchangers in Solar Sea Power Plants", Carnegie-Mellon University, (April, 1977).

2. S. K. Combs, An Experimental Study of Heat Transfer Enhancement for Ammonia Condensing on Vertical Fluted Tubes, ORNL-5356 (January, 1978).

3. TRW, "Ocean Thermal Energy Conversion Power System Utilizing Advanced, High-Performance Heat Transfer Technicques, Volume II", TRW SAN/1570-1 (January, 1978).

PROGRAM LISTING

```
00100       PROGRAM GTEC1(INPUT,OUTPUT,TAPE5=INPUT,TAPE6=OUTPUT)
00110 C
00120 C     MAIN PROGRAM - INITIALIZES PARAMETERS,INPUTS DATA
00130 C     AND CALLS OPTIMIZATION SUBROUTINE.
00140 C
00150       COMMON/REN/REDB,RETB,REBC,RRATIO
00160       COMMON/TIAL/THICKC,THICKB,CON
00170       COMMON/NH3D/HB(4),HF(4),SB(4),SF(4),VB(4),VF(4),PZ(4),X(4)
00180       COMMON/COST/C,CBXT,CCXT,CCWT,CCUPT,CWUPT,CMOOR,
00190 +     CTURBT,CSPT,CFPT,CRPT,CGENT
00200       COMMON/POWER/PN,PG,CUP,WUP
00210       COMMON/TEMP/TH,TC,DTH,DTC,T1,T2
00220       COMMON/DIM/H,DC,DH,NH,NC,HTB,HTC,CTL,BTL,
00230      1RKC,RKH,RKBX,RKCX,CL,PI,NCP
00240       COMMON/DIA/DWB,DWC,DB,BDC,DOB,DOC
00250       COMMON/PAR/PKW1,PKW2,PKW3,PKW4,BP1,BP2,BP3,BP4
00260 +     ,PKW2T,PKW4T,PKW1T,PKW3T
00270       COMMON/EVAL/PAR(6),DPAR(6),WMAX,WPB
00280       COMMON/ARRR/ARR
00290       COMMON/FAB/C11,C22,B11,B22
00300       COMMON/PRM/A(210),IWF
00310       COMMON/EFF/ETAP,ETAT,ETAG,XW
00320       COMMON/WXI/QAS,QRS,UB,UC,DT1,DT2
00330       COMMON/RAN/P1,P2,YA,EPSR,PWF,WWF,VA1,
00340 +     VA2,VA3,DHI,DHA,PWFT
00350       COMMON/WXO/VAH,VAC,AB,AC,WTUB,WTUC,EPSB,EPS
00360 +     C,UAB,UAC
00370       COMMON/WTC/FFB,FFC,WWFB,WWFC,WWALLC,WWALLB,WSUB,WSWC
00380       COMMON/OPTIONS/NMOD,NOP,NXM,NXUP,NAFP,NARP,NAT
00390       COMMON/NEXT/NEXT
00400       COMMON/AA/A11(14)
00410       COMMON/WAT/EM(12),CM(12)
00420       COMMON/LAB/EL(12),CL11(12)
00430       DIMENSION NA(36)
00440       REAL NTUB,NTUC
00450       DATA NOP,FAB/1,1./
00460       DATA NA/1,1,1,2,2,1,
00470 +     2,2,1,2,2,1,
00480 +     4,2,1,2,2,1,
00490 +     1,1,2,3,3,2,
00500 +     2,1,2,3,3,1,
00510 +     4,1,1,2,2,1/
00520       DATA RKC,RKCX,RKH,RKBX/3.1,0.70,1.85,0.70/
00530       DATA ETAP,ETAT,ETAG/0.804,0.85,0.98/
00540       DATA H,NH,NC,DH,DC,NCP/3000.,1,1,20.,50.,4/
00550       DATA BTL,CTL/26.5,29.0/
00560       DATA DWB1,DWC1,DB1,DC1,DOB1,DOC1/.87965,.889,.91,.91,
00561 +     .99,.99/
00570       DATA DTH,DTC/5.9,6.2/
00580       DATA CON,THICKC,THICKB/11.5,.04716,.05623/
00590       DATA C11,B11,C22,B22/1.31,1.65,2*0.0/
00600       DATA DPAR/2.,100.,2*0.1,2*1./
00610       DATA VDC,VCL,VDTH,VDTC,VBTL,VCTL/2.,200.,2*0.1,2*1./
00620       DATA PI,IWF,PN1,WMAX/3.14159265,1,10.5,10/
00630       DATA FFB,FFC/0.0001,0.0001/
00640       DATA ARR,DT1,DT2,XW/1.46,0.0,0.1,1./
00650       A11(14)=10HCASE NO 17
00660 C     NAMELIST INPUT
00670       NAMELIST/INPUT/H,DC,DTH,DTC,PN1,IWF,NH,NC,CTL,BTL,
00680 +     RKC,RKH,RKBX,RKCX,ETAP,ETAG,DPAR,NCP,FFB,FFC,
00690 +     DWB1,DWC1,DB1,DC1 ,DOB1,DOC1,NOP,A11,ETAT,
00700 +     XW,ARR,DT1,DT2,C11,C22,B11,B22,CON,THICKC,THICKB
00710       NAMELIST/PARA/DC,CL,DTH,DTC,BTL,CTL,VDC,VCL,VDTH,VDTC,VBTL,
00711 +     VCTL,NEXT
00720  10   READ(5,INPUT)
00730       DOB=DOB1/12.
00740       DOC=DOC1/12.
00750       DWB=DWB1/12.
00760       DWC=DWC1/12.
00770       DB=DB1/12.
00780       DDC= DC1/12.
00790 C     FOR OPTIONS A,B,C,D,E,F  NOP IS EQUAL TO
00800 C     1, 2, 3, 4, 5, 6,  RESPECTFULLY
00810       I=(NOP-1)*6
00820       NMOD=NA(I+1)
00830       NXM=NA(I+2)
00840       NXUP=NA(I+3)
00850       NAFP=NA(I+4)
00860       NARP=NA(I+5)
00870       NAT=NA(I+6)
00880  15   CALL BT(H,TH,TC)
00890       PAR(1)=DC
00900       PAR(2)=H-100.
00910       PAR(3)=DTH
```

```
      PAR(4)=DTC
      PAR(5)=DTL
      PAR(6)=CTL
      T1=TH-(TH-TC)/4.
      T2=TC+(TH-TC)/4.
      CALL RANKINE
      PN=PN1/NMOD
      PG=1.4*PN
      DISPLAY*    DTH      DTC      DTL      CTL      COST*
   20 CALL OPTIMIZ
C     DISPLAY* *
C     DISPLAY* *
C     ENTER THE VALUE OF NEXT
      READ(5,PARA)
      IF(NEXT.EQ.10)GO TO 10
      IF(NEXT.EQ.1) GO TO 20
      IF(NEXT.EQ.3) GO TO 30
      PAR(1)=DC
      PAR(2)=CL
      DPAR(1)=VDC
      DPAR(2)=VCL
      PAR(3)=DTH
      PAR(4)=DTC
      PAR(5)=DTL
      PAR(6)=CTL
      DPAR(3)=VDTH
      DPAR(4)=VDTC
      DPAR(5)=VDTL
      DPAR(6)=VCTL
      GO TO 20
   30 CONTINUE
      CALL PRINT1
      GO TO 10
      END
      SUBROUTINE EVAL(J)
C
C     EVAL IS A "MASTER" SUBROUTINE WHICH EVALUATES OPERATING
C     PARAMETERS AND COST OF A SPECIFIED DESIGN.
C
      COMMON/OPTIONS/NMOD,NOP,NXH,NXUP,NAFP,NARP,NAT
      COMMON/REN/REDB,RETB,REBC,RRATIO
      COMMON/COST/C.CBXT.CCXT,CCUT,CCUPT,CWUPT,CHOOR,
     * CTURBT,CSPT,CFPT,CRPT,CGENT
      COMMON/POWER/PN,PG,CUP,UUP
      COMMON/CHOH/RHOC,RHOB,PHUC,PHUB,CPB,
     * CPC,TKB,TKC
      COMMON/TEMP/TH,TC,DTH,DTC,T1,T2
      COMMON/DIM/H,DC,DH,HH,HC,HTB,HTC,CTL,BTL,
     *)RKC,RKH,RKBX,RKCX,CL,PI,NCP
      COMMON/DIA/DUB,DUC,DB,DBC,DOB,DOC
      COMMON/PAR/PKW1,PKW2,PKW3,PKW4,DP1,DP2,DP3,DP4
     * ,PKW2T,PKW4T,PKW1T,PKW3T
      COMMON/EVAL/PAR(6),DPAR(6),NMAX,NPG
      COMMON/PRN/A(210),IUF
      COMMON/EFF/ETAP,ETAT,ETAG,XU
      COMMON/HXI/QAS,QRS,UB,UC,DT1,DT2
      COMMON/RAN/P1,P2,YA,EPSR,PWF,UWF,VA1,
     * VA2,VA3,DHI,DHA,PWFT
      COMMON/HH3B/HB(4),HF(4),SB(4),SF(4),VB(4),VF(4),PZ(4),X(4)
      COMMON/HXO/VAH,VAC,AB,AC,NTUB,NTUC,EPSB,EPS
     * C,UAB,UAC
      COMMON/HTC/FFB,FFC,HWFB,HWFC,HWALLC,HWALLB,HSUB,HSUC
      COMMON/VEL/VELCP,VELC,VELHP,VELB
      REAL NTUB,NTUC
      NPG=1
      DC=PAR(1)
      CL=PAR(2)
      DTH=PAR(3)
      DTC=PAR(4)
      DTL=PAR(5)
      CTL=PAR(6)
      CALL BT(CL+100.,TH,TC)
      IF(J.GT.2) GO TO 10
      CALL RANKINE
   10 CONTINUE
      NPG=NPG+1
      CALL CWATER(TC+DTC/2.,TKC,CPC,PHUC,RHOC)
      CALL CWATER(TH-DTH/2.,TKB,CPB,PHUB,RHOB)
      CALL HX(PG)
      IF (UAC.LT.0.9E20) GO TO 20
      C=2.E10
      RETURN
   20 CONTINUE
      CALL UCALC(UAB/NXH,AB,CPB,PHUB,TKB,
```

```
01770 +     RHOB,DUB,DB,DOB,FFB,VAH/NXM,2,BTL,UB,
01780      +XN,PB,QRS,WUF)
01790       NTB=XN
01800       CALL UCALC(UAC/NXM,AC,CPC,PMUC,TKC,
01810 +     RHOC,DUC,DDC,DOC,FFC,VAC/NXM,1,CTL,UC,
01820      +XN,PB,QRS,WUF)
01830       NTC=XN
01840 15    CALL PDROP(NC,VAC*NMOD,BC,CL+300.,0.01,RKC,DP1,PKW1,VELCP,RH
01850 +     OC,PMUC,1)
01860       PKW1T=PKW1/(NMOD)
01870       CALL PDROP(NTC,VAC/NXM,BUC,CTL+1.,0.0001,RKCX,DP2
01880 +     ,PKW2,VELC,RHOC,PMUC,2)
01890       PKW2T=PKW2*NXM
01900       CALL PDROP(NH,VAH/NXM,BH,300.,0.02,RKH,DP3,PKW3,VELHP,
01910 +     RHOB,PMUB,3)
01920       PKW3T=PKW3*NXM
01930       CALL PDROP(NTB,VAH/NXM,BUB,BTL+3.5,0.0001,RKBX,DP4
01940 +     ,PKW4,VELB,RHOB,PMUB,4)
01950       PKW4T=PKW4*NXM
01960       PP1=(PKW1T+PKW2T+PKW3T+PKW4T)/1000
01970       RRATIO=RETB/(RETB-REBB)
01980       PP22=PWFT*RRATIO*((BTL+20.)/(144*VF(3))+5.)/(PZ(1)-PZ(3))
01990       PP2=(PWFT*1.1*PB+PP22*PB+PKW1T*1.33/DP1)/1000.
02000       PP=PP1+PP2
02010       IF(ABS((PB-PP-PN)/PN).LT.0.001)GO TO 100
02020       PB=PB-1.3*(PB-PP-PN)
02030       IF(PB.GT.2.*PN)GO TO 110
02040       IF(NPB.EQ.100)GO TO 110
02050       GO TO 10
02060 100   CONTINUE
02070       CALL COST
02080       RETURN
02090  110  C=1.E10
02100       RETURN
02110       END
02120       SUBROUTINE RANKINE
02130 C
02140 C     RANKINE COMPUTES RANKINE CYCLE PARAMETERS,GIVEN
02150 C     WORKING FLUID AND OPERATING TEMPERATURES.
02160 C
02170       COMMON/OPTIONS/NMOD,NOP,NXM,NXUP,NAFP,NARP,NAT
02180       COMMON/TEMP/TH,TC,DTH,DTC,T1,T2
02190       COMMON/HXI/QAS,QRS,UB,UC,DT1,DT2
02200       COMMON/EFF/ETAP,ETAT,ETAG,XW
02210       COMMON/RAN/P1,P2,YA,EPSR,PWF,WWF,VA1,
02220 +     VA2,VA3,DHI,DHA,PWFT
02230       COMMON/DTDP/DTDP(2,3)
02240       COMMON/PRM/A(210),IWF
02250       COMMON/NH3D/HG(4),HF(4),SG(4),SF(4),VG(4),VF(4),PZ(4),X(4)
02260       DATA DTDP/0.44,0.58,0.74,0.95,0.55,0.69/
02270 333   X(1)=T1
02280       X(2)=T1+DT1
02290       X(3)=T2
02300       X(4)=T2-DT2
02310       DO 11 I=1,4
02320       CALL THERMO(X(I),VF(I),VG(I),HF(I),HG(I),SG(I),SF(I),PZ(I))
02330 11    CONTINUE
02340       P1=PZ(1)
02350       P2=PZ(3)
02360       WPI=144./778.16*(P1-P2)*VF(4)
02370       WPA=WPI/0.72
02380       QA=HG(1)-HF(4)-WPA
02390       YI=(SG(3)-SG(1))/(SG(3)-SF(3))
02400       DHI=(HG(1)-(HG(3)-YI*(HG(3)-HF(3))))*(P1-
02410 +     P2-0.1)/(P1-P2)
02420       EPSR=(DHI-WPA)/(QA)
02430       DHA=ETAT*DHI
02440       YA=(DHA+HG(3)-HG(1))/(HG(3)-HF(3))
02450       DHG=ETAG*DHA
02460       PWF=WPA*1000./DHG
02470       PWFT=PWF
02480       WWF=3412.*1000./60./DHG
02490       VA1=WWF*VG(1)
02500       VA2=WWF*(YA*VF(3)+(1.-YA)*VG(3))
02510       QAS=QA*WWF*60.
02520       QRS=(HG(1)-HF(4)-DHA)*WWF*60.
02530       VA3=WWF*VF(4)
02540       RETURN
02550       END
02560       SUBROUTINE THERMO(X1,VF1,VG1,HF1,HG1,SG1,SF1,P11)
02570 C
02580       COMMON/PRM/A(210),IWF
02590       P11   =FX(1,X1)
02600       VF1=FX(2,X1)
```

```
02610       VB1=FX(3,X1)
02620       HF1=FX(4,X1)
02630       HG1=FX(5,X1)
02640       SF1=FX(6,X1)
02650       SG1=FX(7,X1)
02660       RETURN
02670       END
02680       SUBROUTINE CWATER(X,TK,CP,PMU,RHO)
02690 C
02700 C
02710 C
02720       DATA C0,C1,R0,R1,R2,T0,T1,P0,P1,P2/.95213,5.4727E-3,
02730 +     6.4131E+1,-6.8811E-4,-4.9417E-5,3.1043E-1,5.2E-4,
02740 +     7.218,-1.0139E-1,4.903E-4/
02750       TK=(T0+T1*X)/3600.
02760       CP=C0+C1*X
02770       RHO=R0+R1*X+R2*X**2
02780       PMU=(P0+P1*X+P2*X**2)/3600.
02790 C
02800 C
02810 C
02820       RETURN
02830       END
02840       SUBROUTINE HX(PB)
02850 C
02860 C     THIS IS A HEAT EXCHANGER SIZING (UA) ROUTINE.
02870 C
02880       REAL NTUB,NTUC
02890       COMMON/TEMP/TH,TC,DTH,DTC,T1,T2
02900       COMMON/HX1/QAS,QRS,UB,UC,DT1,DT2
02910       COMMON/OPTIONS/NMOD,NOP,NXM,NXUP,NAFP,NARP,NAT
02920       COMMON/HX0/VAH,VAC,AB,AC,NTUB,NTUC,EPSB,EPS
02930 +     C,UAB,UAC
02940       COMMON/CHOH/RHOC,RHOB,PMUC,PMUB,CPB,
02950 +     CPC,TKB,TKC
02960       CWH=PB*QAS/DTH
02970       VAH=CWH/(CPB*RHOB*3600.)
02980       IF((TH-DTH).LT.(T1-DT1+0.001)) GO TO 10
02990       UAB=CWH*ALOG((TH-T1)/(TH-DTH-DT1-T1
03000 +     ))*DTH/(DTH+DT1)
03010       GO TO 11
03020 10    UAB=1.E20
03030       RETURN
03040 11    CONTINUE
03050       NTUB=UAB/CWH
03060       EPSB=1.-EXP(-NTUB)
03070 30    CONTINUE
03080       CWC=PB*QRS/DTC
03090       VAC=CWC/(CPC*RHOC*3600.)
03100       IF((TC+DTC).GT.(T2-0.001)) GO TO 20
03110       IF((TC+0.001).GT.(T2-DT2)) GO TO 20
03120       UAC=CWC*ALOG((T2-TC-DT2)/(T2-TC-DT
03130 +     ))*DTC/(DTC+DT2)
03140       GO TO 41
03150 20    UAC=1.E20
03160       RETURN
03170 41    CONTINUE
03180       NTUC=UAC/CWC
03190       EPSC=1.-EXP(-NTUC)
03200 40    CONTINUE
03210       RETURN
03220       END
03230       FUNCTION FX(N,X)
03240 C
03250 C     COMPUTE THERMODYNAMIC PARAMETERS BY POLYNOMIAL APPROX.
03260 C
03270       COMMON /PRM/ A(10,7,3), M
03280       FX = A(8,N,M)
03290       DO 5 I=1,7
03300    5  FX = A(8-I,N,M) + X*FX
03310       RETURN
03320       END
03330       BLOCK DATA
03340 C
03350 C     THERMODYNAMIC DATA CORRELATIONS FOR THREE WORKING FLUIDS.
03360 C
03370       DIMENSION A(210)
03380       COMMON /PRM/ AN(10,7,3), M
03390       EQUIVALENCE (A,AN)
03400 C           NH3,   M=1
03410 C           R12/31,  M=2
03420 C           C3H8,   M=3
03430       DATA (A(I),I=1,70)/84.133493,-3.9453629,.15738164,-.1913845E-2,
03440      D.1422349E-5,.18339454E-6,-.11502025E-8,3*0.,
```

```
     D.024006455,.31671989E-4,.19186155E-7,7*0.,
     D8.5193668,-.15928666,1.3131055E-3,-4.3466241E-6,6*0.,
     D43.487815,1.0582983,6.0084034E-4,7*0.,
     D611.76387,.32369748,-1.0868347E-3,7*0.,
     D.097824697,.23223434E-2,-.13707722E-5,7*0.,
     D1.3331697,-.18926911E-2,.27186791E-5,7*0./
      DATA (A(I),I=141,210)/38.230987,.7607506,.0053448139,.20438083E-4,
     D6*0.,.028539S,.49614286E-4,8*0.,
     D2.599814,-.042940313,.33701757E-3,-.11431079E-5,6*0.,
     D22.295251,.57566684,.2100919E-3,.17800981E-5,6*0.,
     D192.37849,.24008895,.6844913E-3,-.1036914E-4,.40020469E-7,5*0.,
     D.051873571,.0011781429,8*0.,.41891072,-.18447649E-3,.69524078E-6,
     D7*0./
      DATA (A(I),I=71,140)/23.525983,.51905623,3.9539428E-3,
     D1.8760553E-5,6*0.,.011383466,1.1766036E-5,4.3291317E-8,7*0.,
     D1.8709644,-.035334956,3.5435288E-4,-2.0419788E-6,5.2201533E-9,
     D5*0.,8.9574725,.23667748,-3.4996582E-6,6.8474216E-7,6*0.,
     D90.829294,.11175462,-1.4016807E-4,7*0.,
     D.02036797,5.0953434E-4,-5.0909091E-7,1.4141414E-9,6*0.,
     D.19859993,-1.5477577E-4,6.6334017E-7,-1.8607124E-9,6*0./
      END
      SUBROUTINE FRICFAC(RE,EOD,FD)
C
C     COMPUTES FRICTION FACTORS USING COLEBROOKS CORRELATION.
C
      COMMON/ARRR/ARR
      INTEGER E
      IF(RE.LT.500000.) GO TO 11
      FD = .316/SQRT(SQRT(RE))
      X = 1./SQRT(FD)
      A = EOD/3.7
      B = 2.51/RE
      DX = 0.
      N = -1
 2    X = X + DX
      U = A + B*X
      IF(U.LE.0.0)GO TO 12
      DYDX = 1. + .86*B/U
      DX = -(X + .86*ALOG(U))/DYDX
      N = N + 1
      IF(ABS(DX/X).GT..001) GO TO 2
      FD = 1./(X*X)
      RETURN
 12   FD=.316/SQRT(SQRT(RE))
      RETURN
 11   CONTINUE
      DATA C1,C2,C3/0.025,-0.7534,1.386/
      REL=ALOG(RE)
      FDL=C1*(REL**2)+C2*REL+C3
      FD=EXP(FDL)
      FD=FD*ARR
 10   CONTINUE
      RETURN
      END
      SUBROUTINE PDROP(N,G,D,EL,EPS,RK,DP,PKW,VEL,RHO,PMU,I)
C
C     COMPUTES PRESSURE DROP AND PUMPING POWER
C     FOR A GIVEN PIPE OR TUBE ARRANGEMENT.
      COMMON/EFF/ETAP,ETAT,ETAG,XU
      VEL = 4.*G/(D*D*3.14159*N)
      IF(I.EQ.2.OR.I.EQ.4)GO TO 10
      VEL=6.
      D=SQRT(4*G/(N*3.14159*VEL))
 10   CONTINUE
      RE = RHO*VEL*D/PMU
      CALL FRICFAC(RE,EPS/D,FD)
      DP = (FD*EL/D + RK)*RHO*VEL*VEL/(2.*144.*32.174)
      PKW = 144.*DP*G/(550.*1.341*ETAP)
      RETURN
      END
      SUBROUTINE BT(H,TH1,TC1)
C
C     TEMPERATURE-DEPTH PROFILE.
C
      TH1=79.
      TC1=39.+39.4*EXP(-(H-100.)/977.)
      TH1=80.
      TC1=40.
      RETURN
      END
      SUBROUTINE OPTIMIZ
C
C     OPTIMIZATION (COST MINIMIZATION) ROUTINE
C     SEQUENTIAL DIRECT SEARCH.
```

```
04290 C
04300       COMMON/OPTIONS/NMOD,NOP,NXM,NXUP,NAFP,NARP,NAT
04310       COMMON/EVAL/PAR(6),DPAR(6),NMAX,NPG
04320       COMMON/COST/C,CBXT,CCXT,CCUT,CCUPT,CUUPT,CMOOR,
04330 +     CTURBT,CBPT,CFPT,CRPT,CGENT
04340       COMMON/NEXT/NEXT
04350       IF(NEXT.EQ.4) GO TO 110
04360 C     DISPLAY* J   PAR(J)      COST*
04370       DO 100 J=3,6
04380       N=1
04390    10 CALL EVAL(J)
04400 C     WRITE(6,25) J,PAR(J),C,NPG
04410    25 FORMAT(I2,2X,F10.3,2X,E10.3,I6)
04420       IF(N.NE.1) GO TO 40
04430    20 C0=C
04440    30 N=N+1
04450       PAR(J)=PAR(J)+DPAR(J)
04460       GO TO 10
04470    40 IF(C.GE.C0) GO TO 50
04480       IF(N.GT.NMAX) GO TO 60
04490       GO TO 20
04500    50 DPAR(J)=-DPAR(J)
04510       PAR(J)=PAR(J)+DPAR(J)
04520       IF(N.EQ.2) GO TO 30
04530    60 CONTINUE
04540   100 CONTINUE
04550   110 CALL EVAL(6)
04560 82    PRINT 80,(PAR(J),J=3,6),C,NPG
04570 80    FORMAT(5F9.2,I6)
04580       RETURN
04590       END
04600       SUBROUTINE COST
04610 C
04620 C     COMPUTES DIRECT COST OF TRADE OFF SENSITIVE COST ELEMENTS.
04630 C
04640       COMMON/COST/C,CBXT,CCXT,CCUT,CCUPT,CUUPT,CMOOR,
04650 +     CTURBT,CBPT,CFPT,CRPT,CGENT
04660       COMMON/OPTIONS/NMOD,NOP,NXM,NXUP,NAFP,NARP,NAT
04670       COMMON/POWER/PN,PB,CWP,UUP
04680       COMMON/TEMP/TH,TC,DTH,DTC,T1,T2
04690       COMMON/DIM/H,DC,DH,NH,NC,NTB,NTC,CTL,BTL,
04700 +     RKC,RKH,RKBX,RKCX,CL,PI,NCP
04710       COMMON/DIA/DWB,DWC,DB,DDC,DOB,DOC
04720       COMMON/PAR/PKW1,PKW2,PKW3,PKW4,DP1,DP2,DP3,DP4
04730 +     ,PKW2T,PKW4T,PKW1T,PKW3T
04740       COMMON/EVAL/PAR(6),DPAR(6),NMAX,NPG
04750       COMMON/PRM/A(210),IUF
04760       COMMON/EFF/ETAP,ETAT,ETAG,XW
04770       COMMON/HXI/QAS,QRS,UB,UC,DT1,DT2
04780       COMMON/RAN/P1,P2,YA,EPSR,PWF,UWF,VA1,
04790 +     VA2,VA3,DHI,DHA,PWFT
04800       COMMON/HXO/VAH,VAC,AB,AC,NTUB,NTUC,EPSB,EPS
04810 +     C,UAB,UAC
04820       COMMON/VEL/VELCP,VELC,VELHP,VELB
04830       COMMON/TURB/K3,V3
04840       COMMON/AA/A11(14)
04850       COMMON/MAT/EM(12),CM(12)
04860       COMMON/LAB/EL(12),CL11(12)
04870       COMMON/FAB/C11,C22,B11,B22
04880       COMMON/REN/REBB,RETB,REBC,RRATIO
04890       REAL NTUB,NTUC
04900 C     IF IC=1  TUBESHEETS CLAD  WHICH IMPLIES EM3=EL3=0.0
04910       IC=2
04920       CZ=0.0
04930       D=DOB*12.
04940       XN=NTB
04950       XL=BTL*3.5
04960       EM(1)=XN*(B11*XL+B22)
04970       EM(2)=1.24*D**2.300*XN**1.150
04980       EM(3)=.105*D**2.500*XN**1.27
04990       IF(IC.EQ.1)EM(3)=0.0
05000       IF(IC.NE.1)EM(2)=0.0
05010       EM(4)=(9.22*D**3.046*XN**1.523)/10000.
05020       EM(5)=.012*D**2.290*XN**1.145*XL
05030       EM(6)=.175*D**2.100*XN**1.05
05040       EM(7)=79.6*D**0.908*XN**0.454
05050       EM(8)=.024*D**2.592*XN**1.296
05060       EM(9)=0.0104*D**2.690*XN**1.345
05070       EM(10)=12.0*D**1.280*XN**0.64
05080       EM(11)=0.053*D**2.090*XN**1.045
05090       EL(1)=28.10*D**0.700*XN**1.0
05100       F=D*XN**0.5-148.
05110       IF(F.LT.0.0)F=0.0
05120       EL(2)=0.457*D**0.680*XN**1.34*(D-0.5)+329.*F**1.5
```

```
05130       EL(3)=0.307*D**0.660*XN**1.33*(D-0.5)+221.*F**1.5
05140       IF(IC.EQ.1)EL(3)=0.0
05150       IF(IC.NE.1)EL(2)=0.0
05160       EL(4)=0.124*D**0.591*XN**1.295*(D-0.5)
05170       EL(5)=3.160*D**1.654*XN**0.827*XL**0.7
05180       EL(6)=172.5*D**1.320*XN**0.66
05190       EL(7)=62.30*D**1.340*XN**0.67
05200       EL(8)=.0962*D**0.756*XN**1.38*(D-0.5)
05210       EL(9)=147.4*D**1.350*XN**0.675
05220       EL(10)=92.30*D**1.270*XN**0.635
05230       EL(11)=27.10*D**1.33*XN**0.665
05240       EL(12)=0.0
05250       EM(12)=0.0
05260       DO 50 I=1,11
05270       EL(12)=EL(12)+EL(I)
05280       EM(12)=EM(12)+EM(I)
05290 50    CONTINUE
05300       CBX=EL(12)+EM(12)
05310       CBXT=CBX*NXM*NMOD
05320       SP1=1.6833*XL*XN*D0B*D0B
05330 C     CONDENSER
05340       D=D0C*12.
05350       XN=NTC
05360       XL=CTL+1.0
05370       CM(1)=XN*(C11*XL+C22)
05380       CM(2)=1.24*D**2.300*XN**1.150
05390       CM(3)=.105*D**2.500*XN**1.27
05400       IF(IC.EQ.1)CM(3)=0.0
05410       IF(IC.NE.1)CM(2)=0.0
05420       CM(4)=(9.22*D**3.046*XN**1.523)/10000.
05430       CM(5)=.012*D**2.290*XN**1.145*XL
05440       CM(6)=.175*D**2.100*XN**1.05
05450       CM(7)=79.6*D**0.908*XN**0.454
05460       CM(8)=0.0
05470       CM(9)=0.0
05480       CM(10)=12.0*D**1.280*XN**0.64
05490       CM(11)=0.053*D**2.090*XN**1.045
05500       CL11(1)=28.10*D**0.700*XN**1.0
05510       F=D*XN**0.5-148.
05520       IF(F.LT.0.0)F=0.0
05530       CL11(2)=0.457*D**0.680*XN**1.34*(D-0.5)+329.*F**1.5
05540       CL11(3)=0.307*D**0.660*XN**1.33*(D-0.5)+221.*F**1.5
05550       IF(IC.EQ.1)CL11(3)=0.0
05560       IF(IC.NE.1)CL11(2)=0.0
05570       CL11(4)=0.124*D**0.591*XN**1.295*(D-0.5)
05580       CL11(5)=3.160*D**1.654*XN**0.827*XL**0.7
05590       CL11(6)=172.5*D**1.320*XN**0.66
05600       CL11(7)=62.30*D**1.340*XN**0.67
05610       CL11(8)=0.0
05620       CL11(9)=0.0
05630       CL11(10)=92.30*D**1.270*XN**0.635
05640       CL11(11)=27.10*D**1.33*XN**0.665
05650       CL11(12)=0.0
05660       CM(12)=0.0
05670       DO 60 I=1,11
05680       CL11(12)=CL11(12)+CL11(I)
05690       CM(12)=CM(12)+CM(I)
05700 60    CONTINUE
05710       CCX=CL11(12)+CM(12)
05720       CCXT=CCX*NXM*NMOD
05730       SP2=1.6833*XL*XN*D0C*D0C
05740       CCWT=42.*CL*PI*DC*NC/4.
05750       CWP=PKW1T*(1.+1.33/DP1)+PKW2T
05760       CCWP=VAC/(NXM*NXWP)*448.6*0.75+50000.
05770       CCWPT=CCWP*NXWP*NMOD*NXM
05780       WWP=PKW3T+PKW4T
05790       CWWP=VAH/(NXM*NXWP)*448.6*0.75+50000.
05800       CWWPT=CWWP*NXWP*NMOD*NXM
05810       K3=1
05820 30    XX=VA3*PG*448.6/(60.*1000.)/NXM/K3
05830       CFP=(7.64*XX-0.304*XX*XX-4.28)*1000.
05840       CFPT=CFP*NAFP*NMOD*NXM
05850       XX=XX*RRATIO
05860       CRP1=(-.045*XX*XX+3.26*XX+12.76)*1000.
05870       CRP2=(-0.6*XX*XX+13.26*XX-27.3)*1000.
05880       CRP=AMAX1(CRP1,CRP2)
05890       CRPT=CRP*NARP*NMOD*NXM
05900       Y=PG/(NXM*NAT)
05910       CTURB=(-0.001*Y*Y+0.082*Y-0.129)*1.E6
05920       CTURBT=CTURB*NMOD*NXM*NAT
05930       CGEN=(0.023*PG+0.3)*1.E6
05940       CGENT=CGEN*NMOD
05950       CMOOR=1.5E6
05960       CSP=(SP1+SP2)*2.*20.
```

```
05970       CSPT=0.0
05980 40    C=(CBXT+CCXT+CSPT+CCUT+CCUPT+CWUPT+CMOOR+CTURBT+CGENT+
05990 +     CFPT+CRPT)/1.E6
06000       RETURN
06010       END
06020       SUBROUTINE UCALC(UA,A,CP,PMU,TK,RHO,DU,D,DO,FF,G,I,TL,U,
06030      +XN,PG,GRS,UWF)
06040       COMMON/ARRR/ARR
06050       COMMON/HTC/FFB,FFC,HWFB,HWFC,HWALLC,HWALLB,HSUB,HSWC
06060 C
06070 C     COMPUTES OVERALL "U" BY NEWTON-RHAPSON ITERATION.
06080       PI=3.1415927
06090       PR=CP*PMU/TK
06100       PR1=(PR**0.33333)*(RHO*DU/PMU)**0.8
06110       C1=4.*G*TL/DU
06120       C2=0.027*TK*PR1*3600.*ARR/DU
06130       X2=(4*G/(PI*DU*DU))**0.8
06140       X1=PI*DU*TL
06150       X3=UA/(X1*X2*C2)
06160       X4=DU*UA/D/X1
06170       X5=UA*FF/X1
06180 C     DISPLAY*C1,C2,X1,X2,X3,X4,X5*
06190 C     DISPLAY C1,C2,X1,X2,X3,X4,X5
06200 C     INITIAL GUESS
06210       XN=4.*G/(PI*DU*DU*6.)
06220 10    CALL NH3HTC(I,TL,XN,D,PG,GRS,UWF,DO,HWF,DHWF)
06230       F1=XN-X3*XN**0.8-X4/HWF-X5
06240       DF1=1-.8*X3/(XN**.2)+X4*DHWF/(HWF*HWF)
06250       XN1=XN-F1/DF1
06260 C     DISPLAY*XN,XN1,F1,DF1,HWF,DHWF*
06270 C     DISPLAY XN,XN1,F1,DF1,HWF,DHWF
06280       IF(ABS((XN-XN1)/XN1).LT.0.001) GO TO 20
06290       XN=XN1
06300       GO TO 10
06310    20 XN=XN1
06320       V=4.*G/(DU*DU*PI*XN)
06330       H=C2*V**0.8
06340       IF(I.EQ.1)HSWC=H
06350       IF(I.EQ.2)HSUB=H
06360       A=X1*XN
06370       U=UA/A
06380 C     DISPLAY*U=*,U,*A=*,A,*V=*,V,*XN=*,XN
06390 C     DISPLAY*N=*,XN,C1,C2,X1,X2,X3,X4,X5
06400 C     DISPLAY*PG,UA,G,HWF*
06410 C     DISPLAY PG,UA,G,HWF
06420 C     DISPLAY* *
06430       IF(U.LT.100.) U=100.
06440       RETURN
06450       END
06460       SUBROUTINE NH3HTC(I,TL,XN,D,PG,GRS,UWF,DO,HWF,DHWF)
06470 C     I=1 IS FOR THE CONDENER
06480       COMMON/REN/REBB,RETB,REBC,RRATIO
06490       COMMON/TIAL/THICKC,THICKB,CUR
06500       COMMON/HTC/FFB,FFC,HWFB,HWFC,HWALLC,HWALLB,HSUB,HSWC
06510       PI=3.14159
06520       IF(I.EQ.1) GO TO 10
06530 C     EVAPORATOR
06540       GO TO 20
06550 C     F1=7200.+6600.*DO-1600*DO*DO
06560 C     F2=0.097-0.233*DO+0.058*DO*DO
06570 C     H=F1*TL**F2
06580 C     RETURN
06590    20 UWF1=UWF*1.0+60
06600 C     INITIAL GUESS
06610       X0=2000.
06620       A=3.17508E8
06630       B=1.44537
06640       C=3.5446282*UWF1/(XN*D)
06650       N=1
06660 100   F5=X0-A*X0**(-B)+C
06670       DF5=1.+A*B*X0**(-B-1)
06680       X1=X0-F5/DF5
06690       IF(ABS((X1-X0)/X1).LT.0.001)GO TO 200
06700       X0=X1
06710       N=N+1
06720       GO TO 100
06730 200   REBB=X1
06740       RETB=A/(X1**B)
06750 C     DISPLAY*NO OF ITERATIONS FOR E HTC=*,N
06760 C     DISPLAY*REBB=*,REBB,*RETB=*,RETB
06770       C1=2.939
06780       C2=0.4151
06790       C3=63.217
06800       C4=1.E6*0.8
```

```
06810       C5=7.04096*0.8
06820       C6=1.8452
06830       F1=((C1*(RETB**C2)-C3)*C4-C5*(REBB**C6))
06840       F2=RETB-REBB
06850       R0=.065/(12.*116.)
06860       H=F1/F2
06870       TH=THICKB/12.
06880       R=TH*D/(CON*(D-TH))
06890       HWALLB=1/R
06900 C     H IS FROM A COMPOSITE CORRELATION
06910 C     THEREFORE RO MUST BE TAKEN OUT TO GET HWFB
06920       HWFB=1./(1/H-R0)
06930       HWF=1/(1/HWFB+R)
06940 C     HWF IS THE COMPOSITE HTC FOR THIS SYSTEM
06950       DF1=(-C1*C2*C4*RETB**C2+C5*C6*REBB**C6)/XN
06960       DF2=-F2/XN
06970       DH=(F2*DF1-F1*DF2)/(F2*F2)
06980       DHWFB=DH/(1.-R0*H)**2.
06990       DHWF=DHWFB/(HWFB*R+1.)**2.
07000       RETURN
07010 C     CONDENSER
07020 10    C1=-3231.62
07030       C2=3.684E8
07040       C3=20129.28
07050       R0=.03125/(12.*116.)
07060       Q=QRS*PG
07070       A=TL*D*PI*XN
07080       DA=A/XN
07090       TH=THICKC/12.
07100       R=TH*D/(CON*(D-TH))
07110       H=C1+C2/(Q/A+C3)
07120       HWFC=1/(1/H-R0)
07130       HWF=1/(1/HWFC+R)
07140       DH=C2*Q/DA/(Q/DA+C3*XN)**2.
07150       DHWFC=DH/(1.-R0*H)**2.
07160       DHWF=DHWFC/(1+R*HWFC)**2.
07170       REBC=3.13606*WWF*PG*60./(XN*D)
07180       HWALLC=1/R
07190       RETURN
07200       END
07210       SUBROUTINE PRINT1
07220 C
07230 C     PRINT RESULTS
07240 C
07250       COMMON/REN/REBB,RETB,REBC,RRATIO
07260       COMMON/COST/C,CBXT,CCXT,CCUT,CCUPT,CWUPT,CMOOR,
07270 +     CTURBT,CSPT,CFPT,CRPT,CGENT
07280       COMMON/OPTIONS/NMOD,NOP,NXM,NXUP,NAFP,NARP,NAT
07290       COMMON/POWER/PW,PG,CWP,WWP
07300       COMMON/TEMP/TH,TC,DTH,DTC,T1,T2
07310       COMMON/DIM/H,DC,DH,NH,NC,NTB,NTC,CTL,BTL,
07320      1RKC,RKH,RKBX,RKCX,CL,PI,NCP
07330       COMMON/DIA/DWB,DWC,DB,DBC,DOB,DOC
07340       COMMON/PAR/PKW1,PKW2,PKW3,PKW4,DP1,DP2,DP3,DP4
07350 +     ,PKW2T,PKW4T,PKW1T,PKW3T
07360       COMMON/EVAL/PAR(6),DPAR(6),NMAX,NPG
07370       COMMON/PRM/A(210),IWF
07380       COMMON/EFF/ETAP,ETAT,ETAG,XW
07390       COMMON/HXI/GAS,QRS,HR,HC,DT1,DT2
07400       COMMON/RAN/P1,P2,YA,EPSR,PWF,WWF,VA1,
07410 +     VA2,VA3,DHI,DHA,PWFT
07420       COMMON/HXO/VAH,VAC,AB,AC,NTUB,NTUC,EPSB,EPS
07430 +     C,UAB,UAC
07440       COMMON/TURB/K3,V3
07450       COMMON/HTC/FFB,FFC,HWFB,HWFC,HWALLC,HWALLB,HSWB,HSWC
07460       COMMON/CHOH/RHOC,RHOB,PWC,PWB,CPB,
07470 +     CPC,TKB,TKC
07480       COMMON /VEL/ VELCP,VELC,VELWP,VELB
07490       COMMON/AA/A11(14)
07500       COMMON/MAT/EM(12),CM(12)
07510       COMMON/LAB/EL(12),CL11(12)
07520       COMMON/ARRR/ARR
07530       COMMON/FAB/C11,C22,B11,B22
07540       REAL NTUB,NTUC
07550       DISPLAY* *
07560       PRINT 133,A11(14)
07570 133   FORMAT(25X,A10)
07580       XNTB=NTB
07590       XNTC=NTC
07600       DSC=0.122*D0C*12.**SQRT(XNTC)
07610       D0C0=D0C*12.
07620       W2=VA2*PG/60./WXM
07630       W3=VA3*PG/60./WXM
07640       QC=QRS*PG
```

```
07660       QB=QAS*PG
07670       U1=VA1*PG/60./NXM
07680       BOBO=DOB*12.
07690       DSB=0.122*DOB*12.*SQRT(XNTB)
07700       BTLT=BTL+3.5
07710       CTLT=CTL+1.
07720       VAH1=VAH*3600.*RHOB
07730       VAC1=VAC*3600.*RHOC
07740       DP11=DP1+1.33
07745       T22=T2-DT2
07750       PRINT 9
07760       PRINT 11,CL
07770       PRINT 12,DH,DC
07780       PRINT 13,NH,NC
07790       PRINT 14,VELHP,VELCP
07800       PRINT 38,VAH1,VAC1
07810       PRINT 16,DP3,DP11
07820       PRINT 15
07830       PRINT 17,REBB,REBC
07840       PRINT 18,RETB
07850       PRINT 19,BTL,CTL
07860       PRINT 20,BTLT,CTLT
07870       PRINT 21,DSB,DSC
07880       PRINT 22,BOBO,BOCO
07890       PRINT 23,HTB,HTC
07900       PRINT 41,B11,C11
07910       PRINT 24,VELB,VELC
07920       PRINT 25,U2
07930       PRINT 26,U1,U3
07940       PRINT 27,AB,AC
07950       PRINT 28,QB,QC
07960       PRINT 29,UB,UC
07970       PRINT 30,HWFB,HWFC
07980       PRINT 31,HWALLB,HWALLC
07990       PRINT 32,HSUB,HSUC
08000       PRINT 40,ARR,ARR
08010       PRINT 33,FFB,FFC
08020       PRINT 39,TH,TC
08030       PRINT 34,DTH,DTC
08040       PRINT 35,DP4,DP2
08050       PRINT 36,T1,T22
08060       PRINT 37,P1,P2
08070 9:    FORMAT(/20X,12HU WATER PIPE,3X,12HC WATER PIPE)
08080 11    FORMAT(25HLENGTH FEET                ,12X,3H300,F15.4)
08090 12    FORMAT(25HDIAMETER FT                ,2F15.4)
08100 13    FORMAT(25HNUMBER OF PIPES            ,2I15)
08110 14    FORMAT(25HH20 VEL FT/S               ,2F15.4)
08120 38    FORMAT(25HWATER FLOW LB/HR           ,2E15.4)
08130 16    FORMAT(25HPRESSURE DROP PSI          ,2F15.4)
08140 15    FORMAT(28X,10HEVAPORATOR,5X,9HCONDENSER)
08150 17    FORMAT(25HBOTTOM REYNOLDS NUM        ,2E15.4)
08160 18    FORMAT(25HTOP REYNOLDS NUM           ,E15.4,12X,3H0.0)
08170 19    FORMAT(25HHEAT TRAN LENGTH FT        ,2F15.4)
08180 20    FORMAT(25HTOTAL LENGTH FT            ,2F15.4)
08190 21    FORMAT(25HSHELL DIAM FT              ,2F15.4)
08200 22    FORMAT(25HTUBE DIAMETER IN           ,2F15.4)
08210 23    FORMAT(25HNUMBER TUBES               ,2I15)
08220 24    FORMAT(25HWATER TUBE VEL FT/SEC      ,2F15.4)
08230 25    FORMAT(25HNH3 ENT FLOW CFS           ,15X,E15.4)
08240 26    FORMAT(25HNH3 EXIT FLOW CFS          ,2E15.4)
08250 27    FORMAT(25HHEAT TRAN AREA SQ. FT.     ,2E15.4)
08260 28    FORMAT(25HHEAT TRANSFERED BTU/HR     ,2E15.4)
08270 29    FORMAT(25HOVERALL BTU/HR/F/FT**2     ,2F15.4)
08280 30    FORMAT(25HNH3 HTC BTU/HR/F/FT**2     ,2F15.4)
08290 31    FORMAT(25HWALL HTC BTU/HR/F/FT**2    ,2F15.4)
08300 32    FORMAT(25HWATER HTC BTU/HR/F/FT**2   ,2F15.4)
08310 33    FORMAT(25HFOULING (FT**2 HR F/BTU)   ,2E15.4)
08320 34    FORMAT(25HCHANGE IN WATER TEMP       ,2F15.4)
08330 35    FORMAT(25HPRESSURE DROP PSID         ,2F15.4)
08340 36    FORMAT(25HNH3 OUTLET TEMP  F         ,2F15.4)
08350 37    FORMAT(25HNH3 OUTLET PRES PSIA       ,2F15.4)
08360       C1=CWP*WMOD /1000.
08370       C2=WWP*WMOD /1000.
08380       PNW=WMOD*PW
08390       PGG=PG*WMOD
08400       C3=PGG-PNW-C1-C2
08410       CHXT=CBXT+CCXT
08420       W4=WWF*PG/60./NXM
08430       W5=PWF*PG
08440       Z1=CPB*RHOB*DTH*VAH*3600.
08450       PEFF=PW*3412*1.E3/Z1
08455       C=C*1.E6
08460       PRINT 42
08470       PRINT 43,PGG,PNW
08480       PRINT 44,C2,C1
```

```
      PRINT 45,C3,U4
      YA1=1.-YA
      PRINT 46,DHA,YA1
      PRINT 47,PEFF,ETAT
      PRINT 48
      PRINT 49,CBXT,CCXT
      PRINT 51,CUUPT,CCUPT
      PRINT 52,CRPT,CFPT
      PRINT 53,CBENT,CTURBT
      PRINT 54,CCWT,CHOOR
      PRINT 55,C,CHXT
   39 FORMAT(25HH2O ENTRANCE TEMP F      ,2F15.4)
   40 FORMAT(25HH2O AREA RATIO           ,2F15.4)
   41 FORMAT(25HTUBE MAT COST $/FOOT     ,2F15.4)
   42 FORMAT(20X,10HCYCLE DATA)
   43 FORMAT(15HGROSS POWER MW ,E10.4,15X,
     +  15HNET POWER MW    ,E10.4)
   44 FORMAT(15HUU PUMPS MW     ,E10.4,15X,
     +  15HCW PUMPS MW     ,E10.4)
   45 FORMAT(15HNH3 PUMPS MW    ,E10.4,15X,
     +  15HEVAPOR LB/SEC   ,E10.4)
   46 FORMAT(15HTURBINE BTU/LB ,E10.4,15X,
     +  15HTUR EX QUALITY ,E10.4)
   47 FORMAT(15HPLANT EFF       ,E10.4,15X,
     +  15HTURBINE EFF     ,E10.4)
   48 FORMAT(20X,10HCOST BREAKDOWN ($))
   49 FORMAT(15HEVAP HE COST    ,E10.4,15X,
     +  15HCON HE COST     ,E10.4)
   51 FORMAT(15HUU PUMP COST    ,E10.4,15X,
     +  15HCW PUMP COST    ,E10.4)
   52 FORMAT(15HNH3 R PUMP      ,E10.4,15X,
     +  15HNH3 F PUMP      ,E10.4)
   53 FORMAT(15HGEN COST        ,E10.4,15X,
     +  15HTURBINE COST    ,E10.4)
   54 FORMAT(15HCW PIPE         ,E10.4,15X,
     +  15HMISCEL          ,E10.4)
   55 FORMAT(15HTOTAL SYSTEM    ,E10.4,15X,
     +  15HTOTAL BOTH HE   ,E10.4)
      A11(1)=10HTUBES
      A11(2)=10HCLAD
      A11(3)=10HUNCLAD
      A11(4)=10HPLATES
      A11(5)=10HSHELL
      A11(6)=10HBOXES
      A11(7)=10HNOZZLES
      A11(8)=10HDIST
      A11(9)=10HBUSTLE
      A11(10)=10HINLETS
      A11(11)=10HSUPPORT
      A11(12)=10HEACH TOTAL
      DISPLAY*                    EVAPORATOR*,
     +  *                         CONDENSER*
      DISPLAY*PART                MATERIAL       LABOR*
     +  ,*        MATERIAL          LABOR*
      DO 10 I=1,12
      PRINT 50,A11(I),EM(I),EL(I),CM(I),CL11(I)
   50 FORMAT(A10,4E15.4)
   10 CONTINUE
      PRINT 1111
 1111 FORMAT(////////)
      RETURN
      END
```

THIS PAGE

WAS INTENTIONALLY

LEFT BLANK

APPENDIX A.2

SYSTEM PERFORMANCE MODEL

TABLE OF CONTENTS

1. INTRODUCTION AND OVERVIEW

2. PROGRAM DESCRIPTION

2.1 Introduction

2.2 The Basic Flow of the Program

2.3 Subroutines and Functions referenced by Main Subroutines Vapor and Liquid

2.3.1 Subroutines and Functions Used in Main Subroutine Vapor

2.3.2 Subroutines and Functions Used in Liquid Side Calculations

2.3.3 Hierarchical Structure of the Program

2.4 Program Flow Charts

2.4.1 Flow Chart of Main Program

2.4.2 Flow Chart of Subroutines Vapor and Liquid

3. INPUT

4. OUTPUT

5. OPERATING PROCEDURES

ATTACHMENT I: SAMPLE CASE

A.1 Standard Output

A.2 TAPE6 (Debug) Output

ATTACHMENT II: DESCRIPTION OF FUNCTIONS AND SUBROUTINES

FIGURES:

2.1 Flow Diagram of Configuration 1

2.2 Flow Diagram of Configuration 2a and 2b

3.1 NAMELIST DATA ($DATAIN) Variables

3.2 NAMELIST DATA ($GEODATA) Variables

4.1 Standard Output

1.0 Introduction and Overview

The Ocean Thermal Energy Conversion Steady State Simulation (OTECSS) computer program was developed to provide an accurate performance model of TRW's PSDI OTEC design's steady state performance. With this simulation as a tool, the performance (power) and, functional parameters (temperatures, pressures, pump suction heads, flow rates etc.) of the plant may be investigated over a wide range of operation conditions.

The OTECSS program was designed to provide the next level of detail beyond the OTEC-II Computer Program in the analysis of OTEC performance. The OTEC-II Program is a design optimization program designed to optimize OTEC cost performance using somewhat simplified models of plant performance consistant with the optimization process. The OTECSS program provides a detailed model of an OTEC design as developed from OTEC-II and other analyses. The OTECSS contains detailed models of the various elements of the OTEC power cycle: Evaporator, condenser, turbine, bypass, pumps, pipes, valves, and bends. The program was developed by TRW and Carnegie Mellon University Consultants. The program is modular in construction and has all important plant parameters as input variables so that present and future designs can be easily studied.

The heat exchangers modeled are of the fluted tube falling film design. The program segements the tubes into a number (nominally 10) of elements and determines the heat transfer for each of the elements. The sum of the evaporation/condensation flow for each element is the total for a single tube. This multiplied by the number of tubes to get the total evaporation or condensation rate. The model assumes that there is no pressure drop in the heat exchanger caused by vapor flow. The amonia entering the evaporator is assumed to be raised to saturation temperature in the header and the water temperature is adjusted for this. Super heat of the liquid in the evaporator header and super cooling in the condenser well is not modeled but should be negligible. Likewise heat transfer through the heat exchanger shells and the various pipes in the system is also not modeled. The water flow through the heat exchangers is constant for this steady state model.

The model for the turbine was developed by Professor Larry Ambs of the University of Massachusetts based on their amonia turbine simulation programs. An optimized single stage turbine was defined for the baseline OTEC conditions using their turbine optimization program. The off design performance was then investigated and the results were curve fit to provide power, outlet pressure, and outlet enthalpy as a function of inlet flow and temperature. Generator efficiency is assumed to be 98% and a 1% turbine bearing loss is allowed for in the program. While the turbine model is felt to be accurate over a wide range, output at less than half or more than 50% greater than nominal may be in error. Variable turbine nozzles are not modeled.

The amonia reflux and condensate pumps are modeled with curve fits to the pump curves shows in Figures 1-1 and 1-2. The curves are valid at the indicated RPM. The head and flow as a function of RPM was developed using the relationship:

$$\frac{n}{n_o} = \frac{Q}{Q_o} = \sqrt{\frac{H}{H_o}}$$

where n_o, Q_o, and H_o are the RPM, flow, and head at the design RPM.

The various control valves are modeled simply with a k factor with which the pressure drop across them is determined. The capability exists to model the k vs angle relationship but this is not used at this time.

The parasitic power required to provide the nominal water flow rates (as input) is an input variable. If different rates are input a new parasitic pumping power is computed as:

$$\text{Power} = \text{Nominal Power}\left(\frac{\text{Flow}}{\text{Flow Nominal}}\right)^{2.8}$$

The OTECSS program selects the proper valve or motor RPM settings on the condensate and reflux (recirculation) lines to achieve equilibrium. Thus, it is not possible to select these valve or RPM settings to observe what will happen to plant performance; they are the dependent variables. Feed rate to the evaporator is an independent variable and the valve or pump setting necessary to achieve a specified flow can be determined.

Program flow in the OTECSS is fairly straightforward. The vapor and liquid portions of the simulation are performed in sequence. First the vapor calculation is performed using the input values of amonia flow, and warm cold water flow. An iterative solution is used in which the evaporation rate and pressure, turbine pressure, enthalpy and quality drops, and condensation rate and pressure are adjusted to reach equilibrium. This is accomplished by adjusting the evaporator pressure until the evaporation rate and the condensation rate (adjusted for turbine outlet quality) are equal to within 1 lb/sec ($\approx .1\%$). The condenser flow and evaporator reflux along with the resepctive pressures are then input to the liquid side. Pump speeds or valve settings are iteratively adjusted, taking into account the pressure drops associated with the fluid flows, to achieve pressure equilibrium.

The following sections of this report describe the program in greater detail, define the input, outputs, and operating procedures and provide a sample case.

Fig. 1-1 EVAPORATOR PUMP & SYSTEM HEAD vs. FLOW

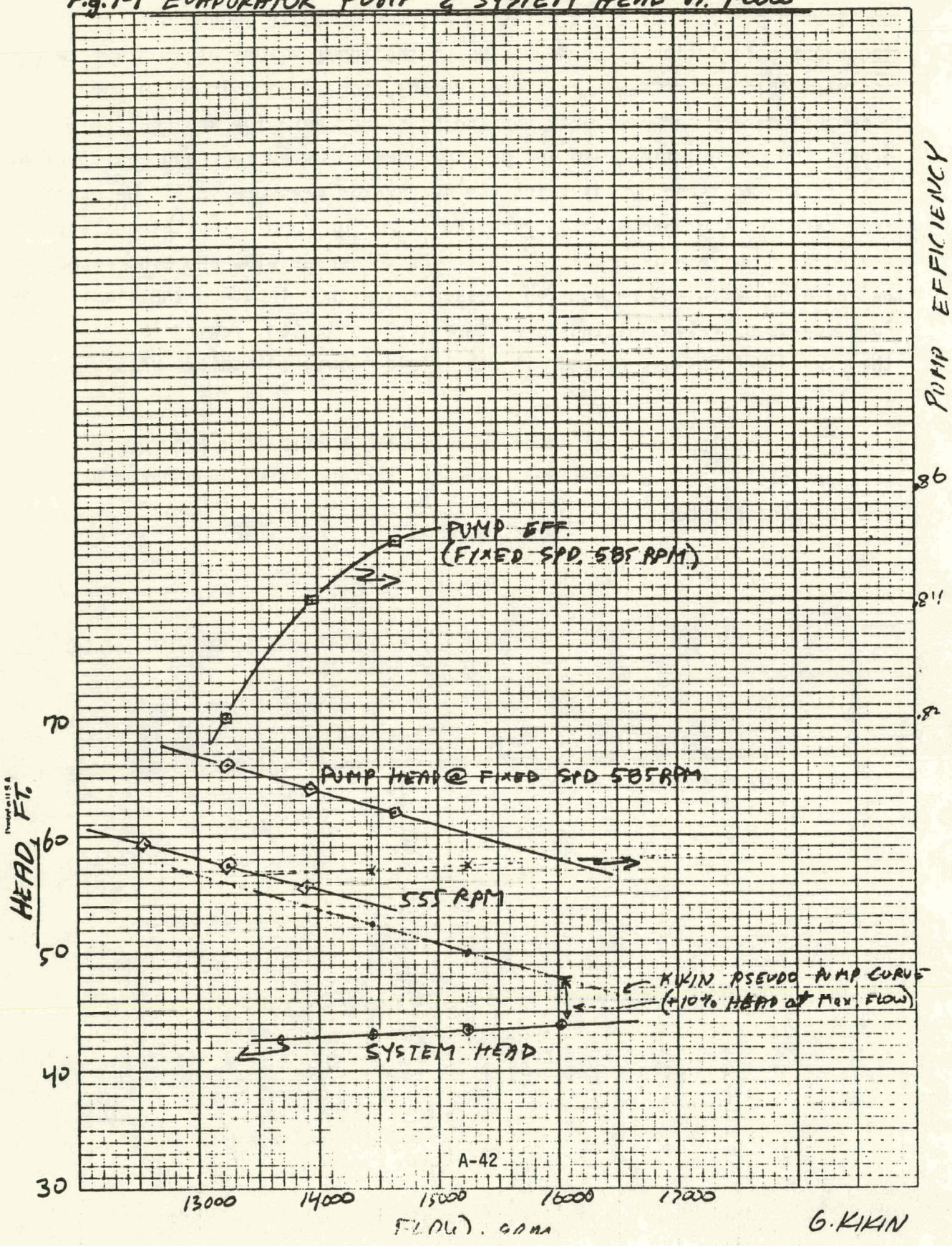

A-42

Fig. 1-2 CONDENSATE PUMP & SYSTEM HEAD vs FLOW

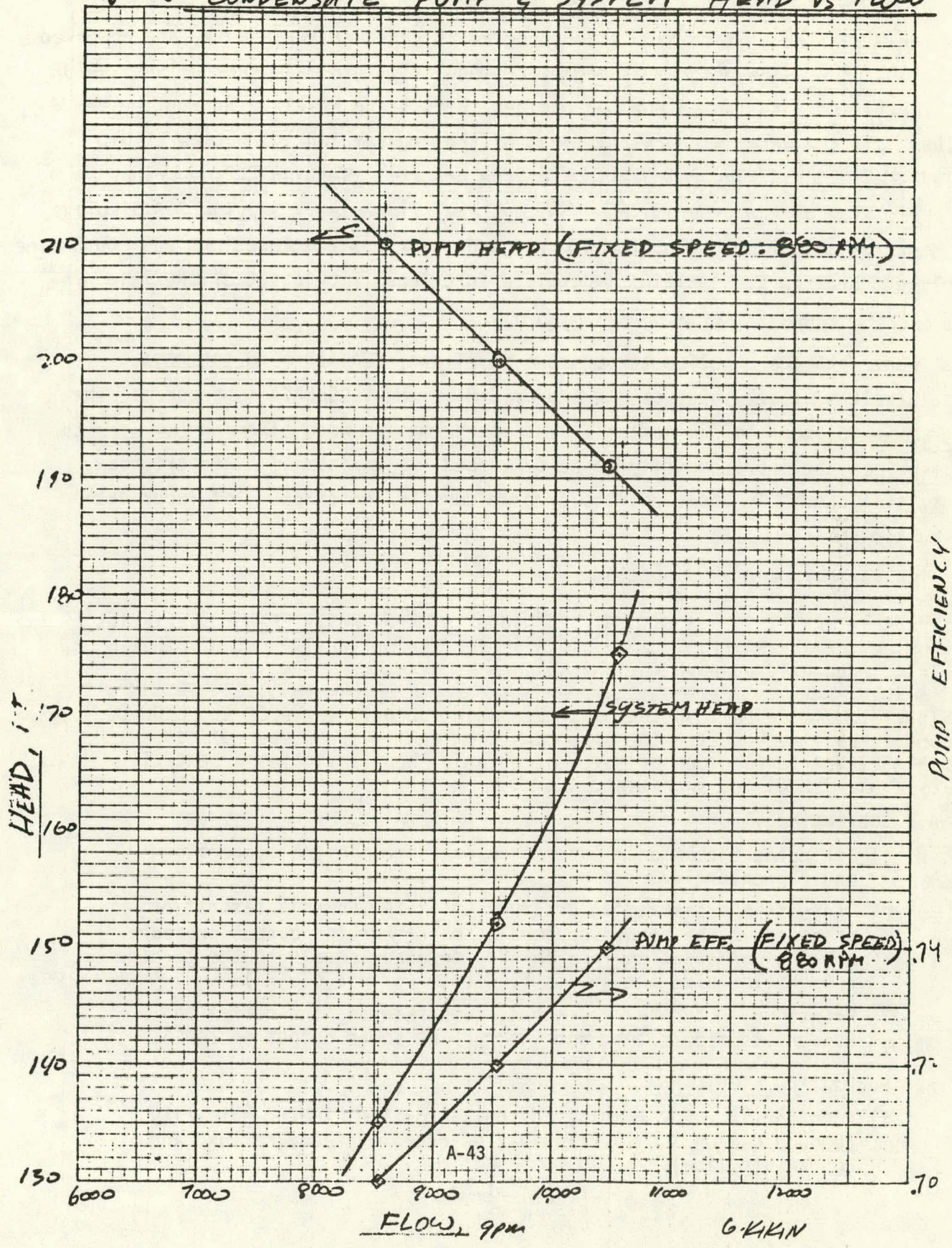

2. PROGRAM DESCRIPTION

2.1 INTRODUCTION

The OTEC Steady State Simulation program is coded in FORTRAN IV, and compiled on the CDC 6600. The program is organized modularly into main subroutines VAPOR and LIQUID, and into two output subroutines BUDGET and MATRIX. Subroutine VAPOR includes all the vapor side calculations of the program and subroutine LIQUID includes all liquid side calculations of the program. Section 2.2 describes the basic flow of the program from the top level flow view. Section 2.3 displays the hierarchical structure of the program and describes the functions and subroutines involved. Section 2.4 contains a detailed functional flow chart of the main program and the subroutines VAPOR and LIQUID.

Input data are supplied through two Namelists, $DATAIN and $GEODATA. Default values of all input data are provided in the BLOCKDATA subprogram. The program is designed to run nominally in a perturbation mode allowing the user to specify just the input quantity to be perturbed. A maximum of nine perturbations is allowed. In addition, the program permits the stacking of input data for multiple cases.

2.2 THE BASIC FLOW OF THE PROGRAM

1. Reads in NAMELIST data $DATAIN for input of frequently changed variables and next reads NAMELIST data $GEODATA for the optional input of other less frequently changed variables.

2. Initiates major DO loop that includes main subroutines VAPOR and LIQUID, and subroutine BUDGET. The loop runs from one to the number of cases (NCASE), perturbing one of seven acceptable input variables repeatedly by a user specified increment.

   a. Subroutine VAPOR

      1) Estimates the ammonia saturation pressures in the evaporator and condenser.

      2) Adjusts the saturation pressure until the ammonia saturation pressure in the condenser equals to the turbine output pressure and the condensation rate in the condenser equals to the turbine output flow plus the bypass flow rate (if not closed).

      3) Prints out saturated pressures, temperatures, the reflux and condensate flow rates, and the turbine power output on TAPE6.

   b. Subroutine LIQUID

      1) Couples the VAPOR results to the subroutine LIQUID, primarily through COMMON/SEAWTR/(liquid flow rates of feed, reflux, and condensate line).

2) Calculates the pump speeds/control valve settings to produce a pressure balance among points P8, P12, and P18 (see Figure 1.1).

3) Calculates the remaining pressures at LIQUID side points.

4) Prints out the pressure profile around the system, the values of the control parameters, the pump powers and NPSH values on TAPE6.

c. Subroutine BUDGET

1) Transmits some of the subroutine LIQUID results to the BUDGET routine through COMMON/PARA/.

2) Prints out the final gross and net power budget on TAPE6.

3. After completion of the DO loop statement, subroutine MATRIX is called in the main program. It displays the output variables of interest.

4. The calculational flow then returns to the start and looks for the next stacked case, or terminates if so instructed.

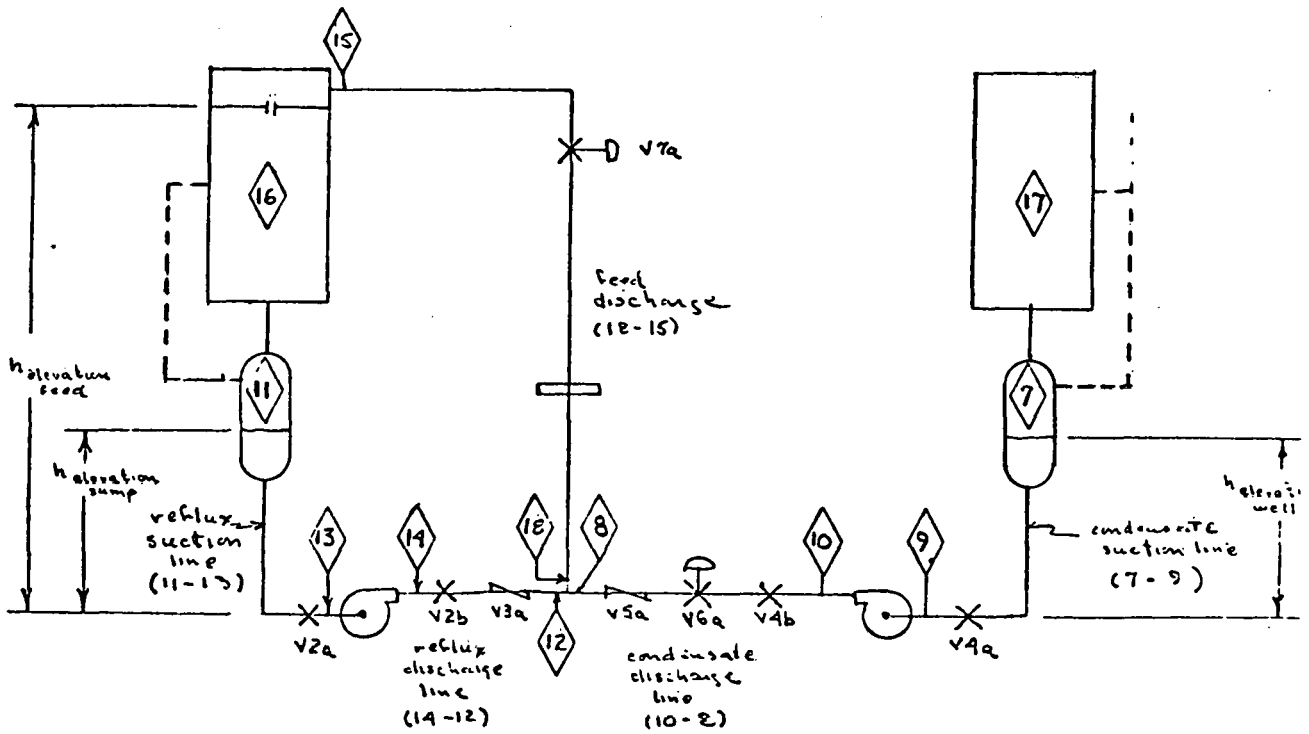

Figure 2.1 Flow Diagram of Configuration 1

Configuration 2a

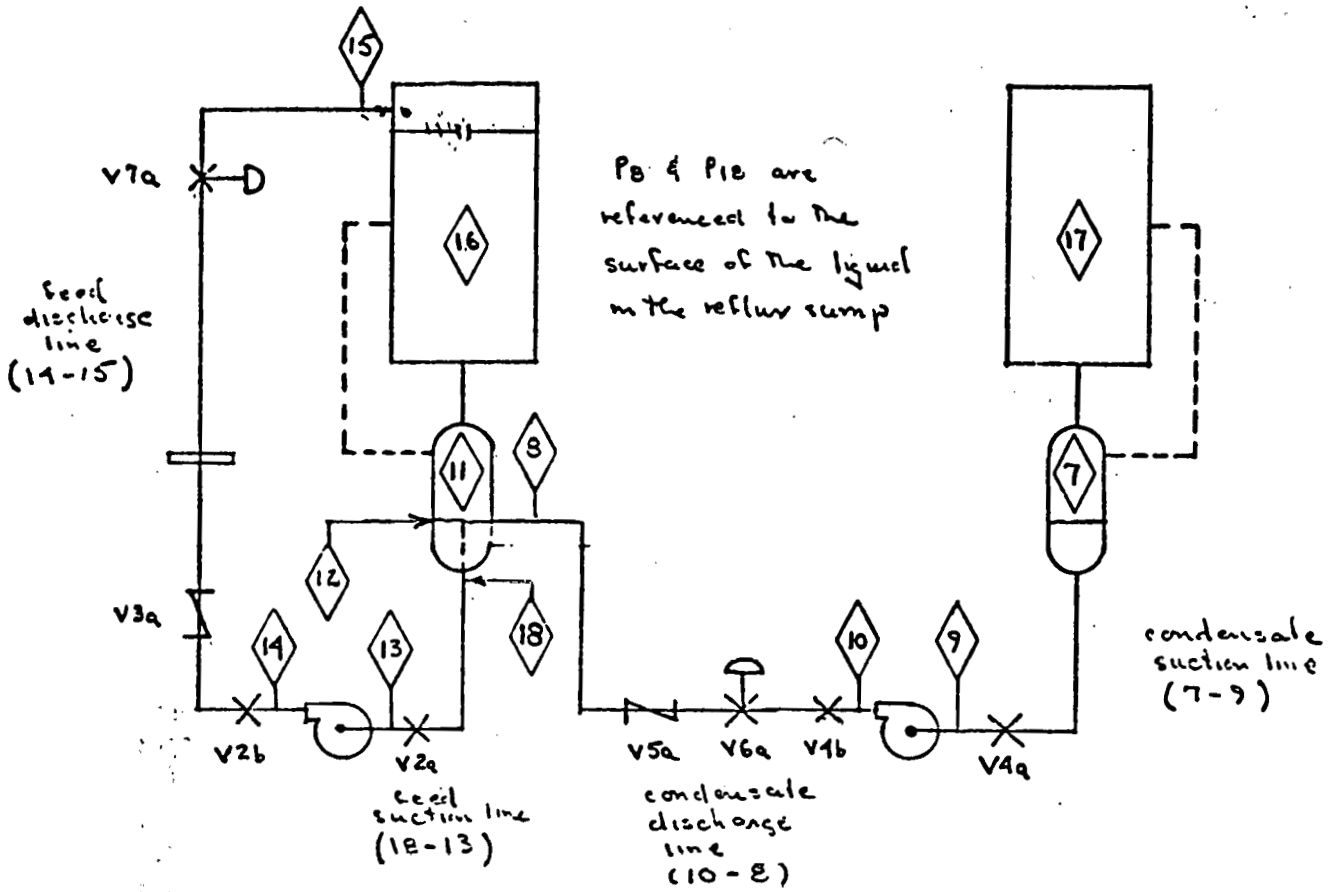

Configuration 2b

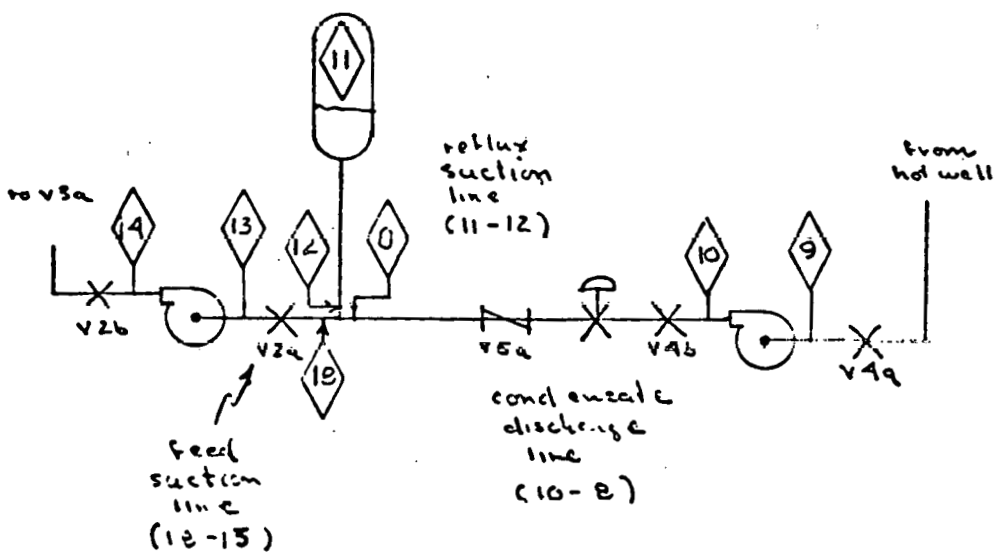

Figure 2.2 Flow Diagram of Configuration 2a and 2b

2.3. SUBROUTINES AND FUNCTIONS REFERENCED BY MAIN SUBROUTINES VAPOR AND LIQUID

2.3.1. Subroutines and Functions Used in Main Subroutine VAPOR

FUNCTIONS		DESCRIPTION
TSAT (P_{sat})	Ammonia Table	Calculates saturation temperature (°F).
PSAT (T_{sat})	Ammonia Table	Calculates saturation pressure (PSIA).
VOLUME (P_{sat})	Ammonia Table	Calculates specific volume of saturated vapor (cu.ft/lb).
HEVAP (M_{WW},M_{NH3},T_{WW},T_{NH3})		Calculates overall local heat transfer coefficient for a segment of an evaporator tube (Btu/°F.sec).
HCOND (M_{CW},M_{NH3},T_{CW},T_{NH3})		Calculates overall local heat transfer coefficient for a segment of a condensate tube (Btu/°F.sec).

SUBROUTINE	DESCRIPTION
EVAP	Calculates the evaporation rate and $\partial ER/\partial P_{sat}$ in the evaporator for specified warm sea water conditions and a specified ammonia feed rate and saturation temperature.
COND	Calculates the condensation rate and $\partial CR/\partial p_{sat}$ in the condenser for specified cold sea water conditons and a specified saturation temperature.
TURBINN	Calculates the output conditions for the turbine and the work done in the turbine for specified inlet conditions and inlet flow rate.

2.3.2 Subroutines and Functions Used in Liquid Side Calculations

FUNCTIONS		DESCRIPTION
PSAT (T_{sat})	Ammonia Table	Calculates saturation pressure (PSIA).
GAMMA (T_{sat})	Ammonia Table	Calculates density of saturated liquid (lbs/ft^3).
P18C1, P18C2A, P18C2B	Calculates pressure drop at control valve V_{7a}	These functions calculate the pressure at points 18, 12, and 8 for the three configurations (see Figure 1.1).
P12C1, P12C2A, P12C2B		
P8C1, P8C2A, P8C2B	Calculates pressure drop at control valve V_{6a}	

SUBROUTINES	DESCRIPTION
VALV7A	Calculates K factor of feed flow control valve.
PUMPRF	Calculates head of reflux pump (ft) and power (KW).
VALV6A	Calculates K factor of condensate flow control valve.
PUMPC	Calculates head of condensate pump (ft) and power (KW).
HEADER	Calculates ΔP in ammonia feed header (ft^3/sec).
SEARCH	Search subroutine to determine the required valve K factors or pump speeds to secure pressure balances in the several legs of the liquid ammonia system.

2.3.3 Hierarchical Structure of the Program

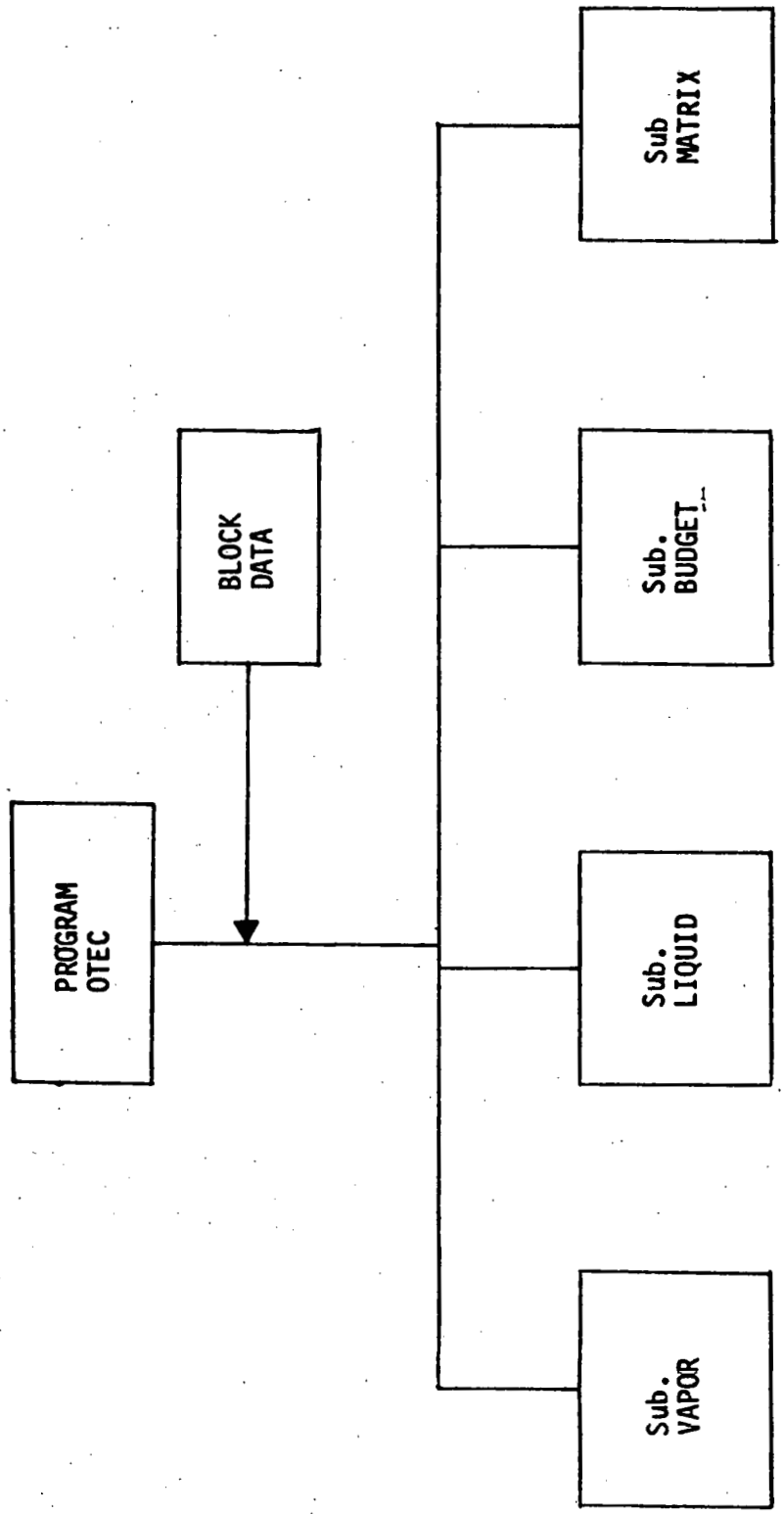

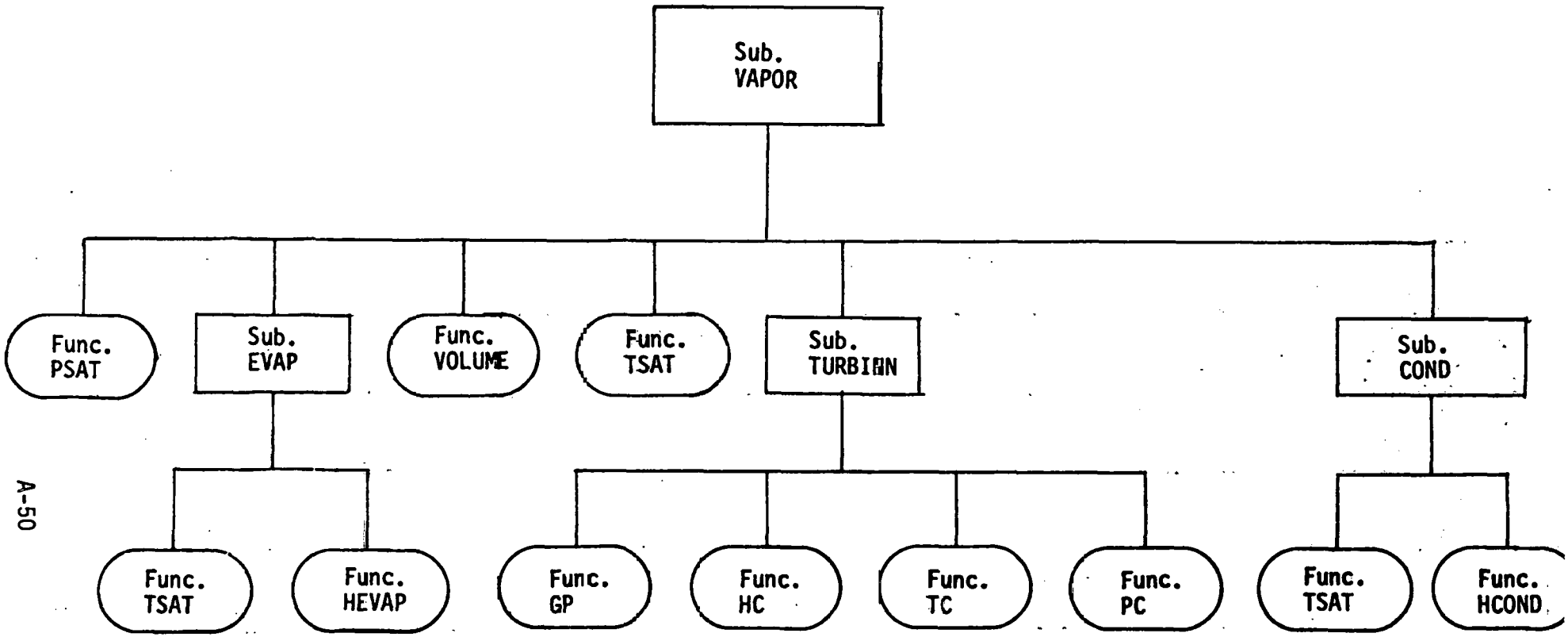
Sub.
VAPOR
Func.
PSAT
Sub.
EVAP
Func.
VOLUME
Func.
TSAT
Sub.
TURBIHN
Sub.
COND
Func.
TSAT
Func.
HEVAP
Func.
GP
Func.
HC
Func.
TC
Func.
PC
Func.
TSAT
Func.
HCOND

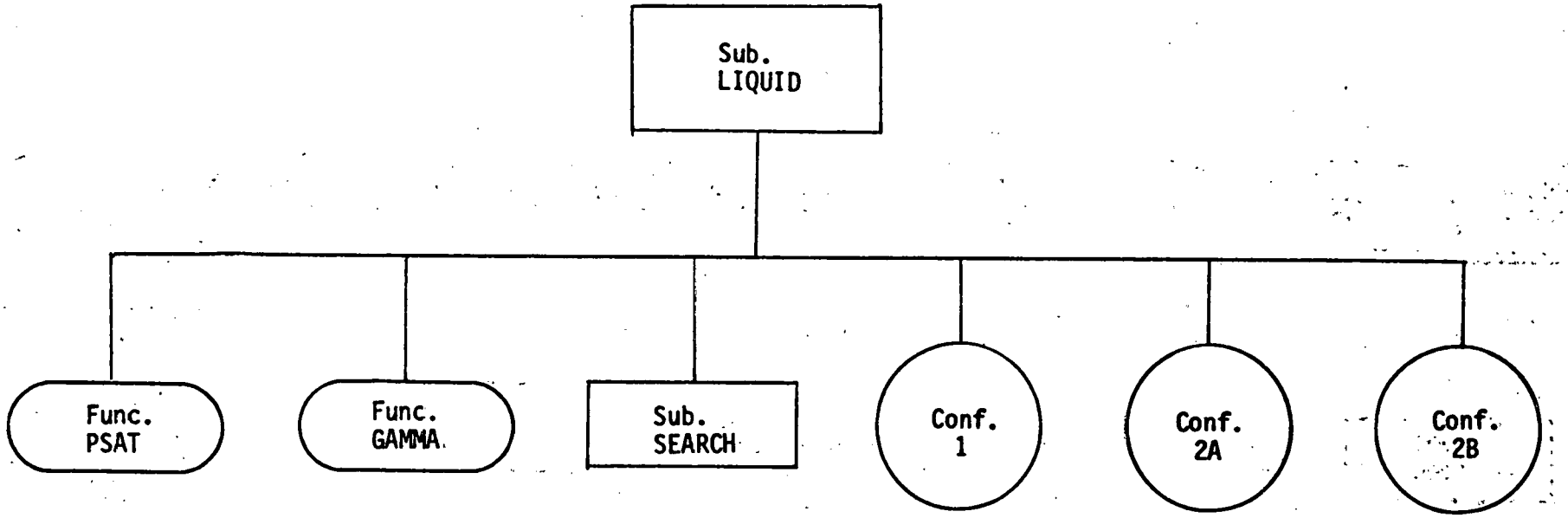
Sub.
LIQUID
Func.
PSAT
Func.
GAMMA
Sub.
SEARCH
Conf.
1
Conf.
2A
Conf.
2B

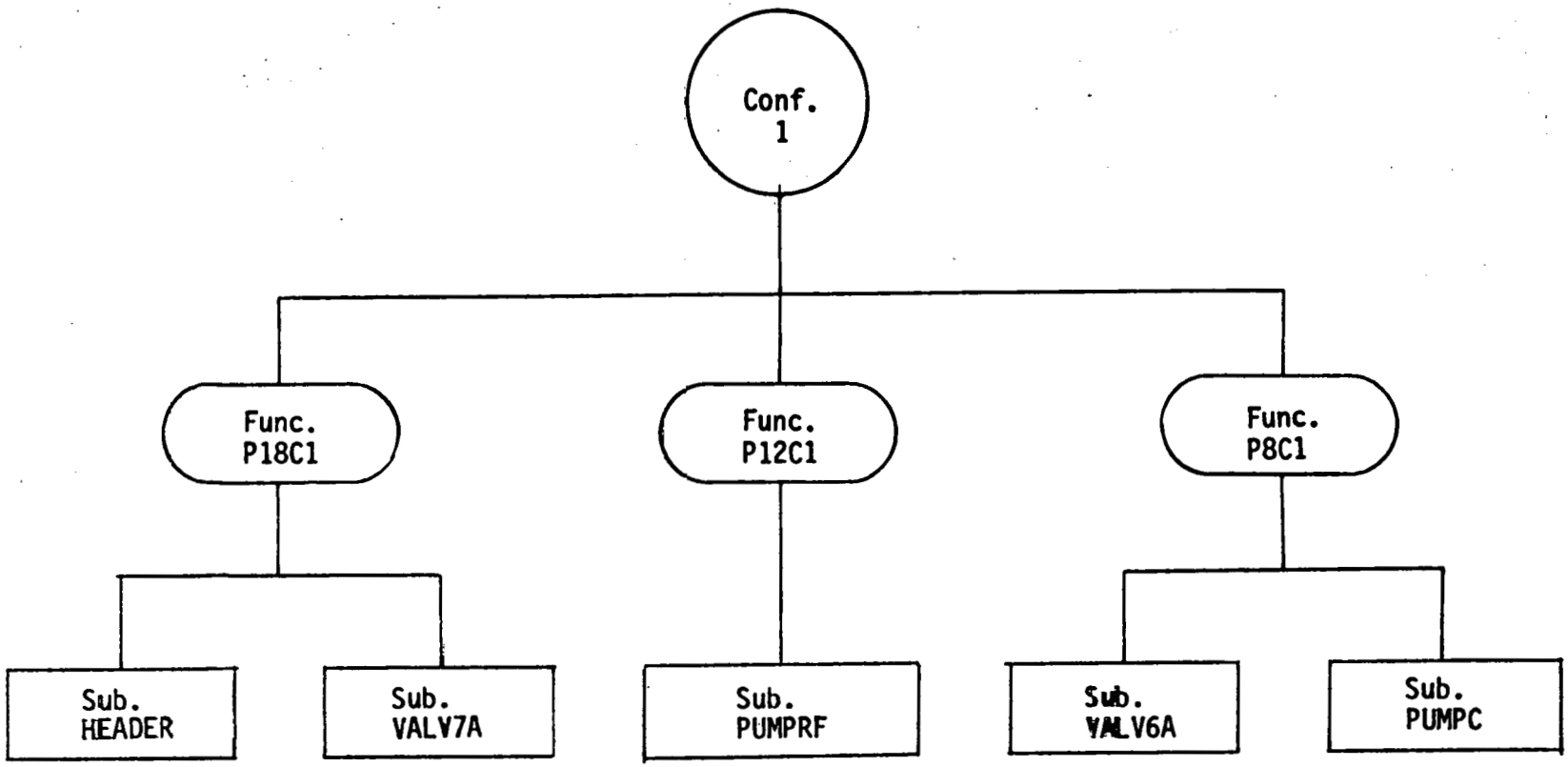
Conf.
1
Func.
P18C1
Func.
P12C1
Func.
P8C1
Sub.
HEADER
Sub.
VALV7A
Sub.
PUMPRF
Sub.
VALV6A
Sub.
PUMPC

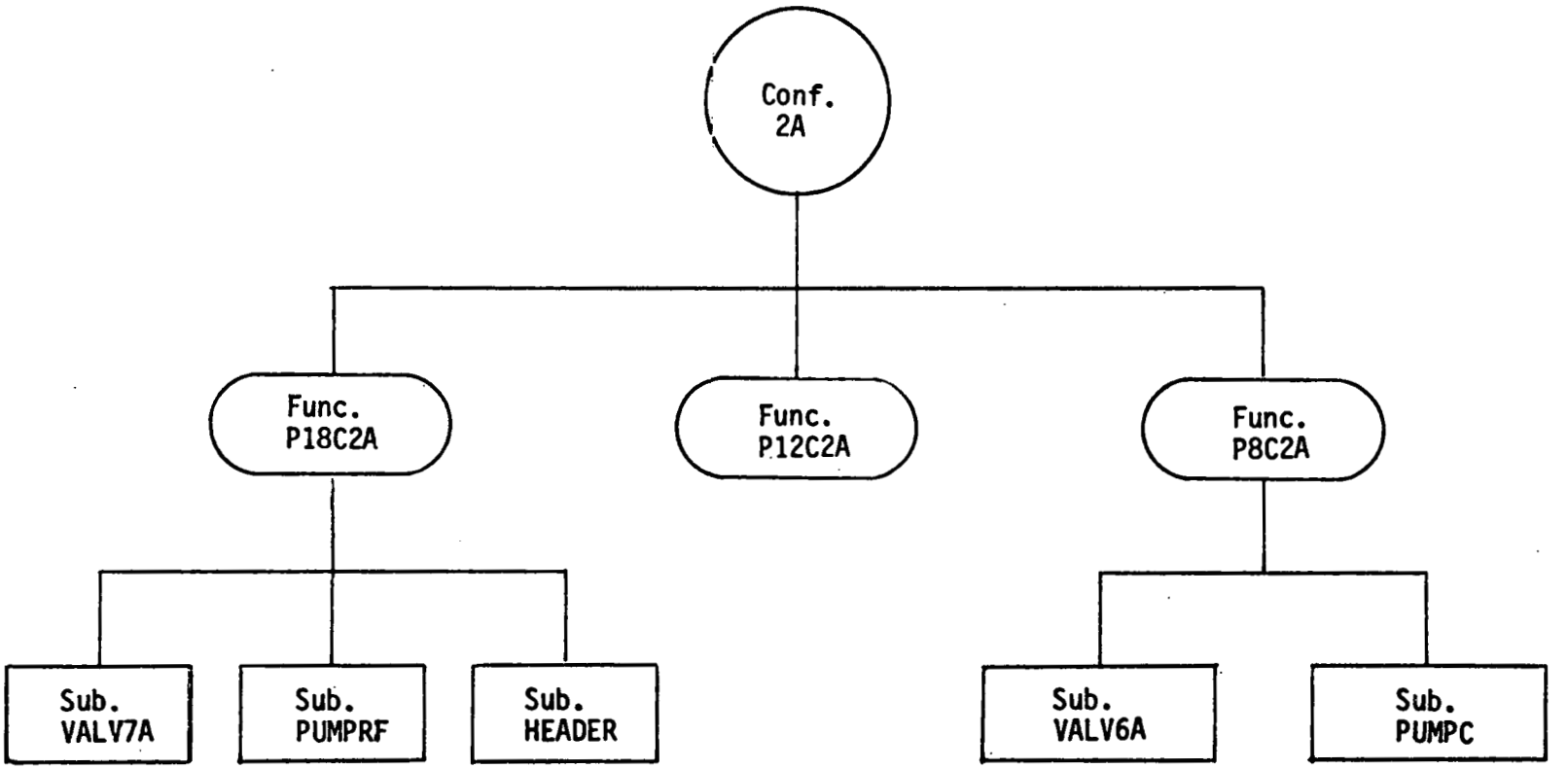
Conf.
2A
Func.
P18C2A
Func.
P12C2A
Func.
P8C2A
Sub.
VALV7A
Sub.
PUMPRF
Sub.
HEADER
Sub.
VALV6A
Sub.
PUMPC

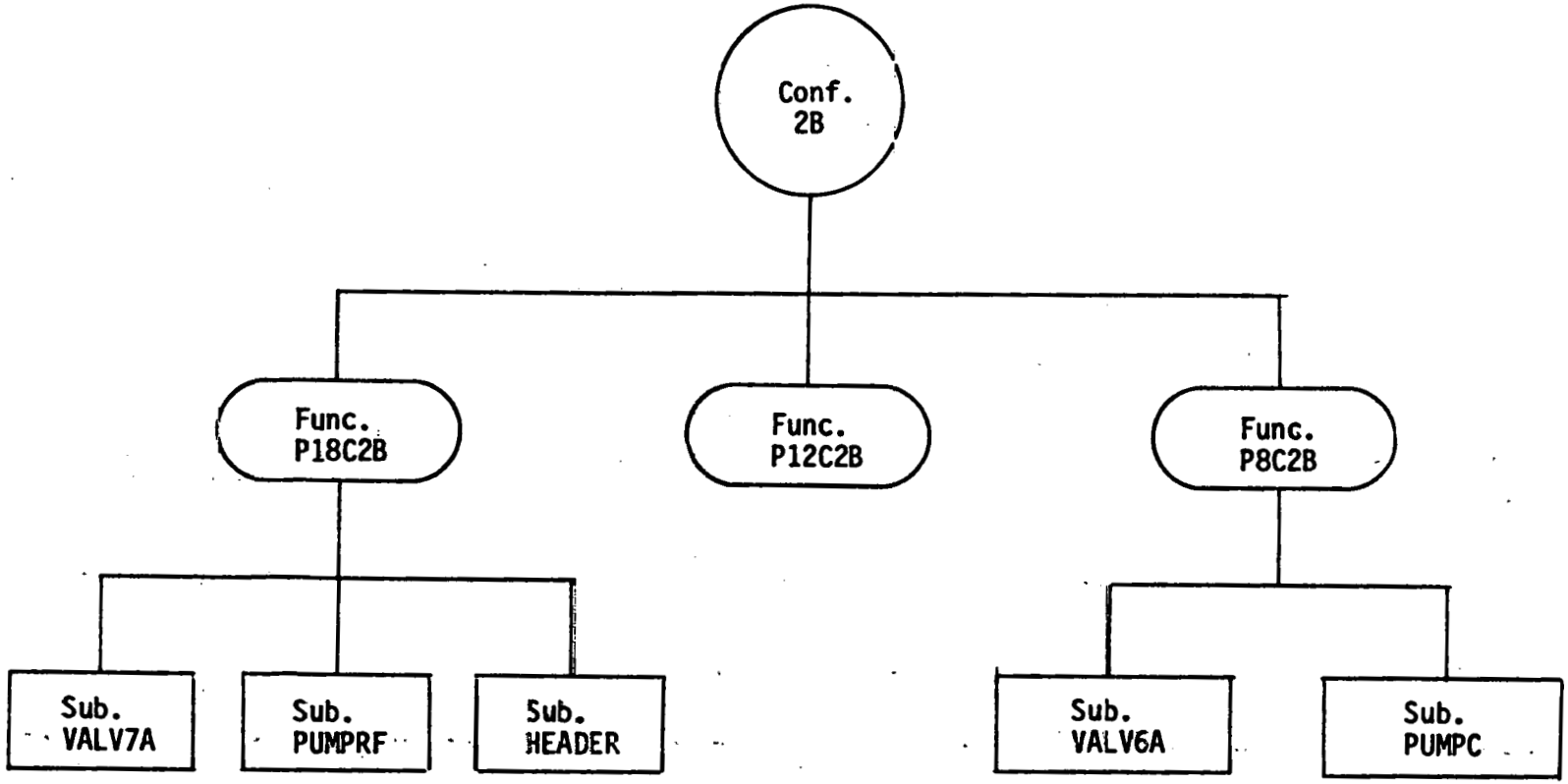
Conf.
2B
Func.
P18C2B
Func.
P12C2B
Func.
P8C2B
Sub.
VALV7A
Sub.
PUMPRF
Sub.
HEADER
Sub.
VALV6A
Sub.
PUMPC

2.4 PROGRAM FLOW CHARTS

2.4.1 Flow Chart of Main Program

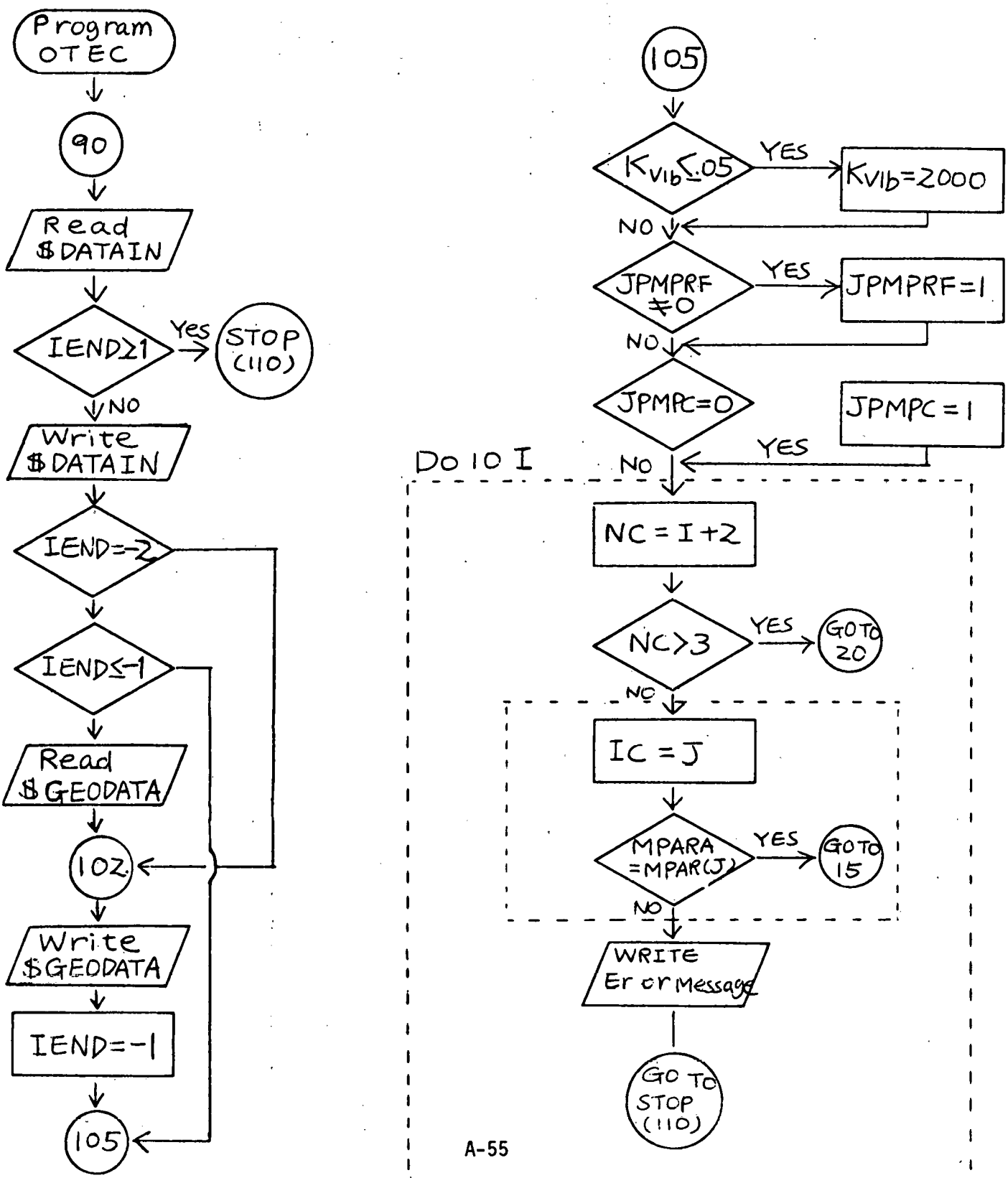

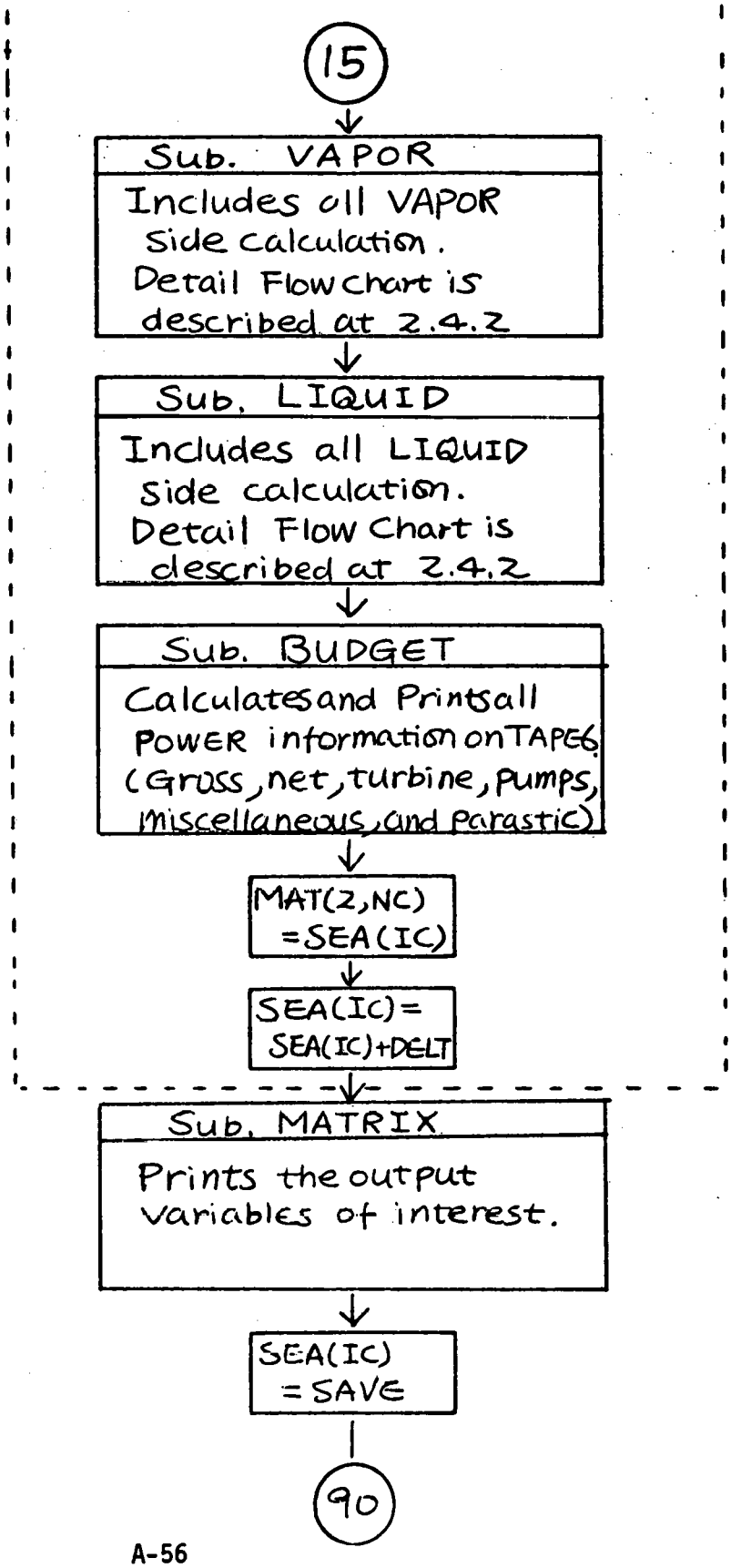
15
Sub. VAPOR
Includes all VAPOR Side calculation. Detail Flowchart is described at 2.4.2
Sub. LIQUID
Includes all LIQUID Side calculation. Detail Flow Chart is described at 2.4.2
Sub. BUDGET
Calculates and Prints all POWER information on TAPE6 (Gross, net, turbine, pumps, miscellaneous, and parastic)
MAT(2,NC) =SEA(IC)
SEA(IC)= SEA(IC)+DELT
Sub. MATRIX
Prints the output variables of interest.
SEA(IC) =SAVE
90

2.4.2 Flow Chart of Subroutines VAPOR and LIQUID

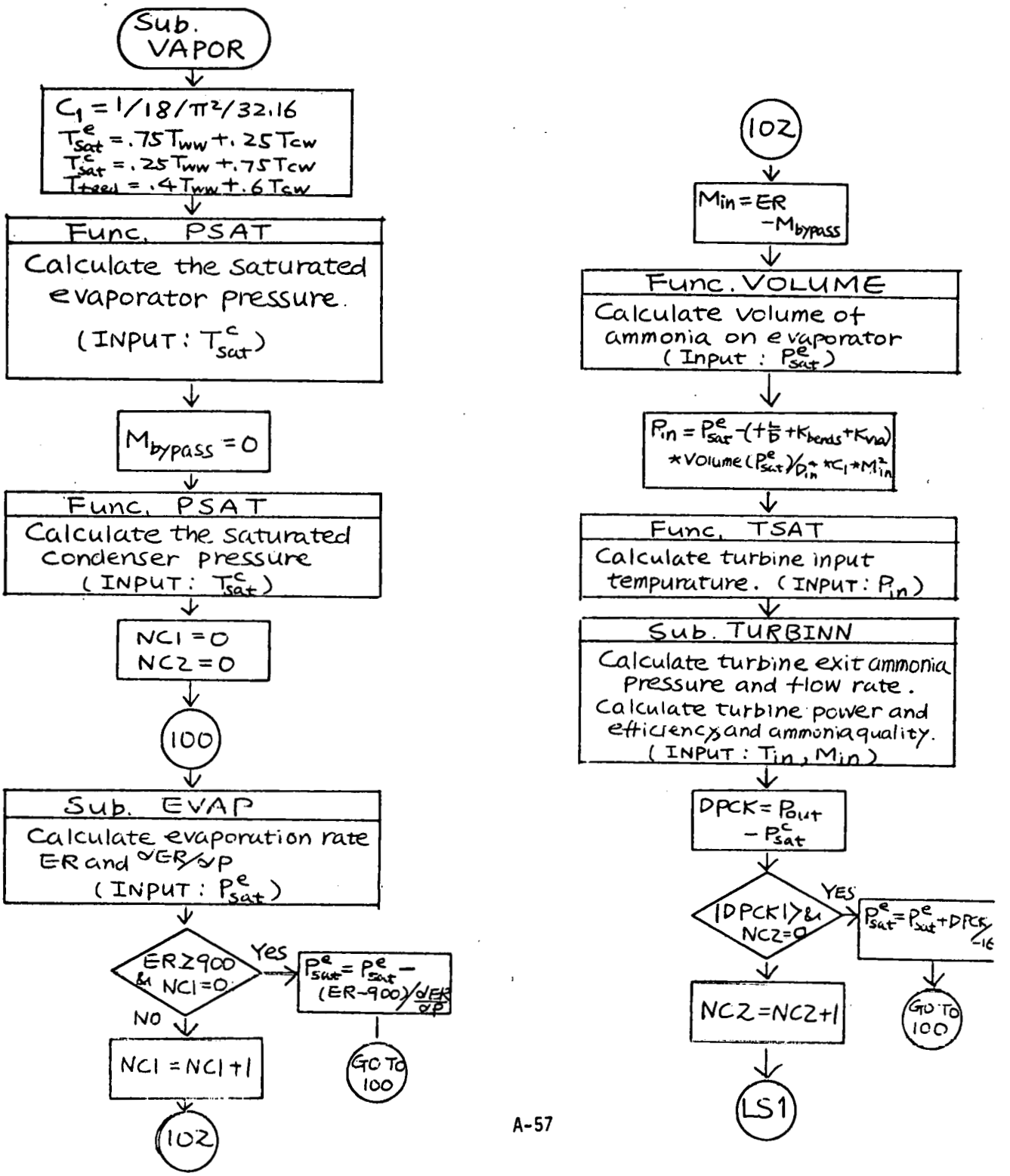

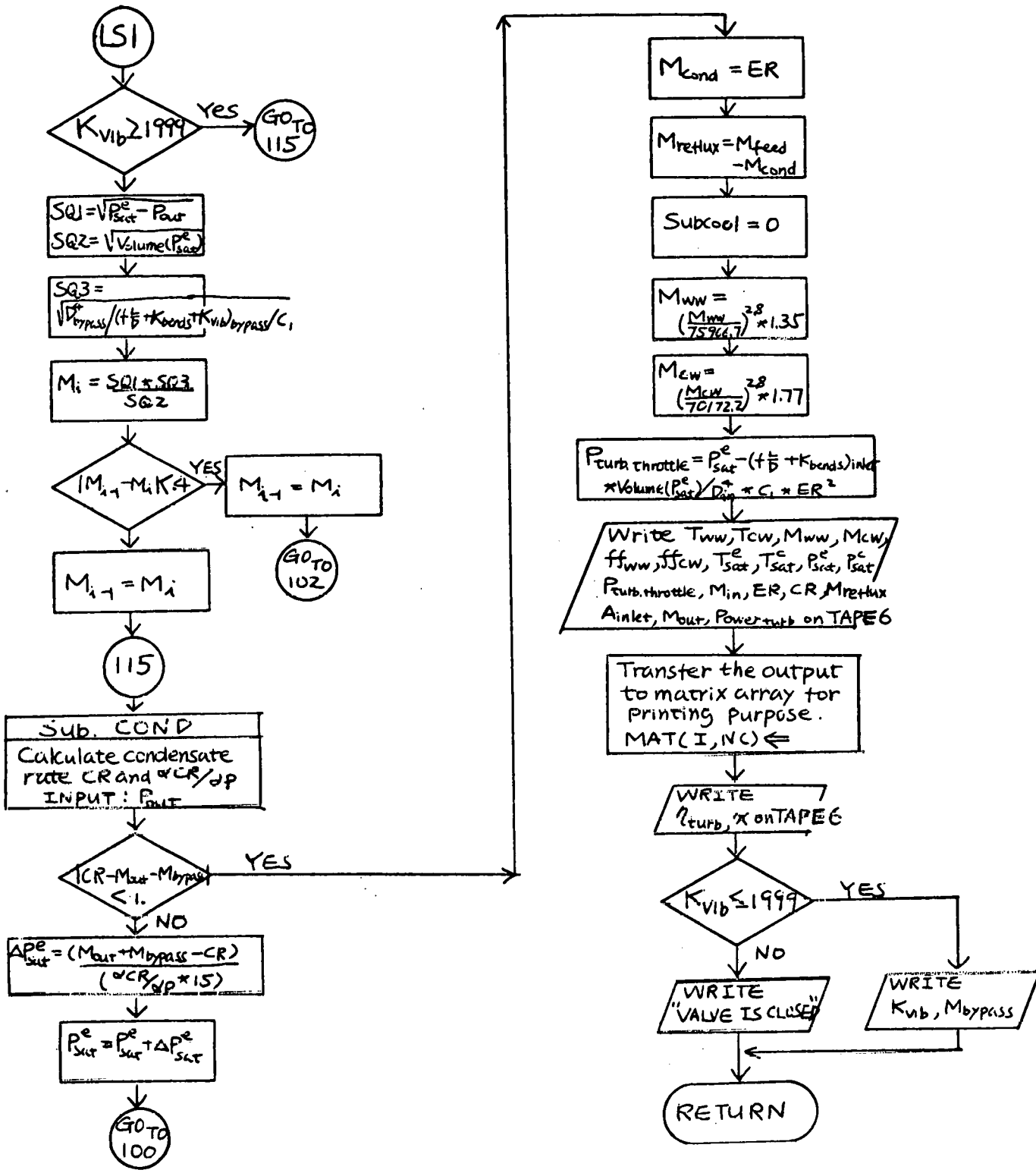
LS1
$K_{vlb} \geq 1999$
YES
GO TO 115
$SQ1 = \sqrt{P^e_{sat} - P_{out}}$
$SQ2 = \sqrt{Volume(P^e_{sat})}$
$SQ3 = \sqrt{P^e_{bypass}/((f\frac{L}{D} + K_{bends} + K_{vlb})_{bypass}/C_1}$
$M_i = \frac{SQ1 * SQ3}{SQ2}$
$|M_{i-1} - M_i| < 4$
YES
$M_{i-1} = M_i$
GO TO 102
$M_{i-1} = M_i$
115
Sub. COND
Calculate condensate rate CR and $\partial CR/\partial p$
INPUT: P_{out}
$|CR - M_{out} - M_{bypass}| < 1.$
YES
NO
$\Delta P^e_{sat} = \frac{(M_{out} + M_{bypass} - CR)}{(\partial CR/\partial p * 15)}$
$P^e_{sat} = P^e_{sat} + \Delta P^e_{sat}$
GO TO 100
$M_{cond} = ER$
$M_{reflux} = M_{feed} - M_{cond}$
Subcool = 0
$M_{ww} = (\frac{M_{ww}}{75966.7})^{2.8} * 1.35$
$M_{cw} = (\frac{M_{cw}}{70172.2})^{2.8} * 1.77$
$P_{turb\ throttle} = P^e_{sat} - (f\frac{L}{D} + K_{bends})_{inlet} * Volume(P^e_{sat}) / D^4_{in} * C_1 * ER^2$
Write $T_{ww}, T_{cw}, M_{ww}, M_{cw}, ff_{ww}, ff_{cw}, T^e_{sat}, T^c_{sat}, P^e_{sat}, P^c_{sat}, P_{turb.throttle}, M_{in}, ER, CR, M_{reflux}, A_{inlet}, M_{out}, Power_{turb}$ on TAPE6
Transfer the output to matrix array for printing purpose.
MAT(I, NC) ⇐
WRITE η_{turb}, π on TAPE6
$K_{vlb} \leq 1999$
YES
NO
WRITE "VALVE IS CLOSED"
WRITE K_{vlb}, M_{bypass}
RETURN

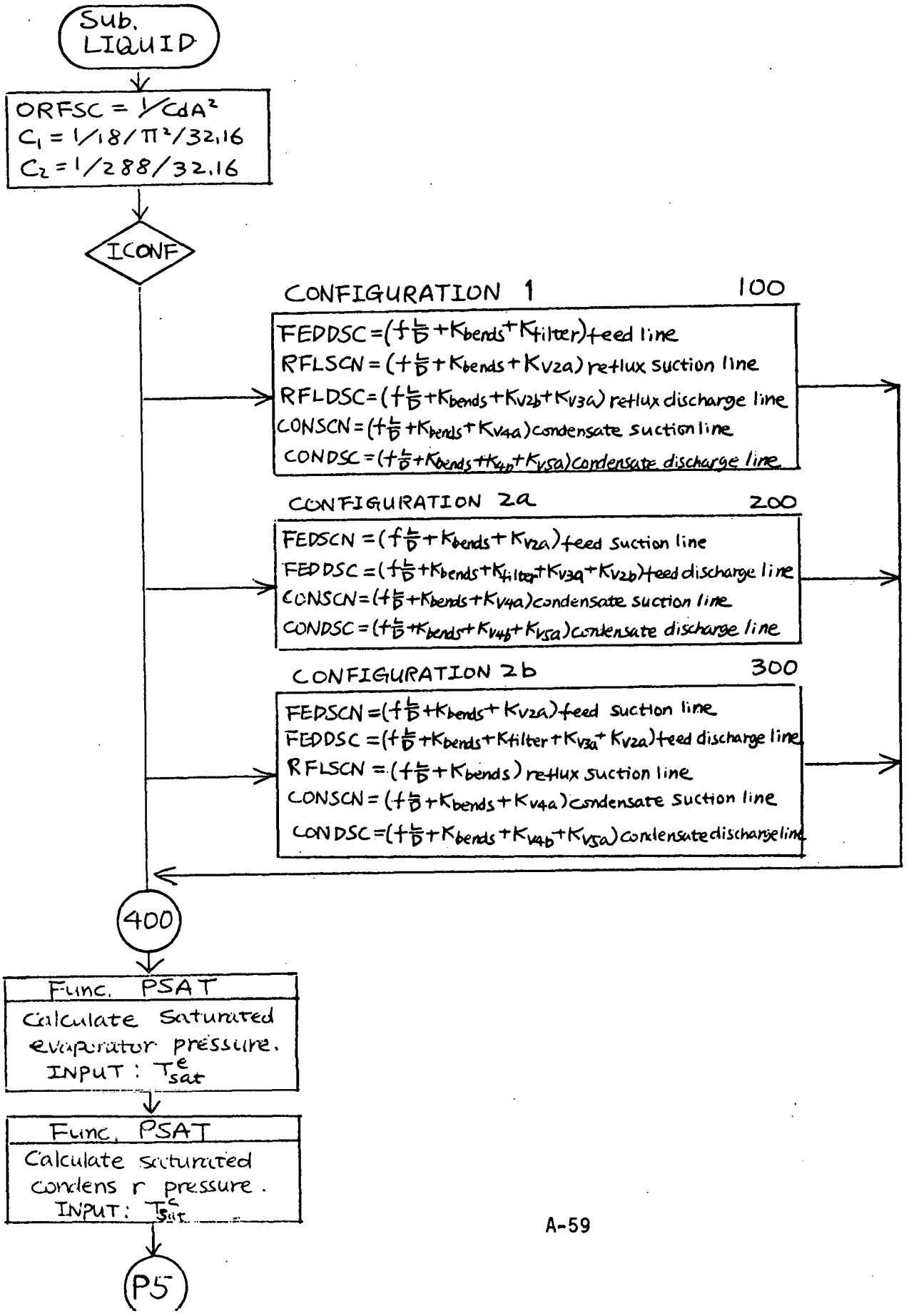
Sub. LIQUID
ORFSC = 1/CdA²
C1 = 1/18/π²/32.16
C2 = 1/288/32.16
ICONF
CONFIGURATION 1
100
FEDDSC = (f L/D + Kbends + Kfilter) feed line
RFLSCN = (f L/D + Kbends + Kv2a) reflux suction line
RFLDSC = (f L/D + Kbends + Kv2b + Kv3a) reflux discharge line
CONSCN = (f L/D + Kbends + Kv4a) condensate suction line
CONDSC = (f L/D + Kbends + Kv4b + Kv5a) condensate discharge line
CONFIGURATION 2a
200
FEDSCN = (f L/D + Kbends + Kv2a) feed suction line
FEDDSC = (f L/D + Kbends + Kfilter + Kv3a + Kv2b) feed discharge line
CONSCN = (f L/D + Kbends + Kv4a) condensate suction line
CONDSC = (f L/D + Kbends + Kv4b + Kv5a) condensate discharge line
CONFIGURATION 2b
300
FEDSCN = (f L/D + Kbends + Kv2a) feed suction line
FEDDSC = (f L/D + Kbends + Kfilter + Kv3a + Kv2a) feed discharge line
RFLSCN = (f L/D + Kbends) reflux suction line
CONSCN = (f L/D + Kbends + Kv4a) condensate suction line
CONDSC = (f L/D + Kbends + Kv4b + Kv5a) condensate discharge line
400
Func. PSAT
Calculate Saturated evaporator pressure.
INPUT: T^e_sat
Func. PSAT
Calculate saturated condenser pressure.
INPUT: T^c_sat
P5

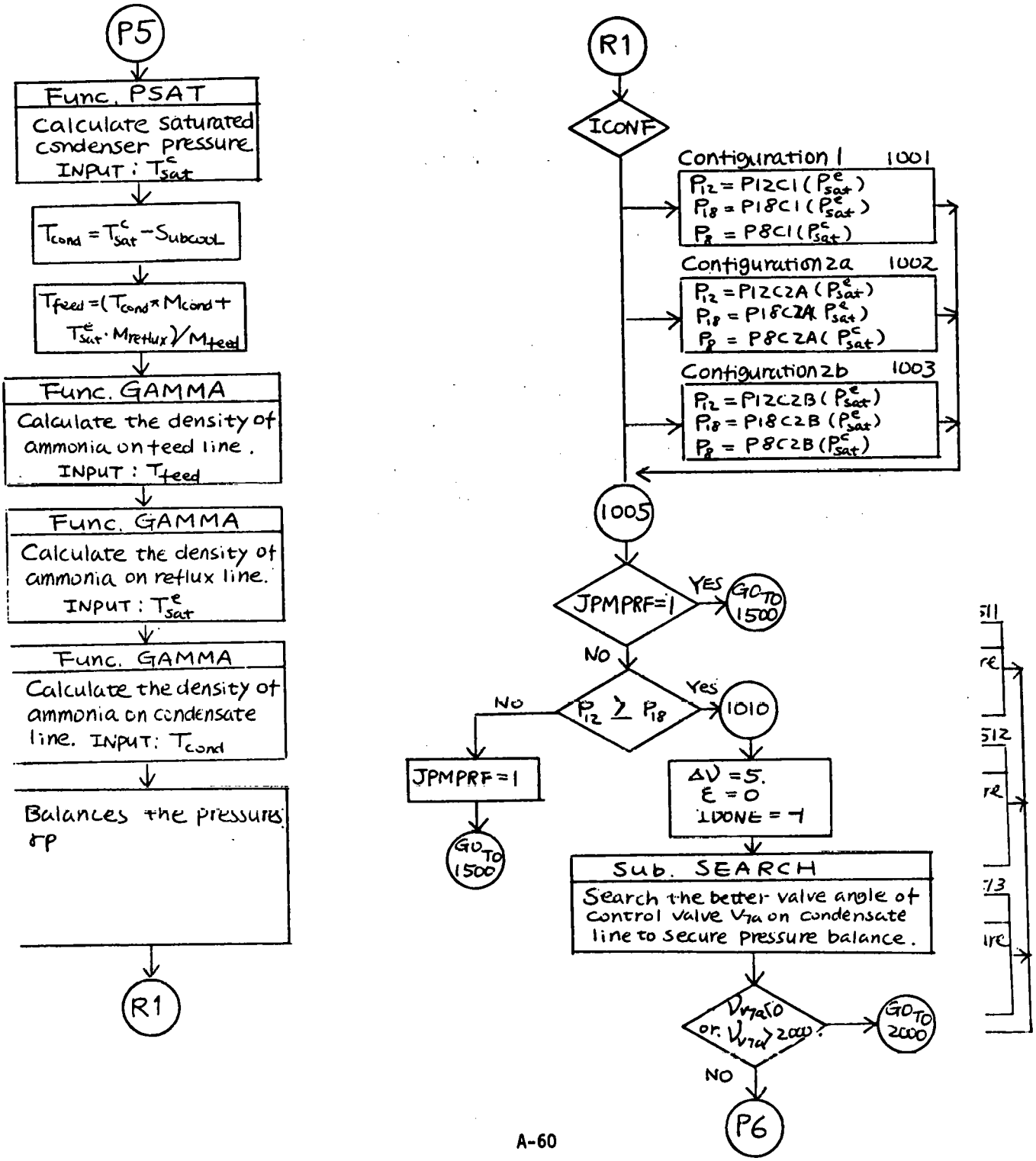
P5
Func. PSAT
Calculate saturated condenser pressure.
INPUT : T^c_{sat}
$T_{cond} = T^c_{sat} - Subcool$
$T_{feed} = (T_{cond} \times M_{cond} + T^e_{sat} \cdot M_{reflux}) / M_{feed}$
Func. GAMMA
Calculate the density of ammonia on feed line.
INPUT : T_{feed}
Func. GAMMA
Calculate the density of ammonia on reflux line.
INPUT : T^e_{sat}
Func. GAMMA
Calculate the density of ammonia on condensate line. INPUT: T_{cond}
Balances the pressure & p
R1
R1
ICONF
Configuration 1 1001
$P_{12} = P12C1(P^e_{sat})$
$P_{18} = P18C1(P^e_{sat})$
$P_8 = P8C1(P^c_{sat})$
Configuration 2a 1002
$P_{12} = P12C2A(P^e_{sat})$
$P_{18} = P18C2A(P^e_{sat})$
$P_8 = P8C2A(P^c_{sat})$
Configuration 2b 1003
$P_{12} = P12C2B(P^e_{sat})$
$P_{18} = P18C2B(P^e_{sat})$
$P_8 = P8C2B(P^c_{sat})$
1005
JPMPRF=1
YES
GO TO 1500
NO
$P_{12} \geq P_{18}$
Yes
1010
NO
JPMPRF=1
GO TO 1500
$\Delta V = 5.$
$\epsilon = 0$
IDONE = 1
Sub. SEARCH
Search the better valve angle of control valve V_{7a} on condensate line to secure pressure balance.
$V_{7a} \leq 0$ or $V_{7a} \geq 200$?
GO TO 2000
NO
P6

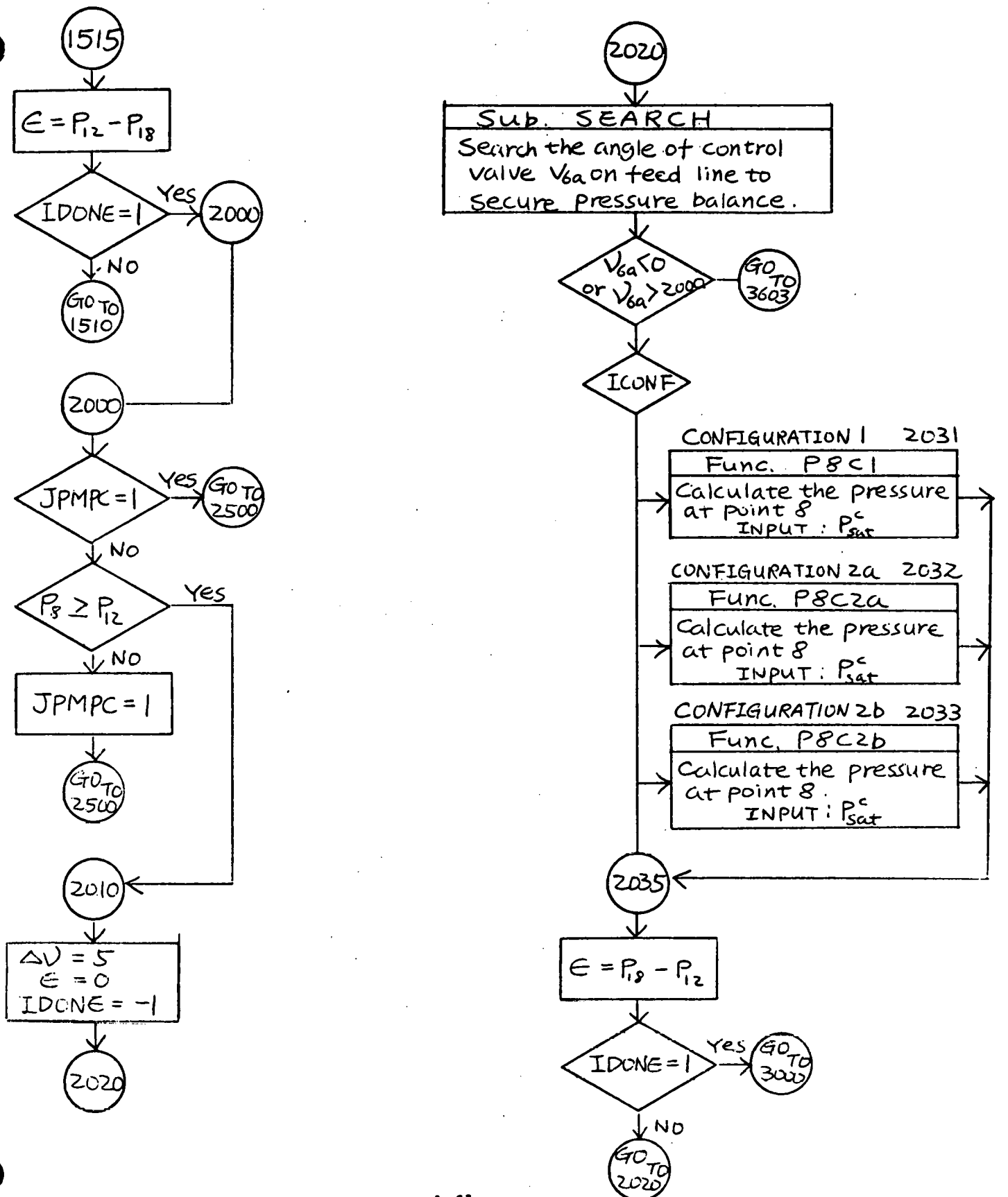
1515
$\epsilon = P_{12} - P_{18}$
IDONE=1
Yes
2000
NO
GO TO 1510
2000
JPMPC=1
Yes
GO TO 2500
NO
$P_8 \geq P_{12}$
Yes
NO
JPMPC=1
GO TO 2500
2010
$\Delta V = 5$
$\epsilon = 0$
IDONE = -1
2020
2020
Sub. SEARCH
Search the angle of control valve V_{6a} on feed line to secure pressure balance.
$V_{6a} < 0$ or $V_{6a} > 2000$
GO TO 3603
ICONF
CONFIGURATION 1 2031
Func. P8C1
Calculate the pressure at point 8
INPUT : P^c_{sat}
CONFIGURATION 2a 2032
Func. P8C2a
Calculate the pressure at point 8
INPUT : P^c_{sat}
CONFIGURATION 2b 2033
Func. P8C2b
Calculate the pressure at point 8.
INPUT : P^c_{sat}
2035
$\epsilon = P_{18} - P_{12}$
IDONE=1
Yes
GO TO 3000
NO
GO TO 2020

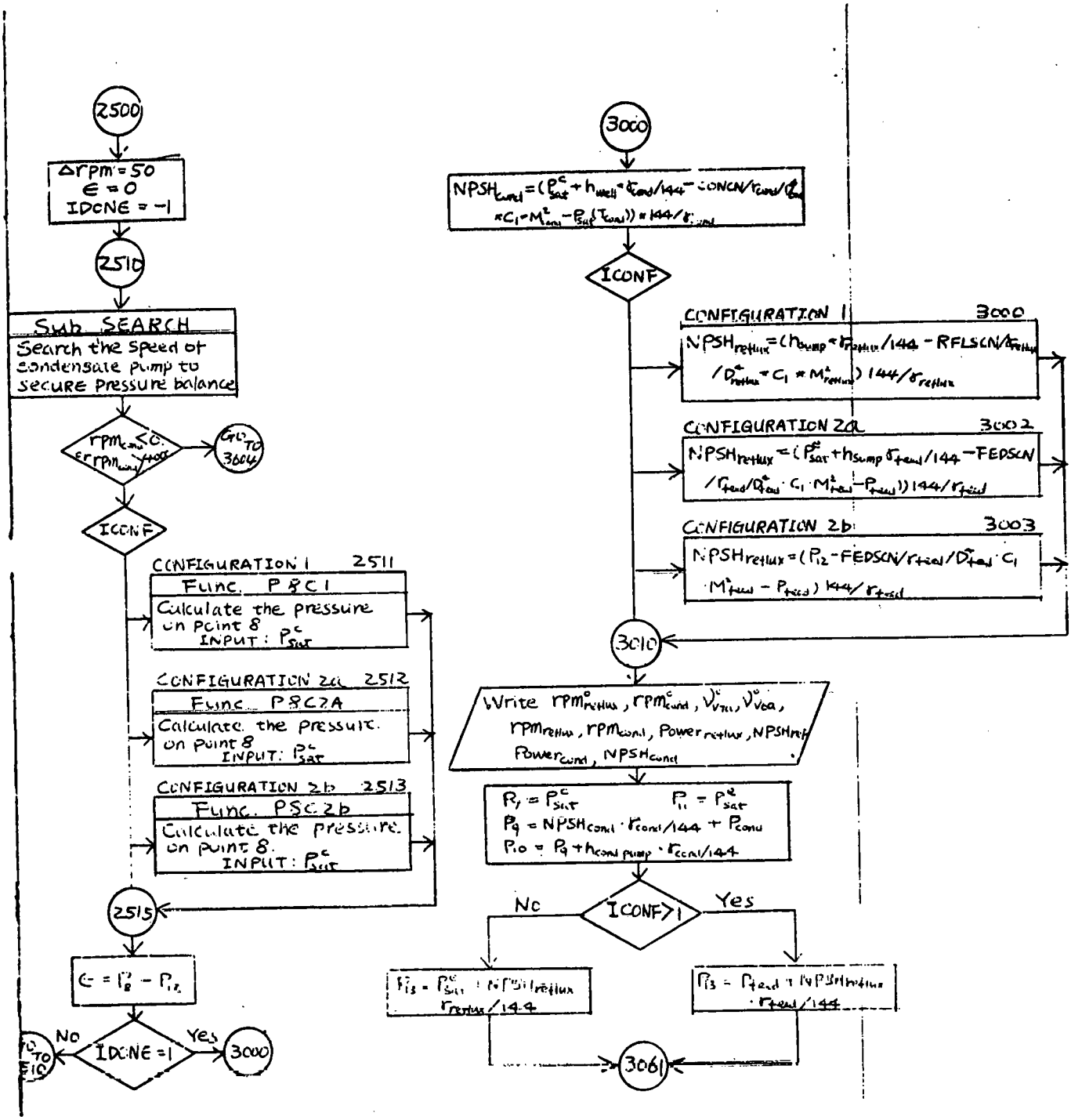
2500
Δrpm = 50
ε = 0
IDONE = -1
2510
Sub SEARCH
Search the speed of condensate pump to secure pressure balance
GO TO 3064
ICONF
CONFIGURATION 1 2511
Func. PSC1
Calculate the pressure on point 8
INPUT: P^c_sat
CONFIGURATION 2a 2512
Func. PSC2A
Calculate the pressure on point 8
INPUT: P^c_sat
CONFIGURATION 2b 2513
Func. PSC2b
Calculate the pressure on point 8.
INPUT: P^c_sat
2515
ε = P'_8 - P_12
No
IDONE = 1
Yes
3000
3000
ICONF
CONFIGURATION 1 3000
CONFIGURATION 2a 3002
CONFIGURATION 2b 3003
3010
Write rpm°_reflux, rpm^c_cond, V̇^c_VRV, V̇^c_VCA, rpm_reflux, rpm_cond, Power_reflux, NPSH_req, Power_cond, NPSH_cond
P_7 = P^c_sat
P_11 = P^c_sat
P_9 = NPSH_cond · ρ_cond/144 + P_cond
P_10 = P_9 + h_cond pump · ρ_cond/144
ICONF>1
No
Yes
3061

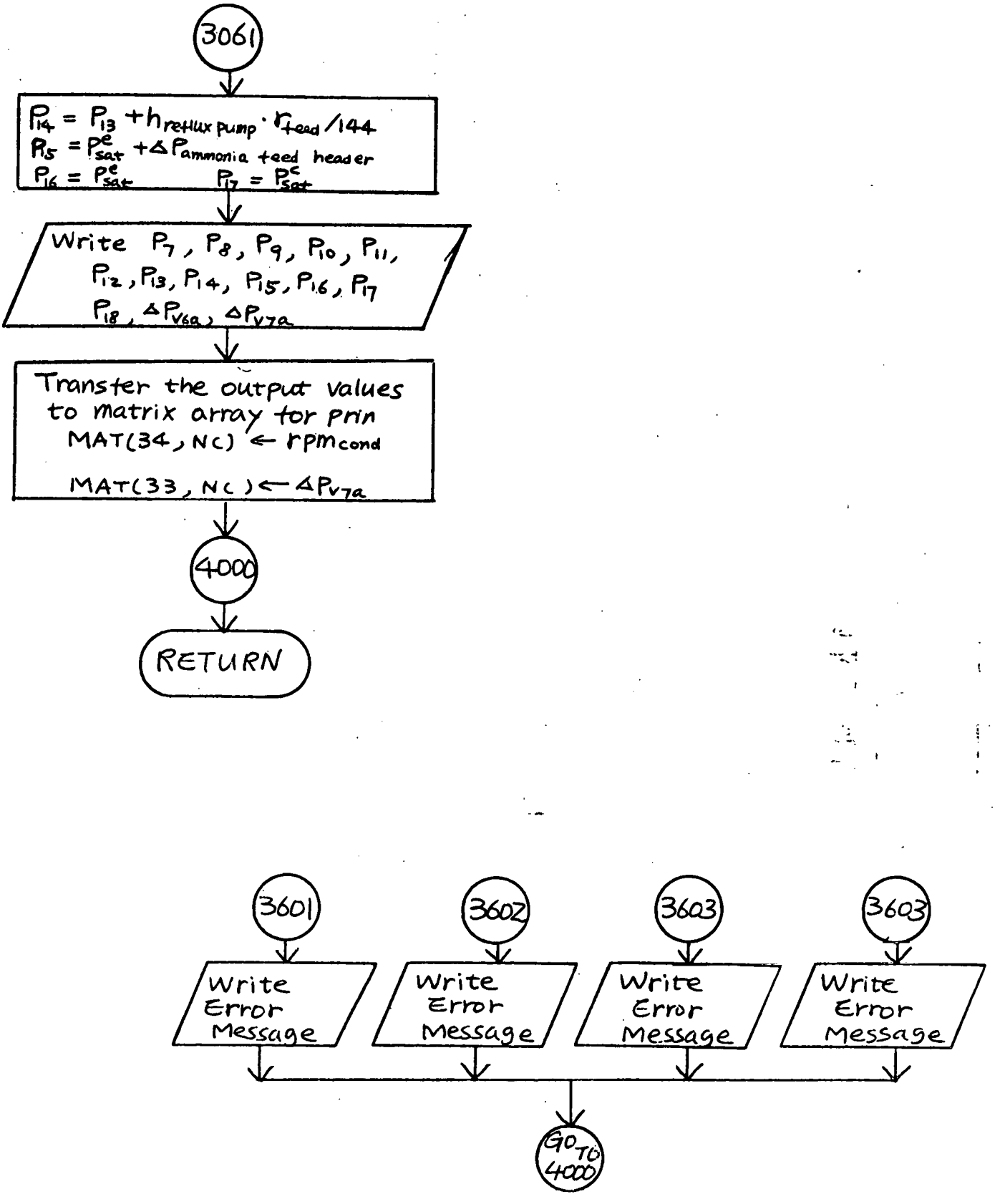
3061
$P_{14} = P_{13} + h_{reflux\ pump} \cdot \gamma_{feed} / 144$
$P_{15} = P^e_{sat} + \Delta P_{ammonia\ feed\ header}$
$P_{16} = P^e_{sat}$
$P_{17} = P^c_{sat}$
Write $P_7, P_8, P_9, P_{10}, P_{11}, P_{12}, P_{13}, P_{14}, P_{15}, P_{16}, P_{17}, P_{18}, \Delta P_{V6a}, \Delta P_{V7a}$
Transfer the output values to matrix array for prin
MAT(34, NC) ← rpm_{cond}
MAT(33, NC) ← ΔP_{V7a}
4000
RETURN
3601
Write Error Message
3602
Write Error Message
3603
Write Error Message
3603
Write Error Message
GO TO 4000

3. INPUT

Input data are supplied through two NAMELISTS labeled $DATAIN and $GEODATA. $DATAIN comprises twenty input variables which it is anticipated will be altered for various test runs: e.g., seawater temperatures, fouling factors, mass flow rates, and so on. $GEODATA comprises forty-eight parameters which it is anticipated will be altered only infrequently between runs; e.g., tube dimensions, pipe elevations, valve K-factors, and so on.

Default values of all input data are provided in the BLOCKDATA subprogram. These values specify the 10 MW "baseline case" for power module steady-state operation. To run the baseline case, input:

```
P$DATAIN
 $END
```

$GEODATA need not be specified. The simulation program permits the stacking of namelist data sets for multiple cases. See variable IEND below.

The program has been designed to run nominally in a parameter perturbation mode. The user specifies only one of 7 acceptable input variables to be perturbed (see MPARA below), the amount of the perturbation (see DELT below) and the number of cases to be run (see NCASE below). The program then executes a nominal case followed by NCASE-1 successive perturbation cases and formats the results of all cases in an easy to read columnar format. Note that in this mode namelist $DATAIN is input once only.

Figures 3.1 and 3.2 following define all input variables.

FORTRAN SYMBOL	ENGINEERING SYMBOL	DEFAULT VALUE	DEFINITION
TWARM	T_{warm}	80.	Temperature of warm sea water (°F).
MWARM	$\dot{M}_{warm}$	75967.	Warm sea water flow rate to evaporator (lbs/sec)
FFWARM	ff_{warm}	.0001	Fouling factor on input diameter of evaporator tubes (ft^2 hr °F/Btu).
TCØLD	T_{cold}	40.	Temperature of cold sea water (°F).
MCØLD	$\dot{M}_{cold}$	70172.2	Cold sea water flow rate to condenser (lbs/sec).
FFCØLD	ff_{cold}	.0001	Fouling factor on input diameter of condenser tubes (ft^2 hr °F/Btu).
ICØNF		2	Liquid side configuration selector. 1 = configuration 1 2 = configuration 2a 3 = configuration 2b
MFEED	$\dot{M}_{feed}$	1324.4	Ammonia feed rate to the evaporator header (lbs/sec).
KV1B	K_{v1b}	2000.	Bypass valve K factor. If KV1B > 1999. or < .05 the valve is closed.
REFRFL	$rpm/_{rfl}$	585.	Specified/initial estimate of reflux/feed pump rotational speed (rpm).
REFCØN	$rpm/_{cond}$	880.	Specified/initial estimate of condensate pump rotational speed (rpm).
REFV7A	$V/_{rfl}$	.2	Specified/initial estimate of ammonia feed flow control valve (V_{7a}).
REFV6A	$V/_{cond}$	.2	Specified/initial estimate of ammonia condensate flow control valve (V_{6a}).
JPMPRF		0	Feed flow control selector. (0 = V_{7a} control valve) (1 = reflux/feed pump)

Figure 3.1 NAMELIST DATAIN ($DATAIN) Variables

FORTRAN SYMBOL	ENGINEERING SYMBOL	DEFAULT VALUE	DEFINITION
JPMPC		1	Condensate flow control selector. (0 = V_{6a} control valve) (1 = condensate pump)
IEND		-2 (on the first case) -1 (subsequent case)	Run termination and namelist control flag. 1 Terminates run 0 Requests namelist GEODATA be read and written -1 Suppresses reading and writing of GEODATA -2 Requests GEODATA be written only
MPARA		'MCØLD'	Hollerith name of input variable to be perturbed. Acceptable names are 'TWARM', 'MWARM', FFWARM', 'TCØLD', 'MCØLD','FFCØLD', 'MFEED'.
DELT		100.	Amount by which MPARA variable is perturbed.
NCASE		1	Number of cases to be run by perturbing variable defined by MPARA: (10 ≤ offline) (5 ≤ terminal)

FORTRAN SYMBOL	ENGINEERING SYMBOL	DEFAULT VALUE	DEFINITION
DIAI	D_{inlet}	5.9	Inside diameter of vapor duct from evaporator to turbine (ft).
FLDI	$f\frac{L}{D}$	.1	The product of the friction factor by the length over diameter ratio of vapor duct from evaporator to turbine.
BENDSI	$K_{bend, etc.}$	.9	K factor of vapor duct from evaporator to turbine (includes exit orifice losses in evaporator).
DIAØ	D_{outlet}	8.0	Inside diameter of vapor duct from turbine to condenser (average value) (ft).
FLDØ	$f\frac{L}{D}$	.1	The product of the friction factor by the length over diameter ratio of vapor duct from turbine to condenser.
BENDSØ	$K_{bend, etc.}$	.3	K factor of vapor duct from turbine to condenser.
DIAB	D_{bypass}	5.5	Inside diameter of vapor bypass duct around turbine (ft).
FLDB	$f\frac{L}{D}$	.45	The product of the friction factor by the length over diameter ratio of vapor bypass duct.
BENDSB	$K_{bend, etc.}$	.45	K factor of vapor bypass duct.
DIAFED	D_{feed}	3.0	Inside diameter of liquid ammonia feed line (ft.)
FLDFS	$f\frac{L}{D}$	.1	The product of the friction factor by the length over diameter ratio of feed suction. line.
BENDFS	K_{bends}	.45	K factor of feed suction line.
FLDFD	$f\frac{L}{D}$	.3	The product of the friction factor by the length over diameter ratio of feed discharge line.
BENDFD	K_{bends}	1.35	K factor of feed discharge line.
HFEED	h_{feed}	54.	Elevation of evaporator orifice plate above pump centerline (ft).
DIARFL	D_{reflux}	3.0	Diameter of liquid ammonia reflux line (ft).
FLDRS	$f\frac{L}{D}$	0.	The product of the friction factor by the length over diameter ratio of reflux suction line.

Figure 3.2 NAMELIST GEODATA ($GEØDATA) Variables

FORTRAN SYMBOL	ENGINEERING SYMBOL	DEFAULT VALUE	DEFINITION
BENDRS	K_{bends}	0.	K factor of reflux suction line.
FLDRD	$f\frac{L}{D}$	0.	The product of the friction factor by the length over diameter of ratio of reflux discharge line.
BENDRD	K_{bends}	0.	K factor of reflux discharge line.
HSUMP	h_{sump}	21.	Elevation of liquid surface in evaporator sump above pump center line (ft).
DIACØN	D_{cond}	2.0	Diameter of liquid ammonia condensate line (ft).
FLDCS	$f\frac{L}{D}$	.3	The product of the friction factor by the length over diameter ratio of condensate suction line.
BENDCS	K_{bends}	.45	K factor of condensate suction line.
FLDCD	$f\frac{L}{D}$	.3	The product of the friction factor by the length over diameter ratio of condensate discharge line.
BENDCD	K_{bends}	1.35	K factor of condensate discharge line.
HWELL	h_{well}	21.	Elevation of liquid surface in condenser hot well above pump centerline (ft).
FILTER	K_{filter}	6.4	K factor of the liquid ammonia feed filter.
CDA	C_dA	1.16	The product of the discharge coefficient and the area of the composite of all of the film forming orifices in the evaporator (ft^2).
KV1A	K_{v1a}	.2	K factor of the valve which is between the outlet of evaporator and inlet of turbine.
KV2A	K_{v2a}	.2	K factor of the valve which is between the sump and reflux/feed pump.
KV2B	K_{v2b}	.2	K factor of the valve which is between the reflux/feed pump and the valve V_{3a}.
KV3A	K_{v3a}	0.	K factor of the valve which is between the valve V_{2b} and screen filter.
KV4A	K_{v4a}	.2	K factor of the valve which is between the hot well and the condensate pump.
KV4B	K_{v4b}	.2	K factor of the valve which is between the condensate pump and control valve V_{6a}.

FORTRAN SYMBOL	ENGINEERING SYMBOL	DEFAULT VALUE	DEFINITION
KV5A	k_{v5a}	0.	K factor of the valve which is between the control valve V_{6a} and sump.
ETUBID	D^e_{ID}	.0733	Evaporator tube effective inside diameter (ft).
ETUBØD	D^e_{OD}	.07583	Evaporator tube effective outside diameter (ft).
ELNGTH	l^e	26.5	Evaporator tube active length (ft).
ENMBR	n^e	42667	Total number of evaporator tubes.
ENSEG	$NSEG^e$	10	Number of length segments into which the evaporator tubes are divided for computational purposes (≤ 20).
CTUBID	D^c_{ID}	.07408	Condenser tube effective inside diameter (ft).
CTUBØD	D^c_{OD}	.07583	Condenser tube effective outside diameter (ft).
CLNGTH	l^c	29.	Condenser tube active length (ft).
CNMBR	n^c	43678	Total number of condenser tubes.
CNSEG	$NSEG^c$	10	Number of segments of length into which the condenser tubes are to be divided for computational purposes (≤ 20).
ARE	AR^e	1.46	Area ratio of evaporator.
ARC	AR^c	1.46	Area ratio of condenser.
THET	t^e	.00469	Thermal thickness of evaporator tube (ft).
THCT	t^c	.00393	Thermal thickness of condenser tube (ft).
CONCT	K^c	11.5	Thermal conductivity of condenser tube (Btu/hr/ft/°F).
CONET	K^e	11.5	Thermal conductivity of evaporator tube (Btu/hr/ft/°F).

4. OUTPUT

The output consists of a printout of the input data sets $DATA and optionally $GEODATA, and a display of the simulation results. The printing of the $GEODATA set is controlled by input IEND in the $DATAIN set. If the name of the variable to be perturbed is input to MPAPA, it is displayed in hollerith representation. If not input, its default value 'MCOLD' is displayed in integer format.

The output is formatted and printed in subroutine MATRIX. The output format has been designed to display 33 variables for up to ten cases for offline print and for up to five cases for remote terminal display. One example of this format appears in Figure 4.1. For debug purposes, Dr. Impink's output is displayed on TAPE6. The variables are self-identified by text. The procedure for obtaining this output is given in Section 5.

The following is a list, with definitions, of the standard output variables displayed in the order of appearance so shown in Figure 4.1.

FORTRAN SYMBOL	ENGINEERING SYMBOL	DEFINITION
	POWER AND EFFICIENCY	
QNET	P_{net}	Net power of the system (MegaWatts).
POWER	$P_{turbine}$	Turbine power (MegaWatts).
QCOLD	$P_{cold\ water}$	Cold sea water pumping power (MegaWatts).
QWARM	$P_{warm\ water}$	Warm sea water pumping power (MegaWatts).
QCOND	P^{c}_{pump}	Ammonia condensate pumping power (MegaWatts).
QRFLX	P^{e}_{pump}	Ammonia feed pumping power (MegaWatts).
QMISC	P_{mis}	Miscellaneous power requirements (MegaWatts).
FFFIC	η	Turbine efficiency (%).
QUAL	X	Ammonia turbine exit quality.

FORTRAN SYMBOL	ENGINEERING SYMBOL	DEFINITION
	FLOW RATES	
M_{feed}	M_{feed}	Ammonia feed rate to the evaporator header (lbs/sec).
ER		Evaporation rate (lbs/sec).
CR		Condensate rate (lbs/sec).
MRFL	M_{reflux}	The evaporator reflux flow rate (lbs/sec).
FLOWIN	TF	Turbine inlet flow rate (lbs/sec).
BYPASS	BP	The resulting bypass flow rate (lbs/sec).
	TEMPERATURES	
TOUTW	$T_{warm\ water}$	The warm water discharge temperature (°F).
TOUTC	$T_{cold\ water}$	The cold water discharge temperature (°F).
TSATE	T_{evap}	Temperature of evaporator (°F).
TSATC	T_{cold}	Temperature of condensor (°F).
	PRESSURES	
PSATE	P_{evap}	Pressure of evaporator (PSIA).
PSATC	P_{cond}	Pressure of condersor (PSIA).
PTHRTL	$P_{turb\ throttle}$	Turbine throttle pressure (PSIA).
RPMRFL	$rpm_{reflux\ pump}$	Reflux feed pump speed (RPM).
ANGV7A	ν°_{V7A}	Feed flow valve angles (°).
NPSHRF	$NPSH_{reflux}$	Reflux feed pump NPSH (feet).
DPV7A	ΔP_{V7A}	The pressure drop across the feed control valve (PSI).
RPMCON	$rpm_{cond\ pump}$	Condensate pump speed (RPM).
ANGV6A	ν°_{V6A}	Condensate flow valve angle (°).
NPSHC	$NPSH_{cond}$	Condensate pump NPSH (feet).
DPV6A	ΔP_{V6A}	The pressure drop across (feet) the the condensate flow control valve (PSI).

FORTRAN SYMBOL	ENGINEERING SYMBOL	DEFINITION
	PRESSURES (continued)	
HEU		Heat transfer coefficient of evaporator (Btu/ F/ft^2/sec).
HCU		Heat transfer coefficient of condenser (Btu/ F/ft^2/sec).

CASE	1	2
VARIABLE MFEED	1324.40	1224.40
POWER & EFFICIENCY	(MEGAWATTS)	
NET POWER	10.33	10.34
TURBINE POWER	14.73	14.73
COLD WATER PUMP	1.77	1.77
WARM WATER PUMP	1.35	1.35
CONDENSATE PUMP	.32	.32
FEED PUMP	.16	.15
MISCELLANEOUS	.50	.50
TURBINE EFFICIENCY%	87.67	87.67
AMMONIA QUALITY %	97.44	97.44
FLOW RATES	(LBS/SEC)	
FEED TO EVAPORATOR	1324.40	1224.40
EVAPORATION FLOW	808.43	808.28
CONDENSATION FLOW	787.47	787.26
REFLUX FLOW	515.97	416.12
TURB INLET FLOW	808.43	808.28
BYPASS FLOW	0.00	0.00
TEMPERATURES	(DEG F)	
WARM WATER DISCHG	74.02	74.05
COLD WATER DISCHG	46.21	46.21
EVAPORATOR	70.20	70.19
CONDENSER	50.31	50.31
PRESSURES	(PSIA)	
EVAPORATOR	129.25	129.23
CONDENSER	89.19	89.19
TURB THROTTLE	129.04	129.02
PUMPS AND VALVES		
FEED PUMP SPEED,RPM	596.56	576.99
FEED ANGLE,DEGREE	.20	.20
FEED NPSH,FEET	123.52	130.44
DF PR FEED VALV,PSI	.02	.02
COND PUMP SPEED,RPM	779.60	779.65
COND ANGLE,DEGREE	.20	.20
COND NPSH,FEET	26.36	26.36
DF PR COND VALV,PSI	0.00	0.00
HEAT TRS COEFF EVAP	905.04	887.93
HEAT TRS COEFF COND	726.81	726.82

Figure 4.1 Standard Output

5. OPERATING PROCEDURES

Approximately 34200 (octal) words of core are needed for loading, and 24400 (octal) words of core are needed for execution on the CDC 6600 at TRW. To run the default case with no variable perturbations takes about one second of central processor time. A typical control file for timeshare execution is:

```
GET,OTEB5,Input file
OTEB5,INPUT=Input file,OUTPUT=PR1
PRINTF,PR1,bldg,room (or courier)
(PRINTF,TAPE6) if debug output is desired
```

A control file for remote batch execution is:

```
ACCOUNT,username,password
NAME,CCC00,badge,last name,first initial
PROBLEM,job number
FLENGTH,34200
PRIORITY,E
BANNER,OUTPUT,bldg.room (or courier)
GET,OTEB5,input file
OTEB5,INPUT=input file
(PRINTF,TAPE6) if debug output is desired
```

ATTACHMENT I

SAMPLE CASE

A.1 STANDARD OUTPUT

OTEC STATIC SIMULATION MODEL

```
$DATAIN
$END
```

```
$DATAIN
TWARM    = 8.0E+01,
MWARM    = 7.59667E+04,
FFWARM   = 1.0E-04,
TCOLD    = 4.0E+01,
MCOLD    = 7.01722E+04,
FFCOLD   = 1.0E-04,
MFEED    = 1.3244E+03,
 NF      = 2,
A  EA    = 2.36,
K/1B     = 2.0E+03,
REFRFL   = 5.85E+02,
REFCON   = 8.8E+02,
REFV7A   = 2.0E-01,
REFV6A   = 2.0E-01,
JPMPRF   = 0,
JPMPC    = 1,
IEND     = -2,
MPARA    = 235098405946710893,
DELT     = 1.0E+02,
RELEASE  = 1,
$END
```

```
$GEODATA
DIAI     = 5.5,
FLDI     = 3.0E-01,
BENDSI   = 4.5E-01,
DIAO     = 7.0,
FLDO     = 3.0E-01,
BENDSO   = 4.5E-01,
DIAB     = 5.5,
FLDB     = 4.5E-01,
BENDSB   = 4.5E-01,
DIAFED   = 3.0,
FLDFS    = 3.0E-01,
BENDFS   = 4.5E-01,
FLDFD    = 3.0E-01,
BENDFD   = 9.0E-01,
HFEED    = 7.0E+01,
DIARFL   = 2.5,
FLDRS    = 0.,
BENDRS   = 0.,
FLDRD    = 0.,
BENDRD   = 0.,
HSUMP    = 2.9E+01,
DIACON   = 2.0,
FLDCS    = 3.0E-01,
BENDCS   = 4.5E-01,
FLDCD    = 3.0E-01,
BENDCD   = 9.0E-01,
HWELL    = 2.7E+01,
FILTER   = 4.0E-01,
CDA      = 1.16,
KV1A     = 2.0E-01,
KV2A     = 2.0E-01,
KV2B     = 2.0E-01,
KV3A     = 0.,
KV4A     = 2.0E-01,
KV4B     = 2.0E-01,
KV5A     = 0.,
ETUBID   = 7.33E-02,
ETUBOD   = 8.25E-02,
ELNGTH   = 2.65E+01,
ENMBR    = 42667,
ENSEG    = 10,
```

```
 CTUBID  = 7.408E-02,
 CTUBOD  = 8.25E-02,
 CLNGTH  = 2.9E+01,
 CNMBR   = 43678,
 CNSEG   = 10,
 ARE     = 1.46,
 ARC     = 1.46,
 THET    = 4.69E-03,
 THCT    = 3.93E-03,
 CONET   = 1.15E+01,
 CONCT   = 1.15E+01,
 $END
```

CASE	1	
VARIABLE MCOLD	70172.20	
POWER & EFFICIENCY		(MEGAWATTS)
NET POWER	10.33	
TURBINE POWER	14.73	
COLD WATER PUMP	1.77	
WARM WATER PUMP	1.35	
CONDENSATE PUMP	.32	
FEED PUMP	.16	
MISCELLANEOUS	.50	
TURBINE EFFICIENCY%	87.67	
AMMONIA QUALITY %	97.44	
FLOW RATES		(LBS/SEC)
FEED TO EVAPORATOR	1324.40	
EVAPORATION FLOW	808.43	
CONDENSATION FLOW	787.47	
REFLUX FLOW	515.97	
TURB INLET FLOW	808.43	
BYPASS FLOW	0.00	
TEMPERATURES		(DEG F)
WARM WATER DISCHG	74.02	
COLD WATER DISCHG	46.21	
EVAPORATOR	70.20	
CONDENSER	50.31	
PRESSURES		(PSIA)
EVAPORATOR	129.25	
CONDENSER	89.19	
TURB THROTTLE	129.04	
PUMPS AND VALVES		
FEED PUMP SPEED,RPM	596.58	
FEED ANGLE,DEGREE	.20	
FEED NPSH,FEET	123.52	
DF PR FEED VALV,PSI	.02	
COND PUMP SPEED,RPM	779.80	
COND ANGLE,DEGREE	.20	
COND NPSH,FEET	26.36	
DF PR COND VALV,PSI	0.00	
HEAT TRS COEFF EVAP	905.04	
HEAT TRS COEFF COND	726.81	

A.2 TAPE6 DEBUG OUTPUT

THE BYPASS VALVE IS CLOSED

LIQUID.SIDE.CHARACTERISTICS

CONFIGUPATION 2A

	REFLUX/FEED PUMP SPEED	CONDENSATE PUMP SPEED	FEED FLOW VALVE ANGLE	COND.FLOW VALVE ANGLE
INPUT	585.00	880.00	.20	.20
ACTUAL	596.58	779.80	.20	.20

PUMP PARAMETERS

	POWER	NPSH
REFLUX/FEED	.16	123.52
CONDENSATE	.32	26.36

PRESSURES

P 7 = 89.73
P 8 = 129.24
P 9 = 96.86
P10 = 137.35
P11 = 129.24
P12 = 129.24
P13 = 136.92
P14 = 153.85
P15 = 134.89
P16 = 129.24
P17 = 89.73
P18 = 129.24

THE PRESSURE DROP ACROSS THE CONDENSATE FLOW CONTROL VALVE (V6A) IS 0.0 PSI
THE PRESSURE DROP ACROSS THE FEED FLOW CONTROL VALVE IS .0 PSI

OVERALL POWER BALANCE

TURBINE THERMAL POWER IS 14.73 MEGAWATTS

GROSS ELECTRICAL POWER IS 14.44 MEGAWATTS

TOTAL PARASITIC LOSSES ARE 4.11 MEGAWATTS, APPORTIONED AS FOLLOWS

COLD SEAWATER PUMPING POWER	1.77 MEGAWATTS
WARM SEAWATER PUMPING POWER	1.35 MEGAWATTS
AMMONIA CONDENSATE PUMPING POWER	.32 MEGAWATTS
AMMONIA FEED PUMPING POWER	.16 MEGAWATTS
MISCELLANEOUS POWER REQUIREMENTS	.50 MEGAWATTS

NET ELECTRICAL POWER IS 10.33 MEGAWATTS

THIS PAGE

WAS INTENTIONALLY

LEFT BLANK

ATTACHMENT II

DESCRIPTION OF FUNCTIONS AND SUBROUTINES

PROGRAM LISTING

These will be furnished at customer's request.

THIS PAGE

WAS INTENTIONALLY

LEFT BLANK

APPENDIX A.3

HYDRAULIC TRANSIENT MODEL

A.3. HYDRAULIC TRANSIENT MODEL

The vertical motion of the hull causes flow transients in the cold and warm water systems, which cause unsteady flow on the waterside of the heat exchangers. In order to examine the nature of the unsteady flow and to determine its effect, a dynamic mathematical model of the water flow was set up and was solved numerically by computer. In the model, the hydraulic features of a 40 MW platform are represented by three subsystems. The cold water pipe and open trough are represented as a single subsystem as shown in Figure 1. The second subsystem consists of a condenser, an evaporator, and their common effluent discharge pipe as shown in Figure 2. The third subsystem includes all of the seawater pumps and is represented by a dimensionless pump characteristic curve as shown in Figure 3. The symbols used to represent these subsystems are defined in Tables 1, 2, and 3, respectively.

Table 1. Symbols Used for Representation of Cold Water Pipe and Open Trough

a_1 = area of horizontal water surface in the trough (constant)

A_1 = cross section area of cold water pipe (constant)

D_r = draft (constant)

= depth from mean sea level to floor of open trough in calm sea with no pumping

D_1 = internal diameter of cold water pipe (constant)

h_1 = elevation of water surface in trough with respect to datum elevation (function of time, positive up from datum)

h_{MSL} = elevation of mean sea level with respect to datum elevation (constant, positive up from datum)

V_1 = absolute velocity of flow in cold water pipe (function of time, positive up pipe into trough)

z_1 = elevation of floor of trough with respect to datum elevation (function of time, positive up from datum)

z_0 = half amplitude of heave of platform

z_1' = value of z_1 in calm sea

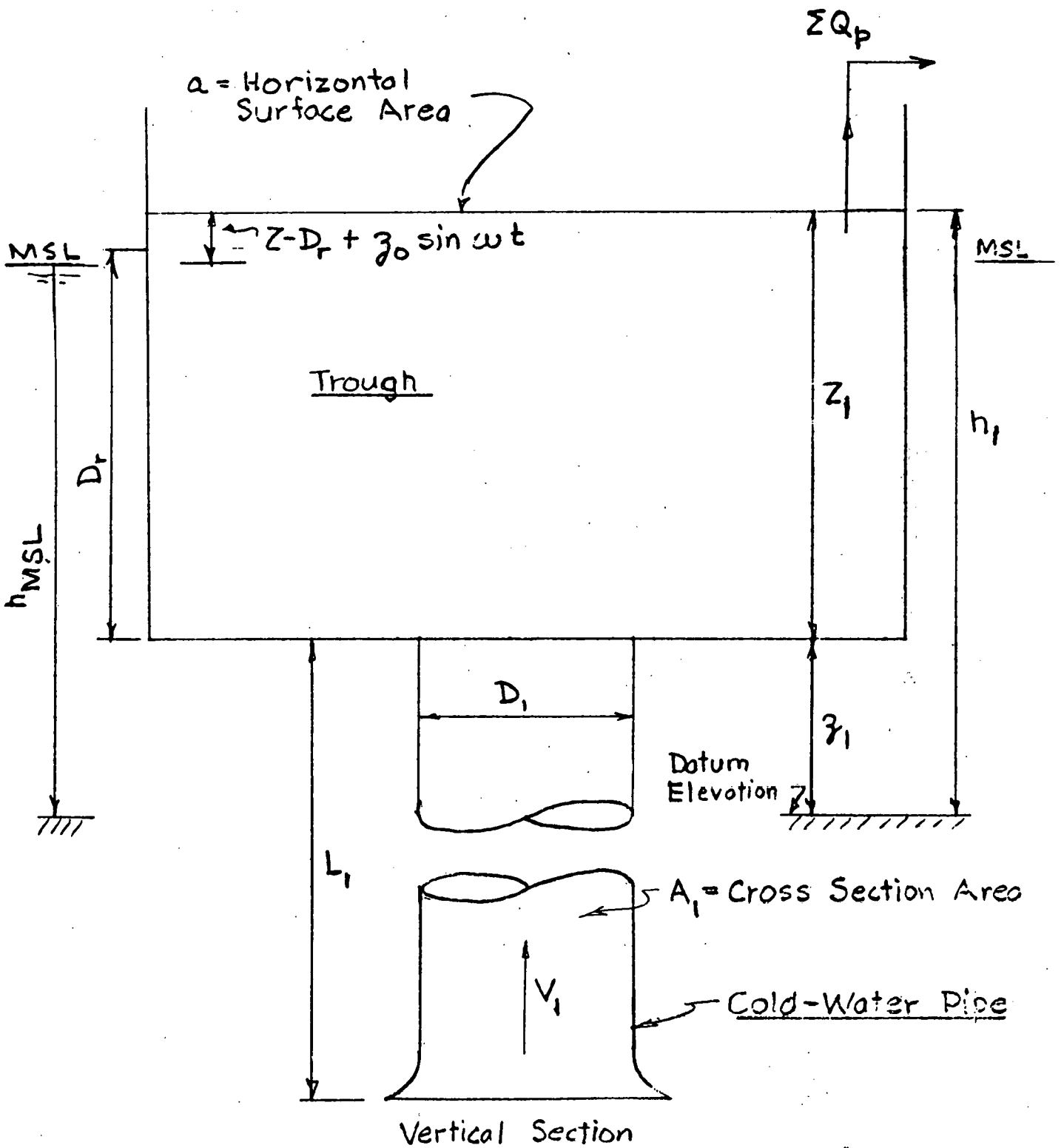

Fig. 1. Cold-Water Pipe and Open Trough

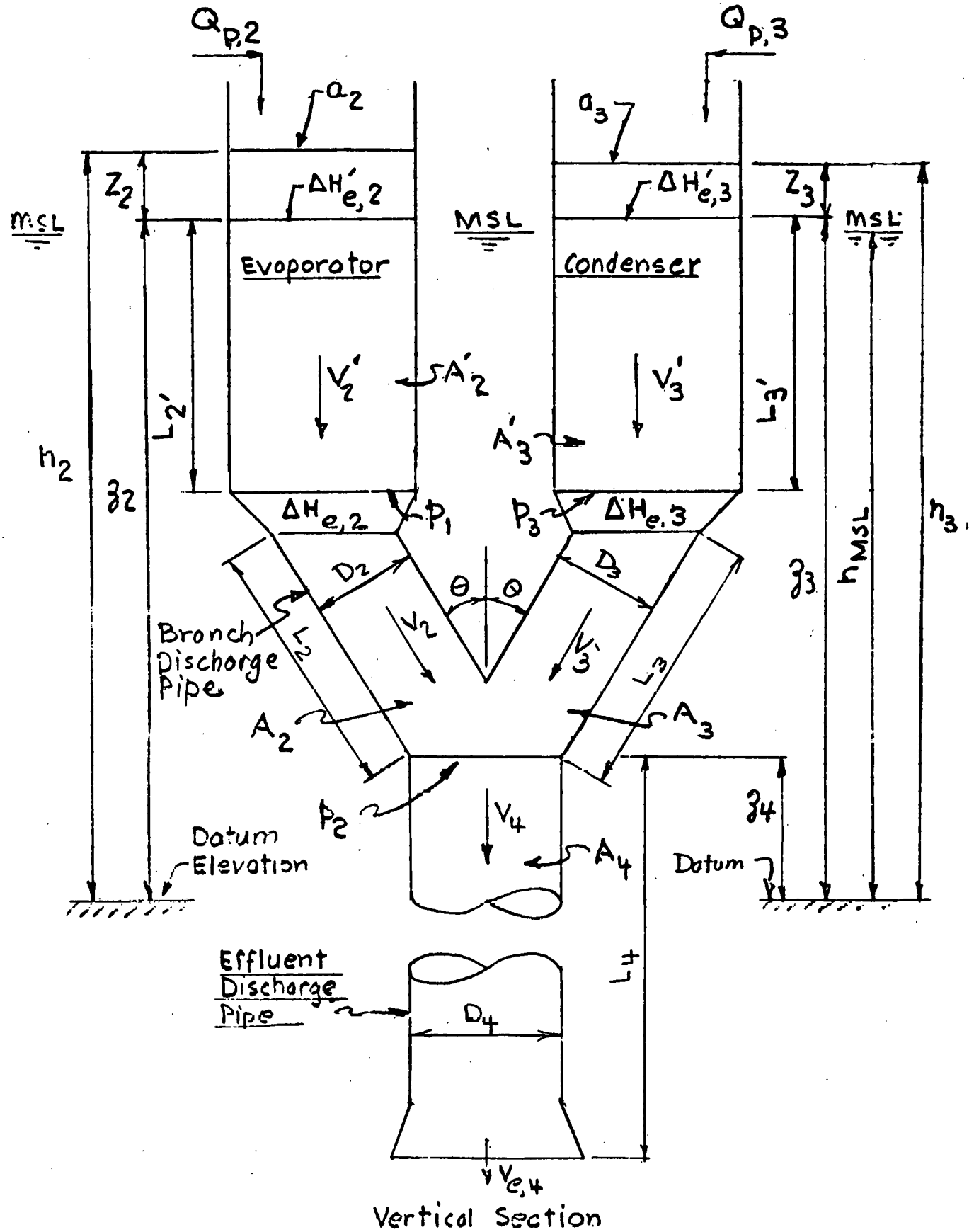

Vertical Section

Fig. 2. Evoporotor, Condenser, and Effluent Discharge Pipe

FIGURE 3

DIMENSIONLESS PUMP CHARACTERISTIC CURVE

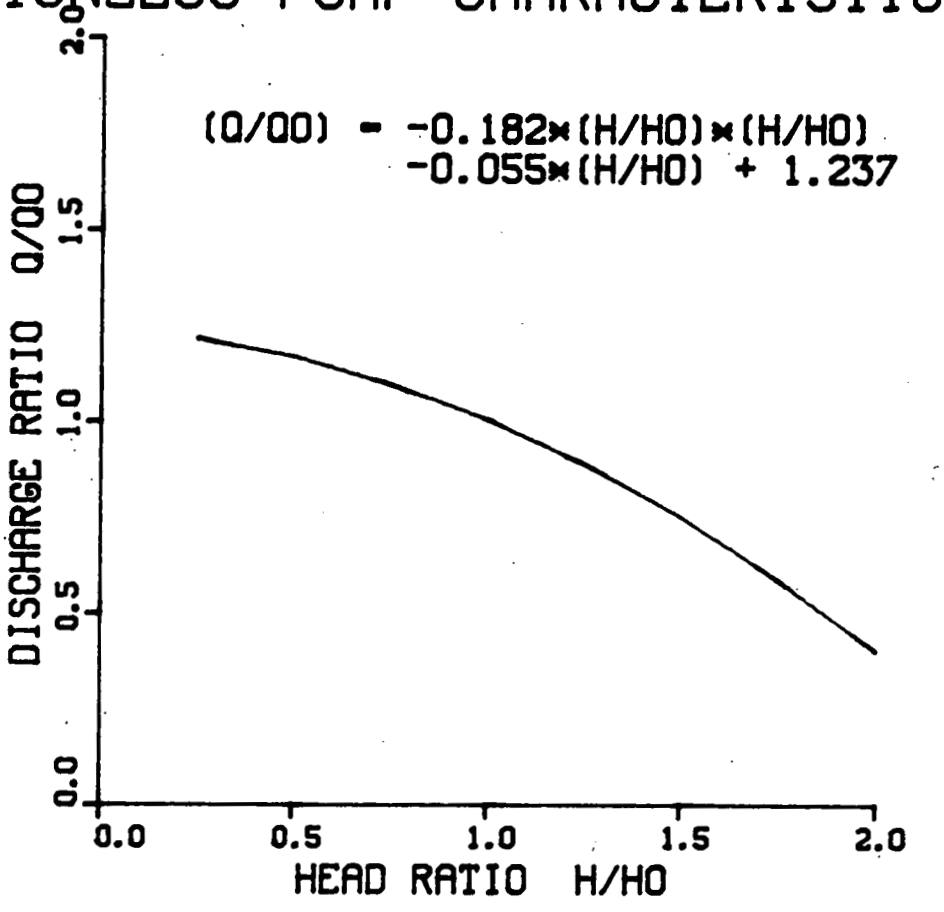

Table 1. Symbols Used for Representation of Cold Water Pipe and Open Trough (Continued)

Z_1 = depth of water in trough (function of time)

ΣQ_p = total rate of flow out of trough through all cold water pumps (function of time)

L_1 = length of cold water pipe from bottom end to floor of trough (constant)

MSL = mean sea level

g = acceleration due to gravity

t = time

$\Delta h_{s,1}$ = difference in static head due to difference between water temperatures inside and outside of cold water pipe

f_1 = Darcy friction factor for cold water pipe

ω = frequency of heave of platform

Table 2. Symbols Used for Representation of Heat Exchangers and Effluent Discharge Pipe

a_2 = area of horizontal water surface in top water box of evaporator (constant)

a_3 = area of horizontal water surface in top water box of condenser (constant)

A_2' = total cross section area of all tubes in evaporator (constant)

A_3' = total cross section area of all tubes in condenser (constant)

A_2 = cross section area of evaporator branch of discharge pipe (constant)

A_3 = Cross section area of condenser branch of discharge pipe (constant)

A_4 = cross section area of combined effluent discharge pipe (constant)

D_2 = diameter of evaporator branch of discharge pipe (constant)

D_3 = diameter of condenser branch of discharge pipe (constant)

D_4 = diameter of combined effluent discharge pipe (constant)

Table 2. Symbols Used for Representation of Heat Exchangers and Effluent Discharge Pipe (Continued)

h_2 = elevation of water surface in top water box in evaporator with respect to datum elevation (function of time, positive up from datum)

h_3 = elevation of water surface in top water box in condenser with respect to datum elevation (function of time, positive up from datum)

$\Delta H'_{e,2}$ = energy loss during flow from top water box into tubes in evaporator (function of velocity V'_2)

$\Delta H'_{e,3}$ = energy loss during flow from top water box into tubes in condenser (function of V'_3)

$\Delta H_{e,2}$ = energy loss during flow from evaporator bottom water box to branch discharge pipe (function of V_2)

$\Delta H_{e,3}$ = energy loss during flow from condenser water box to branch discharge pipe (function of V_3)

L'_2 = length of flow path through evaporator tubes and bottom water box (constant)

L'_3 = length of flow path through condenser tubes and bottom water box (constant)

L_2 = length of evaporator branch discharge pipe (constant)

L_3 = length of condenser branch discharge pipe (constant)

L_4 = length of combined discharge pipe (constant)

p_1 = pressure at bottom tubesheet of evaporator (function of time)

p_3 = pressure at bottom tubesheet of condenser (function of time)

p_2 = pressure at junction of branch discharge pipes (function of time)

$Q_{p,2}$ = rate of flow pumped into top water box of evaporator (function of time)

$Q_{p,3}$ = rate of flow pumped into top water box of condenser (function of time)

V'_2 = absolute velocity of flow in evaporator tubes (function of time, positive toward discharge outlet)

V'_3 = absolute velocity of flow in condenser tubes (function of time, positive toward discharge outlet)

Table 2. Symbols Used for Representation of Heat Exchangers and Effluent Discharge Pipe (Continued)

V_2 = absolute velocity of flow in evaporator branch discharge pipe (function of time, positive toward discharge outlet)

V_3 = absolute velocity of flow in condenser branch discharge pipe (function of time, positive toward discharge outlet)

V_4 = absolute velocity of flow in combined discharge pipe (function of time, positive toward discharge outlet)

$V_{e,4}$ = absolute velocity at outlet end of combined discharge pipe (function of time, positive out of pipe)

z_2 = elevation of evaporator top tubesheet with respect to datum (function of time, positive up from datum)

z_3 = elevation of condenser top tubesheet with respect to datum (function of time, positive up from datum)

z_4 = elevation of junction of branch interceptors with respect to datum (function of time, positive up from datum)

Z_2 = depth of water in top water box of evaporator (function of time)

Z_3 = depth of water in top water box of condenser (function of time)

α = coefficient (constant)

β = coefficient (constant)

θ = angle between vertical and branch discharge conduit (constant)

γ = unit weight of water (constant)

$\Delta H'_{f,2}$ = friction losses in evaporator tubes (function of V'_2 and time)

$\Delta H'_{f,3}$ = friction losses in condenser tubes (function of V'_3 and time)

$\Delta H_{f,2}$ = friction losses in evaporator branch discharge pipe (function of V_2 and time)

$\Delta H_{f,3}$ = friction losses in condenser branch discharge pipe (function of V_3 and time)

$\Delta H_{f,4}$ = friction losses in combined discharge pipe (function of V_4 and time)

Table 3. Symbols Used for Representation of Pumps

H	= head delivered by pump (function of time)
H_0	= head delivered by pump at steady state in calm sea (constant)
Q	= rate of flow pumped (function of time)
Q_0	= rate of flow pumped at head H_0 with steady state and calm sea (constant)
z_0'	= half amplitude of wave motion driving the heave of the platform (constant)

For each subsystem, the flow in each component is described by equation of continuity and momentum. The former are written in terms of velocities relative to the hull, pipes, tubesheets, etc. The momentum equations are written in terms of absolute velocities relative to fixed space, except for the terms that determine entrance and friction losses. These terms are written with the same relative velocities used in the continuity equations. The absolute velocities are needed for terms involving momentum and acceleration.

For the cold water pipe and open trough, the continuity equation is concerned primarily with the trough while the momentum equation is concerned primarily with the pipe. The continuity equation is

$$A_1(V_1 - \frac{dz_1}{dt}) - \Sigma Q_p = a_1 \frac{dZ_1}{dt} \qquad (1)$$

while the momentum equation is

$$-\frac{L_1}{g}\frac{dV_1}{dt} = z_1 + Z_1 - h_{MSL} + \Delta h_{s,1} + \frac{V_1^2}{2g} + \frac{f_1 L_1}{2gD_1}(V_1 - \frac{dz_1}{dt})^2 \qquad (2)$$

In order to guarantee that the friction force always acts in the correct direction, the square of the relative velocity in equation (2) can be replaced by $|(V_1 - dz_1/dt)|(V_1 - dz_1/dt)$. However, since no reversal of flow in the pipe was anticipated this elaboration was not used.

The elevation, z_1, can be divided into a static term, z_1', and an oscillating term, $z_0 \sin \omega t$. The first gives the value of z_1 in a calm sea, while the second is a sinusoidal representation of the heave of the platform. With this division the values of z_1 and Z_1 always satisfy the equation

$$z_1 + Z_1 - h_{MSL} = Z_1 - D_r + z_0 \sin \omega t \tag{3}$$

Substitution of equation (3) in equation (2) leads to

$$-\frac{L_1}{g}\frac{dV_1}{dt} = Z_1 - D_r + z_0 \sin \omega t + \Delta h_{s,1} + \frac{V_1^2}{2g} + \frac{f_1 L_1}{2gD_1}\left(V_1 - \frac{dz_1}{dt}\right)^2 \tag{4}$$

Continuity equations for the heat exchangers are similar to those for the trough. The equations for the evaporator and condenser are respectively

$$Q_{p,2} - A_2'\left(V_2' + \frac{dz_2}{dt}\right) = a_2 \frac{dZ_2}{dt} \tag{5}$$

$$Q_{p,3} - A_3'\left(V_3' + \frac{dz_3}{dt}\right) = a_3 \frac{dZ_3}{dt} \tag{6}$$

The velocities in the tubesheet can be eliminated using the continuity equations between heat exchanger and branch discharge pipe. That is

$$A_2'\left(V_2' + \frac{dz_2}{dt}\right) = A_2\left[\left(V_2 \cos\theta + \frac{dz_2}{dt}\right)^2 + \left(V_2 \sin\theta\right)^2\right]^{1/2} \tag{7}$$

and

$$A_3'\left(V_3' + \frac{dz_3}{dt}\right) = A_3\left[\left(V_3 \cos\theta + \frac{dz_3}{dt}\right)^2 + \left(V_3 \sin\theta\right)^2\right]^{1/2} \tag{8}$$

Substitution of equations (7) and (8) into equations (5) and (6), respectively, leads to the following overall equations for each interceptor and branch discharge pipe.

$$Q_{p,2} - A_2\left[\left(V_2 \cos\theta + \frac{dz_2}{dt}\right)^2 + \left(V_2 \sin\theta\right)^2\right]^{1/2} = a_2 \frac{dZ_2}{dt} \tag{9}$$

$$Q_{p,3} - A_3\left[\left(V_3 \cos\theta + \frac{dz_3}{dt}\right)^2 + \left(V_3 \sin\theta\right)^2\right]^{1/2} = a_3 \frac{dZ_3}{dt} \tag{10}$$

Finally flow in the branches is related to flow in the combined discharge pipe by the following continuity equation

$$A_2\left[\left(V_2 \cos\theta + \frac{dz_2}{dt}\right)^2 + (V_2 \sin\theta)^2\right]^{1/2}$$

$$+ A_3\left[\left(V_3 \cos\theta + \frac{dz_3}{dt}\right)^2 + (V_3 \sin\theta)^2\right]^{1/2} = A_4\left(V_4 + \frac{dz_4}{dt}\right) \qquad (11)$$

The momentum equations for the heat exchangers and discharge pipes are similar to those for the trough and cold water pipe. However, the equations for the individual components must be written in terms of intermediate pressures p_1, p_2, and p_3. For the heat exchangers, the equations become:

$$-\frac{L'_2}{g}\frac{dV'_2}{dt} = -L'_2 + \frac{V_2'^2}{2g} + \frac{p_1}{\gamma} - \alpha_2\frac{V_1'^2}{2g} - Z_2 + \Delta H'_{e,2} + \Delta H'_{f,2} \qquad (12)$$

$$-\frac{L'_3}{g}\frac{dV'_3}{dt} = -L'_3 + \frac{V_3'^2}{2g} + \frac{p_3}{\gamma} - \alpha_3\frac{V'^2_3}{2g} - Z_3 + \Delta H'_{e,3} + \Delta H'_{f,e} \qquad (13)$$

In these equations α_i and β_i are defined by

$$\alpha_i = \frac{A_i'}{A_B}\left(1 - \frac{A_i'}{A_B}\right) \qquad \beta_i = \left(\frac{A_i}{A_B}\right)^2 \qquad (14)$$

in which A_B is the cross section area of the bottom water box of the heat exchanger. The equations for the branch discharge pipes become

$$\frac{p_2}{\gamma} - \frac{p_3}{\gamma} + (1 - \beta_2)\frac{V_2^2}{2g} - L_2\cos\theta + \Delta H_{e,2} + \Delta H_{f,2} = -\frac{L_2}{g}\frac{dV_2}{dt} - \frac{V_2^2}{g}(1 - \sqrt{\beta}_2\cos\theta) \qquad (15)$$

and

$$\frac{p_1}{\gamma} - \frac{p_3}{\gamma} + (1 - \beta_3)\frac{V_3^2}{2g} - L_3 \cos\theta + \Delta H_{e,3} + \Delta H_{f,3} =$$

$$-\frac{L_3}{g}\frac{dV_3}{dt} - \frac{V_3^2}{g}(1 - \sqrt{\beta}_3 \cos\theta) \qquad (16)$$

Equations 12 and 13 can be combined with 15 and 16 respecitvely to yield the following overall equation from the top water boxes to the junction of the branch discharge pipes.

$$-\frac{L'_2}{g}\frac{dV'_2}{dt} - \frac{L_2}{g}\frac{dV_2}{dt} = \frac{P_2}{\gamma} - L_2 \cos\theta - Z_2 + \frac{V_2^2}{g}(1 - \sqrt{\beta}_2 \cos\theta)$$
$$+ (1 - \alpha_2)\frac{V'^2_2}{2g} + (1 - \beta_2)\frac{V_2^2}{2g} + \Delta H'_{e,2} + \Delta H'_{f,2} + \Delta H_{f,2} + \Delta H_{e,2} \qquad (17)$$

$$-\frac{L'_3}{g}\frac{dV'_3}{dt} - \frac{L_3}{g}\frac{dV_3}{dt} = \frac{P_2}{\gamma} - L'_3 - L_3 \cos\theta - Z_3 + \frac{V_3^2}{g}(1 - \sqrt{\beta}_3 \cos\theta)$$

(18)

$$+ (1 - \alpha_3)\frac{V'^2_3}{2g} + (1 - \beta_3)\frac{V_3^2}{2g} + \Delta H'_{e,3} + \Delta H_{e,3} + \Delta H'_{f,3} + \Delta H_{f,3}$$

The momentum equation for the combined discharge pipe also requires the intermediate pressure p_2 at the junction. The equation is:

$$-\frac{L_4}{g}\frac{dV_4}{dt} = h_{MSL} - z_4 - \frac{p_2}{\gamma} + \frac{V_{e,4}^2}{2g}$$

$$+ \frac{V_4^2}{2g} + \Delta H_{f,4} - \frac{1}{g}\left(\frac{A_2}{A_4}\right)V_2^2 \cos\theta - \frac{1}{g}\left(\frac{A_3}{A_4}\right)V_3^2 \cos\theta \qquad (19)$$

In the current form of the dynamic model, the momentum and dynamics of the seawater pumps and their motors are not considered. Each pump is represented by an approximate characteristic curve that gives delivered head as a function of discharge. For the cold water pump, the delivered head H_3 is the difference $h_3 - h_1$ between water surface elevations in the open trough and the top water box of the condenser. This difference is given by

$$H_3 = h_3 - h_1 = Z_3 - Z_1 + D_r \tag{20}$$

For the warm water pump, the delivered head H_2 is equal to the difference between h_2 and the sea outside the hull. If the wave motion that drives the heave of the platform is represented by $z_o' \sin \omega t$, the delivered head on the warm water pump is given by

$$H_2 = h_2 - z_o' \sin \omega t = Z_2 + (z_o - z_o') \sin \omega t \tag{21}$$

At any time the delivered head is determined from the values of Z_1, Z_2, and Z_3 and Equation 20 or 21. The value of flow is then obtained from the characteristic curve for the pump.

The use of only one curve for each pump is equivalent to the assumption that the pump operates at constant speed as the head changes. The change in pump torque and pump speed due to variation in head has been ignored.

As already shown in Figure 3, a dimensionless pump curve is used. The same curve is used for cold and warm water. For each pump, the values of H_0 and Q_0 are the delivered head and discharge, respecitvely, for steady state in a calm sea.

In addition to the pump curve, there is a relationship between flow rates $Q_{p,3}$ and ΣQ_p. Since all of the flow is pumped to the condensers comes from the trough

$$\Sigma Q_p = 4\, Q_{p,3} \tag{22}$$

Equations 1, 4, 7, 8, 9, 10, 11, 17, 18, 19, 20, 21, 22, and the two pump characteristic curves for cold and warm water form a set of 15 equations with 15 variables V_1, V_2', V_2, V_3', V_3, V_4, Z_1, Z_2, Z_3, $Q_{p,2}$, $Q_{p,3}$, ΣQ_p, p_2, H_2 and H_3. By differentiation and substitution, Equation 7, 8, 11, 17, 18 and 19 are reduced to two equations in V_3 and V_2, and the variables V'_2, V'_3, V_4 and p_2 are eliminated. The result is two equations with the functional form

$$C_{1,1} \frac{dV_3}{dt} + C_{1,2} \frac{dV_2}{dt} = C_{1,0} \tag{23}$$

$$C_{2,1} \frac{dV_3}{dt} + C_{2,2} \frac{dV_2}{dt} = C_{2,0} \tag{24}$$

In addition, Equation 22 is used to eliminate $Q_{p,3}$. The set is reduced to 10 equations, 1, 4, 9, 10, 20, 21, 23, 24 and two pump curves. The 10 variables are V_1, V_2, V_3, Z_1, Z_2, Z_3, $Q_{p,2}$, $Q_{p,3}$, H_2 and H_3. This set of 10 equations and variables is solved numerically by computer. Values of the variables at time t are used in the equations to calculate the values after an increment Δt of time.

In 8 of the equations and variables, an explicit method of solution is used. In each equation only one variable is allowed to change during Δt. The other variables are treated as constants with values that they have at time t. The equation is then solved independently for the value of the one variable that changes. In Equation 1, for example, all variables except Z_1, are treated as constants with values from time t. The equation is solved independently for the change in Z_1, during Δt. Similarly, Equation 4 is solved independently for the change in V_1. The changes during Δt are added to the values of the variables at t to obtain values at $t + \Delta t$. For a pump curve, the value of H at t is used to determine Q_p at t. The value of Q_p then remains constant until $t + \Delta t$.

Equation 23 and 24 are solved implicitly, that is V_3 and V_2 both change during Δt, and the equations are solved simultaneously for the changes. The changes are then added to values at t to obtain values at $t + \Delta t$. Since Equation 23 and 24 represent the 6 original equations 7, 8, 11, 17, 18 and 19, all 6 equations are essentially solved simultaneously.

PREPARED _____ REPORT NO. PAGE

CHECKED _____

MODEL _____

VARIABLE NAME	FORTRAN NAME	VARIABLE NAME	FORTRAN NAME	VARIABLE NAME	FORTRAN NAME
a_1	A	L_4	L4	z_2	GZ2
a_2	AWB2	L_2'	LE	z_3	GZ3
a_3	AWB3	L_3'	LC	z_4	GZ4
A_1	A1	P_1	P1	Z_1	Z1
A_2	A2	P_2	P2	Z_2	Z2
A_3	A3	P_3	P3	Z_3	Z3
A_4	A4	ΣQ_P	QP	$\Delta H_{e,2}$	HE2
A_2'	AE	$Q_{P,2}$	QP2	$\Delta H_{e,3}$	HE3
A_3'	AC	$Q_{P,3}$	QP3	$\Delta H_{e,2}'$	HEE
D_1	D1	t	T	$\Delta H_{e,3}'$	HEC
D_2	D2	V_1	V1	$\Delta H_{f,2}$	HF2
D_3	D3	V_2	V2	$\Delta H_{f,3}$	HF3
D_4	D4	V_3	V3	$\Delta H_{f,4}$	HF4
D_r	DR	V_4	V4	$\Delta H_{f,2}'$	HFE
f_1	F1	V_2'	VE	$\Delta H_{f,3}'$	HEC
g	G	V_3'	VC	$\Delta h_{s,1}$	DHS
h_{msL}	HMSL	$V_{e,4}$	VED	Δt	DT
H_0	HO	z_0	ZH1		
L_1	L1	z_1	GZ1		
L_2	L2				
L_3	L3				

VARIABLE NAME	FORTRAN NAME	VARIABLE NAME	FORTRAN NAME	VARIABLE NAME	FORTRAN NAME
β	BETA	$\frac{dz_4}{dt}$	DG24		
θ	THETA				
ω	W	$\frac{dz_1}{dt}$	D21		
α	AIPHA				
$\frac{dv_1}{dt}$	DV1	$\frac{dz_2}{dt}$	D22		
$\frac{dv_2}{dt}$	DV2				
$\frac{dv_3}{dt}$	DV3	$\frac{dz_3}{dt}$	D23		
$\frac{dv_4}{dt}$	DV4				
$\frac{dv_2'}{dt}$	DVE				
$\frac{dv_3'}{dt}$	DVC				
$\frac{dz_1}{dt}$	DG21				
$\frac{dz_2}{dt}$	DG22				
$\frac{dz_3}{dt}$	DG23				

```
00100        PROGRAM ENWAT(INPUT,OUTPUT,TAPE5=INPUT,TAPE6)
00110        COMMON/COM1/ZH0,TH,PI,TMAX,G,DHS,HMSL,DR,F1
00120        COMMON/COM2/D4,D3,D2,D1,DE,DC
00130        COMMON/COM3/L4,L3,L2,L1,LE,LC
00140        COMMON/COM4/A4,A3,A2,A1,AE,AC,A
00150        COMMON/COM5/QP,QP2,QP3,GZ,DGZ,D2GZ,GZ4
00160        COMMON/COM6/DWB2T,DWB3T,AWB2T,AWB3T,THETA
00170        COMMON/COM7/Z,V1,Z2,V2,Z3,V3,V4,VE,VC,VED
00180        COMMON/COM8/DZ,DV1,DZ2,DV2,DZ3,DV3,DV4,
00190     +  DVE,DVC
00200        COMMON/COM9/HEE,HFE,HE2,HF2,HEC,HFC,HE3,HF3,HF4
00210        COMMON/COM10/DT1,CFLOW,NMAX
00220        EQUIVALENCE (D2GZ,D2GZ2,D2GZ3,D2GZ4)
00230        EQUIVALENCE (DGZ,DGZ2,DGZ3,DGZ4)
00240        DATA L,DR/5,63./
00250        DATA PI,ZH0,TH,TMAX/
00260       +3.1415927,10.7,16.19,100./
00270        DATA D1,A,L1,G,DHS,DT1,EPS/
00280       +30.505,5893.,2950,32.174,3.,.2,.02/
00290        DATA HMSL,D4,D3,D2,DE1,DC1/0.0,22.03,15.2525,15.8975,
00300     +  .87965,0.889/
00310        DATA L4,L3,L2,LE,LC/270,2*40,2*30/
00320        DATA DWB2T,DWB3T,QP20,QP30/2*27.,1191.0,1096.3/
00330        DATA DWB2B,DWB3B/2*27./
00340        DATA CFLOW,NMAX,NPRINT/0.0,62,0/
00350        NAMELIST/INPUT/PI,ZH0,TH,Z0,V10,TMAX,
00360     +  D1,A,L1,G,DHS,DT1,EPS,L,DR,D4,D3,D2,DE1,DC1,
00370     +  L4,L3,L2,Z20,Z30,V20,V30,CFLOW,DWB2T,DWB3T,NMAX,
00380     +  NPRINT
00390 17     READ(5,INPUT)
00400        IF(L.EQ.65)GO TO 65
00410        IF(L.EQ.64)GO TO 18
00420        DE=DE1/12.
00430        DC=DC1/12.
00440        CALL CAL10(A1,D1,A4,D4,1)
00450        CALL CAL10(A2,D2,AE,DE,42667)
00460        CALL CAL10(AWB2T,DWB2T,AWB3T,DWB3T,1)
00470        CALL CAL10(AWB2B,DWB2B,AWB3B,DWB3B,1)
00480        CALL CAL10(A3,D3,AC,DC,43678)
00490        CALL CAL11(BETA2,A2,AWB2B,ALPHA2,AE)
00500        CALL CAL11(BETA3,A3,AWB3B,ALPHA3,AC)
00510        DT=DT1
00520        QP3=QP30
00530        QP2=QP20
00540        QP=4.*QP3
00550        Z2=0.0
00560        Z3=0.0
00570        V1=QP/A1
00580        V2=QP2/A2
00590        V3=QP3/A3
00600        THETA=PI/6.
00610        N=1
00620        NN=1
00630        T=-1.0
00640 16     CONTINUE
00650 C      IF(T.EQ.2.0.OR.T.EQ.4.0)DT=2.*DT
00660        IF(T.NE.-1.0.AND.T.LT.0.0)T=0.0
00670        CALL  HEAVE(T)
00680        IF(T.EQ.-1.0)GO TO 20
```

```
00690       CALL FLOW(Z3-Z+DR,QP3,H30,QP30)
00700       CALL FLOW(Z2-CFLOW*DGZ,QP2,H20,QP20)
00710       QP=4.*QP3
00720 20    CONTINUE
00730       CALL FRICFAC(V1-DGZ,EPS/D1,F1,D1,1.70906E-5)
00740       CALL CAL1(F22,THETA,V2,DGZ2)
00750       CALL CAL2(DZ2,F22*A2,QP2,AWB2T)
00760       CALL CAL1(F33,THETA,V3,DGZ3)
00770       CALL CAL2(DZ3,F33*A3,QP3,AWB3T)
00780       CALL CAL3(VE,F22*A2,0.0,DGZ2,AE)
00790       CALL CAL3(VC,F33*A3,0.0,DGZ3,AC)
00800       CALL CAL3(V4,F22*A2,F33*A3,DGZ4,A4)
00810       VED=V4/2.
00820       CALL FRICFAC(V4+DGZ,0.01/D4,F4,D4,1.26150E-5)
00830       CALL FRICFAC(V3+DGZ,0.01/D3,F3,D3,1.70906E-5)
00840       CALL FRICFAC(V2+DGZ,0.01/D2,F2,D2,0.97915E-5)
00850       CALL FRICFAC(VE+DGZ,0.0001/DE,FE,DE,0.97915E-5)
00860       CALL FRICFAC(VC+DGZ,0.0001/DC,FC,DC,1.70906E-5)
00870       CALL PDROP(HEE,VE+DGZ,0.3,HE2,V2+DGZ,0.25)
00880       CALL PDROP(HEC,VC+DGZ,0.3,HE3,V3+DGZ,0.25)
00890       CALL PDROP(HFE,VE+DGZ,FE*LE/DE,HFC,VC+DGZ,FC*LC/DC)
00900       CALL PDROP(HF2,V2+DGZ,F2*L2/D2,HF3,V3+DGZ,F3*L3/D3)
00910       CALL PDROP(HF4,V4+DGZ,F4*L4/D4,XXX,0.0,0.0)
00920       CALL CAL5(CC1,CC2,CC3,D2GZ2,D2GZ3,D2GZ4,
00930 +     AE,AC,A4)
00940       CALL CAL6(CF4,CF3,CF2,CF1,LE,L2,Z2,
00950 +     VE,V2,ALPHA2,BETA2,HEE,HFE,HE2,HF2)
00960       CALL CAL6(CG4,CG3,CG2,CG1,LC,L3,Z3,
00970 +     VC,V3,ALPHA3,BETA3,HEC,HFC,HE3,HF3)
00980       IF(T.GT.-1.0) GO TO 14
00990       Z=-(GZ+DHS-DR+V1*ABS(V1)/(2.*G)+
01000 +     (F1*L1/2./G/D1)*(V1)*ABS(V1))
01010       Z2=CF4
01020       Z3=CG4
01030       CF4=0.0
01040       CG4=0.0
01050       H30=Z3-Z+DR
01060       H20=Z2
01070 14    CONTINUE
01080       CALL CAL4(CA1,CA2,A2,AE,F22,V2,THETA,DGZ2,D2GZ2)
01090       CALL CAL4(CB1,CB2,A3,AC,F33,V3,THETA,DGZ3,D2GZ3)
01100       CALL CAL7(CH1,CH2,CH3,CH4,CF1,CF2,
01110 +     CF3,CF4,CC1,CC2,CC3)
01120       CALL CAL7(CI1,CI2,CI3,CI4,CG1,CG2,
01130 +     CG3,CG4,CC2,CC1,CC3)
01140       CALL CAL8(CX1,CX2,CX3,CH1,CH2,CH3,CH4,
01150 +     CA1,CA2,CB1,CB2)
01160       CALL CAL8(CY1,CY3,CY2,CI1,CI2,CI3,CI4,
01170 +     CB1,CB2,CA1,CA2)
01180       CALL CAL9(DV2,DV3,CX1,CX2,CX3,CY1,CY2,CY3)
01190       CALL DIFF(T)
01200       IF(T.EQ.0.0.OR.T.EQ.-1.)GO TO 13
01210       IF(N.EQ.L)GO  TO 13
01220       N=N+1
01230       T=T+DT
01240       CALL INT(DT,T)
01250       GO TO 16
01260 13    N=1
01270       CALL PLOT(T,NN)
01280       NN=NN+1
01290 15    T=T+DT
01300       CALL INT(DT,T)
01310       IF(NN.LE.NMAX)GO TO 16
01320       IF(NPRINT.NE.0)GO TO 18
01330       GO TO 17
01340 18    CALL PRINT(T,NPRINT)
```

```
01350       GO TO 17
01360 65    CONTINUE
01370       END
01380       SUBROUTINE INT(DT,T)
01390       COMMON/COM7/Y(10)
01400       COMMON/COM8/F(9)
01410       DO 10 I=1,6
01420 10    Y(I)=Y(I)+DT*F(I)
01430       RETURN
01440       END
01450       SUBROUTINE HEAVE(T)
01460       COMMON/COM1/ZH0,TH,PI,TMAX,G,DHS,HMSL,DR,F1
01470       COMMON/COM3/L4,L3,L2,L1,LE,LC
01480       COMMON/COM5/QP,QP2,QP3,GZ,DGZ,D2GZ,GZ4
01490       COMMON/COM6/DWB2T,DWB3T,AWB2T,AWB3T,THETA
01500       IF(T.EQ.-1.0)GO TO 10
01510       IF(T.LE.10.0)ZH1=ZH0*T/10.
01520       W=2.*PI/TH
01530       GZ=ZH1*SIN(W*T)
01540       GZ4=GZ-(LE+L2*COS(THETA))
01550       DGZ=W*ZH1*COS(W*T)
01560       D2GZ=-W*W*ZH1*SIN(W*T)
01570       RETURN
01580 10    GZ=0.0
01590       DGZ=0.0
01600       D2GZ=0.0
01610       GZ4=-(LE+L2*COS(THETA))
01620       RETURN
01630       END
01640       SUBROUTINE DIFF(T)
01650       COMMON/COM1/ZH0,TH,PI,TMAX,G,DHS,HMSL,DR,F1
01660       COMMON/COM2/D4,D3,D2,D1,DE,DC
01670       COMMON/COM3/L4,L3,L2,L1,LE,LC
01680       COMMON/COM4/A4,A3,A2,A1,AE,AC,A
01690       COMMON/COM5/QP,QP2,QP3,GZ,DGZ,D2GZ,GZ4
01700       COMMON/COM7/Z,V1,Z2,V2,Z3,V3,V4,VE,VC,VED
01710       COMMON/COM8/F(9)
01720       F(1)=(A1/A)*(V1-DGZ)-QP/A
01730       F(2)=-(G/L1)*(GZ+Z+DHS-DR+V1*ABS(V1)/(2.*6)+
01740 +     (F1*L1/2./G/D1)*(V1-DGZ)*ABS(V1-DGZ))
01750       RETURN
01760       END
01770       SUBROUTINE FRICFAC(V1,EDD,FD,D1,XNU)
01780 C
01790 C     COMPUTES FRICTION FACTORS USING COLEBROOKS CORRELATION.
01800       RE=ABS(V1)*D1/XNU
01810       IF(RE.LT.500000.) GO TO 11
01820       FD = .316/SQRT(SQRT(RE))
01830       X = 1./SQRT(FD)
01840       A = EDD/3.7
01850       B = 2.51/RE
01860       DX = 0.
01870       N = -1
01880  2    X = X + DX
01890       U = A + B*X
01900       IF(U.LE.0.0)GO TO 12
01910       DYDX = 1. + .86*B/U
01920       DX = -(X + .86*ALOG(U))/DYDX
01930       N = N + 1
01940       IF(ABS(DX/X).GT..001) GO TO 2
01950       FD = 1./(X*X)
01960       RETURN
01970 12    FD=.316/SQRT(SQRT(RE))
01980       RETURN
01990 11    CONTINUE
02000       DATA C1,C2,C3/0.025,-0.7534,1.386/
```

```
02010       REL=ALOG(RE)
02020       FDL=C1*(REL**2)+C2*REL+C3
02030       FD=EXP(FDL)
02040       FD=FD*1.46
02050 10    CONTINUE
02060       RETURN
02070       END
02080       SUBROUTINE CAL1(F3,THETA,V,DGZ)
02090 C     THIS COMPUTES MAGNITUDE OF HX VELOCITY
02100       F1=V*COS(THETA)+DGZ
02110       F2=V*SIN(THETA)
02120       F3=SQRT(F1*F1+F2*F2)
02130       RETURN
02140       END
02150       SUBROUTINE CAL2(DX,F,QP,AWB)
02160 C     COMPUTES EQUATIONS NO. 1 AND 2.
02170       DX=(QP-F)/AWB
02180       RETURN
02190       END
02200       SUBROUTINE CAL3(V,F3,F2,DGZ,A)
02210 C     COMPUTES EQUATIONS 6,7, AND 8.
02220       V=(F3+F2)/A -DGZ
02230       RETURN
02240       END
02250       SUBROUTINE CAL4(C1,C2,A2,AE,F2,V2,THETA,DGZ,D2GZ)
02260 C     COMPUTES COEFFICIENTS FOR EQUATIONS 9 AND 10 IN
02270 C     THE FORM OF EQUATIONS 14 AND 15.
02280       X1=A2/AE/F2
02290       C2=X1*(V2+DGZ*COS(THETA))
02300       C1=X1*(V2*D2GZ*COS(THETA)+DGZ*D2GZ)-D2GZ
02310       RETURN
02320       END
02330       SUBROUTINE CAL5(CC1,CC2,CC3,D2GZ2,D2GZ3,D2GZ4,
02340 +     AE,AC,A4)
02350 C     COMPUTES COEFFICIENTS OF EQUATION NO. 11
02360 C     IN THE FORM OF EQUATION 11B
02370       CC1=AE/A4
02380       CC2=AC/A4
02390       CC3=CC1*D2GZ2+CC2*D2GZ3-D2GZ4
02400       RETURN
02410       END
02420       SUBROUTINE CAL6(CF4,CF3,CF2,CF1,LEX,L2X,Z2X,
02430 +     VEX,V2X,ALPHA,BETA,HEEX,HFEX,HF2X,HF2X)
02440 C     COMPUTES COEFFICIENTS OF EQUATIONS 12 AND 13
02450 C     IN THE FORM OF EQUATION 12B
02460       COMMON/COM1/ZH0,TH,PI,TMAX,G,DHS,HMSL,DR,F1
02470       COMMON/COM2/D4,D3,D2,D1,DE,DC
02480       COMMON/COM3/L4,L3,L2,L1,LE,LC
02490       COMMON/COM4/A4,A3,A2,A1,AE,AC,A
02500       COMMON/COM5/QP,QP2,QP3,GZ,DGZ,D2GZ,GZ4
02510       COMMON/COM6/DWB2T,DWB3T,AWB2T,AWB3T,THETA
02520       COMMON/COM7/Z,V1,Z2,V2,Z3,V3,V4,VE,VC,VED
02530       COMMON/COM8/DZ,DV1,DZ2,DV2,DZ3,DV3,DV4,
02540 +     DVE,DVC
02550       COMMON/COM9/HEE,HFE,HE2,HF2,HEC,HFC,HE3,HF3,HF4
02560       HT=HEEX+HFEX+HE2X+HF2X
02570       C1=HMSL-GZ4+HF4-Z2X
02580       C2=(VED*VED/2.-V4*V4/2.+V4*V4)/G
02590       C3=-(A2*V2*V2+A3*V3*V3)*COS(THETA)/G/A4
02600       C4=V2X*V2X*(1.-SQRT(BETA)*COS(THETA))/G
02610       C5=((1.-ALPHA)*VEX*VEX+(1.-BETA)*V2X*V2X)/2./G
02620       CF4=C1+C2+C3+C4+C5+HT-LEX-L2X*COS(THETA)
02630       CF3=-L4/G
02640       CF2=-L2X/G
02650       CF1=-LEX/G
```

```
02660       RETURN
02670       END
02680       SUBROUTINE CAL7(CH1,CH2,CH3,CH4,CF1,CF2,
02690  +    CF3,CF4,CC1,CC2,CC3)
02700  C    COMPUTES COEFFICIENTS OF EQUATIONS NO. 16 AND 17.
02710       CH1=CF1+CF3*CC1
02720       CH2=CF2
02730       CH3=CF3*CC2
02740       CH4=CF4-CF3*CC3
02750       RETURN
02760       END
02770       SUBROUTINE CAL8(CX1,CX2,CX3,CH1,CH2,CH3,CH4,
02780  +    CA1,CA2,CB1,CB2)
02790  C    COMPUTES COEFFICIENTS OF EQUATIONS 18 AND 19.
02800       CX1=CH1*CA1+CH3*CB1-CH4
02810       CX2=CH1*CA2+CH2
02820       CX3=CH3*CB2
02830       RETURN
02840       END
02850       SUBROUTINE CAL9(DV2,DV3,X1,X2,X3,Y1,Y2,Y3)
02860  C    SOLVES EQUATIONS 20 AND 21.
02870       X6=Y2-Y3*X2/X3
02880       X7=Y3*X1/X3-Y1
02890       DV2=X7/X6
02900       DV3=(X1+X2*DV2)/(-X3)
02910       RETURN
02920       END
02930       SUBROUTINE PDROP(H1,V1,X1,H2,V2,X2)
02940       G=32.174
02950       H1=X1*V1*ABS(V1)/G/2.
02960       H2=X2*V2*ABS(V2)/G/2.
02970       RETURN
02980       END
02990       SUBROUTINE CAL10(A1,D1,A2,D2,N)
03000       PI=3.1415927
03010       A1=PI*D1*D1/4.
03020       A2=PI*D2*D2*N/4.
03030       RETURN
03040       END
03050       SUBROUTINE CAL11(BETA,A,AB,ALPHA,AX)
03060       BETA=(A/AB)**2.
03070       ALPHA=(AX/AB)*(1.-AX/AB)
03080       RETURN
03090       END
03100       SUBROUTINE PLOT(T,I)
03110       COMMON/COM1/ZH0,TH,PI,TMAX,G,DHS,HMSL,DR,F1
03120       COMMON/COM2/D4,D3,D2,D1,DE,DC
03130       COMMON/COM3/L4,L3,L2,L1,LE,LC
03140       COMMON/COM4/A4,A3,A2,A1,AE,AC,A
03150       COMMON/COM5/QP,QP2,QP3,GZ,DGZ,D2GZ,GZ4
03160       COMMON/COM6/DWB2T,DWB3T,AWB2T,AWB3T,THETA
03170       COMMON/COM7/Z,V1,Z2,V2,Z3,V3,V4,VE,VC,VED
03180       COMMON/COM8/DZ,DV1,DZ2,DV2,DZ3,DV3,DV4,
03190  +    DVE,DVC
03200       COMMON/COM9/HEE,HFE,HE2,HF2,HEC,HFC,HE3,HF3,HF4
03210       COMMON/COM10/DT1,CFLOW,NMAX
03220       COMMON/COM11/X(100),YV11(100),YV22(100),YV33(100)
03230       COMMON/COM12/YDD(100),YZ2(100),YZ3(100),YDGZ(100)
03240       COMMON/COM13/YVCC(100),YVEE(100),YV44(100)
03250       YDGZ(I)=DGZ
03260       X(I)=T
03270       YV11(I)=V1-DGZ
03280       YV22(I)=V2+DGZ
03290       YV33(I)=V3+DGZ
03300       YV44(I)=V4+DGZ
03310       YDD(I)=Z-DR
```

```
03320         YZ2(I)=Z2
03330         YZ3(I)=Z3
03340         YVCC(I)=VC+DGZ
03350         YVEE(I)=VE+DGZ
03360         IF(I.EQ.NMAX)GO TO 20
03370         RETURN
03380 20      CONTINUE
03390         WRITE(6,36)CFLOW,DT1
03400 36      FORMAT(//5X,6HCFLOW=,F12.9,5X,4HDT1=,F12.9)
03410         WRITE(6,37)
03420         WRITE(6,34)(X(J),YV11(J),YVEE(J),YVCC(J),J=1,NMAX)
03430         WRITE(6,35)
03440         WRITE(6,34)(X(J),YDD(J),YZ2(J),YZ3(J),J=1,NMAX)
03450 34      FORMAT(4F15.9)
03460 35      FORMAT(//5X,4HTIME,11X,9HDRAW DOWN,6X,10HEVAP DEPTH,5X,
03470 +       10HCOND DEPTH)
03480 37      FORMAT(//5X,4HTIME,11X,8HV1-DZ/DT,7X,8HVE+DZ/DT,
03490 +       7X,8HVC+DZ/DT)
03500         RETURN
03510         END
03520         SUBROUTINE FLOW(H,QP,H0,QP0)
03530         DATA A,B,C/-1.82E-01,-5.5E-02,1.237/
03540         X=H/H0
03550         QP=(C+B*X+A*X*X)*QP0
03560         RETURN
03570         END
03580         SUBROUTINE PRINT(T,NPRINT)
03590         COMMON/COM1/ZH0,TH,PI,TMAX,G,DHS,HMSL,DR,F1
03600         COMMON/COM2/D4,D3,D2,D1,DE,DC
03610         COMMON/COM3/L4,L3,L2,L1,LE,LC
03620         COMMON/COM4/A4,A3,A2,A1,AE,AC,A
03630         COMMON/COM5/QP,QP2,QP3,GZ,DGZ,D2GZ,GZ4
03640         COMMON/COM6/DWB2T,DWB3T,AWB2T,AWB3T,THETA
03650         COMMON/COM7/Z,V1,Z2,V2,Z3,V3,V4,VE,VC,VED
03660         COMMON/COM8/DZ,DV1,DZ2,DV2,DZ3,DV3,DV4,
03670 +       DVE,DVC
03680         COMMON/COM9/HEE,HFE,HE2,HF2,HEC,HFC,HE3,HF3,HF4
03690         COMMON/COM10/DT1,CFLOW,NMAX
03700         COMMON/COM11/X(100),YV11(100),YV22(100),YV33(100)
03710         COMMON/COM12/YDD(100),YZ2(100),YZ3(100),YDGZ(100)
03720         COMMON/COM13/YVCC(100),YVEE(100),YV44(100)
03730         PRINT 10
03740         DO 100 I=1,NPRINT
03750         V1=YV11(I)+YDGZ(I)
03760         VE=YVEE(I)-YDGZ(I)
03770         VC=YVCC(I)-YDGZ(I)
03780         V4=YV44(I)-YDGZ(I)
03790         Z=YDD(I)+DR
03800         QP4=A4*YV44(I)
03810         QPC=AC*YVCC(I)
03820         QPE=AE*YV22(I)
03830         QP=4.*QPC
03840 12      PRINT 11,X(I)
03850         PRINT 13,V1,VE,VC,V4
03860         PRINT 14,YV11(I),YVEE(I),YVCC(I),YV44(I)
03870         PRINT 15,Z,YZ2(I),YZ3(I)
03880         PRINT 17,QP,QPE,QPC,QP4
03890         PRINT 16,YDD(I)
03900 100     CONTINUE
03910 11      FORMAT(20HTIME,SECONDS          ,F13.4)
03920 13      FORMAT(20HSTATIONARY VEL,FT/S   ,4E13.4)
03930 14      FORMAT(20HRELATIVE VEL FT/S     ,4E13.4)
03940 15      FORMAT(20HWATER DEPTH FT        ,3E13.4)
03950 17      FORMAT(20HFLOW RATE CFS         ,4E13.4)
03960 16      FORMAT(20HDRAW DOWN FT          ,E13.4,/)
03970 10      FORMAT(///20X,3X,10HCW PIPE     ,3X,10HEVAPORATOR,3X,
03980 +       10HCONDENSER ,3X,9HEXIT PIPE)
03990         RETURN
04000         END
```

APPENDIX B

WATER SYSTEM DYNAMICS STUDIES

THIS PAGE

WAS INTENTIONALLY

LEFT BLANK

APPENDIX B.1
SUMMARY

B.1.1 INTRODUCTION, PURPOSE, AND SCOPE

B.1.1.1 Introduction

The work described below is a study of the dynamics of the flow in the cold and warm water system, and it is part of Tasks b and c in the Statement of Work Number 1981-LB-7.088. The work is concerned primarily with transients and oscillations in flow caused by:

1. Operation including startup, shutdown, load rejection, and equipment failure.

2. Hull motion due to the sea state including vertical motion (heave), horizontal motion (surge and sway), and rotation about horizontal axes (roll and pitch).

B.1.1.2 Purpose

The purposes of the work described are:

1. To determine the nature and approximate magnitude of transients and oscillations in pressures, velocities, and water surfaces in the distribution system.

2. To interpret the significance of the transients and oscillations in the system design.

3. To recommend design features to reduce or modify the transients and oscillations in instances where they are unacceptable.

B.1.1.3 Scope

Three types of water distribution systems were considered. They are:

1. A completely closed conduit distribution system.

2. A decoupled conduit distribution system.

3. An open trough distribution system.

Not all of the items of operation and hull motion mentioned above were considered for each type of system. Some were not appropriate for some systems and some were beyond the scope of work at this time. Even for those considered, the nature of the flow was determined qualitatively and the magnitude approximated roughly.

A much more accurate determination of the nature and magnitude of the dynamic effects is possible, but it requires the simultaneous solution of systems of nonlinear equations. Such solutions would have to be obtained numerically by computer and are beyond the scope of work at this time. In some cases, the distribution system was represented by simpler systems in order to obtain approximate solutions. In other cases, the nonlinear terms were linearized. When absolutely necessary, a small amount of numerical solution was done by hand calculator.

B.1.2 CONDUIT DISTRIBUTION SYSTEMS

B.1.2.1 Completely Closed Conduit System

In the completely closed conduit water system, the total path from intake to discharge is a closed conduit with no openings to the atmosphere. This alternative was examined for both the cold and warm water systems, but most attention was given to the former. The long vertical cold water supply conduit makes the cold water system more crucial.

The cold water system examined first corresponds to one of the early design options in which the modules are laid out in a single line and the hull is long and narrow. When the system was reexamined later in the work, the length of horizontal pipe, from the vertical supply conduit to the pumps, was changed to correspond more closely to a later option such as Option A with a square hull. The results obtained and the conclusions reached will be similar for either configuration.

The dynamics of flow in the completely closed cold water system were examined for the following situations:

1. Pump startup
2. Vertical hull motion in Sea State 6.

The major problem in pump startup in this type of system is the maximum drop in suction head at the starting pump before sufficient water arrives from the vertical supply conduit. If the suction head falls too low, it will cause cavitation of the pump. The cavitation could continue for several minutes after starting. For feasible configuration

and geometry of the cold water system, the only parameter that can be adjusted to avoid the problem is the rate of increase of the pump speed and rate of flow for the starting pump. The slower the increase, the less the drop in suction head. For a configuration with 16 cold water pumps and a linear rate of increase in flow rate, cavitation might occur if the starting pump reaches full speed in less than 15 seconds. In starting the pumps sequentially, the suction head decreases at the pumps already running, as well as at the starting pump. Therefore, cavitation can be caused at the pumps already running, as well as the one starting.

The decrease in suction head at the pumps already running means a decrease in flow rate. This decrease in flow also means a decrease in flow at the heat exchangers already operating. Therefore, rapid starting of pumps in the completely-closed system can interfere with power generation in units already running.

To examine the dynamic effect of vertical hull motion on the flow in the completely-closed conduit system, the system was approximated by an inverted U-tube with both legs down in the water and a pump in the upper end of one leg. One leg represented the vertical cold water supply column. The other leg represented the hydraulic equivalent of the heat exchangers and vertical discharge pipes in parallel. The horizontal section between the two legs represented the hydraulic equivalent of the pipes from the supply conduit to the heat exchangers in parallel.

The heave and vertical accelerations for Sea State 6 were incorporated into a sinusoidal variation of hull elevation with time. This variation in elevation was applied to the inverted U-tube representing the system. The nonlinear equations for the fluid motion in the tube with the pump operating were linearized and solved.

The pressures and velocities resulting from Sea State 6 were estimated. At certain times in the hull motion, pressures in conduits can have a maximum value from 16 to 60 psi. Pressures of this magnitude occurred in the top of the condenser on the cold water side. For a mean velocity of 7 fps, at steady state, the mean velocity at Sea State 6 is reduced by about 4 percent to 6.7 fps. The variation in velocity at this sea state is from 6.0 to 7.4 or $\pm$10 percent.

B.1.2.2 Decoupled Closed Conduit System

In one early design, the closed conduit system for cold water is decoupled by disconnecting the conduits at the pumps. Instead of a vertical conduit connected to the pump intake, the vertical conduit is larger than the pump and extends up around it to form an open standpipe. The pump is located inside the standpipe, which serves as the forebay or suction well for the pump. The dynamics of flow in this system were examined for the following situations:

1. Pump startup
2. Vertical hull motion in Sea State 6.

The dynamics of startup in the decoupled system are the same as in the completely-closed system if water-surface elevation in the standpipe is substituted for suction head at the pump. The fall in the water level in the standpipe is equivalent to the decrease in suction head. The occurrence of cavitation and the variation of flow in the heat exchangers are similar for both systems. The problems are avoided in both systems by limiting the rate of increase in pump speed during pump starting. However, the limit is not quite the same for both. The standpipe in the decoupled system holds a larger volume of water than the pump conduit in the completely-closed system. Because of the storage, the drop in water level in the uncoupled system is less than the decrease in suction head in the completely-closed system for the same rate of increase in pump speed. A pump starting the decoupled system can be brought up to full speed in about 10 seconds.

In the decoupled system, the vertical hull motion does not produce the high pressures produced in the completely-closed system. However, the variation in flow through the heat exchanger is much larger. The rise and fall of water surface in the standpipe around the pump is of the same order as the heave of the hull. That is, ± 8 to 10 feet from the mean elevation at Sea State 6. This variation causes a similar variation in head on the pumps. This amount of change in head will change the flow rate pumped by ± 33 percent.

B.1.3 DYNAMICS OF FLOW IN THE OPEN TROUGH SYSTEM

B.1.3.1 Problems Considered

For examination of the dynamics of flow in the open trough system, Design Option A was used. The dynamics were examined for the following items:

1. Pump startup
2. Vertical hull motion (heave)
3. Horizontal hull motion (surge)
4. Rotation about horizontal axes (pitch and roll).

The problems identified in this examination were:

1. Standing waves in the open trough
2. Vertical motion of water surfaces in the trough and on top of the heat exchangers
3. Variation in pump head and rate of flow through heat exchanger.

All of the problems identified were less severe or more easily avoided than the problems associated with the two alternative systems. For this reason, among several others, the open trough system is the alternative selected. The dynamics of this alternative are discussed more fully in the next section.

B.1.3.2 Startup

In the open trough of the cold water system, the dynamic response to pump startup has two aspects analogous to aspects of the two alternative systems. These are the motion of fluid at the vicinity of the starting pump and the effect on other pumps.

In the open trough, the water surface does not drop in the same manner as water level in the standpipe or suction head in the pump conduit. As soon as the water falls at one location in the trough, water from other locations rushes to the first forming a surface wave. Because the depth

and the area of the vertical cross section of the trough are so large, the waves formed by starting one pump are small. If the largest pump anticipated in the design were brought up to speed instantaneously, the resulting surface wave in the trough would have a height of less than 1 foot. Thus, there is no limit on how fast the pumps are brought up to speed.

However, if several pumps were started at the same time and each one brought up to full speed instantaneously, difficulties could occur. Depending on the location of the pumps in the trough, the surface wave formed could be significant. Furthermore, the inertia of the vertical supply conduit limits the rate at which the flow in that conduit can increase. Therefore, instantaneous startup of several pumps simultaneously would remove a significant amount of water from the trough and lower the water level in the trough by 10 feet or more before the inflow from the supply conduit could catch up. Therefore, pumps should be started sequentially with at least 100 seconds between starting successive pumps, but each pump can be started instantaneously.

The startup of the warm water pumps presents no difficulties. The warm water troughs are connected to the open sea through openings in the hull. If these openings are large enough, water rushes into the trough quickly enough to prevent significant fall in water level in the trough. However, the pumps in one trough should be started sequentially.

B.1.3.3 Standing Waves in the Trough

The surge and pitch of the hull can produce standing shallow water waves in the trough. At certain frequencies, the waves are in resonance with the hull motion, and the amplitude increases without limit until the waves break. For the length of trough in Design Option A, the fundamental resonant frequency is about 14 seconds, while it is about 17 seconds for the longer trough in Option B. Without hydraulic model tests or detailed numerical computations, it is difficult to predict the maximum amplitude of the waves in resonance before they break. Based on values of wave steepness, the amplitude of the standing waves could be as great as 7 feet. These amplitudes can occur in relatively calm sea when the frequency of the surge and pitch are suitable for resonance.

The amplitude of the standing waves in resonance can be reduced and controlled by gated walls or bulkheads across the trough. The gates in the walls would be adjustable and controlled as part of operation. Whether two or four walls are required would have to be determined by hydraulic model studies along with other aspects of operation. By opening various gates in the walls, the trough can be detuned and the resonant waves broken up. It is estimated that gated walls can reduce the maximum amplitude of the standing waves to 2 feet.

B.1.3.4 Vertical Motion of Water Surface

The heave of the hull and vertical movement of the open trough cold water system produces vertical motion of the water in the trough relative to the hull. It also produces vertical motion of the water in the top water box of the heat exchanger relative to the top tube sheet. If there were no friction losses in the vertical supply conduit, and the horizontal area of the trough were the same as the cross section area of the conduit, the water column in the conduit would not move in space due to its inertia. The motion of the water relative to the conduit and trough would be exactly equal and opposite to the vertical hull motion. The same would be true in the heat exchangers if the horizontal area of the top water box equalled the cross-sectional area of the discharge conduit and there were no friction losses. Relative to the trough or water box the vertical motion of the water in them would have an amplitude of 21 feet in Sea State 6.

The area ratios and friction losses that actually occur reduce this amplitude significantly. In order to estimate the reduced amplitude, the equations of motion were set up for vertical flow in the supply conduit and trough and in the heat exchanger and discharge conduit. Design Option A and a constant rate of pumping were assumed, and other simplifying assumptions were made. The equations were solved numerically for a limited number of time increments using a hand calculator. From these calculations it was estimated that the amplitude of vertical motion of the water surface in the trough relative to the trough in Sea State 6 is 6 feet. That is, the water surface stays within ± 3 feet of the steady level for a calm sea. For Design Option B, the amplitude would be a little less. In the heat exchanger, the motion of the water surface relative to the tube sheet stays within ± 1 foot of the steady level for a calm sea.

If it is desired to reduce the vertical motion in the trough even further the adjustments of gates in the walls across the trough can be used. More detailed computation or hydraulic model studies would be necessary to determine how much additional reduction is possible.

In the warm water trough the heave doesn't cause vertical motion of the water in the trough relative to the trough. At the surface of the sea, the water surface goes up and down with the hull. However, there is similar motion due to roll. When one side of the hull goes up or down due to roll, the sea goes down or up with respect to the trough. The depth of water in the warm water trough decreases or increases accordingly. For Design Option A, the magnitude of the change is ± 3 feet, which is similar to the motion in the cold water trough. In Design Option B, the change is a little less.

B.1.3.5 Variation in Pump Head and Heat Exchanger Flow

The combination of the vertical motion in the trough and heat exchanger can change the head on the cold water pumps by ± 4 feet in either the cold or warm water system. This change of head causes a change in flow rate of ± 10 to 12 percent.

Since a constant rate of flow was assumed for the computation of vertical motion, the results are in error, but the error is conservative. When the pump head increases, the flow rate decreases, the water level on the heat exchanger falls, and the pump head starts to decrease again. The opposite happens when the pump rate decreases. Therefore, the variation in pump head will tend to decrease the vertical motion that causes the variation.

The variation in pump flow rate and the vertical motion of water in the heat exchanger and discharge conduit produce a total variation in flow rate through the heat exchanger. The conservative assumption is that the maximum change due to pump flow rate occurs with the maximum due to vertical motion. This would cause the flow rate to vary by 20 to 30 percent.

THIS PAGE

WAS INTENTIONALLY

LEFT BLANK

APPENDIX B.2

COMPLETELY CLOSED CONDUIT SYSTEMS

B.2. COMPLETELY CLOSED CONDUIT SYSTEMS

B.2.1 BASIC FEATURES AND SIMPLIFIED REPRESENTATION

B.2.1.1 Design Features Considered

Figure 1 shows an elevation and side view of the design of a cold water distribution system used as an example of a completely closed conduit system. Cold water passes through the vertical supply conduit and the lateral conduit to the pump conduit where the pump causes an increase in pressure. The motion through these three conduits is caused by the total head at the suction side of the pump being below mean sea level. The total head at the discharge side of the pump is above sea level and forces the flow through the pump discharge conduit, heat exchanger, and vertical discharge conduit. The complete path from cold water intake to discharge is closed conduit with no openings to the atmosphere.

Figure 2 shows the warm water system used as an example of a completely closed system. Warm water passes from the trough through the pump conduit, pump discharge conduit, heat exchanger and vertical discharge conduit. Although the conduit system is simpler, it is still completely closed from intake to discharge.

B.2.1.2 Simplified Representation

For analysis of certain problems, the completely closed conduit system can be approximated by an inverted U-tube as shown in Figure 3 for the cold water system. The longer vertical leg, 1, represents the vertical cold water supply column. The horizontal section, 2, represents the hydraulic equivalent of most of the conduits between the supply conduit and the heat exchanger, while the shorter vertical leg, 3, represents the hydraulic equivalent of all of the heat exchangers and vertical discharge columns. For convenience, the equivalent of the pumps is placed near the top of the longer leg, but it could be placed almost anywhere in the U-tube. The length of a leg is represented by L and the cross-section area by A as shown.

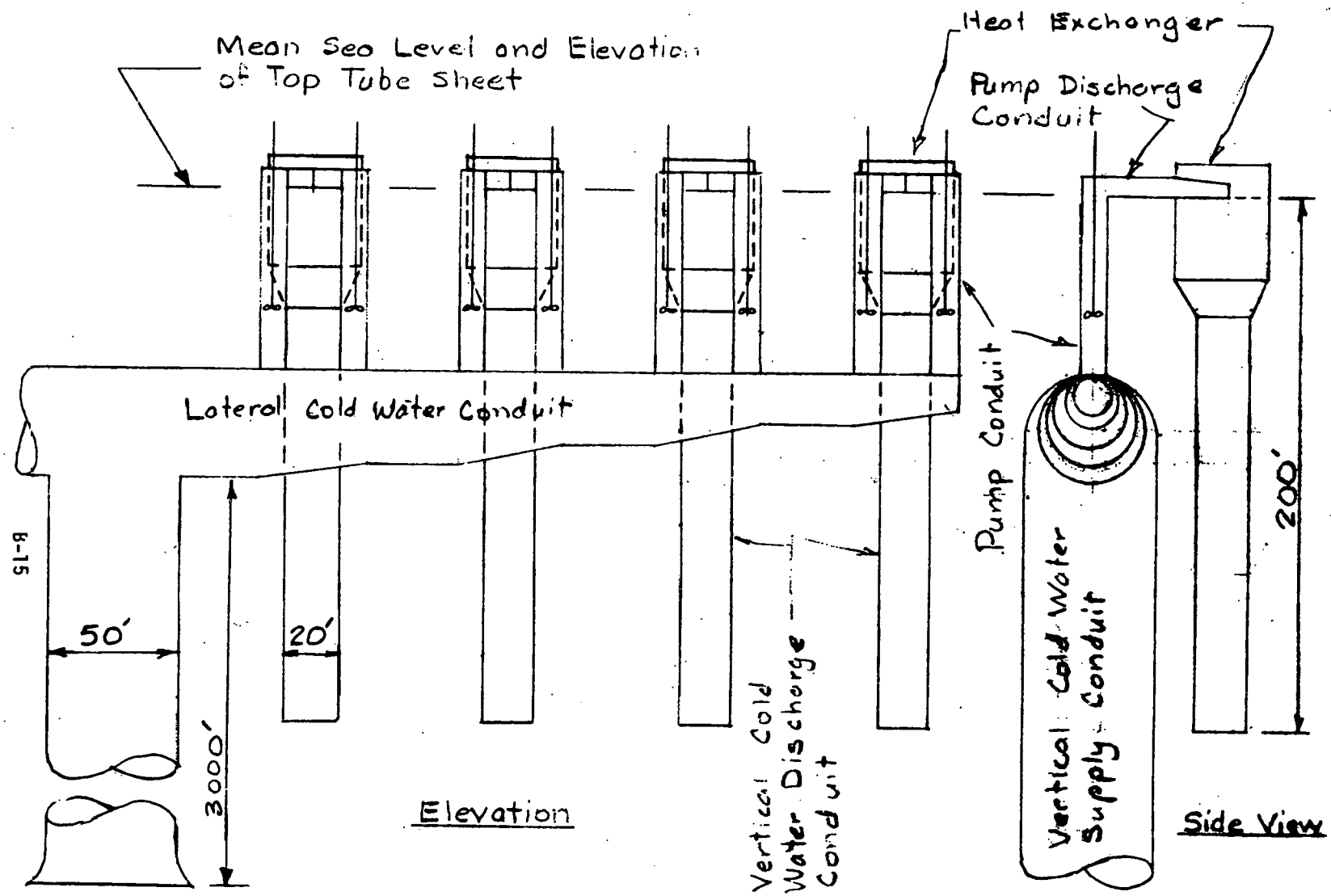

Fig. 1 Cold Water Distribution, Completely Closed Conduit

Scale 1"=50'

BY _____ DATE 2-6-77 SUBJECT _____
CHKD. BY _____ DATE _____
JOB NO. _____ SHEET NO. 2-2 OF _____

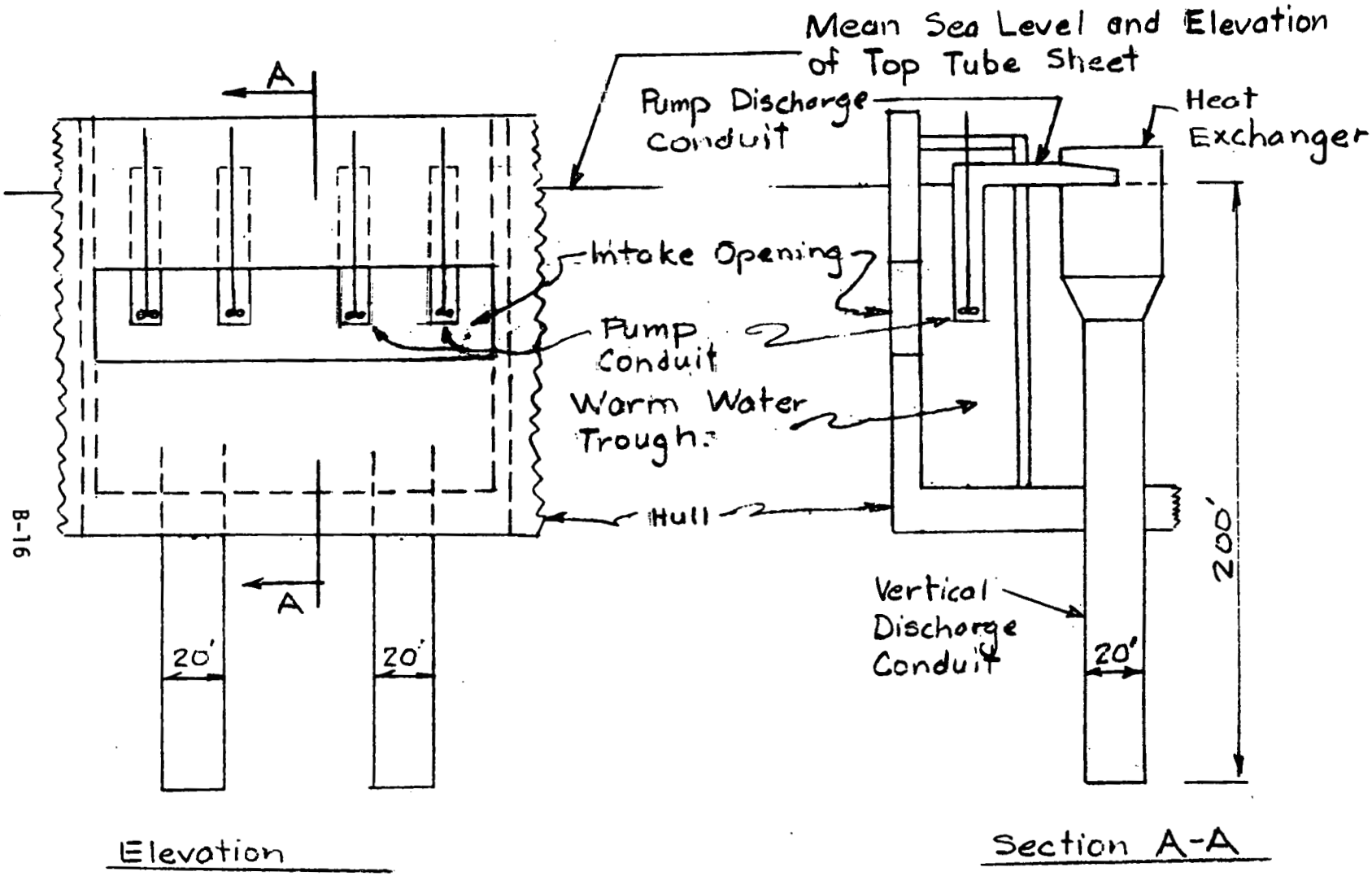

Fig 2 Warm Water Distribution

Scale 1"=50'

BY _____ DATE 27 XII 77 SUBJECT _____
CHKD. BY _____ DATE _____
SHEET NO. 2-4 OF _____
JOB NO. _____

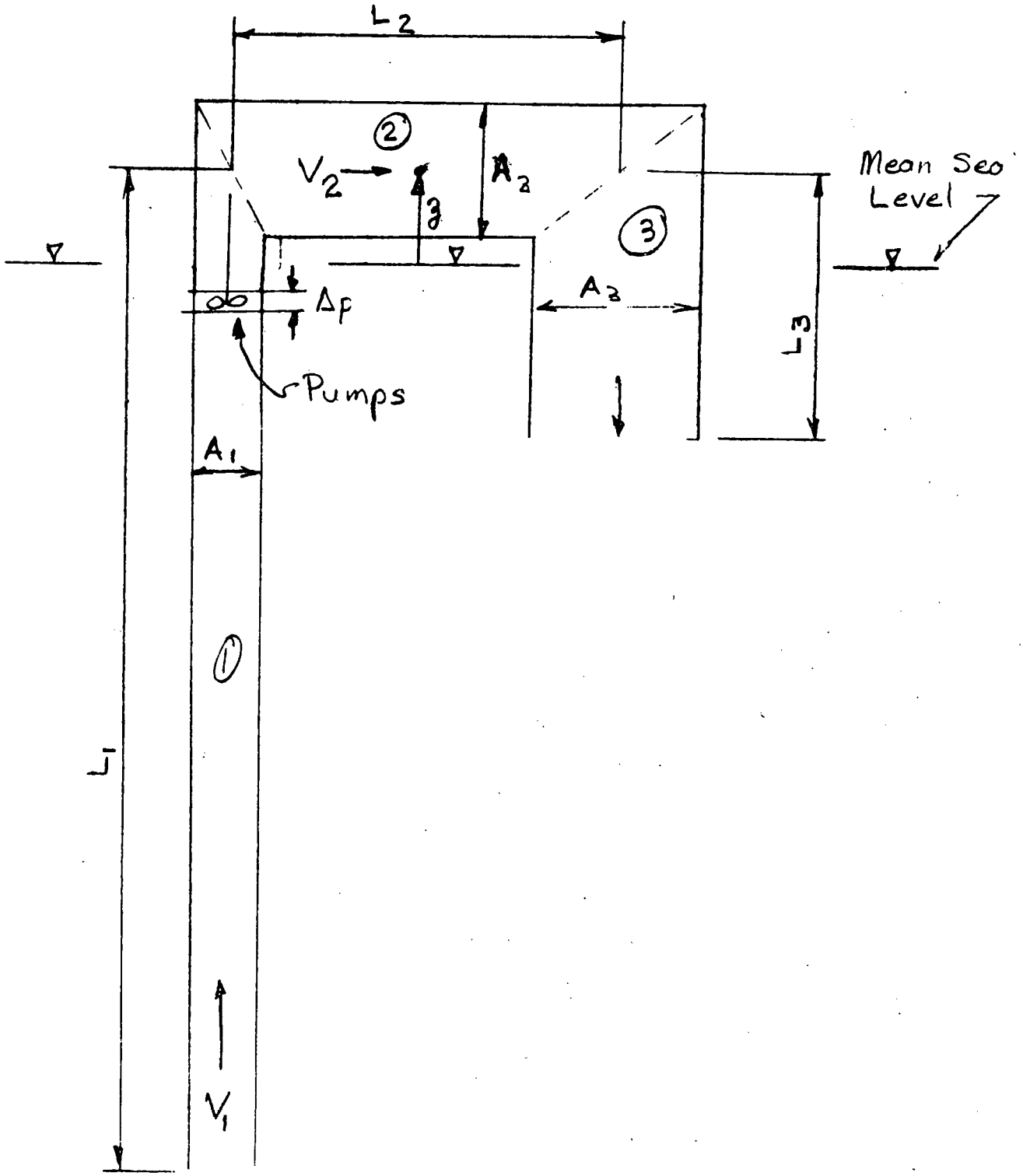

Fig. 3 Inverted U-tube as Approximation of Completely Closed Control System

B.2.2 STARTUP

B.2.2.1 General

In startup, the system with completely closed conduits is similar to one with decoupled conduits. Before a unit is started up the surface of the water in the pump conduits and heat exchanger must be at or near mean sea level, and there must be empty space in the top of the pump discharge conduit and the heat exchanger. The unit is not closed until the space is filled with water.

B.2.2.2 Starting One Cold Water Pump With All Units Off

When all units are off, water is standing in the pump conduits with the water surface near mean sea level as just described. In the heat exchanger there is little or no water above the top tube sheet. When the pump starts, therefore, it will be pumping against less head than at normal operation. As a result, the flow rate will be greater than normal operation.

On the suction side of the starting pump the piezometric head is below mean sea level. A pressure gradient is created in the lateral conduit because the water level in other pump conduits is still at or near sea level. Therefore, water in the lateral conduit begins to flow toward the pump conduit where the pump is being started. Because of the inertia of the water in the long vertical supply conduit, that conduit does not supply water to flow in the lateral conduit. As a result, water flows from other pump conduits to the conduit of the pump being started. This causes the water in all pump conduits to be drawn down.

Figure 4 shows the pattern of water surface elevations in pump conduits and flow in the lateral conduit a short time after starting the first pump with all others off. The line drawn through water surfaces in the pump conduits is the hydraulic grade line along the lateral conduit. Where the hydraulic grade line passes over the top of the vertical supply column, the difference between the line and mean sea level is the head available to accelerate flow in the column. Therefore, the acceleration in the column cannot be significant until the water surfaces in all the

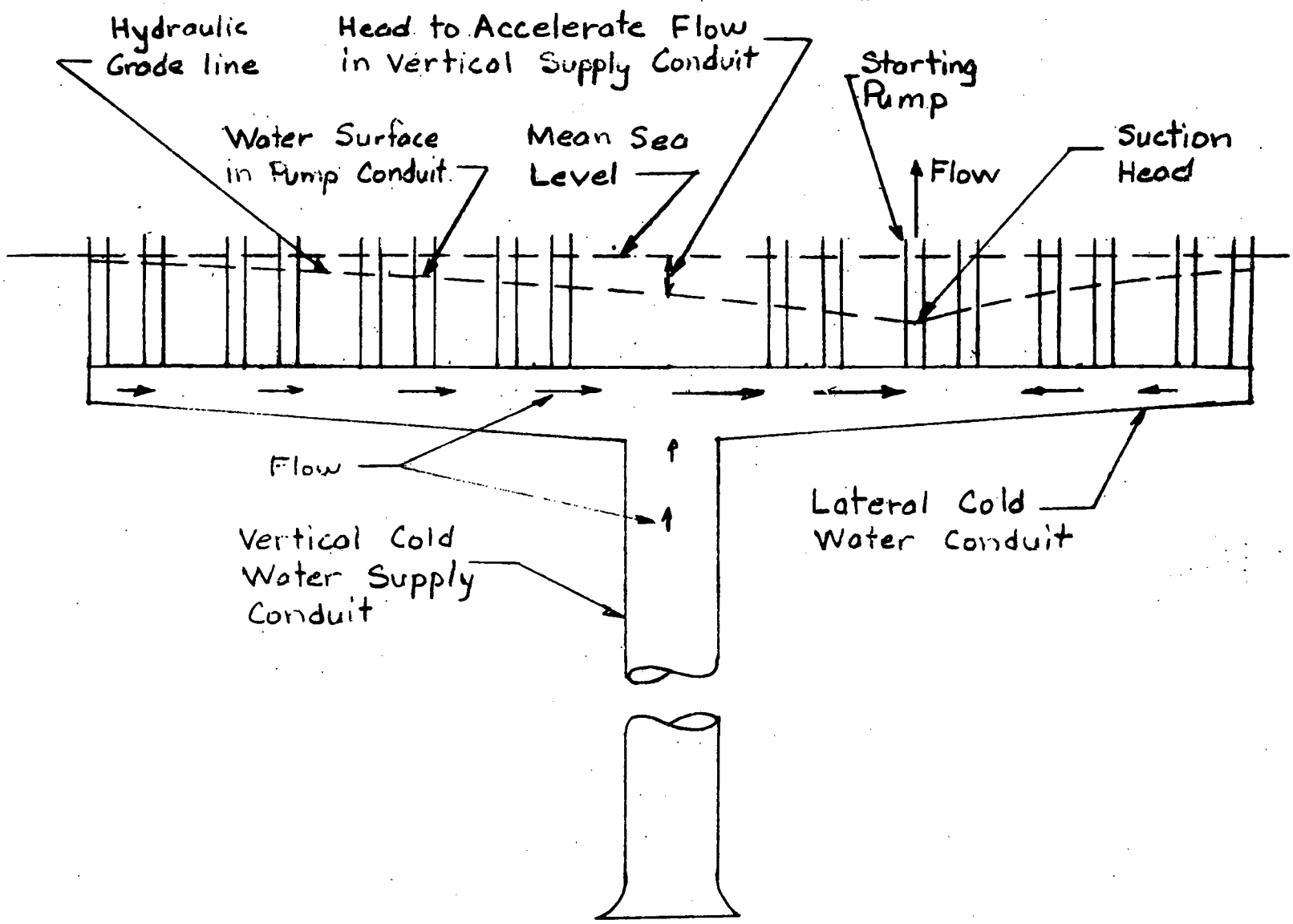

Fig. 4 Hydraulic Grade Line and Flow Shortly After Starting First Pump

BY_____ DATE_____
CHKD. BY_____ DATE_____
SUBJECT_____
SHEET NO. 2-11 OF_____
JOB NO._____

pump conduits are low enough to have a low hydraulic grade line. By then the suction head in the conduit of the pump being started will be low enough for the pump to cavitate.

The drop in suction head and hydraulic grade line is part transient and part steady state. Right after the pump starts, most of the difference between mean sea level and the hydraulic grade line corresponds to acceleration of flow. This part is the transient. At stady state, the flow rate in the vertical column is equal to the rate of pumping, and the difference between mean sea level and the hydraulic grade line corresponds to friction losses. At some time during the transient, the hydraulic grade line drops to a level much lower than that corresponding to steady state. It is at these greatest values of draw down that cavitation is most likely. The cavitation could last several minutes.

B.2.2.3 Approximate Analysis for Starting First Pump

If the shape of the hydraulic grade line in Figure 4 can be assumed, it is possible to develop an approximate analysis of the flow resulting from starting the first pump. With such an assumption, the volume of water withdrawn from the pump columns can be related to the elevation of the hydraulic grade line above the top of the cold water supply conduit. A possible assumption is shown in Figure 5. The example represented is for the pump that experiences the greatest drop in suction head. It was selected because it is conservative and because the analysis will serve for startup of other pumps as well as the first.

The pump shown is the one furthest from the vertical supply conduit. Because it is the first pump, the friction losses in the lateral supply conduit are low enough to cause negligible slope in the hydraulic grade line even when the rate of flow at the pump is up to full value. The slope of the hydraulic grade line is caused primarily by acceleration of flow in the lateral supply conduit. Between the vertical supply conduit and the starting pump the grade line is linear with a constant slope. Rough estimates can be made for the drop in the grade line between vertical conduit and the starting pump. Based on the diameters and length of the vertical and horizontal conduits, it is estimated that the drop in the

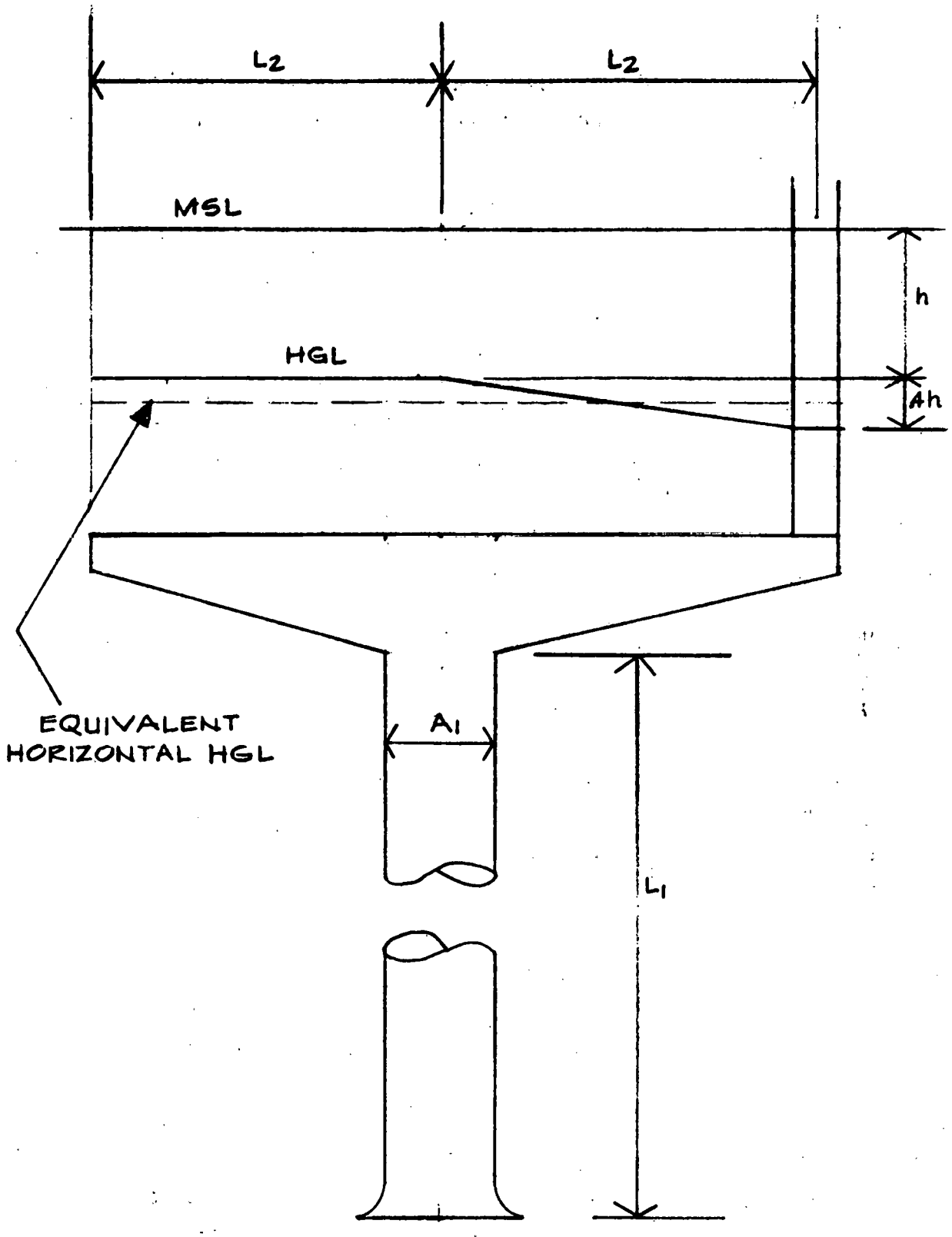

FIG. 5. HYDRAULIC GRADE LINE FIRST PUMP STARTING IN THE COMPLETELY CLOSED SYSTEM

grade line is about 40 percent of the difference between mean sea level and the hydraulic grade line above the vertical conduit. Letting the difference be h, the drop is 0.4h. On the opposite side of the vertical conduit, the acceleration in the lateral conduit is assumed to be negligible, and the hydraulic grade is assumed to be straight and horizontal.

With this assumed grade line, the change in average water-surface elevation in the pump conduits is 1.1dh when the change in h is dh. The corresponding change in total volume in the pump conduits is the product of the average change and the total horizontal area of water surface in these conduits. The water surface moves in 15 of the 16 pumps. Only the suction head changes in the starting pump. For 15 conduits, each with a diameter of 10 feet, the change in volume is $1.1(15)25\pi dh$ or $412.5\pi dh$ ft^3.

The rate of change in h is equal to the difference between the rate of flow into the pump conduits and the rate of flow out of them. The former is equal to the rate of flow, Q_1, in the pump conduit while the latter is equal to the rate of pumped flow, Q_p. Thus the continuity equation for the sum of the pump conduits is

$$Q_1 - Q_p = 412.5\pi\frac{dh}{dt} \tag{1}$$

in which t is the time in seconds.

The difference, h, is the head available to change the flow rate, Q_1, in the vertical conduit. Let h be positive when the hydraulic grade line is above mean sea level and Q_1 be positive when the flow in the conduit is up. For this convention, the momentum equation for flow in the conduit is

$$-h - \Delta h_s - \frac{V_1|V_1|}{2g} - \Delta H_f = \frac{L_1}{g}\frac{dV_1}{dt} = \frac{L_1}{gA_1}\frac{dQ_1}{dt} \tag{2}$$

in which

Δh_s = static head due to difference between the water temperature inside the conduit and in the surrounding water outside

V_1 = flow velocity in the vertical supply conduit

ΔH_f = head losses due to friction

L_1 = length of vertical supply conduit

A_1 = cross section area of vertical supply conduit

g = acceleration due to gravity.

Some terms in the equation can be dropped. For the first pump starting, the flow is a small percentage of the total flow for all pumps. In addition, the water inside the vertical conduit has not been displaced by colder water. Therefore, the terms Δh_s, ΔH_f, and $V_1|V_1|/2g$ are negligible. The equation becomes

$$-h = \frac{L_1}{gA_1}\frac{dQ_1}{dt} \tag{3}$$

The continuity equation can be differentiated and substituted into the momentum equation to give

$$-h = \frac{L_1}{gA_1}(412.5\pi\frac{d^2h}{dt^2} + \frac{dQ_p}{dt}) \tag{4}$$

The derivative, dQ_p/dt, indicates the effect of the rate of starting the pump. For simplicity assume that the method of starting the pump produces a linear rate of increase in Q_p. That is

$$Q_p = qt \tag{5}$$

The differential equation then becomes

$$\frac{L_1}{gA_1}412.5\pi\frac{d^2h}{dt^2} + h = -\frac{L_1}{gA_1}q \tag{6}$$

The coefficients in this equation can be evaluated from the following data

L_1 = 3000 feet

$A_1 = (50)^2\pi/4 = 625\pi ft^2$

The equation becomes

$$61.49\frac{d^2h}{dt^2} + h = -0.0474q \tag{7}$$

For the initial conditions

$h = dh/dt = 0 \qquad @\ t = 0$

the solution is

$$h = -0.0474q\left(1 - \cos\frac{t}{7.842}\right) \tag{8}$$

The fundamental period of the motion is 49.27 seconds. If the linear increase in Q_p continues long enough the minimum value of h occurs at 24.64 seconds.

This solution is valid until the pump reaches full speed. The following table shows the values of h and dh/dt when the pump reaches full flow rate in various times.

Startup Time In Seconds	q Ft^3/Sec^2	h (Feet)	dh/dt
1	860.000	-0.331	-0.661
5	172.000	-1.602	-0.619
10	86.000	-2.889	-0.497
15	57.330	-3.629	-0.326
20	43.000	-3.730	-0.141
25	34.400	-3.261*	
30	28.667	-2.718*	

As a first approximation, assume that Q_p is constant after the pump reaches full speed. The differential equation of h becomes

$$61.49\frac{d^2h}{dt^2} + h = 0 \tag{9}$$

The initial conditions for this equation are the values, h_o and dh_o/dt, at the time, t_o, when the pump reaches full flow rate. These conditions are the values in the above table. The solution of the equation is

*Minimum h occurs when $t/7.842 = \pi$ or $t = 24.64$ seconds.

$$h = 7.842 \frac{dh_o}{dt} \sin \frac{(t-t_o)}{7.842} + h_o \cos \frac{(t-t_o)}{7.842} \quad (10)$$

The lowest point occurs when dh/dt is zero, that is

$$\frac{dh}{dt} = \frac{dh_o}{dt} \cos \frac{(t-t_o)}{7.842} - \frac{h_o}{7.842} \sin \frac{(t-t_o)}{7.842} = 0 \quad (11)$$

$$\tan \frac{(t-t_o)}{7.842} = \frac{7.842}{h_o} \frac{dh_o}{dt} \quad (12)$$

The following table gives the minimum values of h based on h_o and dh_o/dt from the table above.

Startup Time t_o (seconds)	$\frac{7.842}{h_o} \frac{dh_o}{dt}$	Time to Minimum h		Minimum h (feet)
		$t-t_o$ (seconds)	t (seconds)	
1	15.684	11.819	12.82	-5.190
5	3.030	9.818	14.82	-5.110
10	1.349	7.316	17.32	-4.851
15	0.704	4.813	19.81	-4.439
20	0.296	2.260	22.26	-3.890
25			24.64	-3.261
30			24.64	-2.781

The minimum h is the maximum drop in suction head at the starting pump. This approximate analysis shows that the maximum does not decrease significantly until the startup time, t_o, approaches half of the fundamental period of the motion. The fundamental period decreases with the cross section area of the pump conduits. Thus, the pumps can be started faster with smaller conduits than with larger ones.

This result is true only for the first one or two pumps. For these, the value of V_1 is small and the terms $V_1^2/2g$ and $\Delta H_{f,1}$ are negligible. Without these terms in the equation, the amplitude of the motion is independent of the horizontal cross section area of storage. A larger area slows down the response of the flow in the vertical conduit without any decrease of the amplitude.

If the diameter of the pump conduits is reduced from 10 feet to 8 feet the fundamental period is reduced to 39.4 seconds. A startup time of 20 seconds would produce the minimum values of maximum drop in suction. Since there is a limit to how small the column can be made, it is unlikely that the startup time can be less than 15 seconds for safe values of minimum h. However, smaller conduits are not beneficial for starting other pumps after the first one or two. As the values of $V_1^2/2g$ and $\Delta H_{f,1}$ become significant, larger conduits reduce the minimum value of h. Therefore, it is better to plan to start the first pump or two more slowly and let them take 25 or 30 seconds to reach full flow rate.

B.2.2.4 Starting One Cold Water Pump With Other Units On

Starting a pump with others already running is similar to starting the first pump. Just before this latest pump starts the water levels or suction heads in the pump conduits all lie on some hydraulic grade line corresponding to flow to the pumps already running. If only one pump is already running, the grade line would look something like that in Figure 4 or 5. When the latest pump starts, its suction head is lowered until the hydraulic grade line is altered enough to cause water to flow to the pump. The inertia of the flow in the vertical cold water conduit causes the flow to respond slowly to the increase corresponding to the latest pump. Therefore, flow to the latest pump comes from reduction in flow to the pumps already running until the flow in the vertical column increases.

As was shown in Figure 4, the whole grade line must be lowered to accelerate flow in the vertical conduit. Thus startup of the latest pump lowers its own suction head and the suction head at all pumps already running. Cavitation can be caused at the latest pump and may be caused at some of the running pumps. Also, the flow rate of all of the running pumps is affected.

The situation changes as the number of pumps already running is increased. The location of the grade line before the latest pump starts is lower when more pumps are running. Therefore, the suction head is already lower at the beginning of the transient caused by starting the latest pump. On the other hand, the terms, $V_1^2/2g$ and $\Delta H_{f,1}$, in the

momentum are significant and reduce the amplitude of the transient. The suction head at the lowest point in the transient is not as far below the value at the beginning of the transient. Also, with less storage effects in the pump conduits, the period of the transient is shorter.

For this stage of the work, it is not feasible to obtain numerical estimates of these changes. The analysis of starting pumps after the first cannot be approximated as easily as for the first pumps. The pump conduits with pumps already running do not provide simple storage. The analysis of the change in flow at these pumps involves the characteristic curves of the pump and the inertia of the pump and motor as well as the momentum of flow in the conduits.

Short of adequate computation, it appears that the reduction in amplitude and period of the transient is a larger effect than the lower hydraulic grade line at the beginning of the transient. After the first one or two pumps, therefore, the time for each pump to reach full flow rate can probably be reduced to 15 seconds. At most, it will be 25 or 30 seconds.

B.2.3 VERTICAL HULL MOTION

B.2.3.1 Sinusoidal Approximation of Hull Motion

Assume that the elevation, z, of the hull above mean sea level can be represented by

$$z = z^* \sin \Omega t \qquad (13)$$

in which

z^* = maximum value of z

Ω = frequency in radians per second

By differentiation the acceleration of the hull is

$$\frac{d^2z}{dt^2} = -\Omega^2 z^* \sin \Omega t \qquad (14)$$

The values of Ω and z^* can be estimated for Sea State 6. The heave of 21.4 feet can be represented by $2z^*$. That is

$$z^* = 10.7 \text{ feet}$$

The maximum acceleration is 0.05g. Therefore

$$\Omega^2 z^* = 0.05g$$

$$\Omega = \left[\frac{0.05(32.2)}{10.7}\right]^{1/2} = 0.388 \text{ radians/sec}$$

The frequency in cycles per second is $0.39/2\pi$ or 0.062 and the period is 16.11 seconds. The equation for z is

$$z = 10.7 \sin 0.388\ t$$

B.2.3.2 Equations for Simplified Representation

The simplified representation of the completely closed system as an inverted U-tube is described in Article 2.1b. This simplification is used to estimate the effect of vertical hull motion on the flow in the completely closed cold water system.

To set up the equations of motion for the flow the following variables and terms are needed:

h_o = hydraulic or piezometric head just outside of entrance to the vertical cold water supply conduit

= depth of entrance of column below mean sea level (negative value because below mean sea level)

$\Delta H_{u,1}$ = head loss at entrance to vertical supply conduit

γ = unit weight of water in the conduits

$\Delta H_{f,1}$ = friction loss in vertical supply conduit

Δp = increase in pressure from suction to discharge side of pump

$\Delta H_{f,2}$ = friction loss in lateral supply and pump conduits

V_2 = velocity in the equivalent to lateral supply and pump conduits

L_2 = length of the equivalent to lateral

V_3 = velocity in the equivalent of condenser and cold water discharge

L_3 = length of condenser and cold water discharge

$\Delta H_{f,3}$ = friction loss in condenser and cold water discharge

$\Delta H_{d,3}$ = head loss and exit loss at outlet of cold water discharge

$\Delta h_{s,2}$ = static head in vertical cold water discharge conduit

Other variables have already been defined in preceding articles.

The momentum equation for the equivalent U-tube is

$$\Delta H_{u,1} + \Delta H_{f,1} - \frac{\Delta p}{\gamma} + \Delta h_{s,1} + \frac{L_1}{g}\frac{dV_1}{dt} + \Delta H_{f,2} + \frac{L_2}{g}\frac{dV_2}{dt} + \Delta H_{f,3} - \Delta h_{s,3} + \Delta H_{d,3} + \frac{L_3}{g}\frac{dV_3}{dt} = 0 \tag{15}$$

The losses are given by

$$\left.\begin{aligned} \Delta H_{u,1} &= C_1 V_1^2/2g \\ \Delta H_{d,3} &= (1+C_3)V_3^2/2g \\ \Delta H_{f,1} &= \frac{f_1 L_1}{2gD_1}(V_1 - \frac{dz}{dt})^2 \\ \Delta H_{f,2} &= \frac{f_2 L_2}{2gD_2} V_2^2 \\ \Delta H_{f,3} &= \frac{f_3 L_3}{2gD_3}(V_3 + \frac{dz}{dt})^2 \end{aligned}\right\} \tag{16}$$

In the expressions for friction loss, f is the friction factor. In the expressions for entrance and exit losses, assume

$$C_1 = C_2 = 0$$

For the given design, the static heads are approximated by

$$\Delta h_{s,1} = 3.0$$

$$\Delta h_{s,2} = 0$$

The continuity equations for the equivalent U-tube are:

$$(V_1 - \frac{dz}{dt})A_1 = V_2 A_2 = (V_3 + \frac{dz}{dt})A_3 \tag{17}$$

These lead to

$$V_2 = \frac{A_1}{A_2} V_1 - \frac{A_1}{A_2}\frac{dz}{dt} \tag{18}$$

$$V_3 = \frac{A_1}{A_3} V_1 - (\frac{A_1 + A_3}{A_3})\frac{dz}{dt} \tag{19}$$

Substitution of the continuity equation into the momentum equation leads to

$$\Delta H_{f,1} + \Delta H_{f,2} + \Delta H_{f,3} + 3 - \Delta p/\gamma + \left(\frac{A_1}{A_3}\right)^2 \frac{V_1^2}{2g} + \left(\frac{L_1}{g} + \frac{A_1}{A_2}\frac{L_2}{g} + \frac{A_1}{A_3}\frac{L_2}{g}\right)\frac{dV_1}{dt}$$

$$= \left[\frac{A_1}{A_2}\frac{L_2}{g} + \left(\frac{A_1 + A_3}{A_3}\right)\frac{L_3}{g}\right]\frac{d^2z}{dt^2} + \frac{1}{g}\frac{A_1}{A_3}\left(\frac{A_1 + A_3}{A_3}\right)V_1\frac{dz}{dt} - \frac{1}{2g}\left(\frac{A_1 + A_3}{A_3}\right)^2\left(\frac{dz}{dt}\right)^2 \quad (20)$$

The friction losses are given by

$$\Delta H_{f,1} + \Delta H_{f,2} + \Delta H_{f,3} = \left[\frac{f_1 L_1}{2gD_1} + \left(\frac{A_1}{A_2}\right)^2\frac{f_2 L_2}{2gD_2} + \left(\frac{A_1}{A_3}\right)^2\frac{f_3 L_3}{2gD_3}\right]\left(V_1 - \frac{dz}{dt}\right) \quad (21)$$

In order to provide a simple approximation, assume that the total area of conduits in parallel, equivalent to conduits 2 and 3 of the U-tube, is each equal to the area of conduit 1. That is

$$A_1 = A_2 = A_3 \quad (22)$$

With this approximation the equation is simplified to

$$\left(1 + \Sigma\frac{fL}{D}\right)\frac{V_1^2}{2g} + 3 + \frac{1}{g}\Sigma L\frac{dV_1}{dt} = \frac{\Delta p}{\gamma} + \frac{V_1}{g}\left(2 + \Sigma\frac{fL}{D}\right)\frac{dz}{dt} - \frac{1}{2g}\left(4 + \Sigma\frac{fL}{D}\right)\left(\frac{dz}{dt}\right)^2 + \frac{1}{g}(L_2 + 2L_3)\frac{d^2z}{dt^2} \quad (23)$$

in which

$$\Sigma\frac{fL}{D} = \frac{f_1 L_1}{D_1} + \frac{f_2 L_2}{D_2} + \frac{f_3 L_3}{D_3} \quad (24)$$

and

$$\Sigma L = L_1 + L_2 + L_3 \quad (25)$$

To linearize the equation, the term V_1^2 is replaced by $|V_1|V_1$ with $|V_1|$ equal to a constant. The constant absolute value was made equal to 7 ft/sec which is the steady value for no vertical hull motion. This value is also used in the coefficient of dz/dt.

The friction losses are based on the average diameters and lengths of the conduits. The data used are given in the following table.

Conduit	L Feet	D Feet	f
1	3000	50	0.010
2	150	20	0.013
3	200	20	

In order to make the head loss through the heat exchanger and discharge tube equal to the design value for no vertical hull motion, it is necessary to have

$$\frac{f_3 L_3}{D_3} = 10.803$$

With these values

$$\Sigma \frac{fL}{D} = 11.5$$

Additional friction loss was added to this value to allow for bends and changes in diameter not included in the value of f_3L_3/D_3. With the additional losses

$$\Sigma \frac{fL}{D} = 13.6$$

The value of ΣL is obtained from the lengths in the table for friction factors. That is

$$\Sigma L = 3350 \text{ feet}$$

The derivatives of hull motion are given by

$$\frac{dz}{dt} = 4.152 \cos 0.388t \qquad (26)$$

$$\frac{d^2z}{dt^2} = -1.61 \sin 0.388t$$

$$\left(\frac{dz}{dt}\right)^2 = 8.62\ (1 + \cos 0.776t)$$

With the preceding numerical values and assumptions, the final linearized equation becomes

$$104.04 \frac{dV_1}{dt} + 1.59\ V_1 = \frac{\Delta p}{62.4} - 27.50\sin 0.388t + 14.08\cos 0.388t - 2.36\cos 0.776t - 5.36 \tag{27}$$

2.3.3 Linear Approximation For Pump Curve

To obtain an expression for $\Delta p/\gamma$, it is assumed that the pump curve is linear in the range of values of Q_1 anticipated in the vertical motion. The linear expression for the curve is

$$\frac{\Delta p}{\gamma} = h_o - (Q_1 - \bar{Q}_1) \frac{dh}{dQ_1} \tag{28}$$

The value of $\bar{Q}_1$ corresponds to a value of 7 ft/sec for $|V_1|$. This expression can also be written

$$\frac{\Delta p}{\gamma} = h_o - (V_1 - 7) \frac{dh}{dV_1} \tag{29}$$

From the pump curves supplied by TRW

$$\frac{\Delta p}{\gamma} = 14.11 - 7.42\ (V_1 - 7) \tag{30}$$

When this expression is substituted in the momentum equation, the resulting equation is

$$104.04 \frac{dV_1}{dt} + 9.01\ V_1 = 60.69 - 27.50\sin 0.388t + 14.08\cos 0.388t - 2.36\cos 0.776t \tag{31}$$

or

$$\frac{dV_1}{dt} + 0.0866\ V_1 = 0.584 - 0.264\sin 0.388t + 0.135\cos 0.388t - 0.0227\cos 0.776t \tag{32}$$

B.2.3.4 Variation in Flow Rate

This equation can be solved directly for V_1. It is in the form

$$\frac{dV_1}{dt} + PV_1 = Q(t) \tag{33}$$

The solution

$$V_1(t) = Ce^{-\int Pdt} + e^{-\int Pdt} \int e^{\int Pdt} Q(t)dt \tag{34}$$

To evaluate the solution

$$\int Pdt = 0.866t$$

$$\int e^{0.866t} Q(t)dt = 6.738\, e^{0.866t} - 0.639\, e^{0.866t} (0.2232 \sin 0.388t - \cos 0.388t) + 0.332\, e^{0.0866t} (\sin 0.388t + 0.2232 \cos 0.388t) - 0.0289\, e^{0.866t} (0.112 \cos 0.776t + \sin 0.776t) \tag{35}$$

$$V_1(t) = Ce^{-0.0866t} + 6.738 + 0.189 \sin 0.388t + 0.713 \cos 0.388t - 0.0289 \sin 0.776t - 0.00324 \cos 0.776t \tag{36}$$

If

$$V_1 = 7 \text{ @ } t = 0$$

then

$$7 = C + 6.738 + 0.713 - 0.00324$$

$$C = 7 - 7.448 = -0.448$$

Therefore,

$$V_1(t) = -0.448\, e^{-0.0866t} + 6.738 + 0.189 \sin 0.388t + 0.713 \cos 0.388t - 0.0289 \sin 0.776t - 0.00324 \cos 0.776t \tag{37}$$

To find the range of velocity variation at steady state, try various points in the cycle of hull motion for $t = \infty$.

$\sin 0.388t = 1$:

$$V_1 = 6.738 + 0.189 + 0.00324 = 6.93 \text{ ft/sec}$$

$\cos 0.388t = -1$:

$$V_1 = 6.738 - 0.713 + 0.00324 = 6.03 \text{ ft/sec}$$

$\sin 0.388t = -1$:

$$V_1 = 6.738 - 0.189 + 0.00324 = 6.55 \text{ ft/sec}$$

$\cos 0.388t = 1$:

$$V = 6.738 + 0.713 + 0.00324 = 7.454 \text{ ft/sec}$$

The range of velocity is approximately 7.454 - 6.03 = 1.42 ft/sec with a mean value of 6.74 ft/sec. This variation is +0.71/6.74 = +10.5 percent. It is also the variation in flow rate.

B.2.3.5 Maximum Pressures

The pressure at the top of the longer leg of the inverted U-tube corresponds to the pressure at the top of the vertical supply conduit, while the pressure at the top of the shorter leg corresponds to the pressure in the top water box of the heat exchanger. These pressures vary during the cycle of vertical hull motion as required to accelerate or decelerate the flow in the conduits. They are related to dV_1/dt by the momentum euqation.

From the solution V(t) in the preceding section,

$$\frac{dV_1}{dt} = 0.040\, e^{-0.0866t} + 0.073\cos 0.388t - 0.277\sin 0.388t - 0.022\cos 0.776t + 0.00251\sin 0.776t \qquad (38)$$

The range of values of this derivation can be determined by evaluating it for different times during the cycle of hull motion. For steady state the exponential term is zero.

$\cos 0.388t = 1$:

$$\frac{dV_1}{dt} = 0.073 - 0.022 = 0.051$$

$\sin 0.388t = 1$:

$$\frac{dV_1}{dt} = -0.277 - 0.022 = -0.299$$

$\cos 0.388t = -1$

$$\frac{dV_1}{dt} = -0.073 - 0.022 = -0.095$$

$\sin 0.388t = -1$

$$\frac{dV_1}{dt} = 0.277 + 0.022 = 0.299$$

At the top of the vertical supply conduit, the head associated with the acceleration is given by

$$h + z = -\frac{3000}{32.2}\frac{dV_1}{dt}$$

At the maximum values of acceleration

$z = 10.7$ ft;

$h = 27.86 - 10.7 = 17.16$ ft

$p = 7.44$ psi

$z = -10.7$ ft

$h = -27.86 + 10.7 = -17.16$ ft

$p = -7.44$ psi

These accelerations and associated pressures are based on the assumption that

$$A_1 = A_2 = A_3$$

If A_2 and A_3 are smaller than A_1, the accelerations and pressures are increased in magnitude. The pressures could be as high as 10 psi or as low as -10 psi.

The pressures due to acceleration, must be added to the pressure created by the pumps for overcoming friction. At some locations between the pump discharge and the heat exchanger, this pressure is 4 to 6 psi. At the top of the vertical hull motion the pressures from acceleration and pumping add total from 14 to 16 psi. At the bottom of the motion, the sum of the two is negative with values between -6 and -4 psi.

These pressures all assume no malfunction of the pumps or closure of valves that might restrict the flow in conduits. Suppose that it is attempted to operate valves and pump speed to maintain a constant flow rate with respect to the conduits. The acceleration of the flow would equal the acceleration of the hull. The pressures associated with these accelerations would be of the order of 60 psi.

The actual pressures lie somewhere between the ultimate value of 60 psi and the value of 14 to 16 psi given above. To estimate them more accurately, it is necessary to consider the control and inertia of the pump and motor.

APPENDIX B.3

DECOUPLED CLOSED CONDUIT SYSTEM

B.3. DECOUPLED CLOSED CONDUIT SYSTEM

B.3.1 BASIC FEATURES

In one early design, the closed conduit system for cold water supply is decoupled by disconnecting the conduits at the pumps. The design is shown in Figure 6. Instead of a vertical conduit connected to the pump intake the vertical conduit is larger than the pump and extends up around it to form an open standpipe. The pump is located inside the standpipe, which serves as the forebay or suction well for the pump. All design features except for the open standpipe are the same as shown in Figure 1 for the completely closed sytem.

B.3.2 DYNAMICS OF FLOW

B.3.2.1 Pump Startup

The dynamics of conduit flow resulting from starting pumps is similar to that described in Subsection 2.2 for the completely closed system. For the decoupled system, the hydraulic grade line in Figure 4 is always defined by the water surface in the standpipes instead of a combination of pump suction head at the pumps running and water surface at those not running. The flow to the latest starting pump comes from storage in the standpipes until the flow rate in the vertical supply column is increased to provide for the latest pump.

The approximations and equations used for the completely closed system in Subsection 2.2 can be used for very rough estimates. As shown in that subsection, the drawdown for starting the first one or two pumps is not decreased significantly unless the time for the pump to reach full flow rate is approximately 1/2 the fundamental period of the motion.

In that subsection it was also shown that the fundamental period depends upon the horizontal cross-section area of the water stored in the pump conduits. For the decoupled system, the period depends upon the horizontal cross-section of the annular space between the pump casing and the standpipe.

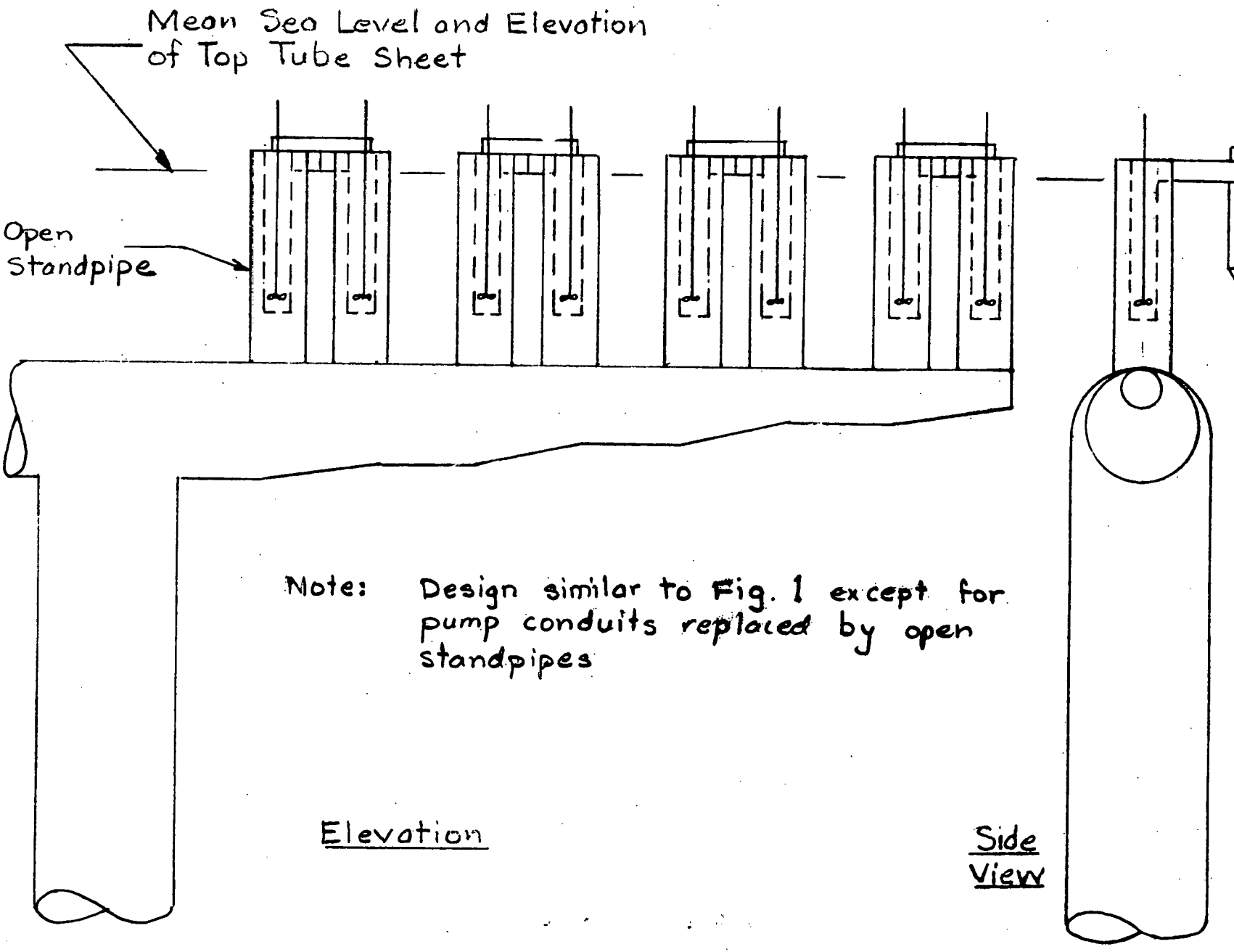

Fig. 6 Cold Water Distribution Decoupled Conduit

Scale 1"=50'

BY DATE 26 JULY 77 SUBJECT
CHKD. BY DATE
SHEET NO. 2-2 OF
JOB NO.

Depending upon the design, the area of the annular space can be less or greater than the cross-section area of the pump conduits in the completely closed system. If the diameters of the pump casing and standpipe are 9 and 13 feet, respectively, the horizontal area of 15 annular spares is 330 π feet. This is less than the total horizontal cross-section area pump conduits used for the computations in Article 2.2c. Therefore, the fundamental period is shorter for the decoupled system and the first pump can be started more quickly.

For pumps after the first one or two, larger standpipes permit more rapid pump start up. If the diameters of the pump casing and standpipe are 9 and 15 feet, respectively, the horizontal area of 15 annular spares is 540 π ft^2. This is significantly more than the total horizontal cross-sectional area of pump conduits in the computations for the completely closed system. Furthermore, there is a storage effect in all 15 stand pipes, regardless of how many pumps are running. Without detailed computations, it appears that most of the pumps in the decoupled system can be brought up to full flow rate in about 10 seconds.

B.3.2.2 Vertical Hull Motion

In the decoupled system, the vertical hull motion does not produce the high pressures produced in the completely closed system. Instead, the motion causes movement of the water surface in the stand pipes around the pumps. The rise and fall of the water surface is of the same order as the motion of the hull. At sea state 6 the change is $\pm$ 8 to 10 feet from the mean elevation.

This variation in elevation of the water surface is a change in the head on the pumps. A change of this magnitude will cause the rate of flow pumped to change by $\pm$ 33%.

APPENDIX B.4

OPEN TROUGH SYSTEM

B.4. OPEN TROUGH SYSTEM

B.4.1 BASIC FEATURES

The open trough system for supply and distribution of cold water is shown in Figure 7. The dimensions shown there are the ones used for preliminary estimates. The system has free water surface at two locations. One is the open trough, and the other is the water box at the top of the condenser.

The warm-water system is similar to that shown in Figure 2 with one difference; the water box at the top of the evaporator has a free surface.

B.4.2 PUMP STARTUP

B.4.2.1 Cold Water System

When a pump is started in the open trough, there is a tendency for the water surface to have the same shape as the hydraulic grade line in Figure 4 for roughly similar reasons. As soon as the water surface falls at the starting pump, however, water from the rest of the trough rushes toward the pump forming a surface wave. The height and speed of the wave can be estimated.

The estimate was made for a case of starting one large pump or several small pumps located near enough to each other to be considered a single point. The flow rate at the starting pumps increased to 3700 ft^3/sec instantaneously. The flow resulting from starting the pumps was treated as a shallow water wave.

For water starting with no velocity and a depth of 80 feet, the wave celerity w corresponding to 3700 ft^3/sec is given by

$$-2(80g)^{1/2} = V + 2w \tag{40}$$

The velocity V and depth Z at the wave are related by

$$60VZ = 3700 \tag{41}$$

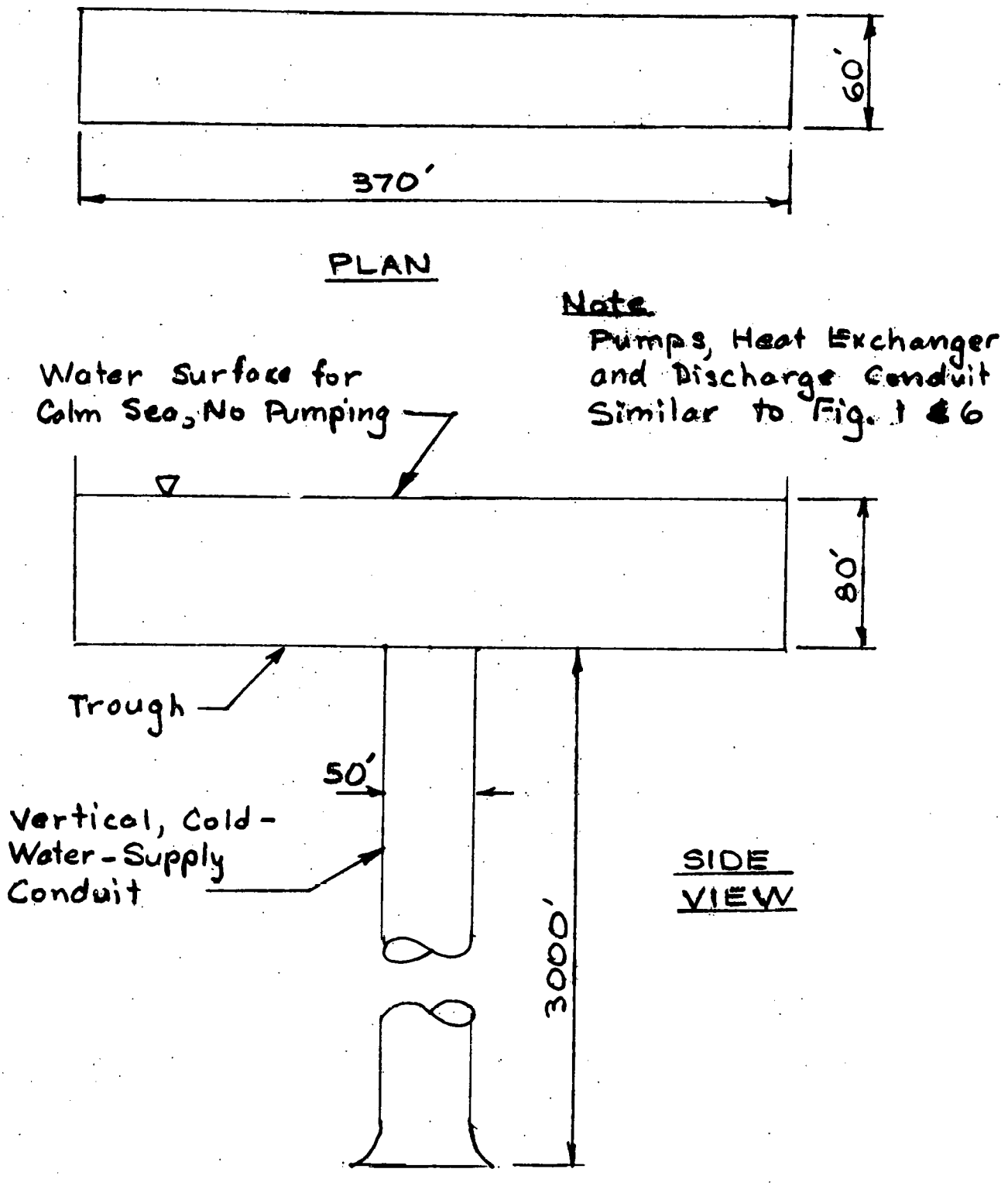

Fig. 7. Open Trough Cold Water Distribution

The depth Z is related to the wave celerity w by

$$w = \sqrt{gZ} \tag{42}$$

These 3 equations are combined to form the following equation

$$\frac{1824.67}{w^2} + 2w = 101.51 \tag{43}$$

By trial and error the solution is

$$w = 50.4 \text{ ft/sec}$$

$$Z = 78.87 \text{ ft}$$

$$V = 0.782 \text{ ft/sec}$$

Therefore the wave is a drawdown or decrease in depth equal to 1.13 feet moving away from the pump at a speed of 49.6 ft/sec.

This case is more extreme than any start up anticipated in an actual design. The flow rate for a single pump will be less than 3700 ft/sec. For a pump that will be selected for design, the wave height will be less than 1 foot.

In addition to surface waves, pump start up can also cause a drop in the water surface in the whole trough. As described for the previous system, the inertia of the water in the vertical supply conduit prevents the flow rate in that conduit from responding immediately to the starting pump. The water for the starting pump comes from the trough, and the whole water surface in the trough falls below the elevation at which it was located before the pump started. Because of the large horizontal area of the trough, the response of the flow in the conduit is slow. The period of the transient motion in the conduit is 204 seconds.

If more than one pump is started within 1/2 of the period, the effect will be the same as one pump with a flow rate equal to the sum of flow rates of all of the pumps started. After starting one pump, the

next should not be started until at least 100 seconds later. However, the time between successive pump starts should not be multiples of the period of 204 seconds. Although there should be sufficient time between successive pump starts, it is not necessary to start up each individual pump slowly. Each pump can be brought up to full flow rate as quickly as desired.

B.4.2.2 Warm Water System

Start-up of the warm water trough presents no difficulties. The warm-water troughs are connected to the open sea through openings in the hull. If these openings are large enough, water enters the trough quickly enough to prevent significant fall in water level in the trough. However, the pumps in any single trough should be started sequentially.

B.4.3 STANDING WAVES IN THE TROUGH

The surge and pitch of the hull can produce standing shallow water waves in the trough. The period of these waves can be determined from the wave celerity given in Article 4.2.1. The period of the shallow water trough is twice the length of time required for the wave to travel the length of the trough. With a length of 370 feet and a celerity of 50.4 ft/sec., the period is 14.7 seconds.

This period is in the range of periods that can be expected for rotation and horizontal motion of the hull. For these periods, the standing waves are in resonance with the hull motion. Even though the sea which is creating the hull motion is relatively calm, the standing waves in the hull at resonance will increase in height until they break. Without hydraulic model tests on detailed numerical computations, it is difficult to predict the maximum height of the waves before they break. Based on values of wave steepness at breaking, the height could be as great as 7 feet.

The amplitude of the standing waves can be reduced by building walls or bulkheads across the trough. The walls would have openings covered by gates so that the total area of opening in each wall can be controlled.

By varying the opening according to the sea state, the natural frequency of the waves in the trough can be kept different from the hull motion and resonance can be avoided. Essentially the trough is detuned.

The design and operation of the gated walls would have to be determined from hydraulic model studies. It is estimated that such walls could limit the maximum amplitude of the standing waves to 2 feet.

B.4.4 VERTICAL MOTION OF WATER SURFACE

B.4.4.1 Equations of Motion

The vertical motion of the hull causes unsteady flow on the cold and warm water systems. This unsteady flow causes the water surfaces in the troughs and in the top water boxes of the heat exchangers to move relative to the troughs and boxes. If the horizontal area of the cold water trough were equal to the cross-section area of the vertical cold water conduit, and if there were no friction losses, the water column in the conduit would not move relative to fixed space because of the inertia of the column. The same could be said of the water columns in the vertical discharge conduits for the heat exchangers. For such a situation, the water surface in the cold water trough and water boxes would remain at mean sea level and appear to move up and down in the trough and boxes. The amplitude of this relative motion would equal the heave of the hull.

The relative motion affects the flow ratio pumped through the heat exchangers. Since the pumps are fixed with respect to the hull, the water surfaces move relative to the pumps and changes the head on the pumps. As a result, the rate of flow pumped to the heat exchangers changes.

The equations for the relative motion are similar to the momentum and continuity equations used in previous sections. The continuity equation for the vertical conduit and open trough or vertical conduit and heat exchanger is

$$A\left(V-\frac{dz}{dt}\right) - \sum Q_p = a\,\frac{dZ}{dt} \qquad (44)$$

Most of the symbols of this equation have been defined previously. The variable a is now the horizontal area of the water surface in the open trough or in the water box at the top of the heat exchanger. The sum of flow for all pumps operating is $\sum Q_p$. The velocity V is the value for the vertical column being considered. The momentum equation is

$$-\frac{L}{g}\frac{dV}{dt} = z + Z + \Delta h_s + \frac{V^2}{2g} + \frac{fL}{2gD}(V - \frac{dz}{dt})^2 \qquad (45)$$

In this equation the V^2 is replaced by $|V|V$ and $(V - dz/dt)^2$ by $|(V - dz/dt)|$ $(V - dz/dt)$ as was done previously.

B.4.4.2 Numerical Solution

In previous sections, similar equations were linearized by assuming that the absolute values in the momentum equation are constant and equal to average values. A similar approach was used for the open trough system, but the results were not reassuring. Therefore, it was decided to do a limited amount of numerical computation.

The equations of motion were written in terms of increments ΔV, ΔZ, and Δt. They become

$$\Delta Z = \left[\frac{A}{a}(V - \frac{dz}{dt}) - \frac{\sum Q_p}{a}\right]\Delta t \qquad (46)$$

$$\Delta V = -\frac{g}{L}\left[z + (Z + \Delta h_s) + V|V|2g \right. \qquad (47)$$

$$\left. + \frac{fL}{2gD}(V - \frac{dz}{dt})\,|V - \frac{dz}{dt}|\right]\Delta t$$

The values of ΔZ and ΔV were computed for a Δt of 2 seconds using the values of V and dz/dt at the beginning of the increment Δt. The computations began with initial values of V and Z, and the values of ΔV and ΔZ were added at the end of each time increment. In the continuity equation, the value of Q_p remained constant. The computation was

carried out in a combination of manual calculations and automatic data processing with a programmable hand calculator.

For the open trough, the initial value of V and Z were 7 fps and 77 feet, respectively. The hull motion was represented by the sine wave derived above for Sea State 6. The values of f, L and D for the vertical cold water conduit are the same as those used in Subsection 2.3.

For the heat exchanger and vertical discharge column, the initial value of V was -5.41 ft/sec. The initial surface elevation h of the water above the top tube sheet was 8.22 feet above mean sea level. This elevation is equal to the head losses for steady flow through the heat exchanger when there is no hull motion and the velocity in the discharge column is -5.41 ft/sec. The value of fL/2gD was 0.265 which corresponds to a head loss of 8.22 feet.

The results of the computations are listed in the following tables. For the open trough the values of V and Z are given, while the values of V and h are given for the heat exchanger. In order to indicate the water velocity relative to the heat exchanger tubes, the values of V - dz/dt are also given for the heat exchanger.

B.4.4.3 Results

The values of h and Z are plotted in Figure 8. Also shown in the figure are the values of Δh_s in the trough, ΔH_f in the veritcal cold-water supply conduit; and the elevation h of the water surface in the top of the heat exchanger when there is no vertical hull motion.

The computations could not be carried far enough to show a complete cycle of the depth in the trough. The fundamental period of the transient motion in the vertical supply conduit is 204 seconds. The computation might have to be continued for 612 seconds or more before the curve for Z begins to repeat. However, it can be assumed that in the first three quarters of a period, the maximum difference between the depth in the trough and the depth that would occur in a calm sea is an indication of one half of the maximum amplitude of the change in depth.

VELOCITY IN VERTICAL SUPPLY CONDUIT AND DEPTH
IN OPEN TROUGH BY NUMERICAL COMPUTATION

t sec	V ft/sec	Z-77 ft	t sec	V ft/sec	Z-77 ft	t sec	V ft/sec	Z-77 ft
0	7.0	0	56	6.08	-2.53	112	7.53	-2.29
2	6.98	-0.72	58	6.07	-1.95	114	7.63	-2.89
4	6.82	-1.24	60	6.21	-1.50	116	7.56	-3.42
6	6.59	-1.27	62	6.45	-1.51	118	7.39	-3.54
8	6.42	-0.82	64	6.65	-2.02	120	7.23	-3.12
10	6.40	-0.17	66	6.72	-2.80	122	7.18	-2.37
12	6.53	0.27	68	6.63	-3.44	124	7.29	-1.66
14	6.64	0.74	70	6.46	-3.63	126	7.51	-1.36
16	6.78	0.78	72	6.32	-3.30	128	7.72	-1.57
18	6.77	0.60	74	6.31	-2.68	130	7.81	-2.13
20	6.61	-0.12	76	6.46	-2.18	132	7.73	-2.64
22	6.38	-1.25	78	6.71	-2.11	134	7.55	-2.76
24	6.21	-0.86	80	6.92	-2.55	136	7.36	-2.34
26	6.18	-0.25	82	7.01	-3.27	138	7.29	-1.58
28	6.30	0.17	84	6.94	-3.88	140	7.37	-0.84
30	6.51	0.12	86	6.78	-4.05	142	7.57	-0.49
32	6.66	-0.43	88	6.64	-3.69	144	7.76	-0.67
34	6.51	-1.05	90	6.62	-3.02	146	7.84	-1.20
36	6.37	-1.69	92	6.77	-2.44	148	7.76	-1.72
38	6.15	-1.86	94	7.02	-2.29	150	7.55	-1.86
40	5.99	-1.53	96	7.25	-2.65	152	7.35	-1.48
42	5.96	-0.97	98	7.34	-3.31	154	7.24	-0.73
44	6.10	-0.56	100	7.28	-3.87	156	7.30	0.02
46	6.32	-0.67	102	7.11	-4.01	158	7.19	-0.60
48	6.49	-1.18	104	6.97	-3.62	160	6.97	-0.84
50	6.53	-1.99	106	6.94	-2.90	162	7.06	-1.50
52	6.42	-2.65	108	7.07	-2.25	164	7.00	-2.17
54	6.23	-2.84	110	7.31	-2.01	166	6.82	-2.48

VELOCITY IN VERTICAL DISCHARGE CONDUIT AND WATER SURFACE ELEVATION IN HEAT EXCHANGER

t sec	V ft/sec	$V - \frac{dz}{dt}$ ft/sec	h ft	t sec	V ft/sec	$V - \frac{dz}{dt}$ ft/sec	h ft
0	-5.41	-9.58	8.22	28	-5.59	-5.28	7.61
1	-2.74	-6.60	6.86	29	-3.83	-5.12	7.65
2	-2.62	-5.59	6.47	30	-2.27	-4.97	7.74
3	-3.52	-5.15	6.41	31	-1.13	-4.84	7.89
4	-4.98	-5.02	6.50	32	-0.61	-4.77	8.07
5	-6.61	-5.06	6.62	33	-0.79	-4.77	8.28
6	-8.07	-5.17	6.74	34	-1.67	-4.87	8.49
7	-9.09	-5.27	6.82	35	-3.11	-5.07	8.67
8	-9.49	-5.31	6.87	36	-4.91	-5.32	8.78
9	-9.20	-5.31	6.90	37	-6.77	-5.57	8.81
10	-8.28	-5.25	6.93	38	-8.40	-5.77	8.76
11	-6.86	-5.15	6.99	39	-9.55	-5.89	8.65
12	-5.16	-5.03	7.07	40	-10.06	-5.91	8.49
13	-3.43	-4.89	7.20	41	-9.87	-5.86	8.33
14	-1.93	-4.76	7.37	42	-9.02	-5.75	8.18
15	-0.87	-4.66	7.58	43	-7.65	-5.61	8.07
16	-0.44	-4.61	7.82	44	-5.95	-5.46	8.00
17	-0.72	-4.64	8.09	45	-4.17	-5.29	7.99
18	-1.68	-4.77	8.34	46	-2.56	-5.12	8.03
19	-3.20	-5.00	8.54	47	-1.36	-4.98	8.12
20	-5.04	-5.27	8.68	48	-0.75	-4.88	8.27
21	-6.91	-5.54	8.73	49	-0.83	-4.87	8.44
22	-8.52	-7.14	8.69	50	-1.62	-4.94	8.62
23	-9.18	-6.41	8.12	51	-3.00	-5.11	8.77
24	-9.81	-5.65	7.80	52	-4.76	-5.35	8.87
25	-9.58	-5.62	7.72	53	-6.62	-5.59	8.89
26	-8.69	-5.54	7.65	54	-8.28	-5.79	8.83
27	-7.29	-5.42	7.61	55	-9.48		8.71

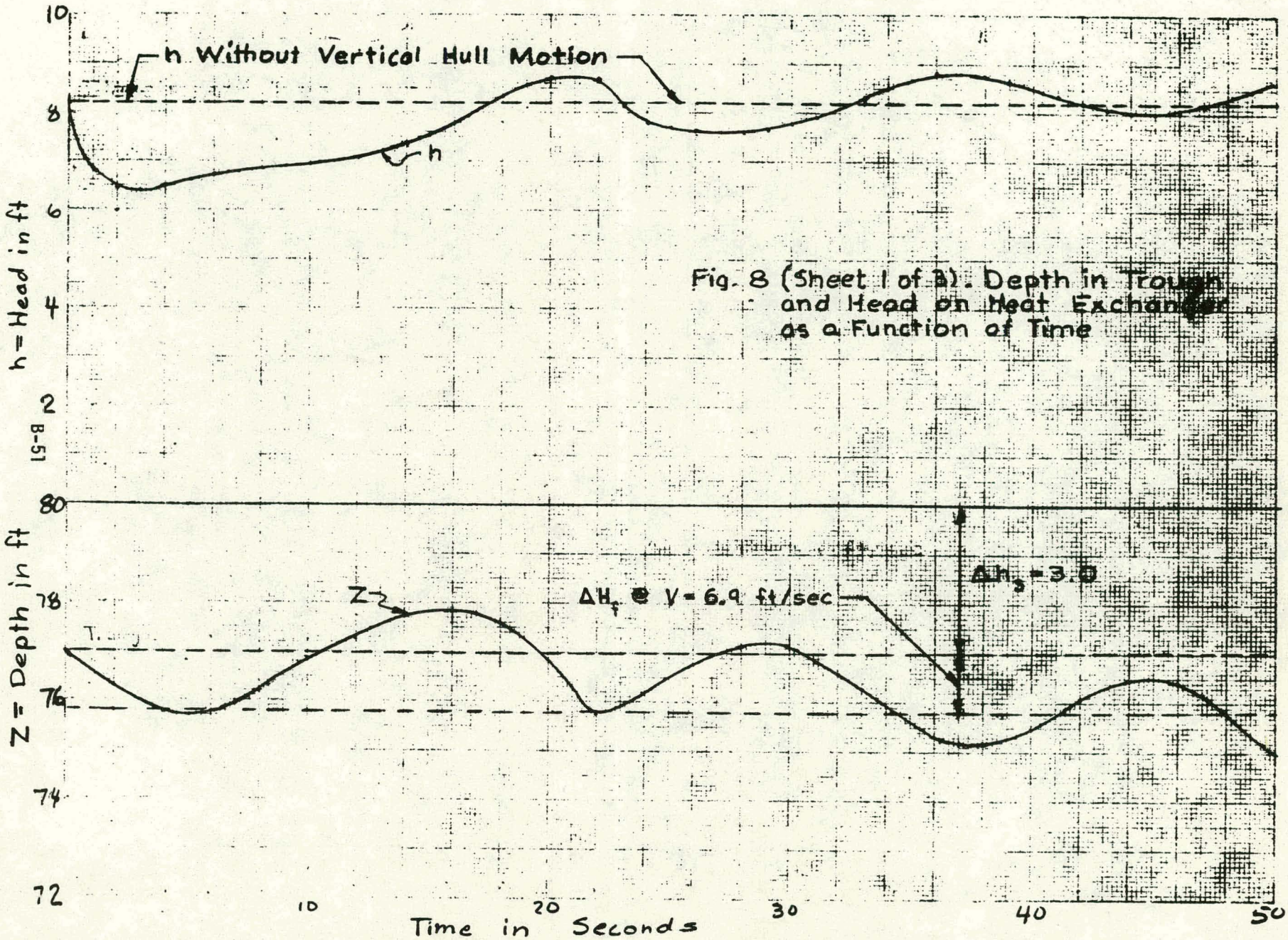

Fig. 8 (Sheet 1 of 2). Depth in Trough and Head on Heat Exchanger as a Function of Time

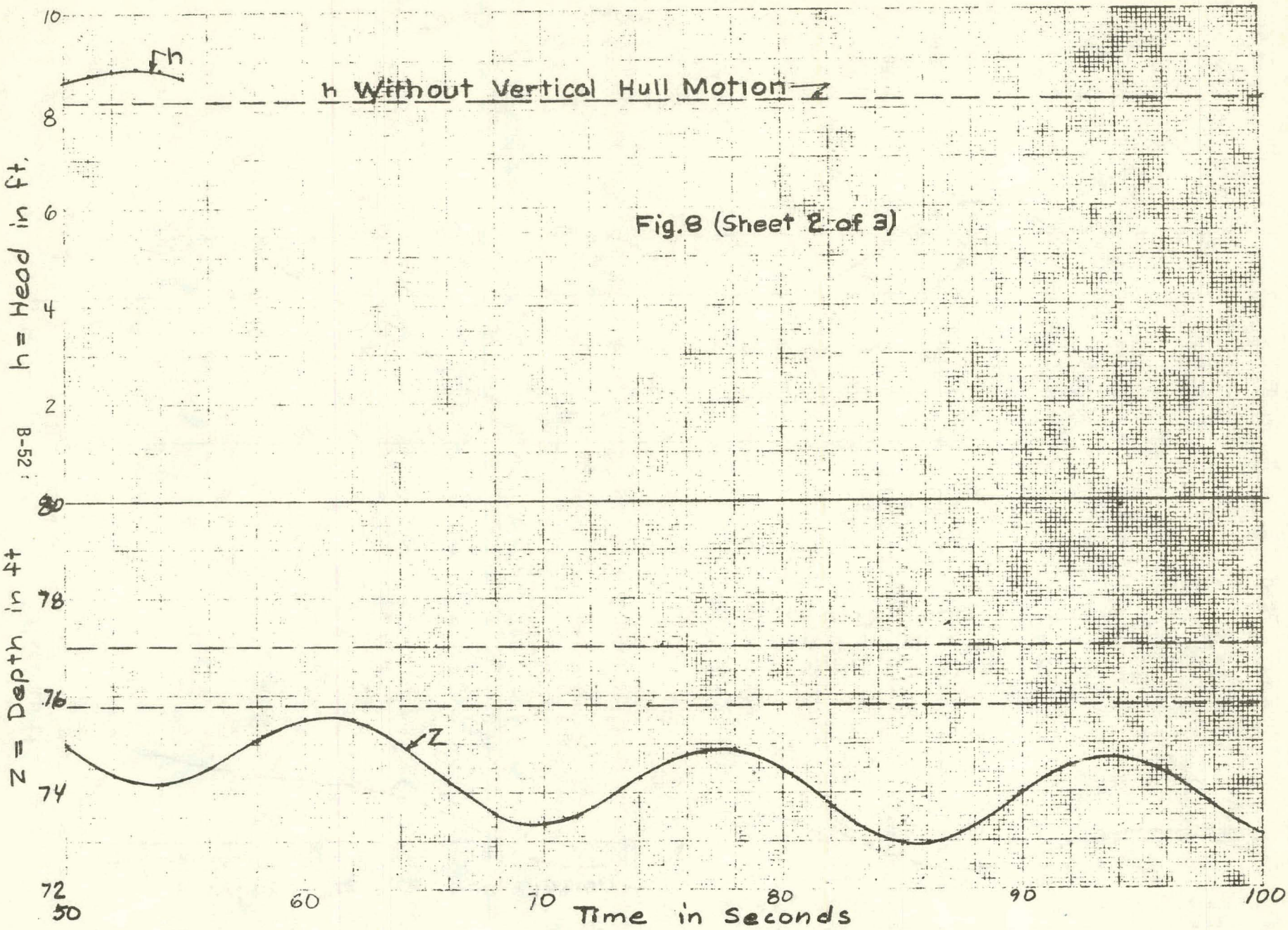

Fig.8 (Sheet 2 of 3)

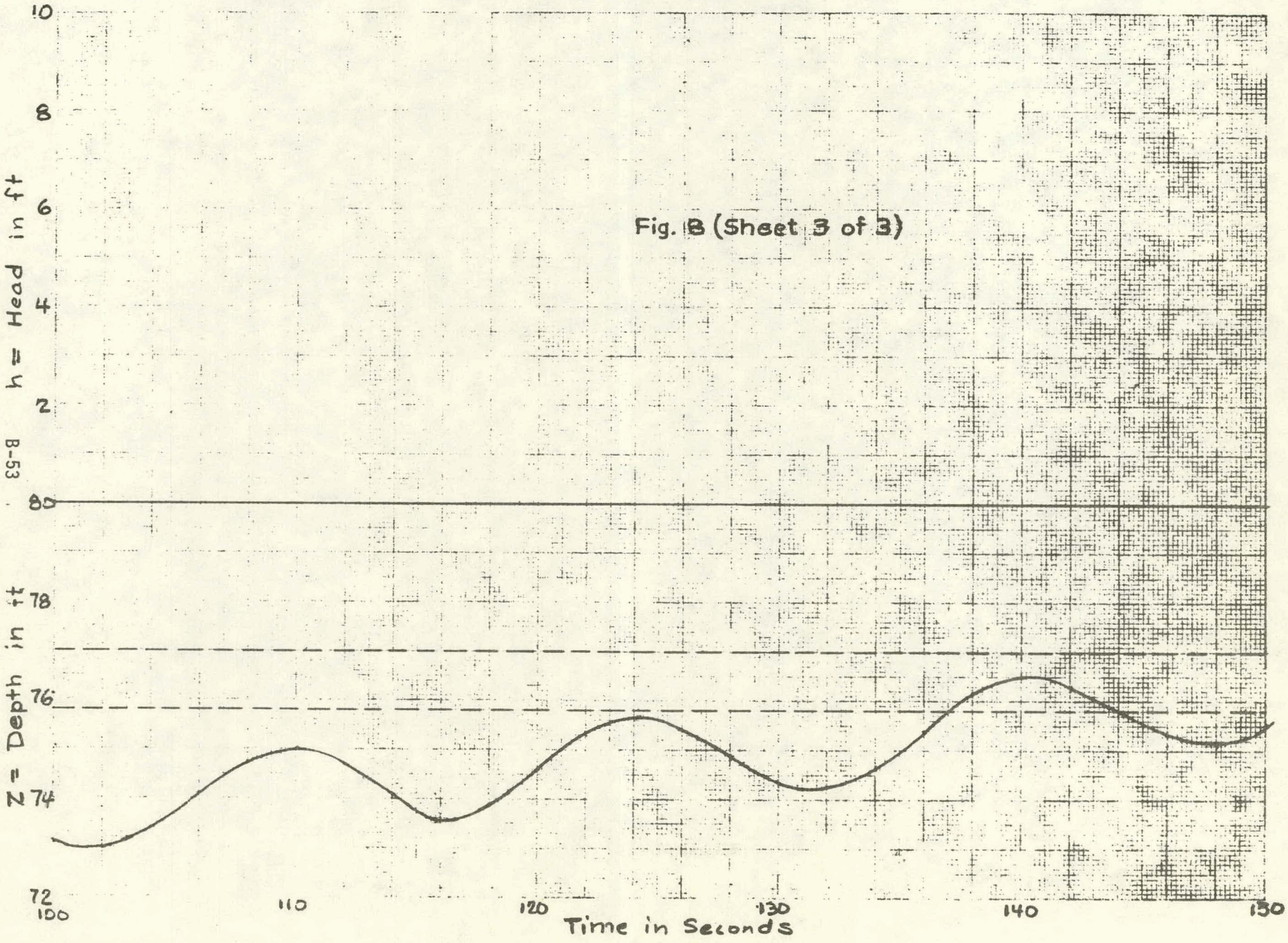
Fig. B (Sheet 3 of 3)
B-53
h = Head in ft
Z = Depth in ft
10
8
6
4
2
80
78
76
74
72
100
110
120
130
140
150
Time in Seconds

APPENDIX C

MISCELLANEOUS PERFORMANCE ANALYSIS

THIS PAGE

WAS INTENTIONALLY

LEFT BLANK

APPENDIX C.1

VARIABILITY OF AMMONIA LOOP PARAMETERS

TRW
DEFENSE AND SPACE SYSTEMS GROUP
ONE SPACE PARK • REDONDO BEACH • CALIFORNIA 90278

INTEROFFICE CORRESPONDENCE

78.6806-PJB-253
PSD-I-262

TO: Distribution

CC:

DATE: 5 May 1978

SUBJECT: Preliminary Analysis of Variability of Ammonia Loop Parameters Due to Annual Overall Temperature Difference Variations

PJB

FROM: P. J. Bakstad

BLDG.	MAIL STA.	EXT.
81	1538	51554

The analysis included in the attached technical note has been prepared to support preliminary design activities. More detailed analyses will be available later during the July-August timeframe, but these will come too late to impact early design decisions. These latter detailed performance models are presently being formulated by Dr. Impink, et al, at CMU under the direction of Dr. Kayton and myself.

The analysis presented gives estimates of the annual variations in ammonia flow, pressure and temperature. These results should be useful in the preliminary design of the instrumentation and control systems, the specifications of ammonia pumps, valves and turbogenerator (these must be sized for maximum flow and power conditions), for the definition of design pressures (e.g., 10% over maximum operating pressure) and pipe sizing.

The analysis indicates that evaporator and condenser operating conditions are set by energy balances and heat transfer rates considering the effect of the turbine representing a flow impedance between the ammonia vapor source (evaporator) and sink (condenser). The analysis shows that the system is stable in the sense that the evaporator and condenser pressures and temperatures will adjust itself to match the turbine impedance (which depends on parameters such as vane position and power demand) to satisfy energy and mass balances.

We are presently assuming that nominal design ΔT is 40°F with annual variations of ± 4°F ($T_H = 80 \pm 4$°F, $T_C = 40$°F constant). Expected variations are shown in a table. Note that the presently ongoing re-optimization will define nominal flow and power for the 10 $MWe_{,net}$ loop. Preliminary results indicate that the gross power at nominal conditions (P_G°) will be about 14.4 MWe, the corresponding nominal ammonia flow rate will be about 825 lb/sec. Table 2 and Eq (10) may then be used to estimate variations.

TRW SYSTEMS GROUP
ONE SPACE PARK • REDONDO BEACH, CALIFORNIA

PREPARED P. BAKSTAD 5/1/78 REPORT NO. PAGE 1/10

CHECKED

MODEL

PRELIMINARY ANALYSIS OF VARIABILITY OF NH_3 LOOP PARAMETERS

1. PURPOSE AND SCOPE

THE PURPOSE OF THIS NOTE IS TO PRESENT A SIMPLIFIED ANALYSIS OF THE VARIABILITY OF THE POWER LOOP PARAMETERS WITH SEASONAL VARIATIONS IN SEAWATER TEMPERATURES. THE ANALYSIS WILL BE SUFFICIENTLY DETAILED TO SUPPORT INITIAL SPECIFICATIONS OF TURBINES AND PUMPS, AND SIZING OF PIPES. (NOTE THAT MAX. FLOW/POWER CONDITIONS MUST BE USED TO SPECIFY THESE ITEMS)

MORE ACCURATE ANALYSES WILL BE AVAILABLE LATER WHEN THE DETAILED STEADY STATE PERFORMANCE AND DYNAMIC MODELS ARE DEVELOPED

2. MODEL AND ASSUMPTIONS

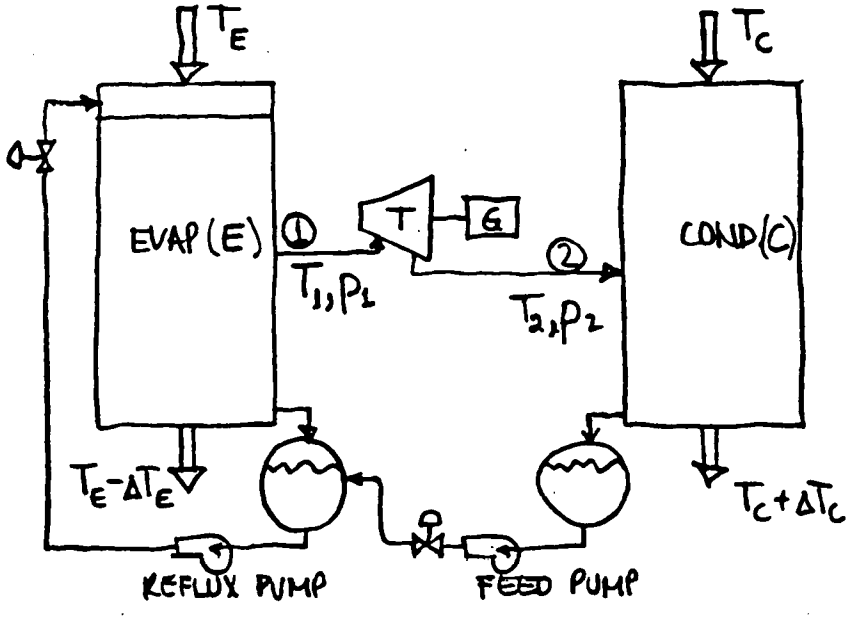

FIG. 1. SIMPLIFIED LOOP SCHEMATIC

THE FOLLOWING EQUATIONS DESCRIBE THE MODEL USED.

HEAT TRANSFER RATE:

TRW SYSTEMS GROUP
ONE SPACE PARK • REDONDO BEACH, CALIFORNIA

REPORT NO.

PAGE 2/10

PREPARED

CHECKED

MODEL

$$Q_E = (UA)_E \frac{(T_E - T_1) - (T_E - \Delta T_E - T_1)}{\ln\left(\frac{T_E - T_1}{T_E - \Delta T_E - T_1}\right)} \qquad (1)$$

$$Q_C = (UA)_C \frac{(T_2 - T_C) - (T_2 - T_C - \Delta T_C)}{\ln\left(\frac{T_2 - T_C}{T_2 - T_C - \Delta T_C}\right)} \qquad (2)$$

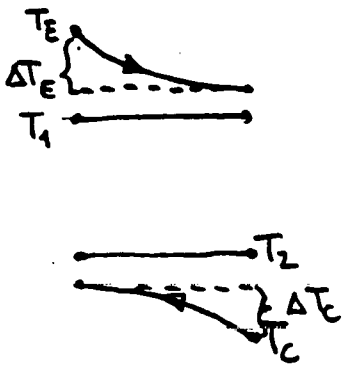

FIG. 2. TEMP. PROFILES

U = OVERALL HEAT TRANSFER COEFF.
A = HEAT TRANSFER AREA
T = TEMPERATURES DEFINED IN FIG. 2

ENERGY BALANCE, WATER SIDE:

$$Q_E = (W_\rho C_p)_E \Delta T_E \qquad (3)$$

$$Q_C = (W_\rho C_p)_C \Delta T_C \qquad (4)$$

$W_\rho C_p$ = HEAT CAPACITY (BTU/HR-°F)
IN ABOVE EQUATIONS: E - EVAPORATOR
C - CONDENSER

THE HEAT RATES ARE RELATED BY A LOOP POWER CONVERSION EFFICIENCY η:

$$Q_C = (1 - \eta) Q_E \qquad (5)$$

AMMONIA FLOW RATE, W IS GIVEN BY:

$$W = \frac{Q_E}{h_g(T_1) - h_f(T_2)} \qquad (6)$$

$h_g(T_1)$ = SPECIFIC ENTHALPY OF SATURATED VAPOR AT T_1
$h_f(T_2)$ = SPECIFIC ENTHALPY OF SATURATED LIQUID AT T_2

TRW SYSTEMS GROUP
ONE SPACE PARK • REDONDO BEACH, CALIFORNIA

PREPARED
CHECKED
MODEL
REPORT NO.
PAGE 3/10

THE TURBINE REPRESENTS AN IMPEDANCE TO VAPOR FLOW FROM EVAPORATOR TO CONDENSER. WE ASSUME FOR THIS ANALYSIS TWO MODELS FOR THIS IMPEDANCE:

$$a)\quad W = C_1\sqrt{\rho_{g_1}(P_1 - P_2)} \tag{7a}$$

$$b)\quad W = C_2 P_1/\sqrt{T_1+460} \approx C_2' P_1 \tag{7b}$$

a) IS AN APPROXIMATE RELATIONSHIP FOR A SUBSONIC NOZZLE

b) IS AN APPROXIMATE RELATIONSHIP FOR A SONIC NOZZLE (CHOKED NOZZLE)

A REFERENCE FOR THESE FORMULAS IS AEROSPACE FLUID COMPONENT DESIGNER'S HANDBOOK VOL 1. 1967 (TRW REPORT AD-809182). SEE ALSO "CRANE, FLOW OF FLUIDS".

ASSUMPTIONS IMPLICIT IN THESE EQUATIONS (1)---(7) INCLUDE:

1. PREHEATING LOAD IS SMALL AND NOT ACCOUNTED FOR IN LOG MEAN ΔT CALCULATION, EQS (1) & (2).
2. THE ENERGY ADDED BY THE REFLUX AND FEED PUMPS AND WORK TO OVERCOME ELEVATION AND FRICTION IS IGNORED IN EQ (6).
3. THE REPRESENTATION OF THE TURBINE IMPEDANCE AS CHOKED OR SUBSONIC NOZZLE IS APPROXIMATE, AT BEST. IT IS OUR CONJECTURE THAT THESE TWO MODELS WILL BRACKET ACTUAL TURBINE CHARACTERISTIC.
4. THE EFFECTS OF VARIABLE INLET VANES HAS NOT BEEN CONSIDERED.

3. DETERMINATION OF $T_1, T_2, \Delta T_E, \Delta T_C$ FOR VARIATIONS IN T_E AND T_C

TO PROCEED THE FOLLOWING ADDITIONAL ASSUMPTIONS WILL BE MADE:

1. $(UA)_E$ AND $(UA)_C$ ARE CONSTANT INDEPENDENT OF SEAWATER TEMPERATURE VARIATIONS. THESE ARE VALID ASSUMPTIONS CONSIDERING 2) BELOW.
2. THE SEAWATER FLOW RATES ARE CONSTANT, THEREFORE $(W\varrho C_p)_E$ AND $(W\varrho C_p)_C$ ARE ESSENTIALLY CONSTANTS.
3. THE POWER CONVERSION EFFICIENCY η IS CONSTANT SUCH THAT

$$\frac{Q_E}{Q_C} = \text{CONSTANT} \tag{8}$$

BY EQUATING EQS(1) AND (3) AND EQS(2) AND(4) RESPECTIVELY WE OBTAIN:

$$\Delta T_E = (T_E - T_1)\left[1 - \exp\left(-\left(\frac{UA}{W\varrho C_p}\right)_E\right)\right] \tag{9}$$

$$\Delta T_C = (T_2 - T_C)\left[1 - \exp\left(-\left(\frac{UA}{W\varrho C_p}\right)_C\right)\right] \tag{10}$$

THEREFORE, DENOTING FROM NOW ON NOMINAL, OR DESIGN, CONDITIONS WITH A SUPERSCRIPT "O":

$$\frac{\Delta T_E}{\Delta T_E^\circ} = \frac{T_E - T_1}{T_E^\circ - T_1^\circ} \tag{11}$$

$$\frac{\Delta T_C}{\Delta T_C^\circ} = \frac{T_2 - T_C}{T_2^\circ - T_C^\circ}, \tag{12}$$

AND USING EQ(8) AND ASSUMPTION 2) ABOVE:

$$\frac{\Delta T_E}{\Delta T_C} = \frac{\Delta T_E^\circ}{\Delta T_C^\circ} \Rightarrow T_2 = T_C + (T_E - T_1)\frac{T_2^\circ - T_C^\circ}{T_E^\circ - T_1^\circ} \tag{13}$$

FINALLY, BY EQUATING EQS(6) AND (7a,b) AND USING NOMINAL CONDITIONS TO ELIMINATE C_1 RESP. C_2 (WHICH

WE ASSUME ARE CONSTANTS) WE OBTAIN

a) FOR THE SUBSONIC NOZZLE ASSUMPTION :

$$\frac{\dfrac{T_E - T_1}{T_E^\circ - T_1^\circ}}{\dfrac{h_g(T_1) - h_f(T_2)}{h_g(T_1^\circ) - h_f(T_2^\circ)}} = \sqrt{\left(\frac{\rho_{g1}}{\rho_{g1}^\circ}\right)\left(\frac{p_1 - p_2}{p_1^\circ - p_2^\circ}\right)} \qquad (14a)$$

b) FOR THE SONIC NOZZLE ASSUMPTION :

$$\frac{\dfrac{T_E - T_1}{T_E^\circ - T_1^\circ}}{\dfrac{h_g(T_1) - h_f(T_2)}{h_g(T_1^\circ) - h_f(T_2^\circ)}} = \frac{p_1}{p_1^\circ} \qquad (14b)$$

EQS (13) AND (14), REPRESENTING TWO EQUATIONS IN TWO UNKNOWNS T_1 AND T_2, HAVE BEEN SOLVED NUMERICALLY FOR DIFFERENT VALUES OF T_E AND T_C USING THE FOLLOWING APPROXIMATIONS FOR THE THERMODYNAMIC RELATIONSHIPS FOR SATURATED AMMONIA :

$$p_1 = p_1^\circ + \Delta T_1 \left(\frac{\partial p}{\partial T}\right)_{1,S} \approx 128.8 + 2.27\,\Delta T_1 \quad \text{(PSIA) AT } 70^\circ F$$

$$p_2 = p_2^\circ + \Delta T_2 \left(\frac{\partial p}{\partial T}\right)_{2,S} = 89.2 + 1.71\,\Delta T_2 \quad \text{(PSIA) AT } 50^\circ F$$

$$h_g = h_g^\circ + \Delta T_1 \left(\frac{\partial h_g}{\partial T}\right)_{1,S} = 629.1 + 0.17\,\Delta T_1 \quad \text{(BTU/LB) AT } 70^\circ F$$

$$h_f = h_f^\circ + \Delta T_2 \left(\frac{\partial h_f}{\partial T}\right)_{2,S} = 97.9 + 1.12\,\Delta T_2 \quad \text{(BTU/LB) AT } 50^\circ F$$

$$\rho_{g1} = \rho_{g1}^\circ + \Delta T_1 \left(\frac{\partial \rho_g}{\partial T}\right)_{1,S} = 0.4325 + 0.0074\,\Delta T_1 \quad \text{(LB/CUFT) AT } 70^\circ F$$

AND

$$\Delta T_1 = T_1 - T_1^\circ$$
$$\Delta T_2 = T_2 - T_2^\circ \qquad (15)$$

TRW SYSTEMS GROUP
ONE SPACE PARK • REDONDO BEACH, CALIFORNIA

REPORT NO. PAGE 6/10

PREPARED
CHECKED
MODEL

A LISTING OF A FORTRAN PROGRAM ACCOMPLISHING THIS (SUBSONIC NOZZLE CASE) IS GIVEN BELOW:

```
00100          PROGRAM SENS(INPUT,OUTPUT)
00110          T10=70.
00120          T20=50.
00130          TE0=80.
00140          TC0=40.
00150          RG10=0.4325
00160          DRG1=0.0074
00170          HG10=629.1
00180          DHG=0.17
00190          HF20=97.9
00200          DHF2=1.12
00210          P10=128.8
00220          DP1=2.27
00230          P20=89.2
00240          DP2=1.71
00250 5        ACCEPT TE,TC
00260          T1=TE-0.25*(TE-TC)
00270 10       T2=TC+(TE-T1)*(T20-TC0)/(TE0-T10)
00280          DT1=T1-T10
00285          DT2=T2-T20
00290          HG1=HG10+DT1*DHG1
00300          HF2=HF20+DT2*DHF2
00310          RG1=RG10+DT1*DRG1
00320          P1=P10+DT1*DP1
00330          P2=P20+DT2*DP2
00340          A=SQRT(RG1*(P1-P2)/(RG10*(P10-P20)))
00350          B=(HG1-HF2)/(HG10-HF20)
00360          T11=TE-(TE0-T10)*A*B
00370          IF(ABS(T11-T1).LT.0.01) GO TO 20
00380          T1=T11
00390          GO TO 10
00400 20       DISPLAY T1,T2
00410          GO TO 5
00420          END
```

4 RESULTS AND DISCUSSION

THE FORTRAN PROGRAM SHOWN ABOVE AND ITS EQUIVALENT FOR THE SONIC NOZZLE CASE (STATEMENT 00340 CHANGED TO A= P1/P10) WERE USE TO GENERATE THE RESULTS IN TABLE 1 (NEXT PAGE) AND FIGURES 1 AND 2.

THE NOMINAL ("0") VALUES ARE $T_E^\circ = 80°F$, $T_1^\circ = 70°F$, $T_2^\circ = 50°F$ AND $T_C^\circ = 40°F$ WHICH IS OUR BASELINE DESIGN. THE TABLE AND FIGURES ALSO SHOW AS A REFERENCE THE RESULT OF THE (1/4, 1/2, 1/4) "RULE", NAMELY

(TEXT CONT. ON PAGE 8)

TRW SYSTEMS GROUP
ONE SPACE PARK • REDONDO BEACH, CALIFORNIA

PREPARED
CHECKED
MODEL

REPORT NO.

		SONIC N.		SUBSONIC N		(1/4, 1/2, 1/4)	
T_E(°F)	T_C(°F)	T_1(°F)	T_2(°F)	T_1(°F)	T_2(°F)	T_1(°F)	T_2(°F)
70.	40.	61.47	48.53	62.37	47.63	62.5	47.5
72.	↓	63.17	48.83	63.87	48.13	64.0	48.0
74.	↓	64.88	49.12	65.40	48.60	65.5	48.5
76.	↓	66.59	49.41	66.94	49.06	67.0	49.0
78.	↓	68.30	49.70	68.47	49.53	68.5	49.5
80.	↓	70.-	50.-	70.-	50.-	70.-	50.-
82.	↓	71.70	50.30	71.53	50.47	71.5	50.5
84.	↓	73.42	50.58	73.09	50.91	73.0	51.0
86.	40.	75.12	50.88	74.62	51.38	74.5	51.5
80.	36.	69.94	46.06	69.41	46.59	69.0	47.0
↓	38.	69.97	48.03	69.71	48.29	69.5	48.5
↓	40.	70.-	50.-	70.-	50.-	70.-	50.-
80.	42.	70.03	51.97	70.30	51.70	70.5	51.5
82.	38.	71.67	48.33	71.25	48.75	71.0	49.0
84.	36.	73.34	46.66	72.51	47.49	72.0	48.0

TABLE 1, NUMERICAL RESULTS

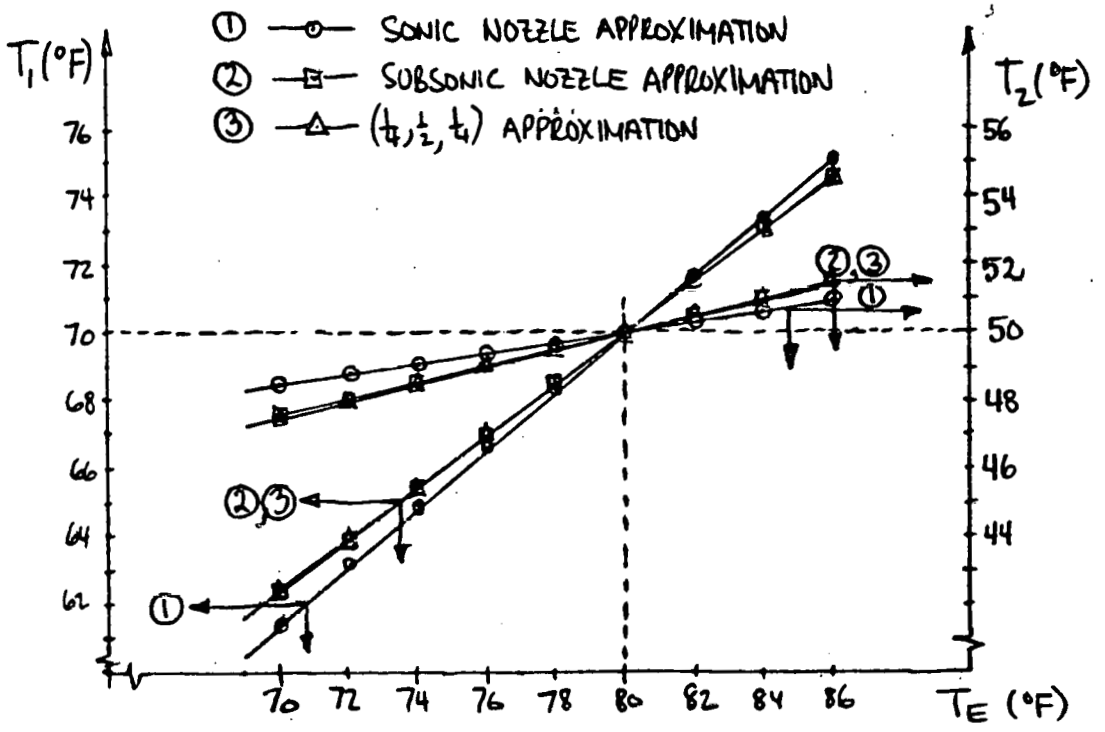

FIG. 2. T_1 AND T_2 FOR VARIATIONS IN T_E, CONSTANT T_C=40°F

TRW SYSTEMS GROUP
ONE SPACE PARK • REDONDO BEACH, CALIFORNIA

PREPARED
CHECKED
MODEL
REPORT NO.
PAGE 8/10

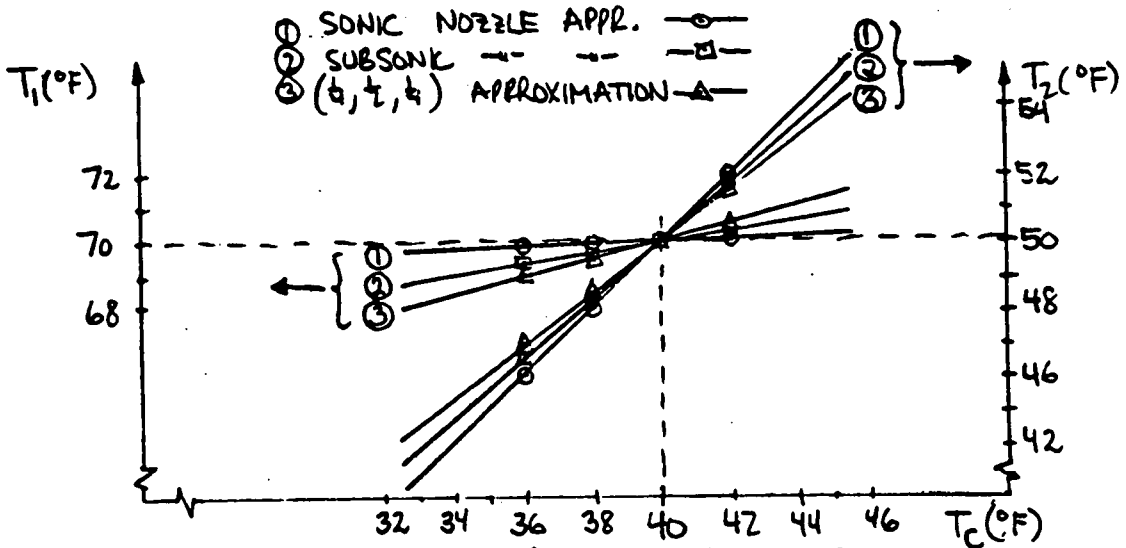

FIG. 3. T_1 AND T_2 FOR VARIATIONS IN T_C, CONST. T_E = 80°F

THAT, APPROXIMATELY, OPTIMUM DESIGN CORRESPONDS TO

$$\left.\begin{aligned} T_E - T_1 &= \tfrac{1}{4}(T_E - T_C) \\ T_1 - T_2 &= \tfrac{1}{2}(T_E - T_C) \\ T_2 - T_C &= \tfrac{1}{4}(T_E - T_C)\ . \end{aligned}\right\} \qquad (16)$$

IF WE MAKE THE ASSUMPTION THAT THE SONIC AND SUBSONIC NOZZLE APPROXIMATIONS BRACKET THE ACTUAL TURBINE, THE RESULTS ABOVE CAN BE USED TO ESTIMATE OFF-DESIGN CONDITIONS OF TEMPERATURES AND FLOW. NOTE THAT THE (1/4, 1/2, 1/4) RULE ALMOST COINCIDES WITH THE SUBSONIC NOZZLE APPROXIMATION.

IF WE ASSUME THAT ANNUAL VARIATIONS IN WARM WATER TEMPERATURE T_E IS ±4°F WITH COLD WATER TEMPERATURE ESSENTIALLY CONSTANT, THEN WE CAN ESTIMATE THE VARIATION IN AMMONIA FLOW PRESSURE AND TEMPERATURE CONDITIONS USING THE VAPOR TABLES AND THE RESULTS SHOWN ABOVE. TABLE 2 SHOWS THE RESULTS.

TRW SYSTEMS GROUP
ONE SPACE PARK • REDONDO BEACH, CALIFORNIA

PREPARED _____ REPORT NO. _____ PAGE 9/10

CHECKED _____

MODEL _____

SEASONAL VARIATIONS IN WARM WATER TEMP. 80±4 °F. CONSTANT COLD WATER TEMP. 40°F	MIN. FLOW CONDITIONS "WINTER" T_E=76°F	NOM. FLOW CONDITIONS T_E=80°F	MAX. FLOW CONDITIONS "SUMMER" T_E=84°F	VARIABILITY (APPROX.) %
EVAPORATOR OUTLET (STATIC)				
NH_3 TEMPERATURE, °F	66.5	70.0	73.5	±5
" PRESSURE, PSIA	121.1	128.8	136.9	±6
" QUALITY, %	≥99	≥99	≥99	
" MASS FLOW, LB/SEC	0.90 w°	w°	1.10 w°	±10
" VOL. FLOW, ACFS	0.95 V°	V°	1.05 V°	±5
CONDENSER INLET (STATIC)				
" TEMPERATURE, °F	49.0	50.0	51.0	±2
" PRESSURE, PSIA	87.5	89.2	90.9	±2

TABLE 2. VARIABILITY OF AMMONIA CONDITIONS

NOTE THAT THE PRESSURE AND TEMPERATURE VARIATIONS ARE BASED ON THE SONIC NOZZLE APPROXIMATION TO THE TURBINE, AND THE MASS AND VOLUMETRIC FLOW RATES ARE, BASED ON THE SUB-SONIC APPROXIMATION. THESE CHOICES MAXIMIZE (OR "WORST-CASE") THESE VARIATIONS.

THE VARIATIONS IN MASS FLOW RATE IS COMPUTED FROM:

$$\left(\frac{w}{w^\circ}\right) = \left(\frac{Q}{Q_0}\right)\left(\frac{h_g^\circ - h_f^\circ}{h_g - h_f}\right) = \left(\frac{T_E - T_1}{T_E^\circ - T_1^\circ}\right)\left(\frac{h_g^\circ - h_f^\circ}{h_g - h_f}\right) . \qquad (9)$$

THE VARIATION IN GROSS TURBINE POWER HAS BEEN CALCULATED BASED ON CONSTANT TURBINE EFFICIENCY. FROM THE THERMODYNAMIC TABLES IT FOLLOWS THAT:

(T_1, T_2)	73, 51	70, 50	67, 49	(°F)
$(\Delta h)_{s=c}$	21.56	19.85	17.99	(BTU/LB)

TRW SYSTEMS GROUP
ONE SPACE PARK • REDONDO BEACH, CALIFORNIA

PREPARED
CHECKED
MODEL
REPORT NO.
PAGE 10/10

USING EQ(9) IT FOLLOWS THAT:

$$\left(\frac{P_G}{P_G^\circ}\right)_{MAX} = 1.196$$
$$\left(\frac{P_G}{P_G^\circ}\right)_{MIN} = 0.815 \qquad (10)$$

NOTE:

- THE TURBO-GENERATOR MUST BE SIZED FOR MAX. POWER.
- AMMONIA PUMPS, PIPES AND VALVES MUST BE SIZED FOR MAX. FLOW.
- THE CONTROL SYSTEMS MUST HANDLE VARIATIONS BETWEEN MIN. AND MAX.. THE RFP REQUIREMENTS INCLUDE CONSIDERATION OF ΔT VARIATIONS OF +4 °F AND −11 °F. THEREFORE, OPERATION AT CONSIDERABLY REDUCED FLOWS, AND EVAPORATOR PRESSURE MUST BE ADDRESSED.

APPENDIX C.2

OPTIMUM DESIGN ΔT

TRW
DEFENSE AND SPACE SYSTEMS GROUP
ONE SPACE PARK • REDONDO BEACH • CALIFORNIA 90278

INTEROFFICE CORRESPONDENCE

78.6806-PJB-254
PSD-I-263

TO: Distribution

CC:

DATE: 5 May 1978

SUBJECT: Optimum Design ΔT^* For OTEC Plants

FROM: P. J. Bakstad

BLDG.	MAIL STA.	EXT.
81	1538	51554

Dr. Abe Lavi* called my attention to an unpublished paper where he showed that the optimum design ΔT^* for an OTEC plant may be less than the annual average ΔT_o. The purpose of the enclosed note is to analyze this conjecture using our own cost and performance models. The result indicates that for an average annual ΔT of 40°F varying sinusordally with $\pm$ 4°F amplitude, the optimum design ΔT^* is 38.1°F. This result is based on the assumption that the warm and cold water flow rates are constant, and that the ammonia pumps, valves, pipes and turbine-generator are sufficiently oversized to handle maximum ΔT ("summer") conditions. However, the sensitivity to $|\Delta T^* - \Delta T_o|$ is so small that the result is of theoretical interest only. Furthermore, we show that the optimum ΔT^* is sensitive to the details of the cost model used.

It is concluded that, at the present state-of-the-art, the design ΔT^* should be selected equal to the annual average ΔT_o. This is the approach we are taking in the PSD-I design. It must be emphasized again that ammonia pumps, valves, pipes and turbogenerator must be sized for maximum ΔT ("summer") conditions.

---

* I believe during the February Miami Conference

PREPARED P. BAKSTAD 4/30/78 REPORT NO. PAGE 1/5

CHECKED

MODEL

OPTIMUM DESIGN ΔT FOR OTEC PLANTS

LAVI (UNPUPLISHED PAPER) HAS SUGGESTED THAT, CONSIDERING ANNUAL VARIATIONS IN THE AVAILABLE $\Delta T = T_{WARM} - T_{COLD}$, THE OPTIMUM DESIGN $\Delta T = \Delta T^*$ MAY BE LESS THAN THE AVERAGE $\Delta T = \Delta T_o$. THIS NOTE INVESTIGATES THIS CONJECTURE, FOLLOWING LAVI'S ANALYSIS USING OUR OWN RECOMMENDED PERFORMANCE AND COST RELATIONSHIPS.

LET ΔT^* BE THE DESIGN ΔT, THEN, AS SUGGESTED BY J. HILBERT ANDERSON, THE PLANT CAPITAL COST IS APPROXIMATED BY

$$C_c = \frac{a}{\Delta T^* - b}, \$ \qquad (1)$$

WHERE $b \approx 23\,^\circ F$, AS SHOWN IN THE PSD CD. REPORT.

THE VARIATION IN PLANT OUTPUT WITH ΔT IS APPROXIMATELY GIVEN BY

$$P_N = P_G^* \left(\frac{\Delta T}{\Delta T^*}\right)^2 - P_L^* \qquad (2)$$

WHERE

P_N = NET POWER, MW

P_G^* = GROSS POWER AT DESIGN $\Delta T = \Delta T^*$, MW

P_L^* = LOSSES, MOST OF WHICH ARE WATER PUMPING WHICH ARE ASSUMED CONSTANT (NO FLOW RATE VARIATION), MW

THE POWER DEPENDENCY IS APPROXIMATELY TRUE, SINCE TO A FIRST APPROXIMATION GROSS POWER IS PROPORTIONAL TO CARNOT EFFICIENCY ($\sim\Delta T$) TIMES HEAT TRANSFERRED ($\sim\Delta T$).

ASSUME FURTHER THAT THE ΔT VARIATION WITH TIME IS SINUSOIDAL:

$$\Delta T(t) = \Delta T_o + \epsilon \cdot \sin\left(\frac{2\pi t}{12}\right) \qquad t \text{ IN MONTHS} \qquad (3)$$

TRW SYSTEMS GROUP
ONE SPACE PARK • REDONDO BEACH, CALIFORNIA

PREPARED
CHECKED
MODEL
REPORT NO.
PAGE 2.5

THE TIME VARIATION OF NET PLANT OUTPUT IS THEN:

$$P_N(t) = P_G^*\left(\frac{\Delta T(t)}{\Delta T^*}\right)^2 - P_L^* \qquad (4)$$

THE ANNUAL AVERAGE IS THEREFORE:

$$\langle P_N \rangle = P_G^* \frac{\Delta T_o^2 + \frac{1}{2}\varepsilon^2}{(\Delta T^*)^2} - P_L^* \qquad (5)$$

NOTE THAT THESE DERIVATIONS ASSUME THAT THE TURBOGENERATOR IS OVERSIZED TO HANDLE MAX. POWER OUTPUT AND ALSO THAT TURBINE EFFICIENCY IS ESSENTIALLY CONSTANT.

THE BUSBAR ENERGY COST C_{BB} ($/KWH) IS NOW, ASSUMING A CONSTANT AVAILABILITY FACTOR:

$$C_{BB} \sim \left[\frac{a}{\Delta T^* - b}\right]\left[\frac{1}{P_G^* \frac{\Delta T_o^2 + \frac{1}{2}\varepsilon^2}{(\Delta T^*)^2} - P_L^*}\right]$$

IF C_{BB} HAS A MINIMUM FOR SOME ΔT^* THE DERIVATIVE MUST BE ZERO:

$$\frac{\partial C_{BB}}{\partial \Delta T^*} = 0$$

OR EQUIVALENTLY

$$\frac{\partial\left(\frac{1}{C_{BB}}\right)}{\partial \Delta T^*} = 0$$

THEREFORE:

$$\left[P_G^* \frac{\Delta T_o^2 + \frac{1}{2}\varepsilon^2}{(\Delta T^*)^2} - P_L^*\right] + \left[\Delta T^* - b\right]\left[P_G^*\left(\Delta T_o^2 + \frac{1}{2}\varepsilon^2\right)(-2)(\Delta T^*)^{-3}\right] = 0$$

TRW SYSTEMS GROUP
ONE SPACE PARK · REDONDO BEACH, CALIFORNIA

PREPARED
CHECKED
MODEL
REPORT NO.
PAGE 3/5

DIVIDE BY P_G^*, MULTIPLY WITH $(\Delta T^*)^3$ AND COLLECT TERMS:

$$\frac{P_L^*}{P_G^*}(\Delta T^*)^3 + \Delta T^*\left[\Delta T_o^2 + \tfrac{1}{2}\varepsilon^2\right] - 2b\left[\Delta T_o^2 + \tfrac{1}{2}\varepsilon^2\right] = 0 \qquad (6)$$

THIS EQUATION CAN BE SOLVED ANALYTICALLY, BUT TRIAL-AND-ERROR SOLUTION IN THE FORM

$$\Delta T^* = \frac{2b\left[\Delta T_o^2 + \tfrac{1}{2}\varepsilon^2\right](P_G^*/P_L^*)}{\left[\Delta T_o^2 + \tfrac{1}{2}\varepsilon^2\right](P_G^*/P_L^*) + (\Delta T^*)^2} \qquad (7)$$

IS EASIER.

EXAMPLE:

$$\frac{P_G^*}{P_L^*} = \frac{1.3}{0.3} = 4.333$$

$b = 23°F$

$\Delta T_o = 40°F$

$\varepsilon = 4°F$

$$\Delta T_{i+1}^* = \frac{320528}{6968 + (\Delta T_i^*)^2} \Rightarrow \Delta T^* = 38.1°F$$

THIS SUGGEST THAT THE OPTIMUM DESIGN ΔT^* IS 38.1 °F WHICH IS 1.9 °F LESS THAN THE AVERAGE SITE ΔT_o. TO INVESTIGATE SENSITIVITY CALCULATE:

$$\frac{C_{BB}(\Delta T^*)}{C_{BB}(\Delta T_o)} = \left[\frac{\Delta T_o - b}{\Delta T^* - b}\right]\left[\frac{\frac{P_G^*}{P_L^*}(\Delta T_o^2 + \frac{1}{2}\varepsilon^2) - \Delta T_o^2}{\frac{P_G^*}{P_L^*}(\Delta T_o^2 + \frac{1}{2}\varepsilon^2)\left(\frac{\Delta T_o}{\Delta T^*}\right)^2 - \Delta T_o^2}\right]$$

WHICH IS THE RATIO OF ENERGY COST FOR DESIGN ΔT^* VERSUS AVERAGE ΔT_o. FOR THE SAMPLE VALUES:

TRW SYSTEMS GROUP
ONE SPACE PARK • REDONDO BEACH, CALIFORNIA

REPORT NO.

PAGE 4/5

PREPARED

CHECKED

MODEL

WE COMPUTE :

ΔT^*	$\frac{C_{BB}(\Delta T^*)}{C_{BB}(\Delta T_0)}$
34	1.0313
36	1.0025
38	0.9940
40	1.0000
42	1.0175
44	1.0449
38.1	0.9939

(C^*_{BB}/C^0_{BB})

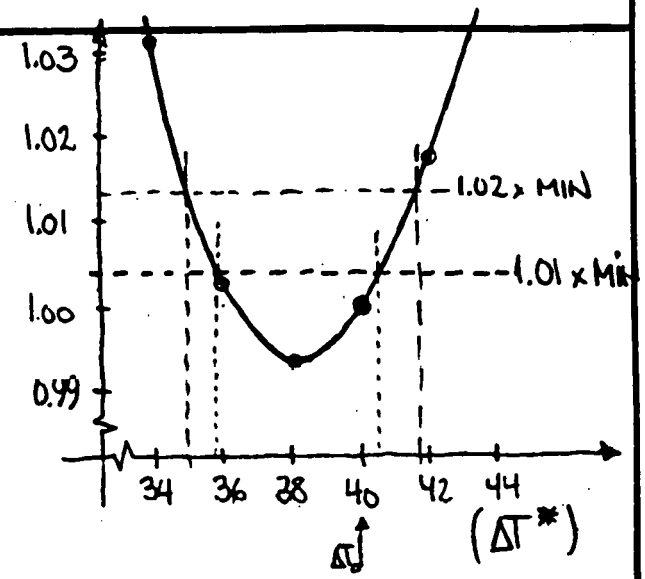

IT FOLLOWS FROM THIS NUMERICAL EXAMPLE THAT ALTHOUGH A THEORETICAL MINIMUM ENERGY COST OCCURS FOR 38.1 °F FOR AN AVERAGE ΔT_0 OF 40 °F, THE SENSITIVITY IS SMALL. THE ENERGY COST AT 40°F IS HIGHER BY ONLY 0.6 PERCENT. (WHICH IS WITHIN THE UNCERTAINTY OF THE MODEL !)

CONCLUSION

DR. LAVI'S CONJECTURE APPEARS MATHEMATICALLY CORRECT. HOWEVER, THE ENERGY COST IS VERY INSENSITIVE TO DESIGN TEMPERATURE AND FOR DESIGN OTHER CONSIDERATIONS OF OFF-DESIGN PERFORMANCE (SUCH AS TURBINE EFFICIENCY) ARE MORE IMPORTANT.

APRIL 30, 78
P.J. Bakstad

ADDENDUM

THE CONCLUSION ABOVE APPEARS SENSITIVE TO THE EXACT COST MODEL. LAVI ASSUMED THAT

TRW SYSTEMS GROUP
ONE SPACE PARK • REDONDO BEACH, CALIFORNIA

PREPARED
CHECKED
MODEL
REPORT NO.
PAGE 5/5

$$C \sim (\Delta T^*)^{-k} \qquad \text{WHERE } 2 \le k \le 3.$$
(LAVI SUGGESTS THAT $k = 2.5$)

FOR THIS CASE:

$$\Delta T^*\Big|_{\substack{\text{MIN}\\ \text{COST LAVI}}} = \sqrt{\left(\frac{P_G^*}{P_L^*}\right)\left(\frac{k-2}{k}\right)\left[(\Delta T_0)^2 + \tfrac{1}{2}\varepsilon^2\right]}$$

IN OUR EXAMPLE:

$$\Delta T^*\Big|_{\substack{\text{MIN}\\ \text{COST, LAVI}}} = \sqrt{\left(\frac{1.3}{0.3}\right)\left(\frac{0.5}{2.5}\right)(1600+8)} = 37.3 \quad \text{FOR } k=2.5$$
$$= 0. \quad (!) \text{ FOR } k=2.$$
$$= 48.2 \quad (!) \text{ FOR } k=3.$$

THE EXPRESSION FOR $C_{BB}(\Delta T^*)/C_{BB}(\Delta T_0)$ BECOMES:

$$\frac{C_{BB}(\Delta T^*)}{C_{BB}(\Delta T_0)} = \left(\frac{\Delta T_0}{\Delta T^*}\right)^k \left[\frac{\frac{P_G^*}{P_L^*}(\Delta T_0^2 + \frac{1}{2}\varepsilon^2) - \Delta T_0^2}{\frac{P_G^*}{P_L^*}(\Delta T_0^2 + \frac{1}{2}\varepsilon^2)\left(\frac{\Delta T_0}{\Delta T^*}\right)^2 - \Delta T_0^2}\right]$$

ΔT^*	C_{BB}^*/C_{BB}^*		
	$k=2$	$k=2.5$	$k=3$
32	0.903	1.010	1.129
36	0.946	0.998	1.052
40	1.000	1.000	1.000
44	1.067	1.017	0.970
48	1.151	1.051	0.959

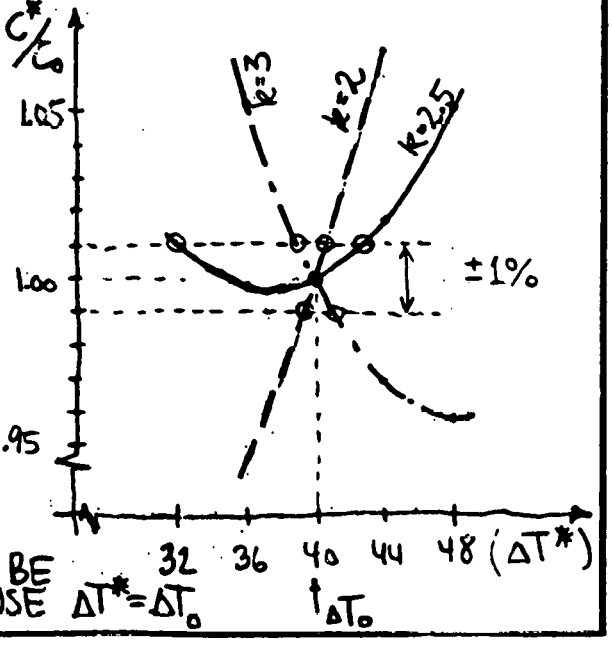

THIS SHOWS:

1) THE LAVI COST ALG.'S WEAKNESS IN ITS SENSITIVITY TO k
2) THE IDEA OF OPTIMIZING DESIGN ΔT^* SHOULD NOT BE PURSUED AT PRESENT, USE $\Delta T^* = \Delta T_0$

APPENDIX D

MATERIALS AND PROCESSES

THIS PAGE

WAS INTENTIONALLY

LEFT BLANK

APPENDIX D.1

TUBE MANUFACTURING

TRW
DEFENSE AND SPACE SYSTEMS GROUP
ONE SPACE PARK • REDONDO BEACH • CALIFORNIA 90278

PSD-1-546
5515.2.78-433

INTEROFFICE CORRESPONDENCE

TO: C. Williamson

CC: P. Edris
C. Feddersen ✓
J. Hsu
F. Jackson
G. Porter
L. Rosales
W. Talon
S. Vincent

DATE: 7 September 1978

SUBJECT: OTEC Tube to Tubesheet Joints — Rubber Expanding Method

FROM: J. Hicks

BLDG.	MAIL STA.	EXT.
01	2080	61486

Reference: (1) IOC PCS-1-488 (same subject) from C. Williamson to J. Hsu, 14 August 1978.

(2) Letter from Hitachi America, Ltd. (same subject) to J. Hicks, 25 August 1978.

(3) Letter from J. Hicks to Hitachi America, Ltd., 7 September 1978.

1. In response to your Reference (1) recommendations, representatives of Materials Engineering met with Mr. K. Ichibashi from Hitachi America (Houston, Texas), who has since supplied the Reference (2) information (copy attached).

2. To facilitate an in-house evaluation of the rubber expanding method, the Reference (3) "cost and delivery" inquiry has been made to Hitachi to supply TRW with twelve sample specimens for testing in our laboratories. Their reply will be forwarded upon receipt.

TRW

7 September 1978

Mr. K. Ichihashi
Hitachi America, Ltd.
3800 Buffalo Speedway, Suite 318
Greenway Plaza
Houston, Texas 77098

Dear Mr. Ichihasi:

This letter is to acknowledge receipt of the proposed licensing agreement for use of the Hitachi Expanding Machine (Rubber Expansion Unit), and the copy of the United States patent for same. This information has been forwarded to our Ocean and Energy Systems Department for their consideration.

We would appreciate further information from your home office relative to having Hitachi provide TRW with twelve single tube models, as illustrated in Figure 9 of the Hitachi "Technical Report of Uniform Tube Expansion (Rubber Expansion)", except the titanium tube wall thickness should be 0.71 mm (0.028 inch) instead of the 1.75 mm (0.069 inch) shown. These twelve specimens would be tested in TRW laboratories relative to retaining force and watertightness. The planning information required is:

- Total cost, including air freight delivery to Los Angeles International Airport
- Estimated delivery schedule (TRW desires delivery by mid-November 1978).

Thank you for your assistance in obtaining the above information.

Sincerely yours,

John S. Hicks

DEFENSE AND SPACE SYSTEMS GROUP OF TRW INC. • ONE SPACE PARK, REDONDO BEACH, CALIFORNIA 90278 • (213) 535 4321

Hitachi America, Ltd.
HOUSTON OFFICE
3800 BUFFALO SPEEDWAY, SUITE 318
GREENWAY PLAZA
HOUSTON, TEXAS 77098

TELEX
77-5965

August 25, 1978
HOU-025-S

Mr. John Hicks
TRW, Inc., Systems Group
Building No. 01, Room 2220
One Space Park
Redondo Beach, California 90278

Dear Mr. Hicks:

I am enclosing our proposal regarding Hitachi Expanding machine (Rubber Expansion Unit) sales, and also the patent copy registered in the United States, for your reference.

The unit is ready for shipment within four (4) months after our receipt of contract.

We would appreciate your comment on this matter. Thank you for your kind attention.

Very truly yours,

HITACHI, AMERICA, LTD.

K. Ichihashi

K. Ichihashi

KI:sp
Enclosures

LICENSE AGREEMENT

1. Grant of License

HITACHI, LTD. grants to Licensee:

1. A nonexclusive and nontransferrable license to use technical information disclosed to licensee by Hitachi, Ltd., in the manufacture and sale of Heat Exchangers throughout the world.

2. A nonexclusive and nontransferrable license under Hitachi, Ltd. patent right throughout the world to manufacture and sell Heat Exchangers.

2. Royalty

1. An initial payment of five million yen (¥ 5,000,000), which shall be applicable to the running royalties specified in No. 2, below.

2. Running royalties in the amount of 1.5 per cent of the net sales price of Heat Exchanger manufactured by Rubber Expanding Unit and sold by licensee during the term of this Agreement.

3. Royalty shall be paid to Hitachi, Ltd. every six months.

3. Hitachi, Ltd. Services

Hitachi, Ltd. furnishes to Licensee:

1. Information helpful to licensee in the manufacture of Heat Exchangers applying Rubber Expansion Unit.

2. Design Method of tube-to-tubesheet construction.

3. Operation manual and explanation sheet of Rubber Expansion Unit.

4. Rubber Expansion Unit

FOB Japan Port Price: ¥ 5,000,000 (five million yen) per one unit.

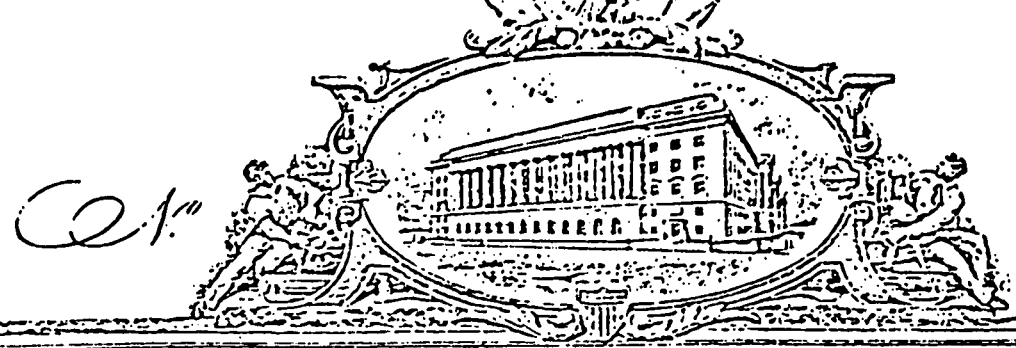

4068372

THE UNITED STATES OF AMERICA

TO ALL TO WHOM THESE PRESENTS SHALL COME:

Whereas, THERE HAS BEEN PRESENTED TO THE

Commissioner of Patents and Trademarks

A PETITION PRAYING FOR THE GRANT OF LETTERS PATENT FOR AN ALLEGED NEW AND USEFUL INVENTION THE TITLE AND DESCRIPTION OF WHICH ARE CONTAINED IN THE SPECIFICATIONS OF WHICH A COPY IS HEREUNTO ANNEXED AND MADE A PART HEREOF, AND THE VARIOUS REQUIREMENTS OF LAW IN SUCH CASES MADE AND PROVIDED HAVE BEEN COMPLIED WITH, AND THE TITLE THERETO IS, FROM THE RECORDS OF THE PATENT AND TRADEMARK OFFICE IN THE CLAIMANT(S) INDICATED IN THE SAID COPY, AND WHEREAS, UPON DUE EXAMINATION MADE, THE SAID CLAIMANT(S) IS (ARE) ADJUDGED TO BE ENTITLED TO A PATENT UNDER THE LAW.

NOW, THEREFORE, THESE Letters Patent ARE TO GRANT UNTO THE SAID CLAIMANT(S) AND THE SUCCESSORS, HEIRS OR ASSIGNS OF THE SAID CLAIMANT(S) FOR THE TERM OF SEVENTEEN YEARS FROM THE DATE OF THIS GRANT, SUBJECT TO THE PAYMENT OF ISSUE FEES AS PROVIDED BY LAW, THE RIGHT TO EXCLUDE [illegible]HERS FROM MAKING, USING OR SELLING THE SAID INVENTION THROUGHOUT THE [illegible]ED STATES.

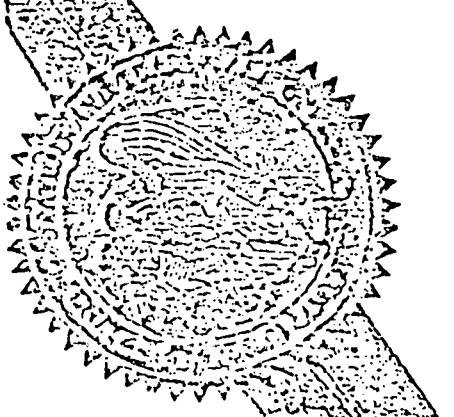

In testimony wherenf *I have hereunto set my hand and caused the seal of the* Patent and Trademark Office *to be affixed at the City of Washington this* seventeenth *day of* January *in the year of our Lord one thousand nine hundred and* seventy-eight, *and of the Independence of the United States of America the two hundredth and* second.

Attest:

Attesting Officer.

D-8

Acting Commissioner of Patents and Trademarks.

United States Patent [19]

Kamohara et al.

[11] 4,068,372

[45] Jan. 17, 1978

[54] TUBE EXPANDER

[75] Inventors: Hideaki Kamohara, Kudamatsu; Toji Nakatui, Hikari; Yuji Yoshitomi, Kudamatsu; Iwao Sasaki, Kudamatsu; Kenji Shimada, Kudamatsu, all of Japan

[73] Assignee: Hitachi, Ltd., Tokyo, Japan

[21] Appl. No.: 768,198

[22] Filed: Feb. 14, 1977

[30] Foreign Application Priority Data

Feb. 18, 1976 Japan 51-15879

[51] Int. Cl.² B23P 17/00

[52] U.S. Cl. 29/727; 29/282; 29/283.5; 72/58; 72/DIG. 14

[58] Field of Search ..... 72/58, 59, 61, 62, DIG. 14; 29/421 R, 523, 727, 283.5, 282, 157.4

[56] References Cited

U.S. PATENT DOCUMENTS

3,152,630	10/1964	Nilsson	72/58 X
3,595,047	7/1971	Fenning	72/58
3,977,068	8/1976	Krips	29/727 X
4,006,619	2/1977	Anderson	72/58 X

Primary Examiner—Leon Gilden

Attorney, Agent, or Firm—Beall & Jeffery

[57] ABSTRACT

Disclosed is a tube expander adapted for use in fixing tubes to a tube plate of a boiler or a multitubular heat exchanger. The expander incorporates an elastic expanding medium adapted to be inserted into a tube to be expanded radially against a wall of a tube-receiving bore of the tube plate. The expander further includes a pressurizing rod passing through the expanding medium, a pressurizing rod head provided at one end of the pressurizing rod, a back-up ring adapted to be supported straddling said tube receiving bore and slidably passed by the pressurizing rod, and seal rings disposed at both sides of the pressurizing rod. The seal rings are made of a hard elastic material of a hardness greater than that of the expanding medium, and each of them is provided with at its portion confronting the end of the expanding medium with a conical recess.

10 Claims, 7 Drawing Figures

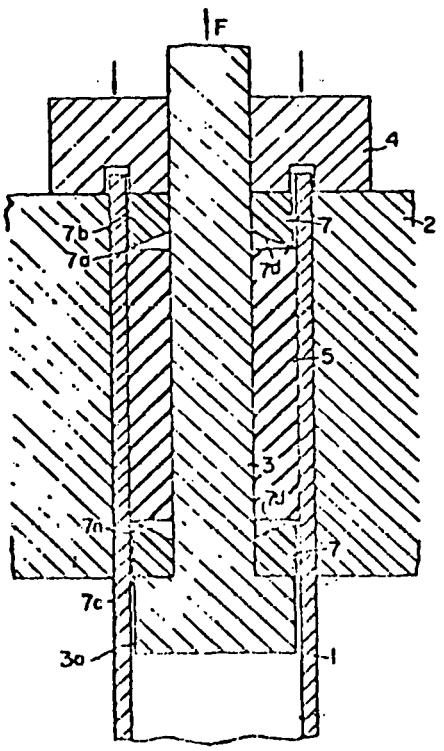

FIG. 1

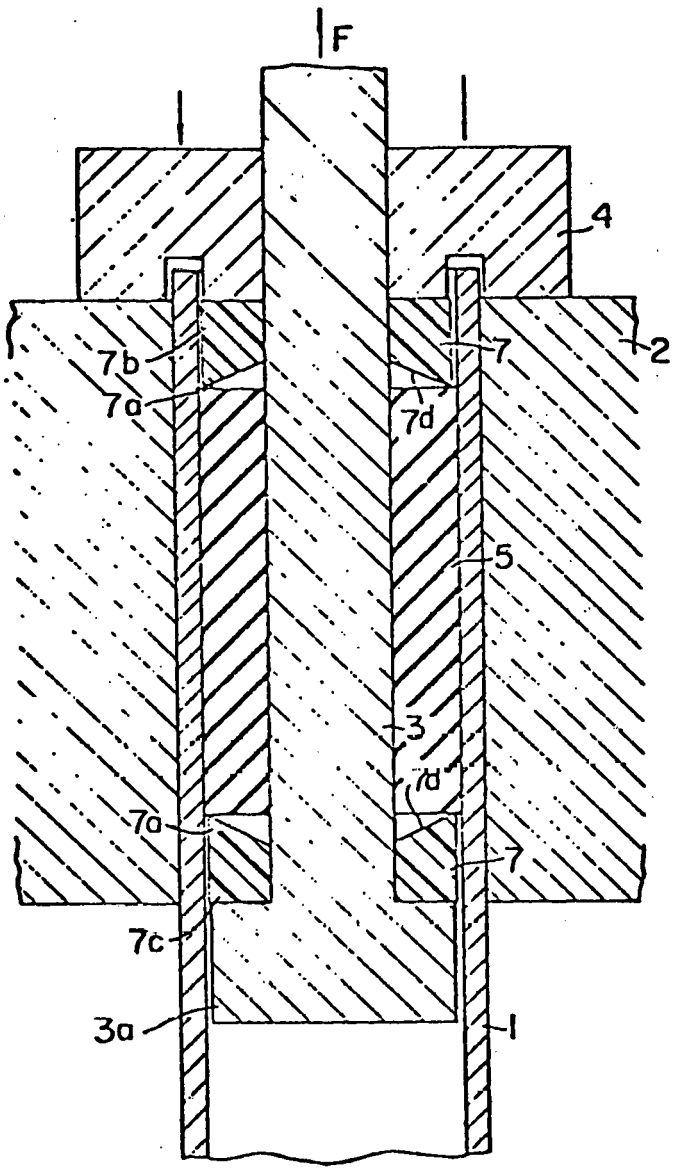

FIG. 2

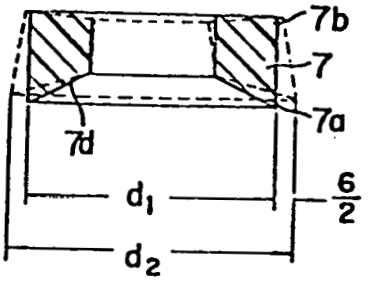
7b
7
7a
7d
d_1
$\frac{6}{2}$
d_2

FIG. 3

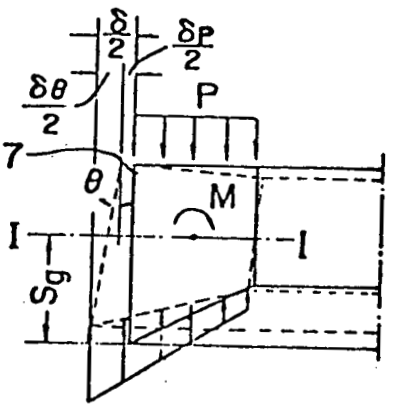
$\frac{\delta}{2}$
$\frac{\delta P}{2}$
$\frac{\delta\theta}{2}$
P
7
θ
M
I
I
S_g

FIG. 4

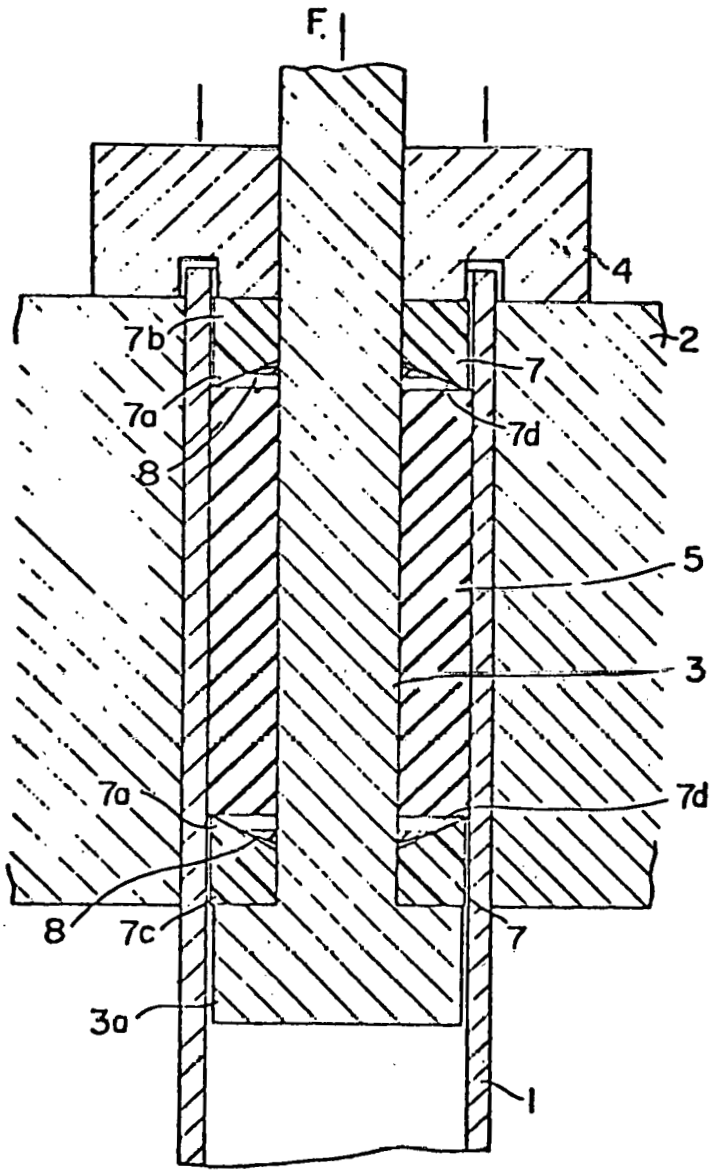

FIG. 5

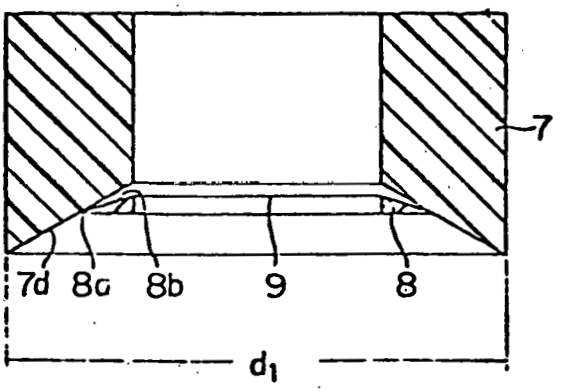

FIG. 6

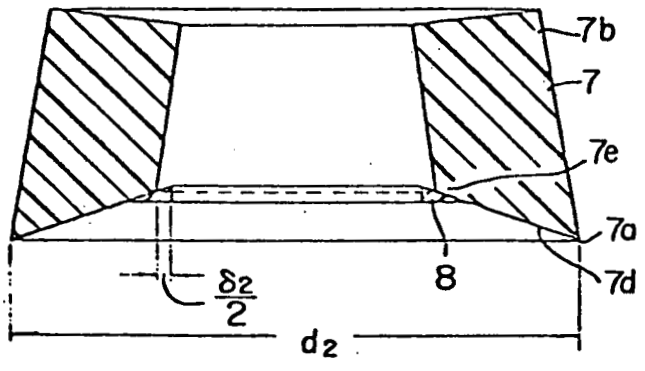

FIG. 7

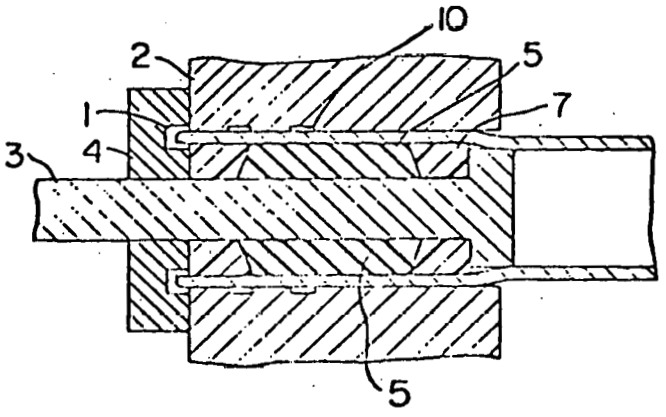

TUBE EXPANDER

BACKGROUND OF THE INVENTION

The present invention relates to a tube expander for fixing tubes to a tube plate of a boiler or multitubular heat exchanger and, more particularly, to a tube expander relying upon a radial expansion of a cylindrical elastic expanding medium inserted into a tube caused by an axial compression of the medium for expanding and fixing the tube to the tube-receiving bore of the tube plate.

In manufacturing boilers and multitubular heat exchanger or the like, such a method of fixing tubes to a tube plate is getting popular as consisted in inserting a cylindrical elastic expanding medium and compressing the medium in the axial direction to cause the later to exert a radical expanding force which in turn acts on the inner peripheral wall of the tube to radially expand and tightly fix the tube to the tube plate.

Conventionally, tube expanders for carrying out the above explained method incorporates a cylindrical elastic expanding medium, a pressurizing rod passing through the medium and a back-up ring adapted to be secured straddling a tube-receiving bore of the tube plate. The pressurizing rod is connected to a piston rod in a hydraulic cylinder. In operation, the hydraulic cylinder exerts a force on a rod-head of the pressurizing rod so that the rod effects an axial compression and a consequent radial expansion of the expanding medium. The radial expansion of the medium in turn expands the tube radially and tightly fits it to the tube-receiving bore of the tube plate.

In those conventional tube expanders, as the tube is radially expanding, a gap left between the inner surface of the tube and a central boss of the back-up ring is also enlarged. Thus, part of the expanding medium inconveniently invades this enlarged gap causing a collapse or deformation of the expanding medium. This unfavorable invasion of the expanding medium takes place also at the end of the pressurizing rod opposite to the back-up ring, where a gap is formed between the rod-head of the pressurizing rod and the tube.

In order to prevent this undesirable collapse of the expanding medium, it has been proposed to put a cylindrical seal ring having parallel end surfaces between the expanding medium and the tube. This seal ring is adapted to expand radially, when compressed axially, to increase its diameter thereby to prevent the collapse of the expanding medium.

The radial deformation or displacement of the seal ring depends on the hardness of the material of the seal ring. A soft seal ring would be collapsed as it is pressed onto the back-up ring, although it may exhibit a large radial displacement to ensure a larger sealing effect. Therefore, the material of the seal ring is selected to have a larger hardness than the expanding medium.

The seal ring is, however, not effective when the expanding pressure reaches 3000 to 4000 kg/cm² as is the case where a large airtightness and a large fixing force is required between the tube and the tube plate, although it can do pretty well for thin tubes. Namely, the larger radial displacement of the seal ring for ensuring the larger sealing effect and the prevention of the collapse of the seal ring are incompatible with each other, since the collapse prevention is ensured only through an enhanced hardness which provides a poor radial displacement.

Under these circumstance, the invention is aiming at overcoming the drawbacks of the prior art by providing an improved tube expander which is free from the collapse of the expanding medium even at a large expanding pressure.

According to the invention, there is provided a tube expander comprising an elastic expanding medium adapted to be received by a tube to be expanded, a pressurizing rod passing through the expanding medium, a rod-head provided at one end of the pressurizing rod, a back-up ring slidingly passed by the pressurizing rod and seal rings made of an elastic material of a hardness greater than that of the expanding medium disposed close to both ends of the expanding medium and slidingly passed by the pressurizing rod, characterized in that a conical recess is formed in at least one seal ring at a portion thereof facing one end surface of the expanding medium.

The described and other objects, as well as the advantageous features of the invention will become clear from the following description of preferred embodiments taken in conjunction with the attached drawings in which:

BRIEF DESCRIPTION OF THE DRAWINGS

FIG. 1 shows a tube expander embodying the present invention received by a tube to be expanded, particularly a cross-section thereof before the expansion,

FIG. 2 is a cross-sectional illustration explaining a deflection of a seal ring incorporated in the tube expander of the invention, when the ring is axially compressed,

FIG. 3 is a cross-sectional illustration explaining the dynamic behavior of the seal ring when it is deflected,

FIG. 4 is a cross-sectional view of another tube expander received by a tube to be expanded, before the expansion,

FIG. 5 is a cross-sectional view of a seal ring incorporated in the tube expander of the invention,

FIG. 6 is a cross-sectional view of the seal ring of FIG. 5 in a deflected state, and

FIG. 7 is a sectional view of another example of the tube plate to which a tube is fixed by means of a tube expander of the invention, after the expansion.

DETAILED DESCRIPTION OF PREFERRED EMBODIMENTS

Referring at first to FIG. 1 which shows a cross-section of a tube expander embodying the invention received by a tube 1 to be expanded before the expansion, the tube expander includes a cylindrical expanding medium 5 made of an elastic material such as silicon rubber or natural rubber, a pressurizing rod 3 passing through the expanding medium 5, seal rings 7 disposed close to the end faces of the expanding medium and slidingly passed by the pressurizing rod 3, the seal rings 7 having conical recesses 7*d* confronting the ends of the expanding medium and being made of urethane rubber, TEFLON, epoxy or the like material, and a back-up ring 4 adapted to be secured to the end face of the tube plate 2 by straddling the tube receiving bore.

The pressurizing rod 3 is connected to a piston housed by a hydraulic cylinder which are not shown in the drawings.

The arrangement is such that an axial force F exerted by the hydraulic cylinder on a rod-head 3*a* of the pressurizing rod 3 compresses the expanding medium 5 axially, whereby a resulting radial expansion of the

medium 5 expands the tube radially to tightly fit it against the tube plate 2.

As mentioned above, the seal rings 7 incorporated in the expander of the invention are provided at their portions confronting the end surfaces of the expanding medium with conical recesses 7*d*. These recesses are intended for causing a larger radial displacement of the seal rings 7 at portions 7*a* thereof contacting the expanding medium than at opposite portions 7*b*, 7*c*, when the seal rings are subjected to axial compression. The seal rings 7 are adapted to assume their original form when relieved from axial load, and are made of an elastic material for an easy insertion and withdrawal to and from the tube 1, and have a hardness larger than that of the expanding medium 5 so as not to be collapsed by the expanding pressure.

In the embodiment of FIG. 1, a seal ring having conical reces 7*d* is provided at each side or end of the expanding medium 5. However, alternatively, the seal ring having conical recess may be situated at only one side of the expanding medium, preferably at the side closer to the pressurizing rod head 3*a* where a comparatively greater load is imparted so as to shift axially, although it is preferable to use the conically recessed seal ring 7 at both sides of the expanding medium, in order to ensure the prevention of the collapse of the expanding medium 5.

Referring next to FIGS. 2 and 3 showing the manner of deflection of the seal rings, as an axial force F is applied to the pressurizing rod 3, as shown in FIG. 1, the force is transmitted through the seal ring 7 to the expanding medium 5. The axial compression exerted on the seal ring 7 appears uniformly on the surface of the seal ring 7 abutting the back-up ring 4 as substantially equally distributed surface pressure *p*, while, on the surface confronting the expanding medium 5, the pressure increases as it radiates from the center of the seal ring, due to the presence of the conical recess 7*d*.

Thus, the seal ring 7 is subjected not only to the compression load but also to a bending moment M, so that the seal ring 7 is deflected to have a profile shown by a broken line.

The maximum radial displacement δ of the seal ring is the sum of a radial displacement δ_p caused by the surface pressure *p* and that δ_θ caused by the bending moment M, as shown in the following equation 1.

$$\delta = \delta_p + \delta_\theta \quad (1)$$

The radial displacements δ_p and δ_θ caused by the surface pressure *p* and the bending moment M are given by the following equations 2 and 3, respectively.

$$\delta_p = (Pd_1/E)\,\mu \quad (2)$$

$$\delta_\theta = 2Sg \cdot \theta = 2Sg\,(MRg/EI) \quad (3)$$

where,

P: surface pressure on the seal ring kg/cm²

Rg: centroidal radius of the cross-sectional of the seal ring mm

E: Young's modulus of the seal ring kg/mm²

Sg: distance of the seal ring from the centroid mm

θ: angular displacement of the seal ring

M: bending moment applied to the seal ring kg-mm/mm

I: moment of inertia of area around an axis 1—1

d_1: the outer diameter of the ring 7 in the relaxed condition

As will be seen from the equations 2 and 3, the surface pressure *p* and the bending moment M becomes larger as the compression load on the seal ring increases. Therefore, the radial displacement of the seal ring at the portion in contact with the expanding medium gets larger as the compression load increases, thereby to ensure a larger sealing effect and to prevent the fluidizing of the seal ring which would cause the collapse of the expanding medium.

A multitubular heat exchanger was produced employing a tube expander of the invention. No collapsing phenomena of the expanding medium (this medium was a soft rubber having a hardness of 65HsA) was observed even by a surface pressure of 3870 kg/cm², and an uniform expansion of the tube was obtained. The inner diameter of the tube was found to have been increased by about 0.5 mm, as a result of the expansion, and the gap between the outer diameter of the expanding medium and the inner diameter of the tube was 1.1 mm at the maximum.

As have been explained, thanks to the adoption of seal rings having conical recesses, a deflection of the seal ring is effected at its portion confronting the expanding medium, not only by a surface pressure but by a bending moment as well, so that a larger sealing effect is obtained promising a larger effect of preventing the collapsing phenomenas of the expanding medium.

The maximum allowable radial displacement of the seal ring can optionally determined, as far as it falls within an acceptable range for the tube-expanding, by suitably selecting the material, shape and dimension of the seal ring.

Therefore, the allowable gap between the wall of the tube-receiving bore of the tube plate and the outer surface of the tube can be made larger as compared with the tube-expansion relying upon conventional seal rings, which contributes to facilitate the insertion of the tube, resulting in a lowered cost of manufacture of the heat exchanger. In addition, the sealing mechanism for the expanding medium is considerably simplified to much facilitate maintenance and inspection of the tube expander.

FIG. 4 shows another embodiment of the invention. A tube expander is shown in section, received by a tube 1 destined to be fitted to a tube plate 2, at a state before the expansion.

The tube expander of this embodiment comprises a pressurizing rod 3 having a head 3*a*, a cylindrical expanding medium 5, a back-up ring 4 and seal rings 7 (hereinafter called conical seal rings 7) having respective conical recesses 7*d*, similarly to the first mentioned embodiment.

The tube expander of this embodiment is characterized by an additional provision of an auxiliary conical seal ring 8 disposed in the conical recess of the seal ring, the auxiliary seal ring having a shape similar to that of the conical recess and being made of the same material as the seal ring.

As will be seen from an enlarged view of FIG. 5, the auxiliary seal ring 8 has an outer peripheral edge 8*a* in contact with the tapered wall of the recess 7*d*. The auxiliary seal ring 8 further has a tapered surface 8*b* confronting the wall of the recess 7*d* of the conical seal ring 7. The tapered surface 8*b* is inclined with respect to a plane normal to the axis of the ring at an angle smaller than that at which the wall of the 7*d* is inclined, so that a slight gap 9 is formed between the two seal rings 7 and 8.

In use, subsequent to an insertion of the tube 1 to the tube-receiving bore of the tube plate 2, the conical seal ring 7, auxiliary seal ring 8, expanding medium 5, another auxiliary seal ring 8 and another conical seal ring 7 are fitted on the pressurizing rod 7 in the mentioned sequence.

The pressurizing rod 3 thus carrying these members is then inserted into the tube 1. A back-up ring 4 for supporting the axial compression during the expansion is then attached.

An axial force F is applied in the same manner as the first mentioned embodiment to cause the radial expansion of the expansion medium and, accordingly, of the tube.

During this operation of expanding, the conical seal ring 7 and the auxiliary seal ring 8 play respective roles as mentioned below. The conical seal ring 7 assumes a shape as shown in FIG. 5, before the expansion, while, during the expansion the conical seal ring 7 is deformed to assume a shape as shown in FIG. 6 by the axial compression force. Thus, the peripheral edge 7*a* of the conical recess 7*d* exhibits a larger radial deformation than the opposite peripheral edge 7*b* of the conical seal ring 7, so as to be strongly pressed against the inner surface of the tube 1, thereby to prevent the collapse of the expanding medium 5.

As a result of a repeated use of the conical seal ring 7, the inner peripheral edge 7*e* of the peripheral edge of the recess 7*d* is deformed radially outwardly, causing a slight gap δ, between itself 7*e* and the pressurizing rod 3. However, this gap is conveniently covered by the auxiliary seal ring 8 which has been axially moved without being deformed substantially.

In general, as the conical seal ring 7 is used for repeated continuous operations, the gap between the peripheral edge 7*e* of the ring and the pressurizing rod 3 is increased considerably, so as to allow the invasion of the fluidized expanding medium. It is remarkable that this plastic flow of the expanding medium 5 is prevented by the provision of the auxiliary seal ring.

Referring to a practical example of the tube expander of the second embodiment, the expanding medium was made from a soft rubber having a hardness of 65 HsA, while the conical seal rings are formed with a hard rubber having a hardness exceeding 95 HsA. These expanding medium and the seal rings are used for expanding tubes having a diameter of 25.4 mm and a thickness of 1.7 mm. Unfavorable plastic flow of the expanding medium was not observed, and efficient and good tube-expanding was confirmed even after 1000 times of operation.

In order to obtain an increased fixing force and watertightness between the tube and the tube plate, the wall of the tube-receiving bore of the tube plate can have a plurality of grooves 10, as shown in FIG. 7. The tube will then firmly gnaw into the grooves to provide an increased force of fixing and enhanced watertightness.

It will be seen from the foregoing description that the tube expander of the present invention incorporates seal rings disposed at both ends of the expanding medium, at least one of the seal rings having a conical recess at a portion thereof confronting a cylindrical recess. The conical recess causes an additional bending moment on the seal ring, when the later is compressed even by a strong expanding pressure, which in combination with the surface pressure resulted by the compression provides a larger radial deflection of the seal ring, thereby to ensure against plastic flow and a consequent collapse of the expanding medium.

What is claimed is:

1. A tube expander having a tubular, elastic expansion medium having axially opposite end surfaces and adapted to be inserted into a tube which, through a radial expansion thereof, is adapted to be fixed to a tube plate; a pressurizing rod passing through said expansion medium; a pressurizing rod head provided at one end of said pressurizing rod; a back-up ring adapted to be supported by an end of said tube plate straddling a tube-receiving bore of said tube plate, said back-up ring being telescopically received by said pressurizing rod; and seal rings each disposed to abut respective ones of said end surfaces of said expansion medium, said seal rings being of an elastic material having a hardness greater than that of said expansion medium and telescopically received by said pressurizing rod, and at least one of said seal rings having a conical recess at its portion confronting the end surface of said expansion medium.

2. A tube expander as claimed in claim 1, wherein said seal ring closest to said pressurizing rod head has said conical recess.

3. A tube expander as claimed in claim 1, wherein seal rings at both sides of said expansion medium have said conical recess.

4. A tube expander as claimed in claim 3, wherein an auxiliary seal ring is disposed in said conical recess of said seal ring.

5. A tube expander as claimed in claim 4, wherein said auxiliary seal ring has a conical shape similar to that of said conical recess of said seal ring.

6. A tube expander as claimed in claim 1, wherein said conical recess increases in axial width radially inwardly from the outermost peripheral edge of each seal ring that provides the sole engagement between the sealing rings and expansion medium prior to expansion and further provides means for exerting a bending moment on said sealing ring so as to radially expand said peripheral edge to a greater extent than the remaining portions of said sealing rings, upon expansion of said expansion ring to effectively seal the annular gap between the sealing ring and the inner diameter of the tube during expansion of the tube against axial flow of the expansion medium between the sealing rings and the tube during expansion.

7. A tube expander as claimed in claim 6, further including an auxiliary ring telescopically received on said pressurizing rod with the inner diameter of said auxiliary ring being close to the outer diameter of said pressurizing rod, said auxiliary ring having a hardness greater than that of said expansion medium, having an outer diameter substantially less than the outer diameter of each of said sealing rings, and constituting means to seal the gap between the pressurizing rod and the adjacent sealing ring as the sealing ring expands outwardly to prevent flow of the expansion medium between the pressurizing rod and the seal ring during expansion.

8. A tube expander as claimed in claim 7, wherein said auxiliary seal ring has one axial face of complimentary shape to the adjacent face of said expansion medium, and an opposite axial face that is conical at an angle with respect to a plane perpendicular to said pressurizing rod to a lesser extent than the adjacent conical face of its seal ring.

9. A tube expander as claimed in claim 1, further including an auxiliary ring telescopically received on

said pressurizing rod with the inner diameter of said auxiliary ring being close to the outer diameter of said pressurizing rod, said auxiliary ring having a hardness greater than that of said expansion medium, having an outer diameter substantially less than the outer diameter of each of said sealing rings, and constituting means to seal the gap between the pressurizing rod and the adjacent sealing ring as the sealing ring expands outwardly to prevent flow of the expansion medium between the pressurizing rod and the seal ring during expansion.

10. A tube expander as claimed in claim 9, wherein said auxiliary seal ring has one axial face of complimentary shape to the adjacent face of said expansion medium, and an opposite axial face that is conical at an angle with respect to a plane perpendicular to said pressurizing rod to a lesser extent than the adjacent conical face of its seal ring.

Tube Enhancement Development

Several alternate processes are being evaluated in an effort to reduce the cost of enhanced tubing for heat exchangers.

During the course of the tube enhancement development program it was decided to investigate processes that required one piece tooling (i.e., male or female). This decision was reached due to the large number of corrugations required (36) and the apparent lack of available space for two piece tooling. As such, isostatic pressing was evaluated.

A male tool was made to the reverse geometry (i.e., desired contour of 36 flutes for production parts on I.D.) because of ease of fabricability (Figure A). A 5052-0 aluminum alloy tube was placed over the die and the ends sealed. The tube was then placed in an isostatic press and pressurized to 60,000 psi. The I.D. of the tube conformed to the outermost contour of the die but not the innermost portion. A cross-section of the resulting shape is shown in Figure B and an overall view shown in Figure C. It was concluded that higher pressures were required. The same procedure was repeated with commercially pure titanium. Very little forming was achieved, as anticipated, due to the higher strength of the titanium. Inasmuch as significantly higher pressures could not be achieved with commercially available isostatic presses, hot pressing was considered. By heating the material to 1500°F to 1800°F it was possible that, due to the lower strength of the material at temperature, the pressures available with existing facilities could be utilized to produre satisfactory results. To this end, superplastic forming (SPF) was evaluated.

The SPF process consisted of heating a die with the desired profile machined into one surface to approximately 1650°F and applying 600 psi pressure (the limit of the equipment). Using this technique the geometry produced is shown in Figures D and E. It was concluded from these efforts that still higher pressures were required to achieve total conformity to the die.

To obtain higher pressures, hot isostatic pressing (HIP) was evaluated. A die with the desired contour machined into one surface was completely encased in a titanium case, evacuated, and sealed. The encased die was then placed
in an isostatic press, the temperature raised to 1650°F and the pressure raised to 15,000 psi. The results are TBD (hopefully by Tuesday 10/19/78).

The production application of this process is envisioned as a multi-cavity heated die into which tubing is placed. The tube(s) will then be internally pressurized with argon gas thereby forcing the tube to conform to the die.

One of the methods employing two piece tooling that was evaluated was roll forming. This process utilizes opposed rolls which roll the corrugated contour into the sheet material. The formed sheet will then be rolled into a tubular shape and fusion welded. Figure F shows a cross-section of corrugated sheet with a 0.132 inch pitch which has been partially formed into a circular cross-section. To date, a pitch of 0.100 inches has been produced which results in 31 corrugations. Figure G shows a cross-section of the corrugations.

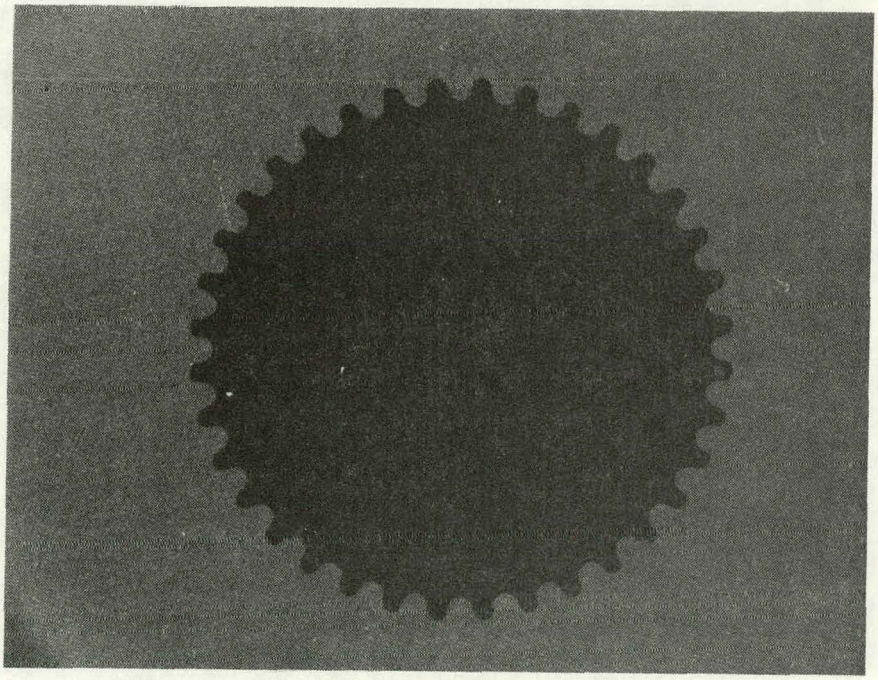

Figure A. Photograph of male die (Mag. 3x)

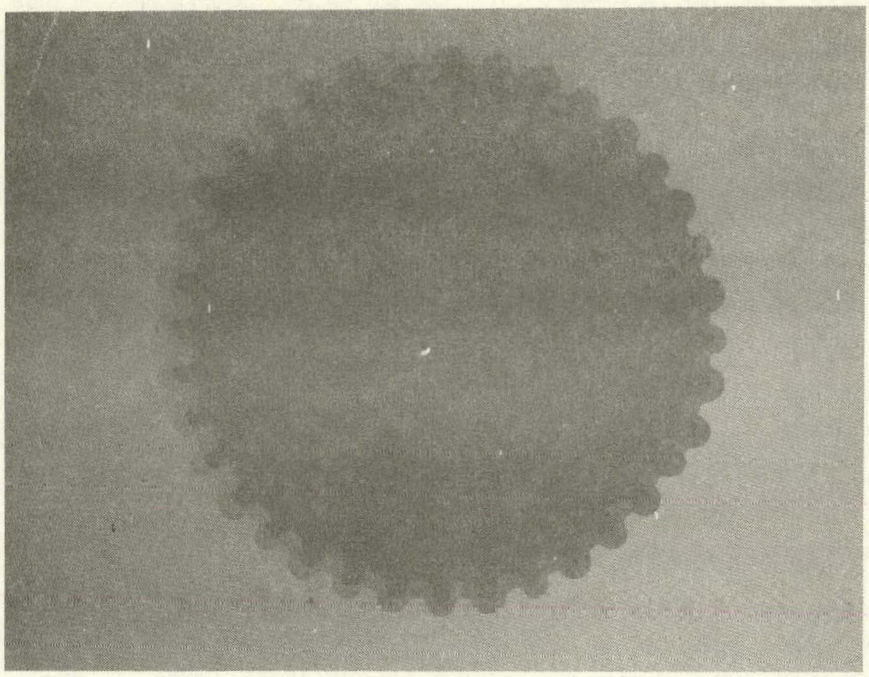

Figure B. Cross-section of 5052-O Aluminum Tube After Isostatic Pressing at 60,000 psi (Mag. 3x)

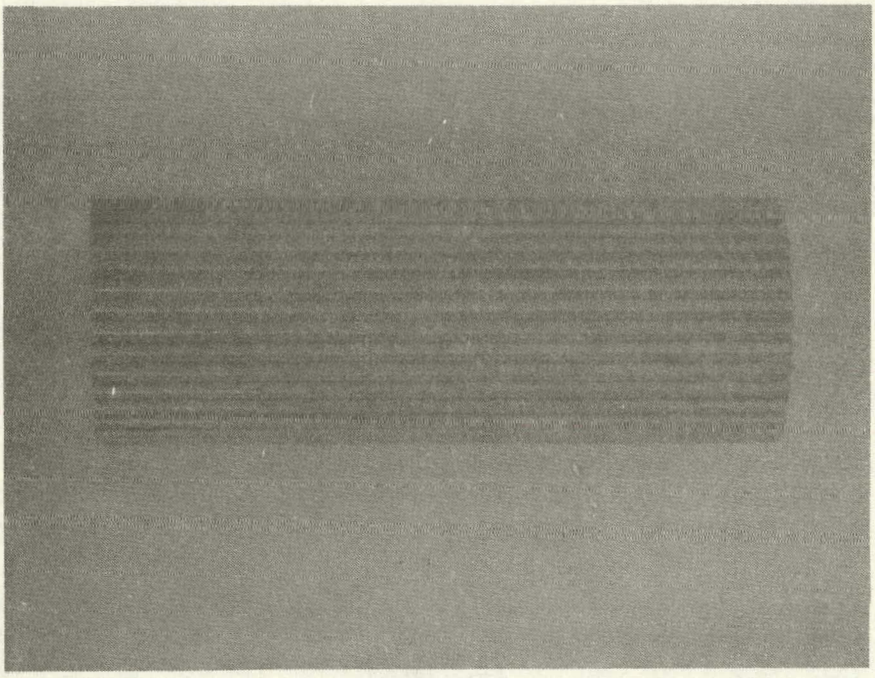

Figure C. View of 5052-O Tube Formed by Isostatic Pressing at 60,000 psi (Mag. 1-1/4x)

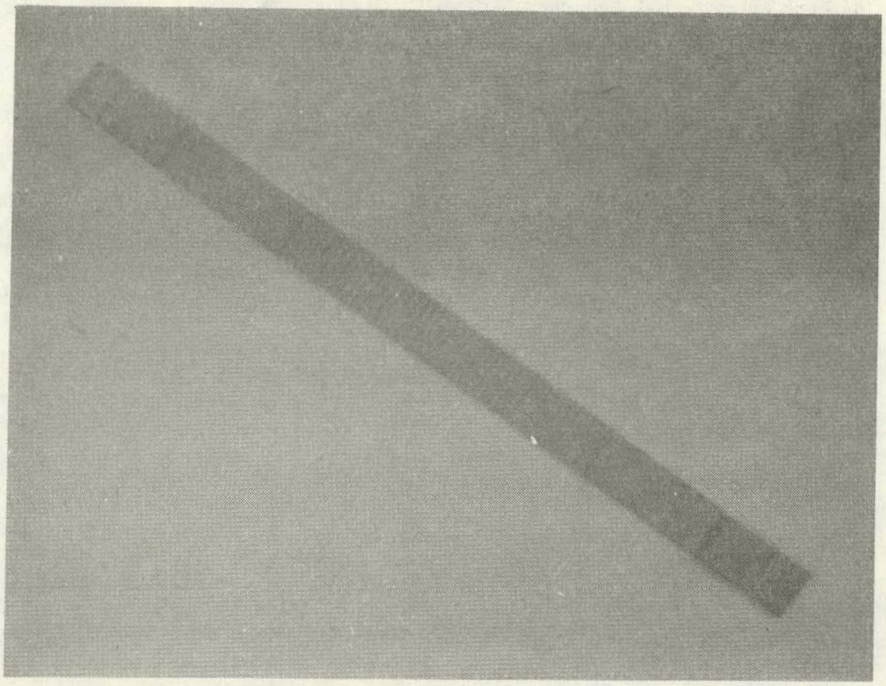

Figure D. View of the Contour Produced by SPF.

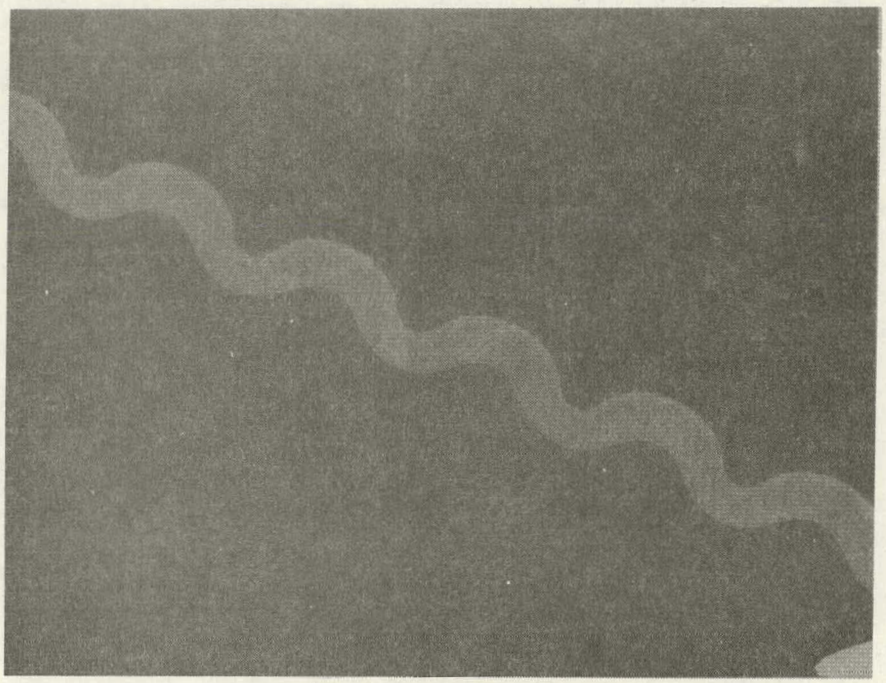

Figure E. Cross-section of Part Shown in Figure D (Mag. 10x)

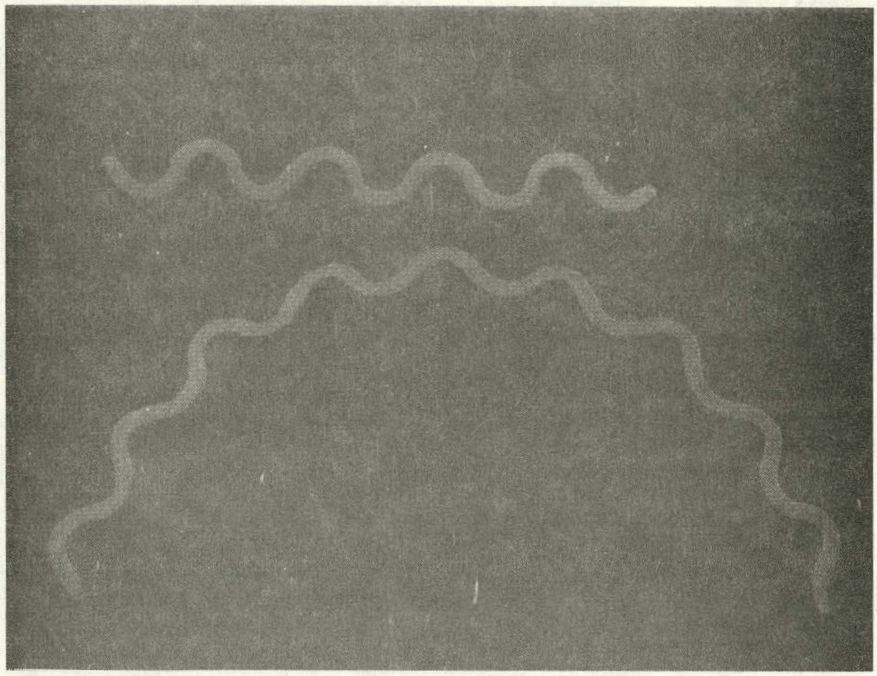

Figure F. Flat Pattern With 0.132 Pitch Rolled Into a Tubular Cross-section (Mag. 5x)

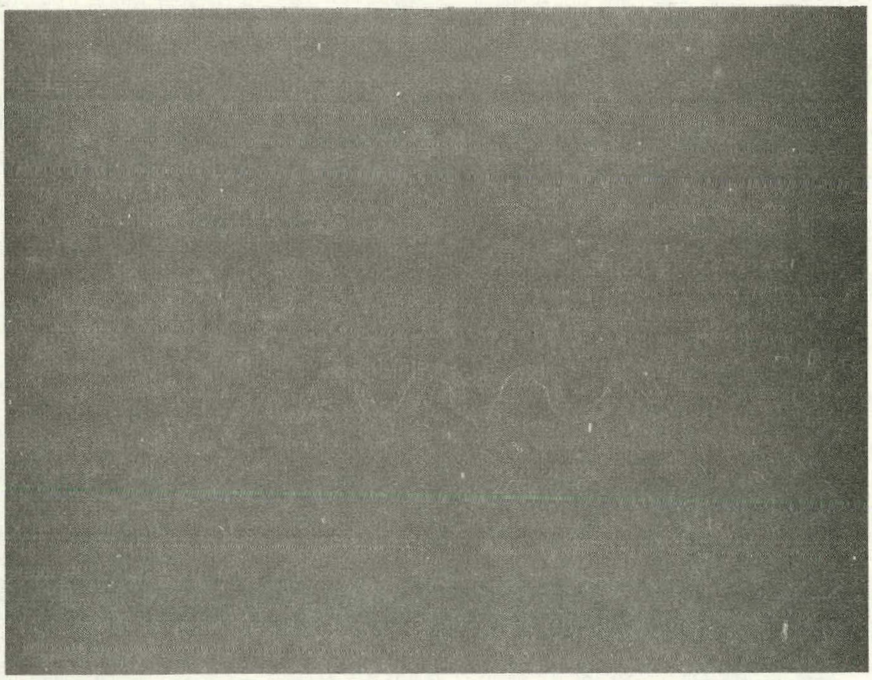

Figure G. Cross-section of Corrugated Sheet With a Pitch of 0.100 Inches (Mag. 5x)

Toshiba High Heat Flux Titanium Tube

Toshiba Research and Development Center

Toshiba Metal Products Division

The generation of power from heat sources with low enthalpy, such as geothermal resources, sea water, low temperature water which is rejected from power stations and factories is becoming increasingly important.

As the energy extraction system mentioned above, fluid from geothermal wells, power stations and factories exchanges heat through a series of heat exchangers to a secondary fluid. For example, freon or isobutane is used. The fluid is evaporated and expanded to turn a turbine to generate electricity. The fluid is then cooled in a condenser using cooling water and then returned to the heat exchanger system.

In this system, the heat exchanger requires ten times more surface area than that of a thermal power plant, because of the low temperature difference between the heat source fluid and a secondary fluid, as well as because of the low heat conducting coefficient of the secondary fluid. According to a trial calculation of the system, the cost of the heat exchangers for 10-MW plant represents approximately 30 percent of the total plant equipment cost. Decreasing the heat exchanger cost is an important factor in the system development.

Toshiba high heat flux tube, introduced in the catalog has been developed for a binary cycle power generation system using hot geothermal water, sea water and so on. The developed process enables fabricating the tube surface in a contoured shape which consists of ridges and valleys for enhancement of heat transfer coefficient. For an example of condensing heat transfer, the appropriate contoured

surfaces utilize surface tension to push the condensate in the drainage channels, as was first pointed out by Gregorig, resulting in enhancing tube heat transfer coefficients. Tube characteristics are as follows:

High heat transfer coefficient

As the condensed film on the tube is pulled into the channels and becomes thinner due to spreading over the contoured surface, condensing heat transfer coefficient of the tube is 8 - 15 times higher than that of a flat tube.

No limitation to tube materials in fabricating the contoured surface

Not only aluminum, copper and their alloys, but also titanium and its alloys and stainless steels, which have superior corrosion resistance to geothermal hot water and sea water, which contains many of corrosive elements, such as Cl^-, SO_4^{--}, NH_4^+ and H_2S gas, can be fabricated into the contoured surface that enhances heat transfer coefficient. Especially, the latter two metals entail difficult fabrication properties.

Economy superiority

Plant cost and space are saved by making the heat exchanger compact.

1. Toshiba high flux tube production method

1.1 Toshiba's fabrication process

The process is illustrated in Fig. 1. First, the plate is cold rolled and the appropriate contoured surface is fabricated. Then,

the plate with the contoured surface is run out in a tubular shape by roll forming and welding.

A precise contoured surface with 1.0mm pitch, suitable for enhancing heat transfer is obtained by the process. This precision manufacturing is difficult by ordinary fabrication process, such as machining, extrusion and drawing. The process is especially suitable for fabricating the contoured surface on titanium and its alloys and stainless steels.

1.2 Tube materials

Due to adoption of Toshiba's process, there is no limitation as to tube materials which can be used in fabrication of the contoured surface. The process is applied economically to titanium and its alloys and stainless steels.

1.3 Contoured surface

The contoured surface is decided by pitch, radius of curvature and depth, as shown in Fig. 2. Contoured surfaces, which are possible to fabricate on titanium and its alloy and stainless steels, are shown in the following.

Pitch	: 0.5 ~ 5 mm
Radius of curvature	: 0.1 ~ 3 mm
Depth	: > 0.3 mm

1.4 Tube types

Tubes with the contoured surfaces outside, inside (shown in Fig. 3A or B), or both sides (the so called doubly fluted tube), can be produced by the process.

2. Toshiba high heat flux titanium tube specifications

An example of the specification is shown in Table 1. The outer diameter of the tube produced in Toshiba is 8mm to 50mm.

3. Toshiba high heat flux titanium tube external appearance

Tubes are shown in Figs. 4A and B.

4. Toshiba high heat flux titanium tube contoured surface

The cross section of Toshiba high flux titanium tube with 1.0mm and 1.5mm in pitch, and 0.5mm in depth are shown in Fig. 5A and B.

5. Toshiba high heat flux titanium tube heat transfer coefficient measurement results

Condensing heat transfer coefficients for tubes which have the same contoured surface as that shown in Figs. 5A and B, are shown in Fig. 6. Compared with a flat titanium tube, the condensing heat transfer coefficient for Toshiba high flux titanium tube is 8 to 15 times higher than that of a flat tube. Heat transfer coefficients were measured in Toshiba Research and Development Center in a vertical state.

6. Toshiba high heat flux titanium tube heat transfer enhancement mechanism

Condensed fluids flow on the contoured surface due to a combination of gravity and surface tension forces, as shown in Fig. 7. In an actual case, as the surface tension force in the horizontal direction is ten times larger than the gravity force in the vertical direction, the condensed fluids on the surface are pulled from the ridges to the valleys and flow in channels in the vertical direction.

For this reason, the condensed films become thinner, resulting in enhancing condensing heat transfer coefficients.

7. Applications

Home electric appliances

Condenser, evaporator for air conditioner

Heat pipes

Heavy electric appliances

Binary cycle power generation and solar sea power plant heat exchanger tube.

Vertical-multi-effect type desalination plant.

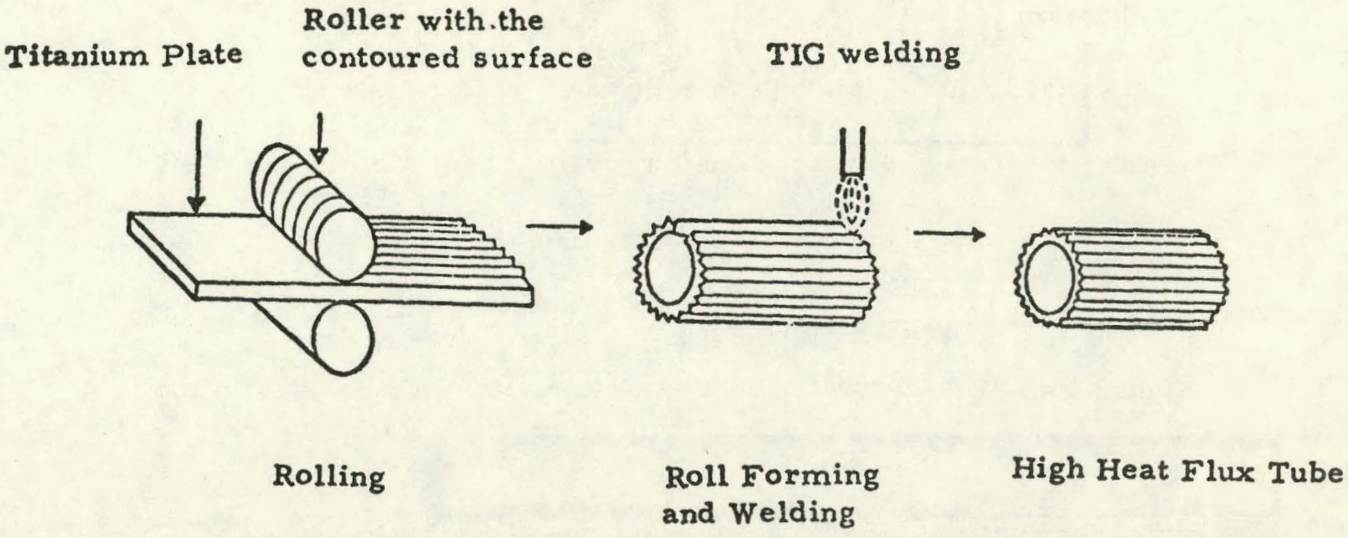

Fig. 1 Toshiba High Heat Flux Titanium Tube Fabrication Process.

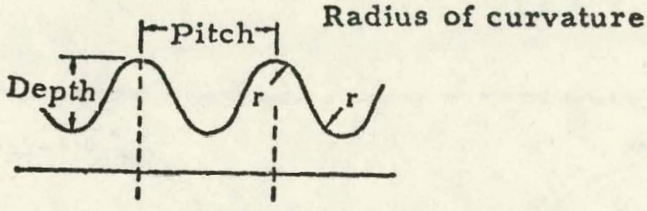

Fig. 2 Contoured Shape

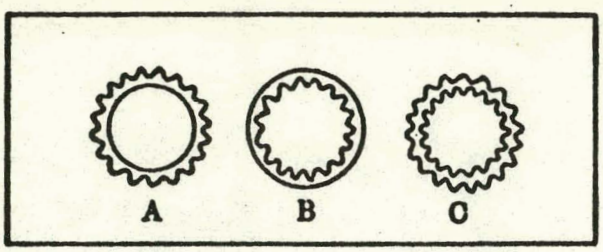

Fig. 3 Tube Types

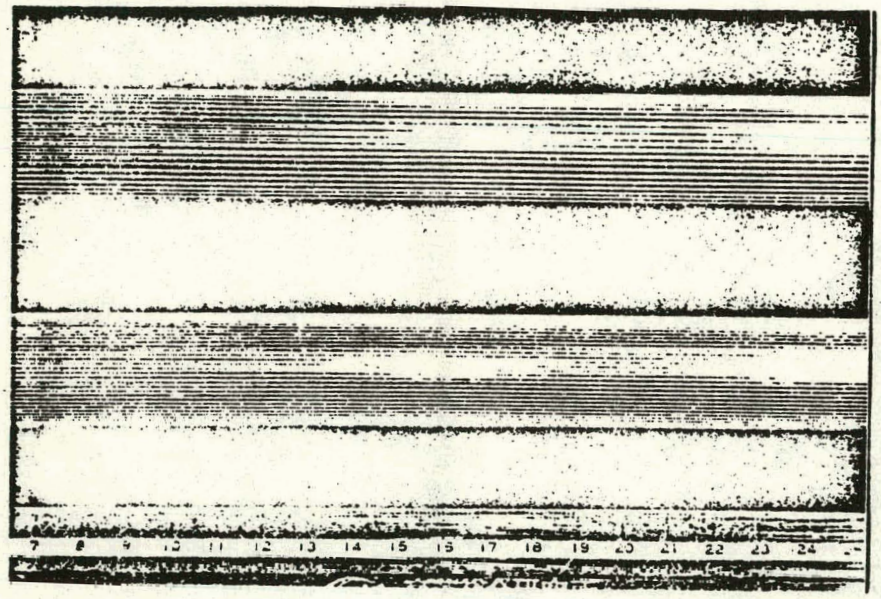

(A) External Appearance

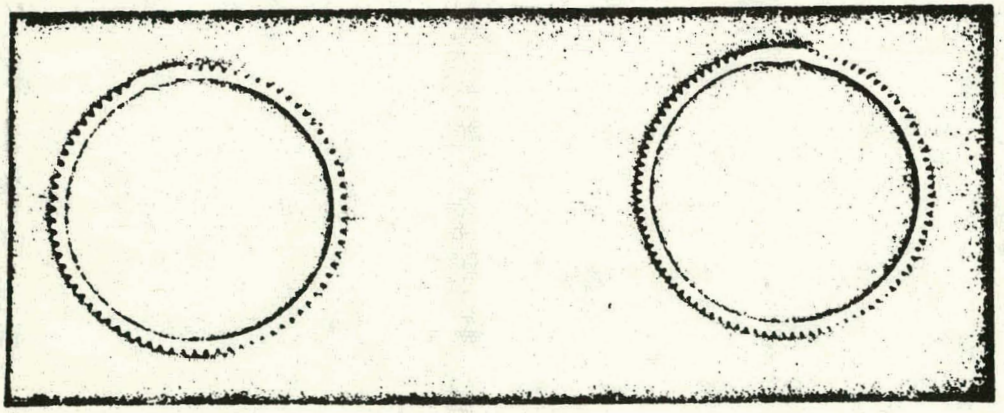

(B) Cross Section

Fig. 4 Toshiba High Heat Flux Titanium Tube

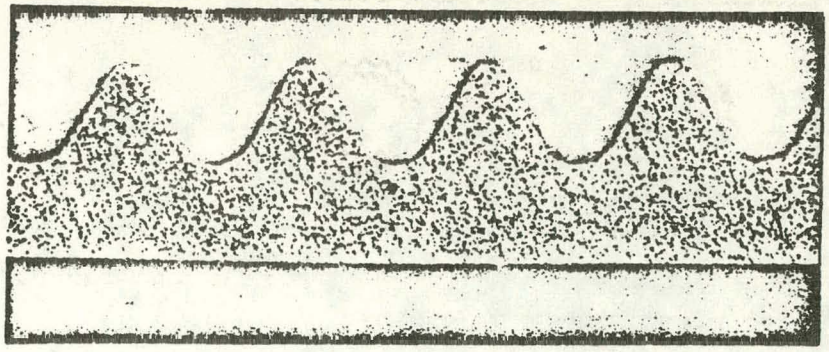

(A) Pitch .04 in., Depth: 0.2 in. x 25

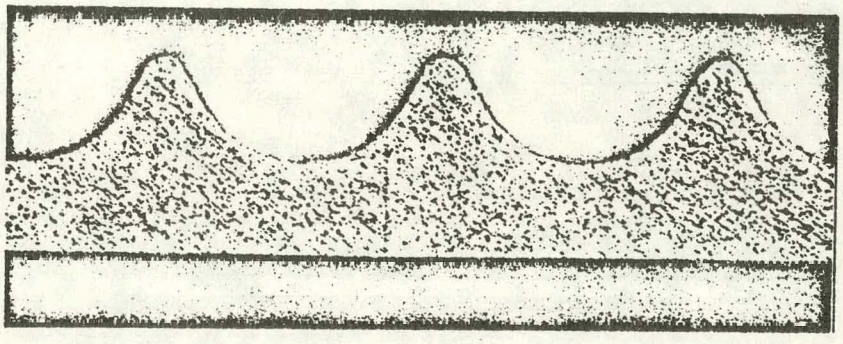

(B) Pitch .06 in., Depth: .02 in. x 25

Fig. 5 Toshiba High Heat Flux Titanium Tube Contoured Surface

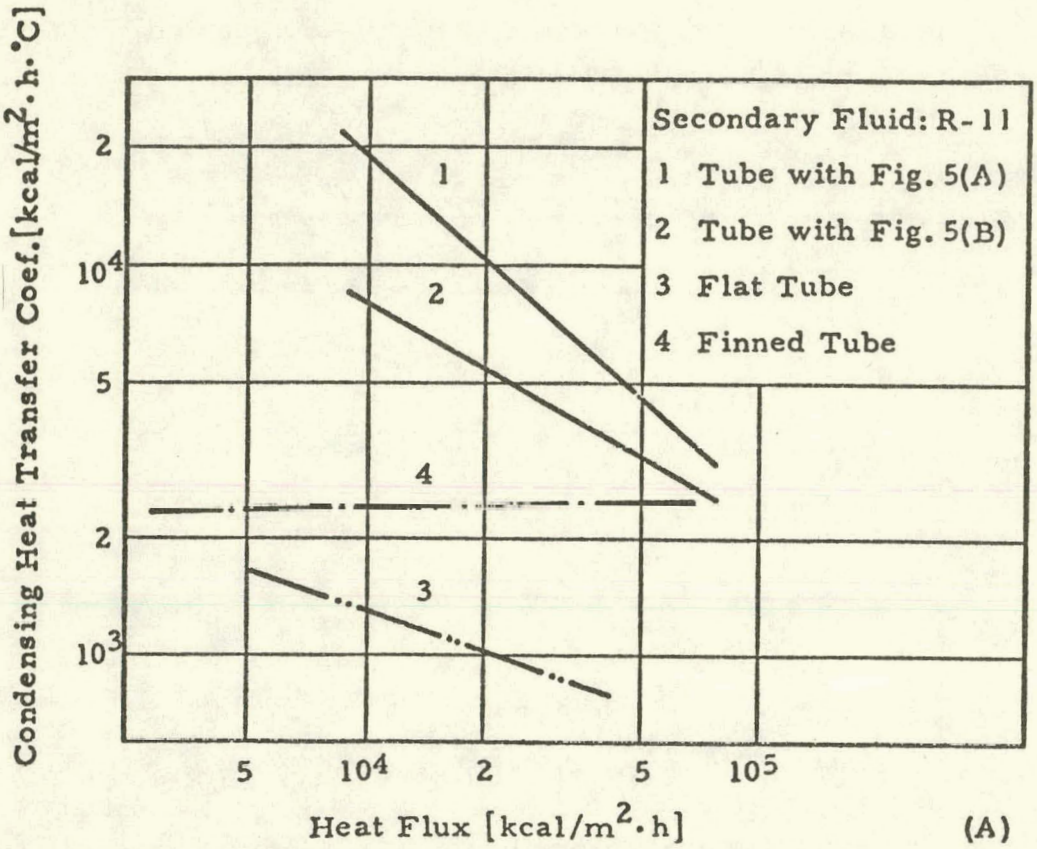

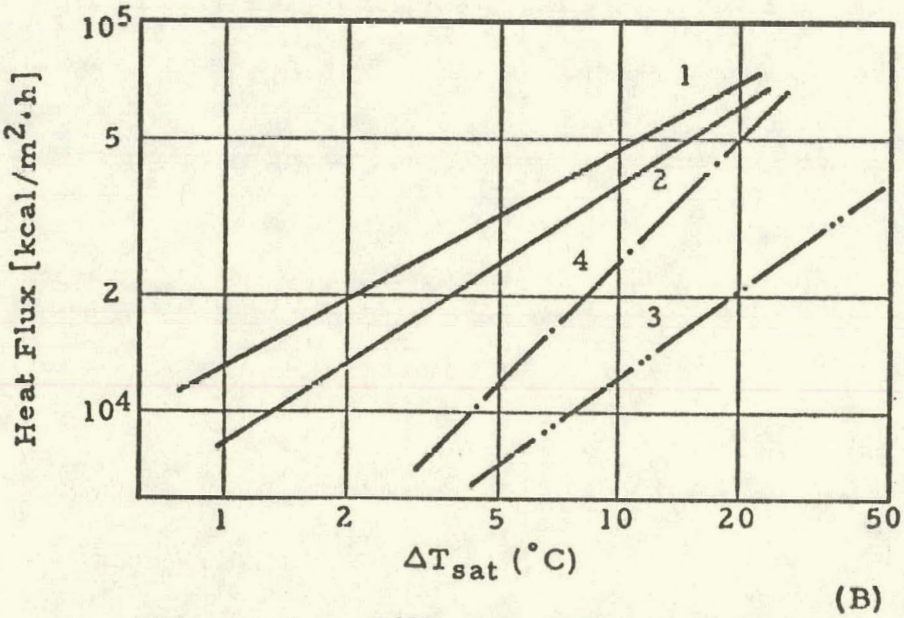

(Temperature Difference Between Tube Surface and Saturated Freon 11 Fluid)

Fig. 6 Measurement Results of Heat Transfer Coefficients of Toshiba High Heat Flux Titanium Tube.

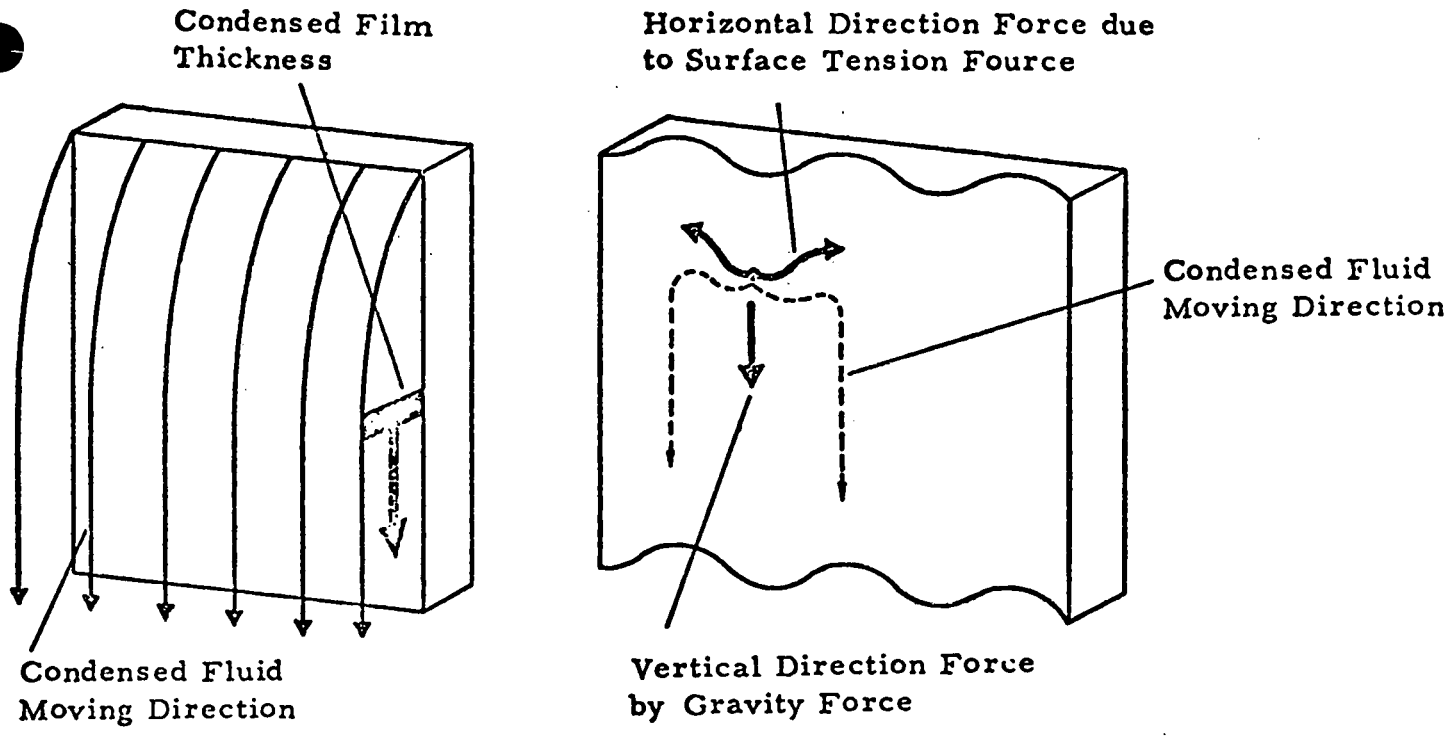

Fig. 7 Toshiba High Heat Flux Titanium Tube
Heat Transfer Enhancement Mechanism

Table 1 Toshiba High Heat Fluex Titanium Tube Specifications.

Types	Dimension	Pitch (p)	Thickness (t)		Outer Diameter (D)	
			Max.	Min.	Max.	Min.
Types A and B	1p x 0.5t x 25.4D	1 ± 0.1	1± 0.06	0.5 ± 0.08	25.4	24.9
	1.5p x 0.5t x 25.4D	1.5± 0.1	1± 0.06	0.5 ± 0.08		
Type C	1p x 0.5t x 25.4D	1 ± 0.1				

Dimensions : mm

BALCKE-DÜRR
Sonderdruck A 31e

from
VGB KRAFTWERKSTECHNIK
Volume 56, No. 7

Hydraulic Expansion — a new method for the anchoring of tubes

H. Krips und M. Podhorsky

Production Programme

Steam Generators	for all capacities, pressures and temperatures to be installed in power stations for fossile fuels, in nuclear power plants, and for waste heat recuperation in industrial plants.
Firing Systems	for all fuels.
Heat Exchangers	to be installed in power stations as well as in chemical and petrochemical industries, for air conditioning and refrigerating systems.
Water Recooling Systems	designed as natural or mechanical draught wet or dry or combined (hybride) cooling towers, package cooling towers, industrial air coolers, complete cooling water supply systems.
Condensers	air-cooled or water-cooled.
Feedwater Tanks	and deaeration plants.
Air Heaters	fluo-gas-heated or steam-heated.
Sanitary and Domestic Equipment	heating systems, ventilation and air conditioning plants, pipework.
Pumps and Compressors	
Conveyor Systems	for furnace residues and bulk materials.
Low Pressure Fans	with low noise level, impeller dia. up to 26 m.
Fin Tubes	made of steel or nonferrous metals.

Hydraulic Expansion
— a new method for the anchoring of tubes

*By H. Krips and M. Podhorsky**

The conventional method of mechanical rolling for expanding tubes into the tube plates of heat exchangers has for some time been the target of justified criticism both from engineers supplying the chemical industry and from those supplying equipment for nuclear plants. The joint between tube and tube plate is an important consideration, both from safety and from process engineering aspects. Pressure-tightness, shaping in the transition area between the anchoring zone and the unstressed tube, and proper sealing of the gap are all essential requirements for the reliability and life of valuable plant components. The conventional method of mechanical rolling expansion does not adequately meet these requirements.

INTRODUCTION

The mechanical deformation produced by rolling the tube walls results in stresses which cannot be accurately determined because of the inherent irregularities of the method. Such stresses make the tube susceptible to, or increase the risk of, corrosion. The end gap cannot be closed by rolling without risking shearing of the tube. Any improvement to this mechanical method can only be partially successful and thus one is compelled to look for a different method.

The hydraulic expansion method described below eliminates the inadequacies encountered in the past. The advantage of a hydraulic method rests in the fact that the working pressure of the liquid can be accurately determined. This affords the necessary consistency of a repetitive process, and thus allows tube anchorage calculations to be performed. Only a method whose results can be calculated beforehand will ensure adequate reliability of the equipment.

In almost all fields, development work leads to equipment of ever increasing unit size, with the number of heat exchanger tubes increasing as the square of the heat exachanger diameter. In view of the great number of tube anchorages, which may total several thousand in a single item of equipment, the reliability of this joint is of decisive importance. The bigger the item of equipment, the more important is its degree of availability, and this depends largely on the pressure-tightness of the individual tubes. Sufficient reliability of the equipment under all operating conditions can only be assured by tube joints meeting superior quality standards. Efforts to improve the quality of conventional mechanically rolled tube joints encounter limits due to physical factors. It is unlikely that substantial further progress will be made in this field in the foreseeable future.

Hydraulic expansion of tubes is a method which, although in its early days, has already yielded good results. Predictability, accurate consistency, ease of handling and the associated economy are major advantages of the hydraulic method. Like rolling, it can be combined with a welding operation. A combination of the hydraulic and mechanical methods might be an interesting proposition for certain designs.

* *Oberingenieur H. Krips and Dr.-Ing. M. Podhorsky, Balcke-Dürr AG, Bochum.*

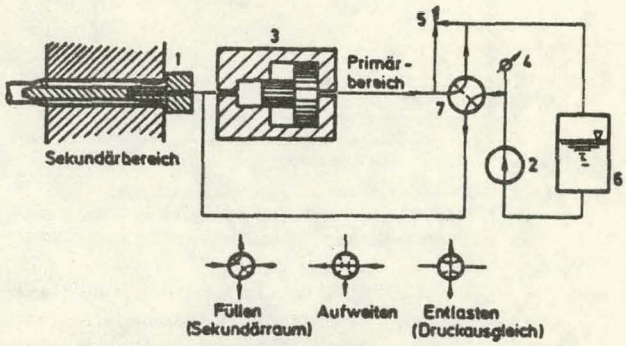

Fig. 1. Diagram of the tube-expansion installation.

Sekundärbereich	= Secondary section
Primärbereich	= Primary section
Füllen	= Fill
(Sekundärraum)	= (secondary space)
Aufweiten	= Expand
Entlasten	= Relieve
(Druckausgleich)	= (pressure equalization)

DESCRIPTION OF THE METHOD

Hydraulic expansion differs from all other known anchoring methods in that the tube is plastically deformed simply by means of a pressurized liquid. Under the pressure exerted by this liquid, the tube material flows until it reaches the wall of the bore. By increasing the pressure further, the tube is pressed against the wall of the receiving bore. The pressure is increased until the bore has been so deformed that the tube disc will lock permanently around the tube as a result of the elastic recovery of the disc when the pressure is removed. The tube expander is simple and neatly arranged as can be seen from Figure 1. It consists of probe 1, pump 2, booster 3, pressure gauge 4, overflow valve 5, hydraulic fluid tank 6 and control valve 7. A mobile tube expander is shown in Figure 2.

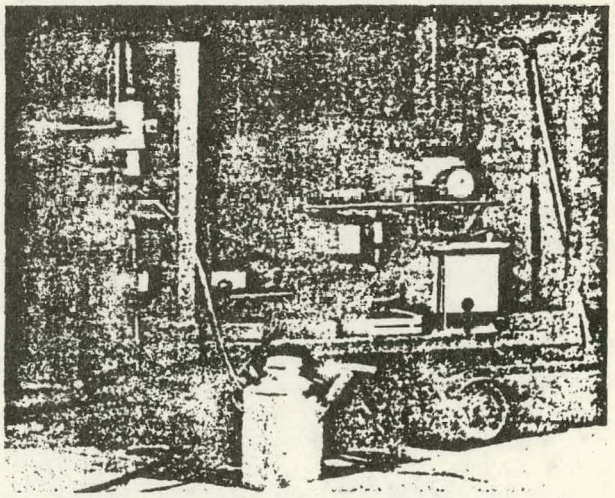

Fig. 2. Mobile tube expander.

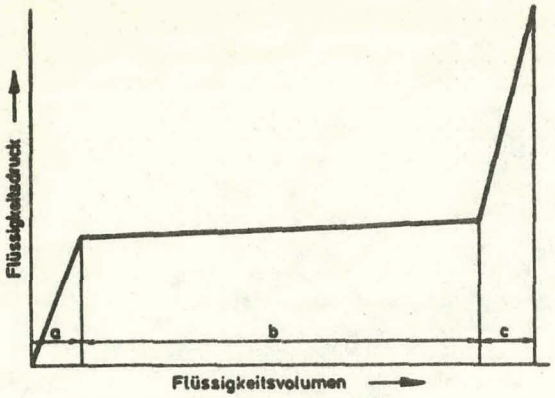

Fig. 3. Deformation during the expansion operation.
Flüssigkeitsdruck = Liquid pressure
Flüssigkeitsvolumen = Liquid volume

The probe 1 inserted in the tube is provided with two sealing elements which limit the range of expansion. Before expansion can commence, the secondary section must be filled with liquid and the booster 3 pushed into its inital position. This is achieved by actuating the control valve 7. The high-pressure pump 2 generates the primary pressure required to operate the equipment. The booster 3 intensifes this pressure to the secondary pressure level required for the tube expansion operation. Since the pressure intensification ratio of the booster is constant, the final pressure in the secondary section must be set by limiting the pressure in the primary section.

The operating pressure in the secondary section is checked by means of pressure gauge 4, which is connected to the primary section. The primary pressure is set by means of overflow valve 5. As soon as the desired maximum pressure has been reached, the overflow valve 5 discharges liquid from the primary section into tank 6. To enable the probe to be withdrawn from the expanded tube, control valve 7 must be operated in order to equalize the pressure between the secondary space and the tank 6.

Figure 3 illustrates the deformation of the tube and tube disc during the expansion operation. The amount of pressurized liquid introduced is a function of the proportions of elastic and plastic expansion occuring in the tube and tube disc. In zone a), the tube is stressed elastically until the yield point is reached. In zone b), the tube material flows until it has bridged the gap between the outside diameter of the tube and the wall of the receiving bore. This plastic flow is usually accompanied by a strain-hardening effect and is reflected in the upward slope of the pressure curves. On reaching zone c), the tube bears against the wall of the receiving bore. From this point onwards, the tube undergoes further plastic deformation, and the tube plate now deforms elastically. The final pressure of zone c) is calculated on the basis of the material selected, the tube disc geometry and the desired adhesion pressure, and it is set on overflow valve 5.

Figure 4 a shows the zone of contact between an expanded tube and the wall of the receiving bore. The roughness of the bore wall and that of the tube surface determine the extraction force. Where a greater extraction force is required, the wall of the hole is provided with a shallow circular recess. The depth of this groove is no more than a few tenths of a millimetre. A tube expanded into a recessed hole is shown in Figure 4 b. This shows clearly how accurately the tube has been formed to the shape of the receiving bore under the high hydraulic pressure applied. The recess is produced in a manner similar to that employed for rolled grooves except that the cutting tool used has very mild contours.

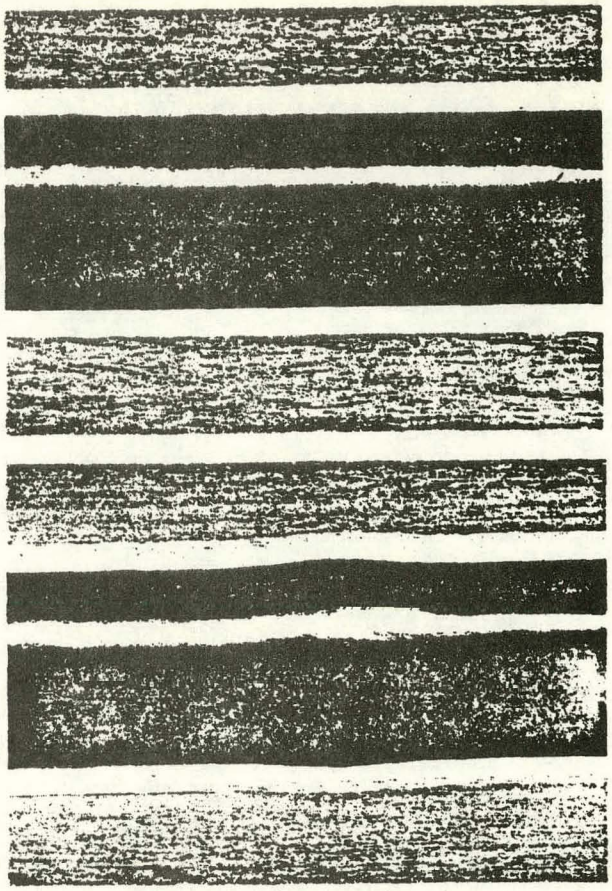

Fig. 4. Expanded tube.
a) in a straight-walled bore
b) in a recessed bore

ADVANTAGE OF THE EXPANSION DEVICE

The pressure probe can be inserted into the tubes without damaging them. The device is easy to handle and move (Figure 5). The insertion depth can be accurately fixed. Operation is by means of a simple lever (Figure 6).

The expansion operation as such does not take more than a few seconds. The probe can be pulled out with ease after the pressure has been removed. The useful life of the sealing elements is, of course, limited.

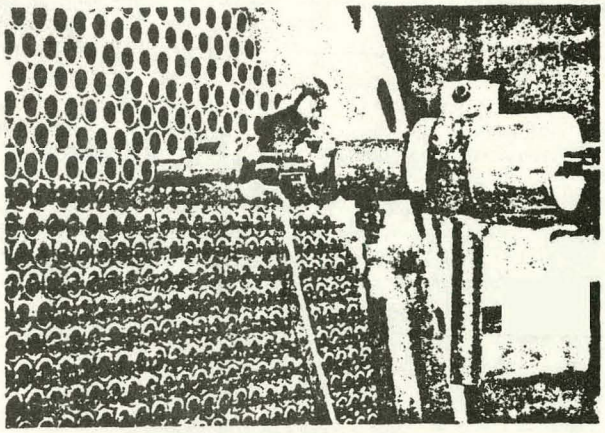

Fig. 5. Hydraulic expansion device.

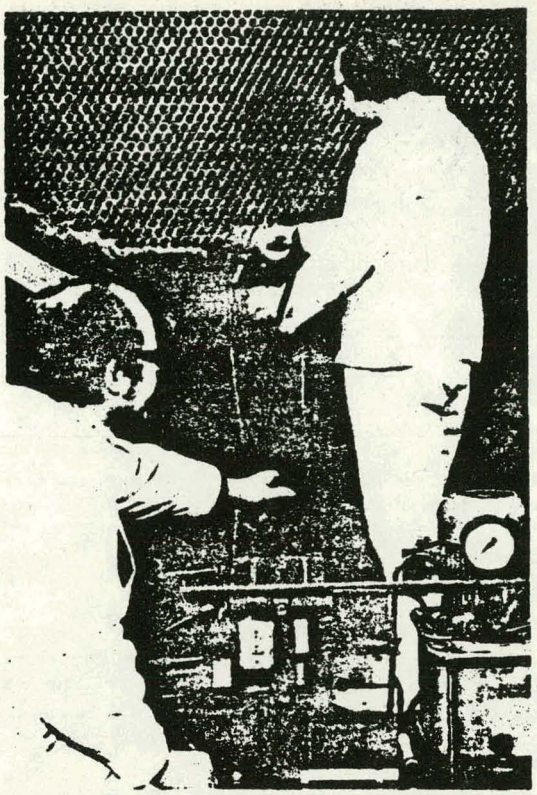

Fig. 6. Handling of the expansion plant.

Replacing these elements is, however, neither difficult nor time-consuming. Each expansion operation verifies at the same time the existence of proper adhesion in the respective tube joint, because adhesion between the tube and the receiving bore is determined exclusively by the selected pressure, which can be checked on the pressure gauge. Check measurements of the diameter of the expanded tube are not only superfluous, but might even lead to wrong conclusions. Thus, with a wall thickness of 2.9 mm, a spacing of 30 mm and a calculated adhesion pressure of 728 bar (see numerical example), an inaccuracy of no more than 0.002 mm in the measurement of the inside diameter would result in an error of 10%.

Since no mechanical tool is involved in deforming the tube, the material will naturally adopt the shape having least internal stress. Bores with adhering revolving shafts are no exception to this rule. This property is of great importance for all materials susceptible to stress corrosion cracking.

The expansion zones can be accurately defined. This permits the gap between tube and tube plate to be avoided, even at the end of the receiving bore on the inner side of the tube plate, the expansion zone being located at the end of the bore. In conventional roll-expanded tube joints the tubes could not be expanded to the end of the bore without risking damage, and thus gaps were left as potential nests of corrosion.

No additional tools are required in cases where contact between tube and tube plate is to extend over great lengths in order to preclude the formation of a heat-insulating gap or to assure continuous adhesion. The difference in time required for expanding a short or long section is negligible.

In tubes which are anchored in two fixed tube plates, axial stresses are produced both in the case of hydraulic expansion and in the case of mechanical roll expansion. These included stresses produce a load on the tube disc. However, the axial stresses produced by hydraulic expansion and those produced by mechanical roll expansion act in opposite directions. Consequently, if hydraulic expansion and mechanical roll expansion are employed in an appropriately matched combination, it is now possible to anchor tubes in apparaturs having two fixed tube plates with balanced stress or a predetermined amount of prestress.

The economy of the new method can only be assessed by comparing it with the conventional roll-expansion method, although the two methods and the different results achieved by them can hardly be compared.

Assuming, for the sake of comparison, that the two methods produce the same effect, the costs of hydraulic tube expansion are slightly lower than those of rolling in two steps, because a comparison clearly favours the hydraulic method as soon as the length to be rolled exceeds 30 mm.

TUBE ANCHORAGE CALCULATION

The hydraulic method provides a clear basis for calculating the expansion pressure required to achieve a desired adhesion pressure.

The adhesion pressure is a measure of the force preventing the tube plate from being extracted from the bore. For the purposes of the following calculation, adhesion pressure will be substituted for the previously used criterion of adhesive expansion.

The thick-walled tube under conditions of dynamically balanced surface loading

Hydraulic expansion produces a dynamically balanced stress field first in the tube and later, approximately, in the tube plate also.

Assume that the longitudinal stress is equal to zero (plane stress). The equilibrium equations for the element are thus considerably simplified. Taking advantage of the convenience afforded by polar coordinates, we have:

$$\frac{d}{dr}(r \cdot \sigma_r) - \sigma_\varphi = 0 \qquad (1)$$

The stress-strain relationships are:

$$\varepsilon_r = \frac{dw}{dr} = \frac{1}{E}(\sigma_r - \mu \cdot \sigma_\varphi) \qquad (2)$$

With the stress function F and the stresses

$$\varepsilon_\varphi = \frac{w}{r} = \frac{1}{E}(\sigma_\varphi - \mu \cdot \sigma_r).$$

$$\sigma_r = \frac{1}{r}\frac{dF}{dr} \qquad (3)$$

$$\sigma_\varphi = \frac{d^2F}{dr^2}$$

the equilibrium condition (1) is fully satisfied. We must therefore apply the compatibility condition

$$\frac{d}{dr}(r \cdot \varepsilon_\varphi) - \varepsilon_r = 0 \qquad (4)$$

With (2) and (3), we obtain the homogenous differential equation

$$\frac{d^3 F}{d r^3} + \frac{1}{r}\frac{d^2 F}{d r^2} - \frac{1}{r^2}\frac{d F}{d r} = 0 \qquad (5)$$

the solution of which can be written as follows:

$$F = A \cdot \lg r + C\, r^2 \qquad (6)$$

The constants A and C are determined from the limiting conditions in accordance with Figure 7. The following applies:

$$\sigma_{r_i} = -p_i \qquad \sigma_{r_a} = -p_a \qquad (7)$$

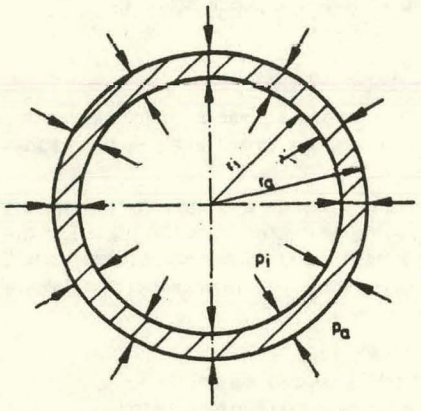

Fig. 7. Loads acting on a tube.

Using (3) and (6) the constants can be expressed as:

$$A = \frac{r_i^2 \cdot r_a^2 (p_a - p_i)}{r_a^2 - r_i^2}; \qquad C = \frac{1}{2}\,\frac{p_i r_i^2 - p_a \cdot r_a^2}{r_a^2 - r_i^2} \qquad (8)$$

The stresses can then be expressed as follows:

$$\sigma_r = \frac{r_i^2 \cdot r_a^2 (p_a - p_i)}{r_a^2 - r_i^2}\,\frac{1}{r^2} + \frac{p_i \cdot r_i^2 - p_a \cdot r_a^2}{r_a^2 - r_i^2}$$
$$\sigma_\Phi = -\frac{r_i^2 \cdot r_a^2 \cdot (p_a - p_i)}{r_a^2 - r_i^2}\,\frac{1}{r^2} + \frac{p_i \cdot r_i^2 - p_a \cdot r_a^2}{r_a^2 - r_i^2} \qquad (9)$$

The stresses are simplified for $p_a = 0$:

$$\sigma_r = \frac{r_i^2 \cdot p_i}{r_a^2 - r_i^2}\left(1 - \frac{r_a^2}{r^2}\right)$$
$$\sigma_\Phi = \frac{r_i^2 \cdot p_i}{r_a^2 - r_i^2}\left(1 + \frac{r_a^2}{r^2}\right) \qquad (10)$$

and for $p_i = 0$:

$$\sigma_r = \frac{r_a^2 \cdot p_a}{r_a^2 - r_i^2}\left(\frac{r_i^2}{r^2} - 1\right)$$
$$\sigma_\Phi = -\frac{r_a^2 \cdot p_a}{r_a^2 - r_i^2}\left(\frac{r_i^2}{r^2} + 1\right) \qquad (11)$$

Up to this point, we have only considered the behaviour of the tube within the elastic range. Hydraulically expanded tubes are, however, deliberately deformed plastically. To calculate the load-bearing capacitiy and behaviour of the tube in the elastic-plastic and plastic ranges, we need a formula for plastic flow. For the purposes of the following calculations, we will use the formula developed by Mises which expresses plastic flow as follows:

$$\sigma_F = \sqrt{3} \cdot \sqrt{I_{2(D\sigma)}} \qquad (12)$$

For the plane stress condition assumed, we can express the load due to internal pressure as follows:

$$\sigma_F = \sqrt{\sigma_r^2 - \sigma_r \cdot \sigma_\Phi + \sigma_\Phi^2} =$$
$$= \frac{p_i \cdot r_i^2}{r_a^2 - r_i^2}\sqrt{3\left(\frac{r_a}{r}\right)^4 + 1} \qquad (13)$$

The internal pressure at which the inner fibre of the tube yields can be calculated from (13):

$$p_i^i = \frac{\sigma_F (u^2 - 1)}{\sqrt{3 \cdot u^4 + 1}} \qquad (14)$$

A further increase in the internal pressure will cause the plastic zone to extend outwards. The outer fibre is reached as a pressure of:

$$p_i^a = \frac{\sigma_F}{2}(u^2 - 1) \qquad (15)$$

The radial shift in the elastic range is calculated from (2) for the load due to p_i:

$$w = \frac{p_i \cdot r}{E} \cdot \frac{1 + \mu}{u^2 - 1} \cdot \left[\left(\frac{r_a}{r}\right)^2 + \frac{1 - \mu}{1 + \mu}\right]$$

and for p_a: (16)

$$w = -\frac{p_a \cdot r}{E} \cdot \frac{1 + \mu}{1 - \frac{1}{u^2}} \cdot \left[\left(\frac{r_i}{r}\right)^2 + \frac{1 - \mu}{1 + \mu}\right]$$

For further considerations, the shift of the outer fibre of the tube significant. If $r = r_a$, then

$$(w)_{r=r_a} = \frac{2 \cdot p_i \cdot r_a}{E \cdot (u^2 - 1)}$$
$$(w)_{r=r_a} = -\frac{p_a \cdot r_a}{E}\left(\frac{u^2 + 1}{u^2 - 1} - \mu\right) \qquad (17)$$

and for $p_i = p_i$ we have:

$$(w)_{r=r_a} = \frac{2 \cdot \sigma_F \cdot r_a}{E \cdot \sqrt{3 \cdot u^4 + 1}} \qquad (18)$$

Thus for $p_i = p_i^a$:

$$(w)_{r=r_a} = \frac{\sigma_F \cdot r_a}{E} \qquad (19)$$

Sample calculation for a tube plate

To obtain a simple analytical solution, we simplify the tube plate geometry as shown in Figure 8. We assume that deformation is limited to that part of the plate which is located within the inscribed circle R_a. Strain measurements performed on a test block have confirmed that this assumption

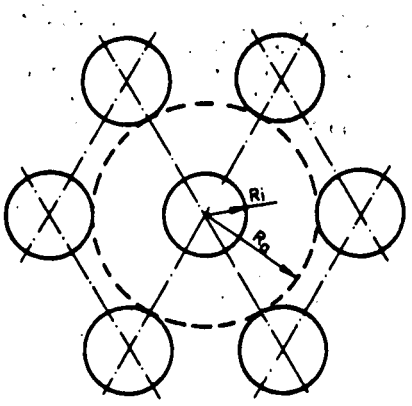

Fig. 8. Simplified tube plate geometry.

yields useful results (Figure 9). Since the aim of the expanding operation is to achieve a permanent contact pressure between the tube and the receiving bore in the tube plate, the following requirement must be satisfied when the pressure has ceased to rise:

$$[(w)_{r=r_a}]\, p_i \leq [(w)_{R=R_i}]_{(p_i - p_i^*)} \qquad (20)$$

After applying the formula derived above, this inequality yields:

$$p_i > \frac{2 \cdot \sigma_{FR}}{\sqrt{3 \cdot u_R^4 + 1}} \cdot \frac{u_p^2 - 1}{u_p^2 (1 + \mu) + 1 - \mu} + \frac{\sigma_{FR} (u_R^2 - 1)}{2} \qquad (21)$$

The right-hand side of equation (21) is called the limiting pressure p_o. It represents the pressure p_i at which the recovery of the tube sheet is equal to the recovery of the tube. In Figure 10, the limiting pressure referred to the yield point of the tube is plotted as a function of the radii. The curve $u_p = 1.0$ shows the specific expansion pressure (p_i^* / σ_{FR}) of the tube, and the curve $u_p = \infty$ shows the relationships in an infinite plate with a single bore.

The following requirement must be satisfied if we wish to avoid plastic deformation of the material between the bores in the tube plate:

$$\left[p_i - \frac{\sigma_{FR} \cdot (u_R^2 - 1)}{2} \right] \cdot \frac{u_p^2 + 1}{u_p - 1} \leq \sigma_{FP} \qquad (22)$$

With $p_i = p_o$ and appropriate transformation, we obtain:

$$\frac{p_o}{\sigma_{FR}} \leq \frac{\sigma_{FP}}{\sigma_{FR}} \cdot \frac{u_p^2 - 1}{u_p^2 + 1} + \frac{u_R^2 - 1}{2} \qquad (23)$$

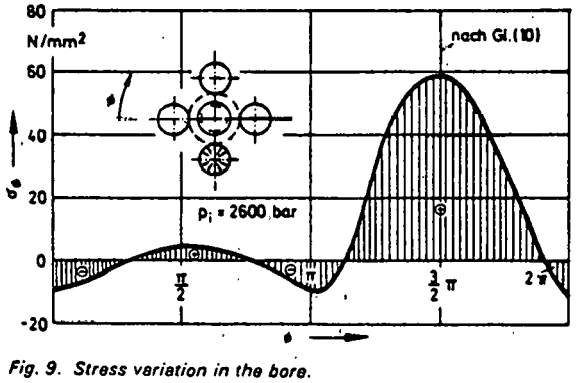

Fig. 9. Stress variation in the bore.

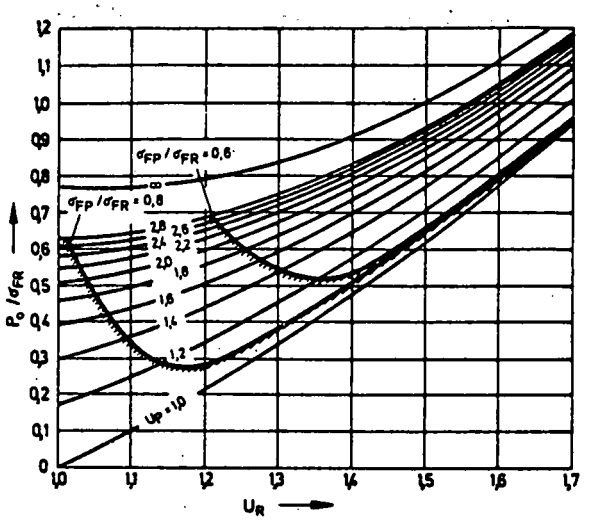

Fig. 10. Specific limiting pressure plotted against tube and tube plate geometry.

$\frac{\delta_{FP}}{\delta_{FR}} = 0.8$ and 0.6 is shown in Figure 10.

With a yield limit condition of $\delta_{FP} - \delta_{FR} < 1$, there are geometries which are so unfavourable that the limiting pressure cannot be reached without the yield point in the tube plate being exceeded.

This limitation of the geometry for

$$\frac{\delta_{FP}}{\delta_{FR}} = 0.8 \text{ and } 0.6$$

is shown in Figure 10.

A very important question which we will now attempt to answer is that of the adhesion pressure persisting between tube and receiving bore under no-load conditions.

According to (16), the expansion of the tube due to the adhesion pressure p_H is

$$w_R = -\frac{p_H \cdot r_a}{E} \cdot \frac{1 + \mu}{1 - \frac{1}{u_R^2}} \left(\frac{1}{u_R^2} + \frac{1 - \mu}{1 + \mu} \right) \qquad (24)$$

and that of the tube plate

$$w_P = \frac{p_H \cdot R_i}{E} \cdot \frac{1 + \mu}{u_p^2 - 1} \left(u_p^2 + \frac{1 - \mu}{1 + \mu} \right) \qquad (25)$$

The expansion of the tube plate model due to the pressure component $(p_i - p_o)$ is:

$$w_P^* = \frac{(p_i - p_o) \cdot R_i}{E} \cdot \frac{1 + \mu}{u_p^2 - 1} \cdot \left(u_p^2 + \frac{1 - \mu}{1 + \mu} \right) \qquad (26)$$

for $R_i = r_a$, the contact formula

$$w_P^* = w_P - w_R \qquad (27)$$

after substitution of the terms (24), (25) and (26) and brief transformation, yields:

$$\frac{p_H}{p_i - p_o} = \frac{1}{1 + \frac{(u_p^2 - 1)}{(u_R^2 - 1)} \cdot \left[\frac{u_R^2 (1 - \mu) + 1 + \mu}{u_p^2 (1 + \mu) + 1 - \mu} \right]} \qquad (28)$$

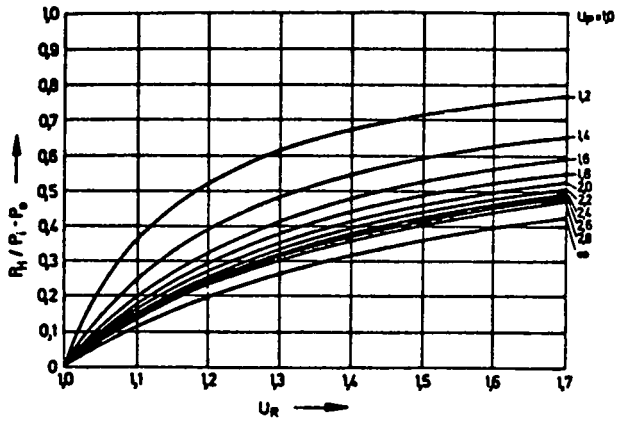

Fig. 11. Specific adhesion pressure plotted against tube and tube plate geometry.

In this calculation, the modulus of elasticity of the tube plate has been equated to that of the tube. The formula (28) is graphically represented in Figure 11 for $\mu = 0.3$. The extraction force for the tube can then be theoretically calculated as

$$P_R = 2 \cdot \pi \cdot r_a \cdot L \cdot p_H \cdot f \qquad (29)$$

Critical comments on the term "adhesive expansion"

In conjunction with the common method of anchoring tubes in a tube plate or similar bodies by mechanical roll-expansion, adhesive expansion is presented as the one and only criterion for the quality of the rolled joint. The approximate values specified for different tube materials in the tube rolling manufacturers' catalogues disregard tube geometry and the clearance between tube and receiving bore. Adhesive expansion is expressed as

$$H = \frac{d_{iA} - D + 2s}{s} \cdot 100 \qquad (30)$$

By substituting $(D - d_{iA}) = 2 S_A$, we have

$$H = 2 \cdot \left(1 - \frac{s_A}{s}\right) \cdot 100. \qquad (31)$$

We shall now examine the behaviour of the tube during the rolling process (Figure 12). The tube expands nonuniformly and contacts the wall of the receiving bore. At this stage, it is not yet possible to create a permament joint between tube and tube plate. Since the volumes are equal before and after contact, it follows that

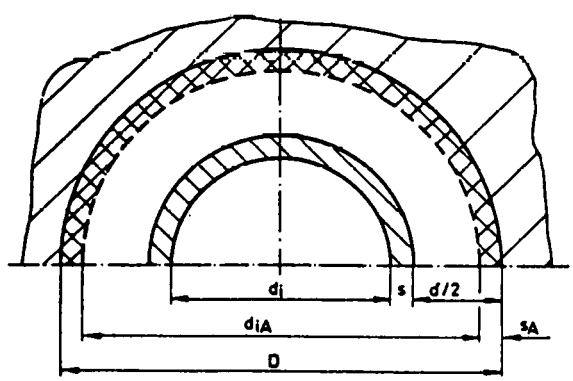

Fig. 12. The tube before and after the rolling operation.

$$\frac{d_i + d_a}{2} \cdot s \cdot L = (d_a + \delta - s_A) \cdot s_A \cdot L - \\ - \Delta \cdot s \cdot \frac{d_i + d_a}{2} \qquad (32)$$

which leads to the quadratic equation

$$s_A^2 - s_A (d_a + \delta) + s \cdot \frac{d_i + d_a}{2} \left(1 + \frac{\Delta}{L}\right) = 0 \qquad (33)$$

and the solution to this is:

$$s_A = \frac{d_a + \delta - \sqrt{(d_a + \delta)^2 - 4 (d_a - s) \cdot \left(1 + \frac{\Delta}{L}\right) \cdot s}}{2} \qquad (34)$$

Substitution of this term in (31) yields an apparent adhesive expansion of

$$H^* = \left\{2 - \left[\frac{d_a}{s} + \frac{\delta}{s} - \right.\right. \\ \left.\left. - \sqrt{\left(\frac{d_a}{s}\right)^2 + 2 \frac{d_a}{s} \cdot \frac{\delta}{s} - 4 \left(\frac{d_a}{s} - 1\right) \left(1 + \frac{\Delta}{L}\right)}\right]\right\} \cdot 100 \qquad (35)$$

Owing to the elongation of the tube during rolling, Δ is negative. The change in tube length depends on several parameters and is unknown for most practical applications. If Δ / L as to 1 in (35) is ignored, the apparent adhesive expansion can be represented graphically. As can be seen from Figure 13, this apparent adhesive expansion depends increases on the tube geometry and clearance. The valur of H* as the clearance increases. The clearance will, however, usually differ from one tube — bore pair to another, which explains the variations of adhesive expansion. The definition of adhesive expansion is obviously unsatisfactory and unreliable. Instead of adhesive expansion, which depends on geometry and clearance, the hydraulic tube expansion method relies on an accurately measurable parameter, namely internal pressure which guarantees uniform tube anchoring for all tubes.

Numerical example

Tube of Incoloy 800, tube plate of 22 NiMoCr 37, triangular spacing 30 mm.

$$\sigma_{FR} = 475 \text{ N / mm}^2$$

$d_i = 16.2$ mm
$d_a = 22$ mm
$D_i = 23.1$ mm
$D_a = 36.9$ mm
$u_R = 1.358$
$u_P = 1.5974$

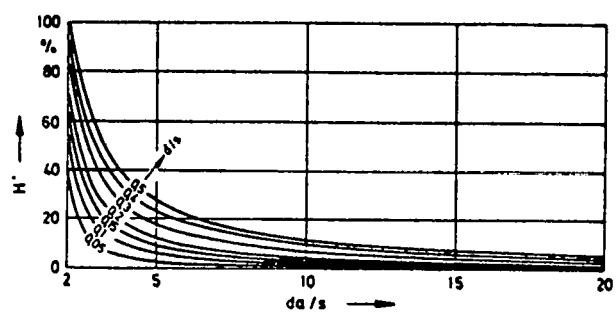

Fig. 13. Apparent adhesive expansion.

From Figure 10, we have for $u_P = 1.0$:

$$\frac{p_o}{\sigma_{FR}} = 0.42$$

Accordingly, the pressure at which the plastic zone has reached the outer fibre of the tube is

$$p_i^0 = 0.42 \cdot 475 \cdot 10 = 1995 \text{ bar.}$$

From Figure 10, we find for the actual tube sheet geometry

$$u_P = 1{,}5974$$

$$\frac{p_o}{\sigma_{FR}} = 0{,}654$$

The limiting pressure is then

$$p_o = 0.654 \cdot 475 \cdot 10 = 3106 \text{ bar.}$$

From Figure 11, we read off the adhesion pressure which persists after the load has been removed:

$$\frac{p_R}{p_i - p_o} = 0.457$$

For example, for $p_i = 4700$ bar:

$$p_H = 0.457\,(4700 - 3106) = 728 \text{ bar.}$$

EXPERIMENT

A number of experiments have been performed to support the theory presented above. One of these experiments will be described and discussed below.

Ten 420 mm long tubes of 22 mm dia × 2.9 mm, made of Incoloy 800, were inserted in a 320 mm thick test block of 22 NiMoCr 37 material. The geometry of the holes and tubes was recorded in three planes.

The pressure applied to expand the tubes ranged between 1950 and 2050 bar. The expansion zone started at a distance of 25 mm from the face of the test block and ended 2 mm behind the rear edge of the test block.

Different final pressures were applied to bring the tubes into contact with the walls of the receiving bores. The change in tube geometry, the reduction in tube length, pressure-tightness and the force required to pull the tube from its receiving bore (extraction force) were measured on completion of the test.

A leak rate of less than $1 \cdot 10^{-7}$ [torr · l · s^{-1}] was verified by a leak test with helium. All of the measured values are plotted graphically in Figure 14. The interdependence of certain parameters is clearly apparent from the graph.

Of particular interest is the relationship between the extraction force, the adhesive expansion and the adhesion pressure P_h calculated in accordance with equation (28). The extraction force P, as well as the positive difference between the adhesive expansion H defined in (30) and the apparent adhesive expansion H* increase with increasing adhesion pressure. This confirms the theory developed above and proves its usefulness in practice. The small extraction forces for tubes 1 and 3 which, according to the theory, ought to be zero are due to inaccuracies of the hole geometry in the longitudinal direction of the hole. Figure 14 proves the justification of the term "apparent adhesive expansion" and shows

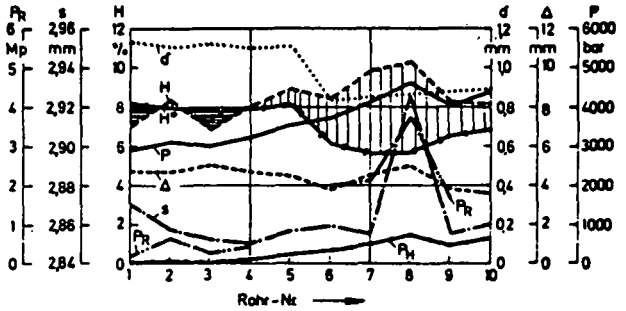

Fig. 14. Test results. Relationship between the actual adhesive expansion and the hydraulic pressure applied.
Rohr-Nr. = Tube No.

how unreliable a check of the joint between tube and tube sheet based on "adhesive expansion" actually is. The strong influence of clearance on apparent adhesive expansion agrees with (35).

PROBLEMS INVOLVED IN STRESS-FREE TUBE ANCHORING IN STRAIGHT-TUBE HEAT EXCHANGERS OR SIMILAR EQUIPMENT WITH TWO FIXED TUBE PLATES

As already mentioned, tubes can be anchored stress-free in tube plates if the hydraulic expansion method is combined with a suitable rolling method, taking advantage of the relationships existing between tube length reduction and clearance in the case of hydraulic expansion and between tube elongation and roller setting in the subsequent rolling operation. These two characteristics can be easily determined by means of a simple pilot test, as shown in Figure 15. It is logical that we shall always endeavour to exactly balance out the reduction in tube length by tube elongation.

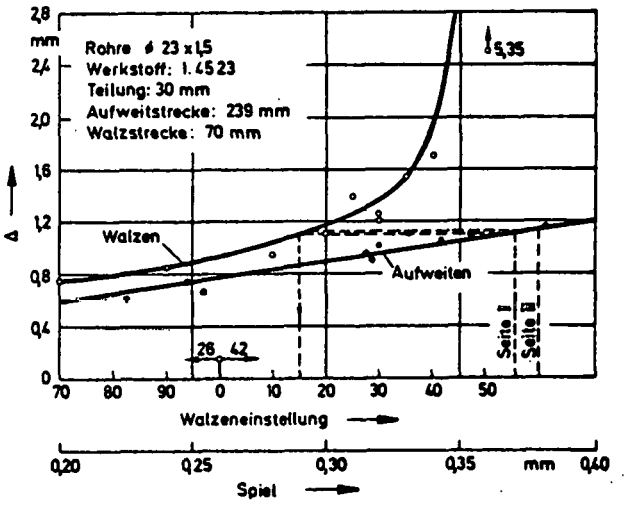

Fig. 15. Change in tube length as a function of roller setting and clearance between tube and tube plate.

Rohre ∅ 23 × 1,5	= Tubes 23 mm dia. × 1.5
Werkstoff: 1.4523	= Material: 1.4523
Teilung: 30 mm	= Spacing: 30 mm
Aufweitstrecke: 239 mm	= Hydr. expanded length: 239 mm
Walzstrecke: 70 mm	= Rolled length: 70 mm
Walzen	= Rolling
Aufweiten	= Hydr. expanding
Walzeneinstellung	= Roller setting
Spiel	= Clearance
Seite I	= Side I
Seite II	= Side II

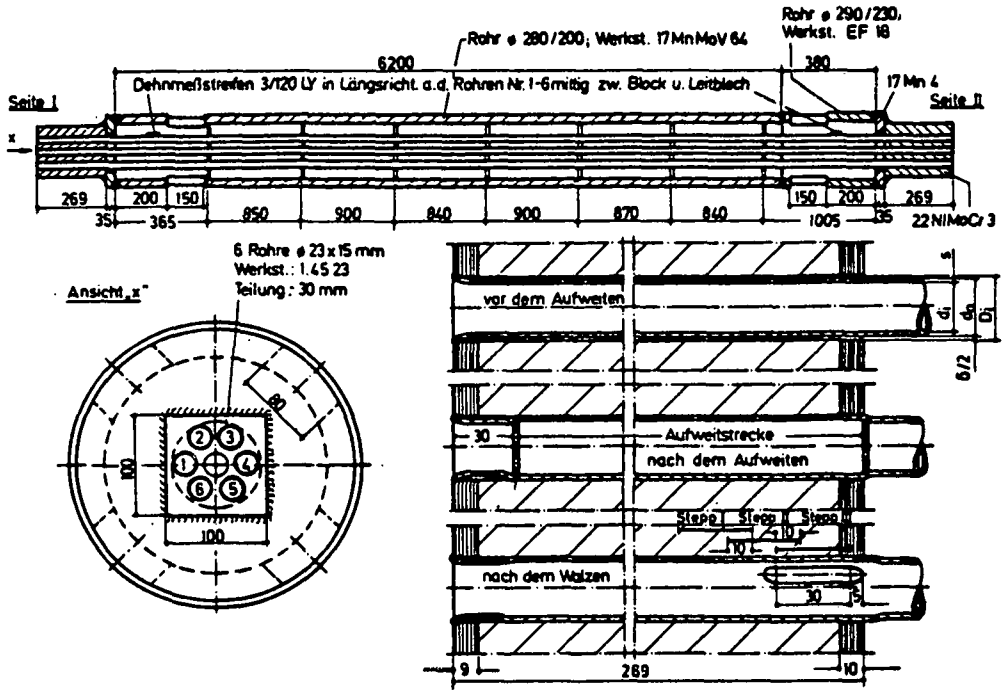

Fig. 16. Test apparatus with two fixed tube plates. Tube 290 dia./230; EF 18 material Tube 280 dia. /200; 17 MnMoV 64 material.
Dehnmeßstreifen 3/120 LY in Längsricht. a.d. Rohren Nr. 1-6mittig zw. Block u. Leitblech
= *Strain gauges 3/120 LY, longitudinally applied to Tubes Nos. 1-6 centrally between block and fin.*
6 Rohre Ø 23 × 15 mm
= *6 tubes 23 dia. × 1,5 mm*
Werkst.: 1.4523 = Material 1.4523
Teilung: 30mm = Spacing: 30 mm
Ansicht „x" = *View "X"*
vor dem Aufweiten = Prior to hydraulic expansion
Aufweitstrecke = Expanded lengths
nach dem Aufweiten = *after hydraulic expansion*
nach dem Walzen = after rolling

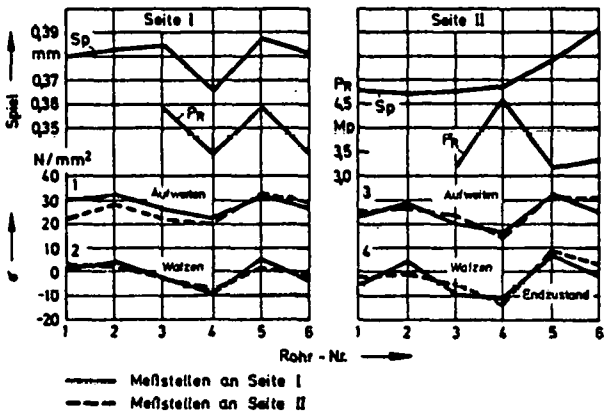

Fig. 17. Results of the extension measurement.
Seite I = Side I
Seite II = Side II
Aufweiten = Expansion
Walzen = Rolling
Endzustand = Final condition
Rohr-Nr. = Tube No.
Meßstellen an Seite I = *Measuring points on side I*
Meßstellen an Seite II = Measuring points on side II
Spiel = Clearance (mm).

We cannot influence the reduction in tube lengths, because it depends exclusively on the clearance. However, the roll setting of the rolling controller and the rolled lengths are variables which, if appropriately selected, will enable us to achieve any desired prestress of the tube, including the special case of stress-free anchorage. Of course, certain tolerances of hole and tube diameter must be expected even in one and the same heat exchanger or similar equipment. It is impossible to measure all bores and associated tubes and then select the required roll setting or rolled length to suit the actual clearance. What we can do, however, is select a statistically representative number of bores and tubes, measure these and then calculate the representative bore diameter, outside diameter of tube and the clearance between tube plate and tubes on the basis of simple drillmatic averages. According to the law of probability, the sum of the tube forces divided by the number of tubes can be expected to yield the desired prestress in the tube, or zero in the case of stress-free anchorage.

To support this theory, a test was performed in which the axial stresses existing in the tubes were measured by means of strain gauges. The test apparatus is shown in Figure 16; the stresses measured after each operation are plotted in Figure 17. It was endeavoured to anchor the tubes in a balanced stress configuration. The expansion zone started at a distance of 30 mm from the face of the tube sheet and ended at the end of the tube emerging from the tube plate. The hydraulic pressure to be applied to expand the tubes was fixed

at 2500 bar. After hydraulically expanding Side I the same side was rolled in three steps, employing the step rolling method (see Figure 16). During this process, the tube was pushed out and a joint was obtained between tube and plate with no gap and balanced stresses. The tubes were then also anchored in the same sequence in Side II.

In the final state (figure 17), the tubes 2 and 5 are subjected to a slight tensile stress while the tubes 1,3,4 and 6 are then subjected to compressive stress. In can be seen that the result is very close to the zero limit which we desired. We can safely assume that with a greater number of tubes the deviation would have been even less.

CONCLUSION

Compared with the conventional method of mechanical roll expansion, the hydraulic method of expanding tubes in tube plates offers numerous advantages which have been discussed in this article. The method is particularly suitable for heat exchangers or similar equipment and tube joints which must satisfy exacting requirements in terms of quality and uniformity of the joint, such as steam generators for nuclear power stations, high and low-pressure feed water heaters for conventional power stations and equipment for the chemical industry. The method presented in this article will enable designers of such equipment to calculate the required expansion pressure in a simple manner. By combining the hydraulic method with mechanical roll expansion for heat exchangers or similar equipment with two fixed tube plates, we can now influence the prestress in straight tubes, although this was previously not possible. This aspect will be found particularly interesting in connection with heat exchangers or other equipment subject to thermal stresses in operation.

SYMBOLS AND ABBREVIATIONS

σ = stress
ε = strain
r = radial coordinate of the tube
R = radial coordinate of the tube plate model
d = tube diameter
D = hole diameter
s = tube wall thickness
E = modulus of elasticity
μ = Poisson' ratio
w = radial displacement
F = stress function
p = pressure
I_2 = second invariant of stress condition
$D\sigma$ = stress deviator
u = ratio of radii (outside/inside)
Δ = reduction in tube length
L = expanded length
f = coefficient of friction
δ = clearance between tube and bore
H = adhesive expansion

INDICES

r = radial direction
Ø = peripheral direction
i = inside
a = outside
F = yield limit
H = adhesion pressure
P = tube plate
R = tube
A = after rolling or hydraulic expansion

LITERATURE

[1] Lehmann, T.: Elemente der Mechanik, Bertelsmann Universitätsverlag, Düsseldorf 1974.

[2] Timoshenko, S.P.: J.N. Goodier: Theory of Elastizity, Mc Graw-Hill Book Company 1970.

[3] Strohmeier, K.: Beitrag zur Berechnung zylindrischer Mehrlagenbehälter für statische Innendruckbelastung, Konstruktion 1974, pages 187–191 and 217–223.

[4] Schweigerer, S.: Festigkeitsberechnung von Bauelementen des Dampfkessel-, Behälter- und Rohrleitungsbaues. Springer 1970, Berlin-Heidelberg-New York.

[5] Dunker, H.W.: Festigkeit von Rohreinwalzungen in Rohrböden. Chem.-Ing.-Technik 1951, Nr. 17/18.

[6] Güllich, J.F.: Bedeutung der thermohydraulischen Verhältnisse für die Korrosionssicherheit von DWE-Dampferzeugern. Atomwirtschaft, February 1975.

[7] Spähn, Wagner, and Steinhoff: Formen, Bedeutung und Erscheinungsbild der Spannungsrißkorrosion. TÜ 14 (1973).

[8] Söhngen, and Faulstich: Festigkeitsuntersuchungen von eingeschweißten Rohren in Rohrböden und Wärmeaustauschern. Schweißen und Schneiden, H. 9, 1964.

[9] Stückrad, J.: Zur Rohr/Rohrboden-Verbindung an Wärmeaustauschern. Chemiker-Ztg./Chem. Apparatur, 90, Volume 1966, No. 17.

[10] Krägeloh, E.: Die Beanspruchung von Lochreihen und die Auswirkung eingewalzter Rohre. Konstruktion 18 (1966), H. 5.

[11] Siebel, E.: Walzverbindungen. Stahl und Eisen, H. 47 (1933).

[12] Class, I.: Überblick über das Gebiet der Spannungsrißkorrosion. Werkstoffe und Korrosion, H. 4, 1965.

[13] Class, I.: Spannungskorrosionsartige Erscheinungen an mechanisch-beanspruchtem Stahl durch diffundierenden Wasserstoff. Werkstoffe und Korrosion, H. 5, 1955.

[14] Möller, W., and Wenzel, H.: Werkstoff- und Fertigungsfragen bei der Herstellung von Geradrohrdampferzeugern. VGB KRAFTWERKSTECHNIK 56 (1976), H. 4.

[15] Schopf, A.: Dampferzeuger in U-Rohr-Bauweise für Kernkraftwerke und ihre Fertigung. VGB KRAFTWERKSTECHNIK 56 (1976), H. 3, p. 137–143.

BALCKE-DÜRR

Sonderdruck A 31 e

R. L. BEYNON & ASSOCIATES
166 Santa Clara Avenue
Oakland, California 94610
Telephone (415) 444-7795

BALCKE-DÜRR
AKTIENGESELLSCHAFT

D-4030 Ratingen 1
Postfach 1240
Telefon (02102) 2001
Telex 08585113

D-4630 Bochum 1
Postfach 100210
Telefon (0234) 6171
Telex 0825808

D-6710 Frankenthal
Postfach 227
Telefon (06233) 6011
Telex 0465228

With effect from end of 1977 please contact our Ratingen office.

APPENDIX D.2

EROSION AND CORROSION CONTROL

TRW
DEFENSE AND SPACE SYSTEMS GROUP
ONE SPACE PARK- REDONDO BEACH • CALIFORNIA 90278

INTEROFFICE CORRESPONDENCE

5515.2.78-416

TO: L. A. Rosales

CC: T. C. Dvorak
J. S. Hicks
M. Kwan

DATE: August 24, 1978

SUBJECT: Tube Sheet Coating and Corrosion Allowance

FROM: M. P. Bianchi

BLDG. 01 MAIL STA. 2230 EXT. 52303

In answer to your request to obtain more information on the neoprene coating used to protect the British Power generating station's condenser tubeplates and waterboxes from saltwater corrosion and silt erosion shown in the April 1978 issue of DuPont's "Elastomers Notebook", I have obtained the following:

1. The manufacturer of the coating is:

   Protective Rubber Coatings (Bristol), Ltd
   Payne's Shipyard, Coronation Rd
   Bristol, England BS 31RP

2. The coating is called "Limpetite" and it is a neoprene coating.

3. The manufacturer has found that at the saltwater-cooled Portishead installation a 1/16-inch coating on the tubeplates, waterboxes, valves, etc. has shown an indefinite life; that is, no degradation other than mechanical damage (the coating is repairable) from maintenance work over the 32 years it has been in service.

4. On that basis, no corrosion allowance is needed and in the U.K. all present power stations under construction will use "Limpetite".

5. Tube entries were also coated for an initial length of three inches with the coating thickness tapering from 0.20 inch to 0 inch. The life of the entry coating at Portishead has been seven years and is extended for one inch every recoat to a maximum of six inches from the end of the tubes.

6. Impressed current cathode protection is not and should not be used with the coating.

7. The surface preparation is by grit-blasting to white metal followed by a brush application of the primer. The coating is then applied with brush or roller in 22 coats to a nominal 1/16-inch final thickness. The process is continuous and the curing time a minimum of ten days.

8. According to their Managing Director, Mr. J. H. Payne, "Limpetite" is not available in the U.S. and, as far as they are concerned, there are no comparable coatings both in the U.S. and the U.K.

Mr. Payne made reference in his Telex of the Central Electricity Generating Board Construction Division in Barnwood, Gloucester, and I am writing them for any further information they may have on this coating.

MPB:cd

Tel. 661344
S.T.D. Code 0272
Telegrams:
Limpetite, Bristol

REGISTERED TRADE MARK

PROTECTIVE RUBBER COATINGS
(BRISTOL) LTD

PAYNE'S SHIPYARD CORONATION ROAD
BRISTOL BS3 1RP

Your Ref.

Our Ref. JHP/PAH

4th September, 1978.

M.P. Bianchi Esq.,
TRW Defense & Space Systems Group,
Building 01,
Room 2230,
One Space Park,
Redondo Beach,
California 90278,
U.S.A.

Dear Mr Bianchi,

We comment upon your letter of August 23rd, 1978.

Limpetite has additionally been used quite widely in Central Electricity Generating Board in the last few years where titanium tubes are fitted to existing "Naval Brass" tube plates. The electro-potential difference between the titanium and the "Naval Brass" is so high that Limpetite is an absolute must. Even new stations under construction were fitted with new brass tube plates until the problem was discovered in some of the older stations where titanium tubes had been fitted on trial. Subsequent new condensers fitted aluminium bronze or aluminium brass tube plates thus reducing the electro-potential difference.

Under specific conditions of aluminium brass tube plates it should be noted no service experience is available as far as we are aware. It is anticipated that Limpetite coatings for the protection of the tube plates will not be necessary. Service conditions may dictate otherwise.

Your specific problem is akin to the first mentioned above where there is a large electro-potential difference between the tubes and the tube plate. We would expect that if it is successful between titanium and "Naval Brass" tube plates it would be equally successful between steel tube plates and presumably titanium or brass tubes.

Cont'd 2/....

★ *Liquid applied, Air cured Synthetic Rubber Coatings*
for protection of all metals against corrosion, erosion and electrolytic action. Applied in liquid, putty or sheet form.

★ *Electricity Generating*
Coatings for main condenser and ancillary cooler water boxes, tube plates and tube entries, water manifolds, valves, coal and ash handling plant. Sea water pumps, strainers and weedgrids.

★ *General and Chemical Engineering*
Coatings for fume ducts, fan casings and impellers, acid vats, storage pressure and vacuum vessels, structures etc.

★ *Marine*
main condenser tube plates, waterboxes, intake and discharge valves, pump casings and impellers. Stern frames, rudder nosings, intake and discharge grills, propeller shafts, diesel engine wet liners, cooling water systems.

★ *Hull Sheathing*
Liquid applied, flexible hull sheathing for steel or wooden boats is completely resistant to marine borers and prevents corrosion. Keeps hull, decks and superstructure watertight

★ *Nylon, P.V.C. Epoxy Phenolic, and Polyurethane Coatings*
for pumps, storage vessels, road and rail tankers, fume ducts, structures, etc.

M.P. Bianchi Esq.,
TRW Defense & Space Systems Group. 4th September, 1978.

Consideration must be given to the design of the tube to tube plate junction at both ends of the tubes. In the case of a floating tube-plate to accommodate the expansion of tubes this presents no problem, but it could present a slightly more difficult problem in the case of fixed tube plates.

In the case of floating tube places the present practice here is for the entry end either to have expanded, bellmouthed, flush tubes with the tube plate coating taken down into the tube entry; or the tubes standing out about ¼" and the coating finished around the outside diameter of the tube. This latter method is that used for the outlet ends where water flow direction would preclude the use of a coating within the tube bore.

In the case of rigid tube plates then presumably the outlet end would be packed in some way allowing the tube to slide through packing on expansion and contraction. In these cases you would use two methods, The simplest seems to be quite effective, namely to coat the tube standing out in exactly the same way as the standout inlet. That is to say, coat around the outside diameter of the tube for a distance of say between ½" and 1". In some cases tubes have pulled through the coating sleeve, yet, under the difference in pressure between the steam side and the cooling water side this has maintained an effective seal. In other cases where the total expansion has remained small the coating has either stretched as necessary or has lifted slightly from the tube plate.

Another method has been used where Neoprene sponge washers have been fitted and a coating applied on the tube plate over the square section washer close fitting to the outside diameter of the tube and on to the outside diameter of the tube thus providing a bellows to accommodate greater movement. The success of this latter method depends to some extent upon the pitch of the tube and the physical accessibility for brushing the coating around the tubes and the washers.

With reference to the second paragraph of your letter Limpetite could be made available in the United States unless there is some Customs ban on its import. In the past we have found the United States Customs requirements to be singularly complicated and we would probably find every component of the three or four components required would have to be submitted for examination and test to U.S. customs Laboratory for classification. It seems to us from our experiences of some time ago that they will not take classifications commonly used throughout Europe and the rest of the world and translate them into their own standard grouping. Your organisation concerned with defence may be able to employ some influence in this respect.

The only literature we have we enclose, which is a general brochure giving illustrations of various applications and a leaflet describing Limpetite A/B; two of the three types of synthetic rubber liquid applied, air cured coatings that we manufacture.

We would imagine that if in the event that you wish to apply materials in the United States it would be best for us to send over a representative who will advise upon initial application. Normally in this country we seldom supply the Limpetite for application by others, except in small private applications, because of the failure so often of professional contractors to appreciate the requirements of Limpetite and to treat it simply as an ordinary paint.

Cont'd 3/....

M.P. Bianchi Esq.,
TRW Defence & Space Systems Group.

4th September, 1978.

It is not untrue to say that the success of Limpetite stems almost as much from our appreciation of the engineering requirements of its application as from the material itself.

We shall be happy to liaise with you on this matter.

Yours truly,

J.H. Payne,
Managing Director.

TRW
DEFENSE AND SPACE SYSTEMS GROUP
ONE SPACE PARK • REDONDO BEACH • CALIFORNIA 90278

INTEROFFICE CORRESPONDENCE 5515.2.78-269

TO: J. W. Denton

CC: P. Edris
E. L. Leventhal
R. O. Pearson
W. I. Rogers
L. A. Rosales
W. J. Tallon, Jr.

DATE: 19 May 1978

SUBJECT: Cathodic Protection of Submerged Heat Exchanger.

FROM: T. C. Dvorak

BLDG. 01 MAIL STA. 2220 EXT. 51900

The customer request to evaluate the impact of submerging the 25 MWe heat exchanger has required that active corrosion preventive measures (i.e. cathodic protection) in addition to the planned passive measures (i.e. coatings) be considered. To this end, the Harco Corporation was contacted and a meeting was arranged.

On May 15, the writer, L. Rosales and L. Leventhal of TRW met with Mr. Robert Deskins, V.P. and Western Region Manager and Steve Jones, Manager of Engineering, Western Region Office of the Harco Corporation. Our design concept was shown to them and the following points were made.

Harco is in the business of providing corrosion engineering services during the design phase of a program. They will review the design, recommend the type of cathodic protection required, prepare plans and specifications for the installation and monitoring of the system after installation.

The method of attachment of the heat exchanger to the hull is very critical. If the joint is electrically conductive and the hull is more noble than the heat exchanger, as would be the case if the hull were concrete, then the exchanger would corrode at a very rapid rate due to the large area ratio of the hull to the heat exchanger. To resolve this issue we must have a better understanding of the hull design, materials of construction, etc.

It was Harco's opinion that the sacrificial anode type of cathodic protection as opposed to induced current was the best method for our application. A cost for this type of system could only be obtained after a detailed design study. The approximate cost for anodes would be one dollar per pound with installation also costing about one dollar per pound (based on off-shore oil platform costs-may be higher for OTEC installations). For an idea of cost, the Exxon oil platform Hondo required 750,000 pounds of sacrificial anodes to provide protection for 10-15 years.

In summary, due to the complex nature of designing an adequate protection system and our lack of experience in this area, we strongly recommend that a company such as Harco, be contracted to provide this service. Our role would be that of technical monitor and point of information exchange. As of this point in time we plan no further activity in this area. Task I, Subtask 5 is now considered complete.

TCD:dj

TRW
DEFENSE AND SPACE SYSTEMS GROUP
ONE SPACE PARK • REDONDO BEACH • CALIFORNIA 90278

INTEROFFICE CORRESPONDENCE

PSD-1-373
5515.2.78-329

TO: Paul Edris

CC: Distribution

DATE: 7 July 1978

SUBJECT: Corrosion Allowance for Carbon Steel in Design of OTEC/PSD-1 Heat Exchanger Shell, Tube Sheets and Water Boxes.

FROM: J. Hicks
BLDG. 01 MAIL STA. 2080 EXT. 61486

References: (1) TRW Conceptual Design Report SAN/1570-1, Volume II, Dated 30 January 1978. (Appendix A - "Heat Exchangers Mechanical Design and Producibility", prepared by C. F. Braun & Co., 10 Januarly 1978.)

(2) DOT/USCG Document CG-116 "Marine Engineering Regulations," dated 1 August 1977.

(3) INCO "Guidelines for Selection of Marine Materials," May 1971.

The following comments are in response to yesterday's inquiry from C. F. Braun & Co. relative to the subject.

1. The corrosion allowance of 1/8-inch for carbon steel as stipulated by C. F. Braun (see Rerference 1, pages A-48 and A49) appears sufficient and proper for the subject heat exchanger components, IF the heat exchanger is not totally immersed in sea water, (see SUMMARY). This conclusion is based on a review of the regulatory requirements, the C. G. Braun proposed design, and general industry guidelines for the selection of marine materials, as outlined below.

2. Code Provisions - Part 54 (Pressure Vessels) of the Reference 2 regulations establishes the requirements for the design, construction and inspection of seaborne heat exchangers. Paragraph 54.01-35 specifically addresses the corrosion allowance to be applied in the design of the pressure portions of pressure vessels. This paragraph is reproduced below; note particularly subparagraphs (b)(1), (b)(4), (d)(1), and (d)(2).

(b) The following information shall be submitted:

(1) Calculations for all pressure containment components including the maximum allowable working pressure, the hydrostatic or pneumatic test pressure, and the intended safety device setting.

(2) Joint design and methods of attachment of all pressure containment components.

(3) Foundations and supports (design and attachment).

(4) Pertinent calculations for pressure vessel foundations and/or supports.

(5) A bill of material meeting the requirements of section VIII of the ASME Code, as modified by this part.

(6) A diagrammatic arrangement drawing of the assembled unit indicating location of internal and external components.

§ 54.01-25 Miscellaneous pressure components (modifies UG-11).

(a) Pressure components for pressure vessels shall be as required by UG-11 of the ASME Code except as noted otherwise in this section.

(b) All pressure components conforming to an accepted ANSI (American National Standards Institute) Standard referred to in an adopted code, specification or standard or in this subchapter shall also be marked in accordance with MSS (Manufacturers' Standardization Society) Standard SP-25.

[CGFR 68-82, 33 F.R. 18828, Dec. 18, 1968, as amended by CGFR 69-127, 35 F.R. 9977, June 17, 1970]

§ 54.01-30 Loadings (modifies UG-22).

(a) The loadings for pressure vessels shall be as required by UG-22 of the ASME Code except as noted otherwise in this section.

(b) In evaluating loadings for certain pressure vessel applications, the Commandant may require consideration of the following loads in addition to those listed in UG-22 of the ASME Code:

(1) Loading imposed by vessel's attitude in roll, list, pitch and trim.

(2) Dynamic forces due to ship motions.

§ 54.01-35 Corrosion (modifies UG-25).

(a) Vessels or portions of vessels subject to corrosion shall be as required by UG-25 of the ASME Code except as noted otherwise in this section.

(b) The pressure portions of pressure vessels shall:

(1) Normally have a corrosion allowance of one-sixth of the calculated thickness, or one-sixteenth inch, whichever is smaller, added to the calculated thickness as determined by the applicable design formula.

(2) Be specifically evaluated in cases where unusually corrosive cargoes will be involved, for the possible increase of this corrosion allowance.

(3) Have no additional thickness required when acceptable corrosion resistant materials are used.

(4) Not normally need additional thickness allowance when the effective stress (either S or SE depending on the design formula used) is 80 percent or less of the allowable stress listed in section VIII of the ASME Code for calculating thickness.

(c) Telltale holes shall not be permitted in pressure vessels containing dangerous fluids, such as acid, poison, corrosives, etc.

(d) Exemption from these corrosion allowance requirements will be granted by the Commandant in those cases where:

(1) The contents of the pressure vessel is judged to be sufficiently noncorrosive; and,

(2) Where the external surface is also protected from corrosion. A suitable vapor barrier is adequate protection, while paint or other thin coatings exposed to weather or mechanical damage are not acceptable.

NOTE: No applied linings except as provided in Part UCL of the ASME Code shall be acceptable.

[CGFR 68-82, 33 F.R. 18828, Dec. 18, 1968, as amended by CGFR 72-59R, 37 F.R. 6163, Mar. 25, 1972]

§ 54.01-40 External pressure (modifies UG-28).

(a) The exemption from external pressure consideration provided by the note under UG-28(f) does not apply.

(b) Vessels which may at times be subjected to partial vacuum due to nature of the contents, temperature, unloading operations, or other facet of employment shall either have vacuum breaker protection or be designed for not less than one-half atmosphere of external pressure.

[CGFR 70-143, 35 F.R. 19606, Dec. 30, 1970]

3. C. F. Braun Proposed Design - Attachment Pages 1 and 2 (from Reference 1) show tube and tubesheet-to-shell details of the C. F. Braun proposed design. It appears that this design complies with the provisions of all four subparagraphs of the Code noted above, IF the heat exchanger is not immersed.

4. Corrosion in Sea Water - Charts from Reference 3 relative to general corrosion rates of unprotected carbon steel in seawater, the galvanic potential of titanium coupled with carbon steel, and other galvanic considerations in the design of tube sheets and water boxes are reproduced below. They are essentially self-explanatory.

Figure 8 – SEAWATER VELOCITY (PIPE AND TUBE RANGES)

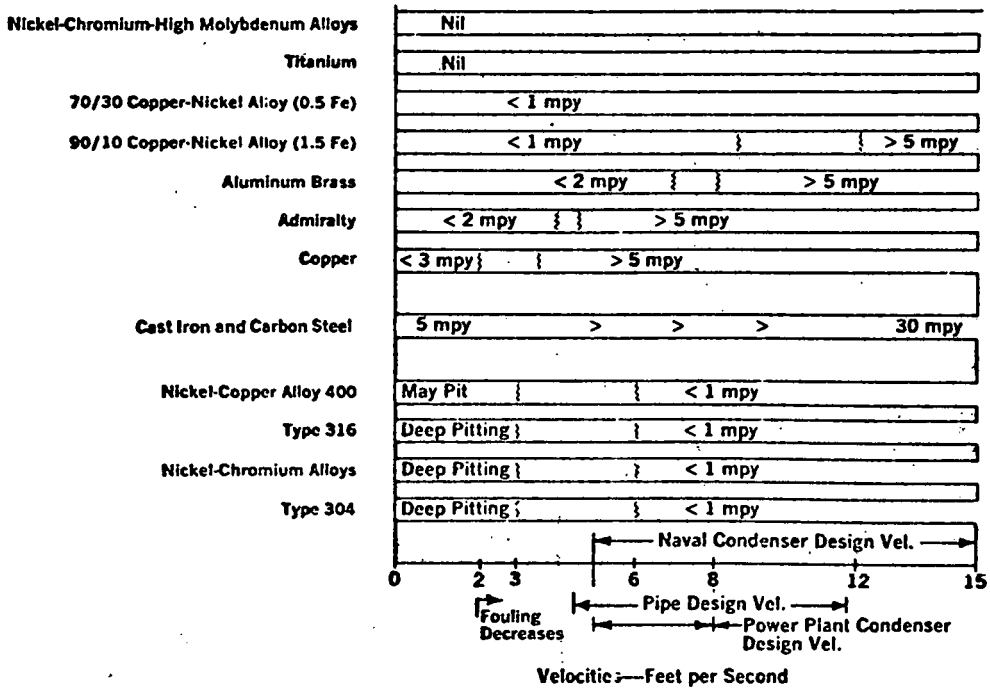

Note, in Figure 8 above, that the general wasting corrosion rate of unprotected carbon steel in seawater can vary from 5 mils/year to 30 mils/years depending on the velocity of the seawater.

Table IV

GALVANIC POTENTIALS IN FLOWING SEAWATER

(VELOCITY = 13 ft. per sec. except where noted)

METAL OR ALLOY	TEMPERATURE, °C			VOLT[3] VS. SATURATED CALOMEL		
Zinc	26			−1.03		
Mild steel	24			.61		
Gray cast iron	24			.61		
Austenitic cast iron[2]		14			.47	
Copper	24			.36		
Admiralty brass	24.6			.36		
Gunmetal	24			.31		
Aluminum brass	24.6			.29		
Admiralty brass		11.9			.30[1]	
Lead-Tin Solder (50-50)		17			.28	
90/10 copper-nickel alloy (1.4 Fe)			6			.24
90/10 copper-nickel alloy (1.4 Fe)		17			.29	
90/10 copper-nickel alloy (1.5 Fe)	24			.22		
70/30 copper-nickel alloy (0.51 Fe)			6			.22
70/30 copper-nickel alloy (0.51 Fe)		17			.24	
70/30 copper-nickel alloy (0.51 Fe)	26.7			.20		
Nickel-copper alloy 400	22			.11		
Nickel	25			.10[1]		
Titanium	27			−.10		
Graphite	24			+.25		
Platinum		18			+.26[1]	

Notes: 1. Seawater velocity = 7.8 ft. per sec.
2. Austenitic nickel ductile cast iron Type D-2 (3.0 C, 1.5–3 Si, 0.7–1.25 Mn, 18–22 Ni, 1.75–2.75 Cr).
3. All values negative vs. saturated calomel reference electrode except those for graphite and platinum.

Note, in Table IV above, that the galvanic couple of titanium with carbon steel in seawater gererates approximately 1/2 volt, with the carbon steel being anodic (sacrificial).

TUBE SHEET

The present trend towards welding tubes to tube sheet and galvanic considerations tend very strongly towards use of the same alloy in the tube sheet as in tubes. This is preferred. Older practice was to use muntz metal or naval brass tube sheets.

Applicable Data

Table V, Selective Corrosion

WATER BOXES

Key Consideration

(1) The water box should not be more noble than the tubing.

Materials Used	Comments
Carbon steel and cast iron	Heavy corrosion of steel provides substantial cathodic protection to copper alloy tube ends and tube sheet.
Carbon steel and cast iron lined with organic lining	Reduces cathodic protection of tube ends. Also forces steel exposed at pinholes and scratches to furnish the full amount of the current required by the galvanic couple with the copper alloy tube sheet and tube ends. Maintenance can be high.
Austenitic nickel cast iron	Good selection. Low corrosion but still protective to copper alloy tube ends and tube sheet.
90/10 copper-nickel alloy (1.5 Fe)	Good selection, when using 90/10 copper-nickel alloy (1.5 Fe) tubes, 70/30 copper-nickel alloy (0.5 Fe) tubes or nickel-copper alloy 400 tubes.
70/30 copper-nickel alloy (0.5 Fe)	Good selection, when using 70/30 copper-nickel alloy (0.5 Fe) tubes and nickel-copper alloy 400 tubes.
Nickel-copper alloy 400	Good selection, when using nickel-copper alloy 400 tubes. Solder wipe when using 70/30 copper-nickel alloy (0.5 Fe) tubes.

Applicable Data

Fig. 10, Galvanic Series
Table IV, Galvanic Series
Fig. 3, Effect of Velocity — Steel
Fig. 4, Effect of Velocity — Zinc
Fig. 5, General Wasting
Fig. 6, Pitting Rates
Fig. 8, Velocity: Pipe and Tube
Table V, Selective Corrosion

5. SUMMARY -

5.1 A corrosion allowance of 1/8-inch for carbon steel in design of the subject components is adequate, if the heat exchanger is not submerged.

5.2 If the OTEC system design requires submergence of the heat exchangers, the corrosion allowance for the pressure vessel components must be increased to a minimum of 1/2-inch, even when protected with an approved marine coating system. (see Code provision 54.01-35 (d)(2), above.)

5.3 Waterbox Coating - It will be noted in the C. F. Braun design (see Figure 6, attached) that a coal tar epoxy coating is proposed for the waterbox coating. Although this coating may be adequate, TRW Materials Engineering suggests that C. F. Braun designers consider another more resilient Neoprene coating system which appears outstanding for this application, and which has a proven 32 year service life. (See attachment pages 3 and 4.)

F W CLEVENGER

FIGURE 5

TRW
SYSTEMS GROUP
REDONDO BEACH, CA

OTEC HEAT EXCHANGERS

5304-100

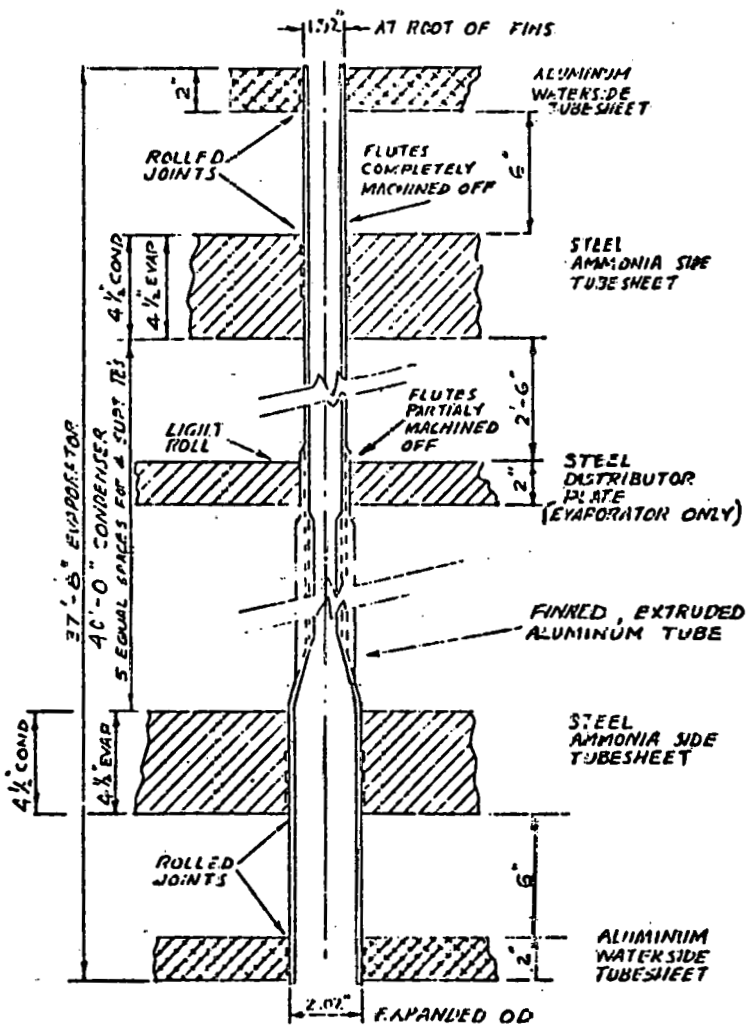

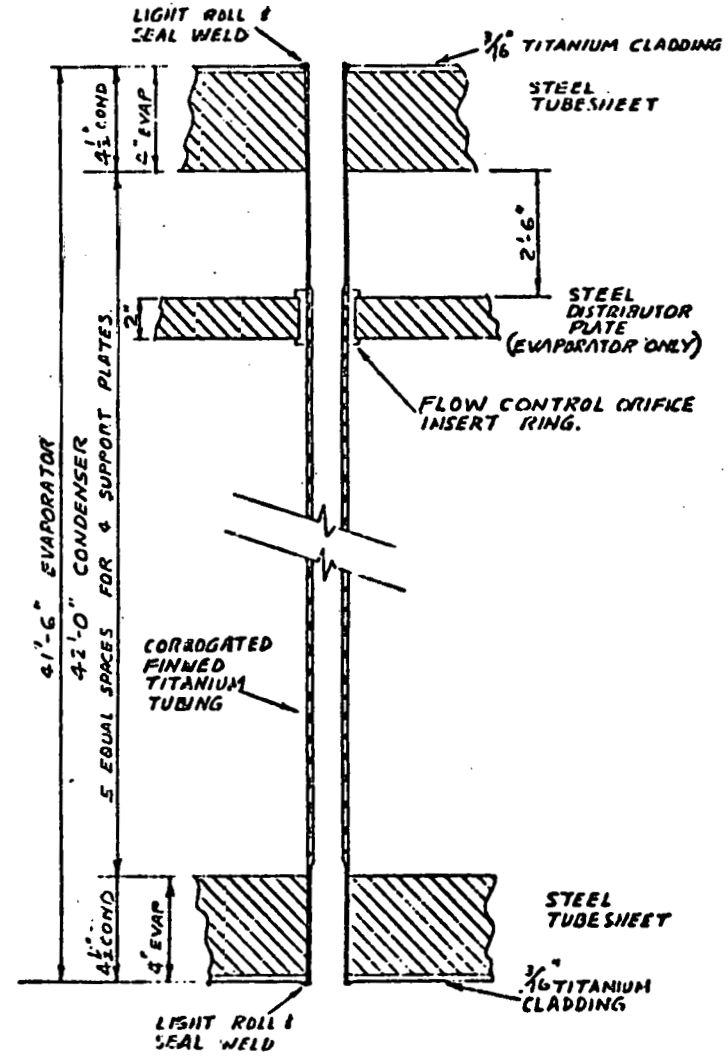

TUBE DETAILS

F W CLEMENS

TRW
SYSTEMS GROUP
REDONDO BEACH, CA

OTEC HEAT EXCHANGERS

FIGURE 6
5308-100

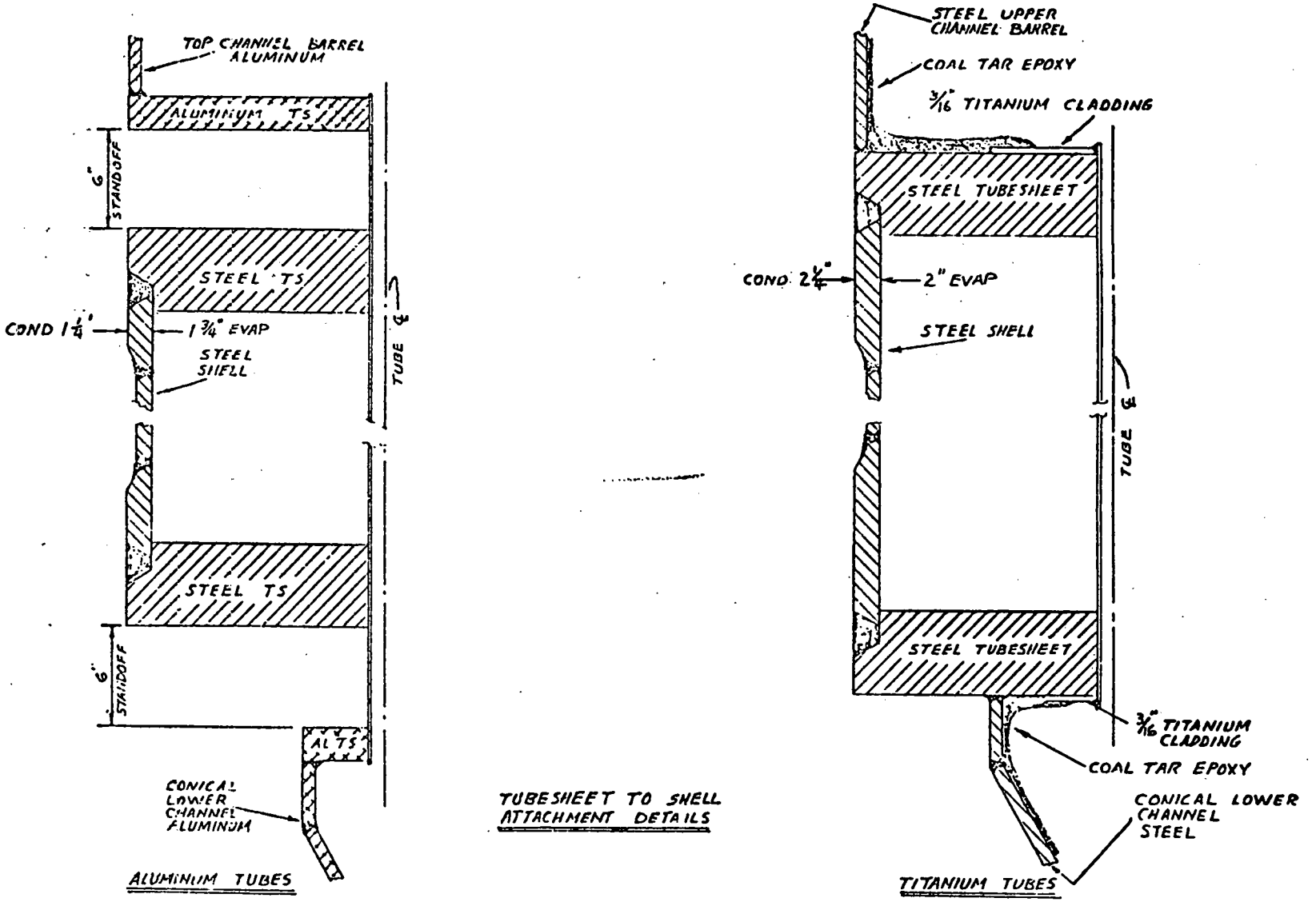

Neoprene Waterbox Coating System

1. Reference: DuPont Elastomers Notebook - Volume 201, April 1978. Neoprene Coating by Protective Rubber Coatings (Bristol) Ltd., England.

2. Application: Portishead "A" Power Station - Bristol, England. Condenser tube plates and waterboxes, coated with Neoprene coating of 60 mils total thickness, exposed to high velocity silted salt water for 32 years. Still in service during March 1978, (See Attachment-4).

3. Coating System Details:

- Surface Preparation - Sandblast to NACE No. 1 white metal blast cleaned surface. (See, SSPC-SP5-63 white metal blast cleaning)
- Prime Coat* - GACO Primer N-11R (inhibitive primer)
- Top Coat* - GACO Neoprene Liquid Lining N-200-1 unit coating thickness = 5 mils Total coating thickness = 60 mils
- Inspection - Electrical continuity test (wet or dry)
- Supplier - GACO Western, Inc.
  8023 E. Slauson Ave.
  Montebello, Calif. 90640
  (213) 254-0536
- Applicator - Parker Brothers
  7044 Bandini
  Los Angeles, Calif.
  (213) 723-8701

* These coating comply with specification MIL-R-15058F, type IV.

RELIABLE PROTECTION FOR 16 YEARS

Neoprene coating, applied in 1946 to condenser water box in English power station, is still successfully combatting corrosion-erosion from tidewater

(Originally published in 1963)

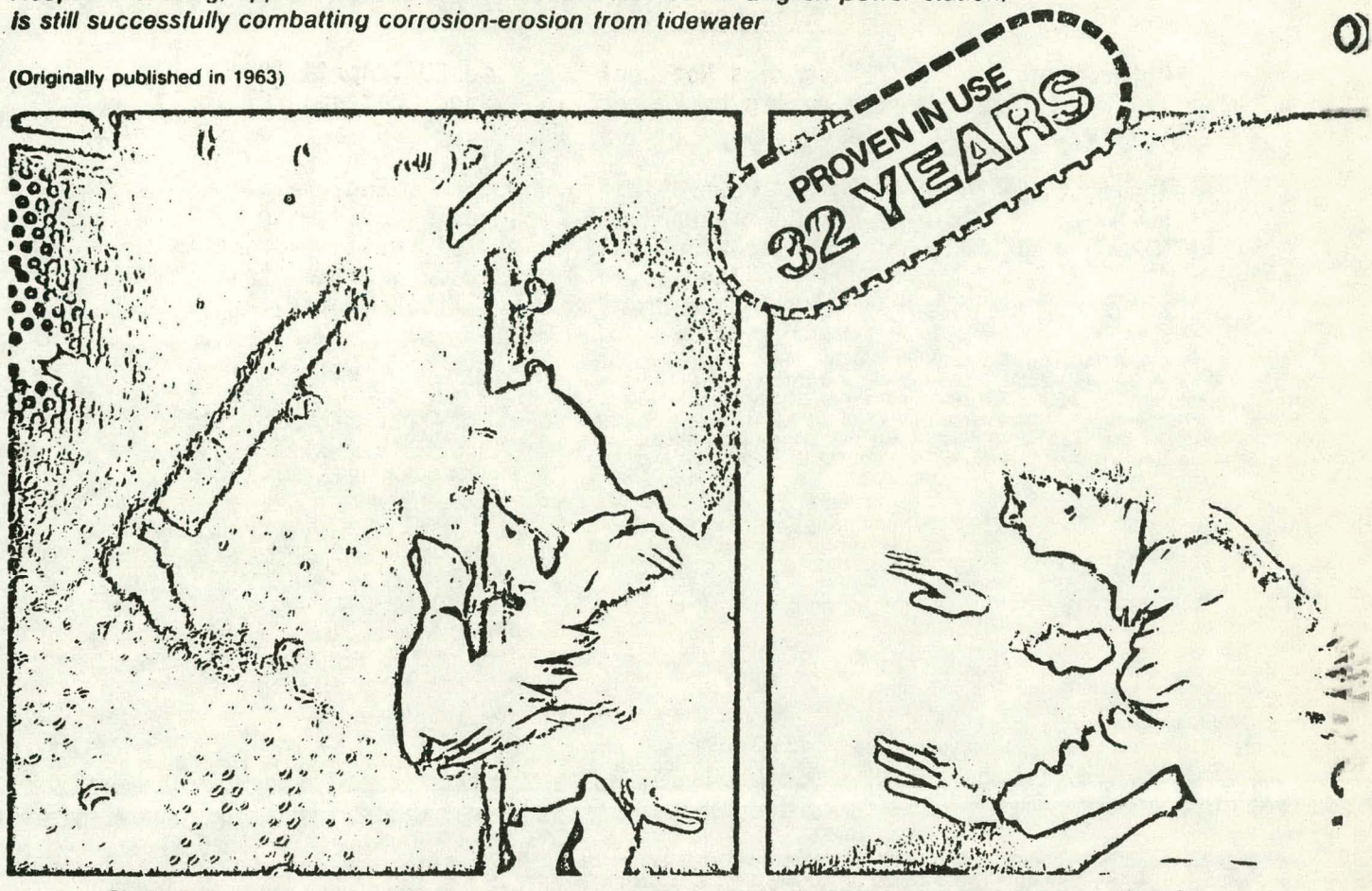

Electrostatic tests and close visual inspection proves Neoprene coating is still firmly attached after years of service.

Sea water is an inexpensive coolant to obtain but engineers at the Portishead "A" Power Station, about 10 miles from Bristol on the Severn Estuary, were painfully aware of how expensive it is to control. Pumped directly from the estuary, millions of gallons of sea water were used per day as the cooling medium in the station's main steam condensers. The supply was convenient and inexhaustible. However, its salt content made it corrosive to metal and the presence of sand and silt intensified this attack by their scouring effect. Condenser tube plates suffered heavy pitting from the cooling water's corrosive-erosive action.

This double-edged hazard to equipment was effectively blunted in 1946 when a protective coating based on Du Pont Neoprene was brush-applied to the condenser tube plates. It was put on the bare metal, to a thickness of about one-sixteenth inch (1.6 mm), after careful surface preparation. Neoprene was chosen for this job because of its well-known resistance to salt water, abrasion, oil and chemicals plus its excellent adhesion to metals and reputation for long life.

The choice has not been regretted. Apart from normal cleaning, the water boxes of the condensers have not been opened up at all for anticorrosion maintenance in the sixteen plus years since the Neoprene coating was put on. This is an important economic advantage because of the considerable expense involved each day a generator is shut down for condenser repairs.

Following the success of this initial coating at Portishead, other stations of the Central Electricity Generating Board in Great Britain have specified the same Neoprene formulation for similar purposes. These include three nuclear power stations as well as a number of conventional facilities.

Equally long life is expected of these installations. When recently inspected, the 1946 Neoprene coating was still resilient and unimpaired. It had every appearance of lasting another sixteen years!

1978 UPDATE

Protective Rubber Coatings (Bristol) Ltd. confirmed, in March, 1978, that the original Neoprene coating indeed was still in service. Occasional repairs to portions mechanically damaged by maintenance workers have been necessary but the major portion of the 1946 coating job is intact after 32 years.

Neoprene coating by
Protective Rubber Coatings (Bristol) Ltd., England Circle Code No. 7

Ameron

DIMETCOTE® 6

MARINE COATING

TYPE: [illegible]

[illegible]

SUITABLE FOR: Ships, Workboats, Barges, Offshore Structures

- ☐ **A SUPERIOR MARINE "PERMANENT" PRIMER**
- ☐ **CAN BE APPLIED AT TEMPERATURES DOWN TO 0°F**
- ☐ **WITHSTANDS WATER CONTACT 15 MINUTES AFTER APPLICATION**
- ☐ **RAPID-CURES AT HUMIDITIES UP TO 99% AND VERY LOW TEMPERATURES**
- ☐ **A SELF-CURING, ALKYL SILICATE-BASED INORGANIC ZINC**

▪ Best inorganic zinc coating for applications in low temperatures, high humidities ▪ Extremely resistant to severe marine environments ▪ Withstands intermittent contact with water, rain or condensation 15 minutes after application ▪ Develops a tough, abrasion-resistant film in approximately 2 hours ▪ Cures to permit topcoating after 24 hours ▪ High metallic zinc content... provides cathodic protection to steel surfaces, including sharp edges, nuts and bolts.

Included in: U.S. Navy Chapter 9190 as a self-curing inorganic zinc silicate coating approved for application to hulls above water line, decks and superstructures of U.S. Navy vessels.

PRINCIPAL AREAS OF USE:

☐ **Barges**
▪ Sides and Rakes ▪ Decks ▪ Deck Piping up to 150°F ▪ Deck Machinery ▪ Cargo Holds ▪ Cargo Tanks ▪ Void Spaces

☐ **Ships, Workboats**
▪ Keel to Light Load Line ▪ Boottopping ▪ Deep Load Line to Rail ▪ Weather Decks ▪ Superstructures ▪ Booms, Masts, King Posts ▪ Deck Piping (Up to 150°F) ▪ Deck Machinery ▪ Cargo Holds ▪ Cargo/Ballast Tanks ▪ Fuel Oil Tanks ▪ Void Spaces and Cofferdams

☐ **Offshore Platforms**
▪ Splash Zone and Submersible Areas ▪ Drilling Areas Subjected to Splash and Spillage of Drilling Muds ▪ Rig Jackets (Including Legs and Columns In and Above Tidal Zone) ▪ Deck Sections

Apply Dimetcote 6 in a single coat, at 2½ mils dry film thickness; badly pitted surfaces may require up to 5 mils, but never apply more than 6 mils. As a permanent primer, Dimetcote 6 will reduce maintenance and eliminate future need for extensive surface preparation when used under recommended Amercoat topcoat systems; obtain specific recommendations, based on service requirements, from the Ameron representative.

RESISTANCE — When Used Without A Topcoat

This chart is only a guide. For specific recommendations, see the Amercoat Coatings Tank Lining Chart.

WEATHER: Outstanding resistance. No loss of protective qualities even after prolonged exposure. Unharmed by ultraviolet light.

TEMPERATURE: Withstands heat up to 600°F (dry).

PETROLEUM: Ideally suited for fumes, splash, spillage or immersion in petroleum hydrocarbons, such as:

Aviation Gasoline	Fuel Oil
Jet Fuel	Motor Gasoline
Kerosene	

SALTS: Prolongs life of topcoat when suitably topcoated and subjected to splash and spillage of neutral salt solutions.

SOLVENTS: Resistant to fumes, splash, spillage or immersion in ketones, aromatic and aliphatic hydrocarbons, chlorinated hydrocarbons (water-free), alcohols, including:

Acetone	Carbon Tetrachloride
Xylene	Isopropyl Alcohol
Toluene	Ether Alcohols
Hexane	

ANIMAL AND VEGETABLE OILS: Suitable for immersion in animal and vegetable oils of free acid content below 2½%.

WATER: Ideally suited for atmospheric exposure to, and (with suitable topcoat) splash or spillage of fresh or salt water.

NOTE: As is true with all inorganic zinc silicate coatings, Dimetcote 6 is not recommended for immersion in, or spillage of, acid or alkali solutions.

FINISH	Matte
COLOR	Reddish Gray to Gray
RECOMMENDED DRY FILM THICKNESS PER COAT	2½ mils
NO. OF COATS REQUIRED	1
TOTAL DRY FILM THICKNESS DIMETCOTE 6	2½ mils
TOTAL VOLUME SOLIDS†	43.7%
THEORETICAL COVERAGE* @ 1 MIL	700 sq. ft. per gal.
THEORETICAL COVERAGE* PER COAT @ 2½ MILS	280 sq. ft. per gal.

*See Amercoat Technical Report on Coverage of Inorganic Zinc Coatings. When computing working coverage, allow for application losses, surface irregularities, etc.

NO. OF COMPONENTS	2
MIXING RATIO	15 lbs. Powder to 3/4 gal. Liquid
POT LIFE	24 hrs. minimum @ 70°F
APPLY OVER	Dry-abrasive blasted steel
APPLY BY	Conventional spray
DRYING TIME	Water-insoluble: 15 min. above 32°F; 15-30 min. @ 0-32°F Abrasion-resistant: 2 hrs. @ 70°F
CURING TIME	To Topcoat: 24 hrs. @ 70°F
TOPCOAT REQUIRED	For specific services
THINNER	Amercoat No. 65 Thinner (70°F or below), No. 101 Thinner (above 70°F). Order 1 gal. per 8 gals. Dimetcote 6
CLEANER	Amercoat No. 65 or No. 101 Thinner. Order 1 gal. per 10 gals. Dimetcote 6
MISCELLANEOUS	Moisture aids in achieving maximum film hardness

TEMPERATURE RESISTANCE	Up to 600°F (dry)
FLASH POINT	70°F Mixed (Tag Open Cup)
COMBUSTIBILITY	Flammable during application; cured film not combustible
WT. PER MIL.-SQ. FT. OF DRY FILM	0.4 oz.
ELECTRICAL CONDUCTIVITY	Weak conductor

PACKAGING	Separate containers make 1 gal. mixture
SHIPPING WEIGHT	Powder—16 lbs. Liquid—7.5 lbs.
GUARANTEED SHELF LIFE FROM SHIPMENT DATE	1 year

†Volatiles Measurement Method

DIMETCOTE® 6 APPLICATION INSTRUCTIONS

SURFACE PREPARATION

STEEL

Round off all rough welds and sharp edges. Remove weld spatter.

Dry-abrasive blast, including all pits and depressions; remove all mill scale, rust, rust scale, grease, paint or foreign matter. Surface profile from abrasive blasting should be similar to that obtained with fresh steel grit (G-40 size), steel shot (S-230 size), graded flint or silica sand (30-60 mesh), under nozzle pressure of 100 psi. If reusing blasting abrasives, clean them of contamination before reusing; do not reuse sand or flint abrasives.

Where an automatic blasting unit is used, its manufacturer should be consulted for "working" abrasive mixtures and line speeds.

OLD OR NEW GALVANIZING

Sweep-blast surface lightly to remove dirt, etc.

Apply Dimetcote 6 as soon as possible to prevent blasted surfaces from rusting. Keep surfaces moisture-free until coated. Keep oil, grease or other organic matter off surface before coating. **Spot reblast** to remove any contamination; solvent-wiping is not satisfactory.

EQUIPMENT REQUIRED

- **Pressure material pot** with mechanical agitator.
- **Separate atomizing** air and fluid pressure regulators.
- **Air Supply:** Compressor capable of continuous volume of 20 CFM at 80 psi minimum to each nozzle. For a moisture-free air supply, a moisture trap (such as DeVilbiss HRE-501 Oil and Moisture Separator) must be in the line between compressor and pressure spray pot and spray gun.
- **Air hose** for gun, 5/16" I.D.
- **Material hose**, ½" I.D.
- **Industrial spray gun**, such as DeVilbiss MBC 2E or 24E with graphite or Teflon needle packing and heavy "mastic" spring; or Binks No. 18 with 66X66P nozzle setup with No. 54-764 graphite or 2-28 Teflon needle packing and No. 54-839 heavy mastic spring.
- **30-60 mesh metal screen.**

SAFETY EQUIPMENT REQUIRED

(In Tanks or Confined Areas Only)

- **Explosion-proof lights** and electrical equipment.
- **Fresh air mask**, such as DeVilbiss P-MPH 527 and MPH 529, connected by ¼" I.D. hose directly to air source.
- **Nonsparking shoes** or tools for workers in area.
- **Exhaust fan** of sufficient capacity to keep solvent vapors below 20% of the explosive limit or ¼% by volume of solvent vapor in air.

Volume of Tank (Gallons)	Required Blower Size* (Cu. Ft./Min.)
500 - 5,000	1,000
5,000 - 20,000	2,000
20,000 - 100,000	5,000
100,000 - 250,000	10,000
500,000	15,000
1,000,000 - 2,000,000	20,000

*All blowers to be suction type.

APPLICATION PROCEDURE

1. **Flush equipment** with Amercoat No. 12 Cleaner to remove moisture from all application equipment; moisture can harden Dimetcote 6 in spray equipment.
2. **Discard desiccant bag** from Powder can.
3. **Stir total contents** of each Powder can slowly into total contents of each Liquid can until well dispersed. **Do not** reverse order. **Do not** vary proportions.
4. **Do not thin** except for workability in conditions such as hot, windy weather, and then with no more than 1 pint of No. 65 or No. 101 Thinner per gallon of mixed Dimetcote 6.
5. **Strain mixture** through 30-60 mesh screen to remove large particles.
6. **Keep mixture in closed container** until ready to use. Dimetcote 6 is sensitive to moisture in the atmosphere. If skinning occurs, remove skin by filtering through cheese cloth or fine mesh screen. Agitate slowly throughout application to maintain uniform suspension.
7. **Remove all dust** from surface to be coated.
8. **Regulate air pressure:** 40-60 psi to gun (with DeVilbiss equipment and 25-ft. hose); 10 psi to pot. **Note:** Required pressures may vary with temperature and hose length.
9. **Keep pressure pot** at approximately same elevation as spray gun.
10. **Make even, parallel passes.** Overlap each pass 50%.
11. **Apply a heavy, wet coat** to obtain proper thickness with no bare areas, pinholes or holidays.
12. **Double-lap spray** all welds, corners, edges, etc.
13. **Clean all spray equipment** immediately after use with Amercoat No. 65 or No. 101 Thinner (not water).
14. **If humidity is extremely low,** spray a water mist to effect rapid curing.
15. **If greater thickness is desired,** recoat when first coat is dry to touch.
16. **Random pinholes and holidays** should be touched up by brush when film is dry to touch. Bare areas should be resprayed.
17. **If damage occurs,** recoat with Dimetcote 6 when film is dry to touch.
18. **If topcoating is required,** allow to dry at least 24 hours.

WARNING: Dimetcote 6 Liquid is flammable and causes skin and eye irritation. Keep away from heat and open flame. Keep container closed. Use with adequate ventilation. Avoid prolonged breathing of vapor. Avoid contact with skin or eyes. Do not take internally. In case of contact, immediately flush skin with plenty of water; for eyes, flush with plenty of water for at least 15 minutes and get medical attention. If used in confined areas, observe the following precautions to prevent hazards of fire or explosion or damage to the health: (1) circulate adequate fresh air continuously during application and drying, (2) use fresh air masks and explosion-proof equipment, (3) prohibit all flames, sparks, welding and smoking.

WARNING: Dimetcote 6 Powder is a harmful dust. Avoid breathing dust. Wash thoroughly before eating or smoking. Keep away from feed or food products.

If welding is to be performed in confined spaces on steel coated with Dimetcote 6, do so in accordance with instructions in U.S.A. Standard Z 49.1—1967, "Safety in Welding and Cutting."

Amercoat
CORROSION CONTROL DIVISION
Home Office BREA, CALIFORNIA 92621

AMERCOAT® 83/84

MARINE COATING

- ☐ **A HIGHLY PROTECTIVE MARINE EPOXY COATING SYSTEM**
- ☐ **PROVIDES FULL PROTECTION IN ONLY TWO COATS**
- ☐ **FORMULATED FOR EXTERIOR HULL PROTECTION**
- ☐ **MEETS U.S. NAVY REQUIREMENTS FOR SUBMARINE HULLS, TOPSIDES AND BOTTOM AREAS**
- ☐ **FULLY COMPATIBLE WITH VINYL ANTI-FOULING TOPCOATS**

- ■ Specially formulated for maximum protection of steel in salt water
- ■ Ready for immersion in 24 hrs.
- ■ Cures at temperatures of 35°F and above
- ■ Available in six standard Navy colors and specified camouflage colors

Conforms to: U.S. Navy Chapter 9190; approved for coating submarine hulls, topsides and bottoms. Also acceptable for bottoms of surface vessels. Proprietary approval for application over post-cured inorganic zinc approved under MIL-P-23236.

PRINCIPAL AREAS OF USE:

☐ **Ships, Workboats**

- ■ **Keel to Light Load Line** — 1 coat of No. 83 Primer, at 2 mils dry film thickness, over Dimetcote 3 or Dimetcote 6. Topcoat with 1 coat of No. 84, at 6 mils dry and 2 coats of Amercoat No. 67 Anti-Fouling, at 3 mils each. **Alternate:** the same system except without Dimetcote 3 or 6 as permanent primer.

☐ **Submarines**

- ■ **Keel to Waterline** — 1 coat of No. 83 Primer, at 2 mils dry, topcoated with 1 coat of No. 84, at 6 mils and 1-2 coats of a Navy-approved antifouling.
- ■ **Topsides** — 1 coat of No. 83 Primer, at 2 mils dry, topcoated with 1 coat of No. 84, at 6 mils.

Where required, U.S. Navy Antifouling Formulas 121/63 or 129/63 or Amercoat No. 67 or No. 70 Anti-Fouling may be applied.

	No. 83 Prime	No. 84 Topcoat
FINISH	Matte	
COLORS	No. 83: Oxide Red. No. 84: Black Navy 3, Gray Navy 7, Gray Navy 11, Ocean Gray Navy 17, Haze Gray Navy 27, White Navy 82 and specified camouflage colors	
RECOMMENDED DRY FILM THICKNESS PER COAT	2 Mils	6 Mils
NO. OF COATS REQUIRED	1	1
TOTAL DRY FILM THICKNESS	2 Mils	6 Mils
THEORETICAL COVERAGE* PER COAT @ 1 MIL	690 Sq. Ft. per Gal.	690 Sq. Ft. per Gal.
THEORETICAL COVERAGE* PER COAT (Sq. Ft./Gal.)	345 @ 2 Mils	115 @ 6 Mils
*When computing working coverage, allow for application losses, surface irregularities, etc.		
NO. OF COMPONENTS	2	2
MIXING RATIO (Parts by Volume)	1 cure: 2 resin	1 cure: 2 resin
MINIMUM POT LIFE	24 hrs. @ 70°F	
APPLY BY	Airless, Conventional Spray; Brush Touchup	
APPLY NO. 83/84 OVER	Blasted Steel; Clean Dimetcote (See other side for repair)	
DRYING TIME	See Application Instructions	
TOPCOATS COMPATIBLE	Vinyl antifouling (Navy Formula 121/63 or 129/63), Amercoat No. 67 or 70 Anti-Fouling	
THINNER AND CLEANER	Amercoat No. 9 HF Thinner--Order 1 gal. per 10 gals. No. 83 and 84	
COMBUSTIBILITY	Chars	
WT. PER SQ. FT. OF TOTAL DRY SYSTEM	Approx. 1.25 oz. @ 8 Mils	
ELECTRICAL CONDUCTIVITY	Nonconductor	
PACKAGING	1's and 5's (Unitized)	
SHIPPING WEIGHT	1's — 13 lbs. 5's — 65 lbs.	1's — 12 lbs. 5's — 59 lbs.
GUARANTEED SHELF LIFE FROM SHIPMENT DATE	1 Year	1 Year

AMERCOAT® 83/84 APPLICATION INSTRUCTIONS

SURFACE PREPARATION

☐ Immersion — Bare Steel

1. **Round off** all rough welds and sharp steel edges. Remove weld spatter.

2. **Dry-abrasive blast**, including all pits and depressions; remove all mill scale, rust, rust scale, grease, paint or foreign matter. **Blast only with** steel grit (G-40 size), steel shot (S-230 size) or graded flint or silica sand (30-60 mesh). **If reusing steel grit or shot**, clean them of contamination before reusing. **Do not** reuse sand or flint abrasives. **Use air of** 100 psi at 200 CFM per blast nozzle.

3. **Apply No. 83 Primer as soon as possible** to prevent blasted surfaces from rusting. Keep moisture, oil, grease or other organic matter off surface before coating. If surface is dry, clean by vacuum brushing or air blow down. If greasy, use solvent or oil cleaner followed by fresh water rinse, then dry thoroughly.

☐ Immersion — Dimetcote Surfaces

1. **Be certain surface is fully cured**, dry and clean.

2. **Wash off any cure crystals**; scrub with water and stiff bristle brush to remove heavy deposits.

☐ **Repair** — No. 83/84 Abraded to Bare Steel

Remove all rust, growth, peeling paint, etc. by spot reblasting, if possible. Otherwise, disc-sand with No. 16 open-coat sandpaper, feathering edges of intact coating.

☐ **Repair** — Abraded No. 84 Topcoat; No. 83 Prime Intact

Scrape and/or lightly sand intact Prime to remove any loosely-adhering coating; feather surrounding edges. Solvent-wipe damaged area.

EQUIPMENT REQUIRED

☐ For Airless Spray —

- **Standard airless spray equipment**, such as **Gray, DeVilbiss** or any others using a 28:1 pump ratio; .015" or .017" tip (for No. 83); .017" or .021" tip (for No. 84). 80-100 psi inbound

☐ For Conventional Spray —

- **Pressure material pot**
- **Separate atomizing air and fluid pressure regulators**
- **Air supply:** compressor capable of supplying a continuous volume of air at 80 psi to nozzle of each gun
- **Air hose** for gun, 5/16" or 3/8" I.D.
- **Material hose**, 1/2" I.D.
- **Industrial spray gun**, such as **DeVilbiss** MBC or JGA with 78 or 765 Air Cap, and "E" Fluid Tip

SAFETY EQUIPMENT REQUIRED
(In Confined Areas Only)

- **Explosion-proof** lights and electrical equipment.
- **Fresh air mask**, such as **DeVilbiss** P-MPH 527 and MPH 529, connected by 1/4" I.D. hose directly to air source
- **Exhaust fan** of sufficient capacity to keep solvent vapors below 20% of the explosive limit or 1/4% by volume of solvent vapor in air

APPLICATION PROCEDURE

1. **Clean all equipment** with No. 9 HF Thinner.

2. **Stir resin and cure** for No. 83 separately. Then mix one part cure into two parts resin (by volume). Stir for about 5 minutes with hand or power mixer. **When ready to apply No. 84**, follow this same mixing procedure.

☐ **If Using Airless Spray Equipment**

a. **At temperatures above 50°F**, thinning is not normally required. **At temperatures of 35-50°F**, thinning may be needed for workability; if so, thin with no more than 1 pint No. 9 HF Thinner per gallon No. 83 or No. 84.

☐ **If Using Conventional Spray Equipment**

a. **At temperatures above 35°F**, thin only for workability, and then with no more than 1 pint No. 9 HF per gallon No. 83 or No. 84.

b. **Regulate air pressure:** 20-25 psi to pot; 60-75 psi to spray gun (with DeVilbiss). **NOTE:** pressure requirements may vary with hose length and temperature.

3. **Apply in even, wet coats**, overlapping each pass 50%. Give special attention to corners, welds, rough areas, edges, etc. Leave no pinholes, bare areas or holidays.

4. **Applying No. 83 Prime — Above 35°F**

a. **Spray one coat** at 2 mils dry film thickness.

b. **Allow No. 83 to dry** at least 2 hrs. @ 70°F (4 hrs. @ 35-50°F) before applying No. 84. No. 83 may be allowed to dry up to 180 days above 35°F before topcoating. If more than 180 days elapse, apply a "mist" coat of No. 83 before topcoating.

5. **Applying No. 84 Topcoat**

At 35-50°F —

a. **Spray on 2 coats**, each at 3 mils dry film thickness. Let dry 4 hrs. between coats.

b. **Allow No. 84 to dry** at least 4 hrs. before applying antifouling. No. 84 may be allowed to dry up to 48 hrs. before applying antifouling.

Above 50°F —

a. **Apply No. 84** in a single coat at 6 mils dry film thickness.

b. **Allow No 84 to dry** at least 4 hrs. before topcoating with antifouling. No. 84 may dry up to 24 hrs. before applying antifouling.

6. **Clean equipment immediately** after application with No. 9 HF Thinner.

☐ Curing No. 83/84 System

1. **Before walking on No. 83/84**, allow system to dry 24 hrs. @ 70°F, 5 days @ 50°F or one week @ 35°F.

2. **Before immersion**, No. 83/84 system must dry at least 24 hrs. above 35°F.

☐ Touchup or Repair

Consult with Amercoat Representative on procedures for touching up or repairing No 83/84 system.

CAUTION: No. 83/84 Resin and Cure are combustible. Keep away from heat and open flame. Keep containers closed. Use with adequate ventilation. Avoid prolonged breathing of vapor. Avoid prolonged and repeated contact with skin. In confined areas, observe the following precautions to prevent hazards of fire or explosion or damage to the health: (1) circulate adequate fresh air continuously during application and drying, (2) use fresh air masks and explosion-proof equipment, (3) prohibit all flames, sparks, welding and smoking.

Amercoat
CORROSION CONTROL DIVISION
Home Office: BREA, CALIFORNIA 92621

THIS PAGE

WAS INTENTIONALLY

LEFT BLANK

APPENDIX D.3

MATERIALS COMPATIBILITY, RECOMMENDED MATERIALS

TRW
DEFENSE AND SPACE SYSTEMS GROUP
ONE SPACE PARK • REDONDO BEACH • CALIFORNIA 90278

INTEROFFICE CORRESPONDENCE

5515.2.78-421

TO: L. A. Rosales CC: Distribution DATE: August 28, 1978

SUBJECT: Ammonia Metering Device Flow Tests

FROM: M. P. Bianchi
BLDG. 01 MAIL STA. 2230 EXT. 52303

INTRODUCTION

A series of flow tests have been run to determine a rough order of magnitude flow rate from the polyethylene metering device proposed for the OTEC falling film heat exchanger tubes. Because of the difficulties in using liquid ammonia for this test, it was decided to use a modeling fluid; that is, one with physical properties similar to liquid ammonia but with a high enough boiling point so that the experiment could be run at room temperature and ambient pressures. Those properties it was desired to simulate were surface tension, density, and viscosity. Ideally, the liquid was to be non-toxic, non-flammable, and was to possess a boiling point as high above room temperature as possible. As will be shown, the latter property had a pronounced effect on the reproducibility of the test. Table I contains a list of some of the candidate fluids, and their properties, proposed for this test. Some candidates, not shown, were rejected since they were not readily available in quantities sufficient for the test. Originally, a water/surfactant solution was developed for heat exchanger tube bundle wetting and distribution tests. The initial requirements for this fluid was that it should possess a contact angle to acrylic (the tube bundle model material) similar to that of liquid ammonia to titanium. The properties of that solution are also shown in Table I. However, as will be discussed later, this fluid does not behave completely like liquid ammonia and the reasons for that will be discussed. Along with the flow rate measurements, the original tests attempted to establish the wetting and distribution of the fluid over the fluted titanium tubes after leaving the metering device. This was unsuccessful largely because the surfactant water mixture was used. Again, the reasons for this will be discussed. Subsequently, isopropyl alcohol was tried and this resulted in complete wetting of the tube which then led us to use it in the metering device tests.

TESTS

A simple flow-rate test set-up was assembled as shown in the sketch of Figure 1. The working principle is as follows:

1. A constant "head" is kept on the metering orifices (see Figures 2 and 3 for details of orifices) by pouring liquid at a rate sufficient to maintain a continuous overflow into the reservoir (Figure 1).

2. After a constant flow down the tube was achieved, a quantity of the fluid was collected over a specified time by means of a beaker held under the tube.

3. The flow-rate was then calculated as the weight of the fluid divided by time taken to collect it.

4. Acetone, isopropyl alcohol and water were the fluids used to measure the flow-rate from the metering device.

RESULTS

The results of the flow-rate measurements from the metering device with the three test fluids are shown in Table II. As can be seen from the results with acetone and isopropyl alcohol, the tests were less than successful. The measurements with water, however, were consistent and showed as good a reproducibility as could be expected from the test set-up. The reason for the decreasing flow rate exhibited by acetone and isopropyl alcohol was temperature. The high evaporation rates, especially of the acetone, caused the device to cool steadily when these fluids were flowing. For example, the temperature during seven consecutive one-minute flow measurements with acetone dropped from $70^{o}F$ to $50^{o}F$. The isopropyl alcohol showed a somewhat slower fall with the temperature dropping from $70^{o}F$ down to $65^{o}F$ over the same number of one-minute flow measurements. Since polyethylene has a large coefficient of expansion (83 to 167 x 10^{-6} in/in/^{o}F), the effect was to cause the orifices in the metering device to shrink a significant amount thus resulting in a steady constriction of these openings. The viscosity also decreased as the temperature dropped, but the change was small and the effect on the flow was probably insignificant.

Both the acetone and the isopropyl alcohol (IPA) completely wet the titanium tube after leaving the orifices in the metering device. Water did not. This was not only because of its higher surface tension, hence poor wettability, but also because the higher density of the water results in a higher momentum when flowing down the tube than that for acetone and IPA. This was the reason for the channeling of the water/surfactant solution even though the surface tension of this fluid is much lower than that of water.

DISCUSSION

The implications of these results to the metering of liquid ammonia with the polyethylene device are difficult to assess. If the device operates at a temperature equal to the installation temperature with little or no variation, the device should work providing, of course, the tube tolerances can be somehow accommodated. Aside from the serious problem of the orifice size change with temperature encountered in our test, we also found that because of the large expansion coefficient differences between the aluminum tube plate (11.7 to 13.7 X 10^{-6} in/in/^{o}F) and the polyethylene metering device, cooling (because of test liquid evaporation) caused a gap to steadily open between the plate and the device which allowed liquid to flow out. The low surface tension of acetone and isopropyl alcohol caused them to wet and spread across the horizontal surface of the tube plate bottom resulting in random dripping from various areas of the plate. In the beginning, this resulted in somewhat erratic measurements if the drops happened to land in our collection beaker. Later we were able to guard against this in our experiment; however, the implications for the OTEC falling film evaporation if cooling occurs, I believe, will have to be looked at. The steel tube sheet proposed for OTEC has an even lower coefficient of expansion than aluminum (approximately 6 to 8 x 10^{-6} in/in/^{o}F) which will result in the same or an even worse gap forming tendency if cooling occurs during operation of the evaporator.

Although not an objective of this test, it was noted that the tube flute ridges were wet by both the acetone and the isopropyl alcohol. However, it was found that the wetting occurred for a greater length with the isopropyl, which we attributed to its higher boiling point hence slower evaporation rate. We did not observe wavefronts in the liquids flowing down the tube which theoretically are supposed to occur on fluted tubes.

CONCLUSIONS

I would like to reiterate that the results of these flow tests on the polyethylene metering device should be considered rough order of magnitude measurements. The difficulties in measurements encountered with the test fluids, as well as problems of fitting the machined metering device without distortion, preclude labeling these tests as definitive.

MPB:cd

Attachments: (1) Table I - Room Temperature Physical Properties
(2) Table II - Flow Rate Measurements
(3) Figure 1 - Cross Sectional Sketch of Flow Rate Measurement Test Set-up
(4) Figure 2 - Polyethylene Metering Device
(5) Figure 3 - Polyethylene Metering Device

TABLE I

ROOM TEMPERATURE PHYSICAL PROPERTIES

FLUID	DENSITY (GMS/CM^3)	VISCOSITY (CENTIPOISE)	SURFACE TENSION (DINES/CM)	BOILING POINT (^oC)
Acetone	0.79	0.34	23.7	56
Isopropyl Alcohol	0.79	2.20	21.7	82
Ethyl Alcohol	0.79	1.20	21.4	78
Hexane	0.66	0.34	18.4	69
Octane	0.70	0.55	21.8	126
Ammonia (Liquid)	0.62	0.16	20	N/A
Water	1.00	1.00	72.8	100
0.1%/Wt QS10/H_2O (Surfactant Solution)	$\cong$1.0	TBD	27.1	$\cong$100

TABLE II

FLOW RATE MEASUREMENTS

FLUID COLUMN HEIGHT: 10 inches

ORIFICE DIMENSIONS: See Figures 2 and 3

FLUID	TEST	TIME (SEC)	WEIGHT (GMS)	FLOW (GMS/SEC)	TEMP. (^{o}F)
Acetone	1	60	300.2	5.0	70
"	2	"	276.5	4.6	
"	3	"	264.7	4.4	
"	4	"	260.7	4.3	
"	5	"	241.0	4.0	
"	6	"	237.0	4.0	
"	7	"	229.1	3.8	50
Isopropyl Alcohol	1	60	145.4	2.4	70
"	2	"	137.5	2.3	
"	3	"	130.4	2.2	
"	4	"	118.5	2.0	
"	5	"	113.8	1.9	
"	6	"	106.7	1.8	
"	7	"	98.8	1.7	64
Water	1	60	260.0	4.3	70
"	2	"	265.0	4.4	
"	3	"	264.0	4.4	
"	4	"	266.0	4.4	
"	5	"	265.0	4.4	70

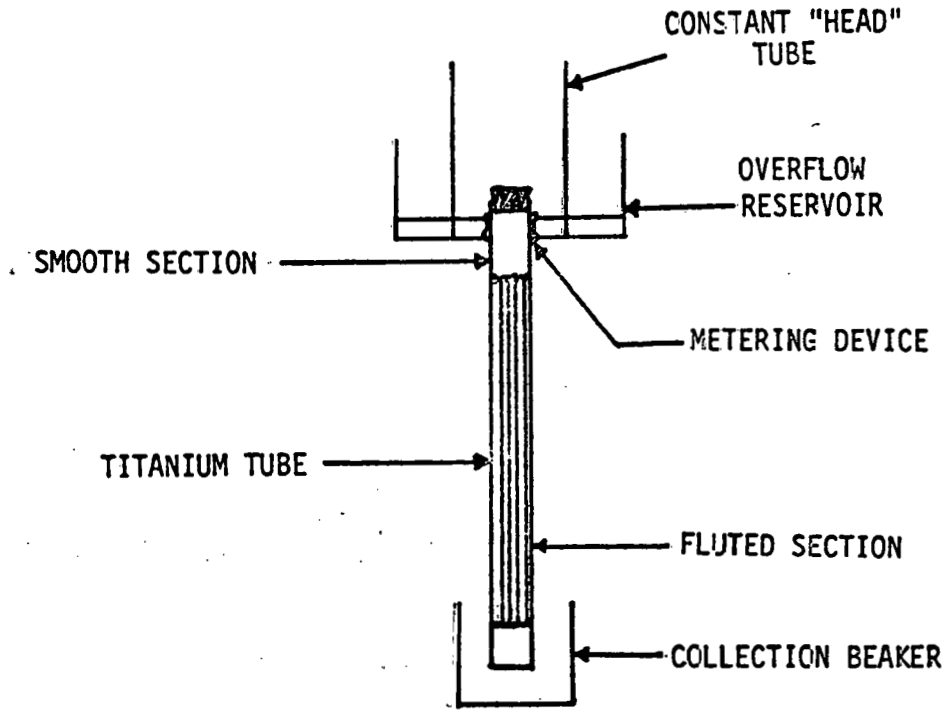

FIGURE 1

CROSS SECTIONAL SKETCH
OF
FLOW RATE MEASUREMENT TEST SET-UP

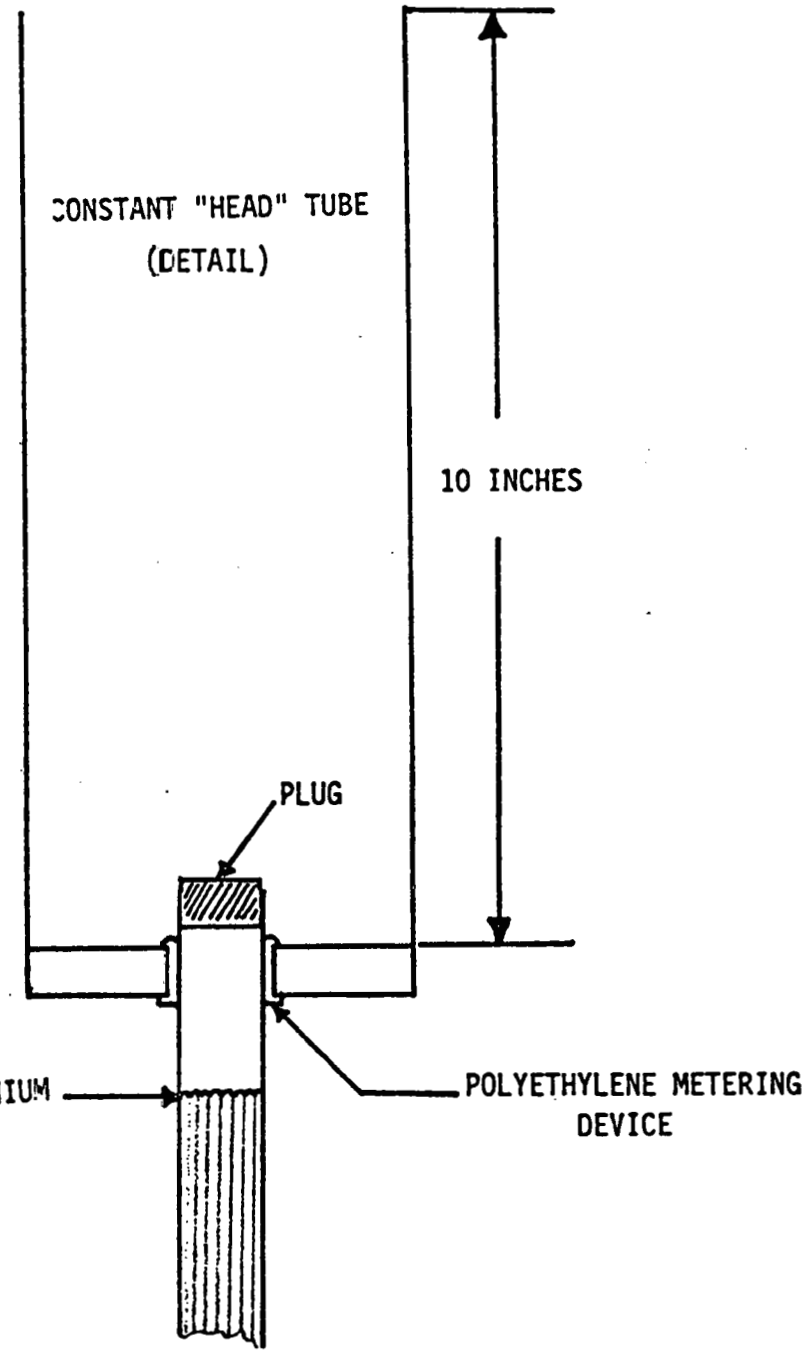

FIGURE 2

POLYETHYLENE METERING DEVICE
DIMENSIONS AND ORIFICE ARRANGEMENT

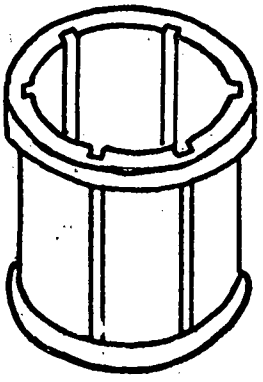

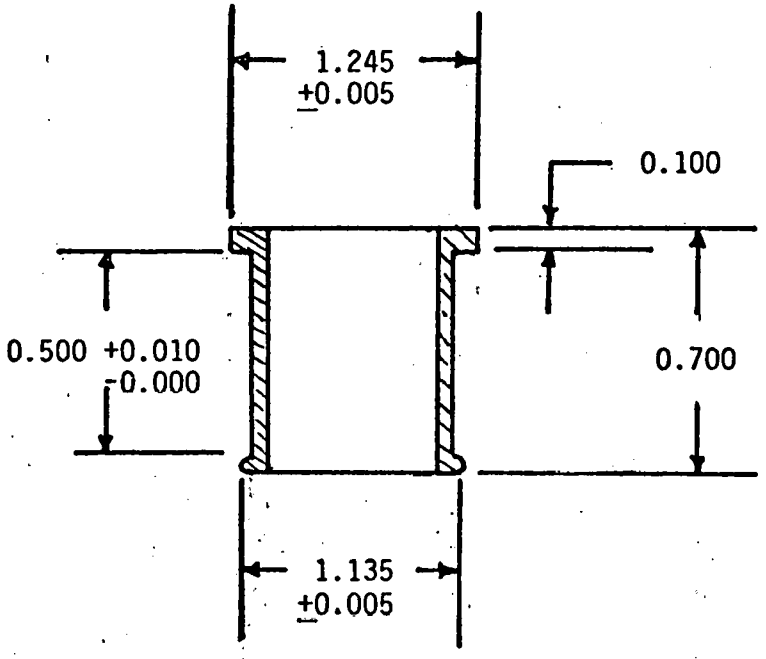

FIGURE 3

POLYETHYLENE METERING DEVICE
ORIFICE DIMENSIONS

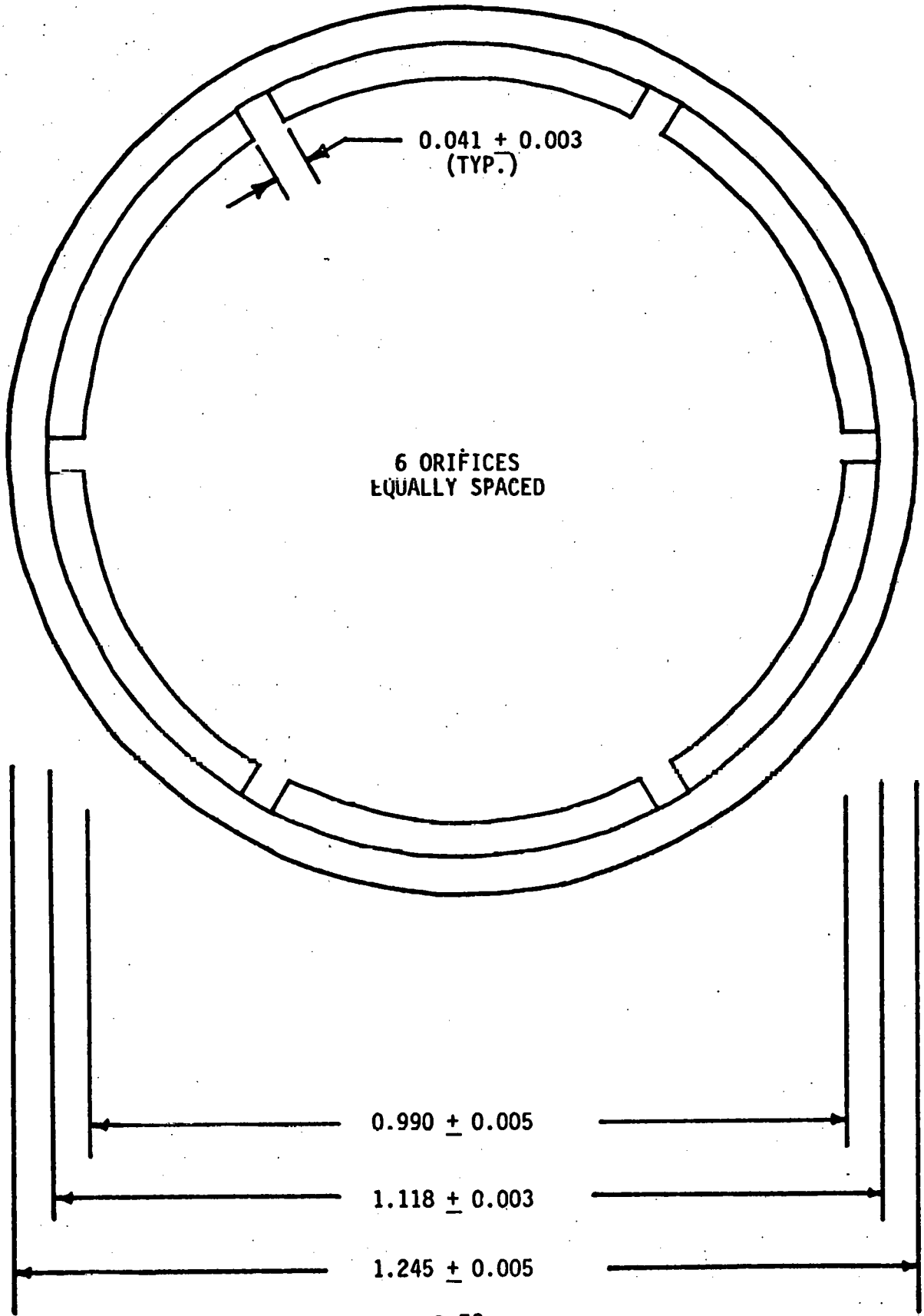

DISTRIBUTION

F. T. Brewen	01/2230
T. C. Dvorak	01/2220
J. S. Hicks	01/2080
M. Kwan	01/2220
W. I. Rogers	01/2230
L. V. Warner	01/2111

MATERIAL SELECTION FOR AMMONIA SERVICE COMPONENTS

PIPING CLASSIFICATION A

CARBON STEEL (AMMONIA SERVICE)

GENERAL	Maximum pressure rating:	150 psig at 100°F
	Minimum temperature:	Minus 28°F
PIPE	1/2 inch through 20 inches:	ASTM A106, Grade B, or API-5L BRG or ASTM A333 GR6 standard weight, seamless or electric-resistance welded.
	Wall thickness for larger diameters:	
	24-36 inches	3/8 (.375) wall thickness.
	60-72 inches	9/16 (.5625) wall thickness.
FITTINGS	2" and smaller:	ASTM A420, WPL6 or ASTM A105, Grade II, ANSI B16.11, 2000#, socket weld, carbon steel.
	2-1/2" and -arger:	ASTM A420, WPL6 or ASTM A234, Grade WPB, ANSI B16.9, same schedule as pipe, butt weld, carbon steel (long radius elbows).
FLANGES		ASTM A350-LF2 or ASTM A181, Grade II, ANSI B16.5, 300#, weld neck or slip on, raised face. Bore to match pipe I.D. Sealing surface finish 500 AARH or less.
GASKETS		Flexitallic Spiral wound type CG.
BOLTS		ASTM A193, Grade B&, ANSI B18.2.
NUTS		ASTM A194, Grade 4, ANSI B18.2 Heavy, semi-finished, hexagonal.

Note: Material for pipe, fittings and flanges shall match.

MATERIAL SELECTION FOR AMMONIA SERVICE COMPONENTS

PIPING CLASSIFICATION B

CARBON STEEL (WELDED) (NITROGEN GAS)

GENERAL	Maximum pressure rating:	275 psig at 100°F
	Minimum temperature:	Minus 20°F
PIPE	1/2 inch through 180 inches:	ASTM A53, Grade B, or ASTM A106 GRB standard weight, seamless or electric-resistance welded.
FITTINGS	2 inches and smaller:	ASTM A420, WPL6 or ASTM A105, Grade II, ANSI B16.11, 2000#, socket weld.
	2-1/2 inches and larger:	ASTM A420, WPL6 or ASTM B16.9, same schedule as pipe, black, but weld (long radius elbows).
FLANGES		ASTM A350-LF2 or ASTM A181, Grade II, ANSI B16.5, 150#, weld neck, raised face with concentric serrations. Bore to match pipe I.D.
GASKETS		Johns-Manville No. 76, i/8 inch thick ring.
BOLTS		ASTM A193, Grade B7, ANSI B18.2.
NUTS		ASTM A195, Grade 4, ANSI B18.2 heavy, semi-finished, hexagonal.

MATERIAL SELECTION FOR AMMONIA SERVICE COMPONENTS

PIPING CLASSIFICATION C

CARBON STEEL (AMMONIA SERVICE)

GENERAL	Maximum pressure rating:	86 psig at 100°F
	Minimum temperature:	Minus 28°F.
PIPE	1/2 inch through 20 inches:	ASTM A106, Grade B, or API-5L GRB or ASTM A333 GR6 standard weight, seamless or electric-resistance welded.
	Wall thickness for larger diameters:	
	94-120 inches	9/16 (.5625) wall thickness.
FITTINGS	2" and smaller:	ASTM A420, WPL6 or ASTM A105, Grade II, ANSI B16.11, 2000#, socket weld, carbon steel.
	2-1/2" and larger:	ASTM A420, WPL6 or ASTM A234, Grade WPB, ANSI B16.9, same schedule as pipe, butt weld, carbon steel (long radius elbows).
FLANGES		ASTM A350-LF2 or ASTM A181, Grade II, ANSI B16.5, 300#, weld neck or slip on, raised face. Bore to match pipe I.D. Sealing surface finish 500 AARH or less.
GASKETS		Flexitallic Spiral wound type CG.
BOLTS		ASTM A193, Grade B7, ANSI B18.2.
NUTS		ASTM A194, Grade 4, ANSI B18.2 Heavy, semi-finished, hexagonal.

Note: Material for pipe, fittings and flanges shall match.

OTEC PSD I AMMONIA CONDENSER SUMP T-2

1	Service LIQUID AMMONIA				Item T-2		
2	Quantity ONE (1) Dia 120 in ID				Length between tangents 26'-6"		horiz YES
3	DESIGN CONDITIONS				OPERATING CONDITIONS		
4	Code ASME SECT. VIII DIV I				Operating pressure		psig
5					Operating temp 50 °F	Liquid sp gravity .625	
6	Design pressure, internal 150 psig				Liquid level for mechanical design is above the bottom TL	9'-0"	
7	At design temperature -28 TO +120 °F						
8	Design pressure, external 7.5 psig						
9	At design temperature -28 TO +120 °F						
10	Corrosion allow 1/8 in						
11	Joint eff, shell 85% ,heads 100%						
12	Wind pressure —						
13	Earthquake — G						
14	Postweld heat treat NO						
15	Radiograph SPOT						
16	Insulation YES thk. 3 in						
17							
18	MATERIAL						
19	Heads SA-516-60 OR APP'VD						
20	Shell SA-516-60 EQUAL						
21	Support CARBON STEEL						
22	Nozzle necks SA-106						
23	Flanges SA-105						
24	Couplings —						
25	Gaskets FLEXITALLIC TYPE CG						
26	Fixed internals —						
27	Removable internals —						
28							
29	SUPPLIED BY SELLER						
30	Type support SADDLES						
31	Manhole cover, hinged YES , w/davit —						
32	Insulation/fireproofing support YES						
33	Clips for ladders and platforms YES						
34	Clips for pipe supts and pipe guides NO						
35	Lifting lugs NO						
36	Surface preparation and paint BLAST						
37	CLEAN PER SSPC SP6						
38	PRIME ORGANIC ZINC						
39	NOZZLES						
40	Mark	No	Size	Rtg Facing	Service		
41	N-1	1	6"	300#	RELIEF		
42	N-2	1	6"	300#	L.L. GUAGE		
43	N-3	1	24"	BW	PUMP		
44	N-4	1	6"	BW	MAKE-UP		
45	N-5	1	24"	BW	PUMP		
46	N-6	1	30"	BW	INLET		
47	M-1	1	18"	300#	MAN WAY		
48							
49							
50							
51							
52							
53							
54							
55							
56							
57							

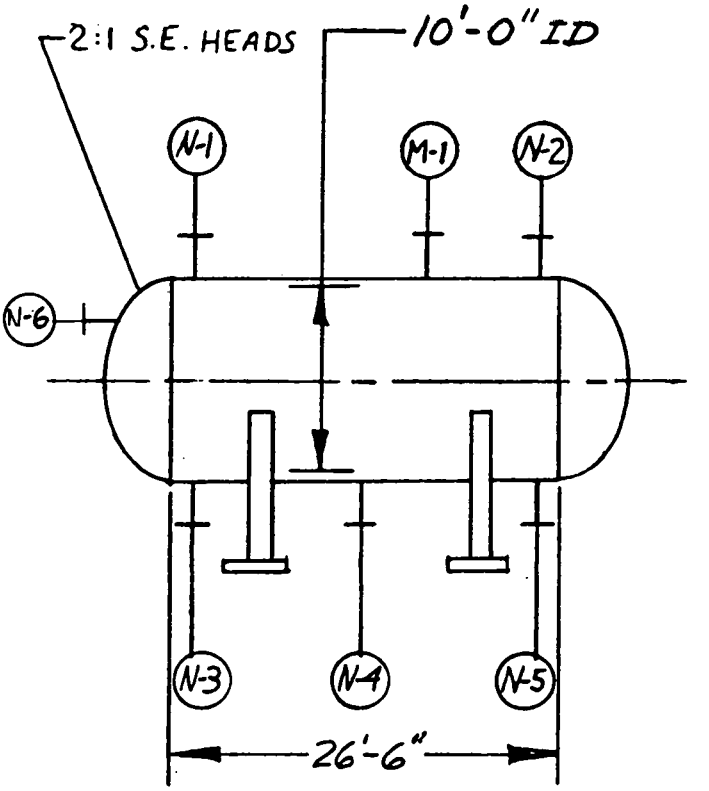

OTEC PSD I AMMONIA EVAPORATOR SUMP T-1

1	Service LIQUID AMMONIA			Item T-1	
2	Quantity ONE (1) Dia 120	in ID	Length between tangents 28'-6"		horiz YES
3	DESIGN CONDITIONS		OPERATING CONDITIONS		
4	Code ASME SECT VIII DIV 1		Operating pressure		psig
5			Operating temp 60 °F	Liquid sp gravity .609	
6	Design pressure, internal 150	psig	Liquid level for mechanical design is above the bottom TL 9'-0"		
7	At design temperature -20 TO +120	°F			
8	Design pressure, external 7.5	psig			
9	At design temperature -20 TO +120	°F			
10	Corrosion allow 1/8	in			
11	Joint eff, shell 85% ,heads 100 %				
12	Wind pressure —				
13	Earthquake —	G			
14	Postweld heat treat NO				
15	Radiograph SPOT				
16	Insulation YES thk. 3"	in			
17					
18	MATERIAL				
19	Heads SA-516-60 OR APP'VD				
20	Shell SA-516-60 EQUAL				
21	Support CARBON STEEL				
22	Nozzle necks SA-106				
23	Flanges SA-105				
24	Couplings —				
25	Gaskets FLEXITALLIC TYPE CG				
26	Fixed internals —				
27	Removable internals —				
28					
29	SUPPLIED BY SELLER				
30	Type support SADDLES				
31	Manhole cover, hinged YES , w/davit YES				
32	Insulation/fireproofing support YES				
33	Clips for ladders and platforms YES				
34	Clips for pipe supts and pipe guides NO				
35	Lifting lugs NO				
36	Surface preparation and paint BLAST CLEAN				
37	PER SSPC SP6, PRIME ORGANIC				
38	ZINC				

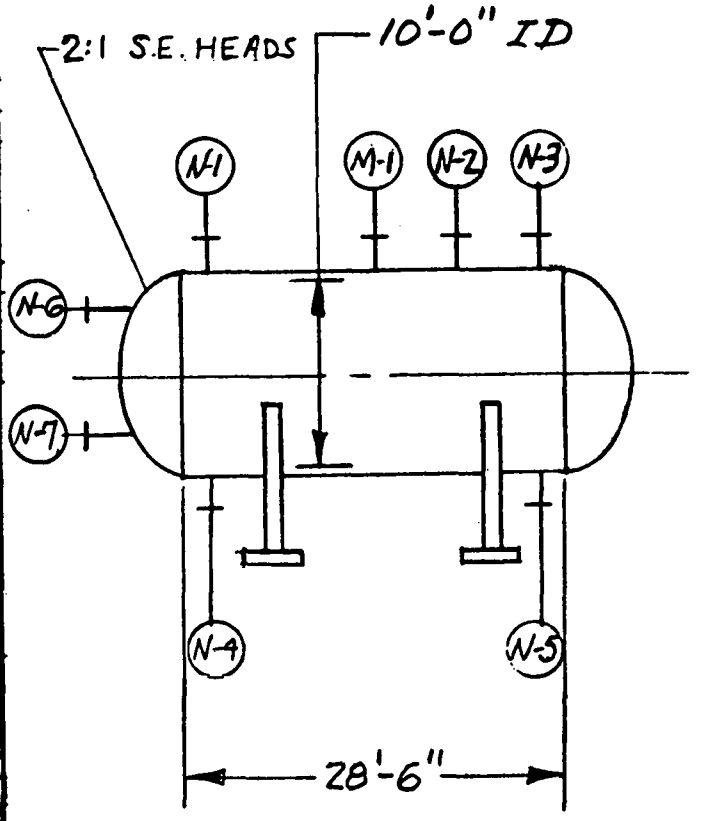

39	NOZZLES				
40	Mark	No	Size	Rtg Facing	Service
41	N-1	1	6"	300#	RELIEF
42	N-2	1	6"	BW	VENT
43	N-3	1	6"	300#	L.L. GAUGE
44	N-4	1	36"	BW	TO PUMP
45	N-5	1	36"	BW	TO PUMP
46	N-6	1	24"	BW	INLET
47	N-7	1	24"	BW	INLET
48	M-1	1	18"	300#	MANWAY
49					
50					
51					
52					
53					
54					
55					
56					
57					

TRW
DEFENSE AND SPACE SYSTEMS GROUP
ONE SPACE PARK- REDONDO BEACH - CALIFORNIA 90278

5515.2.78-427

INTEROFFICE CORRESPONDENCE

TO: L. A. Rosales CC: T. C. Dvorak, J. Hicks DATE: 29 August 1978

SUBJECT: NH_3 Compatibility of Steel FROM: M. Kwan

BLDG. 01 MAIL STA. 2220 EXT. 51901

A literature search was conducted on ammonia compatibility of steels considered for OTEC application. Most of the available experimental data [1-4] on stress-corrosion cracking (SCC) in anhydrous ammonia has been performed on high strength, quenched and tempered steels (such as ASTM A517) used to construct ammonia cargo tanks. These steels, having yield strengths of approximately 100 ksi, have demonstrated their susceptibility to SCC in air contaminated liquid ammonia. Susceptibility to SCC is dependent on a number of factors including the operating temperature, strength of the steel, post-weld heat treatment, and purity of ammonia. Experimental and service experience have shown that the addition of 0.2% water in ammonia inhibits the SCC of these high strength steels.

With respect to the OTEC unit, the addition of 0.2% water to the ammonia may mean a 1 to 2 percent degradation in performance. In addition, the candidate steels being considered for OTEC application have significantly lower yield strengths (Table I). Kawamoto and Kenjo [5] conducted tests on three steels of different strengths where specimens were subjected to 4-point fulcra bending at applied stresses of 40%, 60%, 80% and 100% of their respective yield strengths and immersed in ammonia tanks at three plants. Test results show that those steels with tensile strengths below about 85 ksi can be considered insusceptible to SCC in liquid ammonia when residual stresses due to welding is on the order of the yield strength of the material. Figure 1 summarizes the SCC susceptibility of several steels as a function of tensile strength and applied stress (5). Furthermore, guildelines established for avoiding SCC in ammonia plants indicate that stress relief heat treatment is preferred, but not required, for steels with less than 50 ksi yield strength and operating at -5°C and above[6]. Kawamoto [5] also conducted in-plant immersion tests on slit-type welded specimens of steel at three strength levels (75 ksi, 81 ksi, and 109 ksi yield strengths) which showed little difference in SCC susceptibility between exposures in gas phase

and liquid phase ammonia. Tests on weleded specimens showed cracks beyond the heat-affected zone perpendicular to the weld line; these results indicate that as-quenched metal such as heat-affected zones may have lower susceptibility to SCC compared to the base metal inspite of the higher tensile strength.

It can be concluded that the steels for OTEC are sufficiently low strength that they can be considered insusceptible to SCC in liquid and vapor phase ammonia.

MK:dk

Table I. MECHANICAL PROPERTIES OF STEELS FOR OTEC

Type of Steel	Ultimate Tensile Strength (ksi)	Minimum Yield Strength (ksi)	% Elongation in 2"
SA516, GR70	70 - 90	38	21
SA515, GR70	70 - 90	38	21
SA283, GRD	60 - 72	33	23
SA285, GRB	50 - 70	27	28

REFERENCES

1. Phelps, E.H., "Causes of Stress-Corrosion Cracking of Steel in Ammonia," Ammonia Plant Safety, Vol. 16, pp 32-38.

2. Loginow, A.W. and E.H. Phelps, "Stress-Corrosion Cracking of Steels in Agricultural Ammonia," Corrosion, Vol. 18, No. 8, pp 299t - 309t (1962) August.

3. Deegan, D.C. and B.E. Wilde, "Stress Corrosion Cracking Behavior of ASTM A517 Grade F Steel in Liquid Ammonia Environments," Corrosion, Vol. 29, No. 8, pp 310 - 315 (1973) August.

4. Tones, D.A., C.D. Kim, and B.D. Wilde, "The Electrochemistry and Mechanism of Stress Corrosion Cracking of Constructional Steel in Liquid Ammonia," Corrosion, Vol. 33, No. 2, pp 50 -55 (1977) February.

5. Kawamoto, T., T. Kenjo and Y. Imasaka, "Study on Stress Corrosion Cracking of Liquid Ammonia Spherical Storage Tank", IHI Engineering Review, Vol. 10, No. 4, October 1977.

6. Clark, W.D. and A. Cracknell, "Safety in Ammonia Plants and Related Facilities Atlantic City: 30 August - 1 September 1976," AIChE Symposium.

Figure 1. SCC susceptibility of high strength steels in liquid ammonia [5]

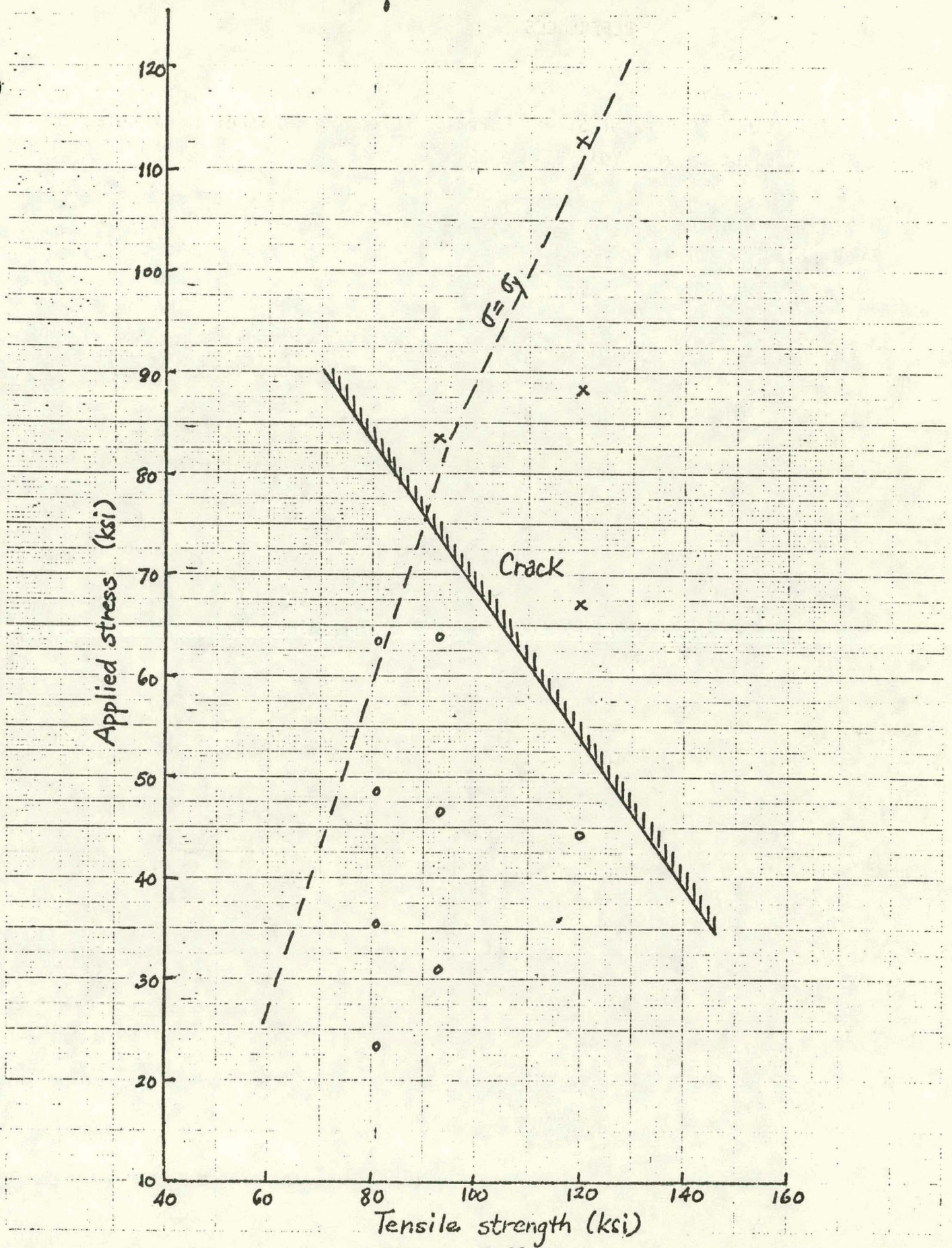

APPENDIX E
DETAILED EQUIPMENT LISTS

THIS PAGE

WAS INTENTIONALLY

LEFT BLANK

APPENDIX E.1

SYSTEM EQUIPMENT LISTS

THIS PAGE

WAS INTENTIONALLY

LEFT BLANK

OTEC EQUIPMENT SUMMARY LIST 10 MWe

REFERENCE DESIGNATOR	DESCRIPTION	SPEC OR DWG NO.	MFG & PART NO.	EST WT. (LB)	DIMENSIONS	SUPPLEMENTAL INFORMATION
E-1	Evaporator	CP-SS14-51 and CFB Spec. No. 5304-100-117 5304-100-117-1	Nooter	451 Ton	26'3"Dia,54'7"H	(L.L)*
C-1	Condenser	Same	Nooter	430 Ton	27'1"Dia,58'7"H	(L.L)
TG-1	Turbine/Generator	CFB Spec. No. 5304-100-135-1	Elliot	100 Ton		Axial turbine, 4-4 1800 RPM, Variable inlet stators (L.L.) 18 MW Generator, 13.8 KV

* (L.L.) = Long Lead

REFERENCE DESIGNATOR	DESCRIPTION	SPEC OR DWG NO.	MFG & PART NO.	EST WT. (LB)	DIMENSIONS	SUPPLEMENTARY INFORMATION	
V-1	Flow Control Valve	CP-EQ2-546		5,200	36" B.W.	Remote	(L.L.)
V-2	Turbine Trip Valve	CP-EQ2-547		8,000	60" B.W.	Remote	(L.L.)
V-3	Turbine By-Pass	CP-EQ2-547		3,600	30" B.W.	Remote	(L.L.)
V-4	Evap. Drain Shut-Off	6850.78-05		2,200	24" B.W.	Remote	(L.L.)
V-5	Cond. Drain Shut-Off	6850.78-05		3,700	30" B.W.	Remote	(L.L.)
V-6	Ammonia Supply	CP-EQ2-544		125	6"-300# ANSI	Remote	
V-7	Ammonia Return	CP-EQ2-544		125	6"-300# ANSI	Remote	
V-8	Ammonia Return	CP-EQ2-544		125	6"-300# ANSI	Remote	
V-9	Recirc. Pump Shut-Off	6850.78-05		4,500	36" B.W.	Manual	(L.L.)
V-10	Recirc. Pump Shut-Off	6850.78-05		5,000	36" B.W.	Remote	(L.L.)
V-11	Feed Pump Shut-Off	6850.78-05		1,900	24" B.W.	Manual	(L.L.)
V-12	Feed Pump Shut-Off	6850.78-05		2,200	24" B.W.	Remote	(L.L.)
V-13	Recirc. Pump Shut-Off	6850.78-05		4,500	36" B.W.	Manual	(L.L.)
V-14	Recirc. Pump Shut-Off	6850.78-05		5,000	36" B.W.	Remote	(L.L.)
V-15	Feed Pump Shut-Off	6850.78-05		1,900	24" B.W.	Manual	(L.L.)
V-16	Feed Pump Shut-Off	6850.78-05		2,200	24" B.W.	Remote	(L.L.)
V-17	Purge and Blowdown	6850.73-05		440	12"-300# ANSI	Remote	
V-18	Non-Cond. Purge	6850.73-05		210	8"-300# ANSI	Remote	
V-19	Purge and Blowdown	6850.73-05		440	12"-300# ANSI	Remote	
V-20	Nitrogen Purge	6850.73-05		10	2"-300# ANSI	Remote	
V-21	Nitrogen Purge	6850.73-05		10	2"-300# ANSI	Remote	
V-22	Cond. Sump Shut-Off	6850.73-05		125	6"-300# ANSI	Remote	
V-23	Evap. Sump Shut-Off	6850.73-05		125	1"-300# ANSI	Remote	
V-24	Ammonia Purification	6850.73-05		8	1"-300# ANSI	Remote	
V-25	Loop Shut-Off Valves	6850.73-05		10	1½"-300# ANSI	Remote	

REFERENCE DESIGNATOR	DESCRIPTION	SPEC OR DWG NO.	MFG & PART NO.	EST WT. (LB)	DIMENSIONS	SUPPLEMENTARY INFORMATION
P-3	Ammonia Recirc. Pump	CP-EQ2-545	Worthington	10,000	41 X 132	250 HP (L.L.)
P-4	Ammonia Recirc. Pump	CP-EQ2-545	20 LNS-28	10,000	41 X 132	250 HP (L.L.)
P-5	Ammonia Feed Pump	CP-EQ2-543	14 LNS-32	6,000		500 HP (L.L.)
P-6	Ammonia Feed Pump	CP-EQ2-543		6,000		500 HP (L.L.)
CV-1	Check Valve	6850.78-05		2,210	24" B.W.	(L.L.)
CV-2	Check Valve	6850.78-05		125	6"-300# ANSI	
PSV-1	Relief Valve	6850.78-05		440	12"-300# ANSI	Set 86 PSIG
PSV-2	Relief Valve	6850.78-05		440	12"-300# ANSI	Set 136 PSIG
PSV-3	Relief Valve	6850.78-05		200	6"-300# ANSI	Set 150 PSIG
PSV-4	Relief Valve	6850.78-05		200	6'-300# ANSI	Set 150 PSIG
PSV-5	Relief Valve	6850.78-05			1"-300# ANSI	Set 150 PSIG
PSV-6	Relief Valve	6850.78-05			1"-300# ANSI	Set 150 PSIG
PSV-7	Relief Valve	6850.78-05			1"-300# ANSI	Set 150 PSIG
PSV-8	Relief Valve	6850.78-05			1"-300# ANSI	Set 150 PSIG
PSV-9	Relief Valve	6850.78-05			1"-300# ANSI	Set 150 PSIG
T-1	Evap. Sump	CP-EQ2-541		52,000	See Spec.	(L.L.)
T-2	Cond. Sump	CP-EQ2-541		52,000	See Spec.	(L.L.)
F-1	Ammonia Filter	6850.78-05		5,000	36" B.W.	W/FLG FOR (L.L.)
F-2	Ammonia Filter	6850.78-05		5,000	36" B.W.	SERVICING (L.L.)
	MISCELLANEOUS CATEGORIES	FOR WEIGHT ESTIMATION				
	Piping, Fittings, Other Piping Loop Materials	6850.78-05		108,000	See Drawing	Field Assembled

OTEC EQUIPMENT SUMMARY LIST 10 MWe

AMMONIA STORAGE, CONDITIONING & SUPPLY SUBSYSTEM

REFERENCE DESIGNATOR	DESCRIPTION	SPEC OR DWG NO.	MFG & PART NO.	EST WT. (LB)	DIMENSIONS	SUPPLEMENTAL INFORMATION
T-101	NH_3 Purification Column	6850.78-06	Riley-Beaird	8,100	Dia = 12",L=324"	Packed with 3/4" Ceramic Saddles(L.L.)
D-100	NH_3 Heel Storage Drum	6850.78-06	Riley-Beaird	135,000	Dia = 168",L=300"	(L.L.)
D-101	Wet NH_3 Storage Drum	6850.78-06	Riley-Beaird	135,000	Dia = 168",L=300"	(L.L.)
D102	Dry NH_3 Storage Drum	6850.78-06	Riley-Beaird	135,000	Dia = 168",L=300"	(L.L.)
D103	NH_3 Reflux Accumulator	6850.78-06	Riley-Beaird	1,100	Dia = 24",L= 36"	(L.L.)
D-104	NH_3 Blowdown Drum	6850.78-06	Riley-Beaird	7,900	Dia = 72", L=120"	(L.L.)
D-105	Recoverec NH_3 Drum	6850.78-06	Riley-Beaird	1,000	Dia = 24", L= 36"	(L.L.)
E-100	NH_3 Overhead Condenser	6850.78-06	Hughes-Anderson	2,100	Dia = 13 1/4", L = 168"	238 Ft^2 (L.L.)
E-101	NH_3 Compressor Condenser	6850.78-06	Hughes-Anderson	1,800	Dia = 12", L=168"	210 Ft^2 (L.L.)
E-102	NH_3 Column Reboiler	6850.78-06	Hughes-Anderson	-	Dia = 19"/36", L = 96"	Part of NH_3 Purification Column 350 Ft^2 (L.L.)
P-100	Evaporator Blowdown Pump	6850.78-06	Sundyne	610		10 GPM - 103 psi - 7.6 HP Motor
P-101	NH_3 Transfer Pump	6850.78-06	Bingham	2,017		500 GPM - 153 psi - 100 HP Motor (L.L.)
P-102	NH_3 Column Feed Pump	6850.78-06	Sundyne	562		10 GPM - 62 psi - 3 HP Motor
P-103	Reflux Pump	6850.78-06	Sundyne	705		10 GPM - 152 psi - 20 HP Motor
P-104	Recovered NH_3 Pump	6850.78-06	Sundyne	332		10 GPM - 45 psi - 3 HP Motor
P-105	NH_3 Blowdown Drum Pump	6850.78-06	Sundyne	585		15 GPM - 216 psi 20 HP Motor

MISCELLANEOUS CATEGORIES - FOR WEIGHT ESTIMATION

REFERENCE DESIGNATOR	DESCRIPTION	SPEC OR DWG NO.	MFG & PART NO.	EST WT. (LB)	DIMENSIONS	SUPPLEMENTAL INFORMATION
	Piping, Fittings & Other Pipe Loop Materials (Ammonia Support)	6850.78-06		38,000		

NITROGEN STORAGE, CONDITIONING & SUPPLY SUBSYSTEM

REFERENCE DESIGNATOR	DESCRIPTION	SPEC OR DWG NO.	MFG & PART NO.	EST WT. (LB)	DIMENSIONS	SUPPLEMENTAL INFORMATION
P-106	Liquid Nitrogen Transfer Pump	6850.78-07	Airco Cryo-genics Duplex	985	1 1/2" - 300# Discharge 3" - 300# Suction	100 GFM, 255 psi (L.L.) 50 HP Motor
P-107	N_2 - Heater Seawater Return Pump	6850.78-07	Bingham 3"x4"x11 1/2"	964	3" - 300# Discharge 4" - 300# Suction	250 GPM, 50 psi 15 HP Motor
P-108	Cold Seawater Pump	6850.78-07	Peerless 8 1b	2,350	6" - 125# ANSI FF Fig	350 GPM, 50 psi 15 HP Motor
P-109	Warm Seawater Pump	6850.78-07	Bingham	2,150	6" - 300# ANSI Discharge 8" - 300# ANSI Suction	1200 GPM, 50 psi 60 HP Motor
E-103	Nitrogen Vaporizer	6850.78-07	TBD	4,300	2" - 2" x 5' x 192" Long Tubes	To be Designed During Final Design (L.L.)
D-106	Liquid Nitrogen Storage Dewar	6850.78-07	TBD	47,000	Dia-122", L-384"	To be Designed and Built (L.L.)
D-107	Liquid Nitrogen Shipping Dewar	6850.78-07	TBD	38,000	Dia- 96",L-396"	To be Designed and Built (L.L.)
	Piping, Fittings and Other Pipe Loop Materials	6850.78-07		12,000		

OTE EQUIPMENT SUMMARY LIST 10 MWe

ELECTRICAL SUBSYSTEM

REFERENCE DESIGNATOR	DESCRIPTION	SPEC OR DWG NO.	MFG & PART NO.	EST WT. (LB)	DIMENSIONS	SUPPLEMENTAL INFORMATION
	ELECTRICAL POWER DISTRIBUTION AND CONTROL	CP-SS14-53				
	15 KV Switchgear	CP-E 2-548	GE/WH	38,000	90"Hx244"Wx78"D	(L.L.)
	480 V Power Transformer	CP-EQ2-551	GE/WH	5,000	90"Hx64"Wx60"D	1500 KVA (L.L.)
	480 V Motor Control Center	CP-EQ2-553	GE/WH	4,800	90"Hx144"Wx20"D	
	480 V Auto Transfer Switch	CP-EQ2-555	GE/WH	650	69"Hx40"Wx16"D	Conduits
	Wiring & Conduit	CP-SS14-53	GE/WH	10,000	NA	Conduits, Condulets, J Boxes, Cables Signal Wire, Misc. Hardware, Etc.
	Local Control Station	CP-SS14-53	GE/WH	1	6"H x 4"W x 2"D	1 Unit per Drive
	INSTRUMENTATION AND CONTROL SUBSYSTEM	CP-SS14-3				
		C F Braun Project Report No. 5304-P Instrument List		25,000	Refer to Spec	Ammonia Power Loop Ammonia Storage Subsystem Nitrogen Storage Subsystem

BIOFOULING CONTROL AND AMMONIA LEAK DETECTION SUBSYSTEM

REFERENCE DESIGNATOR	DESCRIPTION	SPEC OR DWG NO.	MFG & PART NO.	EST WT. (LB)	DIMENSIONS	SUPPLEMENTAL INFORMATION
	BIOFOULING CONTROL SUBSYSTEM	CP-SS14-47				
	Tube Cleaning Subsyster	CP-SS14-45	TBD	10,000		(L.L.)
	Positioner	CP-EQ2-556	TBD	4,000	13'5"H,33'L,27'W	
	Tube Cleaning Head	CP-EQ2-557	TBD	1,000	32'H, 1.5'D	(L.L.)
	Controller/Recorder	CP-EQ2-558	TBD	50		
	Electrolytic Seawater Chlorinator	CP-EQ2-542		4,300		
	AMMONIA LEAK DETECTION SUBSYSTEM	CP-SS14-48	TBD	4,500		Many Small Packages
	Air Monitor, (Ammonia Detector) Infrared Analyzer		Beckman Model Set	750	3'W x 3'D x 2'5"H	Includes Remote Sensing Equipment

APPENDIX E.2

SPECIAL SUPPORT EQUIPMENT LIST

E.2. SPECIAL SUPPORT EQUIPMENT LIST

Following is a preliminary list of identified special support equipment. The list does not necessarily represent the total items of this nature required and is expected to change during final design. Some of the equipment required to support the operation of an OTEC Modular Application Power System (MAPS) were considered important enough to be treated as separate subsystems because of their specific interface requirements with components of the MAPS.

Equipment required for operational support activities are as follows:

- Tube Cleaner

  Described in Appendix C

- Leak Detection Equipment

  Described in Appendix H

- Ammonia Resupply System

  A ship, barge, or work boat mounted tank for transporting ammonia to an OTEC platform.(not part of this contract).

- Nitrogen Resupply System

  A vacuum jacketed tank capable of being transported by ship, barge or work boat to an OTEC platform. Approximate capacity - 8,000 gallons.

- Startup Power Unit

  An 11.5 MVA power source is required for initial startup of a 10 MWe MAPS module. The requirements for this are described in Section 2.10 of the PDR. This unit is not part of this contract.

- Standby Power

  A 563 KVA power source is required to permit orderly shutdown at the 10 MWe MAPS module during system shutdowns This requirement is described in Section 2.10 of this PDR. This unit is not part of this contract. It is anticipated that this power will be available from the platform's main power source.

- Primary Crane for Installation of Heat Exchangers, Turbine Generator and Other Heavy Components

  A 150 ton crane is required for installation of Heat Exchangers as described in Section 2.1.1 of this PDR. This crane may be part of the OTEC platform or it may be provided by a separate service and installation ship. It is not part of this contract.

- Material Handling Equipment for Other Components of the MAPS Module

  Various on-board hoists, cranes, and monorails may be rquired for installation, servicing and replacement of MAPS major components, such as pump, valves and filters. These items have not been defined but will be in the final design. (TBD)

- Heat Exchanger Shipping Fixtures

  Special shipping fixtures will be required for transporting of the heat exchangers from the point of manufacture to the final place of installation. These fixtures are TBD. They will be defined and designed as part of the heat exchangers final design.

THIS PAGE

WAS INTENTIONALLY

LEFT BLANK

APPENDIX E.3

MACHINERY TOOLS AND SPARE PARTS LIST, 10 MWe

E.3. MACHINERY TOOLS AND SPARE PARTS LIST, 10 MWe

The special machinery equipment will consist of handling equipment for the evaporator, condenser, and tube cleaner (slings, etc.) and hydraulic tube expanding equipment for the initial fabrication and subsequent repairing of tube-to-tube sheet joints. Special tools for maintenance of the turbine generator are listed below. They will be shipped with the unit and are priced as part of the turbine-generator unit.

The machinery and equipment, to be fabricated separately from equipment list items, are listed below

	Component Supported	Support Equipment	No. Required	Weight
1.	Evaporator and Condenser	Lifting and Positioning Fixture	1	
2.	Tube Cleaning Posittioner	Lifting Fixture	1	
3.	Tube Cleaning Head	Lifting Fixture	1	
4.	Evaporator and Condenser	Hydro Expanding Tool	2	
5.	Turbine Generator	Inner Casing Removal Rails Centering Rings Endwall Counterweight		

Other items may be identified during final design. Conventional tools required for normal maintenance are not included as they are expected to be the standard commercially available tools carried as workman's tools.

Spare parts will be defined during the final design and will consist of such things as circuit breakers, motors, tubing plugs, pump and valve seals, stem and shaft packing, tube cleaner brushes, instrumentation sensors and the like.

APPENDIX E.4

LONG LEAD TIME PROCUREMENT, 200 kWe AND 10 MWe

E.4 LONG LEAD TIME PROCUREMENT LIST, 200 kWe AND 10 MWe

The Phase II, master milestone schedule, Task 1.1.8 places DOE procurement and fabrication authorization at Phase II go-ahead plus 5 months. Long lead items are defined as those items which must be purchased in advance of the fifth month milestone to guarantee integration into the deliverable hardware package prior to scheduled hardware delivery, Task 1.1.11 on the fourteenth month.

The identifiable long lead items, requiring procurement authorization prior to the scheduled authorization date (Phase II go-ahead plus 5 months) are listed below.

Long Lead Item	Expected Procurement or Fabrication Time (Month)	Need Date Based on Phase II Go-Ahead (Month)
Heat Exchanger Test Article Condenser	12	14
Heat Exchanger Test Article Evaporator	12	14
Heat Exchanger Tubes, 0.2 MWe	TBD	8
Evaporator Recirculation Pump	12	14
Evaporator Sump	14	14
Flow Control Valve	10	14
Filter Unit	8	14

Remaining deliverable items are currently available within 9 months after award of contract (Task 1.1.8).

The Phase II, master milestone schedule, Task 2.1.7 places DOE procurement and fabrication authorization at the end of the sixth month of Phase II activity. This master milestone schedule is used to define long lead items as those items which must be purchased in advance of the sixth month milestone to guarantee integration into the deliverable hardware package prior to scheduled hardware delivery, Task 2.1.10, on the twenty-fourth month.

The identifiable long lead items, requiring procurement authorization prior to the scheduled authorization date (Phase II go-ahead plus 6 months) are indicated on the OTEC Equipment Summary List, 10 MWe, of this Appendix Section E-1, by the symbol L.L. in the supplemental information column.

Remaining deliverable items are currently available within 18 months after award of contract (Task 2.1.7).

APPENDIX F
TURBINE DESIGN STUDIES

THIS PAGE

WAS INTENTIONALLY

LEFT BLANK

APPENDIX F.1

TURBINE PRELIMINARY DESIGN ANALYSIS

F.1 TURBINE PRELIMINARY DESIGN ANALYSIS

Contained herein are the results of an unconstrained analysis of the optimum geometry for ammonia turbines operating between 70°F inlet state and 50°F outlet state. For multistage turbines, only the first stage analysis is given based on equal loading for each stage. Power output is 14 MWe overall with 1% bearing losses and a generator efficiency of 98%. This analysis was performed by Dr. Ambs of University of Massachussetts, consultant to TRW.

Single Stage Single Flow

```
? $TURBINE TB=70.,TC=50.,GP=14.,RND=3600.,DELD=.04,SH=.04,TBH=.04 $END

TURBINE DESIGN FOR  14.00  MEGAWATTS    AMMONIA          WORKING FLUID

STATE POINTS-----T(F),P(PSIA),H(BTU/LBM),V(CUFT/LBM),S(BTU/LBM-F)
                    STATION 3    STATION 2    STATION 1    EVAPORATOR
  TEMPERATURE         50.0000      62.9488      68.4022      70.0000
  STATIC PRESSURE     89.3447     113.7277     125.4049     128.9944
  TOTAL PRESSURE      89.9809     125.4078     126.2579
  STATIC ENTHALPY    611.8146     623.6296     628.8471     629.1218
  TOTAL ENTHALPY     612.1920     629.2218     629.2218
  SP. VOLUME           3.2053       2.5867       2.3728
  ENTROPY              1.2188       1.2165       1.2163       1.2139
  QUALITY               .9745        .9918       1.0000
  VISCOSITY          .232E-01     .238E-01     .240E-01
RELATIVE STATE PROPERTIES
  TOTAL PRESSURE     113.0038     118.3674
  TOTAL ENTHALPY     612.5784     612.5784
PRESSURE RATIO    1.4132

SPECIFIC SPEED       137.9737
SPECIFIC DIAMETER      1.1984
EFFICIENCIES            .8842  TURBOGENERATOR   .9800  GENERATOR   .0100  BEARING LOSS
ROTATIONAL SPEED RPM    3600
MASS FLOW LBM/SEC    803.2858
MACHINE REYNOLDS NO.    .2803E+09
DISK RE. NO.            .3076E+08
STATOR BLADE RE. NO.    .2364E+08
ROTOR BLADE RE. NO.     .4487E+08
STATOR THETA RE. NO.    .3305E+05
ROTOR THETA RE. NO.     .5838E+05
REACTION                .6933

GEOMETRY SPECIFICATION-LENGTH IN FEET
            ROTOR EXIT    ROTOR INLET    STATOR INLET
  DIAMETER     5.5381         4.9751         4.7649
  B. HEIGHT    1.4718         1.3222         1.2663
                          ROTOR          STATOR
  PITCH                   1.3586          .7548
  AXIAL WIDTH              .2569          .4193
  CAMBER LINE LENGTH      1.4138          .9772
  CHORD LENGTH            1.4138          .8877
  TRAILING EDGE THICKNESS  .0589          .0529
  STAGGER ANGLE          10.4678        28.1868
  INLET ANGLE            24.2459        90.0000
  OUTLET ANGLE            6.6289        15.0000
  NO. BLADES             10.0000        18.0000
RATIOS
  ASPECT                   .9606          .6714
  SOLIDITY                 .9610          .8502
  RADIUS                   .4685
  BL. HEIGHT/DIAM.         .2658
GAS FLOW ANGLES  EXIT   85.0489  UNDER TURNING    2.7733
CLEARANCE        TIP      .0589  ROTOR HOUSING     .2215

VELOCITIES IN FT/SEC AT MEAN SQUARE DIAMETER OF   4.3245 FEET
                    STATION 3    STATION 2    STATION 1
  ABSOLUTE          137.4569     529.1111     136.9440
  AXIAL COMP.       136.9440     136.9440
  TANGENTIAL COMP.   11.8634     511.0821
  RELATIVE          838.2693     333.4779
  TANGENTIAL COMP.  827.0077    -304.0622
  PERIPHERAL        815.1443
DIMENSIONLESS DESIGN RATIOS
  BLADE JET SPEED RATIO    .842782          FLOW COEF       .168000
  BLADE LOADING COEF       .703946          SPEED WORK COEF 1.420564
  SPECIFIC SPEED          1.069563          SPECIFIC DIAM   2.853484
  EXIT VELOCITY/SPOUTING   .020197

CALCULATED EFFICIENCY BASED ON THEORETICAL WORK
    TOTAL TO TOTAL   .920882  TOTAL TO STATIC   .902282
CALCULATED EFFICIENCY BASED ON SUMMATION OF LOSSES
    TOTAL TO TOTAL   .920788  TOTAL TO STATIC   .902190
```

Single Stage Double Flow

```
? $TURBINE TB=70.,TC=50.,GP=7.,RND=3600. $END


TURBINE DESIGN FOR   7.00  MEGAWATTS     AMMONIA            WORKING FLUID

STATE POINTS-----T(F),P(PSIA),H(BTU/LBM),V(CUVT/LBM),S(BTU/LBM-F)
                    STATION 3     STATION 2     STATION 1     EVAPORATOR
  TEMPERATURE         50.0000       62.0012       69.5016       70.0000
  STATIC PRESSURE     89.3447      111.7869      127.8664      128.9944
  TOTAL PRESSURE      90.1708      126.7407      128.9944      128.9944
  STATIC ENTHALPY    610.8638      621.8647      629.0368      629.1218
  TOTAL ENTHALPY     611.3530      629.1218      629.1218      629.1218
  SP. VOLUME           3.1994        2.6220        2.3285
  ENTROPY              1.2169        1.2150        1.2146        1.2139
  QUALITY               .9727         .9887        1.0000        1.0000
  VELOCITY            156.0035      156.0035      156.0035        0.0000
  VISCOSITY           .232E-01      .237E-01      .241E-01
RELATIVE STATE PROPERTIES
  TOTAL PRESSURE      110.5454      114.1622
  TOTAL ENTHALPY      611.7320      611.7320
PRESSURE RATIO    1.4438

SPECIFIC SPEED         92.7090
SPECIFIC DIAMETER       1.4642
EFFICIENCIES             .8858  TURBOGENERATOR   .9800  GENERATOR   .0100  BEARING LOSS
ROTATIONAL SPEED RPM    3600.
MASS FLOW LBM/SEC     385.4524
MACHINE REYNOLDS NO.    .1969E+09
DISK RE. NO.            .5235E+08
STATOR BLADE RE. NO.    .1527E+08
ROTOR BLADE RE. NO.     .2449E+08
STATOR THETA RE. NO.    .2037E+05
ROTOR THETA RE. NO.     .2987E+05
REACTION                .6174

GEOMETRY SPECIFICATION-LENGTH IN FEET
              ROTOR EXIT          ROTOR INLET     STATOR INLET
  DIAMETER      4.6367              4.1975          3.9556
  B. HEIGHT      .6277               .5682           .5355
                          ROTOR         STATOR
  PITCH                    .6710         .3863
  AXIAL WIDTH              .1884         .2146
  CAMBER LINE LENGTH       .7266         .5001
  CHORD LENGTH             .7266         .4544
  TRAILING EDGE THICKNESS  .0251         .0227
  STAGGER ANGLE          15.0250       28.1868
  INLET ANGLE            40.4967       90.0000
  OUTLET ANGLE            9.0474       15.0000
  NO. BLADES             19.0000       33.0000
RATIOS
  ASPECT                  1.1577         .7997
  SOLIDITY                 .9234         .8502
  RADIUS                   .7293
  BL. HEIGHT/DIAM.         .1354
GAS FLOW ANGLES  EXIT   85.4542  UNDER TURNING     2.3011
CLEARANCE         TIP     .0251  ROTOR HOUSING      .1855

VELOCITIES IN FT/SEC AT MEAN SQUARE DIAMETER OF    4.0579 FEET
                    STATION 3     STATION 2     STATION 1
  ABSOLUTE          156.4958      602.7511      156.0035
  AXIAL COMP.       156.0035      156.0035
  TANGENTIAL COMP.   12.4032      582.2129
  RELATIVE          792.7941      240.2253
  TANGENTIAL COMP.  777.2937     -182.6776
  PERIPHERAL        764.8905
DIMENSIONLESS DESIGN RATIOS
  BLADE JET SPEED RATIO    .775408          FLOW COEF       .203955
  BLADE LOADING COEF       .831591          SPEED WORK COEF 1.202514
  SPECIFIC SPEED           .718674          SPECIFIC DIAM   3.486152
  EXIT VELOCITY/SPOUTING   .025169

CALCULATED EFFICIENCY BASED ON THEORETICAL WORK
    TOTAL TO TOTAL    .927222  TOTAL TO STATIC    .903884
CALCULATED EFFICIENCY BASED ON SUMMATION OF LOSSES
    TOTAL TO TOTAL    .927244  TOTAL TO STATIC    .903906
```

TWO STAGE SINGLE FLOW

```
? $TURBINE TB=70.,TC=60.,GP=7.,RND=1800. $END


TURBINE DESIGN FOR   7.00  MEGAWATTS    AMMONIA            WORKING FLUID

STATE POINTS-----T(F),P(PSIA),H(BTU/LBM),V(CUFT/LBM),S(BTU/LBM-F)
                    STATION 3     STATION 2     STATION 1     EVAPORATOR
  TEMPERATURE         60.0000       66.2448       69.7664       70.0000
  STATIC PRESSURE    107.7721      120.6804      128.4648      128.9944
  TOTAL PRESSURE     108.2306      128.1615      128.9944      128.9944
  STATIC ENTHALPY    620.0880      625.7298      629.0820      629.1218
  TOTAL ENTHALPY     620.3178      629.1218      629.1218      629.1218
  SP. VOLUME           2.7088        2.4496        2.3180
  ENTROPY              1.2153        1.2144        1.2142        1.2139
  QUALITY               .9861         .9947        1.0000        1.0000
  VELOCITY           106.6541      106.6541      106.6541        0.0000
  VISCOSITY          .236E-01      .239E-01      .241E-01
RELATIVE STATE PROPERTIES
  TOTAL PRESSURE     120.7656      122.1919
  TOTAL ENTHALPY     620.5716      620.5716
PRESSURE RATIO    1.1969

SPECIFIC SPEED       102.6137
SPECIFIC DIAMETER      1.3831
EFFICIENCIES            .8866  TURBOGENERATOR   .9800  GENERATOR   .0100  BEARING LOSS
ROTATIONAL SPEED RPM   1800.
MASS FLOW LBM/SEC    777.5841
MACHINE REYNOLDS NO.    .2468E+09
DISK RE. NO.            .5675E+08
STATOR BLADE RE. NO.    .1899E+08
ROTOR BLADE RE. NO.     .3362E+08
STATOR THETA RE. NO.    .2510E+05
ROTOR THETA RE. NO.     .4050E+05
REACTION                .6390

GEOMETRY SPECIFICATION-LENGTH IN FEET
          ROTOR EXIT          ROTOR INLET    STATOR INLET
  DIAMETER     6.8237          6.4890          6.3123
  B. HEIGHT    1.0979          1.0441          1.0156
                          ROTOR         STATOR
  PITCH                  1.1447         .6784
  AXIAL WIDTH             .2900         .3769
  CAMBER LINE LENGTH     1.2253         .8782
  CHORD LENGTH           1.2253         .7979
  TRAILING EDGE THICKNESS .0439         .0418
  STAGGER ANGLE         13.6891       28.1868
  INLET ANGLE           35.1557       90.0000
  OUTLET ANGLE           8.3766       15.0000
  NO. BLADES            16.0000       27.0000
RATIOS
  ASPECT                 1.1160         .7642
  SOLIDITY                .9342         .8502
  RADIUS                  .6782
  BL. HEIGHT/DIAM.        .1609
GAS FLOW ANGLES  EXIT   83.8138  UNDER TURNING     2.3870
CLEARANCE        TIP      .0439  ROTOR HOUSING      .2729

VELOCITIES IN FT/SEC AT MEAN SQUARE DIAMETER OF    5.830. FEET
                    STATION 3     STATION 2     STATION 1
  ABSOLUTE           107.2788      412.0797      106.6541
  AXIAL COMP.        106.6541      106.6541
  TANGENTIAL COMP.    11.5604      398.0384
  RELATIVE           571.0868    0 185.2277
  TANGENTIAL COMP.   561.0392     -151.4405
  PERIPHERAL         549.4788
DIMENSIONLESS DESIGN RATIOS
  BLADE JET SPEED RATIO    .791516          FLOW COEF       .194100
  BLADE LOADING COEF       .798088          SPEED WORK COEF 1.252994
  SPECIFIC SPEED           .795455          SPECIFIC DIAM   3.293264
  EXIT VELOCITY/SPOUTING   .023881

CALCULATED EFFICIENCY BASED ON THEORETICAL WORK
    TOTAL TO TOTAL   .926803  TOTAL TO STATIC   .904670
CALCULATED EFFICIENCY BASED ON SUMMATION OF LOSSES
    TOTAL TO TOTAL   .926859  TOTAL TO STATIC   .904725
```

Two Stage Double Flow

```
? $TURBINE TB=70.,TC=60.,GP=3.5,RND=3600.,SH=.04,DELD=.04,TBH=.04 $END

TURBINE DESIGN FOR   3.50  MEGAWATTS     AMMONIA            WORKING FLUID

STATE POINTS-----T(F),P(PSIA),H(BTU/LBM),V(CUFT/LBM),S(BTU/LBM-F)
                    STATION 3     STATION 2     STATION 1     EVAPORATOR
  TEMPERATURE         60.0000       66.7442       69.4912       70.0000
  STATIC PRESSURE    107.7721      121.7616      127.8429      128.9944
  TOTAL PRESSURE     108.1445      127.9572      128.2762
  STATIC ENTHALPY    620.4691      626.4335      629.0350      629.1218
  TOTAL ENTHALPY     620.6560      629.2218      629.2218
  SP. VOLUME           2.7108        2.4315        2.3290
  ENTROPY              1.2161        1.2148        1.2146        1.2139
  QUALITY               .9868         .9959        1.0000
  VISCOSITY           .236E-01      .240E-01      .241E-01
RELATIVE STATE PROPERTIES
  TOTAL PRESSURE     122.1416      124.5291
  TOTAL ENTHALPY     620.6996      620.6996
PRESSURE RATIO    1.1903

SPECIFIC SPEED       140.4547
SPECIFIC DIAMETER      1.1610
EFFICIENCIES           .8740  TURBOGENERATOR   .9800  GENERATOR   .0100  BEARING LOSS
ROTATIONAL SPEED RPM    3600
MASS FLOW LBM/SEC    399.2135
MACHINE REYNOLDS NO.    .1796E+09
DISK RE. NO.            .1435E+08
STATOR BLADE RE. NO.    .1320E+08
ROTOR BLADE RE. NO.     .2642E+08
STATOR THETA RE. NO.    .2070E+05
ROTOR THETA RE. NO.     .3779E+05
REACTION                .6985

GEOMETRY SPECIFICATION-LENGTH IN FEET
            ROTOR EXIT    ROTOR INLET    STATOR INLET
  DIAMETER     4.1181         3.9001         3.8170
  B. HEIGHT    1.2361         1.1707         1.1457
                          ROTOR          STATOR
  PITCH                    .9852          .5795
  AXIAL WIDTH              .1717          .3219
  CAMBER LINE LENGTH      1.0278          .7503
  CHORD LENGTH            1.0278          .6816
  TRAILING EDGE THICKNESS  .0494          .0468
  STAGGER ANGLE           9.6174        28.1868
  INLET ANGLE            22.7836        90.0000
  OUTLET ANGLE            6.0583        15.0000
  NO. BLADES             10.0000        17.0000
RATIOS
  ASPECT                   .8315          .5822
  SOLIDITY                 .9585          .8502
  RADIUS                   .3997
  BL. HEIGHT/DIAM.         .3002
GAS FLOW ANGLES  EXIT   88.9047  UNDER TURNING    3.2039
CLEARANCE        TIP      .0494  ROTOR HOUSING     .1647

VELOCITIES IN FT/SEC AT MEAN SQUARE DIAMETER OF    3.1359 FEET
                    STATION 3     STATION 2     STATION 1
  ABSOLUTE            96.7163      373.6149       96.6987
  AXIAL COMP.         96.6987       96.6987
  TANGENTIAL COMP.     1.8489      360.8843
  RELATIVE           600.7871      249.7045
  TANGENTIAL COMP.   592.9541     -230.2210
  PERIPHERAL         591.1052
DIMENSIONLESS DESIGN RATIOS
  BLADE JET SPEED RATIO    .856681          FLOW COEF       .163590
  BLADE LOADING COEF       .681289          SPEED WORK COEF 1.467806
  SPECIFIC SPEED          1.150812          SPECIFIC DIAM   2.764315
  EXIT VELOCITY/SPOUTING   .019648

CALCULATED EFFICIENCY BASED ON THEORETICAL WORK
    TOTAL TO TOTAL   .909729  TOTAL TO STATIC   .891855
CALCULATED EFFICIENCY BASED ON SUMMATION OF LOSSES
    TOTAL TO TOTAL   .909762  TOTAL TO STATIC   .891888
```

THREE STAGE SINGLE FLOW

```
RNH

? $TURBINE TB=70.,TC=63.3,GP=4.67,RND=1800. $END


TURBINE DESIGN FOR   4.67  MEGAWATTS    AMMONIA           WORKING FLUID

STATE POINTS-----T(F),P(PSIA),H(BTU/LBM),V(CUFT/LBM),S(BTU/LBM-F)
                    STATION 3    STATION 2    STATION 1    EVAPORATOR
  TEMPERATURE         63.3000      67.8387      69.8659      70.0000
  STATIC PRESSURE    114.4535     124.1576     128.6902     128.9944
  TOTAL PRESSURE     114.7337     128.5564     128.9944     128.9944
  STATIC ENTHALPY    623.1281     627.1770     629.0989     629.1218
  TOTAL ENTHALPY     623.2613     629.1218     629.1218     629.1218
  SP. VOLUME           2.5680       2.3886       2.3141
  ENTROPY              1.2149       1.2142       1.2141       1.2139
  QUALITY               .9907        .9969       1.0000       1.0000
  VELOCITY            80.7574      80.7574      80.7574       0.0000
  VISCOSITY          .238E-01     .240E-01     .241E-01
RELATIVE STATE PROPERTIES
  TOTAL PRESSURE     124.7612     125.8381
  TOTAL ENTHALPY     623.4917     623.4916
PRESSURE RATIO    1.1270

SPECIFIC SPEED       135.0860
SPECIFIC DIAMETER      1.2097
EFFICIENCIES            .8822  TURBOGENERATOR   .9800  GENERATOR   .0100  BEARING LOSS
ROTATIONAL SPEED RPM   1800.
MASS FLOW LBM/SEC    778.6768
MACHINE REYNOLDS NO.    .2295E+09
DISK RE. NO.            .2722E+08
STATOR BLADE RE. NO.    .1668E+08
ROTOR BLADE RE. NO.     .3799E+08
STATOR THETA RE. NO.    .2443E+05
ROTOR THETA RE. NO.     .5023E+05
REACTION                .6902

GEOMETRY SPECIFICATION-LENGTH IN FEET
            ROTOR EXIT          ROTOR INLET    STATOR INLET
  DIAMETER     6.4287              6.2000          6.1026
  B. HEIGHT    1.6490              1.5904          1.5654
                              ROTOR          STATOR
  PITCH                       1.5884          .8360
  AXIAL WIDTH                  .3057          .4645
  CAMBER LINE LENGTH          1.6551         1.0824
  CHORD LENGTH                1.6551          .9833
  TRAILING EDGE THICKNESS      .0660          .0636
  STAGGER ANGLE              10.6434        28.1868
  INLET ANGLE                24.7551        90.0000
  OUTLET ANGLE                6.7305        15.0000
  NO. BLADES                 10.0000        19.0000
RATIOS
  ASPECT                      1.0037          .6183
  SOLIDITY                     .9597          .8502
  RADIUS                       .4870
  BL. HEIGHT/DIAM.             .2565
GAS FLOW ANGLES  EXIT   81.4767  UNDER TURNING    2.6542
CLEARANCE        TIP      .0660  ROTOR HOUSING     .2571

VELOCITIES IN FT/SEC AT MEAN SQUARE DIAMETER OF    5.0561 FEET
                    STATION 3    STATION 2    STATION 1
  ABSOLUTE            81.6593     312.0226      80.7574
  AXIAL COMP.         80.7574      80.7574
  TANGENTIAL COMP.    12.1029     301.3907
  RELATIVE           495.2575     192.8578
  TANGENTIAL COMP.   488.6290    -175.1353
  PERIPHERAL         476.5261
DIMENSIONLESS DESIGN RATIOS
  BLADE JET SPEED RATIO     .838932          FLOW COEF       .169471
  BLADE LOADING COEF        .710422          SPEED WORK COEF 1.407613
  SPECIFIC SPEED           1.047178          SPECIFIC DIAM   2.880375
  EXIT VELOCITY/SPOUTING    .020668

CALCULATED EFFICIENCY BASED ON THEORETICAL WORK
    TOTAL TO TOTAL    .919247  TOTAL TO STATIC    .900248
CALCULATED EFFICIENCY BASED ON SUMMATION OF LOSSES
    TOTAL TO TOTAL    .919161  TOTAL TO STATIC    .900164
```

```
$TURBINE TB=70.,TC=63.3,GP=2.33,RND=1800.,DELD=.04,TBH=.04,SH=.04 $END

TURBINE DESIGN FOR   2.33  MEGAWATTS     AMMONIA            WORKING FLUID

STATE POINTS-----T(F),P(PSIA),H(BTU/LBM),V(CUFT/LBM),S(BTU/LBM-F)
                    STATION 3     STATION 2     STATION 1     EVAPORATOR
  TEMPERATURE         63.3000       67.3680       69.6678       70.0000
  STATIC PRESSURE    114.4535      123.1229      128.2417      128.9944
  TOTAL PRESSURE     114.7829      128.3690      128.6060
  STATIC ENTHALPY    623.2172      626.8845      629.0652      629.1218
  TOTAL ENTHALPY     623.3738      629.2218      629.2218
  SP. VOLUME           2.5685        2.4070        2.3219
  ENTROPY              1.2151        1.2145        1.2144        1.213*
  QUALITY               .9908         .9965        1.0000
  VISCOSITY          .238E-01      .240E-01      .241E-01
RELATIVE STATE PROPERTIES
  TOTAL PRESSURE     123.0178      124.0301
  TOTAL ENTHALPY     623.3907      623.3907
PRESSURE RATIO    1.1237

SPECIFIC SPEED        96.2231
SPECIFIC DIAMETER      1.4331
EFFICIENCIES           .8872  TURBOGENERATOR   .9800  GENERATOR   .0100  BEARING LOSS
ROTATIONAL SPEED RPM   1800
MASS FLOW LBM/SEC    389.7925
MACHINE REYNOLDS NO.   .1620E+09
DISK RE. NO.           .4101E+08
STATOR BLADE RE. NO.   .1139E+08
ROTOR BLADE RE. NO.    .2034E+08
STATOR THETA RE. NO.   .1605E+05
ROTOR THETA RE. NO.    .2594E+05
REACTION               .6246

GEOMETRY SPECIFICATION-LENGTH IN FEET
            ROTOR EXIT     ROTOR INLET     STATOR INLET
  DIAMETER     5.4007         5.2283          5.1350
  B. HEIGHT     .7788          .7539           .7405
                          ROTOR          STATOR
  PITCH                    .8181          .4750
  AXIAL WIDTH              .2241          .2639
  CAMBER LINE LENGTH       .8811          .6150
  CHORD LENGTH             .8811          .5587
  TRAILING EDGE THICKNESS  .0312          .0302
  STAGGER ANGLE          14.7356        28.1868
  INLET ANGLE            38.4902        90.0000
  OUTLET ANGLE            8.9541        15.0000
  NO. BLADES             18.0000        31.0000
RATIOS
  ASPECT                  1.1313          .7410
  SOLIDITY                 .9285          .8502
  RADIUS                   .7116
  BL. HEIGHT/DIAM.         .1442
GAS FLOW ANGLES  EXIT    89.3805  UNDER TURNING     2.3548
CLEARANCE        TIP       .0312  ROTOR HOUSING      .2160

VELOCITIES IN FT/SEC AT MEAN SQUARE DIAMETER OF    4.6871 FEET
                    STATION 3     STATION 2     STATION 1
  ABSOLUTE          88.5382      342.0655       88.5331
  AXIAL COMP.       88.5331       88.5331
  TANGENTIAL COMP.    .9573      330.4099
  RELATIVE         451.4732      142.2490
  TANGENTIAL COMP. 442.7075     -111.3403
  PERIPHERAL       441.7502
DIMENSIONLESS DESIGN RATIOS
  BLADE JET SPEED RATIO    .781163          FLOW COEF       .200414
  BLADE LOADING COEF       .819382          SPEED WORK COEF 1.220431
  SPECIFIC SPEED           .745916          SPECIFIC DIAM   3.412251
  EXIT VELOCITY/SPOUTING   .024513

CALCULATED EFFICIENCY BASED ON THEORETICAL WORK
    TOTAL TO TOTAL   .928011  TOTAL TO STATIC   .905263
CALCULATED EFFICIENCY BASED ON SUMMATION OF LOSSES
    TOTAL TO TOTAL   .928032  TOTAL TO STATIC   .905283
```

FOUR STAGE SINGLE FLOW

```
? $TURBINE TB=70.,TC=65.,GP=3.5,RND=1800. $END


TURBINE DESIGN FOR   3.50  MEGAWATTS     AMMONIA            WORKING FLUID

STATE POINTS-----T(F),P(PSIA),H(BTU/LBM),V(CUFT/LBM),S(BTU/LBM-F)
                    STATION 3     STATION 2     STATION 1     EVAPORATOR
  TEMPERATURE         65.0000       68.3314       69.8970       70.0000
  STATIC PRESSURE    118.0173      125.2477      128.7605      128.9944
  TOTAL PRESSURE     118.2482      128.6543      128.9944      128.9944
  STATIC ENTHALPY    624.7809      627.6273      629.1042      629.1218
  TOTAL ENTHALPY     624.8877      629.1218      629.1218      629.1218
  SP. VOLUME          2.4996        2.3701        2.3129
  ENTROPY             1.2149        1.2141        1.2140        1.2139
  QUALITY              .9933         .9976        1.0000        1.0000
  VELOCITY           70.7927       70.7927       70.7927        0.0000
  VISCOSITY         .239E-01      .240E-01      .241E-01
RELATIVE STATE PROPERTIES
  TOTAL PRESSURE     125.8908      126.8743
  TOTAL ENTHALPY     624.5660      624.5660
PRESSURE RATIO    1.0930

SPECIFIC SPEED       169.3222
SPECIFIC DIAMETER      1.0989
EFFICIENCIES            .8563  TURBOGENERATOR   .9800  GENERATOR   .0100  BEARING LOSS
ROTATIONAL SPEED RPM   1800.
MASS FLOW LBM/SEC    807.5588
MACHINE REYNOLDS NO.   .2269E+09
DISK RE. NO.           .1021E+08
STATOR BLADE RE. NO.   .1513E+08
ROTOR BLADE RE. NO.    .2915E+08
STATOR THETA RE. NO.   .2397E+05
ROTOR THETA RE. NO.    .4205E+05
REACTION               .6789

GEOMETRY SPECIFICATION-LENGTH IN FEET
            ROTOR EXIT          ROTOR INLET    STATOR INLET
  DIAMETER     6.3162              6.1505          6.0758
  B. HEIGHT    2.2107              2.1527          2.1265
                              ROTOR          STATOR
  PITCH                      1.4649          .9156
  AXIAL WIDTH                 .2422          .5086
  CAMBER LINE LENGTH         1.5325         1.1853
  CHORD LENGTH               1.5325         1.0768
  TRAILING EDGE THICKNESS     .0884          .0861
  STAGGER ANGLE              9.0937        28.1868
  INLET ANGLE               21.9965        90.0000
  OUTLET ANGLE               5.6994        15.0000
  NO. BLADES                10.0000        16.0000
RATIOS
  ASPECT                      .6932          .5002
  SOLIDITY                    .9559          .8502
  RADIUS                      .3000
  BL. HEIGHT/DIAM.            .3500
GAS FLOW ANGLES  EXIT  104.5116  UNDER TURNING    3.8429
CLEARANCE         TIP     .0884  ROTOR HOUSING     .2526

VELOCITIES IN FT/SEC AT MEAN SQUARE DIAMETER OF    4.6629 FEET
                    STATION 3     STATION 2     STATION 1
  ABSOLUTE            73.1256      273.5220       70.7927
  AXIAL COMP.         70.7927       70.7927
  TANGENTIAL COMP.   -18.3235      264.2019
  RELATIVE           427.0361      189.0073
  TANGENTIAL COMP.   421.1273     -175.2489
  PERIPHERAL         439.4508
DIMENSIONLESS DESIGN RATIOS
  BLADE JET SPEED RATIO    .896609          FLOW COEF       .161094
  BLADE LOADING COEF       .621962          SPEED WORK COEF 1.607816
  SPECIFIC SPEED          1.312575          SPECIFIC DIAM   2.616492
  EXIT VELOCITY/SPOUTING   .022260

CALCULATED EFFICIENCY BASED ON THEORETICAL WORK
    TOTAL TO TOTAL   .893674  TOTAL TO STATIC   .873781
CALCULATED EFFICIENCY BASED ON SUMMATION OF LOSSES
    TOTAL TO TOTAL   .893719  TOTAL TO STATIC   .873825
```

FOUR STAGE DOUBLE FLOW

```
? $TURBINE TB=70.,TC=65.,GP=1.75,RND=1800.,SH=.04,DELD=.04,TBH=.04 $END

TURBINE DESIGN FOR   1.75  MEGAWATTS    AMMONIA           WORKING FLUID

STATE POINTS-----T(F),P(PSIA),H(BTU/LBM),V(CUFT/LBM),S(BTU/LBM-F)
                    STATION 3    STATION 2    STATION 1    EVAPORATOR
  TEMPERATURE         65.0000      68.3332      69.9443      70.0000
  STATIC PRESSURE    118.0173     125.2518     128.8680     128.9944
  TOTAL PRESSURE     118.2550     128.9773     129.1239
  STATIC ENTHALPY    624.5992     627.5876     629.1123     629.1218
  TOTAL ENTHALPY     624.7091     629.2218     629.2218
  SP. VOLUME           2.4987       2.3699       2.3110
  ENTROPY              1.2145       1.2140       1.2139       1.2139
  QUALITY               .9929        .9976       1.0000
  VISCOSITY          .239E-01     .240E-01     .241E-01
RELATIVE STATE PROPERTIES
  TOTAL PRESSURE     125.3978     126.2203
  TOTAL ENTHALPY     624.7855     624.7854
PRESSURE RATIO    1.0941

SPECIFIC SPEED       113.5684
SPECIFIC DIAMETER      1.3125
EFFICIENCIES            .8865  TURBOGENERATOR   .9800  GENERATOR   .0100  BEARING LOSS
ROTATIONAL SPEED RPM   1800
MASS FLOW LBM/SEC    379.1503
MACHINE REYNOLDS NO.    .1498E+09
DISK RE. NO.            .2856E+08
STATOR BLADE RE. NO.    .1133E+08
ROTOR BLADE RE. NO.     .2255E+08
STATOR THETA RE. NO.    .1669E+05
ROTOR THETA RE. NO.     .3023E+05
REACTION                .6603

GEOMETRY SPECIFICATION-LENGTH IN FEET
             ROTOR EXIT    ROTOR INLET    STATOR INLET
  DIAMETER     5.1318        4.9977         4.9353
  B. HEIGHT     .9815         .9559          .9439
                          ROTOR          STATOR
  PITCH                  1.0306          .5825
  AXIAL WIDTH             .2386          .3236
  CAMBER LINE LENGTH     1.0874          .7542
  CHORD LENGTH           1.0874          .6851
  TRAILING EDGE THICKNESS  .0393         .0382
  STAGGER ANGLE          12.6747        28.1868
  INLET ANGLE            30.6042        90.0000
  OUTLET ANGLE            7.9119        15.0000
  NO. BLADES             13.0000        23.0000
RATIOS
  ASPECT                  1.1079          .7168
  SOLIDITY                 .9478          .8502
  RADIUS                   .6175
  BL. HEIGHT/DIAM.         .1913
GAS FLOW ANGLES  EXIT   86.3239  UNDER TURNING    2.4045
CLEARANCE        TIP      .0393  ROTOR HOUSING     .2053

VELOCITIES IN FT/SEC AT MEAN SQUARE DIAMETER OF    4.2647 FEET
                    STATION 3    STATION 2    STATION 1
  ABSOLUTE            74.1818     286.0268      74.0292
  AXIAL COMP.         74.0292      74.0292
  TANGENTIAL COMP.     4.7563     276.2807
  RELATIVE           413.3752     145.8411
  TANGENTIAL COMP.   406.6924    -125.6554
  PERIPHERAL         401.9361
DIMENSIONLESS DESIGN RATIOS
  BLADE JET SPEED RATIO    .808555          FLOW COEF       .184181
  BLADE LOADING COEF       .764804          SPEED WORK COEF 1.307524
  SPECIFIC SPEED           .880375          SPECIFIC DIAM   3.125036
  EXIT VELOCITY/SPOUTING   .022269

CALCULATED EFFICIENCY BASED ON THEORETICAL WORK
    TOTAL TO TOTAL   .925198  TOTAL TO STATIC   .904594
CALCULATED EFFICIENCY BASED ON SUMMATION OF LOSSES
    TOTAL TO TOTAL   .925184  TOTAL TO STATIC   .904581
```

FIVE STAGE SINGLE FLOW

```
RNH

? $TURBINE TB=70.,TC=66.,GP=2.8,RND=1200.,$END


TURBINE DESIGN FOR   2.80  MEGAWATTS     AMMONIA            WORKING FLUID

STATE POINTS-----T(F),P(PSIA),H(BTU/LBM),V(CUFT/LBM),S(BTU/LBM-F)
                      STATION 3     STATION 2     STATION 1     EVAPORATOR
  TEMPERATURE          66.0000       68.6927       69.9189       70.0000
  STATIC PRESSURE     120.1531      126.0519      128.8103      128.9944
  TOTAL PRESSURE      120.3304      128.7471      128.9944      128.9944
  STATIC ENTHALPY     625.5472      627.9461      629.1080      629.1218
  TOTAL ENTHALPY      625.6279      629.1218      629.1218      629.1218
  SP. VOLUME            2.4594        2.3567        2.3120
  ENTROPY               1.2145        1.2140        1.2140        1.2139
  QUALITY                .9944         .9981        1.0000        1.0000
  VELOCITY             62.7898       62.7898       62.7898        0.0000
  VISCOSITY           .239E-01      .240E-01      .241E-01
RELATIVE STATE PROPERTIES
  TOTAL PRESSURE      126.4867      127.0128
  TOTAL ENTHALPY      625.7709      625.2708
PRESSURE RATIO    1.0736

SPECIFIC SPEED       130.4387
SPECIFIC DIAMETER      1.2289
EFFICIENCIES            .8836  TURBOGENERATOR   .9800  GENERATOR   .0100  BEARING LOSS
ROTATIONAL SPEED RPM   1200.
MASS FLOW LBM/SEC    783.1835
MACHINE REYNOLDS NO.    .2048E+09
DISK RE. NO.            .2729E+08
STATOR BLADE RE. NO.    .1525E+08
ROTOR BLADE RE. NO.     .3517E+08
STATOR THETA RE. NO.    .2238E+05
ROTOR THETA RE. NO.     .4662E+05
REACTION                .6855

GEOMETRY SPECIFICATION-LENGTH IN FEET
            ROTOR EXIT          ROTOR INLET    STATOR INLET
  DIAMETER     7.2974              7.1434         7.0754
  B. HEIGHT    1.7649              1.7277         1.7112
                              ROTOR          STATOR
  PITCH                      1.8244          .9602
  AXIAL WIDTH                 .3665          .5334
  CAMBER LINE LENGTH         1.9007         1.2431
  CHORD LENGTH               1.9007         1.1294
  TRAILING EDGE THICKNESS     .0706          .0691
  STAGGER ANGLE             11.1179        28.1868
  INLET ANGLE               25.6867        90.0000
  OUTLET ANGLE               7.0395        15.0000
  NO. BLADES                10.0000        19.0000
RATIOS
  ASPECT                     1.0769          .6537
  SOLIDITY                    .9598          .8502
  RADIUS                      .5163
  BL. HEIGHT/DIAM.            .2419
GAS FLOW ANGLES  EXIT   81.1215  UNDER TURNING    2.4737
CLEARANCE        TIP       .0706  ROTOR HOUSING     .2919

VELOCITIES IN FT/SEC AT MEAN SQUARE DIAMETER OF    5.8072 FEET
                      STATION 3     STATION 2     STATION 1
  ABSOLUTE             63.5512      242.6010       62.7898
  AXIAL COMP.          62.7898       62.7898
  TANGENTIAL COMP.      9.8085      234.3346
  RELATIVE            379.9127      144.8604
  TANGENTIAL COMP.    374.6880     -130.5449
  PERIPHERAL          364.8796
DIMENSIONLESS DESIGN RATIOS
  BLADE JET SPEED RATIO    .832660          FLOW COEF       .172084
  BLADE LOADING COEF       .721166          SPEED WORK COEF  1.386644
  SPECIFIC SPEED          1.011153          SPECIFIC DIAM    2.926124
  EXIT VELOCITY/SPOUTING   .021032

CALCULATED EFFICIENCY BASED ON THEORETICAL WORK
    TOTAL TO TOTAL   .921053  TOTAL TO STATIC   .901681
CALCULATED EFFICIENCY BASED ON SUMMATION OF LOSSES
    TOTAL TO TOTAL   .921001  TOTAL TO STATIC   .901630
```

FIVE STAGE DOUBLE FLOW

```
$TURBINE TB=70.,TC=66.,GP=1.4,RND=1800.,TBH=.04,SH=.04,DELD=.04 $END

TURBINE DESIGN FOR   1.40  MEGAWATTS    AMMONIA            WORKING FLUID

STATE POINTS-----T(F),P(PSIA),H(BTU/LBM),V(CUFT/LBM),S(BTU/LBM-F)
                      STATION 3    STATION 2    STATION 1    EVAPORATOR
  TEMPERATURE          66.0000      68.8482      70.0922      70.0000
  STATIC PRESSURE     120.1531     126.3990     129.2039     128.9944
  TOTAL PRESSURE      120.3399     129.2931     129.4016
  STATIC ENTHALPY     625.4209     627.9628     629.1374     629.1218
  TOTAL ENTHALPY      625.5059     629.2218     629.2218
  SP. VOLUME            2.4588       2.3503       2.3052
  ENTROPY               1.2142       1.2138       1.2137       1.2139
  QUALITY                .9941        .9981       1.0000
  VISCOSITY           .239E-01     .241E-01     .241E-01
RELATIVE STATE PROPERTIES
  TOTAL PRESSURE      126.6905     127.3948
  TOTAL ENTHALPY      625.5922     625.5922
PRESSURE RATIO    1.0770

SPECIFIC SPEED        128.2254
SPECIFIC DIAMETER       1.2386
EFFICIENCIES             .8849  TURBOGENERATOR   .9800  GENERATOR   .0100  BEARING LOSS
ROTATIONAL SPEED RPM     1800
MASS FLOW LBM/SEC     368.2197
MACHINE REYNOLDS NO.     .1424E+09
DISK RE. NO.             .2000E+08
STATOR BLADE RE. NO.     .1034E+08
ROTOR BLADE RE. NO.      .2455E+08
STATOR THETA RE. NO.     .1605E+05
ROTOR THETA RE. NO.      .3435E+05
REACTION                 .6825

GEOMETRY SPECIFICATION-LENGTH IN FEET
            ROTOR EXIT    ROTOR INLET    STATOR INLET
  DIAMETER     4.9671         4.8563         4.8095
  B. HEIGHT    1.1672         1.1411         1.1301
                            ROTOR          STATOR
  PITCH                     1.2488          .6244
  AXIAL WIDTH                .2586          .3469
  CAMBER LINE LENGTH        1.2986          .8084
  CHORD LENGTH              1.2986          .7344
  TRAILING EDGE THICKNESS    .0467          .0456
  STAGGER ANGLE            11.4871        28.1868
  INLET ANGLE              26.1833        90.0000
  OUTLET ANGLE              7.2985        15.0000
  NO. BLADES               10.0000        20.0000
RATIOS
  ASPECT                    1.1126          .6436
  SOLIDITY                   .9617          .8502
  RADIUS                     .5300
  BL. HEIGHT/DIAM.           .2350
GAS FLOW ANGLES  EXIT    84.9251  UNDER TURNING    2.3944
CLEARANCE        TIP      .0467  ROTOR HOUSING     .1987

VELOCITIES IN FT/SEC AT MEAN SQUARE DIAMETER OF    3.9751 FEET
                      STATION 3    STATION 2    STATION 1
  ABSOLUTE             65.2336     251.0551      64.9778
  AXIAL COMP.          64.9778      64.9778
  TANGENTIAL COMP.      5.7704     242.5006
  RELATIVE            385.9302     147.2606
  TANGENTIAL COMP.    380.4208    -132.1498
  PERIPHERAL          374.6504
DIMENSIONLESS DESIGN RATIOS
  BLADE JET SPEED RATIO    .829629          FLOW COEF       .173436
  BLADE LOADING COEF       .726444          SPEED WORK COEF 1.376568
  SPECIFIC SPEED           .993996          SPECIFIC DIAM   2.949089
  EXIT VELOCITY/SPOUTING   .020867

CALCULATED EFFICIENCY BASED ON THEORETICAL WORK
    TOTAL TO TOTAL   .922178  TOTAL TO STATIC   .902935
CALCULATED EFFICIENCY BASED ON SUMMATION OF LOSSES
    TOTAL TO TOTAL   .922142  TOTAL TO STATIC   .902900
```

APPENDIX F.2

ELLIOTT'S TURBINE STUDY

THIS PAGE

WAS INTENTIONALLY

LEFT BLANK

DESIGN STUDY OF AN AMMONIA EXPANDER/GENERATOR SET FOR OCEAN THERMAL ENERGY CONVERSION APPLICATION

TRW ORDER NO. G27617LNEE

TRW PROJECT NO. 1981-LN-8.190

AUGUST 25, 1978

FINAL REPORT

Elliott Company - Division of Carrier Corporation
900 North Fourth Street
Jeannette, Pennsylvania 15644

Principal Investigator

Charles H. Kostors

Arthur J. Miller

John E. Claydon

Thomas J. Elliott

Prepared For
TRW Defense and Space Systems Group
One Space Park
Redondo Beach, California 90278

THIS PAGE

WAS INTENTIONALLY

LEFT BLANK

CONTENTS

		PAGE
Tables		F-22
Figures		F-23
SECTION		
1	SUMMARY	F-27
2	INTRODUCTION	F-29
3	GAS PROPERTIES AND CALCULATION METHOD	F-30
	Gas Properties	F-30
	Calculation Method	F-31
4	EXPANDER AERODYNAMIC DESIGN	F-37
	Design Optimization	F-40
	Performance Maps	F-49
	Blade Path Design	F-52
	Variable Nozzle	F-53
	Diffuser Design	F-55
	Moisture Loss	F-57

SECTION		PAGE
5	EXPANDER MECHANICAL DESIGN	F-87
	Rotor	F-89
	Bearings	F-90
	Seals	F-91
	Casing and Maintenance	F-92
	Moisture Erosion	F-96
	Rotor Blades	F-98
6	GENERATOR DESIGN AND ANALYSIS	F-106
	Generator Design	F-106
	Coupling Design	F-107
7	CONTROLS	F-112
	Valve Sizing	F-112
	Valve Characteristics	F-113
	Control Scheme	F-114
	Future Work	F-118
8	LUBE AND SEAL SYSTEM	F-121
	Flow Requirements	F-121
	Components	F-122
	Auxiliary Requirements	F-127
	Degasifier System	F-128
9	SUBSYSTEM DESIGN	F-129
	Cross Section Layout	F-129
	String Arrangement	F-130
	Lube and Seal Oil Schematic	F-131

SECTION		PAGE
10	MISCELLANEOUS	F-138
	Protection Equipment	F-138
	Instrumentation	F-139
	Materials	F-142
	Codes	F-143
	Scalability	F-144
ATTACHMENT 1	REFERENCES	F-155
ATTACHMENT 2	NOMENCLATURE & DEFINITIONS	F-157

TABLES

TABLE		PAGE
2-1	Turbine Inlet and Outlet Conditions	F-28
3-1	Comparison of NBS Circular 142 to B-W-R	F-35
3-2	Expander Thermodynamic Conditions	F-36
6-1	Generator Data	F-109
8-1	Oil Requirements	F-121
8-2	Auxiliary Services	F-127
9-1	Expander Blade Geometry	F-132
9-2	Expander/Generator Component Weights	F-133
10-1	Thermodynamic Instrumentation Requirements	F-149
10-2	Instrumentation	F-150
10-3	Materials of Construction	F-152
10-4	Scaled Expanders	F-153

FIGURES

FIGURES		PAGE
4-1	Normalized Efficiency for Single Stage - Idealized	F-58
4-2	Normalized Efficiency for Two Stage - Idealized	F-59
4-3	Normalized Efficiency for Three Stage - Idealized	F-60
4-4	Normalized Efficiency for Four Stage - Idealized	F-61
4-5	Normalized Efficiency for Five Stage - Idealized	F-62
4-6	L/D versus Base Diameter - Idealized Blades	F-63
4-7	Normalized Efficiency for Three Stage - Real Blades	F-64
4-8	Normalized Efficiency for Four Stage - Real Blades	F-65
4-9	Normalized Efficiency for Five Stage - Real Blades	F-66
4-10	Normalized Efficiency for 31 Base Diameter - Real Blades	F-67
4-11	L/D versus Base Diameter - Real Blades	F-68
4-12	Normalized Efficiency for Single and Double Flow Design - Real Blades	F-69
4-13	Normalized Efficiency for Single Stage, Single Flow Design - Idealized Blades	F-70
4-14	Normalized Efficiency for Radial Inflow Design	F-71
4-15	Flow Correction	F-72
4-16	Generator Output for 89.2 psia Exhaust	F-73
4-17	Generator Output Correction versus Exhaust Pressure	F-74

FIGURES		PAGE
4-18	Generator Output Correction versus Generator Output	F-75
4-19	Generator Output Expanded Plot	F-76
4-20	Generator Output Expanded Plot	F-77
4-21	Generator Output Expanded Plot	F-78
4-22	Generator Output Expanded Plot	F-79
4-23	Seasonal Variation in Expander Efficiency	F-80
4-24	Velocity Triangles First Stage	F-81
4-25	Velocity Triangles Second Stage	F-82
4-26	Velocity Triangles Third Stage	F-83
4-27	Velocity Triangles Fourth Stage	F-84
4-28	Effect of Exhaust Diffuser Recovery Factor	F-85
4-29	Effect of Moisture Loss Factor	F-86
5-1	Labyrinth Seal	F-100
5-2	Dry Carbon Seal	F-101
5-3	Bushing Seal	F-102
5-4	Face Seal with Shutdown Features	F-103
5-5	Variable Nozzle Linkage	F-104
5-6	Goodman Diagram	F-105
6-1	Generator Efficiency	F-111
7-1	Control Schematic	F-120
9-1	Expander Cross Section Layout	F-134
9-2	Expander Blade Path	F-135

FIGURES

		PAGE
9-3	String Arrangement	F-136
9-4	Oil Schematic	F-137
10-1	Normalized Efficiency 10, 22.5, and 40 MW(e)	F-154
B-1	Blade Terminology	F-161
B-2	Turbine Stage Diameters	F-162

THIS PAGE

WAS INTENTIONALLY

LEFT BLANK

SECTION 1

SUMMARY

A design and optimization study for a 14.4 MWe gross expander/generator set operating with ammonia gas as the motive fluid for an ocean thermal energy conversion process (OTEC) has been completed. The prime consideration in this design study dictated that the hardware remain within the state-of-the-art.

A barrel type axial flow expander (See Figure 9-1) was designed to operate on saturated ammonia vapor at inlet conditions of 128.8 psia/70°F to an exhaust pressure of 89.2 psia with a weight flow of 825 pounds mass per second.* Variable parameters included the number of stages, the operating speed, the disc base diameter and the type of expander. The gas properties as used for this expander design were qualified by comparison to NBS circular 142 and making minor corrections to the final results as indicated.

The expander, which resulted in an optimized expander/generator set, was a four stage double flow axial flow machine direct connected to a four-pole synchronous generator developing 15040 KW at 13.8 KV for the above conditions. The 640 KW increase in power output is due to an

*TRW presented new mass flow data, which is 2.8 percent less, at an August 14, 1978 meeting at Elliott Company. No revisions have been made to this report as a result of this new data.

expander efficiency of 89.6 percent compared to a minimum efficiency of 85 percent projected by TRW.

The blading used for the expander is proprietary state-of-the-art high performance blading. Blade stresses and frequencies were checked to verify the mechanical integrity before a final decision could be made on the staging.

The proposed control system includes variable nozzles for the first expander stage; the variable nozzles provide for increased power developed at off-design conditions compared to fixed nozzles.

The safe handling and containing of ammonia vapor was critically important in determining the mechanical design. Special attention was given to joint leakage and shaft seals to provide psoitive sealing.

Operation with ammonia vapor as the motive fluid requires that materials which are not susceptible to stress corrosion cracking be used in the expander construction.

SECTION 2

INTRODUCTION

The purpose of this study is to present a manufacturable ammonia expander/generator set with optimized performance based on nominal conditions provided by TRW, Inc. These and the maximum and minimum extremes to be accommodated by the expander are shown in Table 2 - 1.

TABLE 2 - 1

TURBINE - INLET AND OUTLET CONDITIONS***

	Minimum Flow ("Winter")	Nominal Flow	Maximum Flow ("Summer")
Inlet Conditions (Total)			
Ammonia Mass Flow, lb/sec	742	825	908
Ammonia Temperature, °F	67.0	70.0	73.0
Ammonia Pressure, psia	122.1	128.8	135.7
Ammonia Quality, %*	99.0	99.0	99.0
Ammonia Vol. Flow, acfs **	1,838	1,907	1,995
Outlet Conditions (Total)			
Ammonia Temperature, °F	49.0	50.0	51.0
Ammonia Pressure, psia	87.5	89.2	90.9

* Saturated Conditions

** Estimated Assuming 100% Vapor

*** TRW presented new mass flow data, which is 2.8 percent less, at an August 14, 1978 meeting at Elliott Company. No revisions have been made to this report as a result of this new data.

The approval to proceed with the study was given by TRW on June 12, 1978 and the work was completed on the designated date of August 25, 1978. Included in the study were five main areas of concern, namely; expander aerodynamic analysis, mechanical analysis, generator design, controls and the lube system.

The properties of the motive fluid, anhydrous ammonia vapor, were specified to be per National Bureau of Standards Circular No. 142, Tables of Thermodynamic Properties of Ammonia (1942); the ammonia is to be continuously filtered through a 40 micron filter and have the water content maintained below 10 parts per million.

Sea state six and sea state nine (non-operational at this condition) were considered for the design of the equipment as specified for this marine application.

The generator design information was supplied by Brown Boveri Corporation, North Brunswick, New Jersey.

Definitions of various symbols and terms used in this report can be found in Appendix B.

SECTION 3

GAS PROPERTIES AND CALCULATION METHOD

GAS PROPERTIES

The Elliott Company uses a modified Benedict-Webb-Rubin (BWR) equation of state for real gas calculations. The requirements for this project specified the gas properties to be used as those defined by NBS circular 142. Therefore, a comparison of the two sources of gas properties must be made to insure the accuracy of our thermodynamic calculations. Table 3 - 1 shows three upstream thermodynamic state points, which were chosen from NBS circular 142 to be as close to the actual performance points as possible without requiring any interpolation. The table also includes for each upstream point an isentropic downstream point, which was selected from circular 142 for the same reasons as were the upstream points. The comparison at these upstream and downstream conditions includes specific volume, quality, and available energy.

For the upstream points saturation values of temperature and volume are given for each pressure. No appreciable difference exists between the BWR and circular 142 values of saturation temperature. The downstream points give values for quality and volume. Notice that the difference in quality is practically zero. The absolute levels of enthalpy are not

particularly important here, but the available energy or isentropic heat drop is important. Tabe 3 - 1 contains a comparison of the available energy for each of the three points considered, with the difference being on the order of one percent. The BWR equation calculates the higher available energy values as well as higher specific volumes, by about one and one half percent. We have adjusted all of our calculations to conform to NBS circular 142.

CALCULATION METHOD

The design point performance and performance maps were calculated on Elliott Company's Multistage Performance Program, which has been developed during the past five years. The program is a modified pitch line analysis based on the Ainley and Mathieson (1)* loss method with many of the improvements as proposed by Dunham and Came (2). In addition, a number of proprietary improvements have been incorporated by Elliott Company.

The Multistage Performance Program calculates the turbine thermodynamic conditions at specific stations within the turbine for a given geometry on the basis of mass flow continuity. The thermodynamic analysis uses only pressure, enthalpy, and specific volume

*Numbers in parentheses refer to references listed in Appendix A.

at each station. The calculations between stations are made from calculated efficiencies and enthalpy differences. The method of calculation requires more computer time than the conventional pressure temperature ideal gas law type performance calculation. However, it has the advantage of being completely independent of gas moisture level, utilizing an equilibrium gas property calculation. The gas properties are calculated with a modified Benedict-Webb-Rubin equation of state.

The Ainley and Mathieson loss method develops the losses on the basis of a pressure loss coefficient, Y, which is defined as the loss of total head pressure divided by the blade exit velocity pressure head. The blade row pressure loss coefficient is the sum of profile, secondary and blade leakage pressure loss coefficients. In addition, if the rotating blades are not shrouded it is typical turbine practice to lash the blades together with either zigzag lashing pins or lashing wires, which present a flow path restriction and, therefore, a performance loss. The lashing pressure loss coefficient is calculated for unshrouded rotating blade rows and then added to the total pressure loss coefficient for that row. The profile loss is due to skin friction over the blade surface and blade incidence angle at blade inlet. The incidence loss used in the calculation of profile loss is the average incidence loss considering the base, mean, and tip incidence. The secondary loss includes both the annulus endwall friction losses and losses due to turning of the flow within the blade passage. The

calculation of both profile and secondary losses closely follow the procedures as outlined in references 1 and 2. Blade leakage loss is the loss associated with flow through the diaphragm shaft packing in the case of a stationary blade or over the rotating shroud or blade tips for a rotating blade row. The calculation of blade leakage loss closely follows the method outlined in reference 2. In addition, the rotating blade tip leakage loss has been modified to account for the blade tip static pressure drop.

After the above losses are calculated, the total pressure loss coefficient is converted to a blade efficiency. The blade efficiency is corrected for moisture loss depending on the mean moisture content of the blade row. The actual moisture loss factor is an input and is considered to be the percent decrease in efficiency per percent of mean blade row moisture as suggested in reference 3. The inlet conditions ahead of each blade row are then calculated from the final blade row efficiency and stage mass flow.

The disc friction and shroud friction losses are calculated with standard Elliott equations, and these losses are added to the stage exit enthalpy. This final stage exit enthalpy is used in the calculation of stage work output.

The pressure carryover between stages is calculated according to the method as suggested in reference 3.

Turbine inlet losses are input as a fraction of turbine inlet pressure. The turbine exhaust losses and the effect of the diffuser on exhaust losses are input as a fraction of last stage rotor blade exit velocity heads. The overall turbine efficiency includes inlet, exhaust, bearing and seal losses.

TABLE 3 - 1

COMPARISON OF NBS CIRCULAR AND BENEDICT-WEBB-RUBIN
EQUATION OF STATE FOR AMMONIA

SOURCE	UPSTREAM CONDITION			ISENTROPIC DOWNSTREAM CONDITION			AVAILABLE ENERGY
	P PSIA	T °F	V ft^3/lbm	P PSIA	QUALITY	V ft^3/lbm	ΔH_s BTU/lbm
POINT 1 (Nominal)							
NBS CIRCULAR 142	128.0	69.65	2.326	89.0	.9701	3.203	19.6
BWR			2.365		.9703	3.248	19.8
DIFFERENCE (%)			1.68		.03	1.41	1.02
POINT 2 (Max.)							
NBS CIRCULAR 142	136.0	73.11	2.193	91.0	.9667	3.134	21.6
BWR			2.231		.9670	3.170	21.89
DIFFERENCE (%)			1.74		.03	1.14	1.36
POINT 3 (Min.)							
NBS CIRCULAR 142	122.0	66.94	2.437	88.0	.9731	3.248	17.7
BWR			2.477		.9735	3.294	17.8
DIFFERENCE (%)			1.64		.04	1.42	.59

TABLE 3 - 2

EXPANDER THERMODYNAMIC CONDITIONS

	Minimum Flow (Winter)	Nominal Flow	Maximum Flow (Summer)
Inlet Conditions (Total)			
Pressure, psia	122.1	128.8	135.7
Enthalpy, BTU/lb	628.54	629.04	629.56
Temperature, °F	67.0	70.0	73.0
Quality, %	0.9999	0.9999	0.9999
Outlet Conditions (Total)			
Pressure, psia	87.50	89.30	90.90
Enthalpy, BTU/lb	612.372	611.233	610.203
Temperature, °F	49.0	50.0	51.0
Quality, %	0.9761	0.9735	0.9711
Expander Mass Flow, lb/sec.	742.	825.	908.
Isentropic Heat Drop, BTU/lb	18.069	19.874	21.637
Total To Static Efficiency, %	89.48	89.60	89.46

SECTION 4

EXPANDER AERODYNAMIC DESIGN

The purpose of the aerodynamic design study is to define the optimum expander design for the specified nominal conditions, and then to determine the expander performance characteristics over the entire seasonal operating range.

The primary consideration in the aerodynamic design of the expander was to achieve an optimum performance level with manufacturable state-of-the-art technology. Therefore, the aerodynamic design and the mechanical design cannot be separated. The first step in the design optimization process involves special blades, hereafter referred to as idealized blades, which do not take into account manufacturability. The second step in the optimization process incorporates proven airfoil designs. In this way, a manufacturable state-of-the-art design is assured, while still being optimized on the basis of idealized blades. Finally, the resulting real blade design is compared to several special cases, including single flow and radial inflow designs.

The use of the idealized blades will give the optimum theoretical design possible. These idealized blades consist of stator blades with 12° blade exit angles at their mean diameters and rotor blades with 15° blade exit angles at their mean diameters. These are considered the minimum possible angles for axial flow turbine blades using state-of-the-art technology. They are also predominantly found on blades having much lower L/D ratios than those examined in this study. These low angles, however unrealistic for the long blade lengths required, will give a high theoretical performance. These small angles will compel the use of longer blades, thereby maximizing L/D ratios. This will have the tendency to raise the stage velocity ratios by raising the mean blade speed, U, in the term U/C$_o$. For a design having fewer stages than the optimum number, this has a tendency to increase the stage velocity ratio toward the value where maximum efficiency occurs (in our case, approximately 0.65). The purpose of using the idealized blades is clearly seen in this light, that is, to create an optimum theoretical design with the fewest number of stages.

As mentioned before, however, the desired end result is a manufacturable aerodynamic design. The above analysis will not supply that, since its aerodynamics have been idealized and removed from real world considerations. To alleviate this problem, the design optimization analysis includes a more limited, but similar study involving actual turbine blades of the type envisioned for the final expander. The most promising designs obtained from the ideal blade study have been

reanalyzed on the basis of actual blades. For the actual blade study the base diameters were chosen to provide optimum performance at a synchronous speed. This is in contrast to the idealized blade optimization study, in which the base diameters were chosen to provide a wide enough range to produce a clear favorite. From this study, an optimum design can be chosen which gives the best choice for base diameter and number of stages.

The idealized and real blade designs have been analyzed at the nominal design point conditions, and the results have been presented in the form of normalized efficiency versus velocity ratio curves. Since the overall isentropic heat drop is fixed by the design point, as is the mass flow, the velocity ratio was varied by changing the shaft speed of the design. Constant speed lines are shown on the figures. In the course of changing speeds with a constant mass flow and isentropic heat drop, blade heights also vary along these velocity ratio curves.

Several restrictions have been set on the analyses described previously. Among these is the condition that only double flow axial designs be considered. Radial inflow expanders will be discussed after the double flow axial units have been analyzed, as will single flow designs. The rationale for initially excluding single flow designs is based on fact that such designs are hampered by high thrust bearing losses. Two single flow designs are included in this study,

so as not to rule them out on the basis of high thrust loads alone. It was felt that this disadvantage would limit the possibilities enough to enable a shorter discussion to suffice.

After the optimized design is achieved, it is analyzed over the entire range of operating conditions given, so that a detailed performance map can be made. This map encompasses the effects of variable nozzles over the entire seasonal range. Variable nozzles, diffuser design, and moisture loss are all discussed in later parts of Section 4.

DESIGN OPTIMIZATION

To optimize the final design, two types of blading are analyzed. The first type is an idealized selection, based on what is considered state-of-the-art minimum gauging angles possible for any blades; 12° for the stator blades and 15° for the rotor blades. These extremely low gauging angles are predominantly used in constant section blading. The second type of blading represents the actual blading chosen for this machine, a modified free-vortex design with stator mean gauging angles of 17 to 19 degrees and rotating blade mean gauging angles of 18 to 20 degrees. Limitations placed on the idealized blades included a maximum L/D ratio of 0.33, which has been shown from experience to be a practical limit. An L/D ratio of 0.290 is the limit for the actual blades chosen, which represents the practical twist limit for this modified free vortex design. Higher L/D ratios are possible at the expense of

increasing pitch line gauging angles. All calculations were made using nominal design point data.

Figures 4 - 1 through 4 - 5 show normalized efficiencies versus velocity ratio for the idealized blades. Each plot was drawn for a specific number of stages, with base diameter and speed being varied on each plot. Also shown is a line representing constant machine speed which indicates the peak base diameter for the shaft speed. The constant speed lines shown correspond to synchronous generator speeds. Predictably, overall peak performance increases with the number of stages and with decreasing base diameters. The latter phenomenon is caused by increasing L/D ratios, which are given in Figure 4 - 6 for the designs represented by the first five figures. The efficiencies were calculated regardless of L/D ratio, so that the curve of maximum L/D ratios must be checked for each of the first five figures. Some or most of those designs shown may violate L/D restrictions.

Figure 4 - 1 shows all one stage designs using the idealized blades. Four base diameters are included on the plot. Figure 4 - 6 shows that for one stage designs, the minimum base diameter that allows a reasonable L/D ratio is 22 inches. The constant speed line of 3600 RPM shows the best base diameter is 31 inches with a normalized efficiency of .955. The next, Figure 4 - 2, shows the two stage designs peaking at or below a 24 inch base diameter for 3600 RPM. However, this point represents an L/D ratio over 0.45. For L/D ratios below

the 0.33 limit, either the 31 inch base diameter design running at 3600 RPM or the 38 inch base diameter design running at 1800 RPM are the best. If gears are considered, the 31 inch base diameter design yields the highest normalized efficiency.

Three stage designs are limited to a minimum base diameter of 29 inches by L/D ratios which, in turn, means that the best efficiency for a three stage design is between a 31 inch or a 38 inch base diameter, running at 1800 RPM. The peak efficiency will be about 99% of the four stage efficiency. The four stage designs shown in Figure 4 - 4 are limited to a 31 inch base diameter by L/D ratio. Any higher efficiency in a four stage design must be obtained with an L/D ratio higher than 0.33. Five stage designs are limited to the two largest base diameters, with the 31 inch base diameter producing an L/D ratio of just over .35. With either of the 38 or 47.5 inch base diameter designs, peak efficiencies at synchronous speed are slightly less than the peak four stage efficiency.

In most of these cases either 1800 RPM or 3600 RPM give the best results, since gears are required otherwise, and gears usually mean a two percent efficiency penalty. The first five figures show that with these idealized blades, the highest efficiency can be obtained with a four stage design. The optimum base diameter appears to be near 31 inches, but this finding must be verified by generating efficiency curves of the actual blades under consideration. Figures 4 - 7 thru 4 - 11 are normalized efficiency versus velocity ratio curves for the

actual blades. Only three, four, and five stages have been considered on more than one base diameter, while one through five stages have been analyzed on a 31 inch base diameter. A plot of maximum L/D ratio versus base diameter is shown on Figure 4 - 11, with the .290 L/D limit previously discussed.

The question naturally arises as to why the idealized blades with their small gauging angles are not used instead of the modified free-vortex blades chosen. The answer lies in the nature of the free-vortex tapered and twisted idealized blade. This type of blading produces a nearly uniform radial distribution of mass flow with the stage reaction increasing from base to tip. Therefore, with increasing L/D ratio and constant mean reaction (constant mean exit angle), the reaction at the base of the vane will decrease and become negative, resulting in severe degradation of blade row efficiency. In addition, mechanical considerations dictate the use of zigzag lashing for very high L/D ratio blades rather than shrouds, resulting in additional degradation of performance. The above problems may be avoided by untwisting the blade sections, but this leads to other performance problems, such as mass flow imbalances in the radial direction. These idealized blades are in reality not desirable, but the point of including them in the optimization study was to favor the highest possible L/D ratios with the lowest possible gauging angles. In this way, an idealized design with the fewest number of stages is found and is then used as a starting point for a real blade study.

The general trend of the idealized blade study is that efficiency increases with increasing number of stages.

Figure 4 - 7 shows three stage designs using real blades. The three base diameters are 27 inches, 31 inches, and 40 inches. The latter base diameter maximizes the three stage design efficiency at 1800 RPM. Higher peak efficiencies can be obtained by going to higher shaft speeds and smaller base diameters. In this event, a gear would be used and a two percent loss would be incurred. Since the improvement is not two percent, the best performance can be obtained from the 40 inch base diameter design. This particular design has much lower efficiency compared to the four and five stage designs because of decreasing L/D ratios. This peak normalized efficiency is .978, which means this design will produce 2.2 percent less power than the four stage design. This works out to be approximately 330 Kilowatts. The 330 KW, valued at $330,000*, can be obtained by adding a fourth stage at the cost of approximately $100,000. For this reason, the three stage design can be discounted. The analysis with the idealized blades agrees with the analysis of the actual blades, in that both show that four stages are the minimum number necessary for peak operation.

*Power is evaluated at $1000 per KW as per TRW on July 7, 1978, Equipment prices are based on current cost levels.

The next Figure 4 - 8 shows four stage, double flow designs on three different base diameters. The smallest base diameter peaks at the highest efficiency, but at a speed other than 1800 RPM or 3600 RPM. The 31 inch base diameter design is at the peak efficiency for 1800 RPM operation. No other synchronous speeds are in the proper range to appear on these velocity ratio curves. Figure 4 - 9 presents similar information for five stage designs, with the 27 inch base diameter giving the highest efficiency for 1800 RPM operation although it exceeds the L/D limits. Figure 4 - 10 is a plot of normalized efficiency versus velocity ratio for all of the 31 inch base diameter designs.

A five stage, double flow design does offer better performance than a four stage design, but caution must be exercised about the value of this small improvement. The 27 inch base diameter design peaks at nearly one percent better in performance, at the same shaft speed as the four stage design. But from our L/D curve, we can see that this design has blades that violate L/D limits, making this design unfeasible. The 31 inch base diameter design is also better than the four stage design, but there are two problems here, the first concerning L/D ratios. The maximum L/D ratio for the five stage design on a 31 inch base diameter is slightly higher than the accepted limit for this blade. This would necessitate a redesign of the blade to be used in this application. The second problem concerns practicality. The five stage design is about three-tenths of

one percent better in efficiency, amounting to about 50 KW. If the price of this power is $1000 per KW, then $50,000 could be saved by going to five stages. But the cost of adding a fifth stage to both ends of the double flow design would cost approximately $100,000, making the five stage design cost inefficient. Critical speed problems can also be avoided by keeping bearing spans to a minimum, which also favors a four stage over a five stage design.

As a result of the first eleven figures in this section, several conclusions can be made. First, four stages are the minimum number of stages to provide peak efficiency. Second, a 31 inch base diameter provides the best efficiency for a four stage, double flow design when operating at 1800 RPM and when limited to the blade profile L/D limit shown on Figure 4 - 11. Another conclusion is that a five stage design yields better efficiency, but when the constraints of this system are applied (L/D ratios, 1800 RPM speed, using a gear for nonsynchronous operation) the gain is marginal. The gain is so small that the cost of adding the fifth stage would be higher than the benefit of the additional power. Critical speed problems will be created by stretching the shaft to accommodate the fifth stage.

So far we have only considered double flow designs, since they eliminate any high thrust bearing losses. Bearings for single flow designs can be quite large since it is accepted practice not to load thrust bearings over 250 psi, and preferably to keep the loading below 200 psi.

Figure 4 - 12 compares a double flow and a single flow design for the 10 MW net system. The single flow design is under some system constraints which limit its efficiency to 1.6 percent less than the double flow. The thrust bearing produces a large loss, but another loss is introduced by having to run at a synchronous speed of 1200 RPM. In peaking the velocity ratio of the single flow design for 1200 RPM operation, the base diameter has been increased and L/D ratios have gone down. This also contributes to the lower efficiency. Measures could be taken to reduce the thrust loading, such as balance holes, but an added performance penalty would result.

Also considered is a single stage, single flow design, the results being shown on Figure 4 - 13. This design concept uses the idealized blades previously discussed for comparative purposes. An important part of a single stage, single flow design is the diffuser, which is the only means of recovering some of the substantial amount of exhaust kinetic energy that would otherwise be wasted. For this reason, efficiency curves for a range of diffuser pressure recovery factors have been included in Figure 4 - 13. The highest value for the pressure recovery factor, 0.7, is based on the maximum area ratio possible, that is, the diffuser exit area is identical to the 126 inch diameter condenser inlet flange area. This area ratio produces a diffuser length well over 40 feet for the optimum recovery factor (11). With this type of diffuser, an overhung design would be necessary, with the bearing compartment being designed into the inlet side of the expander. The

probability of obtaining a pressure recovery factor of 0.7 is considered to be very small, even with such a design.

As noted on Figure 4 - 13, the base diameter is 31 inches, which produces an L/D ratio of 0.33. Since it is considered impossible to successfully use a shroud with the L/D ratio being so high, these efficiency curves reflect this difference between the four-stage, double flow and the one-stage, single flow designs. The normalized efficiency of the one-stage, single flow design is more than two percent lower than preferred design, indicating that additional stages do a better job of converting energy to power than a diffuser. Other disadvantages of the one one-stage, single-flow design include the difficult inlet case design and the requirement of more exotic blade materials to handle the higher stresses.

The final topic under consideration in the optimization study is that of using radial inflow expanders. Many different types of systems for radial inflow expanders are possible, but state-of-the-art technology limits the choices to one. No wheel diameter over 52 inches was chosen, since this is approximately the largest radial inflow wheel size now being considered. Because of the low available heat energy, only single stage designs were chosen. For the nominal conditions given, a synchronous speed of 3600 RPM gives the best range of velocity ratios for the wheel diameters studied. The only design choice left undecided at this point is the number of ways the flow must be divided.

46 inch wheel running at 3600 RPM may be designed for one-fourth of the total mass flow. For one-half the total mass flow, the inlet blade heights get large, and the exducer outside diameter approaches the wheel tip diameter. This results in an impractical design for high efficiency. Considering these facts, four-flow, single stage radial inflow expanders of various wheel diameters and running at various speeds were analyzed. Minimum angles were assumed at stator and rotor exits to maximize efficiency. The results are shown in Figure 4 - 14. Notice that the 46 inch wheel produces the peak efficiency for synchronous operation, and that this point is less than 2 percent lower than the peak efficiency for nonsynchronous operation, making a gear-driven generator unattractive. All performance levels are considerably lower than those obtained with the optimum axial flow designs. Therefore, a radial-inflow design is undesirable for this application.

PERFORMANCE MAPS

The TRW/OTEC ammonia expander performance maps were developed in the form of a four step nomograph of a type agreed to by both TRW and Elliott Company. These performance maps will give the generator output in megawatts (MW) from the following three known quantities: expander inlet pressure, exhaust pressure, and mass flow. The expander inlet conditions are fixed at the saturation line in all cases. In addition, the performance maps incorporate the effects of variable first stage stator blades.

The perforamcne maps consist of Figures 4 - 15 through 4 - 18; in addition, Figures 4 - 19 through 4 - 22 represent Figure 4 - 16 on an expanded scale to facilitate greater accuracy.

The purpose of Figure 4 - 15 is to correct the actual expander mass flow to a flow with an exhaust pressure of 89.2 psia.

Figure 4 - 16 is a plot of corrected output in MW for an expander with an exhaust pressure of 89.2 psia plotted against mass flow.

The output found from Figure 4 - 16 can be corrected to any exhaust pressure using Figure 4 - 17. This figure corrects output for exhaust pressure, and includes the effect of expander efficiency, and generator efficiency.

A generator with improved performance was located at the time of final writing of this report and after the performance maps were developed. Therefore, Figure 4 - 18 has been added to correct to the new generator efficiency level.

The procedure for finding the generator output from the expander mass flow, inlet pressure, and exhaust pressure is as follows:

1) Enter Figure 4 - 15 at the actual exhaust pressure and inlet pressure to determine the flow correction factor.

2) Divide the actual flow by the flow correction factor found in step 1.

3) Using the corrected mass flow found in step 2, determine the corrected output for the exhaust pressure of 89.2 psia from Figure 4 - 16.

4) Enter Figure 4 - 17 at the actual exhaust pressure and inlet pressure to determine the generator output correction factor.

5) Multiply the generator output found in step 3 by the correction factor found in step 4 to determine the corrected output.

6) Enter Figure 4 - 18 at the corrected output found in step 5 to determine the generator efficiency correction factor.

7) Multiply the generator output found in step 5 by the generator efficiency correction factor found in step 6.to determine the net generator output for the actual operating conditions.

The performance levels obtained from these maps include the following losses:

1) An inlet loss of 1.4 inlet flange velocity heads. The nominal inlet flange velocity is 103 feet per second.

2) An exhaust loss of 0.8 last stage blade exit velocity heads. The nominal exhaust flange velocity is 55 feet per second.

3) Expander bearing and seal losses of 55.2 KW.

BLADE PATH DESIGN

The four stage double flow TRW/OTEC ammonia expander was designed for optimum performance at the specified nominal conditions, which insures the maximum expander performance over the entire operating range. The maximum performance change of 0.16 percent occurs between nominal (spring, fall) and summer conditions as shown in Figure 4 - 23. The final expander design has shrouded rotor blades for optimum performance resulting in an expander design point flange-to-flange efficiency of 89.60 percent. The generator efficiency at the design point conditions is 97.03 percent, resulting in an overall expander/generator efficiency of 86.94 percent with a generator output of 15040 KW.

The proposed expander utilizes modified free-vortex blading on a 31 inch base diameter. Both stator blades and rotor blades are a tapered and twisted design so that they are properly optimized along the entire blade height. The blade heights ranges from 10.2 inches for the first row stator to 12.3 inches for the fourth row rotor blade. The blading is a reaction type where the average reaction ranges from 3 percent at the base to 63 percent at the tip. A blade path cross section is shown in Figure 9 - 2. The diameters, axial widths, and gauging angles for each stage are given in Table 9 - 1. Velocity triangles, shown on Figures 4 - 24 through 4 - 27, are presented for the nominal conditions at the base, mean, and tip sections for each of the four stages.

It is preferred to use shrouded rotor blades with two 0.03 inch radial clearance tip seals to minimize rotor blade tip leakage and maximize performance. However, the use of shrouded blades in an ammonia atmosphere is still under investigation. If the use of shrouds are ruled out due to material problems, then zigzag lashing pins must be used to lash the blades, reducing the performance by 1.4 percent.

Stator blade leakage along the shaft will be minimized with labyrinth diaphragm seals. Each diaphragm seal will contain eight straight teeth with 0.03 radial clearance.

VARIABLE NOZZLE

As mentioned earlier, the perforamnce map calculations have been made with the assumption that variable first stage nozzles would be incorporated into the final design. In this section the net power gain from the variable nozzles will be compared to their additional cost. To determine the net power gained, the machine design with the nominal point first stage nozzle angle was analyzed at the minimum and maximum flow points. Without variable nozzles, an inlet pressure lower than 122.1 psia is necessary to maintain the mass flow for the minimum condition, resulting in a lower value of pressure energy available to the expander. At the maximum condition, however, a nonvariable nozzle means that a small percentage of the mass flow must be bypassed which, in turn, means that less mass flow is available to produce power. In both cases in which nonvariable nozzles

are used, less power is produced than a comparable case in which variable nozzles are used. In neither case, however, is the change in power directly attributable to a significant change in expander efficiency. The net power gained by using variable nozzles is 150 KW at the minimum point and 252 KW at the maximum point.

The variation from maximum to nominal to minimum flow conditions is essentially a 360 degree sine wave. To determine the average values of net power gained, the sine wave must be integrated and then substituted by a rectangle of equal area. This rectangle will have a height of .637 relative to a sine wave height of 1.0. The average value of net power gained for each part of the sine wave variation in conditions (each 180 degrees) is obtained by multiplying the maximum and minimum flow condition values of net power gained by .637. This yields average values of 96 KW for the minimum part of the cycle and 160 KW for the maximum part of the cycle. The arithmetic average gives the overall cycle average value of net power gained by using variable nozzles. This value is 128 KW. At $1000 per KW, this gives a savings of $128,000 gained by using variable nozzles. Since the cost is roughly $55,000 for both sides of the double flow machine, the variable nozzles will save money over the life of the machine, in addition to providing better control over the unit as outlined in Section 7.

Variable nozzles also provide for better matching of the ammonia expander cycle to particular site conditions, as well as enable one

expander design to be employed at a variety of locations.

Since efficiency is almost constant over the entire range of operating conditions with one set of variable nozzles, the use of variable nozzles in more than one stage will not increase efficiency. Additional complexity of construction and cost are not considered worthwhile.

DIFFUSER DESIGN

The expander last stage exhaust diffuser is designed for an exit to inlet area ratio of 1.61, and has an exit pressure recovery factor of 0.315. Combining both pressure loss in the exhaust diffuser and pressure loss between diffuser exit and the turbine exhaust flange, an estimated 0.8 fourth stage blade exit velocity heads are lost within the expander exhaust hood. Figure 4 - 28 shows a plot of normalized expander efficiency versus exhaust diffuser pressure recovery factor.

The exhaust diffuser design is optimum from a standpoint of its aerodynamic performance versus its effects on expander costs. Increasing the diffuser from the present mean radius of 24 inches to 36 inches will improve nominal expander output by 0.075 percent yielding an additional 11.3 KW. To obtain the additional output, the bearing span and casing diameter will have to be increased approximately 24 inches at an estimated increase in expander cost of $115,000. The increase in expander output is only worth $11,300

evaluated at $1000 per KW. Therefore, use of an improved exhaust diffuser is not cost effective.

The exhaust flange velocity, averaging 55 feet per second, will not have a uniform velocity profile at the exhaust flange. Some of the pressure calculated to be lost within the exhaust hood, in our performance studies, may be recovered by development of a uniform velocity profile. In addition, a uniform velocity profile is necessary to insure minimum loss in downstream elbows or transitions. It should be emphasized that the performance levels quoted in this report are without pressure recovery, and that pressure recovery may slightly improve performance levels.

To develop a uniform exhaust velocity profile it is recommended that a minimum of six expander flange pipe diameters of straight pipe be utilized between exhaust flange and the first pipe elbow or transition. This will insure maximum expander exhaust pressure recovery, in addition to minimizing pressure loss in downstream elbows or transitions. If it is necessary to elbow the exhaust pipe before the development of a uniform velocity head then corner vanes should be used in the pipe.

None of the velocity head lost within the exhaust hood will be recovered by the transition from the 94 inch inside diameter exhaust flange to the 126 inch inside diameter plant condensate pipe. In

addition, care should be exercised in the design of the transition so that a minimum pressure loss occurs. The pressure loss can be kept to a reasonable value by having a smooth transition which is a minimum of five pipe diameters in length (11).

MOISTURE LOSS

A moisture loss factor of one percent for each percent of mean blade row moisture was used in this performance analysis. This is a value which is normally used in high pressure steam turbines. Therefore, this level seems reasonable for the four stage high pressure high reaction design proposed. This moisture loss factor may even be conservative when ammonia drop sizes are compared with those of steam. The maximum stable drop size in ammonia, at 90 psia pressure, calculated on the basis of Weber number, is less than one third (0.199 microns) the size occurring in steam (0.609 microns) for the same conditions.

The effect of moisture loss factor on normalized turbine efficiency is shown in Figure 4 - 29. It should be noted that the aerodynamic loss is greater than that given by the moisture loss factor since the moisture loss is applied to each blade row during the calculation. The moisture loss is applied before the completion of the calculation of each blade row thermodynamic conditions.

FIGURE 4-1

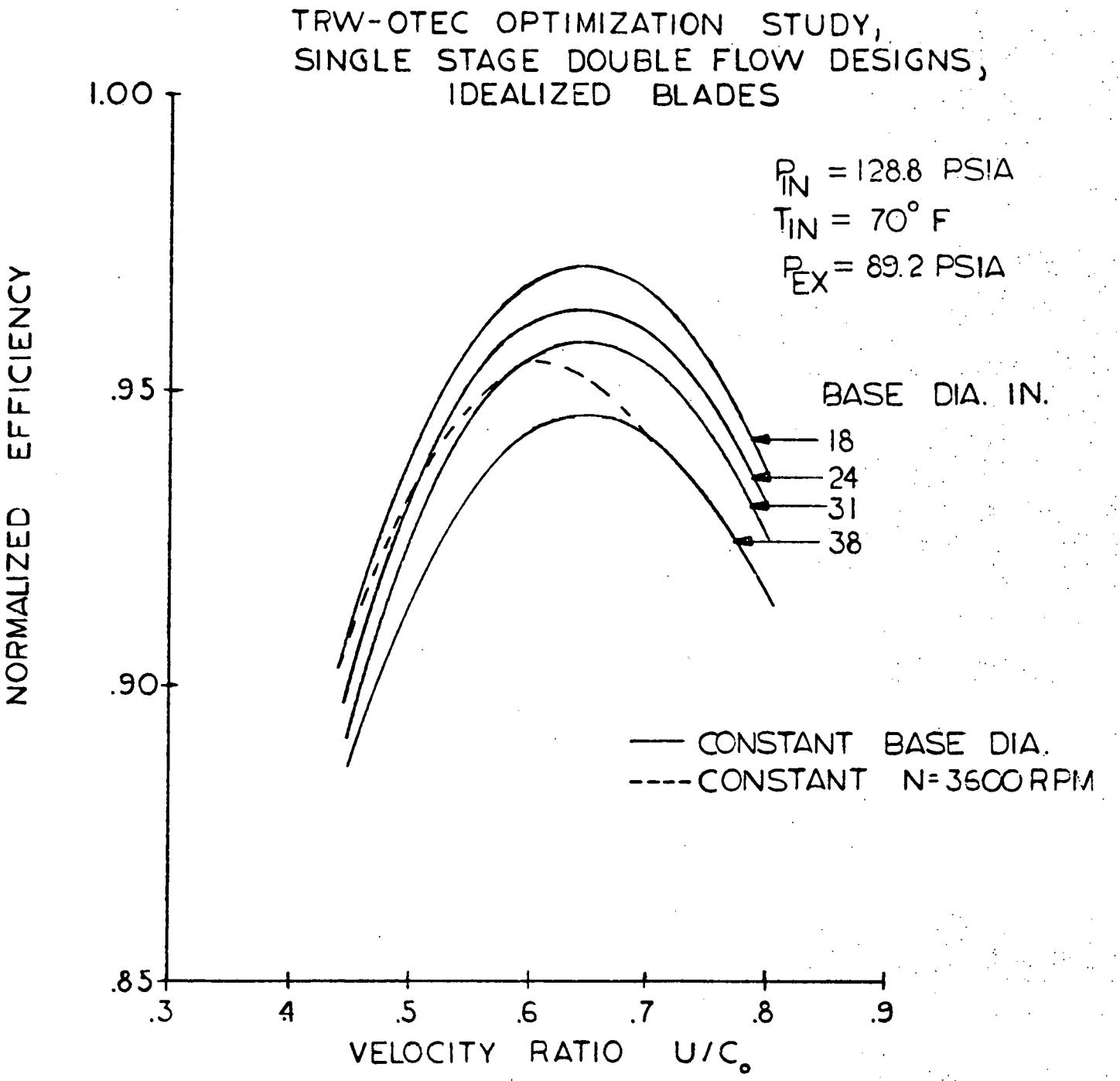
TRW-OTEC OPTIMIZATION STUDY,
SINGLE STAGE DOUBLE FLOW DESIGNS,
IDEALIZED BLADES
P_{IN} = 128.8 PSIA
T_{IN} = 70° F
P_{EX} = 89.2 PSIA
BASE DIA. IN.
18
24
31
38
CONSTANT BASE DIA.
CONSTANT N=3600 RPM
NORMALIZED EFFICIENCY
1.00
.95
.90
.85
.3
.4
.5
.6
.7
.8
.9
VELOCITY RATIO U/C$_o$

FIGURE 4-2

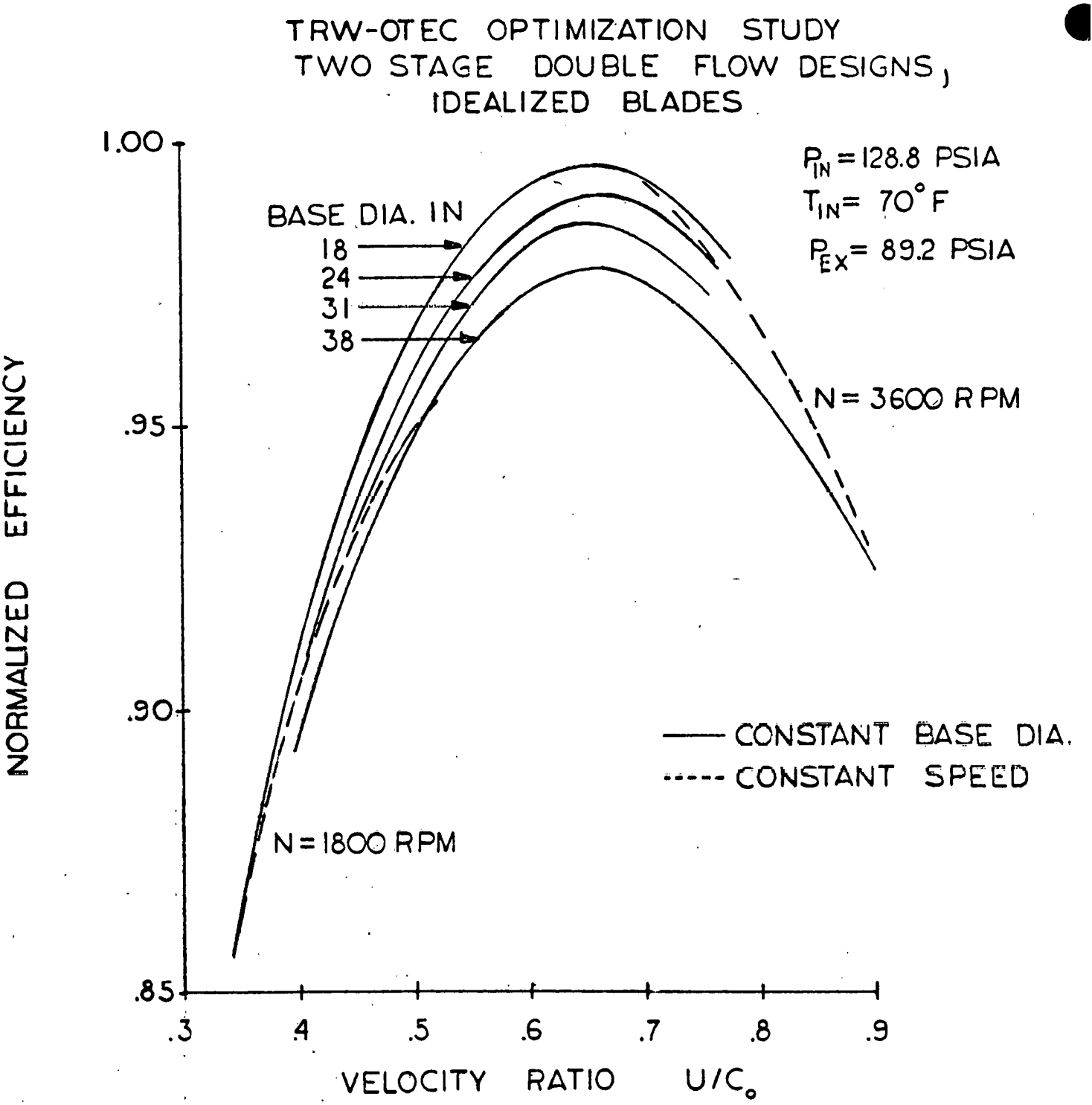
TRW-OTEC OPTIMIZATION STUDY
TWO STAGE DOUBLE FLOW DESIGNS,
IDEALIZED BLADES
1.00
.95
.90
.85
NORMALIZED EFFICIENCY
BASE DIA. IN
18
24
31
38
P_{IN} = 128.8 PSIA
T_{IN} = 70° F
P_{EX} = 89.2 PSIA
N = 3600 RPM
N = 1800 RPM
CONSTANT BASE DIA.
CONSTANT SPEED
.3
.4
.5
.6
.7
.8
.9
VELOCITY RATIO U/C_o

FIGURE 4-3

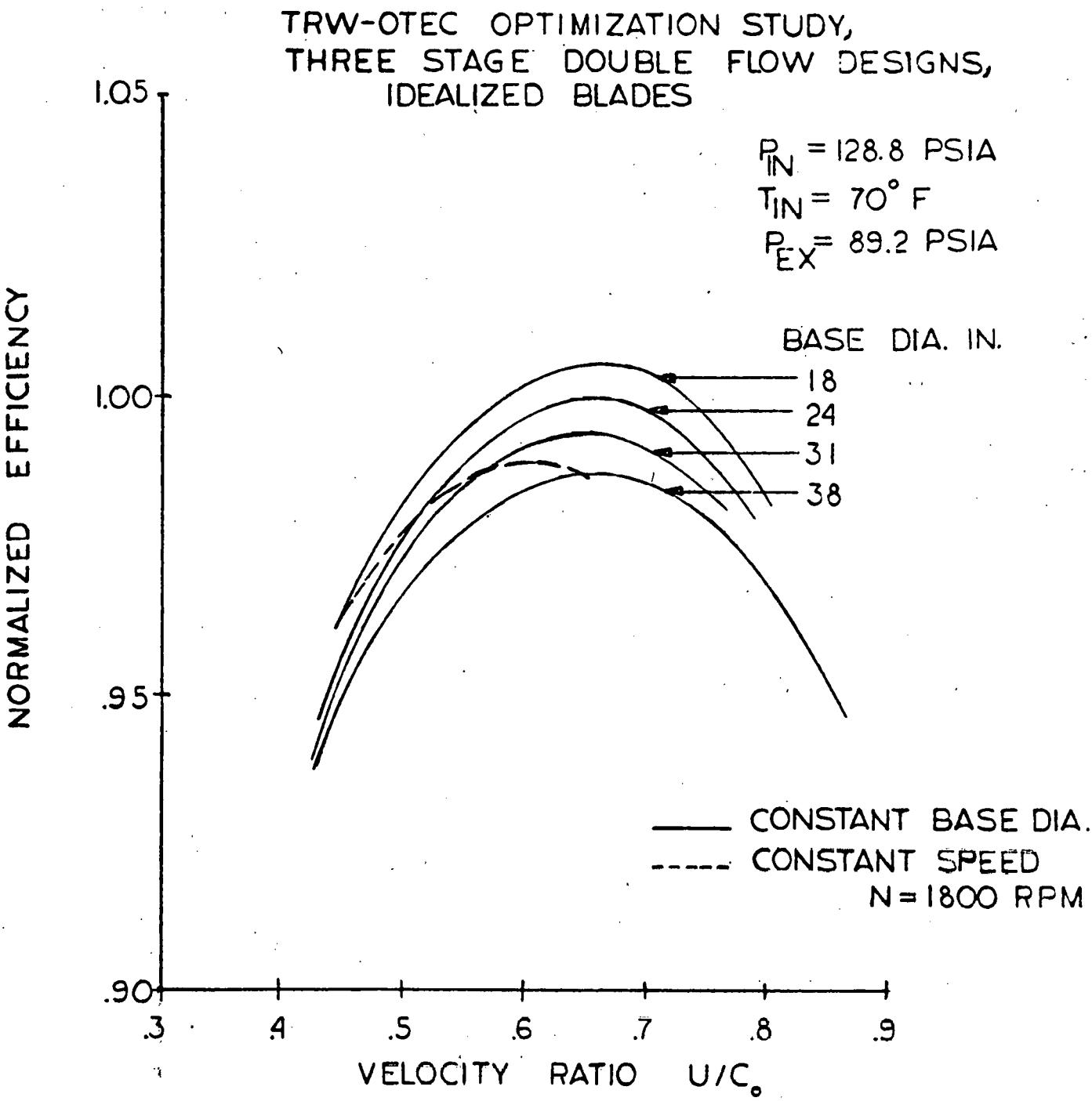
TRW-OTEC OPTIMIZATION STUDY,
THREE STAGE DOUBLE FLOW DESIGNS,
IDEALIZED BLADES
P_{IN} = 128.8 PSIA
T_{IN} = 70° F
P_{EX} = 89.2 PSIA
BASE DIA. IN.
18
24
31
38
CONSTANT BASE DIA.
CONSTANT SPEED
N = 1800 RPM
NORMALIZED EFFICIENCY
1.05
1.00
.95
.90
.3
.4
.5
.6
.7
.8
.9
VELOCITY RATIO U/C$_o$

FIGURE 4-4

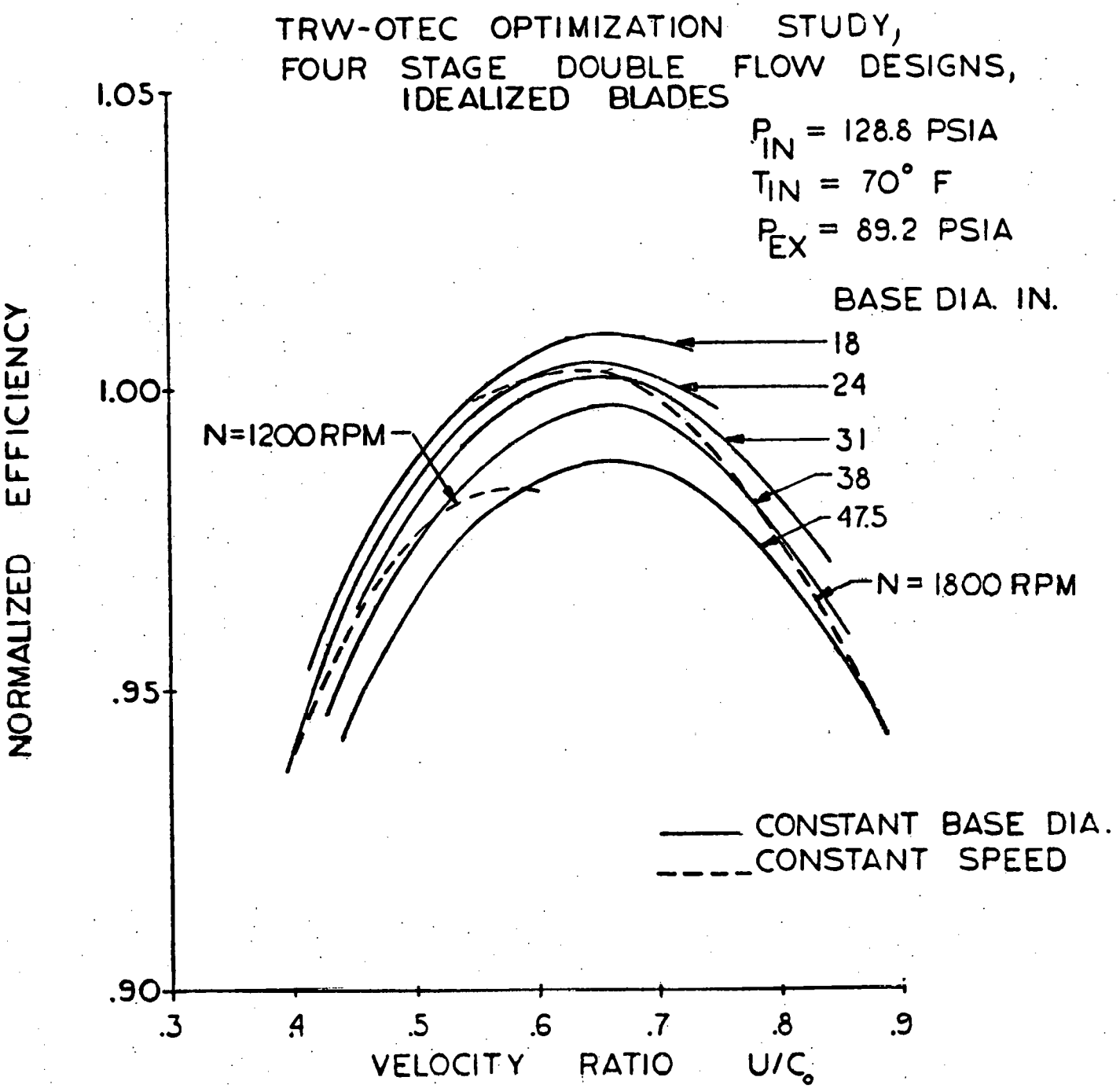
TRW-OTEC OPTIMIZATION STUDY,
FOUR STAGE DOUBLE FLOW DESIGNS,
IDEALIZED BLADES
P_{IN} = 128.8 PSIA
T_{IN} = 70° F
P_{EX} = 89.2 PSIA
BASE DIA. IN.
18
24
31
38
47.5
N=1200 RPM
N = 1800 RPM
CONSTANT BASE DIA.
CONSTANT SPEED
NORMALIZED EFFICIENCY
1.05
1.00
.95
.90
.3
.4
.5
.6
.7
.8
.9
VELOCITY RATIO U/C$_o$

FIGURE 4-5

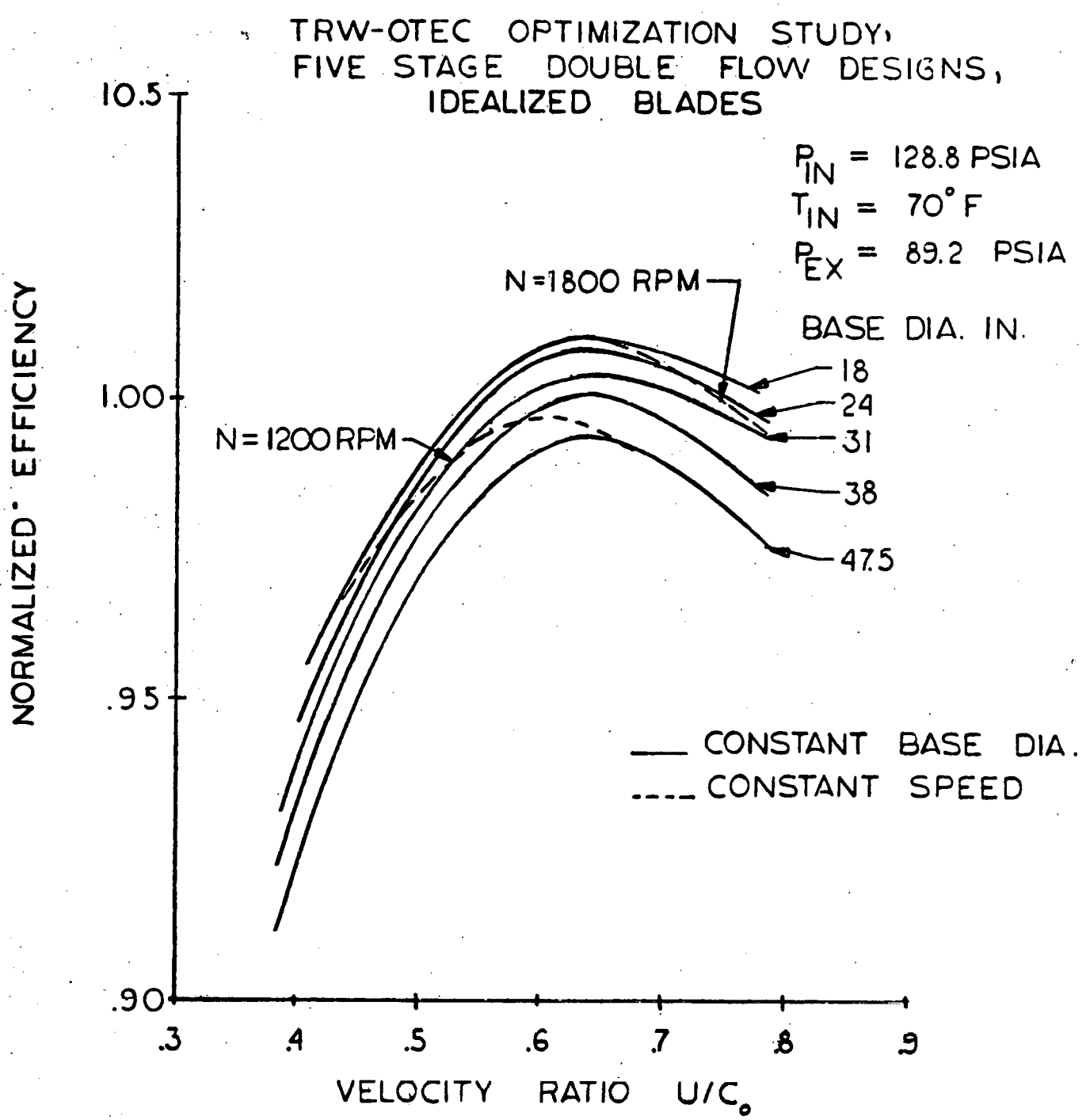
TRW-OTEC OPTIMIZATION STUDY,
FIVE STAGE DOUBLE FLOW DESIGNS,
IDEALIZED BLADES
P_{IN} = 128.8 PSIA
T_{IN} = 70° F
P_{EX} = 89.2 PSIA
BASE DIA. IN.
18
24
31
38
47.5
N=1800 RPM
N=1200 RPM
CONSTANT BASE DIA.
CONSTANT SPEED
NORMALIZED EFFICIENCY
10.5
1.00
.95
.90
.3
.4
.5
.6
.7
.8
.9
VELOCITY RATIO U/C$_o$

FIGURE 4-6

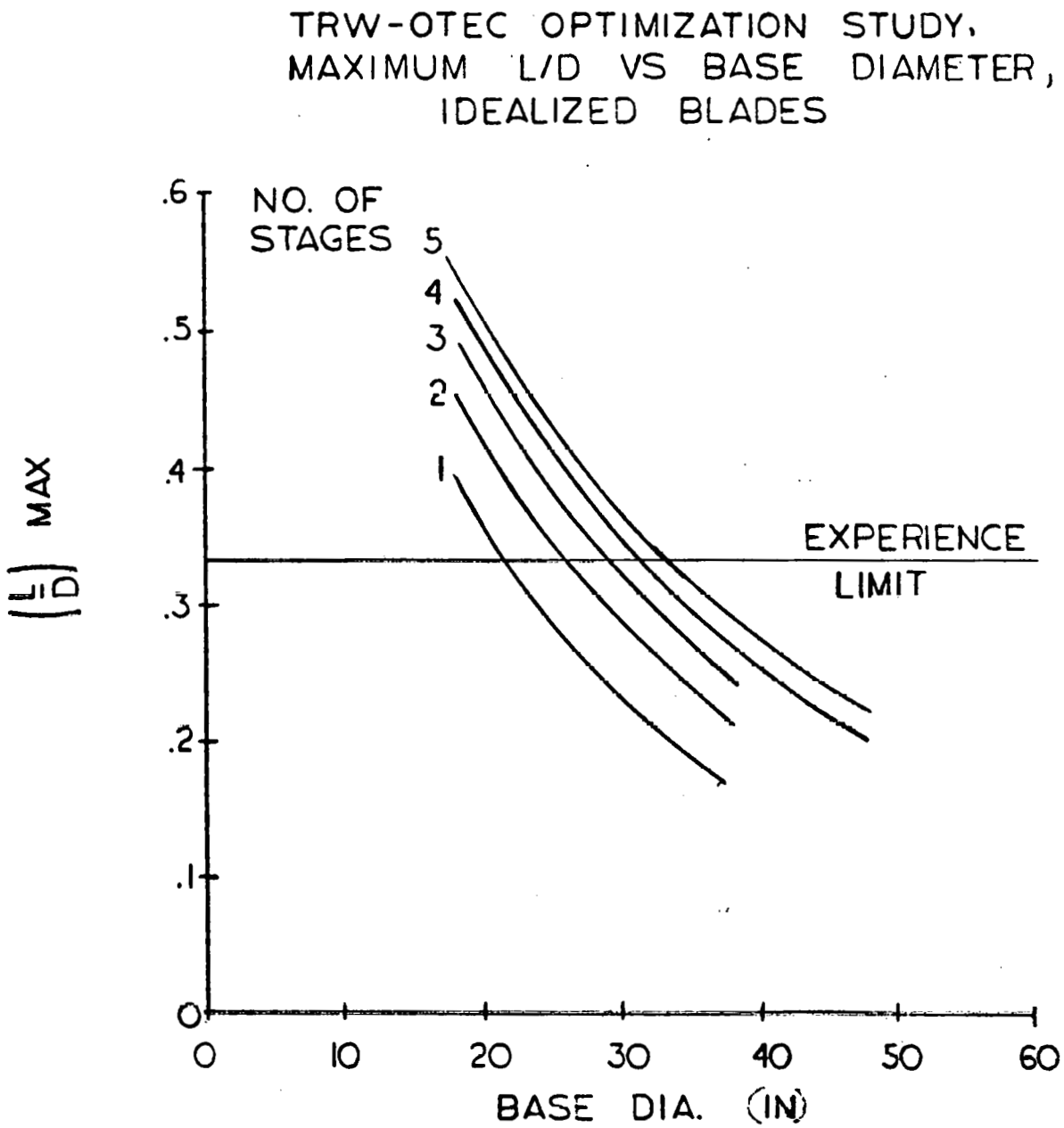
TRW-OTEC OPTIMIZATION STUDY,
MAXIMUM L/D VS BASE DIAMETER,
IDEALIZED BLADES
NO. OF STAGES
5
4
3
2
1
EXPERIENCE LIMIT
(L/D) MAX
.6
.5
.4
.3
.2
.1
0
0
10
20
30
40
50
60
BASE DIA. (IN)

FIGURE 4-7

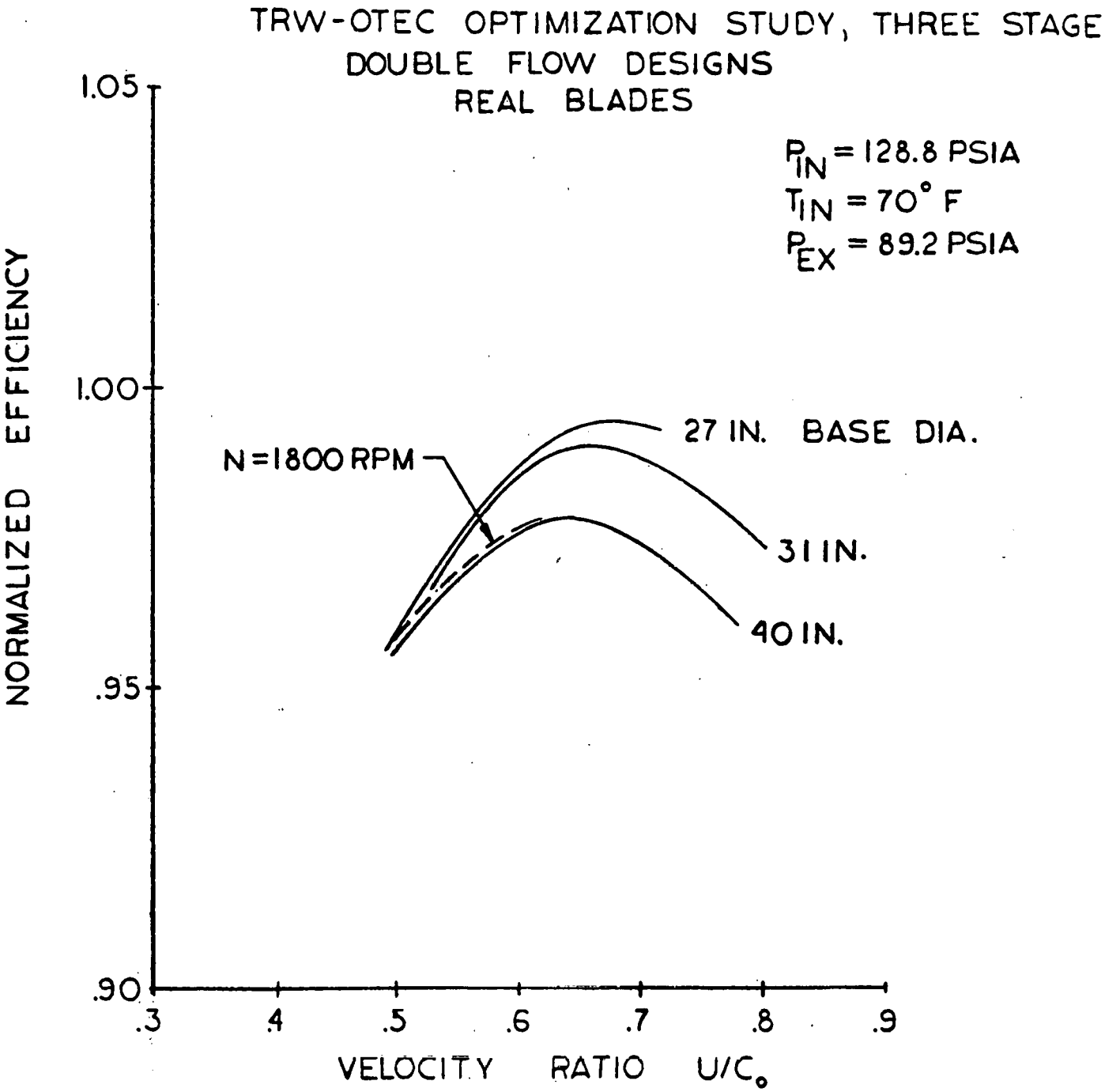
TRW-OTEC OPTIMIZATION STUDY, THREE STAGE
DOUBLE FLOW DESIGNS
REAL BLADES
P_{IN} = 128.8 PSIA
T_{IN} = 70° F
P_{EX} = 89.2 PSIA
NORMALIZED EFFICIENCY
1.05
1.00
.95
.90
N=1800 RPM
27 IN. BASE DIA.
31 IN.
40 IN.
.3
.4
.5
.6
.7
.8
.9
VELOCITY RATIO U/C$_o$

FIGURE 4-8

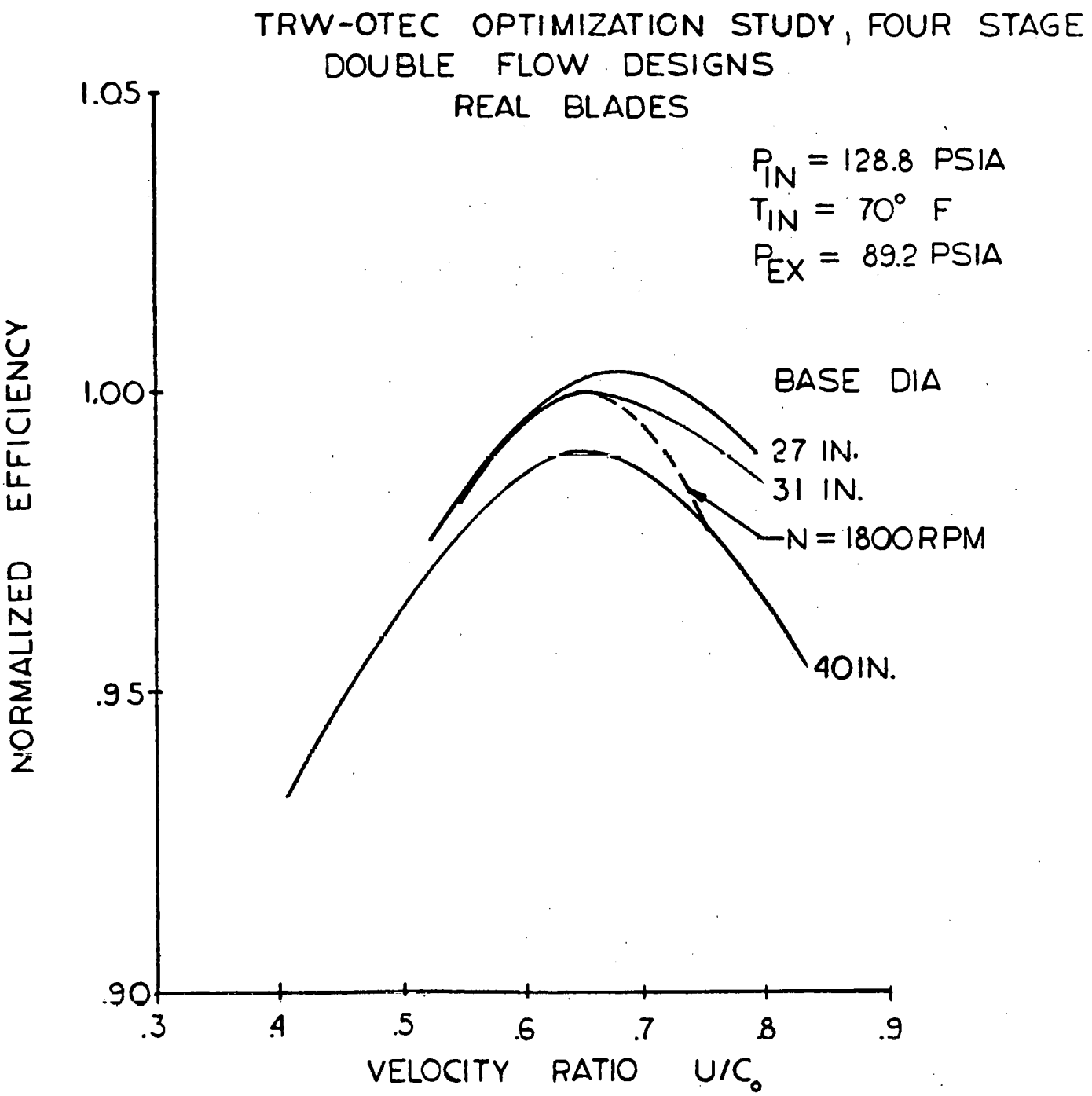
TRW-OTEC OPTIMIZATION STUDY, FOUR STAGE
DOUBLE FLOW DESIGNS
REAL BLADES
P_{IN} = 128.8 PSIA
T_{IN} = 70° F
P_{EX} = 89.2 PSIA
BASE DIA
27 IN.
31 IN.
N = 1800 RPM
40 IN.
NORMALIZED EFFICIENCY
1.05
1.00
.95
.90
.3
.4
.5
.6
.7
.8
.9
VELOCITY RATIO U/C$_o$

FIGURE 4-9

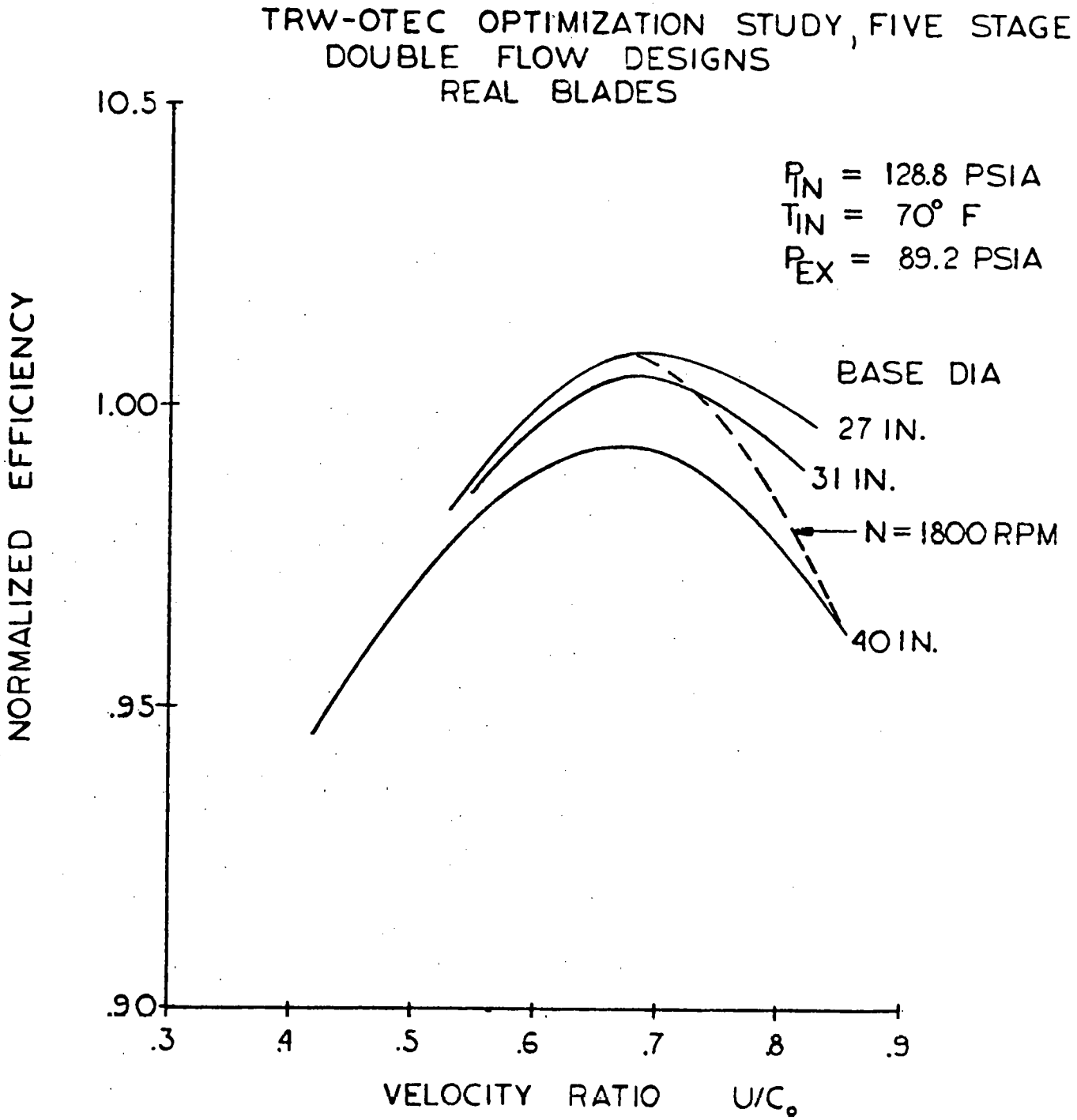
TRW-OTEC OPTIMIZATION STUDY, FIVE STAGE
DOUBLE FLOW DESIGNS
REAL BLADES
P_{IN} = 128.8 PSIA
T_{IN} = 70° F
P_{EX} = 89.2 PSIA
BASE DIA
27 IN.
31 IN.
N = 1800 RPM
40 IN.
NORMALIZED EFFICIENCY
10.5
1.00
.95
.90
.3
.4
.5
.6
.7
.8
.9
VELOCITY RATIO U/C$_o$

FIGURE 4-10

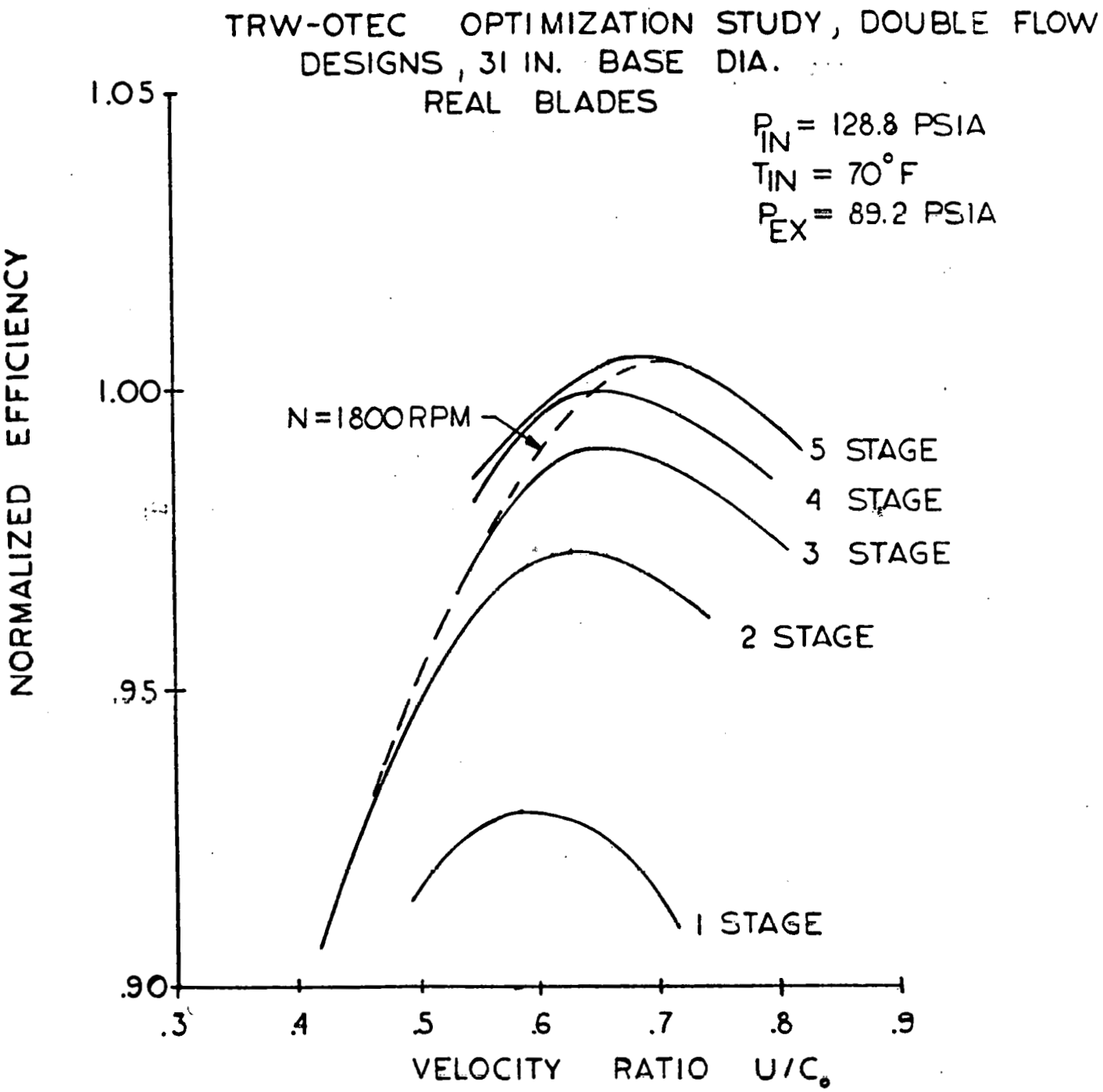
TRW-OTEC OPTIMIZATION STUDY, DOUBLE FLOW DESIGNS, 31 IN. BASE DIA.
REAL BLADES
P_{IN} = 128.8 PSIA
T_{IN} = 70° F
P_{EX} = 89.2 PSIA
NORMALIZED EFFICIENCY
1.05
1.00
.95
.90
N=1800 RPM
5 STAGE
4 STAGE
3 STAGE
2 STAGE
1 STAGE
.3
.4
.5
.6
.7
.8
.9
VELOCITY RATIO U/C$_o$

FIGURE 4-11

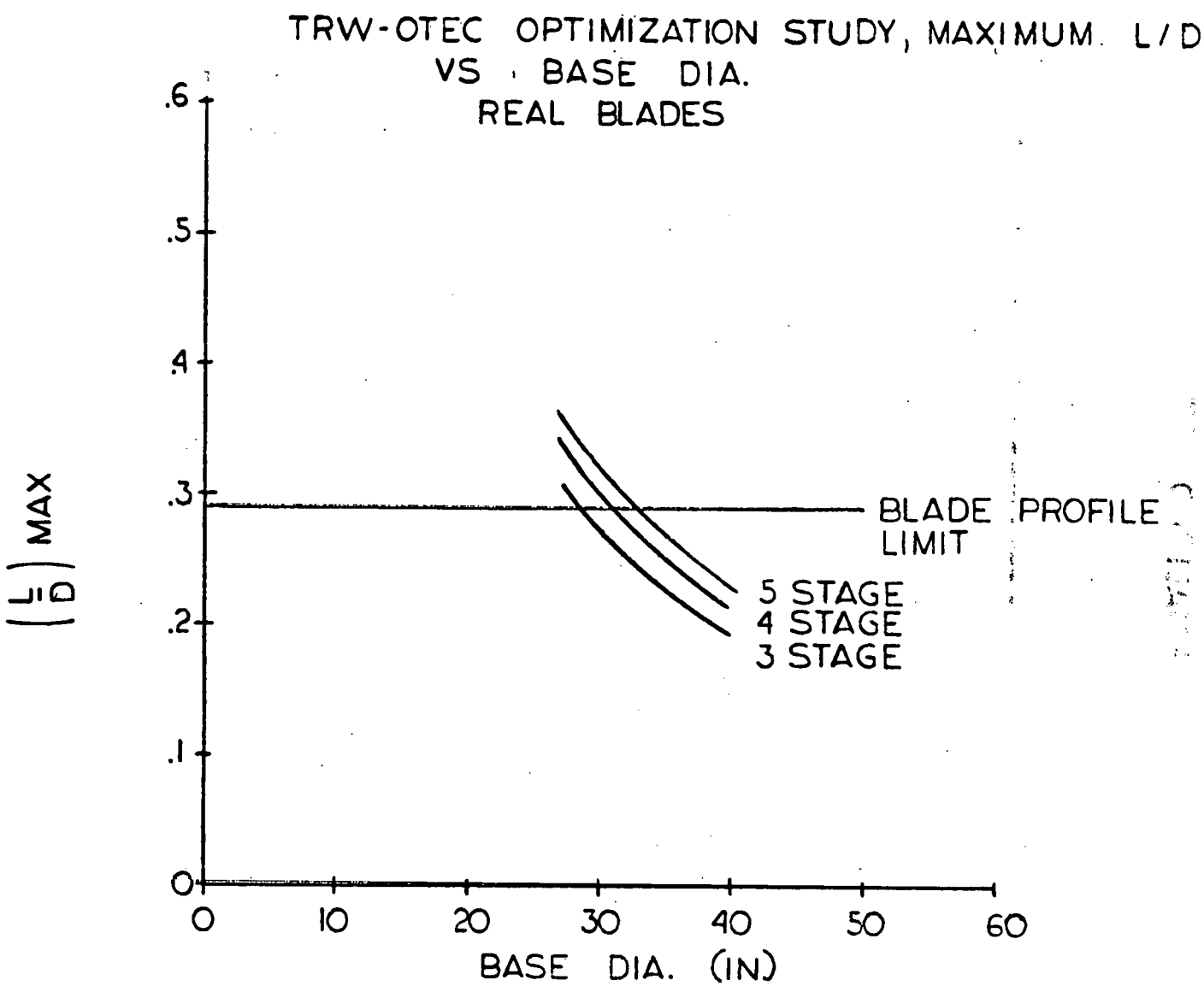
TRW-OTEC OPTIMIZATION STUDY, MAXIMUM L/D VS BASE DIA.
REAL BLADES
(L/D) MAX
.6
.5
.4
.3
.2
.1
0
BLADE PROFILE LIMIT
5 STAGE
4 STAGE
3 STAGE
0
10
20
30
40
50
60
BASE DIA. (IN)

FIGURE 4-12

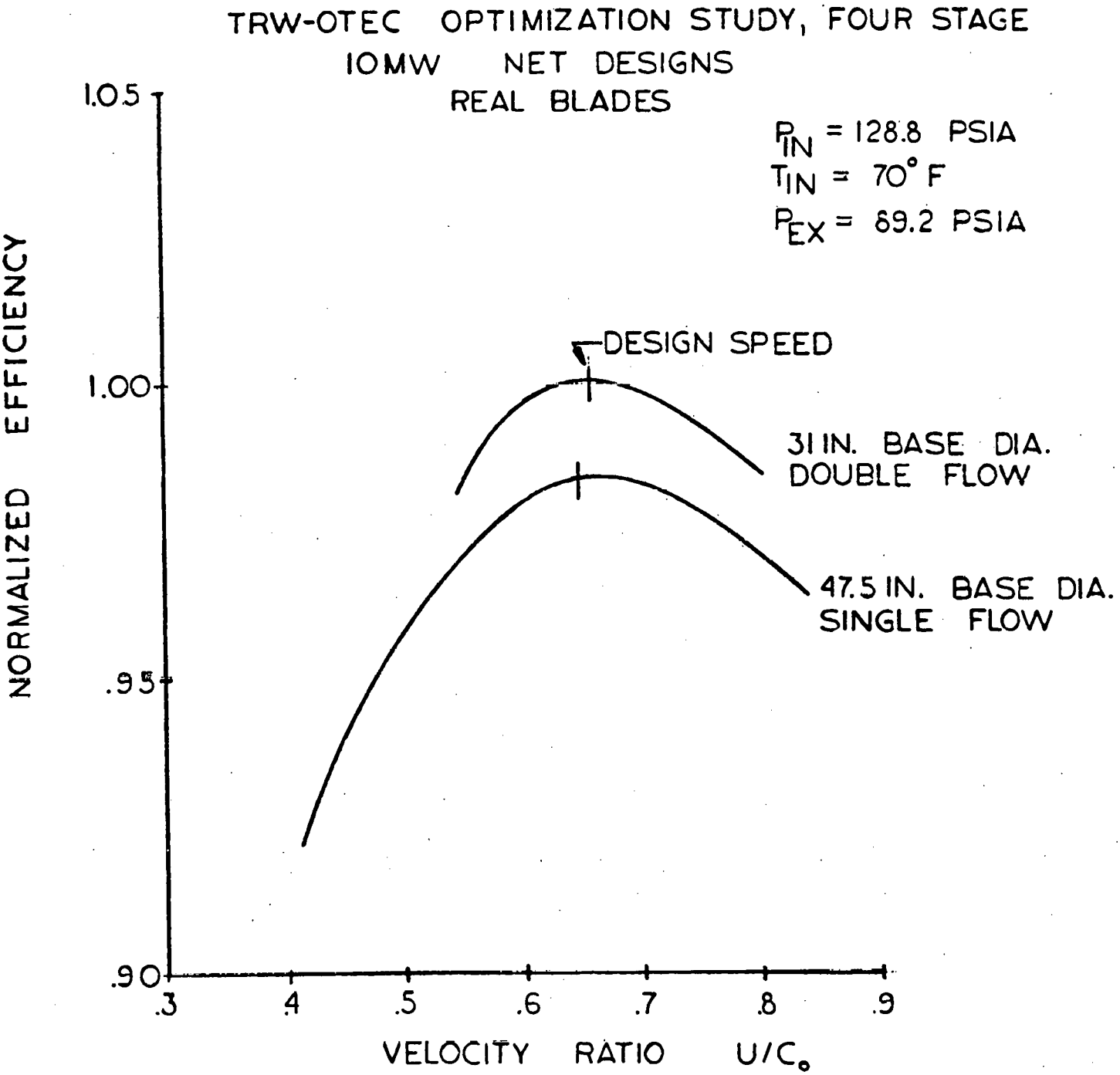
TRW-OTEC OPTIMIZATION STUDY, FOUR STAGE
10MW NET DESIGNS
REAL BLADES
P_{IN} = 128.8 PSIA
T_{IN} = 70° F
P_{EX} = 69.2 PSIA
DESIGN SPEED
31 IN. BASE DIA.
DOUBLE FLOW
47.5 IN. BASE DIA.
SINGLE FLOW
NORMALIZED EFFICIENCY
1.05
1.00
.95
.90
.3
.4
.5
.6
.7
.8
.9
VELOCITY RATIO U/C₀

FIGURE 4-13

TRW/OTEC OPTIMIZATION STUDY
SINGLE STAGE, SINGLE FLOW DESIGNS
IDEALIZED BLADES
BASE DIAMETER = 31 IN.

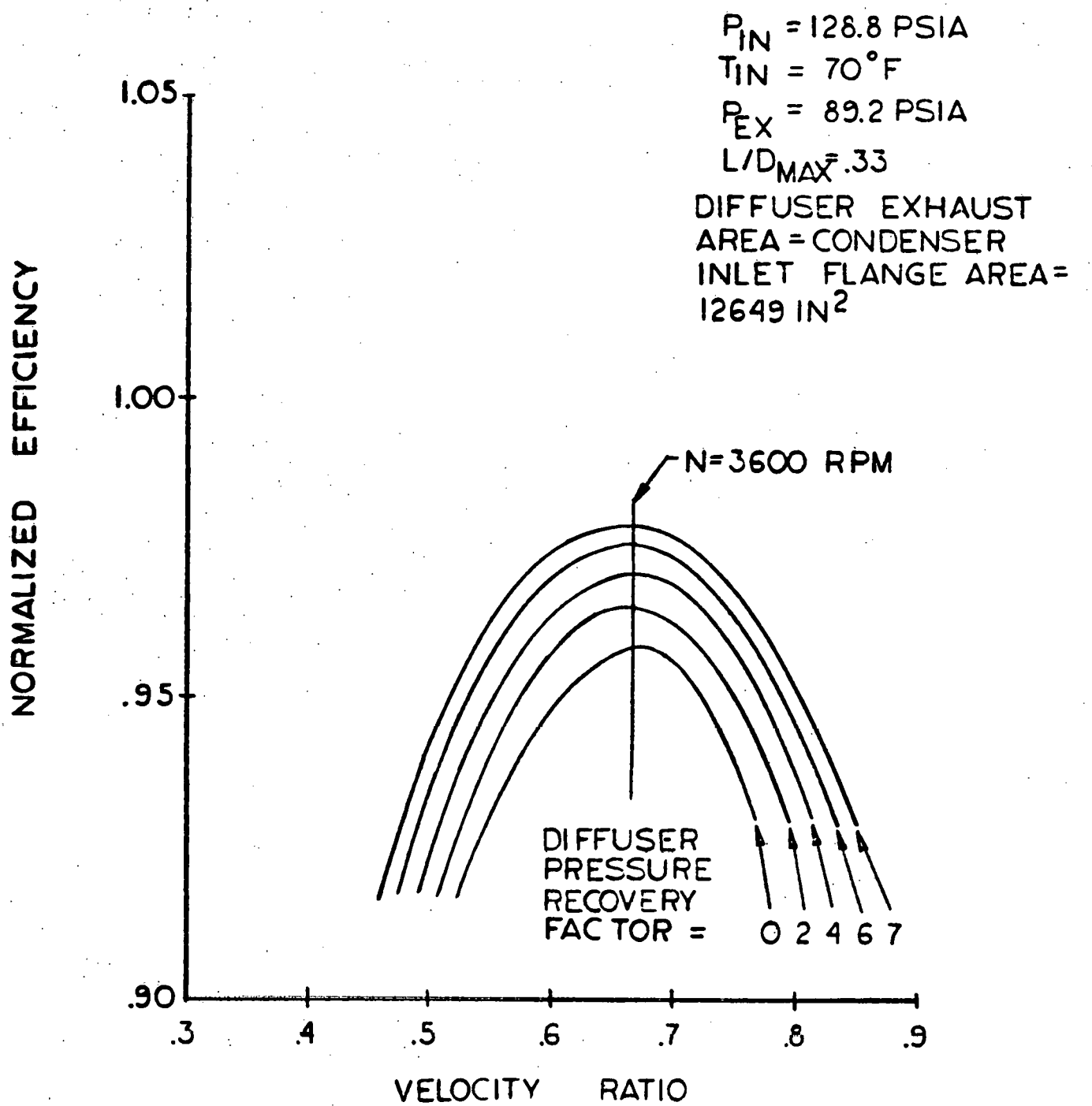

FIGURE 4-14

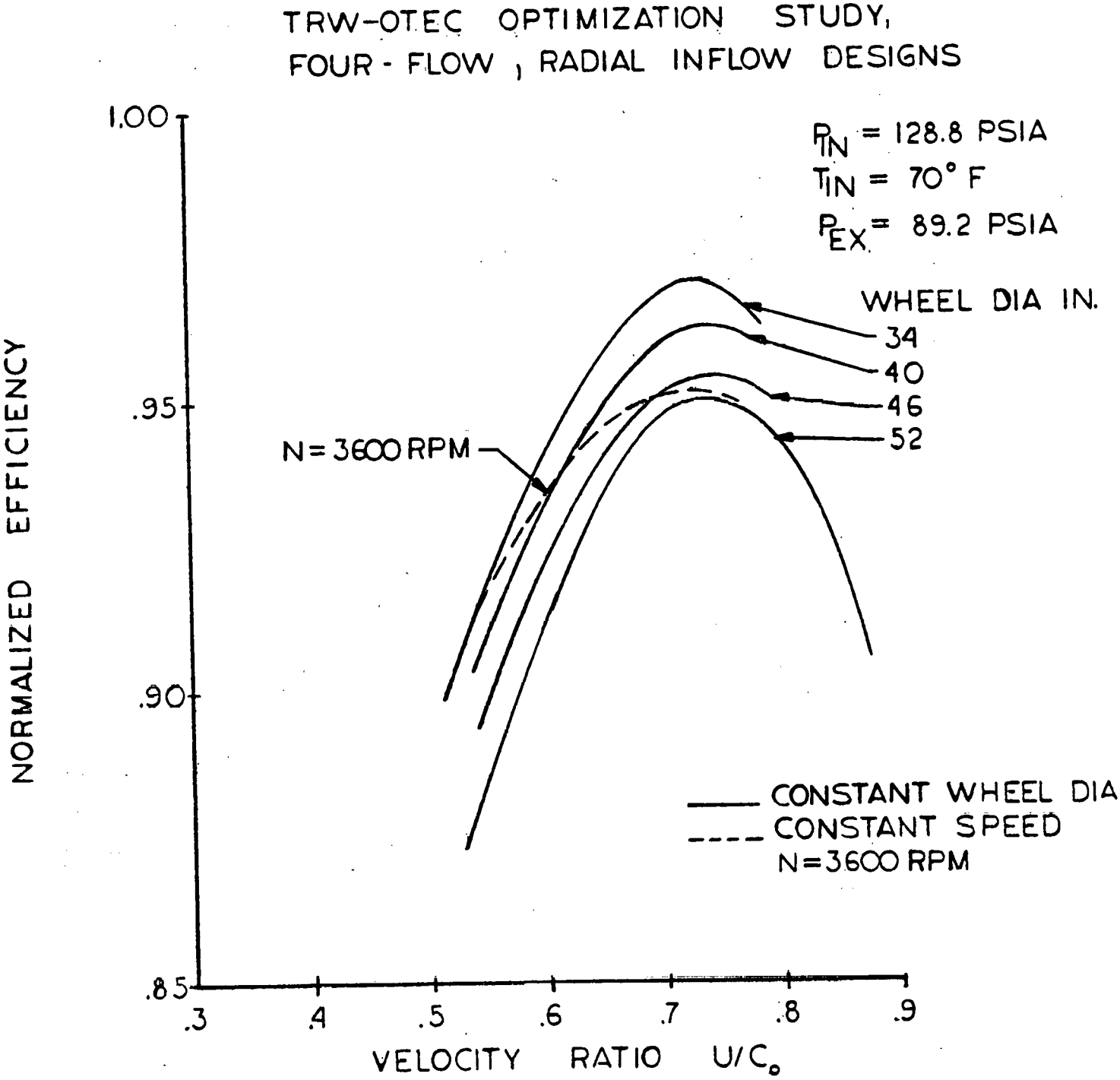
TRW-OTEC OPTIMIZATION STUDY,
FOUR-FLOW, RADIAL INFLOW DESIGNS
P_{IN} = 128.8 PSIA
T_{IN} = 70° F
P_{EX} = 89.2 PSIA
WHEEL DIA IN.
34
40
46
52
N = 3600 RPM
CONSTANT WHEEL DIA.
CONSTANT SPEED
N=3600 RPM
NORMALIZED EFFICIENCY
1.00
.95
.90
.85
.3
.4
.5
.6
.7
.8
.9
VELOCITY RATIO U/C_o

FIGURE 4-15

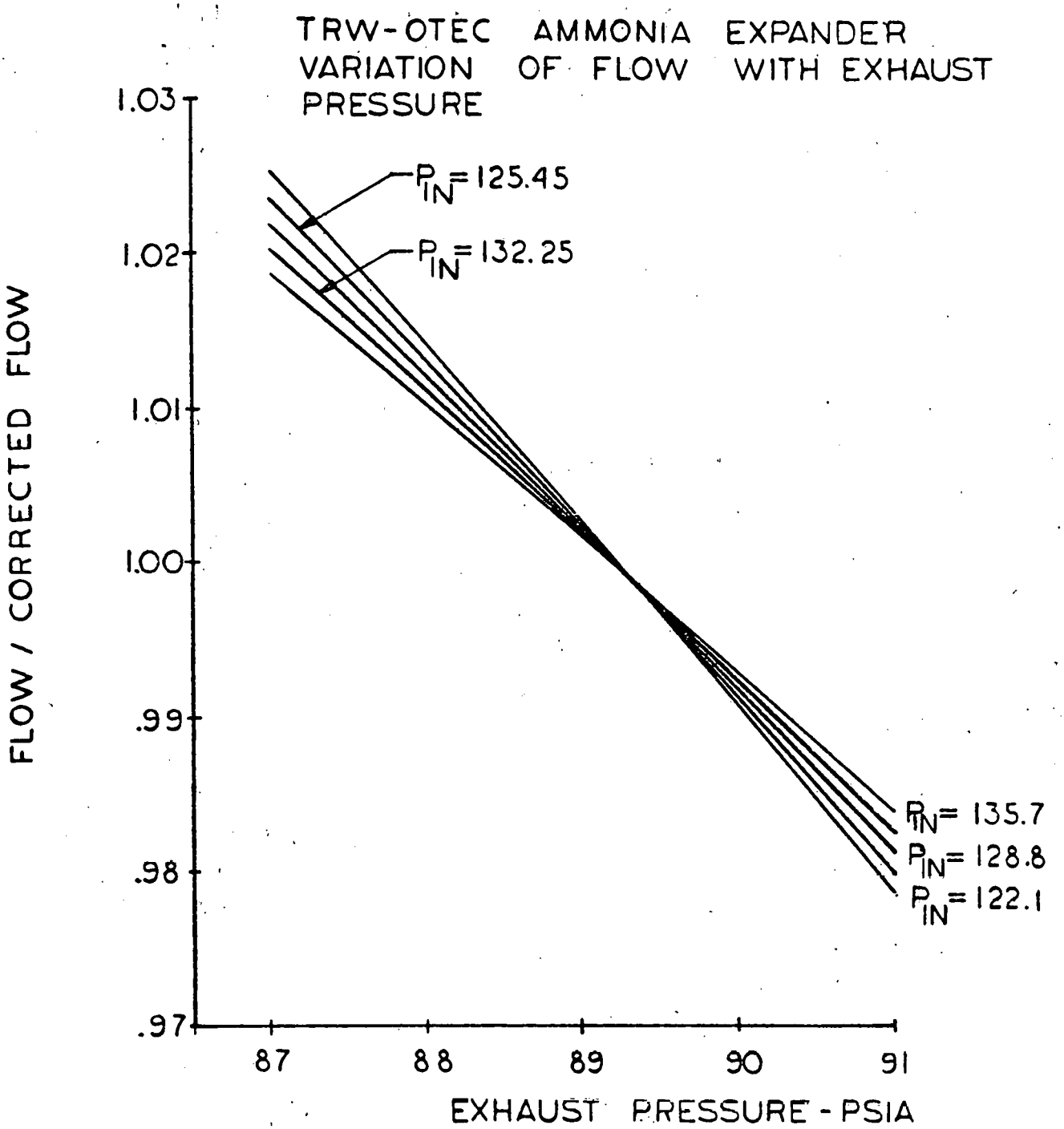
TRW-OTEC AMMONIA EXPANDER
VARIATION OF FLOW WITH EXHAUST PRESSURE
FLOW / CORRECTED FLOW
1.03
1.02
1.01
1.00
.99
.98
.97
P_{IN} = 125.45
P_{IN} = 132.25
P_{IN} = 135.7
P_{IN} = 128.8
P_{IN} = 122.1
87
88
89
90
91
EXHAUST PRESSURE - PSIA

FIGURE 4-16

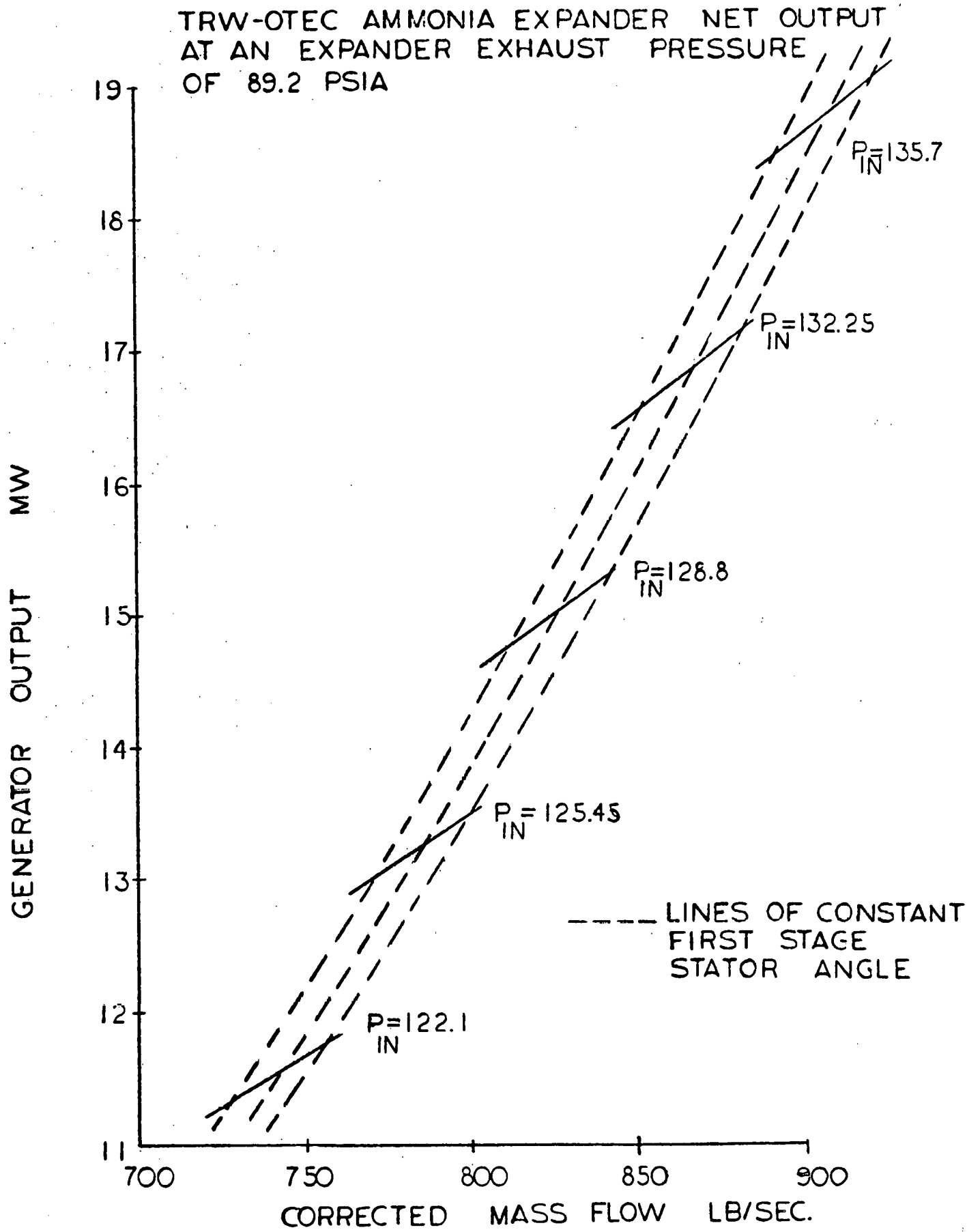
TRW-OTEC AMMONIA EXPANDER NET OUTPUT AT AN EXPANDER EXHAUST PRESSURE OF 89.2 PSIA
GENERATOR OUTPUT MW
19
18
17
16
15
14
13
12
11
700
750
800
850
900
CORRECTED MASS FLOW LB/SEC.
P IN = 135.7
P IN = 132.25
P IN = 128.8
P IN = 125.45
P IN = 122.1
LINES OF CONSTANT FIRST STAGE STATOR ANGLE

FIGURE 4-17

TRW-OTEC AMMONIA EXPANDER VARIATION OF NET OUTPUT VS EXHAUST PRESSURE

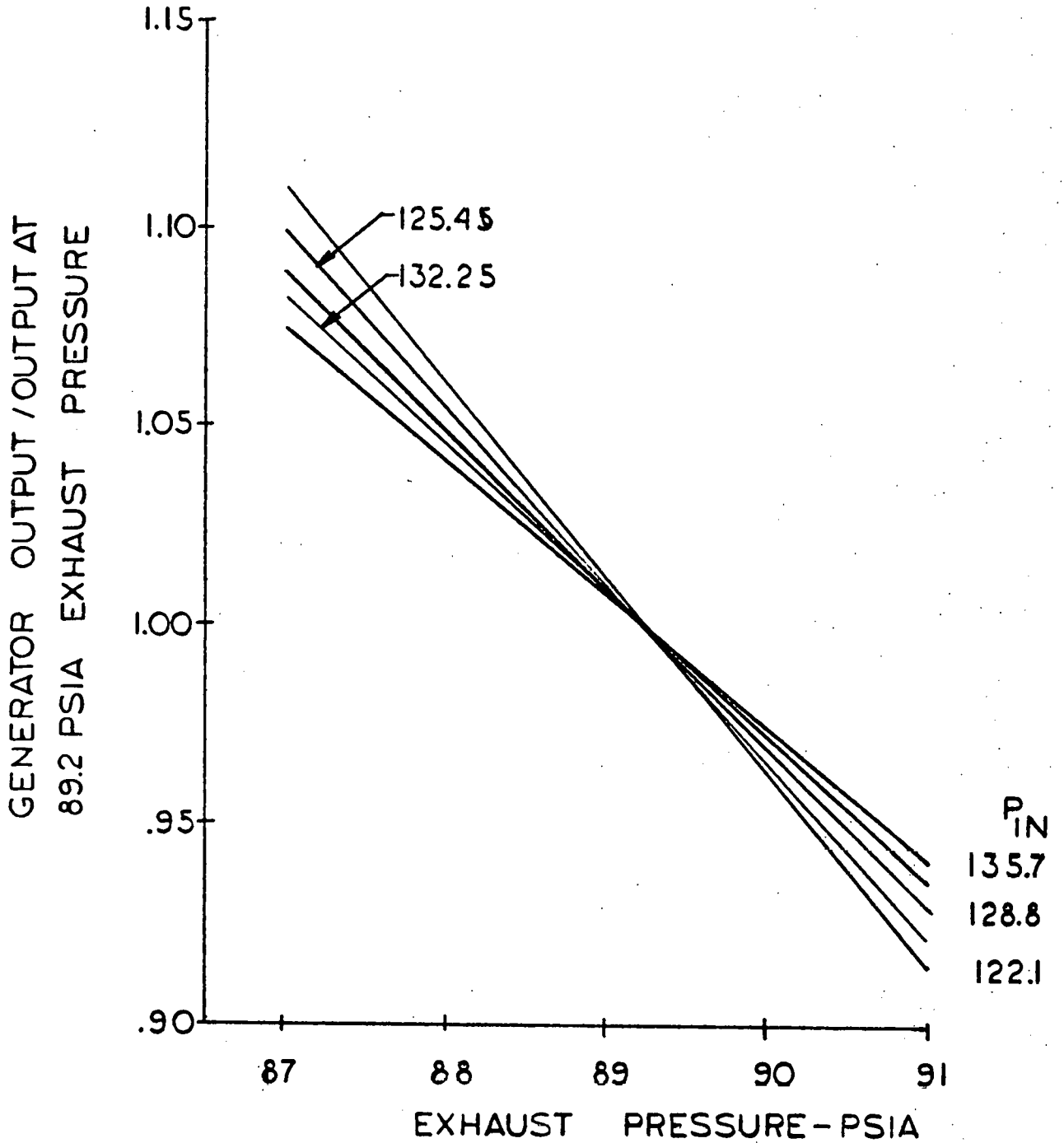

FIGURE 4-18

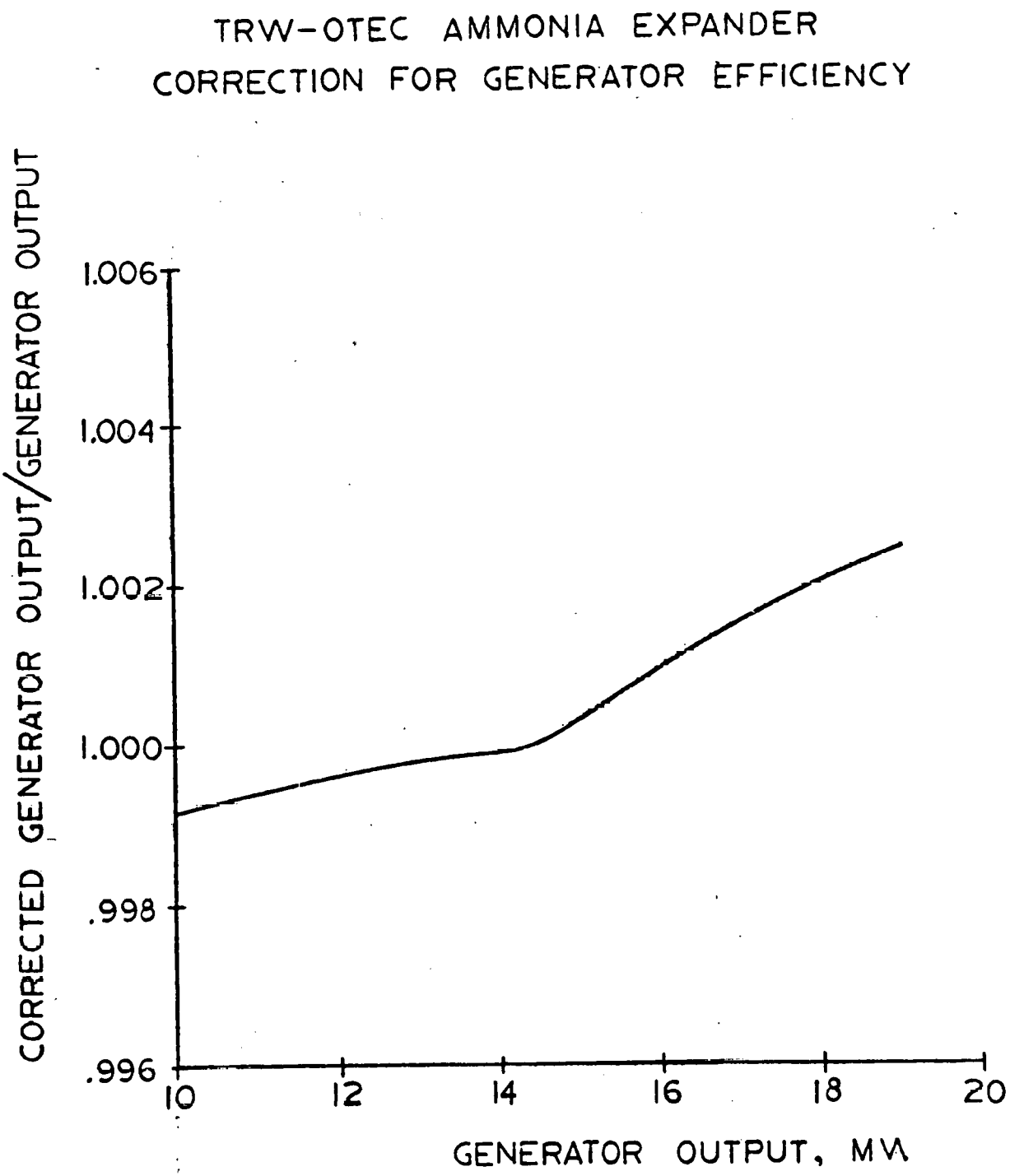
TRW-OTEC AMMONIA EXPANDER
CORRECTION FOR GENERATOR EFFICIENCY
CORRECTED GENERATOR OUTPUT/GENERATOR OUTPUT
1.006
1.004
1.002
1.000
.998
.996
10
12
14
16
18
20
GENERATOR OUTPUT, MW

FIGURE 4-19

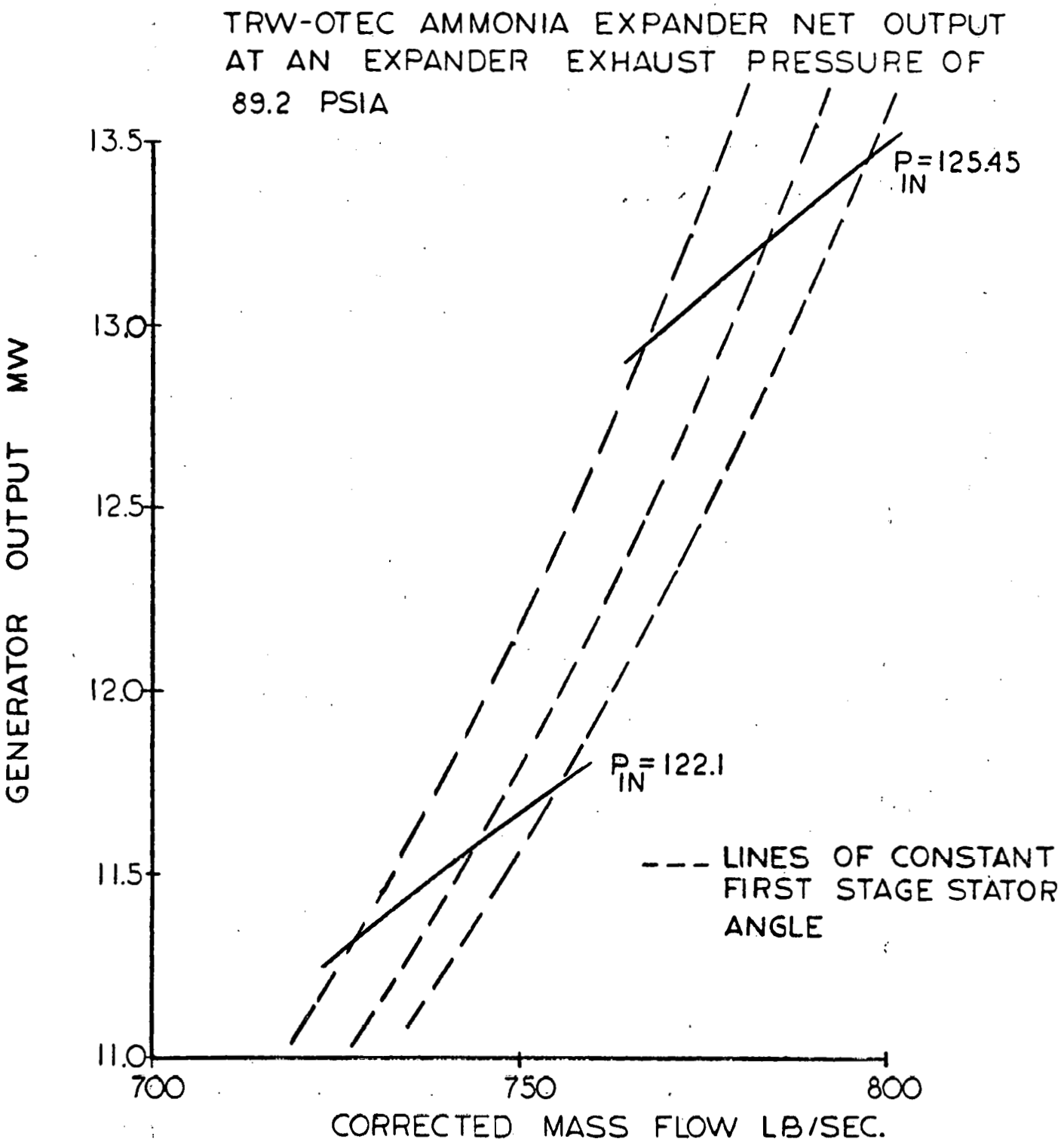
TRW-OTEC AMMONIA EXPANDER NET OUTPUT AT AN EXPANDER EXHAUST PRESSURE OF 89.2 PSIA
GENERATOR OUTPUT MW
13.5
13.0
12.5
12.0
11.5
11.0
700
750
800
CORRECTED MASS FLOW LB/SEC.
P IN = 125.45
P IN = 122.1
--- LINES OF CONSTANT FIRST STAGE STATOR ANGLE

FIGURE 4-20

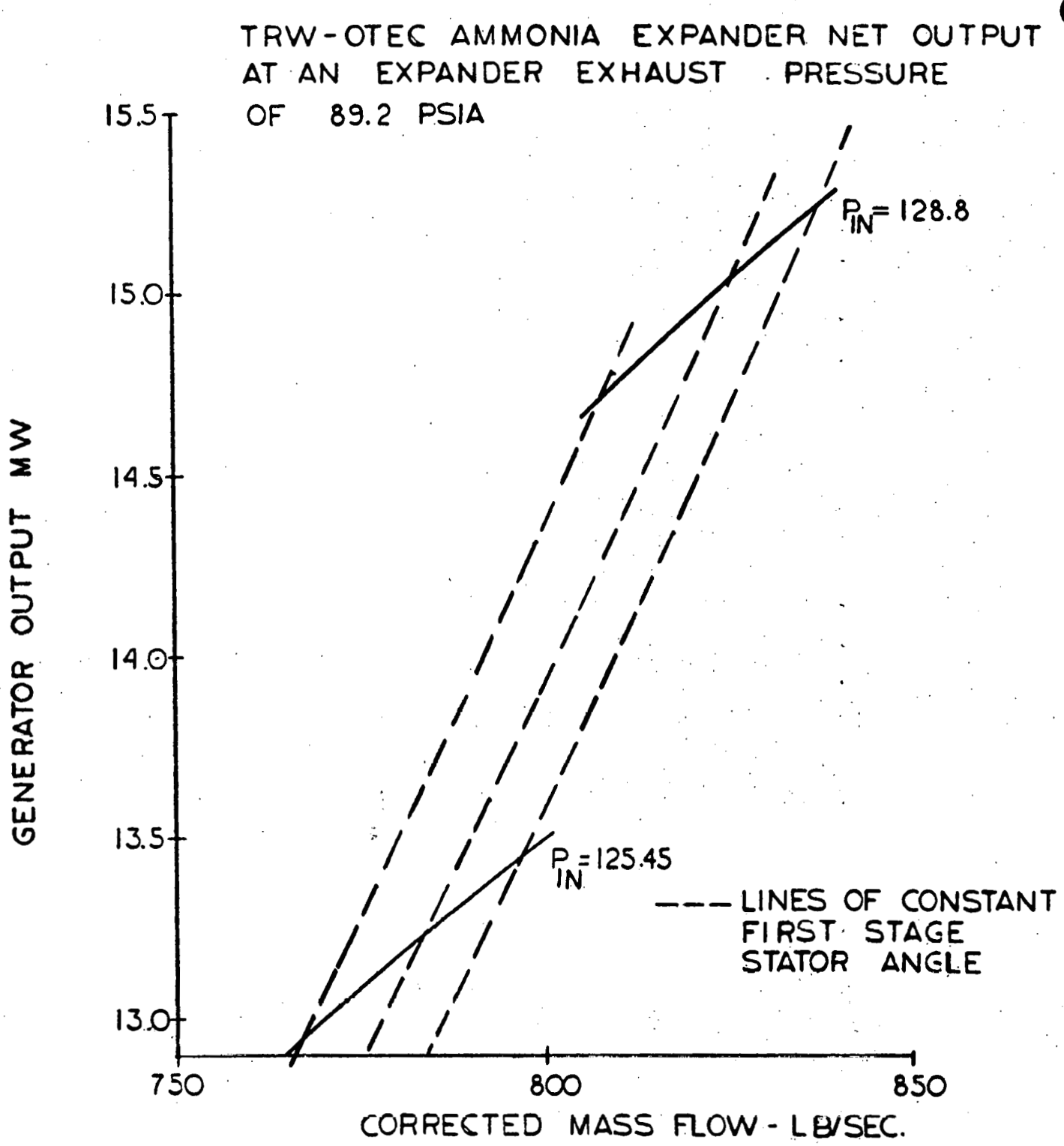
TRW-OTEC AMMONIA EXPANDER NET OUTPUT AT AN EXPANDER EXHAUST PRESSURE OF 89.2 PSIA
GENERATOR OUTPUT MW
15.5
15.0
14.5
14.0
13.5
13.0
750
800
850
CORRECTED MASS FLOW - LB/SEC.
P_{IN} = 128.8
P_{IN} = 125.45
--- LINES OF CONSTANT FIRST STAGE STATOR ANGLE

FIGURE 4-21

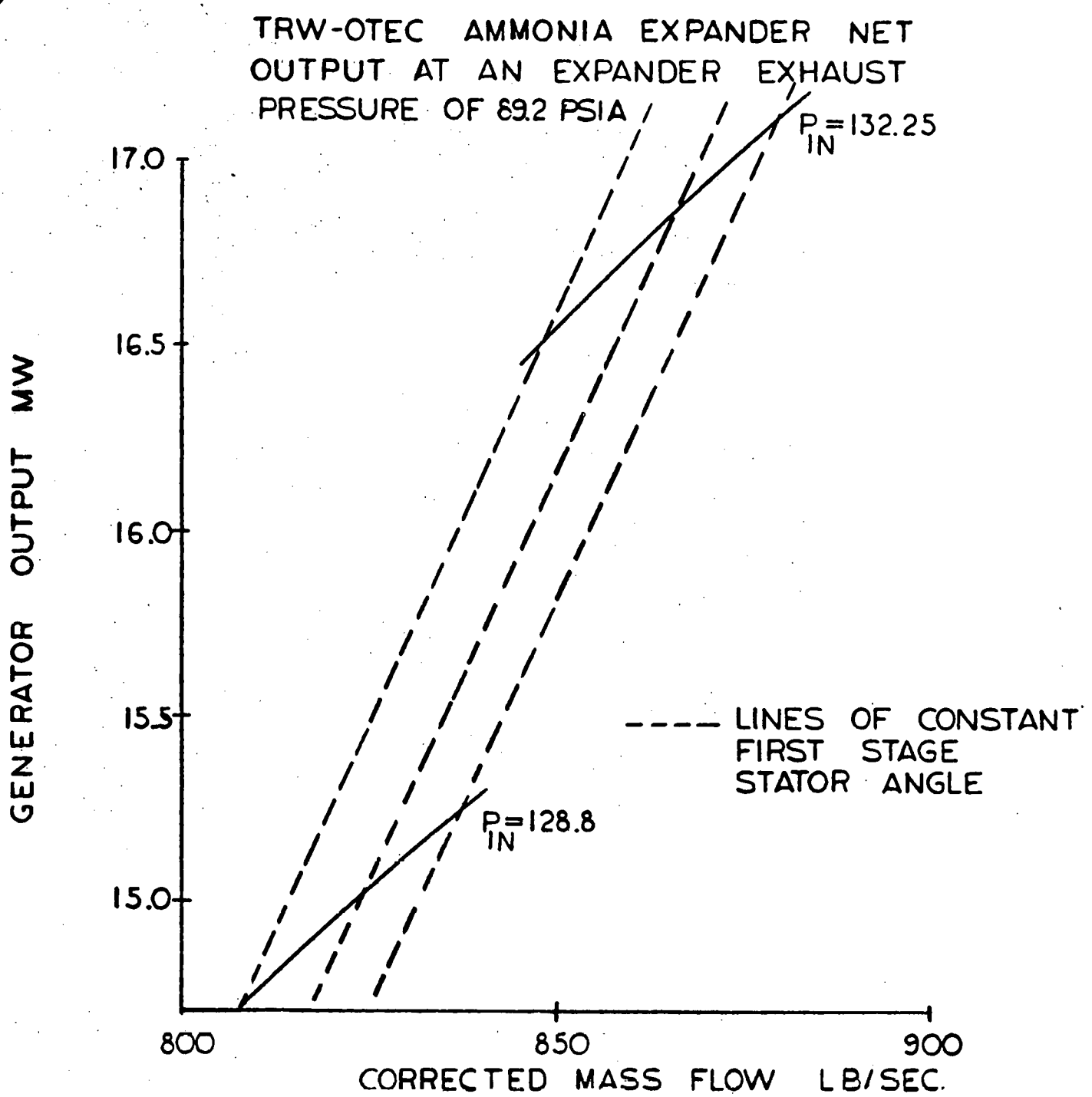
TRW-OTEC AMMONIA EXPANDER NET OUTPUT AT AN EXPANDER EXHAUST PRESSURE OF 89.2 PSIA
P_{IN}=132.25
P_{IN}=128.8
17.0
16.5
16.0
15.5
15.0
GENERATOR OUTPUT MW
800
850
900
CORRECTED MASS FLOW LB/SEC.
---- LINES OF CONSTANT FIRST STAGE STATOR ANGLE

FIGURE 4-22

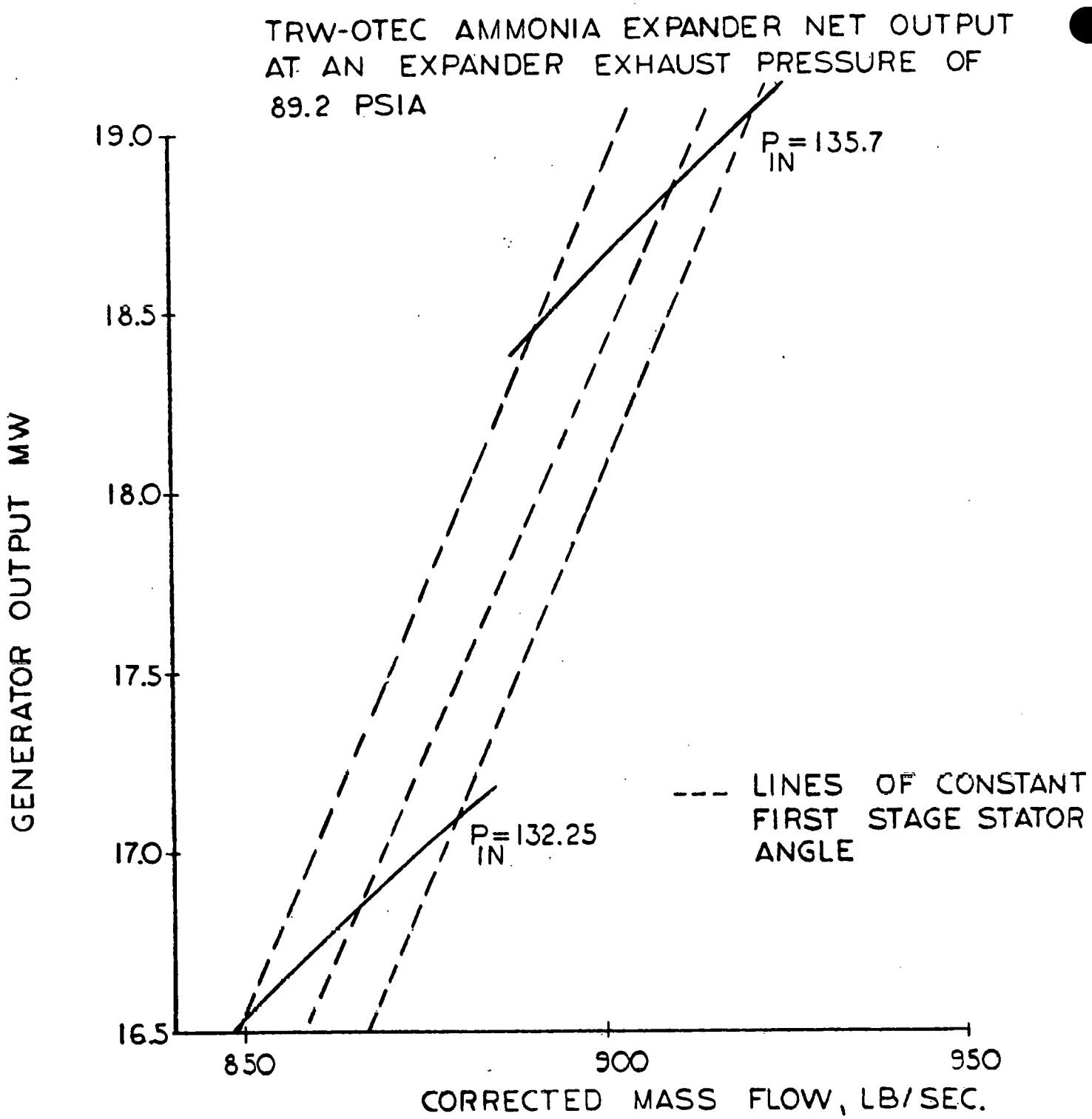
TRW-OTEC AMMONIA EXPANDER NET OUTPUT AT AN EXPANDER EXHAUST PRESSURE OF 89.2 PSIA
GENERATOR OUTPUT MW
19.0
18.5
18.0
17.5
17.0
16.5
850
900
950
CORRECTED MASS FLOW, LB/SEC.
P IN = 135.7
P IN = 132.25
--- LINES OF CONSTANT FIRST STAGE STATOR ANGLE

FIGURE 4-23

TRW-OTEC AMMONIA EXPANDER
SEASONAL VARIATION IN EXPANDER
EFFICIENCY WITH VARIABLE FIRST
STAGE STATOR ANGLE

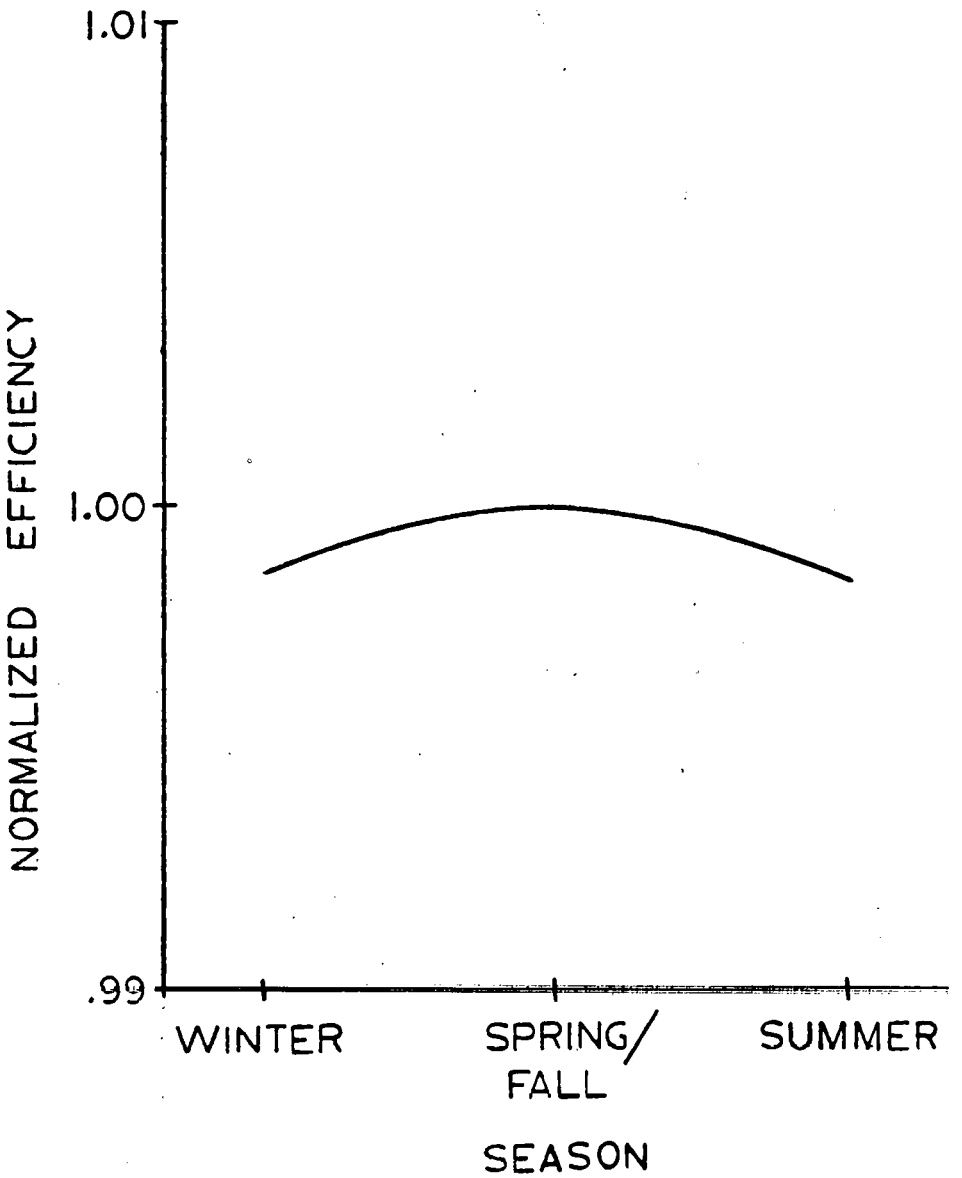

FIGURE 4-24

TRW-OTEC FIRST STAGE VELOCITY TRIANGES AT DESIGN CONDITIONS

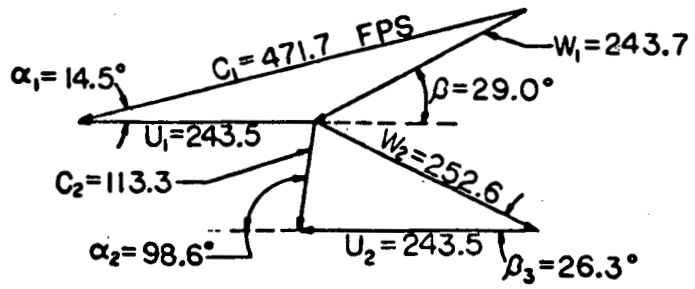

BASE

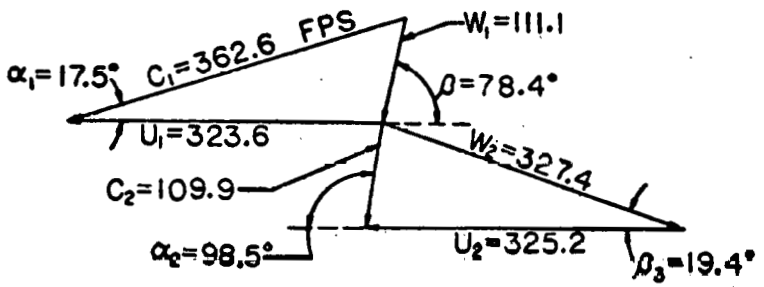

MEAN

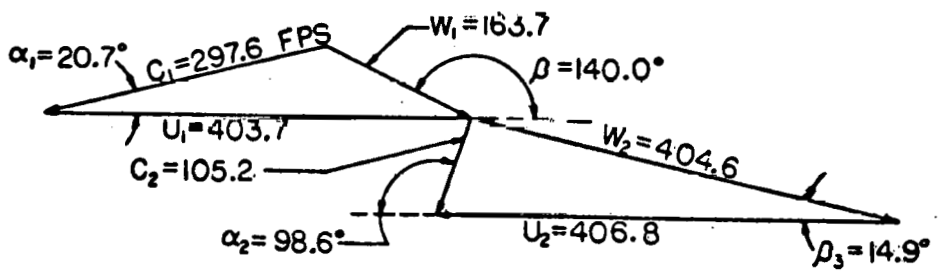

TIP

FIGURE 4-25

TRW-OTEC SECOND STAGE VELOCITY TRIANGLES AT DESIGN CONDITIONS

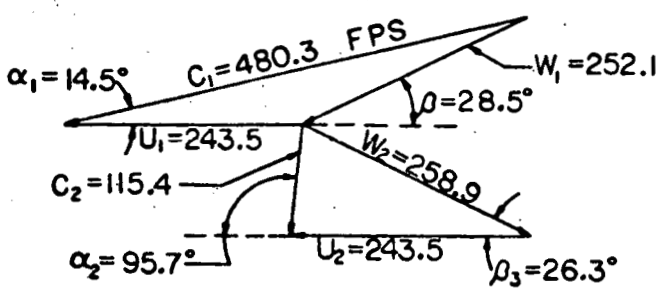

BASE

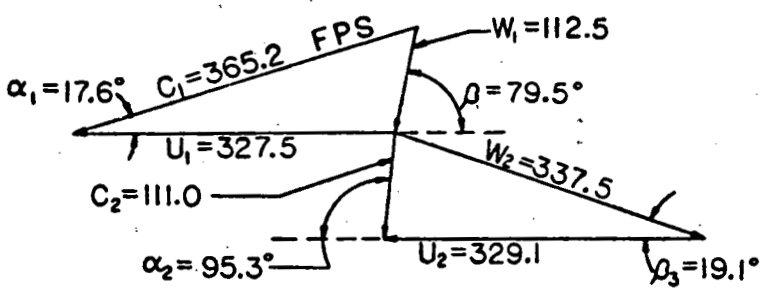

MEAN

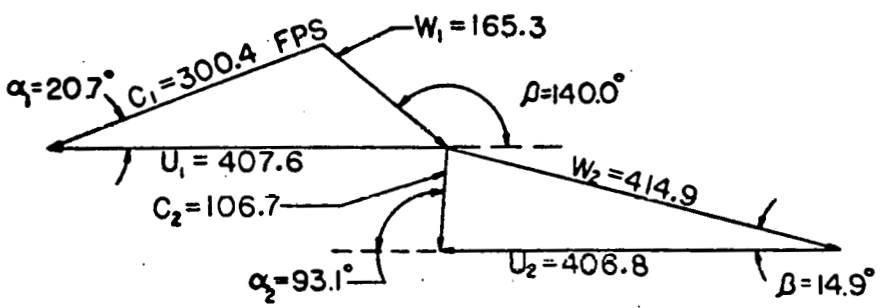

TIP

FIGURE 4-26

TRW-OTEC THIRD STAGE VELOCITY TRIANGLES AT DESIGN CONDITIONS

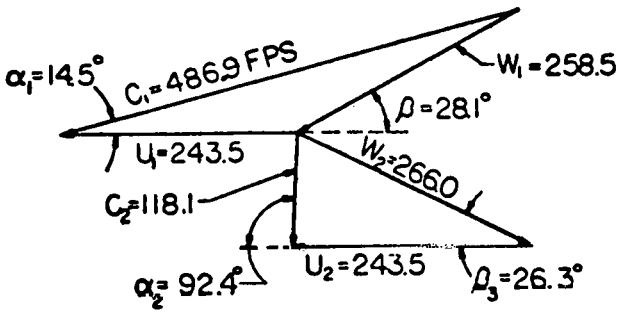

BASE

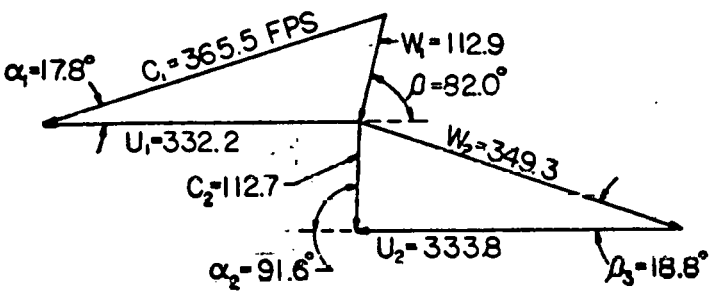

MEAN

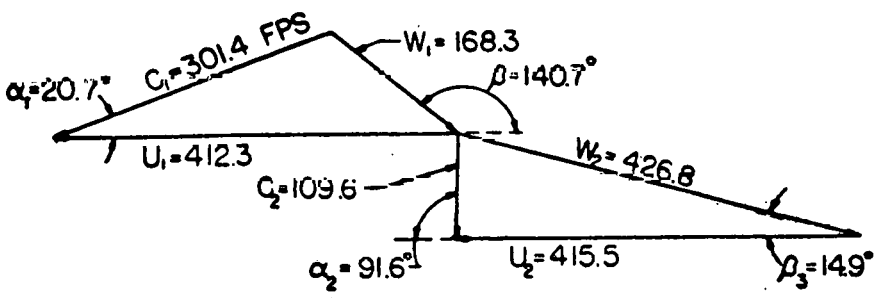

TIP

FIGURE 4-27

TRW-OTEC FOURTH STAGE VELOCITY TRIANGLES

AT DESIGN CONDITIONS

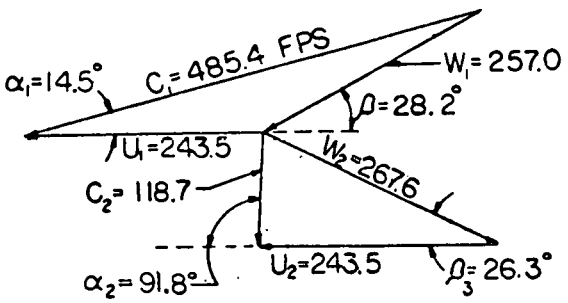

BASE

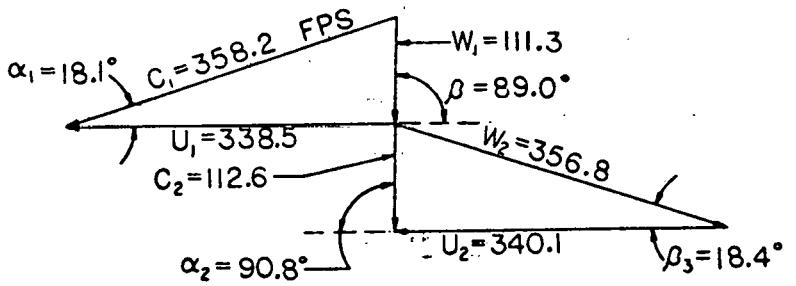

MEAN

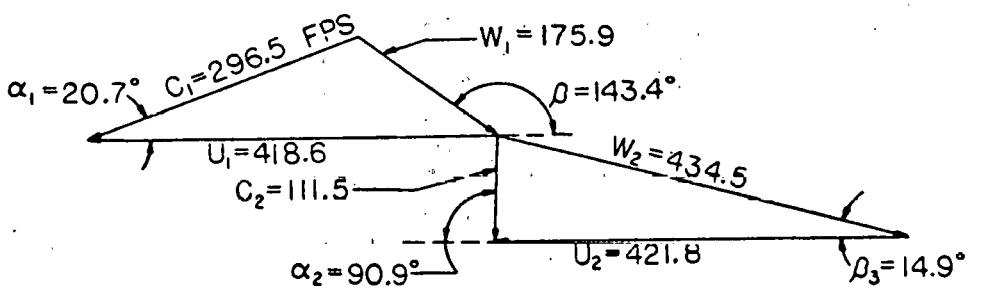

TIP

FIGURE 4-28

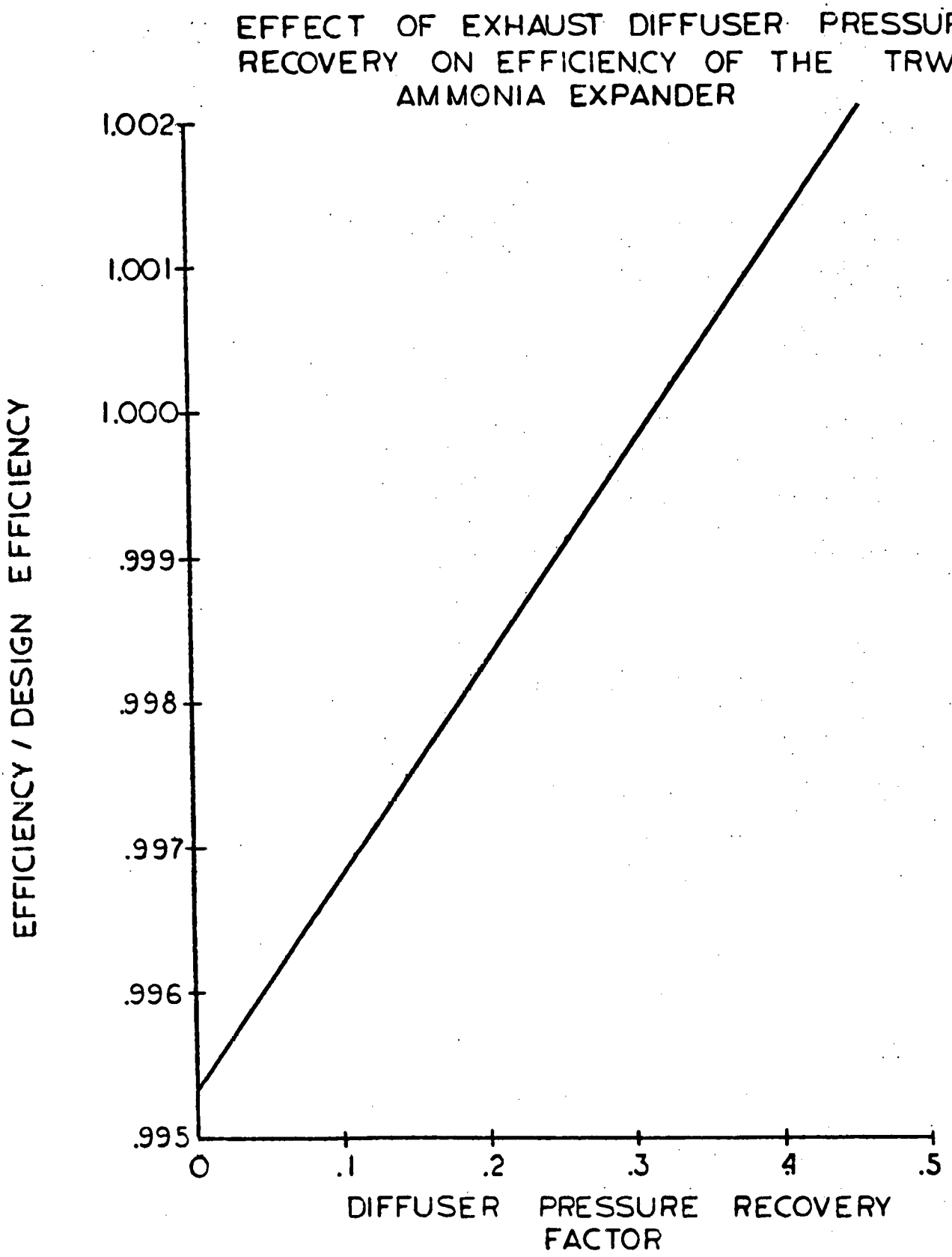
EFFECT OF EXHAUST DIFFUSER PRESSURE RECOVERY ON EFFICIENCY OF THE TRW-OTEC AMMONIA EXPANDER
EFFICIENCY / DESIGN EFFICIENCY
1.002
1.001
1.000
.999
.998
.997
.996
.995
0
.1
.2
.3
.4
.5
DIFFUSER PRESSURE RECOVERY FACTOR

FIGURE 4-29

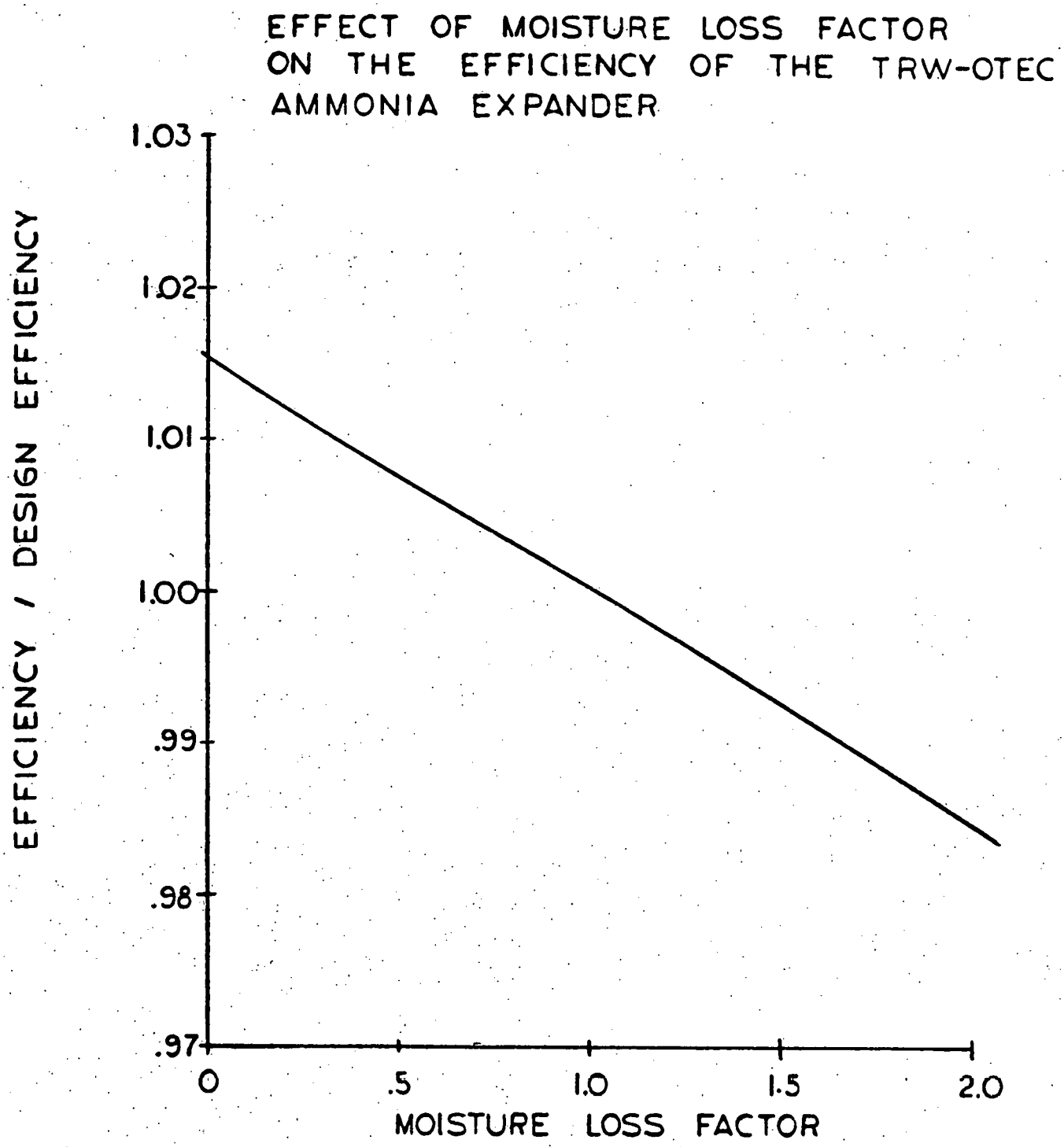
EFFECT OF MOISTURE LOSS FACTOR ON THE EFFICIENCY OF THE TRW-OTEC AMMONIA EXPANDER
EFFICIENCY / DESIGN EFFICIENCY
1.03
1.02
1.01
1.00
.99
.98
.97
0
.5
1.0
1.5
2.0
MOISTURE LOSS FACTOR

SECTION 5

EXPANDER MECHANICAL DESIGN

Prior to the start of any design effort, design objectives must be established. The following objectives were established for the mechanical design of the ammonia expander:

--- Expander is to drive a synchronous generator and operate at a speed consistent with the aerodynamic design.

--- Positive casing sealing is required to contain the toxic ammonia gas.

--- The shaft end seals should not leak the ammonia gas to the atmosphere in the event of loss of pressurized seal oil.

--- Assembly and disassembly of the expander internals should not disturb the generator, nor the inlet and exhaust gas piping.

--- Bearings and seals shall be inspected or replaced without disturbing the main casing.

--- Blading shall be suitable for the required loadings.

The above objectives can be attained by the following:

--- Design the rotor bearing system such that no harmful or objectionable frequencies are within $\pm$ 20 percent of the operating speed.

--- Utilize barrel construction on the expander casing to provide full continuous sealing at the joints.

--- Utilize a contact type seal with shutdown features for virtual leakproof condition with zero sealing oil pressure.

--- Design the barrel-type expander such that the internal parts are removable from one end utilizing simple assembly and disassembly fixtures.

--- Utilize acceptable stress analysis techniques to qualify the blading.

The results of the conceptual design effort are shown in the cross-section layout of the expander, Figure 9 - 1.

ROTOR

Construction

The rotor construction shown on the layout utilizes separate disc assemblies shrunk onto the shaft to maintain concentricity and keyed to transmit the torque. An alternate method is to make the discs integral with shaft. Preliminary investigation indicates that the key disc shrink area may be conducive to stress corrosion cracking in the atmosphere. Further investigation of the stress corrosion potential is required before a final determination of the rotor construction can be made.

Critical Speed

The initial design objective was to make a stiff shaft design where the operating speed is below the first critical speed. Due to the desire to optimize thermodynamic performance, however, the mechanical design gave way. The result is a flexible shaft design with the operating speed between the first and second critical speeds, which are approximately 1300 rpm and 2700 rpm, respectively. The flexible shaft design allows for:

--- Better axial spacing for the inlet channel and for the diffuser at the blade path exhaust.

--- Better placement of the seals and bearings for maintenance accessibility.

--- Smaller bearings and seals requiring less oil flow and power loss.

There are no anticipated difficulties in running the expander between its first and second critical speeds. This is common practice for turbine/generator applications.

BEARINGS

Journal Bearings

The journal bearings should be 10-1/2 inch diameter by 7 inch wide cylindrical bearings and provide a stiffness of approximately 5×10^5 pounds per inch. These journal bearings are adequate considering loading, sea state conditions and critical speed. The bearing retainers are spherically seated to facilitate alignment of the bearings to the shaft. An alternate bearing configuration would be a five shoe tilt pad type, but for this rotor at 1800 rpm the better choice would be cylindrical bearings.

Thrust Bearing

A 55.1 square inch thrust bearing is recommended to accommodate the generator thrust loading due to magnetic misalignment and the thrust due to manufacturing tolerances on the blade rows on either side of the double flow unit. The thrust bearing is a self-equalizing Kingsbury type that is double acting to provide positive positioning of the rotor. The thrust collar is removable from the shaft for ease of maintenance, but does not require removal to change the seal for this particular design size.

SEALS

Four basic types of rotor-casing seals, shown in Figure 5 - 1 through 5 - 4, are used in turbines and compressors for minimizing the amount of motive fluid leaking out along the shaft. These are:

--- Labyrinth Seals

--- Dry Carbon Ring Seals

--- Bushing Seals

--- Face Seals

For this unit the labyrinth type seal was ruled out because it permits leakage of large quantities of the motive fluid. The dry carbon ring type seal has a lower leakage rate than the labyrinth type, but it will also permit leakage of the motive fluid to the atmosphere upon shutdown. The bushing type seal is used predominantly for very high

pressures and would have a large amount of seal oil leakage compared to the face seal. Looking at all factors for this ammonia expander application, the face type seal is recommended for use in this design.

For applications where no gas leakage to the atmosphere can be tolerated, a highly refined contact type face seal with shutdown features and a proven record of performance in process gas compressor installations should be used. During idle periods, shutdown pistons automatically lock the face seal ring. This permits the seal oil system to be shutdown with no ammonia gas leakage even though the expander is still pressurized.

CASING AND MAINTENANCE

The ammonia expander has five major components, namely; the outer casing barrel, the endwalls, inner casing assembly, the rotor assembly, and the two bearing cases. The inner casing assembly can be further broken down to include a stator housing, three diaphragm assemblies for each direction of flow, a diaphragm seal assembly for each diaphragm, a set of variable nozzles for each direction of flow, an inner guide ring for each set of variable nozzles, and variable nozzle linkage. A cross-section layout of the ammonia expander is shown in Figure 9 - 1.

The outer casing, which is of the barrel-type construction to provide full continuous sealing at the joints, has an outside diameter of 120 inches and an overall length of 181-1/2 inches. The 60 inch Class 175 flat faced inlet flange is fabricated to the outer casing thru a transition section and is located on the top vertical centerline 94 inches above the horizontal centerline of the machine. Note that the transition from the round inlet to the obround intersection with the outer barrel provides for the required flow area to maintain low fluid velocities and at the same time minimizes the bearing centerline distance. In a similar fashion there is a transition from the barrel section to the 96 inch Class 175 flat faced exhaust flanged 94 inches below the expander horizontal centerline.

The entire expander is provided with true centerline support by four support feet and keys to maintain the axial centerline. Once aligned at the site, the outer casing will not need to be removed from its foundation; thus the inlet and exhaust joints would not normally be broken.

The endwalls are bolted to the outer casing to provide sealing at the vertical joint. The endwall at the coupling end will not need to be removed once it is aligned to the outer casing. The endwall at the thrust end will require removal for assembly/disassembly purposes when any internal maintenance is desired. In addition to containing the motive fluid in the axial direction, the endwalls also accept

the stationary parts of the face seal that keeps the ammonia from escaping along the shaft to the atmosphere.

The function of the stator housing is to support and position the stationary diaphragms and to direct the flow from the inlet through the rotor to the exhaust. This casing is horizontally split and is fabricated from two half castings, which are welded to the inlet guide vanes to form the top and bottom halves.

The variable nozzles are connected through linkage to a common ring. Therefore, only a single rod penetrates the outer casing for each of the two rows of variable nozzles. The rod will be surrounded by a bushing and O-rings to prevent leakage of any ammonia to the atmosphere. Variable nozzles for axial flow steam turbines are not generally used because control valves have been historically used for part load conditions and high temperatures can create serious deformation problems at the operating pressures. Variable stators have been used very successfully throughout the industry on axial flow compressors for decades. Typical control linkage for an axial flow compressor is shown in Figure 5 - 5. This type of control has exhibited a high level of reliability with a minimum of maintenance.

The rotor assembly is positioned in the casing and provides the means of efficiently converting the energy of the ammonia motive fluid to usable power.

The two bearing cases, which are attached to the endwalls, provide a means of supporting and positioning the rotor.

Normal maintenance turnaround for the ammonia expander would be expected to be:

--- Twelve months for the first turnaround.

--- Twenty-four to thirty-six for subsequent turnarounds.

The first turnaround will require approximately three men for six shifts to make a complete inspection of bearings, seals, rotating element and stationary parts. Subsequent turnarounds of approximately four men for two shifts will involve inspection of only the bearing and seals. Full turnaround including the rotor inspection, similar to the first turnaround, should be conducted every five or six years. Service life of the expander can be expected to be similar to steam turbine generator drives.

The expander should be designed for minimum disassembly for maintenance on the bearings and seals. The bearings can easily be inspected by the removal of the top half bearing cases without disturbing the alignment. The face seals with shutdown features require the disassembly of the bearing cases and on the drive end the coupling must also be removed.

Special tools and fixtures should be provided for the disassembly of the complete expander. These fixtures would include rails to remove the inner casing, a centering ring to maintain concentricity between the rotor and inner casing during insertion, an endwall counterweight for stabilization during disassembly and provisions for eyebolts to remove the bearing cases. Also, a complete instruction book containing a detailed description of assembly and disassembly procedures should be supplied. Normally, the instruction book will include data on trouble shooting as well as alignment methods and spare parts lists.

The lube oil console maintenance and inspection should follow vendor recommendations. Components such as pumps and coolers should be inspected at each turnaround. Filters, reservoir tank oil level, oil pressures, and the temperatures should be checked on a daily basis to insure proper operation. The instrumentation gages, thermocouples, readouts, etc., should be inspected and calibrated at six month intervals.

Maintenance procedures for the synchronous generator should follow the manufacturer's recommendations.

MOISTURE EROSION

The proposed four stage ammonia expander should suffer no significant moisture erosion damage at the specified operating conditions. Consequently, protection of the leading edges of the rotating

blades with the use of stellite strips is not required. Also, due to the low levels of moisture and low velocities encountered in this design, stationary moisture collectors are unnecessary.

The above conclusions are based on calculations of surface tension, maximum stable droplet size, and the erosion coefficient for the ammonia expander as compared to steam turbine experience. At 90 psia pressure, the surface tension of water (.0032 LBF/FT) is 2.0 times greater than it is for ammonia (.0016 LBF/FT); therefore, the apparent hardness exhibited on impact of an ammonia droplet is much less than a water droplet at similar conditions. Similarly, the maximum stable droplet size on the basis of a Weber number calculation is more than three times larger in steam (.609 micron) than it is in ammonia vapor (.199 micron), therefore, the smaller ammonia drops will cause less erosion damage than the larger water drops would cause at similar conditions. The erosion coefficient from the equation

$$E = 4.1072 \times 10^{-6} \frac{K Y_o U^3_{TIP}}{P_o}$$

was calculated for each rotating blade of the ammonia expander at nominal conditions. In the above equation K is a constant, which depends on the distance from the stator blade trailing edge to the rotor blade leading edge and on the thickness of the stator blade trailing edge. The value Y_o is the fraction moisture level ahead of the stage, and U_{TIP} is the speed at the tip of the rotating blade in feet per second.

P_o is the stage inlet static pressure in pounds per square inch absolute. The maximum erosion coefficient, which occurs on the fourth stage with 2 percent moisture ahead of the stage, was calculated to be .003. The threshold of significant erosion danger is at a coefficient of 8 or greater based on steam turbine experience. For example, a typical last stage of a large steam turbine with a moisture of 8 percent has an erosion coefficient of 30 or more.

ROTOR BLADES

The rotating element is the critical item in any piece of rotating equipment. Consequently, Elliott is compelled to insure that the design of the blading is both adequate and practical from a mechanical viewpoint and at the same time keep a watchful eye on optimizing the aerodynamic performance. The proposed expander design has attained these objectives.

Although all four rotor blades have been analyzed only the results for the fourth row, which has the highest stresses and lowest frequency, are presented in this report.

The direct tensile stress at the base of the vane of the last rotor blade row for the nominal operating conditions is 3255 psi and the gas bending stress, which is a maximum at the leading edge, is 5566 psi. Therefore, the maximum total steady state stress if 8821 psi. With these values and properties of annealed AISI Type 403 material,

a Goodman Diagram can be constructed. The Goodman Diagram provides a means of qualifying rotating parts and is an accepted standard in the industry. Figure 5 - 6 is the Goodman Diagram for the fourth row rotor blade. The diagonal solid line represents the failure line for annealed AISI Type 403 material at the blade temperature with a 1.667 stress concentration factor applied to the alternating stress. Actual stress values to the right of this line indicate the blade will fail. As you can see, the combination of stresses for the blade in question is well to the left of this diagonal line, and therefore, there is a certain amount of margin in the design. To determine the amount of margin in a design Elliott calculates a ratio termed the Goodman Factor. The Goodman Factor is just the allowable alternating stress at the blade total steady state stress divided by the actual blade bending stress. For this particular blade the Goodman Factor is 3.3. From historical data, Elliott has found the blades with Goodman Factors of 2.5 and larger will not experience failures due to these stresses for this type of staging.

The rotating blades should be designed so that its natural frequency exceeds the low multiples of the operating speed and does coincide with the nozzle passing frequency. Since the fundamental material frequencies of the rotating blades range from 8 to 11 times the operating speed, no blade vibratory problems are anticipated.

FIGURE 5-1

LABYRINTH SEAL

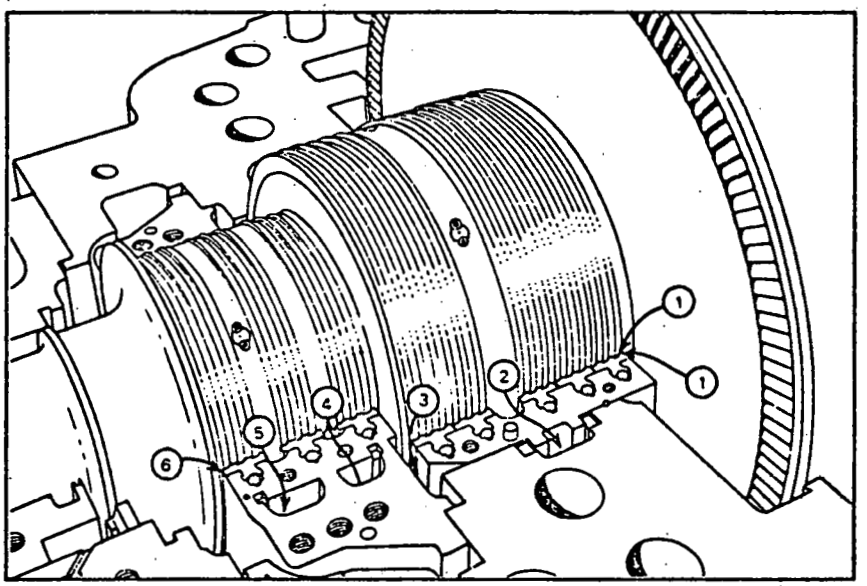

FIGURE 5-2

DRY CARBON RING SEAL

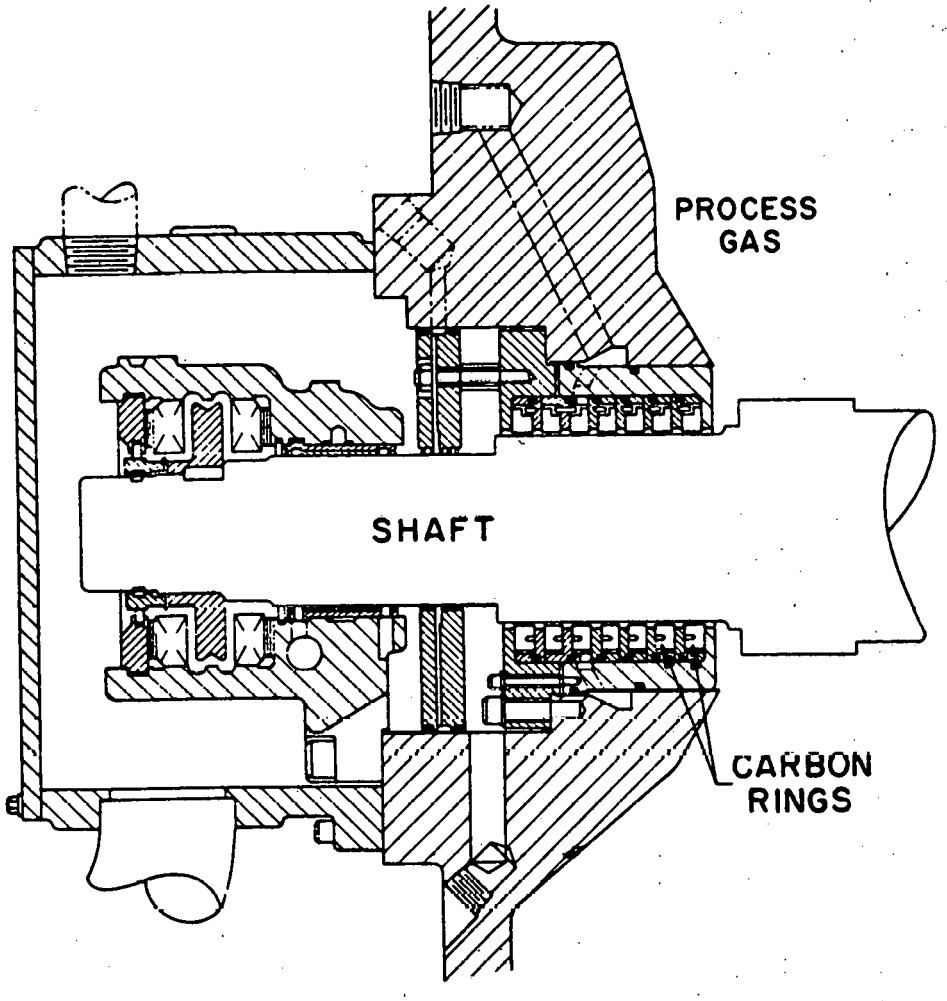

FIGURE 5-3

BUSHING SEAL

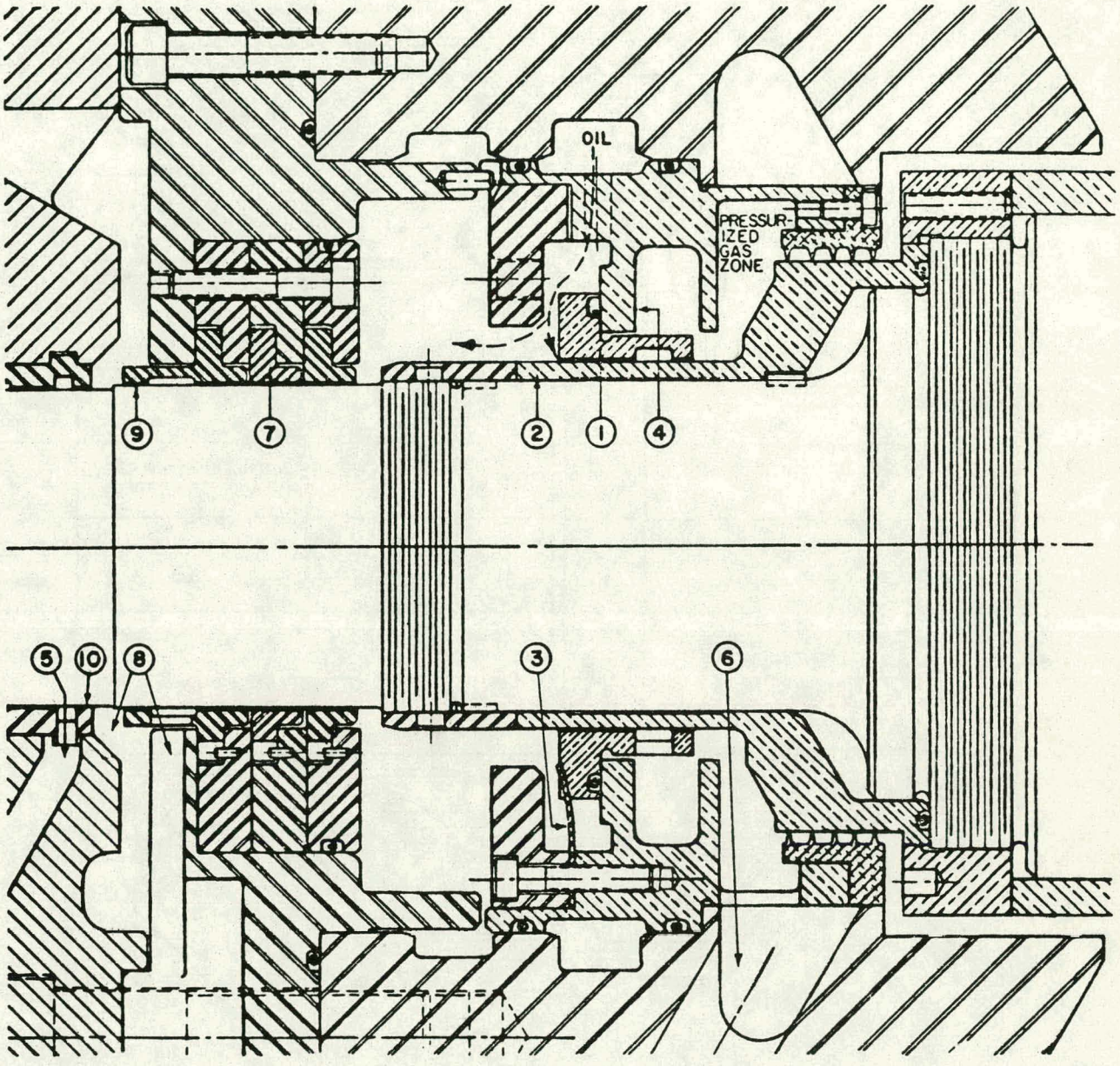

1. STATIONARY SEAL SLEEVE
2. ROTATING SHAFT SLEEVE
3. SPRING
4. SEAL CASING PARTITION
5. BEARING OIL DRAIN LINE
6. GAS AND CONTAMINATED OIL DRAIN
7. FLOATING BABBITT-FACED STEEL RING
8. SEAL OIL DRAIN LINE
9. WIPER RING
10. BEARING WIPER RING

FIGURE 5-4

FACE SEAL WITH SHUTDOWN FEATURES

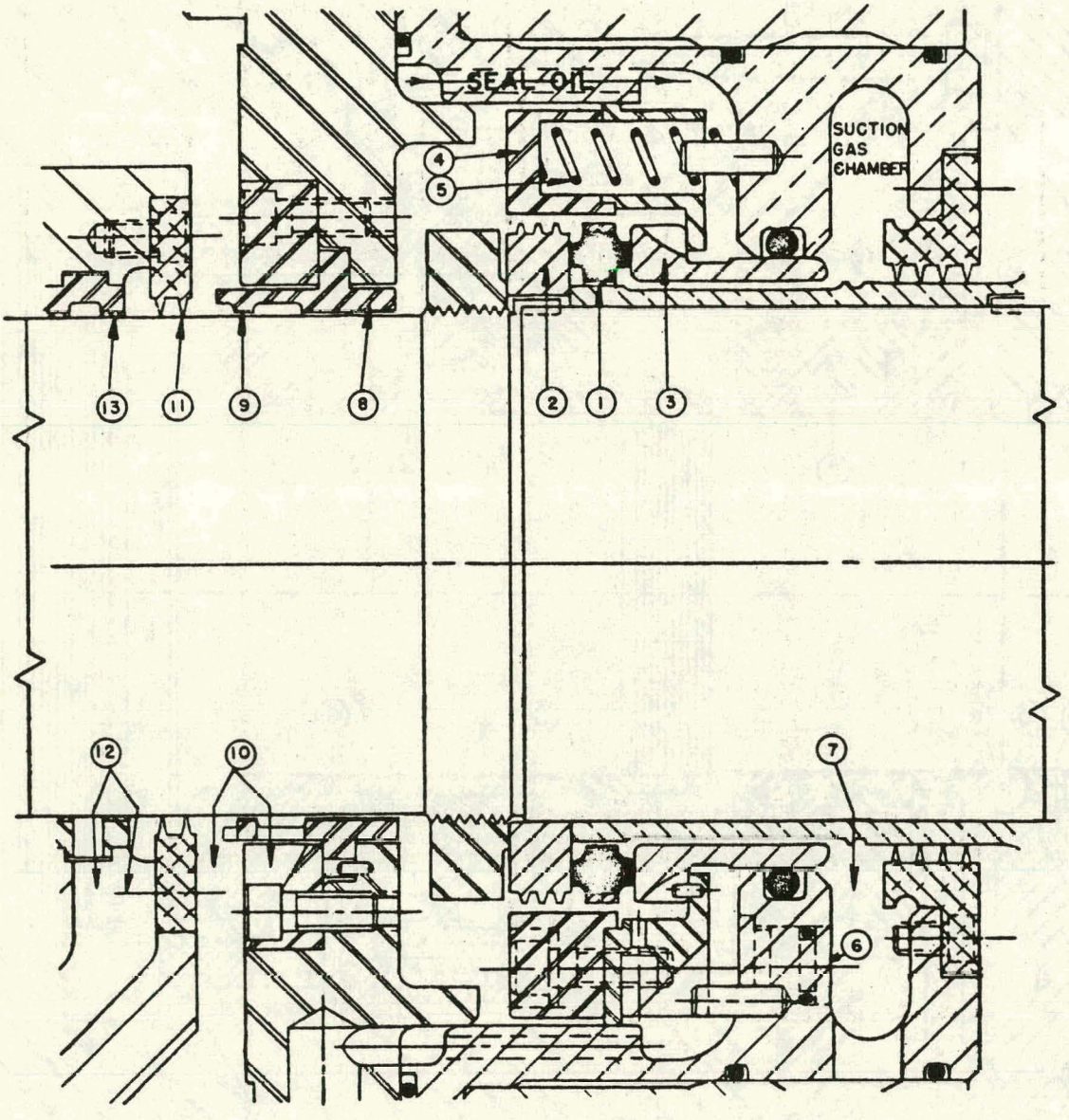

1. ROTATING CARBON RING
2. ROTATING SEAL RING
3. STATIONARY SLEEVE
4. SPRING RETAINER
5. SPRING
6. SHUTDOWN SEAL PISTON
7. GAS AND CONTAMINATED OIL DRAIN
8. FLOATING BABBITT-FACED STEEL RING
9. SEAL WIPER RING
10. SEAL OIL DRAIN LINE
11. SECONDARY WIPER RING LABYRINTH
12. BEARING OIL DRAIN LINE
13. BEARING WIPER RING

FIGURE 5-5

VARIABLE NOZZLE LINKAGE

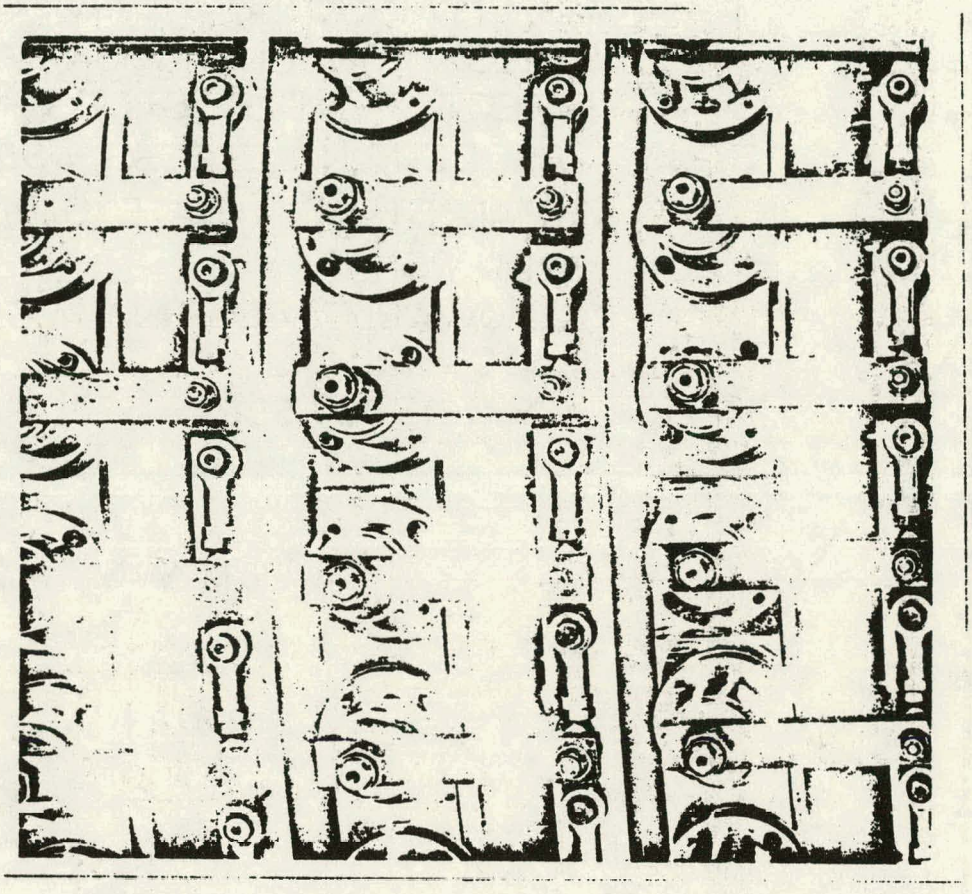

FIGURE 5-6

TRW-OTEC AMMONIA EXPANDER
GOODMAN DIAGRAM

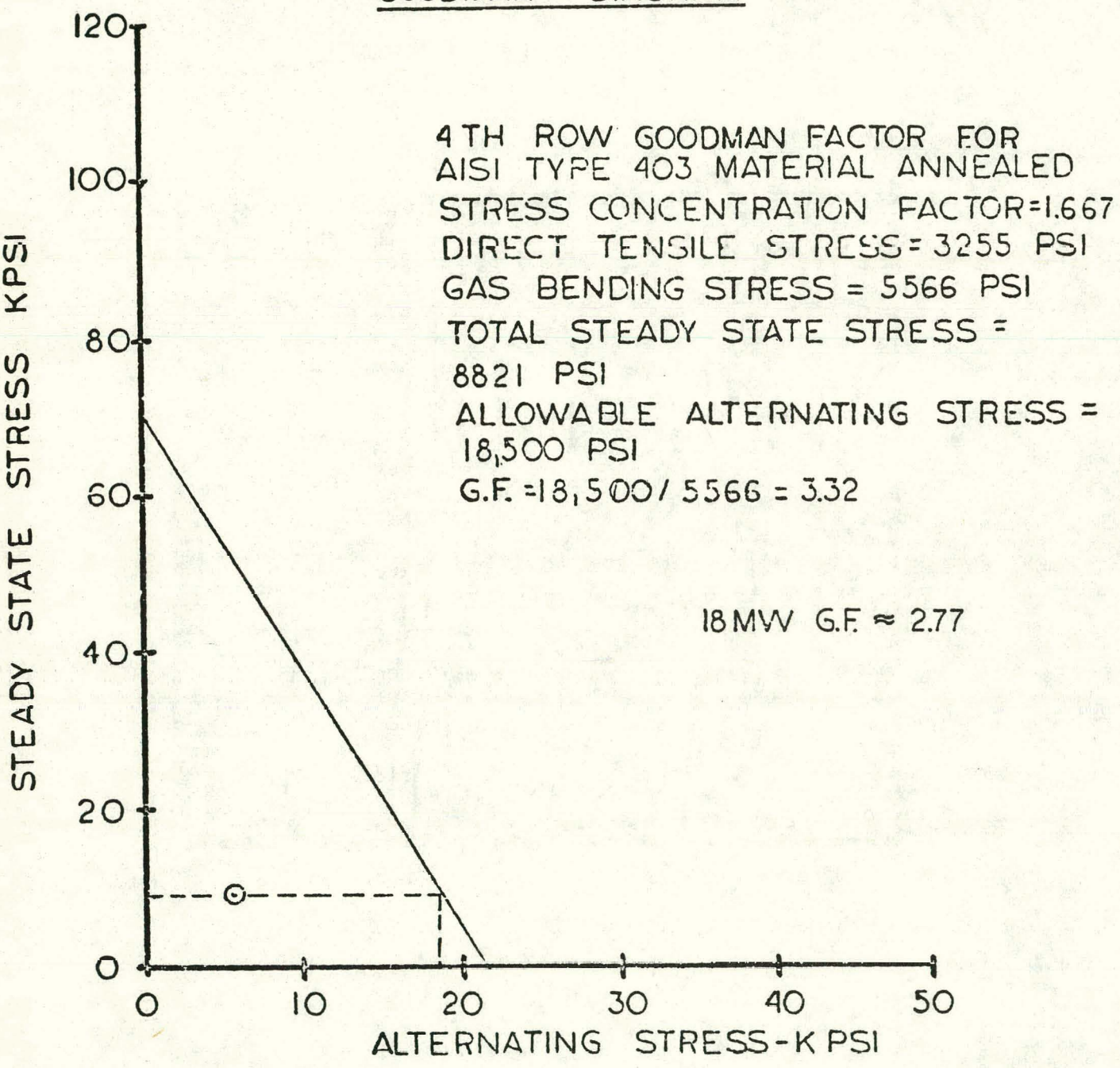

SECTION 6

GENERATOR DESIGN AND ANALYSIS

GENERATOR DESIGN

The Brown Boveri Model WG1000 db 4L generator presented is a 4-pole synchronous generator with a TEWAC (total enclosed water to air cooled) enclosure. Data for this generator is presented in Table 6 - 1. Generator overall efficiency versus load is shown in Figure 6 - 1.

The generator design is such that the service factor is 1.00 at full load of 18.0 MW. A load limiter should be included in the control scheme to prevent a generator overload condition.

Since this generator is only 97.2 percent efficient at full load, inquiries were made for a hydrogen cooled synchronous generator for this service. It was anticipated that efficiencies of 98 percent, or slightly higher, could be obtained. Both Brown Boveri and Westinghouse, however, have responded that they do not offer hydrogen cooled 2, 4 or 6-pole synchronous generators below the 25 to 35 MW range.

Generator vendors were not requested to design a hydrogen cooled

synchronous generator for this particular application. If all development costs for a hydrogen cooled generator were to be absorbed by one unit, the development costs should not exceed the value of the additional power produced. Thus, if a generator manufacturer would be amenable to expend the required design effort, the cost of the hydrogen cooled unit should not exceed the TEWAC generator by more than $150,000.

COUPLING DESIGN

Three types of couplings have been considered for the ammonia expander/generator string, namely; a solid coupling, a gear type coupling and a diaphragm type coupling.

The solid coupling would be the least expensive type. It has the disadvantage, however, that there are no provisions in the design to accommodate offset or misalignment between the expander and generator. Precise alignment requiring many additional man-hours of time would be necessary and any initial cost advantage would quickly disappear. In addition, the barrel construction of the expander dictates that the coupling hub on the expander shaft must be removed to dissasemble the expander. The possibility of getting the coupling hub back on the shaft exactly as it was before removal is highly improbable. Therefore, the solid coupling is not recommended.

A gear type coupling would provide for limited end float, and

could accommodate reasonable offset and misalignment between the two units. A verbal quote has been obtained for a number 9 Koppers gear type coupling at $7500.

A diaphragm type coupling would also be acceptable because it can provide for limited end float, offset and misalignment. A verbal quote of $8000 has been obtained from Bendix for their model 67E516.

Although both the gear and diaphragm type couplings are suitable for this design application, the diaphragm coupling is recommended because it does not require lubrication and allows for bearing case and seal removal.

TABLE 6-1

GENERATOR DATA

Type	Synchronous
Manufacturer	Brown Boveri Corp.
Rated (KW)	18,000
Synchronous Speed (RPM)	1,800
Rated Voltage	13,800
No. of Phases/Frequency	3/60
Power Factor	0.8 Lagging
Service Factor	1.00
Efficiency % (at 4/4, 3/4, 1/2 Load)	97.2, 96.9, 96.2
Insulation Class	F
Max. Temp. Rise (Winding, over 40°C)	80°C
Excitation Type	Brushless
Excitation DC Voltage (at F.L.)	112
Excitation Response	2.0
Short Circuit Ratio	0.55
Short Term Thermal Capability (balance current)	100 Sec.
Short Term Thermal Capability (short current at machine terminals)	
Unbalanced (Line to Neutral)	30 Sec.

T A B L E 6 - 1 (cont...)

GENERATOR DATA

Wave Form Deviation, Max. %	0.8
Calculated Transient and Subtransient Reactance	27% 21%
Enclosure	TEWAC-Weatherproof
Cooling Water Inlet nemp. (Max.), °F	85
Cooling Water Outlet Temp. °F	95
Cooling Water Requirements (GPM)	295
Lube Oil Pressure (PSIG)	15 - 18
Lube Oil Requirements (GPM)	8
WK^2 of Machine ($LB-FT^2$)	24620 generator/exciter
Permissive Overspeed (RPM)	2250
Vibration Max., (MILS) peak-to-peak	1.5 approx.
Noise Level, dB (A)	84 + 3 dB (A) tol.
Weight (lbs.) net/shipping	86640/100500
Overall Dimensions	

Reactive Power Capacity

20	40	60	80	100	% of Load
14.4	14	13.3	12.4	11.2	MVA

FIGURE 6-1

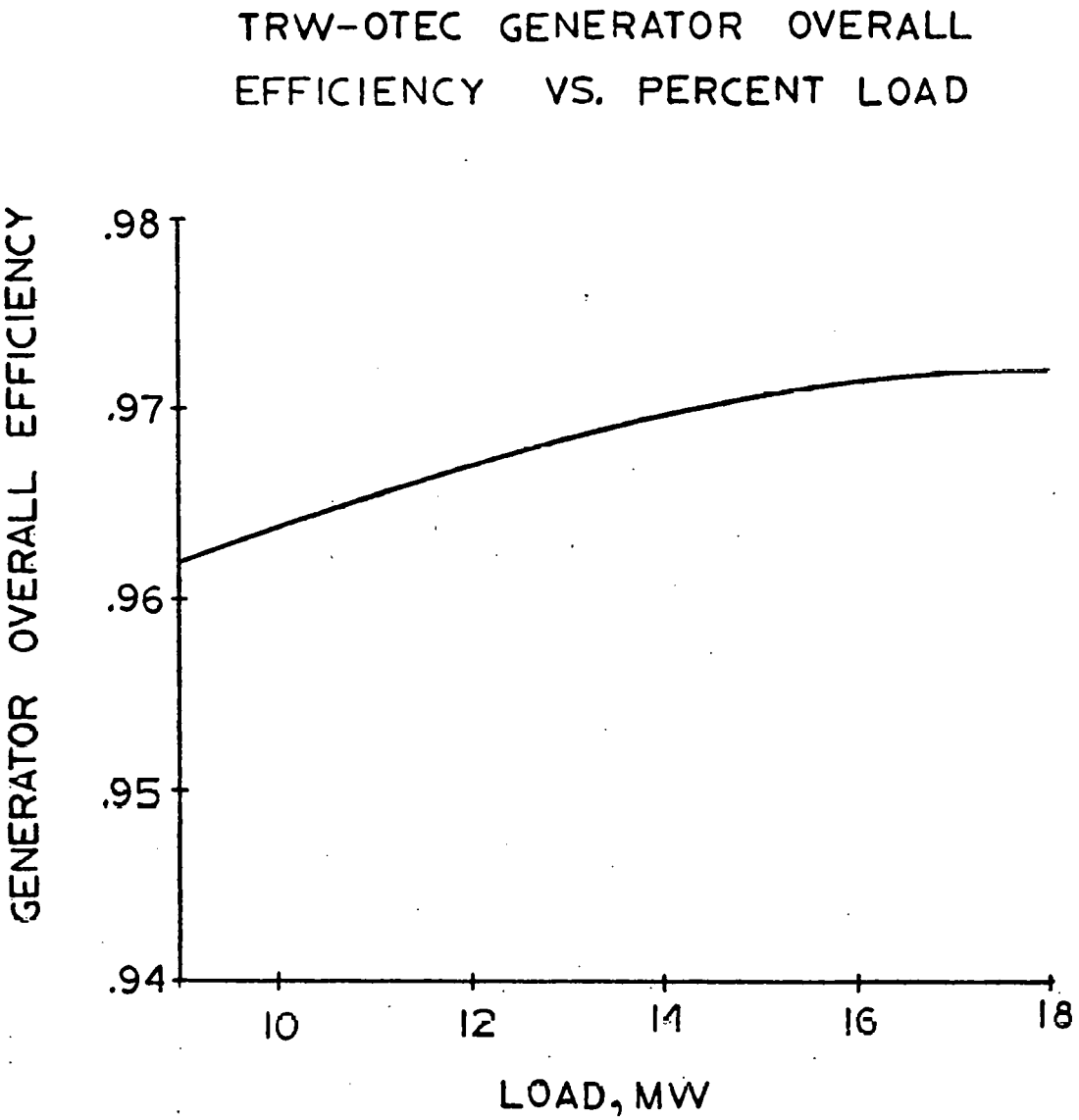
TRW-OTEC GENERATOR OVERALL EFFICIENCY VS. PERCENT LOAD
GENERATOR OVERALL EFFICIENCY
.98
.97
.96
.95
.94
10
12
14
16
18
LOAD, MW

SECTION 7

CONTROLS

VALVE SIZING

Two ammonia gas control valves have been investigated and sized for the expander operation, namely the emergency trip valve ahead of the expander and a bypass valve around the expander. The trip valve will be the equivalent of a 60 inch diameter to match the expander inlet size and should be as close to the inlet flange as possible so that the maximum overspeed of the string can be minimized. The bypass valve need only be the equivalent of a 30 inch diameter because the full pressure drop can be taken across it during start-up, shutdown or during an emergency trip out.

Governor valve requirements for speed control using fixed inlet nozzles in place of speed and load controlled variable inlet nozzles have not been investigated due to the limited time frame for this study. However, no difficulties are anticipated if this arrangement should be preferred. As discussed in Section 4, load controlled variable inlet nozzles are justified for maximizing seasonal output. Speed controlled variable nozzles can also satisfy synchronizing and grid

isolation requirements assuming that the variable nozzles can be designed to control the flow from no load to maximum power conditions.

VALVE CHARACTERISTICS

It is desirable to have a single 60 inch butterfly type trip valve close as quickly as possible. But if it were to slam shut, the valve seat would be damaged and eventually not perform its function. One approach to solve the quick trip problem is to have the valve close quickly to the point where it is only 5 percent open, and ease it closed for the remaining portion. Typical closing times of commercially available hydraulic operated 60 inch diameter butterfly valves are of the order of 3 to 5 seconds. This is not fast enough to prevent overspeeding of the expander/generator on an electrical full load dump. The preferred choice is a swing through type valve designed with a 0.5 second response time to close the valve. This valve would cost about $75,000 and should have hydraulic actuation. Although a detailed calculation of the system was not possible with the information available, it is estimated that the above response times are adequate.

The bypass valve is a 30 inch butterfly valve with 0 to 70 degrees travel and a cost of $31,900. Since tight shutoff and not fast closing is a requirement for this duty, the valve has a 5 second stroking speed from full open to full closed. The important characteristic of this valve is that it can fully open at the time of an emergency tripout in one second or less. This action will divert the motive fluid around the expander.

CONTROL SCHEME

Control of the expander/generator string covers the three basic phases of start-up/shutdown, steady state, and emergency trip. This system is rather unique due to the characteristics of this process, the requirement to limit the generator output, and the requirement to maximize expander output at any steady state condition. A simplified block schematic of the proposed control system is shown in Figure 7 - 1.

The basic elements of the OTEC ammonia cycle are: 1) the condenser for taking the ammonia vapor and converting it into liquid; 2) the ammonia pump for adding pressure head to the liquid; 3) the vapor generator which extracts heat from the warm sea water and transfers it to the ammonia for vaporization; 4) the expander which expands the ammonia vapor to extract energy and convert it to mechanical power; and, 5) the generator which converts the mechanical power to electrical power.

The control system requires a storage and makeup system so that the closed loop can be supplied with the desired amount of motive fluid as operating conditions vary.

The ammonia pump takes liquid from the condenser and pumps it to the vapor generator. Liquid ammonia is converted to a gas in the vapor generator as it passes through. Ammonia vapor passes through

the emergency trip valve and on to the expander variable nozzles, which are tied to the load-speed control. The exhaust flow from the expander goes to the condenser. The level control will maintain level in the condenser pump by bleeding fluid from the makeup system as needed. A bypass valve in a loop around the expander enables the entire loop to operate as a closed system during start-up without the expander rotating.

On start-up the expander trip valve would be closed. The cold sea water pump and warm sea water pump would then be activated.

Activation of the ammonia pump would raise the liquid level in the vapor generator to the desired level with the excess being diverted to the makeup system. Vapor would start to be generated and the system pressure would increase to the saturation pressure attainable with the warm sea water. Eventually, the steady state quantity of ammonia vapor would be generated.

Next, the variable nozzles are set to minimum setting and the trip valve is opened to admit a nominal amount of vapor through the expander.

When enough torque is developed to overcome frictional forces, the expander/generator string will come up to some minimum speed. The variable nozzles will be gradually opened and the bypass valve partially

closed until synchronous speed is attained. The variable nozzles will be used to synchronize the generator.

After synchronization load will gradually be applied to the string by opening the variable nozzles the required amount; the expander bypass valve will gradually be closed until it is completely shut.

Normal shutdown would basically be the reverse of the start-up procedure. Shutdown of the warm sea water pump would remove the heat source and vaporization would cease.

The requirement to maximize power at any steady state condition dictates a unique type of control, which is only possible if variable nozzles are provided and the generator is base loaded. The control would be as follows:

The generator is loaded to the desired capacity with the speed control. The load control is then transferred from manual to automatic operation. In the automatic mode, the load control actuates the variable nozzles a predetermined amount at preset time intervals. Initially, there is no movement of the variable nozzles until the dead band of the controls is exceeded. When the variable nozzle position exceeds this dead band, the load control will sense the increase (or decrease) in power output and will increase (or decrease) the speed set point of

the speed control. The load controller, however, is "smart" in that if power output drops instead of increasing it will reverse operation to decrease (or increase) the speed set point. This is a slow response activity compared to the speed control.

The dead band, proportional band and reset on the speed setting must be adjusted and tuned on site to match the response of the system.

For nonbase loaded operations the control would be as follows:

The generator produces the power required by the load. If the generator load drops below the set point, speed control will want the speed returned to 1800 rpm. Therefore, it will cause the variable nozzles to quickly close and provide less power. If the load is increased, the speed will drop below 1800 rpm and the nozzles will be quickly opened to return the speed to the set point.

The above control scheme has been reviewed with Woodward Governor Company and it seems practical, although there are no known applications of this kind. If the generator output exceeds its rating, a load limiter will decrease the variable nozzle setting, thereby reducing the mass flow to the expander based on the heat source characteristics. Thus, the power input to the generator will be reduced. The load limiter signal could be a part of the load control and will override the maximization of power signal to the variable nozzles.

For the safety of personnel and equipment redundancy has been included in the overspeed trip devices.

If there is a loss of generator load while it is on the line a signal will cause the emergency trip valve to close, the variable nozzles to go to minimum setting, and the expander bypass valve to completely open. This type of emergency is most serious, and thus, safety measures should be instituted at the earliest possible time.

The speed signal from the expander electronic speed counter provides back-up by initiating the above three actions at 3% (1854 rpm) overspeed.

The mechanical overspeed trip on the expander shaft, set at 10% (1980 rpm) overspeed, provides another means to initiate the above sequence of events.

FUTURE WORK

Several facets of the control area are recommended for future analysis.

The speed and load control is believed to be reasonable and feasible but a more detailed investigation is in order.

The variable nozzle minimum setting has to be studied along with

the expander bypass valve area to determine the minimum idle speed after breakaway.

The maximum overspeed of the string with maximum load dump needs to be studied for the actual valve response times, taking into account stored energies and system characteristics assuming the emergency signal occurs at 1800 rpm, at 1854 rpm, and at 1980 rpm.

The variable nozzle requires study to determine if it can provide tight shutoff in the required time, thus eliminating the emergency trip valve. While this is appealing, Elliott does not feel that this can be accomplished without compromising performance. This compromise, however, is minimized with a multistage design.

Also, it might be possible to eliminate the expander bypass valve. This evaluation would require an extensive study of the cycle dynamics. It may not be possible to synchronize the generator at system part load. In addition, the process upsets on the trip out of the string may be intolerable.

OTEC PROPOSED CONTROL SCHEMATIC

FIGURE 7-1

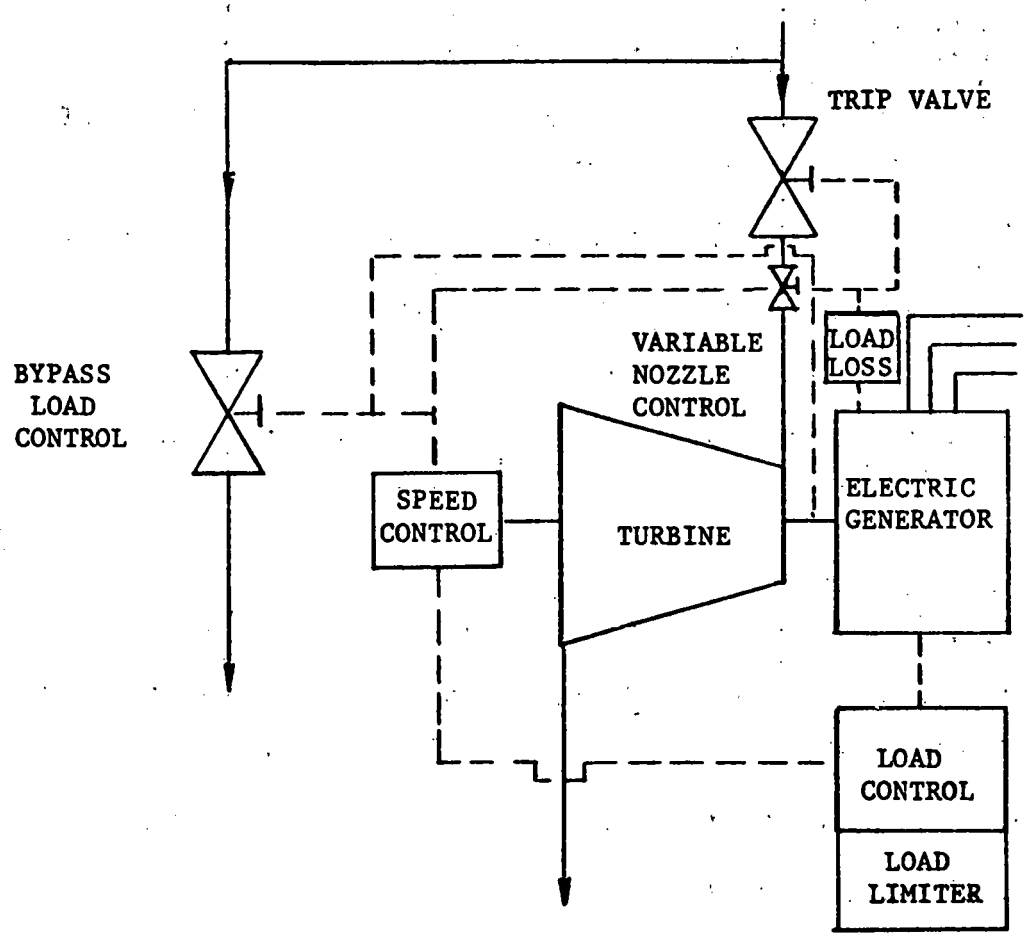

SECTION 8

LUBE AND SEAL SYSTEM

FLOW REQUIREMENTS

Lube and seal oil flow requirements are as follows in Table 8 - 1.

TABLE 8 - 1

		GPM MAX/NORMAL	PRESSURE PSIG
Expander			
Journal Bearings		12.5	15 - 18
Thrust Bearing		11	15 - 18
Iso-Carbon Seals		12.5	125 MAX
Expander Total		36	
Generator Journals Total		8	15 - 18
Controls (Estimated)			
Variable Nozzles	With accumulators for each servomotor	15/10	125
Trip Valve		15/10	125
Bypass Valve		15/10	125
Total Controls		45/30	
Total String Requirements		89/74	

Lubricants utilized in ammonia expanding equipment have a unique requirement for chemical compatibility. Undesirable reactions such as congealing or formation of deposits should not occur. Ordinarily this need can be met by a choice of a straight uninhibited mineral oil. Either a straight naphthenic or a pour point depressed parafinic oil would be suitable for the subject service; the oil should be of a good quality, and pass the oxidation test ASTM D943 for 3000 hours minimum. For the design of this lube console ARCO Ideal Oil S-150, which has an oxidation life of 4000 hours, has been used.

COMPONENTS

API 614, with some Elliott exceptions, was used throughout for the design of the lube system. Due to the ammonia atmosphere and salt water cooling water, no copper or copper bearing alloys will be in contact with the oil or atmosphere. The coolers and filters are ASME Code design and the coolers are TEMA "C" design. Electrical components will be good for NEMA Class 1, Group D, Division 2 areas. All switches are single-pole, double-throw type.

The schematic for this console is shown in Figure 9 - 4. The components in the lube system are reviewed below.

The oil reservoir is designed to insure an undisturbed positive suction for the oil pumps. The reservoir capacity, based on normal flow, is determined through API 614 requirements of a 5 minute working capacity

between minimum operating level and suction-loss level and an 8 minute retention capacity below the minimum operating level. A rundown capacity, capable of holding the total volume of oil in the piping and components, is provided above the maximum operating level. Free board is provided above rundown level. The reservoir is equipped with an internal baffle separating the return lines from the pump suction lines to help prevent vortexing at the pump suction. Each pump suction nozzle is equipped with an antiswirl plate as well. A dessicant-type breather vented through a stack is provided to protect the tank from overpressure. Purge connections are also provided. A level indicator and a level alarm switch are provided to warn the operator of an accidental loss of oil.

The A.C. motor driven main and auxiliary oil pumps are horizontally mounted screw type positive displacement pumps in order to provide essentially pulsation-free oil to the equipment. The drivers are sized to permit the pumps to start up with 1000 SSU oil (40°F) and reach the relief valve set point without burning out the drivers. The pumps are sized to individually supply the necessary oil flows at the required pressures so that if one pump becomes inoperative, the other pump will supply the equipment requirements. Relief valves are provided on each pump discharge line to protect the oil console against overpressure. A D.C. motor driven centrifugal oil pump acts as a back-up for the bearing oil supply for emergency coastdown.

Twin shell and tube type oil coolers are provided to remove the

friction generated heat from the oil and maintain acceptable oil temperatures at the unit. The oil is maintained at a pressure higher than the cooling water to prevent water leaking into the oil. Twin oil filters of a nominal 10 micron rating are provided downstream of the coolers to insure a clean oil supply to the bearings and seals. The filter media is replaceable cotton-cotton matrix cartridges.

A transfer valve is located between the cooler-filter sets. This 6-ported valve permits a change over from one cooler-filter set to the other without bypassing any oil or interrupting the delivery of oil to the seals and bearings. This permits maintenance on the idle cooler-filter set.

A differential pressure indicating switch is provided across the cooler-filter-transfer valve package to indicate the dirty-filter cartridge condition.

A separate single oil filter is provided in the emergency oil supply to the bearings. A differential indicator is provided to indicate the dirty-filter cartridge condition.

Temperature and differential pressure switches notify the operator of a filter or cooler problem.

A pressure switch is located in the main oil header to automatically

start the auxiliary oil pump motor upon loss of header pressure.

A pneumatically controlled back-pressure regulator maintains a constant header pressure downstream of the coolers and filters by dumping the excess oil to the reservoir. This valve is selected to control the header pressure with either one or two of the oil pumps running.

Self-operated pressure regulating valves pass the required flow at the required pressure to the expander bearings and to the generator bearings. A pneumatic operated regulator is provided to pass the required flow and to follow the required differential pressure across the expander shaft seals. A pneumatic operated regulator is also provided to pass the desired flow to the control accumulators. Each regulator station is complete with isolating gate valves and bypass and vent globe valves to provide for maintenance of the valves without disturbing the unit.

Redundant pressure switches and differential pressure switches are installed in the bearing oil feed lines and seal oil feed lines, respectively, to protect the unit on loss of oil. They operate on a "majority rules" basis to eliminate accidental trip out of the string. Alarm switches are also connected to these lines to prompt for operator attention. An alarm switch is connected to the control oil feel line to indicate loss of pressure.

A contaminated seal oil drainer is provided for each of the flat face seals. These drainers permit the separation of free ammonia vapors from the oil and venting of the ammonia vapors to a collector system. The contaminated oil is discharged to the degassing tank.

A degassing tank equipped with an electrical heater separates the entrained ammonia from the oil and vents it to a collector system.

Thermometers are locally mounted at normal points of interest. Thermocouples may be used in lieu of thermometers or in parallel with them for remote read-out stations.

Pressure gages are also locally mounted at normal points of interest, as shown on the schematic, with pressure transducers in lieu of, or in parallel with the pressure gages. Pressure switches are mounted locally.

Sight flow indicators are normally provided in each lube oil drain to provide visual verification of oil flow.

Drain lines from the units should have a minimum slope of 1/4 inch per foot of pipe length to satisfy land-based installations plus an additional amount of slope required to drain the oil during sea state 6 conditions. If the lube console is located about 20 feet below the expander/generator string level, there should be ample slope for these

adverse conditions. Additional pump head capability will be required if the pump discharge is more than 25 feet below the bearing feed elevation.

AUXILIARY REQUIREMENTS

Requirements for auxiliary servics are outlined in Table 8 - 2.

TABLE 8 - 2

AUXILIARY SERVICES

Lube Console	
Cooling Water	100 gpm @ 85°F
Control Air	15 psig
Pump Power	20 HP normal/30HP max.
Emergency DC Power	8 HP normal/15HP max.
Instrumentation	120 V 1ϕ 60Hz 2KW
Expander	
Instrumentation	120 V 1ϕ 60Hz 2KW
Controls	120 V 1ϕ 60Hz 1 KW
Generator	
Cooling Water	295 gpm @ 85°F

DEGASSIFICATION

A degasifying system for the lube and seal oil is recommended to minimize contaimination of the oil with ammonia. The systems consists of a small degassing tank, usually located on top of the oil reservoir equipped with an electrical heater, to separate the entrained ammonia from the oil and pass it to the collector system or vented to a stack above deck level.

SECTION 9

SUBSYSTEM DESIGN

CROSS-SECTION LAYOUT

Figure 9 - 1 shows the cross-section layout of the four stage double flow ammonia expander for 14.4 MWe at the nominal conditions. The expander is a flexible shaft design with a 151 inch bearing span. Flow enters at the top center of the expander and is distributed circumferentially before it turns axially to feed both sets of blading of the double flow design. After passing through the four stages the ammonia is efficiently diffused to exhaust pressure where the two flows are joined before exiting thru the common exhaust flange on the bottom vertical centerline. The overall shaft-end to shaft-end length is 197 inches with a 120 inch diameter of the outer casing. The casing and shaft lengths are nearly equal. The 60 inch diameter inlet is 94 inches from the horizontal centerline and the 96 inch exhaust flange is also 94 inches from the horizontal centerline.

The stages are located between the journal bearings and flat face shaft seals with the thrust bearing, and speed control devices, located outboard of the journal bearing on the nondrive end.

In Figure 9 - 2 data pertaining to the blade path is shown. This layout contains blade data such as number of blades and diameters. Table 9 - 1 contains additional data such as blade axial widths and gauging angles. Any and all blade data not shown in Figure 9 - 2 or in Table 9 - 1 is proprietary to Elliott Company.

STRING ARRANGEMENT

Arrangement of the expander, generator and coupling are shown in Figure 9 - 3 with appropriate overall dimensions. Pertinent details of each component can be found elsewhere in this report. Weights of major parts are in Table 9 - 2. If the components are shipped separately, a 50 ton crane will be required to lift the expander outer casing. If everything is mounted on a baseplate and lifted at the same time, a 150 ton crane will be required; since the baseplate is not included in any of these weights, it is assumed that it will not weigh more than 33000 pounds.

Straight removal of the generator rotor from the exciter end will require 13 more feet of space assuming the exciter portion of the rotor is not removed from the generator shaft. Sixteen and one half feet are needed to remove the expander rotor from the thrust end of the expander casing. The above procedure permits removal of either rotor without disturbing the other unit. It is recommended that a set down work area of 38 feet wide by 24 feet long be provided at the thrust end of the expander. This same area can be used for generator repairs, if desired,

provided the generator parts can be moved past the expander casing. Otherwise, an area 20 feet wide by 20 feet long will be needed for set down and work space for generator parts. Head room under the crane hook to the top of the generator sole plates of 17-1/2 feet is needed for 18.0 MWe TEWAC generator with cooler mounted on top of the generator.

LUBE AND SEAL OIL SCHEMATIC

Figure 9 - 4 shows the lube and seal oil system schematic. The major components include the reservoir, pumps, filters, coolers, regulators, relief valves, pressure switches, receivers and vacuum degassing tank. A more detailed description of the lube and seal system can be found in Section 8.

TABLE 9 - 1

TRW - OTEC DOUBLE FLOW AMMONIA

EXPANDER BLADE GEOMETRY FOR 1800 RPM

STAGE	TYPE	BLADES PER ROW	BASE DIA. IN.	MEAN DIA. IN.	TIP DIA. IN.	BASE GAUGING ANGLE	MEAN GAUGING ANGLE	TIP GAUGING ANGLE	BASE AXIAL WIDTH	MEAN AXIAL WIDTH	TIP AXIAL WIDTH
1	ROTOR	68	31.0	41.40	51.8	25.51	19.47	15.46	2.45	1.49	.97
	STATOR	38	31.0	41.20	51.4	14.57	17.57	20.42	3.05	3.60	4.15
2	ROTOR	68	31.0	41.90	52.8	25.51	19.23	15.18	2.45	1.46	.94
	STATOR	38	31.0	41.70	52.4	14.57	17.72	20.68	3.05	3.63	4.20
3	ROTOR	68	31.0	42.50	54.0	25.51	18.96	14.85	2.45	1.41	.91
	STATOR	38	31.0	42.30	53.6	14.57	17.88	20.95	3.05	3.66	4.26
4	ROTOR	68	31.0	43.30	55.6	25.51	18.58	14.43	2.45	1.35	.87
	STATOR	38	31.0	43.10	55.2	14.57	18.12	21.25	3.05	3.70	4.35

TABLE 9 - 2

EXPANDER GENERATOR COMPONENT WEIGHTS

	Weight - Pounds
Expander	
Outer Casing	99,400
Endwalls (2)	31,380
Inner Casing Assembly	36,950
Rotor Assembly	12,870
Total Expander Weights	180,600
Generator including Exciter	
Stator	49,400
Rotor	24,250
Cooler	12,990
Total Generator Weights	86,640
Total String Weights	267,240

FIGURE 9-1

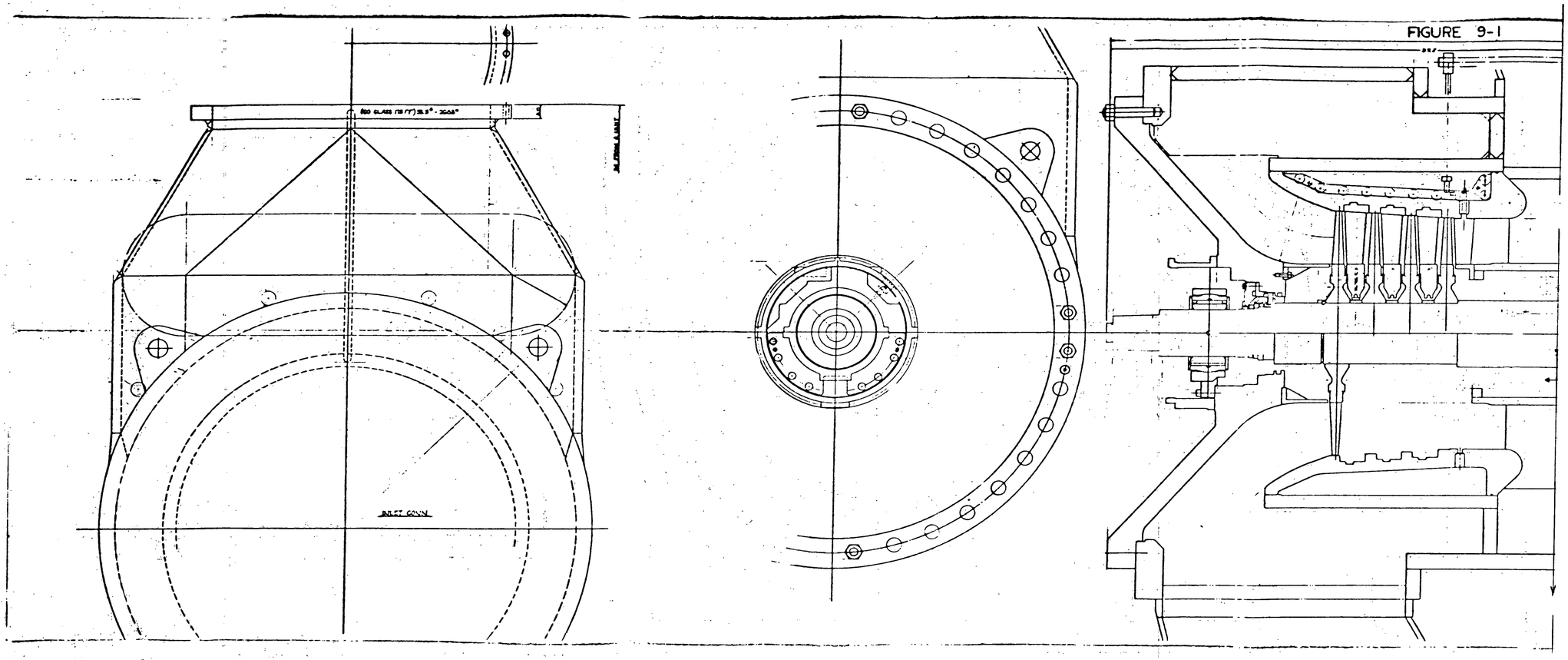

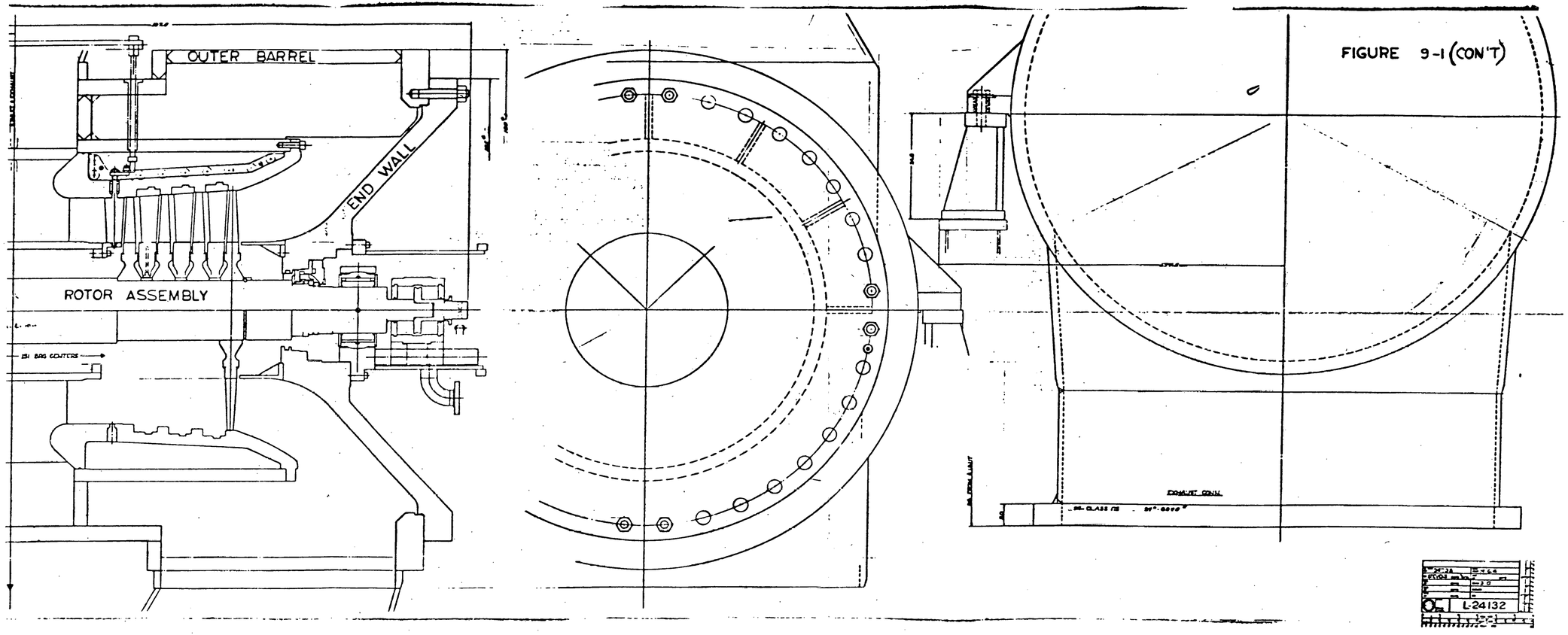

FIGURE 9-1 (CON'T)

TRW-OTEC DOUBLE FLOW AMMONIA EXPANDER BLADE PATH

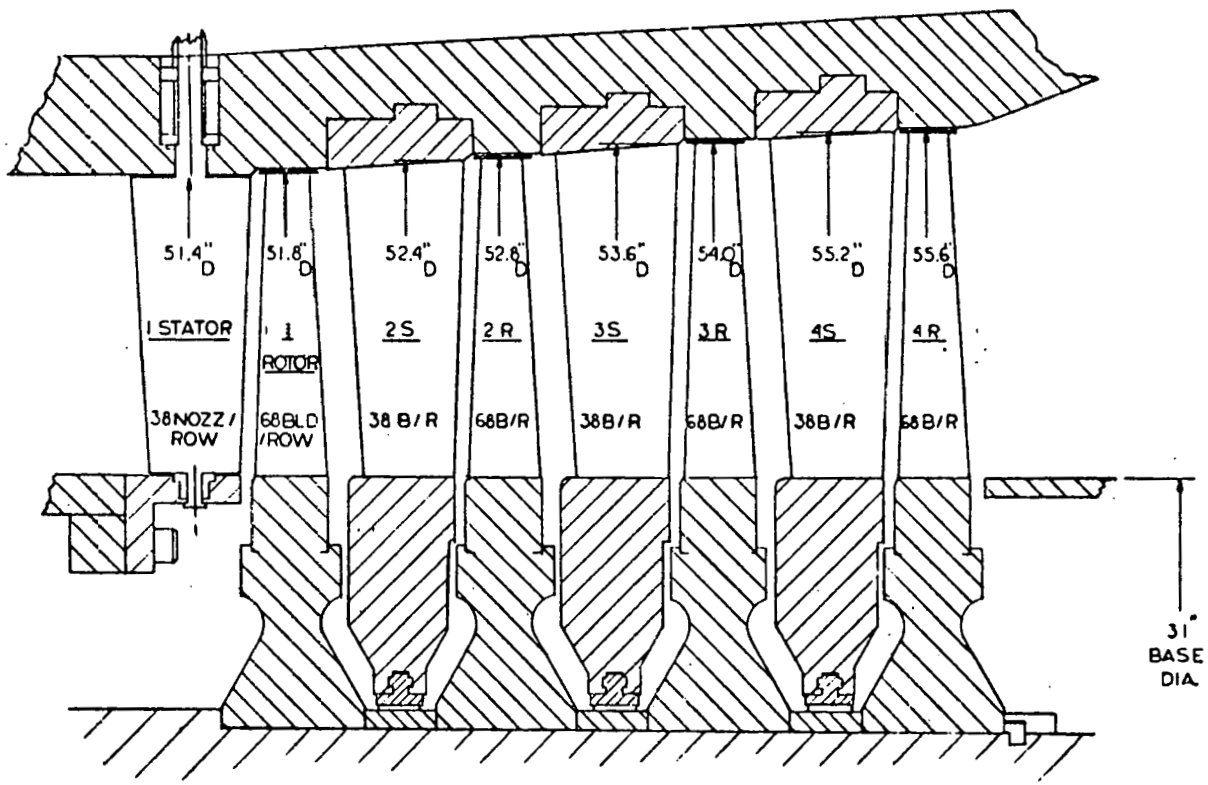

FIGURE 9-2

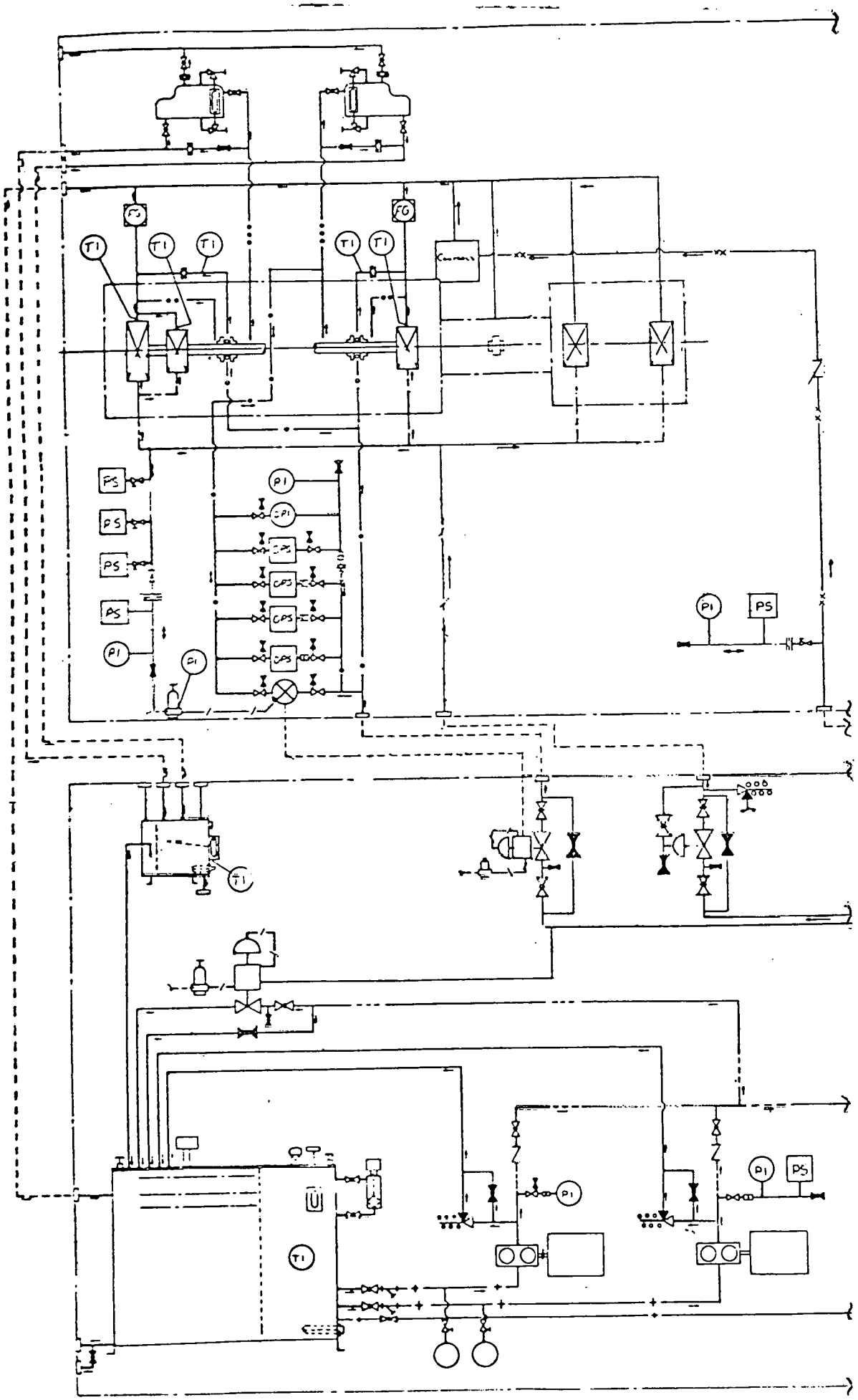
FG
TI
PS
PI

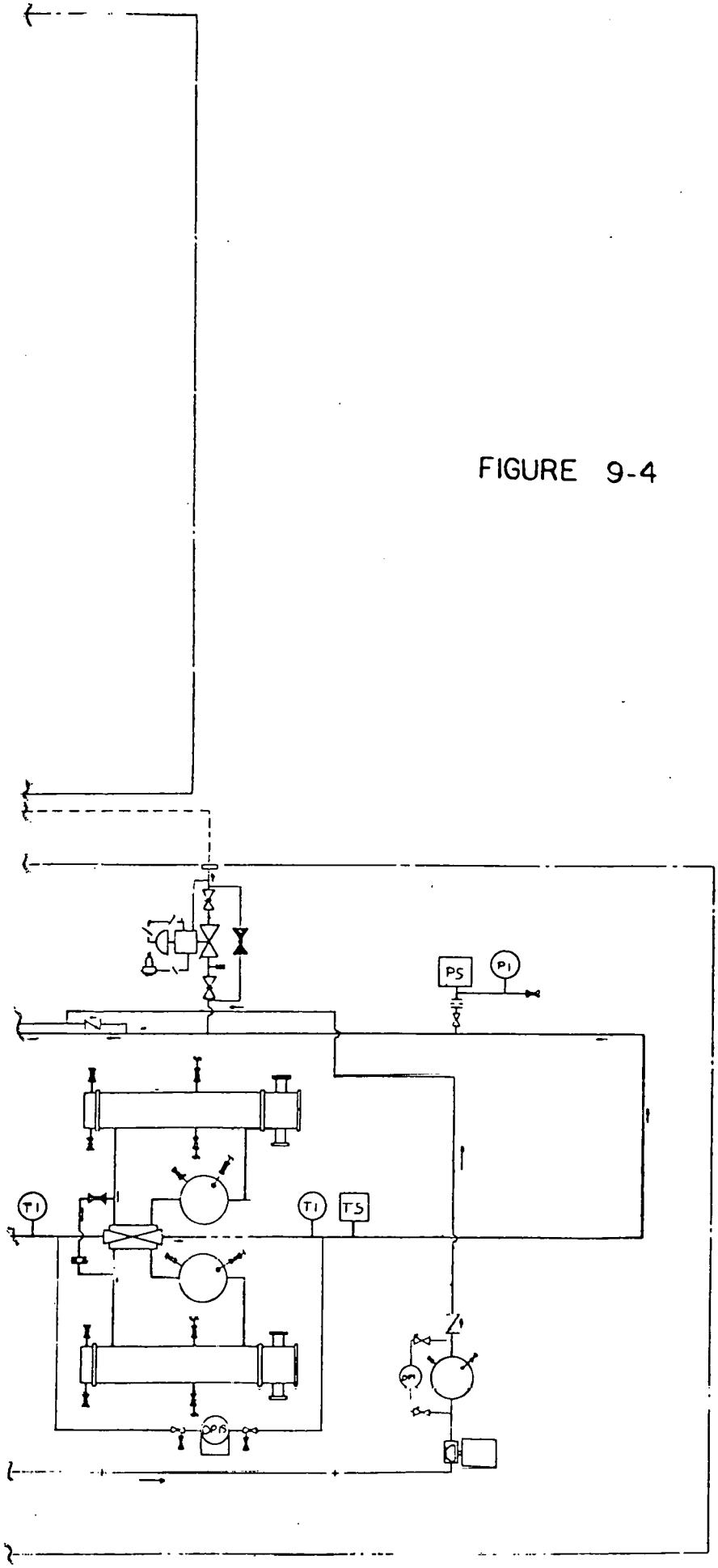

FIGURE 9-4

TRW-OTEC

SCHEMATIC DIAGRAM, OIL FLOW

THIS PAGE

WAS INTENTIONALLY

LEFT BLANK

SECTION 10

MISCELLANEOUS

PROTECTION EQUIPMENT

It is of primary importance that all equipment be provided with overspeed protection when there is a potential that the driver may develop more power than the driven equipment. For this application, one example of an excess of power situation is loss of electric load with a three phase fault on the synchronous generator. At that moment the expander continues to develop the steady state power, but the only load is the train inertia; consequently the speed rapidly increases. Included on the thrust end of the ammonia expander shaft is a pin type overspeed trip. As speed is increased a spring-opposed pin in the expander shaft extension is thrown outward by excessive speed until it hits a striker plate. The movement of the striker plate permits a preloaded cylinder to move and open oil ports which allow a small amount of bearing oil to dump into the bearing case drain. The loss of oil pressure in a small feed line is sensed by a pressure transducer, which signals the trip valve ahead of the expander to shut off the motive fluid and open the bypass valve. The mechanical trip speed setting is to be ten percent above the operating speed, or 1980 rpm. This expander will also be equipped with a manually operated trip so that it may be tripped at any speed simply by turning the trip handle. See Section 7 for additional overspeed protection devices.

INSTRUMENTATION

Mechanical Instrumentation

The expander will be provided with mechanical instrumentation to continuously monitor the performance of the mechanical components and indicate malfunctions.

The expander will be equipped with proximity type vibration probes and read-out devices to monitor shaft vibration. Two probes will be provided at each bearing, 90 degrees apart, for the measurement of the horizontal and vertical vibration components. If the need arises, these probes can also be connected to suitable equipment to determine the journal orbits.

A proximity probe will be provided for measuring the axial position of the expander to indicate possible thrust bearing failure.

A magnetic type speed pick-up will read interruptions from a 60 tooth gear. This device will provide a speed signal to the speed-load control system. It will also be used as an electronic overspeed trip to signal the trip valve ahead of the expander to shut off the motive fluid at three percent above the operating speed, or 1854 rpm.

Thermocouples, or RTD's, will be provided in journal and thrust bearings to monitor bearing metal temperature. Additionally, locally

mounted thermometers will be placed in the oil drains of the journal bearing, thrust bearing and seals for measurement of throw-off temperature. A higher than normal temperature reading may indicate impending bearing or seal failure.

Locally mounted pressure gages will be mounted in the inlet piping to monitor the lube oil pressure and seal oil pressure.

All of the above instrumentation has been extensively used and is accepted practice for rotating equipment in many industries.

Thermodynamic Instrumentation

Pressure measuring devices at the inlet and exhaust flanges will be used to monitor expander conditions. Position of the variable first row stator blades will be determined from an indicator mounted on the external linkage.

Pressure taps located just ahead of each stationary blade will be used during the initial evaluation. These interstage readings will not be used to determine the performance of the expander per se, but might be of assistance to the manufacturer if a question involving performance arises. Further study of the pressure taps to devise a method of purging the lines will be necessary due to the two phase conditions which will be encountered.

For the initial gas rate evaluation of the expander, three additional items pertaining to the motive fluid are required. Devices to measure quality at the inlet and exhaust flanges in conjunction with the pressure measurements, will provide state point data of the ammonia motive fluid. A flow measuring device of suitable accuracy is the third required item. To obtain the necessary accuracy the flow meter must be on the liquid side of the ammonia cycle just after the condenser. To have a valid expander flow value steps msut be taken to insure that the expander bypass valve is closed, and that there are no other leakage paths between the flow meter and the expander inlet.

To complete the gas rate evaluation of the expander/generator system, a high quality calibrated wattmeter to measure generator power output is required. This meter should be retained for monitoring the long-term operation.

A list of the thermodynamic instrumentation required for initial evaluation and long-term operation is contained in Table 10 - 1. Table 10 - 2 is a detailed list of instrumentation for the components of the string.

Gas composition checks should be performed periodically to monitor contaminates and quality of the motive fluid. The gas composition of the motive fluid should be determined with sufficient accuracy for every gas rate evaluation test.

MATERIALS

The preliminary material selections for the major components of the ammonia expander are listed in Table 10 - 3. This listing varies from the usual materials of construction for the specified conditions due to their susceptibility to stress corrosion in the ammonia atmosphere.

For the rotating components the materials proposed are of the same composition as those usually employed for steam turbines. The conditions of heat treatment, however, are different. In conventional steam turbines these materials would be heat treated to a yield strength in the range of 80,000 - 100,000 psi. In this case, in order to improve resistance to stress corrosion cracking, the annealed condition will be used. In this condition, the yield strength will be approximately 30,000 - 50,000 psi, which is sufficient for the application. The problem of stress corrosion cracking of materials of construction in this environment requires further study. Revisions to present selections may be made as a result of such additional investigations.

CODES

The following is a listing of codes and standards applicable to the expander, generator and the lube system.

American National Standards Institute (ANSI)

B1.1: Unified Screw Threads

B2.1: Pipe Threads

B16.5: Steel Pipe Flanges and Flanged Fittings

B16.11: Forged Steel Fittings, Socket-Welding and Threaded

B31.3: Petroleum Refinery Piping

American Petroleum Institute (API)

API 605 Flanges

API 612 Special Purpose Steam Turbines

API 614 Lubrication and Seal Oil Systems

API 617 Centrifugal Compressors

American Socity of Mechanical Engineers (ASME)

Boiler and Pressure Vessel Code:

Section VIII, Division 1, Unfired Pressure Vessels

Section IX, Welding Qualifications

American Society for Testing and Materials (ASTM)

A106 Specification for Seamless Carbon Steel Pipe for High Temperature Service

A193 Specification for Alloy-Steel Bolting Materials for High-Temperature Service

A194 Specification for Carbon and Alloy Steel Nuts for for Bolts for High-Pressure and High-Temperature Service

A266 Specification for Carbon Steel Drum Forgings

A307 Specification for Low-Carbon Steel Externally and Internally Threaded Standard Fasteners

E109 Dry Powder Magnetic Particle Inspection

E125 Reference Phtographs for Magnetic Particle Testing of Ferrous Castings

E138 Wet Magnetic Particle Inspection

National Electrical Manufacturer's Association (NEMA)

SM-21 Turbines, Mechanical Drive Service Multi-Stage

MG-1 Motors and Gears

ISl.1 Enclosures for Industrial Controls and Systems

Tubular Exchange Manufacturer's Association, Inc. (TEMA C)

National Fire Protection Association (NFPA)

Bulletin No. 70: National Electrical Code, Article 500 "Hazardous Location"

SCALABILITY

The scalability of the expander/generator set is controlled by both machines. Since the intention is to use existing generator designs to the maximum extent possible without unduly penalizing the expander, the scalability emphasis will be on the expander.

Brown Boveri Corporation has indicated that they can provide a 4-pole synchronous generator up to 50 MVA. This means that with a 0.8 lagging power factor and 1.0 service factor that the maximum generator power is 40 MW or 53,600 horsepower. Consequently, one of these large

4-pole generators with electronic excitation and double ended shaft can be driven by duplicate ammonia expanders to the design set forth in this study. The maximum single train plant size using a 4-pole generator is, therefore, 30 MW(e) gross.

Four stage double flow ammonia expanders can be scaled from the 15 MW(e) gross units for this study to larger capacities. The first item to consider in scaling is that the use of a gear in the string adds an undesirable parasitic loss of 1-1/2 to 2 percent. To eliminate this loss all we have to do is scale the expanders to operate at a speed which matches a generator speed. Therefore, expanders have been scaled to operate at 1200 rpm and 900 rpm; see Table 10 - 4.

To optimize performance at 1200 rpm, the scaled unit will have to operate at the same velocity ratio as the 1800 rpm unit. Consequently, the scaled pitch diameter will have to be 1.5 times (1800 ÷ 1200) the 1800 rpm unit's pitch diameter. If we retain the same L/D ratio the new scaled base diameter will also be 1.5 times the 4-pole unit, or 46.5 (1.5 x 31) inches. Since pitch diameter and blade length have both increased by 50 percent, the 1200 rpm expander flow passing capacity will be 2.25 times (1.5 x 1.5) the 1800 rpm unit. Efficiency will be just slightly higher for the larger machine as shown in Figure 10 - 1. Plant capacity for the one 46.5 base diameter expander driving a 6-pole generator will be 33.75 MW (e) gross. Once again, if the generator is double ended, two 46.5 inch base diameter expanders can drive one

generator for a 67.5 MW(e) gross plant. At this time, it is important to note that the controls to balance two expanders will be somewhat more involved; the maximization of power feature will require particular attention.

In a similar fashion an expander could be scaled to operate at the 8-pole speed of 900 rpm. The capacity of this unit would be 4 times the 1800 rpm unit. Therefore, the plant capacity would be 60 MW(e) gross for the single body and 120 MW(e) gross if duplicate units are attached to each end of the generator shaft. It has been assumed that 8-pole generators are available for the required output.

This scaling necessarily limits the available output power, since it is done on the basis of synchronous running speed. If synchronous generator operation is required, the optimum scales of the 15 MW(e) gross design are the two previous designs discussed, the 33.75 MW(e) gross and the 60 MW(e) gross. For any other required power, lower efficiency will result. A direct scale of the 15 MW(e) gross design to any other power in the range of 25 MW(e) gross to 75 MW(e) gross will operate at nonsynchronous speed and a gear, along with its 2 percent power loss, would have to be employed. This gear loss is responsible for lower efficiencies at other than optimum scales.

The units in the range of 25 MW(e) gross to 75 MW(e) gross would be scaled on the basis of power output, with the speed being scaled

later. For a 25 MW(e) gross power output, the scaling factor would be 25 ÷ 15, or 1.667. The pitch diameter and the base diameter would both be scaled by the square-root of 1.667, since the L/D ratios would be constant. This results in a base diameter of 40 inches. The speed would be scaled by the inverse of the square root of 1.667 in order to maintain the proper velocity ratio. This resulting speed is 1394 RPM. A 75 MW(e) gross power output unit would be scaled similarly, except the scale factor would be 5.00 (75 ÷ 15). The new base diameter would be 69.3 inches (31 x 2.236) and the new operating speed would be 805 RPM (1800/2.236).

Each scaled design of the 15 MW(e) gross unit will be the highest performing design for their own particular scaled speed. This does not necessarily mean that a scaled design running at a scaled, nonsynchronous speed cannot be out performed by another design running at a synchronous speed. It is possible for a nonscaled design running at a synchronous speed driving a synchronous generator to produce more power than a scaled design running at a nonsychronous speed driving through a gear to a synchronous generator. The latter incurs a performance penalty from the gear, possibly lowering its output power below that of the former. If the generator can be run at a nonsynchronous speed for any reason, the scaled design running at a scaled speed will be the most efficient for any desired gross power output.

So far, this discussion of scalability has considered only the

thermodynamic aspects. Manufacturability must also be considered in the determination of maximum expander size. The 15 MW(e) gross output expander set forth in this study is approaching the limits of this manufacturer's plant capabilities. It is felt that any of these scaled units are within the worldwide state-of-the-art of manufacturability.

TABLE 10 - 1

THERMODYNAMIC INSTRUMENTATION REQUIREMENTS

ITEM	REQUIREMENT	
	INITIAL	LONG-TERM
FLOW METER	YES	YES
INLET PRESSURE	YES	YES
INLET QUALITY	YES	YES
EXHAUST PRESSURE	YES	YES
INTERSTAGE PRESSURE AHEAD OF EACH STATOR	YES	NO
COMPOSITION	YES	YES

TABLE 10 - 2

INSTRUMENTATION

Area of Use or Type of Instrument	Recommended Quantity	Signal Type
Mechanical Instrumentation		
Lube Oil Console Instrumentation		
1) Oil Reservoir Level Alarm Switch	1	Voltage
2) Differential Pressure Indicator Switch	1	Voltage
3) Temperature Switch	1	Voltage
4) Pressure Switch	7	Voltage
5) Differential Pressure Switch	4	Voltage
5) Temperature Indicator	9	Voltage
7) Pressure Indicator	6	Voltage
3) Differential Pressure Indicator	2	Voltage
Expander		
1) Overspeed Trip Pressure Transducer	1	Voltage
2) Magnetic Speed Pickup	1	Frequency
3) Bentley Vibration Probes	4	Voltage
4) Bentley Axial Position Probe	1	Voltage
5) Bearing Thermocouples or RTD's	6	Voltage

T A B L E 10 - 2 (cont.)

INSTRUMENTATION

Area of Use or Type of Instrument	Recommended Quantity	Signal Type
Generator		
1) Stator RTD's	6	Voltage
2) Bearing RTD's	2	Voltage
3) Cooling Air RTD's	3	Voltage
4) Cooling Water RTD's	1	Voltage
5) Cooling Water Leakage Detector	1	Voltage
6) Bentley Vibration Probes	4	Voltage
7) Walt Meter For Generator Load	1	Binary Coded Decimal
Thermodynamic Instrumentation		
1) Inlet Pressure Transducers	4	Voltage
2) Exhaust Flange Pressure Transucers	4	Voltage
3) Interstage Pressure Transducers	12	Voltage
4) Liquid Ammonia Calibrated Venturi Tube		
a) Pressure Transducers	8	Voltage
b) Thermoccuples	2	Voltage

TABLE 10 - 3

MATERIALS OF CONSTRUCTION

FOR MAJOR COMPONENTS

OF AMMONIA EXPANDER

PART	MATERIAL	FORM	MIN. YIELD - psi
OUTER CASING BARREL	SA-516 GRADE 60	PLATE	32,000
ENDWALLS	SA-226 CLASS 1	FORGED	30,000
	SA-516 GR 60	PLATE	32,000
STATOR HOUSING	SA-216 GR WCB	CAST	36,000
DIAPHRAGMS	SA-516 GR 60	PLATE	32,000
STATOR BLADES	AISI TYPE 405	BAR	25,000
ROTOR BLADES	AISI TYPE 403 ANNEALED	BAR	35,000
DISCS	AISI 4140 ANNEALED	FORGED	50,000
SHAFT	AISI 4140 ANNEALED	FORGED	50,000

TABLE 10 - 4

SCALED EXPANDERS

GROSS OUTPUT MW(e)	SPEED RPM	BASE DIAMETER INCHES	RELATIVE THRUPUT
15	1800	31.0	1.0
33.75	1200	46.5	2.25*
60	900	62.0	4.0 *
25	1394	40.0	1.667*
75	805	69.3	5.0 *

*Assumes synchronous generators are available at these speeds for the required output with the same efficiency as the 15 MW(e) gross unit.

FIGURE 10-1

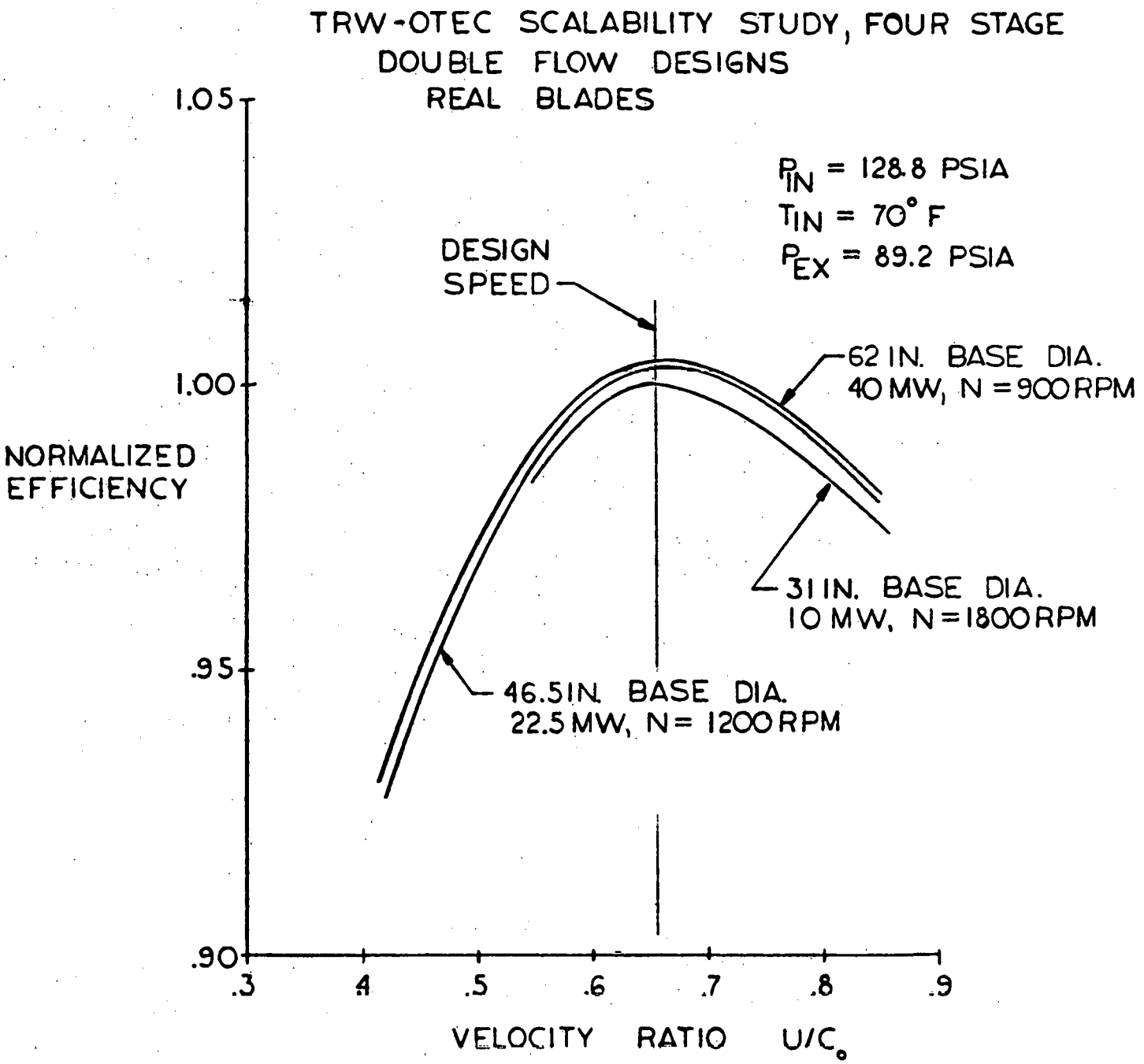
TRW-OTEC SCALABILITY STUDY, FOUR STAGE
DOUBLE FLOW DESIGNS
REAL BLADES
P_{IN} = 128.8 PSIA
T_{IN} = 70° F
P_{EX} = 89.2 PSIA
DESIGN SPEED
62 IN. BASE DIA.
40 MW, N = 900 RPM
31 IN. BASE DIA.
10 MW, N = 1800 RPM
46.5 IN. BASE DIA.
22.5 MW, N = 1200 RPM
NORMALIZED EFFICIENCY
1.05
1.00
.95
.90
.3
.4
.5
.6
.7
.8
.9
VELOCITY RATIO U/C$_o$

ATTACHMENT 1

REFERENCES

1. Ainley, D.C. and Mathieson, G.C.R., "A Method of Performance Estimation for Axial-Flow Turbines", British Aeronautical Research Council, R & M 2974, 1951.

2. Dunham, J. and Came, P.M., "Improvements to the Ainley-Mathieson Method of Turbine Performance Prediction", ASME Paper 70-GT-2, 1970.

3. Craig, H.R.M and Cox, H.J.A., "Performance Estimation of Axial Flow Turbines", Proceedings of The Institution of Mechanical Engineers, 1970 - 71.

4. Silver, H.F. and Nydahl, J.E., Introduction to Engineering Thermodynamics, West Publishing Company, 1977.

5. Reisweber, R.C., "Supercharger Diffuser Development", Elliott Company, TM 272, 1965.

6. Hench, J.E. and Johnston, J.P., "Two-Dimensional Diffuser Performance with Subsonic, Two-Phase, Air-Water Flow, ASME Paper 71-FE-30, 1971.

7. Shepherd, D.G., Principles of Turbomachinery, The Macmillan Company, 1956.

8. More, M.J. and Sieverding, C.H., Two-Phase Steam Flow In Turbines and Separators, Hemisphere Publishing Corporation, Washington, 1976.

9. Handbook of Chemistry and Physics, 45th Edition, 1964 - 65.

10. Claydon, J.E., "Moisture Erosion", Elliott Company Letter, April 14, 1975.

11. Sawyer's Gas Turbine Engineering Handbook, Second Edition, 1972.

12. Liquid Rocket Engine Turbines, NASA - SP-8110, January, 1974.

ATTACHMENT 2

NOMENCLATURE

SYMBOLS

C_o	Isentropic velocity, $C_o = 223.77 \sqrt{\Delta H_o}$ (ft./sec.)
C	Absolute velocity (ft./sec.)
L/D	Ratio of blade height to mean blade path diameter
N	Shaft speed (rpm)
P	Pressure (psia)
T	Temperature (°F)
U	Mean blade speed (ft./sec.)
U/C_o	Velocity ratio
V	Specific volume ($ft.^3/lbm.$)
W	Relative velocity (ft./sec.)
α	Fluid absolute angle measured from tangential plane, at stator exit
β	Fluid relative angle measured from tangential plane, at rotor inlet
β_3	Fluid relative angle measured from tangential plane, at rotor inlet
ΔH_o	Isentropic heat drop (BTU/lbm.)

SUBSCRIPTS

IN	At expander inlet
EX	At expander exhaust
1	At stator exit or rotor inlet
2	At rotor exit

DEFINITIONS

Axial Width ---- The axial width is the maximum width of the blade in the axial direction at the specified section as shown in Figure B-1.

Base Diameter -- The base diameter of a blade is the minimum diameter of the blade where the blade joins the hub as shown in Figure B-2.

Free-Vortex ---- Free-vortex flow is flow with a specified variation in the absolute tangential velocity within the blade path with diameter such that radial inflow equilibrium is maintained. For this type of flow the axial velocity is constant across the entire blade path while the tangential velocity decreases linearily with diameter. Therefore, as the diameter increases across the blade row the stage reaction constantly increases.

Gauging Angle -- The blade gauging angle is defined as the design blade fluid exit angle, and is calculated as the arcsine of the blade throat divided by blade pitch distance. See Figure B-1 for a pictorial representation of the gauging angle.

Mean Diameter -- The diameter of the blade suction half way between (average) the blade base and tip suctions.

Normalized Efficiency ---- Normalized efficiency is defined as being the calculated efficiency divided by the efficiency of a four stage, 31 inch base diameter design with similar blading.

Pitch ---------- The distance between similar points on adjacent blades in the circumferential direction as shown in Figure B-1.

Stage Reaction - The ratio of energy transfer in the rotor resulting from a static pressure change to the total energy transfer in the stage.

Throat --------- The minimum flow area between adjacent blades as shown in Figure B-1.

Tip Diameter --- The tip diameter is the highest or last blade section as shown in Figure B-2.

Velocity Ratio - (12) The velocity ratio for a single stage configuration is $\frac{U}{C_o} = \frac{\text{pitchline velocity}}{\text{theoretical spouting velocity}}$; however, for a multistage turbine design, the numerator of the velocity-ratio term represents the square root of the sum of the squares of the pitchline velocities of each stage. Therefore, the precise expression for velocity ratio for either a single stage or multistage turbine is $\sqrt{\Sigma U^2}/C_o$. However, the velocity ratio will be consistently expressed as U/C_o, it being understood that for a multistage turbine $U = \sqrt{\Sigma U^2}$.

FIGURE B-1

BLADE TERMINOLOGY

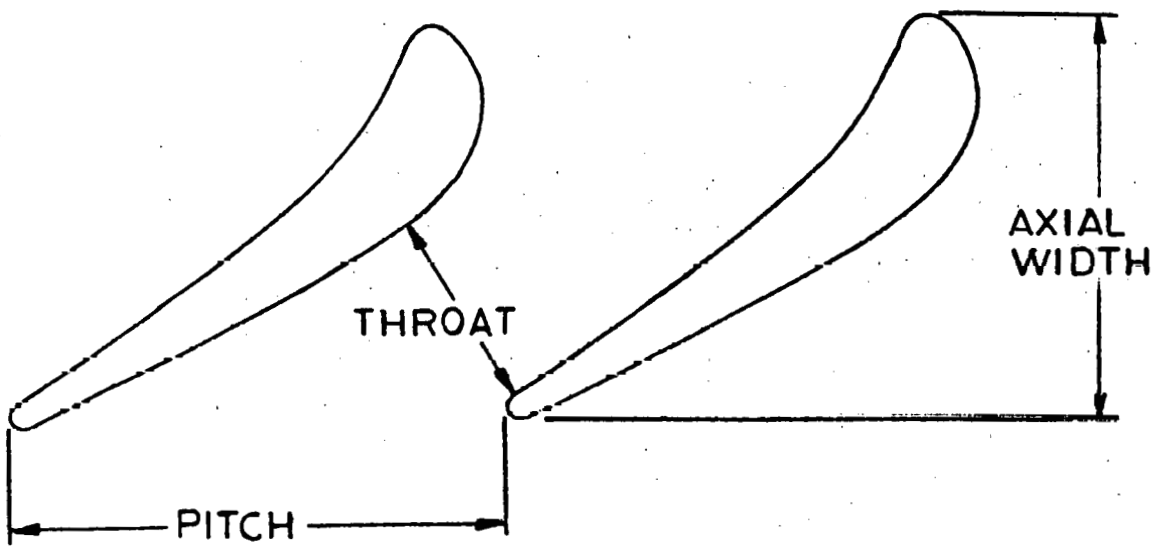

$$\text{GAUGING ANGLE} = \text{ARCSIN}\left(\frac{\text{THROAT}}{\text{PITCH}}\right)$$

FIGURE B-2

TURBINE STAGE DIAMETERS

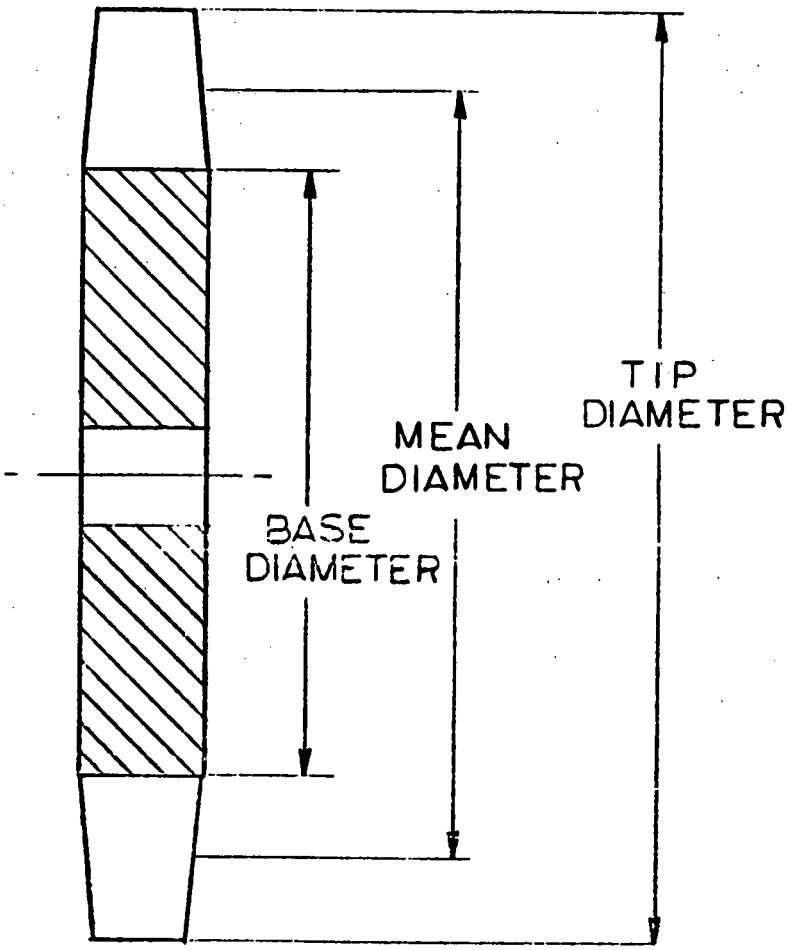

APPENDIX G

TUBE CLEANER DESIGN

THIS PAGE

WAS INTENTIONALLY

LEFT BLANK

APPENDIX G.1

HYDRAULIC TUBE CLEANER ANALYSIS

G.1. HYDRAULIC TUBE CLEANER ANALYSIS

SCOPE

This analysis investigates the design parameters of the hydraulic tube cleaner. The analysis was required for the preliminary design. The following parameters were studied:

- Tube dimensions
- Water volume and weight
- Piston size
- Flow area
- Pump head
- Required power
- Flow rate
- Bouyancy
- Slippage flow rate

PREPARED C Williamson 4/2/78 REPORT NO. PAGE 1A

CHECKED

MODEL

Hydraulic Tube Cleaner

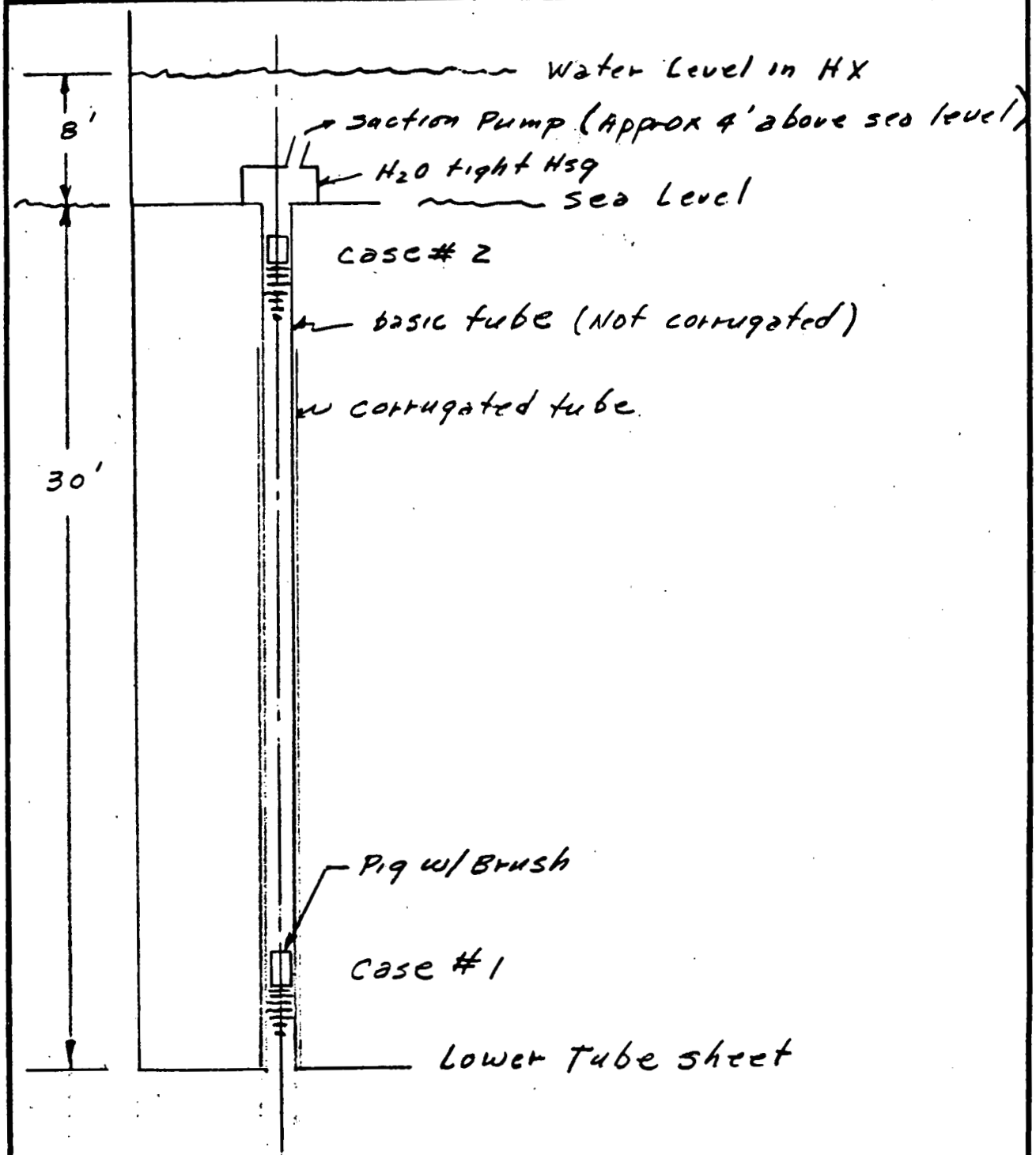

Hydraulic Tube cleaning concept

Tube Dimensions

1.00" OD Basic X 0.031 wall (E) x 0.026" wall (C)
0.990 " Finished
0.866 ID "
0.037 Inner Fill depth
0.883 Equiv H_2O dia.; $A_e = \frac{\pi}{4}(.883)^2 = 0.6124\ IN^2$
36 Flutes

Volume of H_2O in a single tube

$$V_t = \frac{\pi}{4}(0.883)^2(30')(12) = 220\ IN^3$$
$$= 0.1276\ Ft^3$$
$$= 0.9543\ gal$$

Size Piston (Pig behind brush)

Assume 1/64 diametral clearance

$$D_p = 0.866 - 0.016 = 0.850$$
$$A_p = \frac{\pi}{4}(0.850)^2 = 0.567\ IN^2$$

Inner Fill Area

Estimated as trapezoid

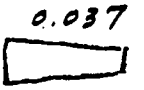

$$A = \frac{1}{2}h(a+b)_{\wedge}^{36} = \frac{1}{2}(0.037)(0.04+0.012)(36)$$
$$= 0.0346\ IN^2\ (Approx)$$

Total Flow Area/tube

$$A_T = 0.567 + 0.0346 = 0.602\ IN^2$$
(should be $0.6124\ IN^2$)

Pump Head to Drive Brush (w/ 60% margin)

Assume brush drag $\cong$ 5 lbs (use 8 lbs)

$$P = F/A = 8/.567 = 14.1\ psid$$
$$= \frac{14.1}{0.433\ \frac{psi}{ft\ H_2O}} = 32.58\ ft\ of\ H_2O$$

Hydraulic cleaner

Wt of H_2O / 100 tubes

$$W = (100)(0.1276)(62.4) = 796 \text{ lbs}$$
$$N \qquad Ft^3$$

Pump Horsepower (w/o slippage past pig)

Assume 20 sec stroke time (one way) ($V \cong 1.5$ fps)

$$w = \frac{796(60)}{20} = 2388 \text{ lbs } H_2O/\text{min}$$

$$W\,HP = \frac{w\,h}{33{,}000} = \frac{2388(32.58)}{33{,}000} = \underline{2.35\ HP}$$

Find Slippage Flow Rate

$$A_s = \underset{(\beta.1)}{0.0346} + \frac{1}{128}\pi\left[\frac{\underset{(0.858)}{0.866} + 0.850}{2}\right]$$

$$" \quad + 0.0211 = \underline{0.0556\ IN^2}$$

$$Q = cA\sqrt{2gh}$$

$c \cong 0.6$; $h = 32.58$; $A = \frac{0.0556}{144} = 3.86 \times 10^{-4}$

$$= 0.6(3.86 \times 10^{-4})\sqrt{2(32.2)(32.58)}$$

$$= 0.0106 \ ft^3/sec \times 62.4 \left(\frac{\#}{ft^3}\right) \times 60 \left(\frac{sec}{min}\right) = \underline{39.72} \ \frac{lb\ H_2O}{min\ tube}$$

Slippage HP Loss

$$W_S HP = \frac{(39.72 \times 100)(32.58)}{33{,}000} = \underline{3.92\ HP}$$

Total HP

$$W HP_T = 3.92 + 2.35 = \underline{6.27\ HP}$$

Basic Flow Rate in Tubes

$v = c_v \sqrt{2gh}$ where: $c_v \cong 0.6$
$h = 8$ ft H_2O
v = fps

$= 0.6 \sqrt{2(32.2)(8)} = 13.62$ fps

$Q = Av$ $A = 0.6124$ in^2
$= 0.0043$ ft^2

$= (0.0043)(13.62) = 0.0579$ ft^3/sec
$= 3.47$ ft^3/min
$\cong 217$ lb/min
$= 3.61$ lb/sec

Flow Rate per tube w/ brush

$v_b = c_v \sqrt{2gh_e}$ $c_v \cong 0.6$

h_e = pump head − head loss due to brush force

$= 32.58 - \frac{5 \text{ lbs}}{0.567 \text{ in}^2} \times \frac{1 \text{ ft}}{0.433 \frac{\text{lb}}{\text{in}^2}}$

$= " - 20.36 = 12.21$ ft H_2O

$v_b = 0.6 \sqrt{2g(20.36)} = 21.73$ fps

$Q = Av_b = \frac{0.6124}{144}(21.73) = 0.092 \frac{\text{ft}^3}{\text{sec}}$
$= 5.54$ ft^3/min
$= 346$ lb/min
$= 5.76$ lb/sec

Potential Bouyancy per IN of Hollow pig length

pig O.D = 0.850
Assume 0.032 wall

$d_i = 0.7860$ $A_i = 0.4852\ IN^2$

$H_2O = 62.4 \frac{\#}{ft^3} = 0.0361 \frac{lb}{in^3}$

Bouyancy $= (0.4852)(0.0361) = 0.0175 \frac{lb}{in.}$
(Negligible)

CASE # 2

Find Slippage Flow Rate in smooth part of tube

Tube OD = 1.000 1.000
wall = .031 x 2 = 0.062
0.938 ID

Flow Area = $\frac{\pi}{4}[0.938^2] - 0.567$ (From p. 1)
$= 0.1240\ IN^2 = 8.6 \times 10^{-4}\ ft^2$

$Q_s = C_v A \sqrt{2gh}$
$= 0.6 (8.6 \times 10^{-4}) \sqrt{2g(32.58)}$
$= 0.0236\ ft^3/sec$
$= 1.47 \frac{lb}{sec}$ $= 88\ lb/min$ / tube
$= 8800\ lb/min$ for 100 tubes

Find Head Developed in Smooth section

Assume Constant Flow Pump @ 2388 + 3972 lb/min
$= 6360\ lb/min$
$= 1.699\ ft^3/sec$

$Q_s = C_v A \sqrt{2gh}$

$h = \frac{1}{2g}\left[\frac{Q}{C_v A_s}\right]^2$

$A_s = 8.6 \times 10^{-4} (10)$
$= 8.6 \times 10^{-2}\ ft^2$ / 100 tubes

$= \frac{1}{64.4}\left[\frac{1.699 \times 10^2}{(0.6)(8.6)}\right]^2$

$= 16.84\ ft\ of\ H_2O$

PREPARED C Williamson 6/2/70 REPORT NO. PAGE 5

CHECKED

MODEL

Hydraulic Tube Cleaner

Globe proposes a "Net Fit" brush serrated to match the convolutes. Brush lengths of from 18" to 2' long are proposed by Globe and brush force of 5 lbs is their estimated drag.

With such brush lengths, it is expected that the slippage flow will be a small fraction of the 39.72 lbs/min estimated on p. 2. Therefore, the force delivered to the brush due to the pump head of 32 1/2 ft will approach the effective H_2O flow area (0.883" dia)

$$F \cong (14.1)(0.883)^2 \frac{\pi}{4} = 8.63 \text{ lbs}$$

Hydraulic Tube Cleaner

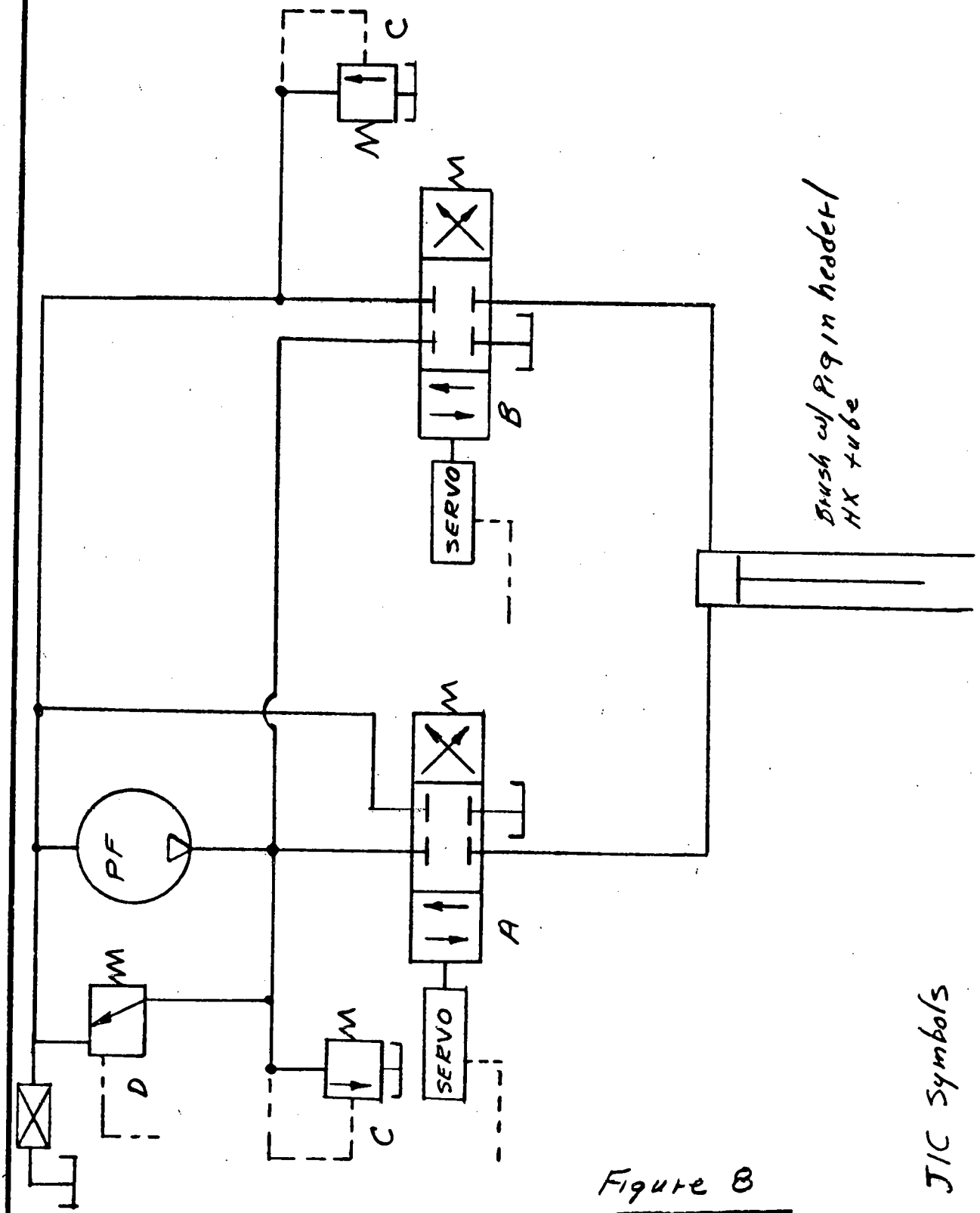

Figure 8

HYDRAULIC CLEANER

VOL OF WATER IN 102 TUBES - 20 SEC

VOL. WATER PER TUBE = 0.9543 GAL (PER WILLIAMSON)

PER 102 TUBES = 97.34 GAL.

FOR 20 SEC. STROKE PUMP FLOW RATE JUST TO FILL TUBES = 3 x 97.34 GAL = 292 GPM

PER WILLIAMSON ASSUME SLIPPAGE FLOW RATE IS ONLY FRACTION OF TUBE VOL. SAY 25%

THEN PUMP CAPACITY = 292 GPM + $\frac{292\ GPM}{4}$ = 365 GPM @ 14

VOL WATER IN 70 TUBES (REMOVE 32 PERIMETER TUBES)

= .9543 x 70 = 66.801 GAL

FOR 30 SEC. STROKE PUMP FLOW TO FILL TUBES

= 66.801 GAL x 2 = 133.602 GPM

ASSUMING SOME SLIPPAGE WILL OCCUR (SAY 10%)

SIZE PUMP TO 150 GPM @ 25 PSI MAX OUTPUT PRESS.

PUMP CAPACITY REQ'D FOR 30 SEC. BRUSH STROKE 102 TUBES

97.34 GAL/30 SEC = 194.68 GPM ASSUMING 25% SLIP FLOW

TOTAL FLOW RATE REQ'D = 195 + $\frac{195}{4}$ = 244 GPM

OUTPUT PRESS = 50 PSI (EST.) SAY **250 GPM**

APPENDIX G.2

OTHER DESIGN CONSIDERATIONS WITH RESPECT TO THE HYDRAULIC TUBE CLEANER

G.2. OTHER DESIGN CONSIDERATIONS WITH RESPECT TO THE HYDRAULIC TUBE CLEANER

SCOPE

Discussions pertaining to the design of the mechanical latch, magnetic latch, passive ultrasonic transducer, active ultrasonic transponder, and nuclear detector device are presented herein. All these discussions consider some device to indicate the bottom of the stroke for the hydraulic tube cleaner.

MECHANICAL LATCH

The mechanical latching system is illustrated in Figure 1. The brush has two pigs located at each end with protruding springs, and one pig in the middle of the brush to contain a latching mechanism. As shown in Figure 1 the two springs are connected with a string which runs in a small tube along with other wires that hold the bristles of the brush. The string is wound around a drum on the latching mechanism (shown as a permanent magnet) in the middle pig.

At the top of the stroke the top spring protrudes from the tube, expands, pulls on the string, and cocks the latch in one position. At the bottom the other spring recocks the latch. The latch itself could be a permanent magnet as shown in Figure 1 whose position could be detected by a simple electronic circuit.

Note that there is no way that the latch could be cocked or recocked during transit unless one end of the brush actually protrudes outside the tube.

Advantages/Disadvantages:

In principle this is a very simple mechanical device which should be 100 percent reliable. However, it may not be as easy to design and build as it appears. For example assembly and sealing of the device would present some challenging problems.

FIG 1 MECHANICAL LATCH

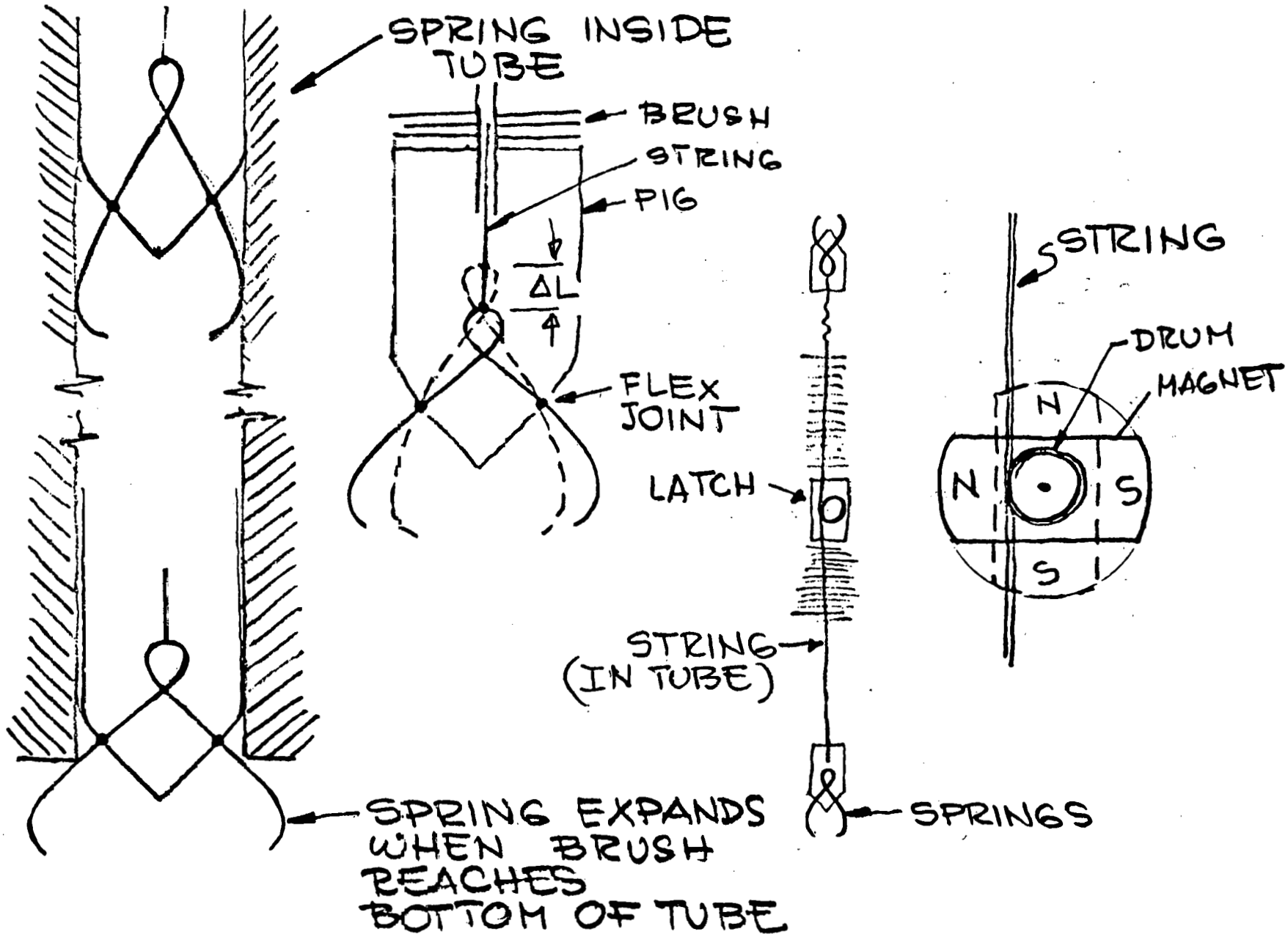

MAGNETIC LATCH

This system contains magnetic latches incorporated in each brush as illustrated in Figure 2. The magnetic latches are set prior to starting the downstroke by an electric magnet and reset by permanent magnets located at the bottom of the tubes. Monitoring the current through the electric magnet during the "set" operation it will be possible to determine whether the magnet has been properly reset by the permanent magnets at the bottom of the stroke.

Disadvantage: Each tube would require a permanent magnet installed at the bottom. Although these magnets could be very cheap (~5¢ each) they would require extensive testing to insure that they last the lifetime of the system. In addition, if some of the magnets failed for some reason, it would be difficult, if not impossible to repair them in situ.

FIG 2
MAGNETIC LATCH

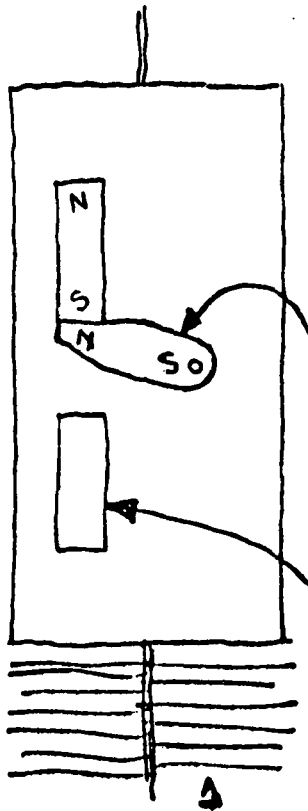

TOP POSITION:

SET LATCH USING EXTERNAL ELECTRIC MAGNET

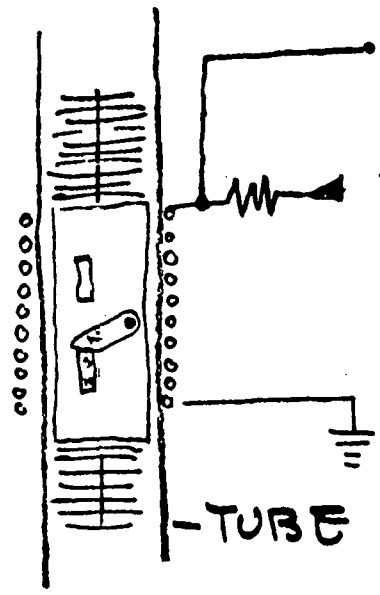

PERMANENT MAGNET LATCH

STEEL BARS

BRUSH

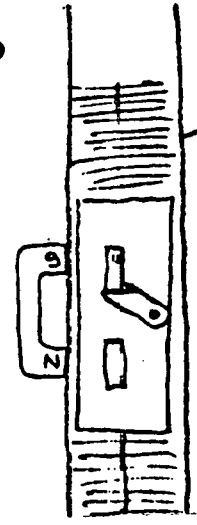

BOTTOM POSITON:

RESET MAGNET USING PERMANENT MAGNET

PASSIVE ULTRASONIC TRANSDUCER

This system incorporates passive ultrasonic transponders in the brushes as shown in Figure 3. The transponders are connected to receiver/transmitter antennas which protrude from the bottom of the brushes. The transponders, in form of a metalic dumbell act like tuning forks when excited by exterior ultrasonic waves. Each brush has a transponder that responds to a different frequency. When the brushes are at the bottom of a stroke with their antennas protruding below the bottom tube sheet an external ultrasonic transducer transmits signals of the appropriate frequencies, and then listens for a return. Thus it would be possible to check that all the brushes have reached the bottom of the stroke.

Advantages: Very simple, inexpensive and possibly perfectly reliable system.

Disadvantages: Would require extensive testing after installation to insure that harmonics and resonances do not give false signals.

FIG 3. ULTRASONIC - PASSIVE

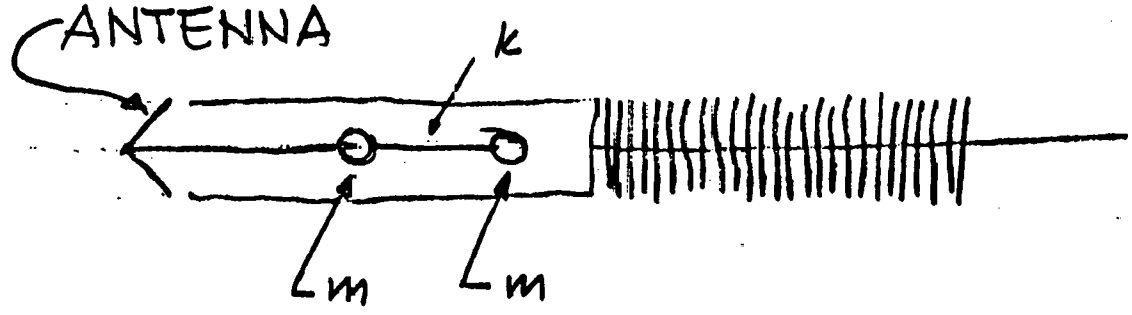

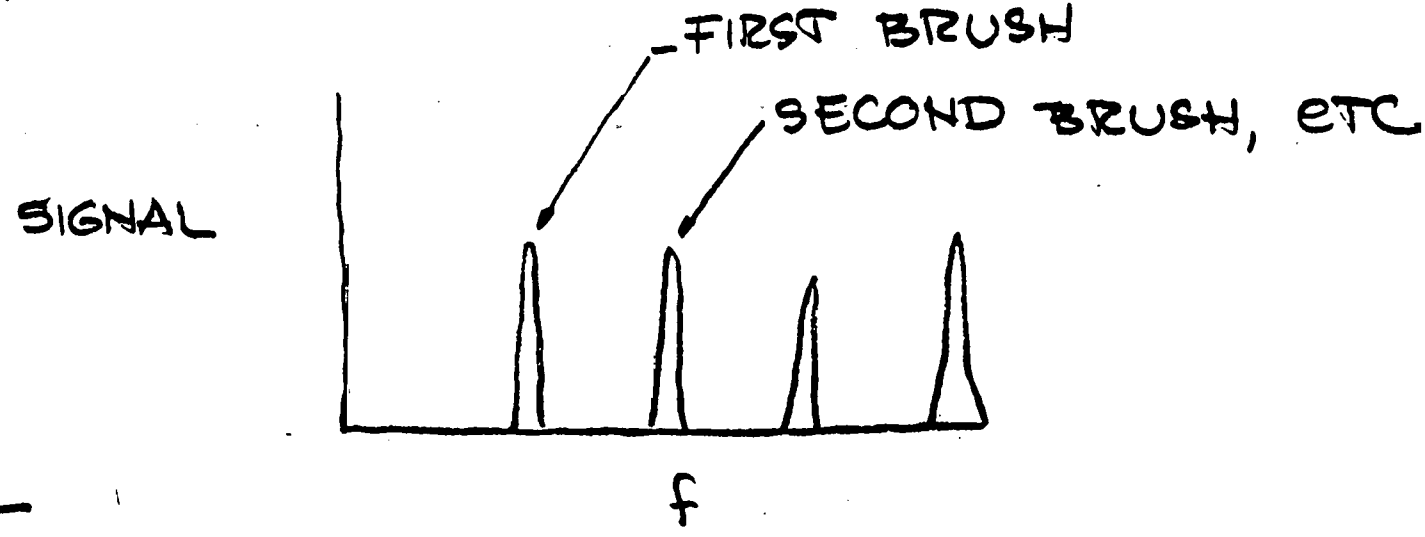

$$f = \frac{1}{2\pi}\sqrt{\frac{k}{m}}$$

ACTIVE ULTRASONIC TRANSPOWER

This device illustrated in Figure 4 consists of an active ultrasonic transmitter and receiver incorporated in each brush. At the start of the cycle the transmitter in each brush is charged up by a magnetic coupling arrangement as illustrated in lower left hand corner of Figure 4. When the brush reaches the bottom of the stroke, the brush stops are arranged so that the transmit/receive antennas protrude through the lower tube sheet. An external ultrasonic transducer located in the chamber below the heat exchanger interrogation could be done by coding each of the brushes with a different signature which the ultrasonic transponders in the brushes recognize and answer to. For example: the external transducer would send out the code for brush #1, receive an answer, the brush #2, etc.

Advantages: The active ultrasonic transponder appears to be the best system for detecting the brushes of all the approaches considered here. The main advantages are that this system should be very reliable and require very little testing or adjustment after installation.

Disadvantages: Some development effort would be required to design the ultrasonic transducers as well as the transducer interrogating system.

ACTIVE ULTRASONIC TRANSPONDER

FIG 4.

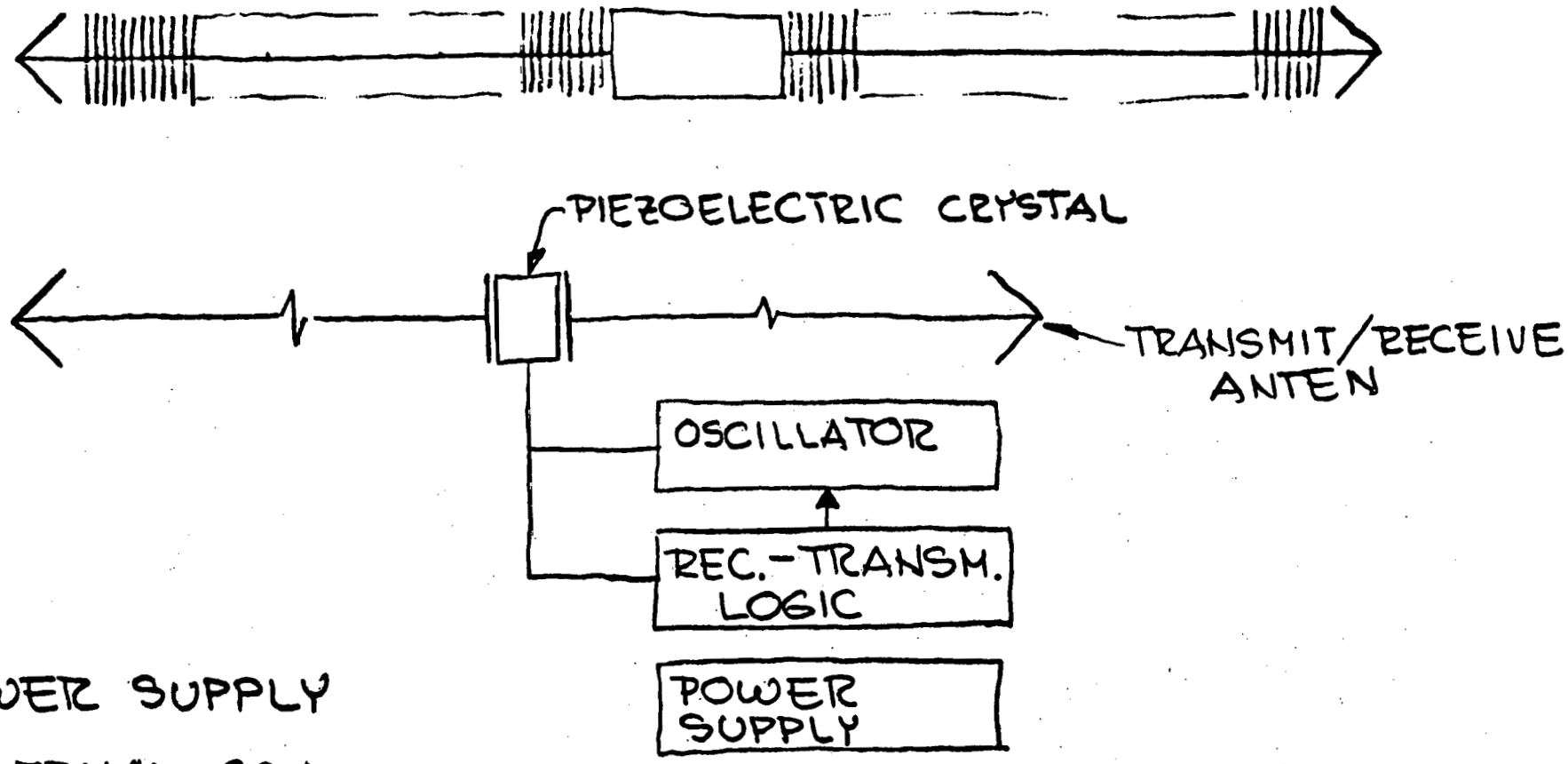

NUCLEAR DETECTOR DEVICE

This scheme, shown in Figure 5 uses an ionization chamber located in a pig attached to the brush and radioisotope sources (such as cobolt-60 or cessium -137) located at the bottom of the tubes. At the start of the stroke the ionization chamber is charged up by external means. When the brush reaches the bottom of the tube the ionization chamber is discharged by the radiation from the radioisotope sources. After the brush is returned back to the brush holder the status of the ionization chamber is interrogated via a magnetic coupling device as illustrated in Figure 5a.

Since the ionization chamber can be discharged only by penetrating nuclear radiation there is virtually no chance that it could discharge before reaching the radioisotope sources at the bottom of the tubes. A very intense cosmic ray shower could have some effect, however, it would be possible to design the system in such a way that the probability of the ionization chamber discharge by cosmic rays would be extremely small.

Advantages: The nuclear detector device should be inexpensive and simple to build. Also it should be very reliable and operate for a long time without maintenance.

Disadvantages. Use of radioisotope sources always presents a practical problem of red tape, safety analyses, etc. Although there should be no real hazard from these radioisotopes, public's lack of understanding of nuclear radiation and sometimes irrational reluctance to accept it makes it difficult to implement nuclear systems in practice.

NUCLEAR DETECTOR
FIG 5.

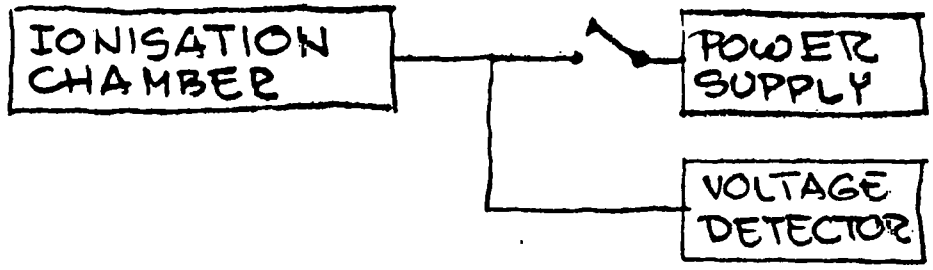

- TOP POSITION – IONISATION CHAMBER IS CHARGED BY EXTERNAL MEANS

- BOTTOM – IONISATION CHAMBER IS DISCHARGED BY RADIATION COMING FROM RADIOISOTOPE SOURCES LOCATED AT THE BOTTOM OF THE TUBES

MAGNETIC COUPLING
FIG 5a

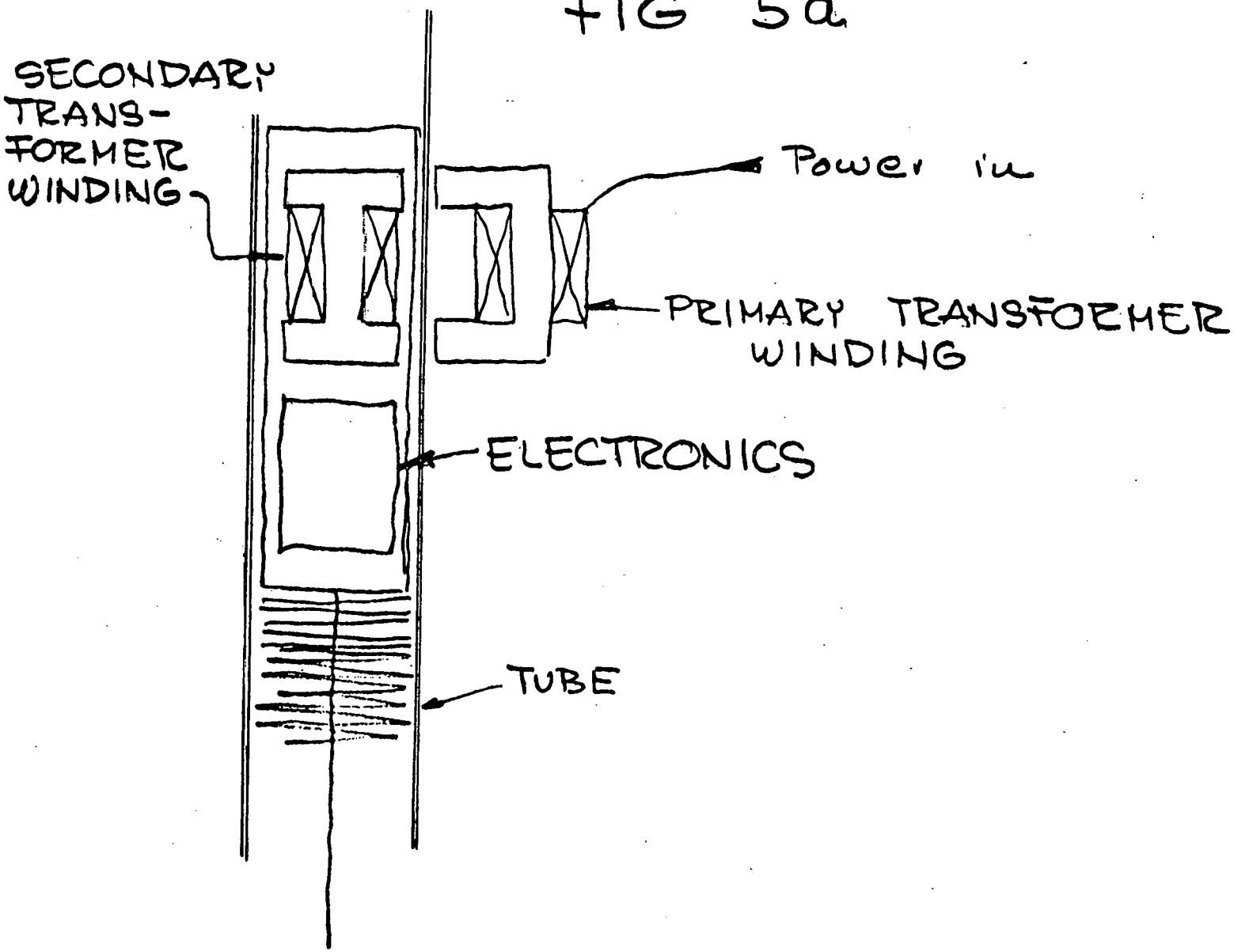

THIS PAGE

WAS INTENTIONALLY

LEFT BLANK

APPENDIX G.3

MAINTENANCE AND OPERATING PLAN INPUTS FOR THE 10 MWe AND THE 0.2 MWe TUBE CLEANERS

TRW
SYSTEMS GROUP
ONE SPACE PARK · REDONDO BEACH · CALIFORNIA 90278

INTEROFFICE CORRESPONDENCE

PSD-I-463
78.6853.6-011

TO: S. Vincent

CC: A.H. Hausrath
W.G. Hample
R. Williams
R. Pearson

DATE: 9 August 1978

SUBJECT: Maintenance and Operating Plan Inputs for the 10 MWe and the 0.2 MWe Tube Cleaners

FROM: C. Williamson

BLDG.	MAIL STA.	EXT.
81	1513	62635

Reference:

1. CP-SS14-45 — Prime Item Development Specification for PSD-1 Heat Exchanger Biofouling Control Subsystem Tube Cleaner
2. CP-EQ2-556 — Critical Item Product Function Specification for the 10 MWe HX Tube Cleaner Positioner
3. CP-EQ2-557 — Critical Item Product Function Specification for the 10 MWe HX Tube Cleaner Cleaner Head
4. CP-EQ2-556 — Critical Item Product Function Specification for the 10 MWe HX Tube Cleaner Controller/ Recorder
5. CP-EQ2-561 — 0.2 MWe HX Tube Cleaner

a) 10MWe HX Tube Cleaner (References 1 thru 4)

1) Operation - The 10 MWe HX tube cleaner has been configured to operate automatically according to the functional flow (Figure 1) and the time line shown in Figure 2 except as noted in Figure 1 and summarized below

a) Move cleaning head to a selected HX under manual control. For the 40 MWe system, interconnecting rails are envisioned. For the 10 MWe system, this movement requires an on-board crane or hoist to position the cleaner to its support pads on the HX. This will require two persons minimum; one to operate the hoist and others to engage the pad locking pins.

b) Position the cleaning head at the start point (under manual controls). This is accomplished by commanding the positioner to seek a specific X-Y position and verifying this location from position indicator readouts. At this point the automatic controls are commanded to take over but the operator will stand by for several cycles to insure proper performance.

c) If an incomplete brush retraction is sensed, the controller shuts down the machine and signals for corrective action. When a crew member is available, he will execute corrective action by proceeding as follows:

- Override the controls to command the brushes to down stroke again in the same position and re-attemp retraction.
- If complete retraction is still not indicated, repeat above at higher (TBD) air pressure in increments of (TBD) up to a maximum of (TBD) pressure.
- If complete retraction is still indicated, the retraction sensor is suspect and maintenance shall be scheduled.

It should be noted that the same procedure shall be followed if locating pin disengagement is not sensed.

2) Maintenance - Reference 1 specifies that the level of repairability shall be such that the vessel maintenance crew can execute maintenance and repairs using multipurpose (tools) and test equipment. Two levels of maintenance are specified. They are:

a) Servicing/maintaining the cleaner in its normal operating position, ie, lubrication, minor adjustments, brush replacement, inspection for degradation, etc.

b) On-deck major maintenance - This entails transporting the cleaner to a open deck service area for disassembly and repairs. To provide access to all parts of the cleaning head, it shall be de-erected to the horizontal position and supported at working level for convenience of repair. Major maintenance shall consist of parts/subassembly replacement/repairs, removal and reapplication of protective coating, reassembly and re installation onto a heat exchanger.

c) Controller servicing/maintenance - The controller/recorder shall be housed inside of a ship bay or compartment immediately adjacent to the heat exchangers to permit line of sight to the tube cleaner. It will not be exposed to the environment such as is the rest of the cleaner subsystem.

Maintenance will require an electrician versed in the operation of the unit and will be performed on location.

b) 0.2 MWe HX Tube Cleaner. (Reference 5)

1) Operation - This unit requires an operater to position the cleaning head into preselected positions for cleaning. Positioning shall be done manually by turning lead screw wheels to pre-identified position in the X and Y matrix. Note in Figure 3 that there are eight discreet X-X positions and 28 Y-Y positions (max). A single operator can set the X-X position, then move to the cleaning head and position it in Y-Y and execute the multiple brush stroking up to 28 times before repositioning in the X-X direction.

The brushes shall be driven pneumatically by the operator operating valves. He will be required to monitor the seven lights signalling completion of the down stroke and seven lights signalling completion of the up stroke.

2) Maintenance - The maintenance of the 0.2 MWe HX Tube Cleaner is as described in A-2-a & b above.

Note: Further details of operation and maintenance will depend on the selected designs as developed by the subcontractor. This document can provide an over view only and will be expanded for the proposal after selection of a subcontractor. The final O&M plan has been identified as a deliverable from the subcontractor.

CW:dp

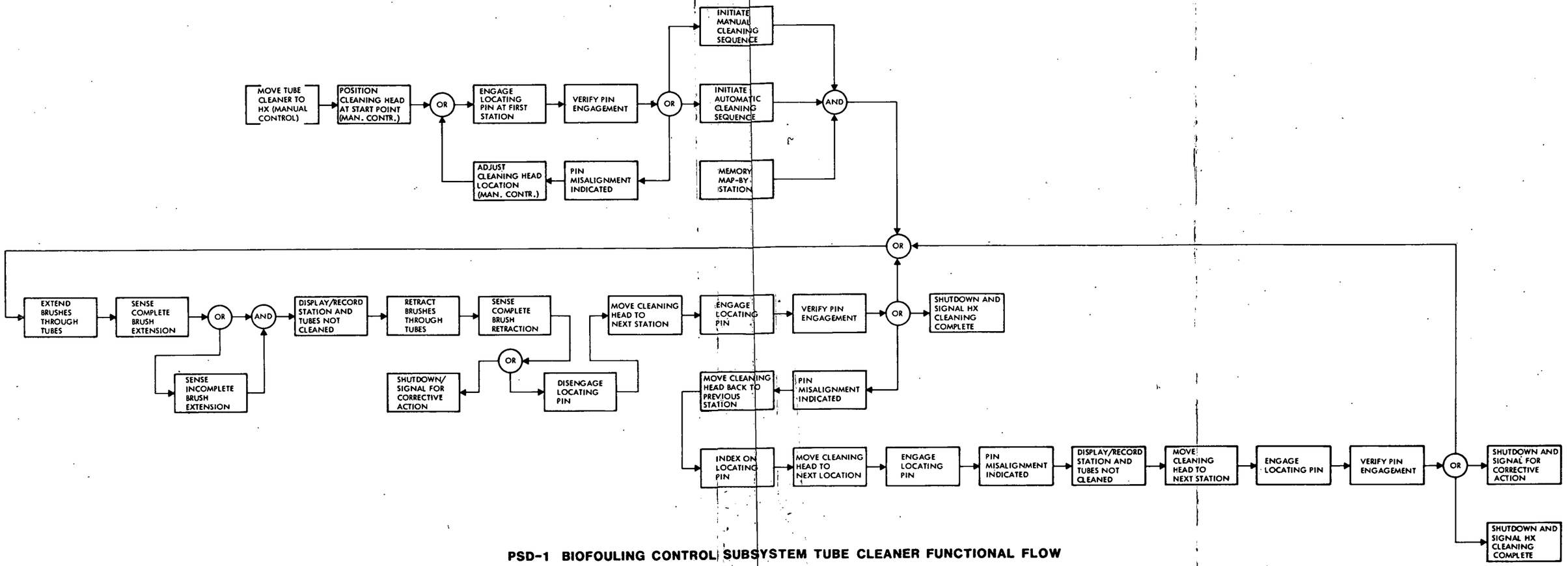

PSD-1 BIOFOULING CONTROL SUBSYSTEM TUBE CLEANER FUNCTIONAL FLOW

Figure 1 PSD-1 Biofouling Control Subsystem Tube Cleaner Functional Flow

THIS PAGE

WAS INTENTIONALLY

LEFT BLANK

APPENDIX G.4

TUBE CLEANER MEASUREMENTS AND CONTROLS

TRW
SYSTEMS GROUP
ONE SPACE PARK · REDONDO BEACH · CALIFORNIA 90278

INTEROFFICE CORRESPONDENCE 78.6853.6-007

TO: R. Williams

CC: S. Vincent
W. Hample
A. Hausrath
M. Nee

DATE: 26 July 1978

SUBJECT: Tube Cleaner Measurements & Controls

FROM: C.E. Williamson

BLDG. 81 MAIL STA. 1513 EXT. 62635

The tube cleaner subsystem is defined by specs CP-SS14-45, CP EQ2-556, 557 & 558. *(Attached) A projected operating time line (Figure 1) and a functional flow (Figure 2) is attached. The subsystem has been designed to normally operate closed loop complete with data recorder. The primary data to be recorded is the location of tubes which arenot accepting the cleaning devices (brushes) to their full stroke and groups of tubes that are skipped by the cleaner. Note that the memory disks will be blanked to negate recording of no-brush-motion where there are no tubes. Following any tube plugging operation, a new disk blank will be required to also negate newly blocked tubes from the record.

Sensors

Within this subsystem, there are sensors to measure the following:

1) Engagement of the cleaning head with the guide pins in the tube sheet. (one sensor)

2) Completion of the down stroke (95 sensors)

3) Completion of the up stoke (95 sensors)

4) Redundant encoders on the X, Y, and Z axes of the positioner

The output from sensor (1) above signals the controller to proceed with stroking the brushes. If a no-go signal is received, the controller directs the cleaning head to retract and return the positioner to the nearest X-Y matrix sensor to verify encoder position information. If on the next attempt a no-go signal is received, the positioner moves to the next location (n+1). If engagement is made, cleaning proceeds and the failure to clean position (n) is recorded. If a no-go signal is received at position (n+1) the system will command shut down and signal for corrective action. The output from sensor (2) is recorded but doesnot interrupt the cleaning sequence. The output from sensors (3) permits the cleaning to proceed. Encoders (4) positions the cleaning head responding to the programmed controller output. If on the second try a no-go is received, shut down/corrective action signal is issued.

From the above, it can be seen that only two types of data are recorded:

1) Failure to position for cleaning an entire group of tubes (95 tubes) and their location in the matrix.

2) Incomplete down stroke of any brush; its group location in the matrix and its position in the group of 95 tubes.

The use of this data is a subject for the system engineers to address but it is our intent that its to be used by the plant operator to plan/ execute maintenance/repair activity.

Controls

The cleaning sequence for a heat exchanger shall be initiated manually by shipboard personnel at a control console. Signals for corrective action will also require attention (not necessarily immediate except in an emergency situation) from ship personnel.

We donot envision the need for a dedicated operator for this subsystem. Also note that the timeline permits completion of cleaning of a single heat exchanger in a 12 hour shift.

Transfer

It is proposed to use a single cleaner for the 10 MWe system for cleaning both the evaporator and the condenser. This will require transfer from one to the other approximately once per week (two transfers per week). It is assumed that this can be accomplished by the regular maintenance crew. Note that a crane will be required for this operation.

For the 40MWe system, two cleaners are envisioned; each dedicated to one side of the ship.

CEW:dp

*Attachments only for R. Williams

TUBE CLEANER TIMELINE

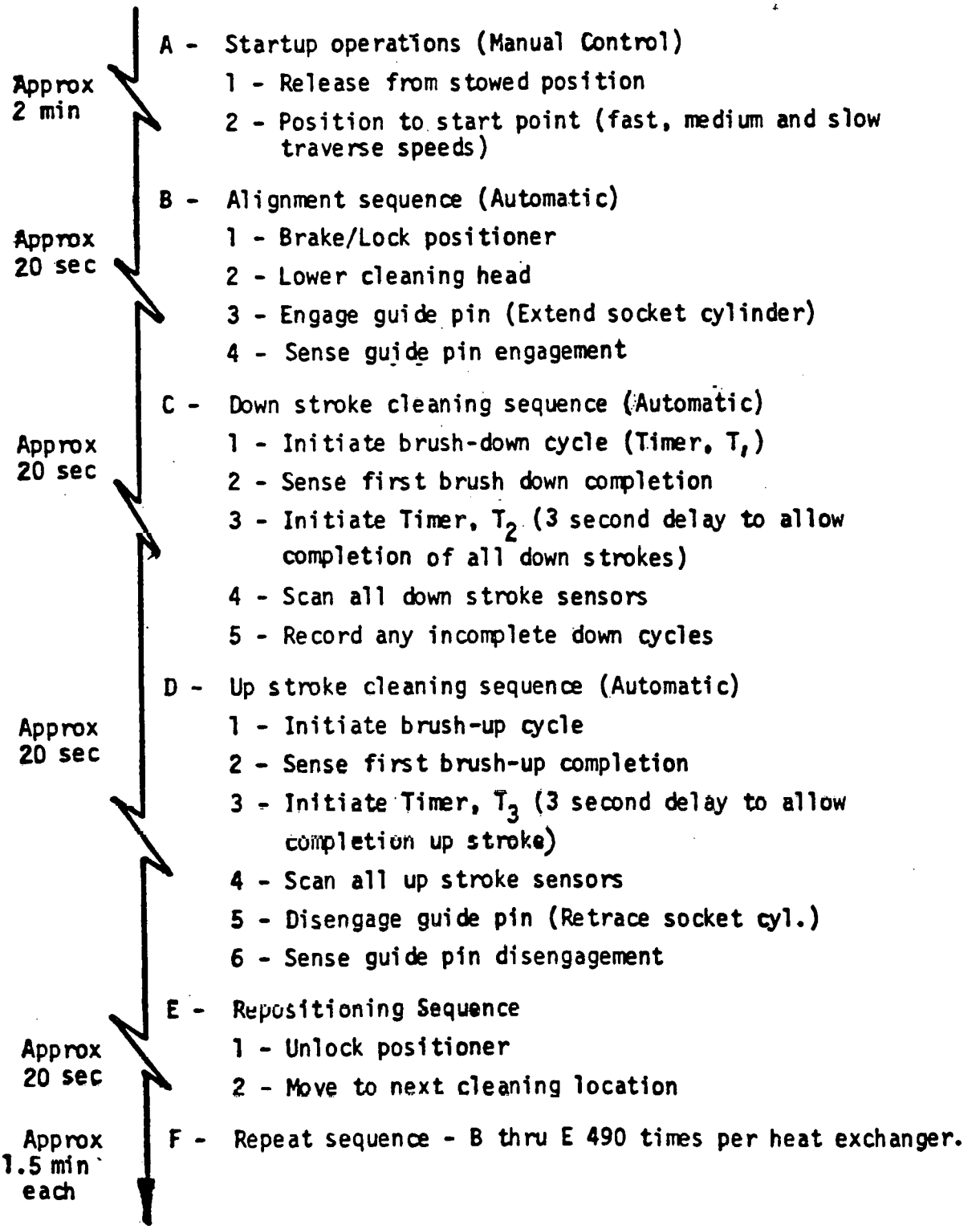

Figure 1

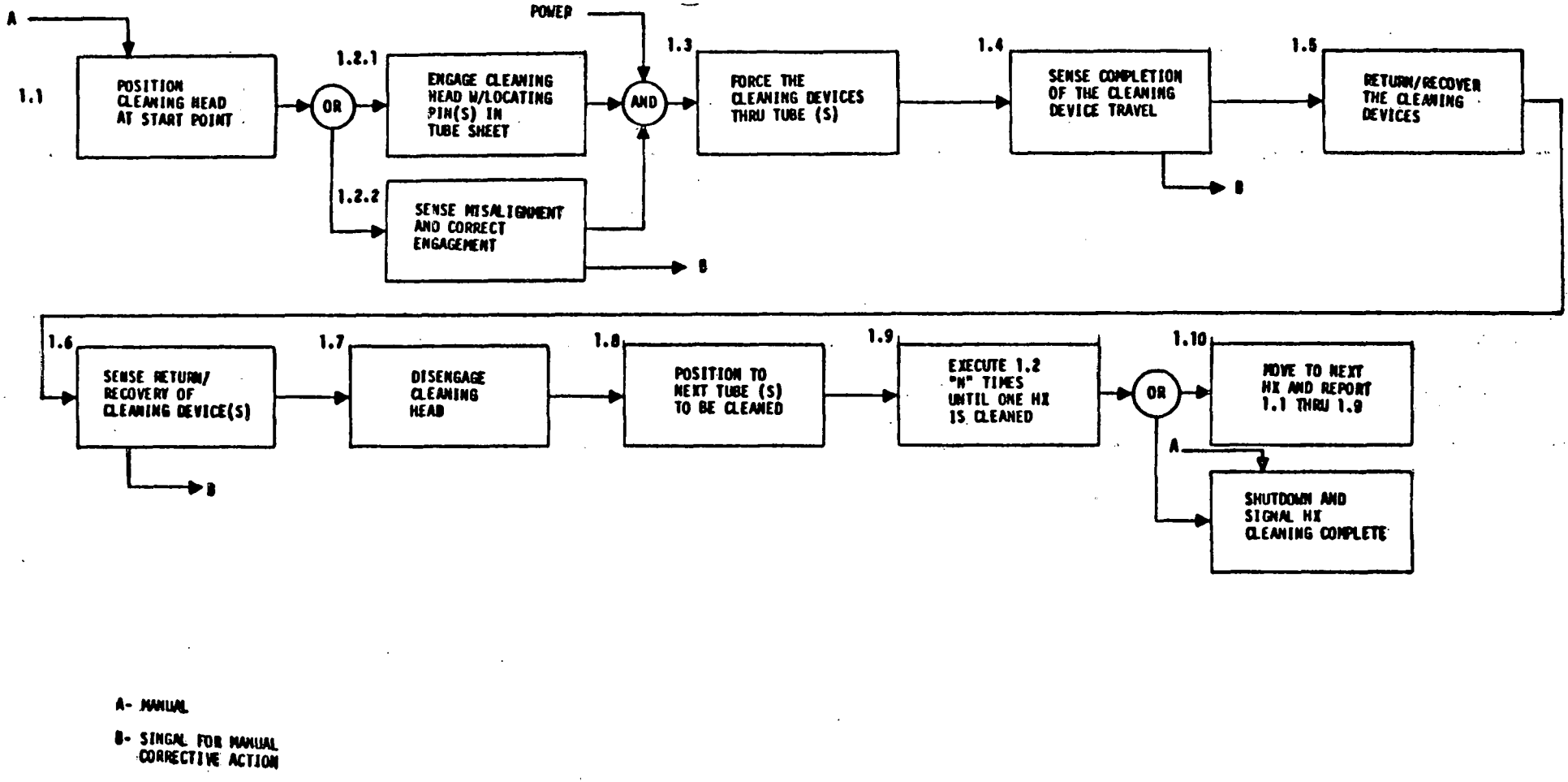

Figure 2. PSD-1 Biofouling Control Subsystem, Tube Cleaner Functional Flow

APPENDIX H

AMMONIA LEAK DETECTION

THIS PAGE

WAS INTENTIONALLY

LEFT BLANK

APPENDIX H.1

OTEC AMMONIA LEAK DETECTION SYSTEM

TRW
DEFENSE AND SPACE SYSTEMS GROUP
ONE SPACE PARK • REDONDO BEACH • CALIFORNIA 90278

INTEROFFICE CORRESPONDENCE

TO: Paul Edris

CC:

4341.AC.78-174
DATE: 8 September 1978

SUBJECT: OTEC Ammonia Leak Detection System

FROM: J. S. Shapiro/ J. Wilson
BLDG. 01 MAIL STA. 2030 EXT. 62451

Attached is our Final Report and Proposal Input regarding the Ammonia Leak Detection System. We feel this report should meet your program requirements quite well and was performed according to our recent PWA. The report is on schedule and the budget was adhered to.

Approved L E Ryan
L. E. Ryan, Section Head
Analytical Chemistry

B. DUBROW
W. CHEW
P. FUKUNAGA
G. GIBSON
A. GRANT
R. JONES
L. KENT
D. REEVES
S. VINCENT

CONTENT

		Pages
1.	INTRODUCTION	H-6
2.	THE SELECTED AMMONIA DETECTION SYSTEM	H-7
3.	OTHER DETECTION SYSTEMS INVESTIGATED BUT ASSESSED AS UNSATISFACTORY	H-9
4.	SAMPLING SYSTEM	H-12
5.	SUMMARY	H-33
	ATTACHMENT 1	H-35
	ATTACHMENT 2	H-36

1. INTRODUCTION

Ammonia is the working fluid in the OTEC PSD-1 module. Because the heat exchangers are submerged and sea water flows through them, any leaks in the tubes or tubesheets or interfaces will release ammonia into sea water. A twofold study has been conducted to determine the best means of detecting ammonia leaks.

The first problem is that of monitoring the heat exchanger discharge streams to determine whether any leak exists. This requires ammonia detection in the 0.1 ppm range, based on an allowable leak rate of 40 pounds/hour NH_3 from the condenser which has 2.5×10^8 pounds/hour water flowing through it. The allowable leak from the evaporator is 50 pounds/hour ammonia. If total mixing between the leaking ammonia and effluent water occurs, the result is a solution 0.16 ppm in ammonia. Because the configuration of the lower water shroud has not been established at this time, calculations have been based on maximum dilution. Technicon Monitor IV equipment can detect ammonia levels as low as 0.01 ppm in sea water; consequently either this instrument or an equivalent one will be used in this application.

The second problem is that of locating the tube or joint that leaks so that repair measures can be instituted. Leak location will be accomplished using the tube cleaning equipment in a modified version for sample collection. Effluents from each bank of 95 tubes will be analyzed as a composite; high ammonia results for any composite will be a signal to search for leaks in that tube bank. The Technicon Monitor IV to be used in this application will be modified to accept new samples every two minutes, which is the cycle time of the tube cleaning equipment.

Once a leaking composite is located, the effluents from individual tubes can be analyzed. The task of feasibly locating individual tube leaks requires complicated and costly valving and TRW recommends the adoption of a simplified system which can narrow the leak to a 19 tube composite. Figure 4.3 in Section 4.1.3 is a schematic of both such systems; the only difference is the number of valves and lines entering the reservoir without previous manifolding.

2. THE SELECTED AMMONIA DETECTION SYSTEM

2.1 THEORY

The specific method for ammonia detection is the Berthelot Reaction, which is in accordance with the procedure for automated analysis in "Methods for Chemical Analysis of Water and Wastes," published by the Water Quality Office of the EPA (Appendix 1, No. 1). In this method samples are treated with alkaline hypochlorite and phenol in the presence of sodium nitroprusside, $Na_2Fe(CN)_5(NO)$. A solution of potassium sodium tartrate and sodium citrate is added to the sample stream to eliminate the precipitation of the hydroxides of calcium and magnesium; the tartrate and citrate ion are good complexing agents. A blue indophenol dye is produced from the ammonia and is measured spectrophotometrically. Both the sensitivity and specificity of the method are well documented. (Appendix 1, No. 2)

2.2 CHOICE OF EQUIPMENT

The Technicon Monitor IV, or a similar type of unit, is the instrument of choice to monitor the level of ammonia in sea water. The Technicon equipment is attractive for the following reasons:

- The company's extensive experience in automated analysis.
- On-the-shelf availability of system sensitive to NH_3 in sea water at 0.01 ppm level.
- Satisfaction of current users of Technicon equipment.

The Monitor IV unit uses the principles of continuous flow analysis developed by Technicon. The delivery of reagents, air and sample is accomplished by a peristaltic pump. The sample stream is continuously drawn into the system. Chemical reactions are performed on the manifold where such functions as mixing, heating, and, when necessary, dilutions, are accomplished. Ultimately, the colored reaction product is measured with a colorimeter.

The analytical system is very flexible and can easily be modified in the field to accommodate a wide ammonia concentration range. Ambient

ammonia concentration in sea water will vary with location, season, temperature, and depth, but 0.03 ppm is a probable maximum (Appendix 1, No. 3). Ammonia levels in each heat exchanger's inlet water will be monitored as a reference and subtracted from effluent readings.

2.2.1 Vendor Qualifications

Technicon provides a one-week training course for operators of their equipment and has a worldwide network of service and support facilities. In addition, we have spoken to numerous laboratories who use their equipment for analyses of sea water and have excellent results. These laboratories included the Public Health Department for the State of California, Scripps Institute of Oceanography and the National Marine Fisheries Service.

2.3 ESTIMATION OF DETECTABLE LEAKS

At the allowable leak rate of 40 pounds/hour of ammonia from the condenser, the effluent will contain 0.16 ppm of ammonia if complete mixing takes place. The Technicon Monitor IV is sensitive to a change of .01 ppm NH_3, which represents about a 6% change in the ammonia leak rate. If a new leak is in a single location, its 95-tube composite will contain about 3 ppm of ammonia. The evaporator has a tolerable maximum leak of 50 pounds/hour of ammonia; hence its detection limit is slightly better than that of the condenser.

Because analysis of the 95-tube composites can detect leaks at a much lower level than analysis of the bulk effluent, periodic composite analyses may be useful in preventive maintenance even when bulk effluent ammonia levels are satisfactory. For example, a 0.4 pound/hour leak in a single tube, which represents 1% of the allowable condenser leak rate but which is too small to be seen in the bulk effluent, would produce an easily detected 0.6 ppm ammonia change in the 95-tube composite.

The process of using a vacuum for sample transfer was evaluated. The solubility of ammonia in water is so high that, until the ammonia level approaches several thousand ppm, the vacuum level of 2 psig required for sampling will not change the ammonia concentration in the system.

3. OTHER DETECTION SYSTEMS INVESTIGATED BUT ASSESSED AS UNSATISFACTORY

3.1 AMMONIA SPECIFIC ION ELECTRODE

Initially the ion selective electrode (ISE) for ammonia was considered a good possibility for the analysis. For maximum sensitivity, solutions to be analyzed by the ISE must be at about pH 11. Above pH 9.2, $Mg(OH)_2$ precipitates from sea water, and adherence of this precipitate would reduce electrode sensitivity significantly over periods of extended use. Disadvantages also include the fact that electrodes currently being used in sea water applications require frequent wiping of the membrane surface with acid solutions to remove precipitates. In addition, the response time of the electrode is quite slow at the levels of ammonia expected in the bulk sample. Technicon, the supplier of the Monitor IV, offers either the ISE or the Berthelot wet chemical method of NH_3 analyses for about the same cost, but for long-term reliable process analysis of ammonia in sea water, Technicon concurs with our recommendation of the Berthelot wet chemical method.

Orion, the manufacturer of an ISE, suggested the possibility of carrying out the analysis at sea water pH (7.8 - 8.3), under which conditions the electrode would sense about 10% of the ammonia present. Such a system would be too insensitive for the bulk analysis mode and would require development work to determine if it is suitable for individual tube analysis. The expected lifetime of an ISE under sea water conditions is still unknown. The situation is further complicated by the fact that the sensitivity of the electrode would vary with sample pH, and it would be necessary to adjust the pH of all solutions to a set value somewhere between ambient pH and the pH at which $Mg(OH)_2$ would begin to interfere.

3.2 pH ELECTRODES

The possibility of monitoring pH changes caused by leaking ammonia was also investigated. Sea water is a highly buffered system due to the presence of approximately 2×10^{-3} M bicarbonate ion. Thus the introduction of ammonia produces much smaller changes in pH than would be seen in fresh water. The high concentration of magnesium ion in sea water (5×10^{-2} M) is another complicating factor. Magnesium hydroxide

precipitates above a pH of about 9.2, serving to reduce even further the change in pH expected from the addition of ammonia.

It was concluded that pH changes are too small to be used for detection of leaks in the bulk mode. Development work would be required to establish the method's suitability for leak location in individual tubes or banks of tubes.

3.3 ION CHROMATOGRAPHY

Another method considered was ion chromatography which used a conductimetric detector. Technical representatives of Dionex Corporation, manufacturer of ion chromotography equipment, said that ammonia can be analyzed by their system only when there is no more than a thousand-fold excess of sodium present. In a sea water medium, ammonia detection would be greatly complicated by the 10^4 ppm interfering concentration of Na^+.

3.4 INFRARED SPECTROPHOTOMETRIC TECHNIQUES

The same ionic interference phenomenon provides a serious drawback for infrared analysis which would have required concentration of the ammonia on a column followed by stripping. A continuous sample technique of this type has yet to be developed.

3.5 MICROCOULOMETRIC ANALYSES

Microcoulometric methods of analyses were sensitive enough for our purposes but process-type equipment for continuous monitoring is not currently available.

3.6 LIGHT SCATTERING TECHNIQUES

It might be possible to locate leaks greater than about 50 ppm NH_3 by monitoring the light scattering which accompanies the formation of the white magnesium hydroxide precipitate at pH values above 9.2. A considerable amount of development work would be necessary to verify the feasibility of this approach.

3.7 INDICATORS

Another possibility which would involve development expense is the addition of a compound such as fluorescein in ppm amounts to the ammonia.

Leaks could then be located by fluorescence detectors at the condenser and evaporator exits.

4. SAMPLING SYSTEM

4.1 GENERAL

As mentioned earlier, a workable systematic system is required for detecting an ammonia leak. It is our proposal to use three modes of operation, classified as

- Bulk outlet sampling
- Composite tube sampling
- Individual tube sampling

Criteria used in decision making included, but were not limited to:

- Fluid mechanics associated with transporting sea water contaminated with ammonia from potential leak sources.
- Detection limit of <0.1 ppm.
- Thorough flushing of each line with solution to be analyzed prior to taking an aliquot.
- The potential leak sources are 1) shell to tube sheet, 2) tube sheet to H-X tube, and 3) H-X tube.
- Use of existing tube cleaning apparatus for sampling sea water (*modified version*)

4.1.1 Bulk Outlet Sampling Mode

The bulk outlet sampling mode consists of aspirating tubes located in the outlet stream of each quadrant of the H-X tube bundle. Samples are withdrawn from each tube by pumping into a mixing reservoir at atmospheric pressure. The reservoir provides a continuous flow sample to an auto-analyzer capable of monitoring the system continuously. When the bulk sample exceeds a recorded preset level, an audio/visual alarm is initiated. The general leak location of the particular quadrant can be determined by sampling the quadrant sampling tubes individually by sequencing the air operated valves. Figure 4-1 shows the bulk outlet sampling mode schematically.

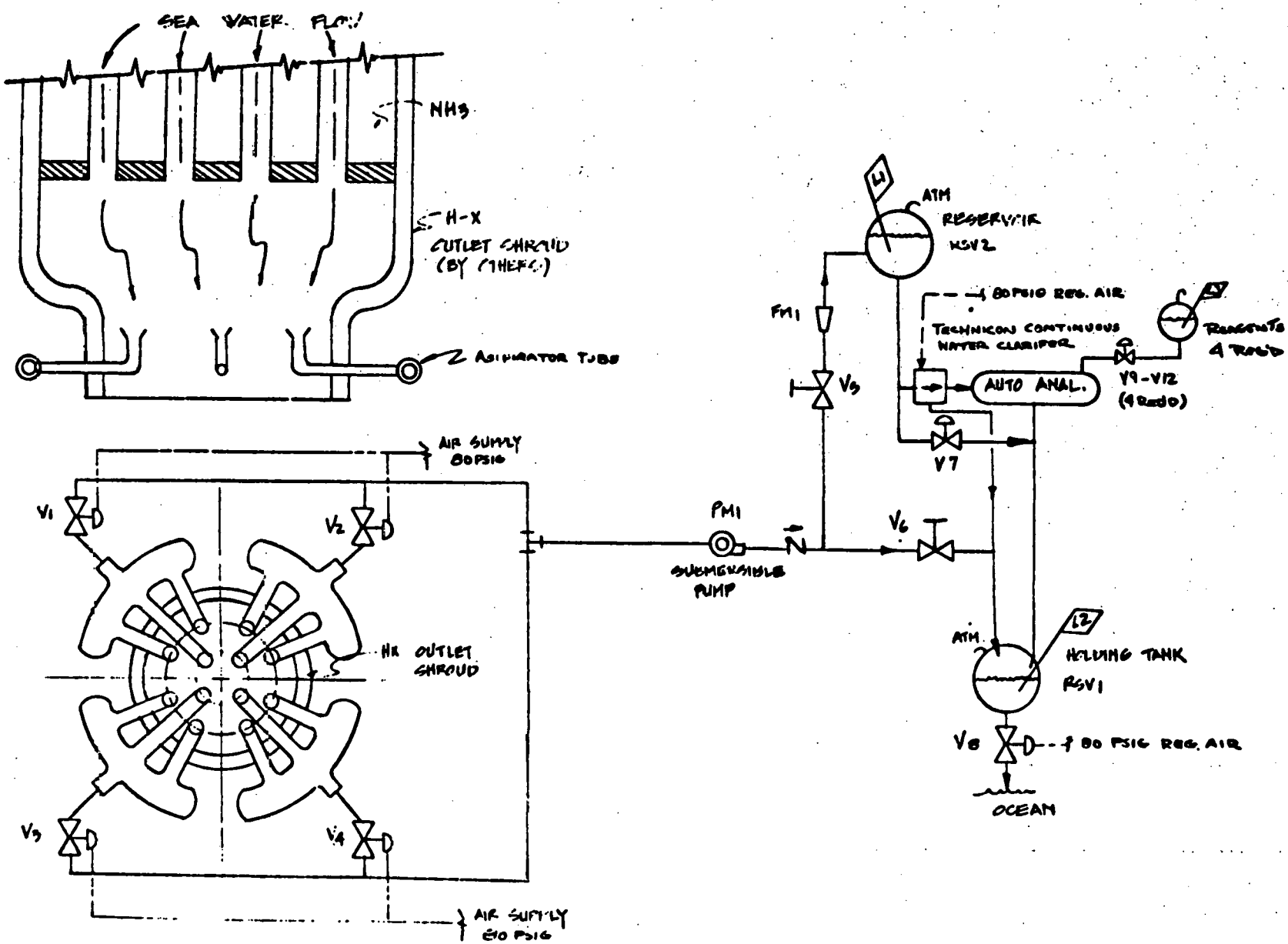

Figure 4-1. Bulk Outlet Sampling - Schematic

4.1.2 Composite Sampling Mode

The composite sampling mode is initiated whenever the bulk sampling system indicates that a leak is present. The concept consists of directing a modified biofouling tube cleaner to the indicated quadrant and sampling a composite of 95 H-X tubes. Sample sea water is taken from each tube and transported to a storage reservoir. Transporting the sample fluid is accomplished by differential pressure from the H-X outlet to a reduced pressure (~2 PSIA) reservoir as shown schematically by Figure 4-2.

Two reservoirs will be provided so that as one reservoir is being analyzed, the other one can be filling with a new sample. This would allow the cleaning head to progress uninterrupted to the next bank of 95 tubes.

Any group of tubes may be sequenced for composite sampling and for narrowing the leak to a specific set of tubes. At that point, a decision would be made either to seal that group of tubes or to continue the sequential analytical approach and perform individual tube sampling.

4.1.3 Individual Tube Sampling

After the initial survey of 95-tube composites, the modified brush cleaning apparatus would return to any bank which showed a level of ammonia higher than a specific preset value. Either individual tubes or a composite sample of from 2 to 95 tubes may be obtained by sequencing the multiplex valving manifold system. During this sequence, only one reservoir would be utilized due to the unique design of our reservoir and sampling mode as shown schematically in Figure 4-3. The unique feature of this mode is the transportation of sea water samples by a single pump (vacuum) and the labeling and storage of these samples for either composite or individual analysis.

If it were feasible to seal off as many as 19 tubes at a time, the system could be greatly simplified by removal of individual valves. Groups of 19 tubes could be sampled as a composite via a manifold, and only one valve would be needed for each 19-tube bank. This would reduce the flexibility of the system, however, and would necessitate manual sampling in the event that location of an individual leaking tube ever became desirable.

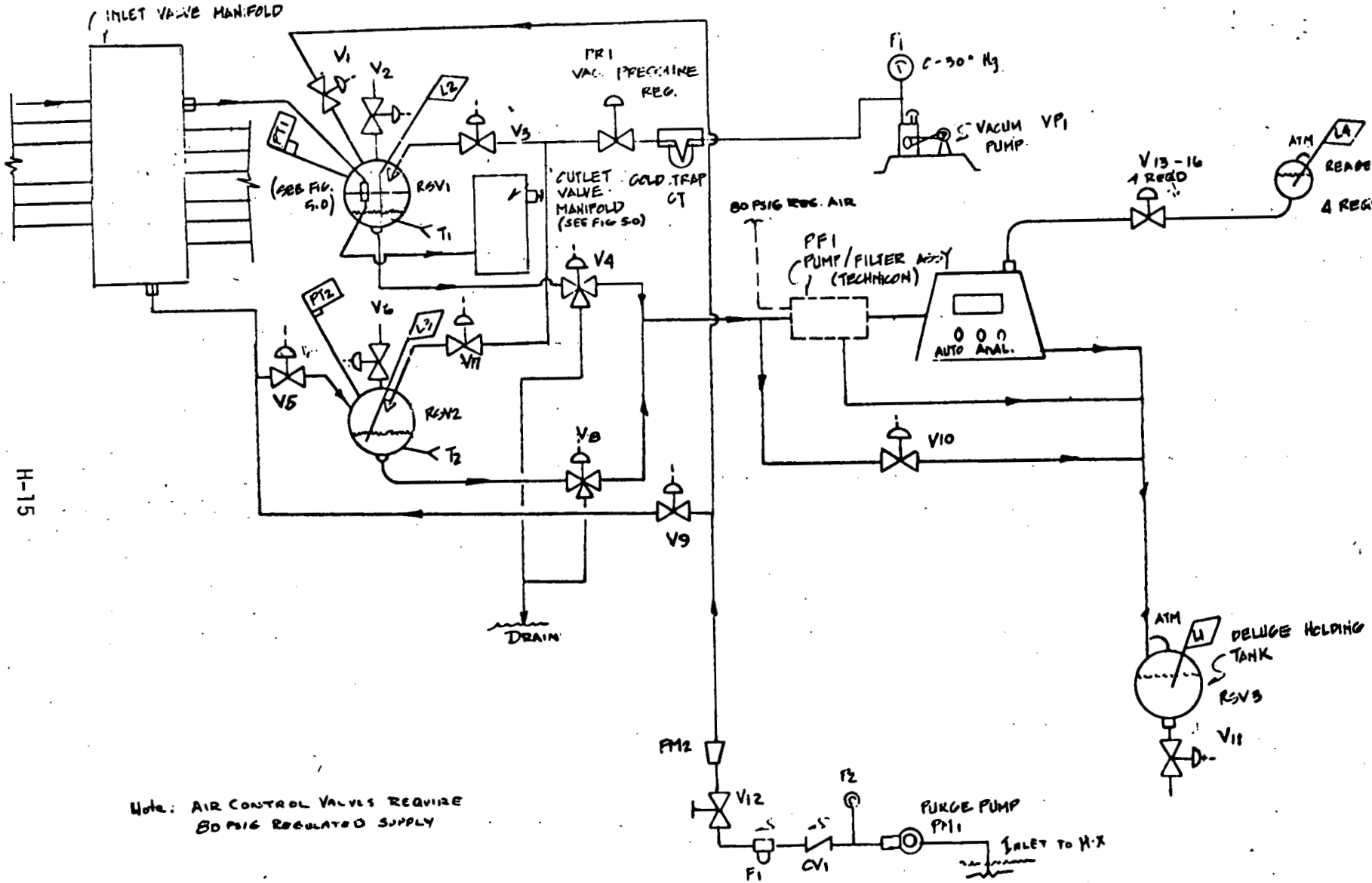

H-15

Figure 4-2. Composite Sampling Mode - Schematic (One Tube Sample Shown)

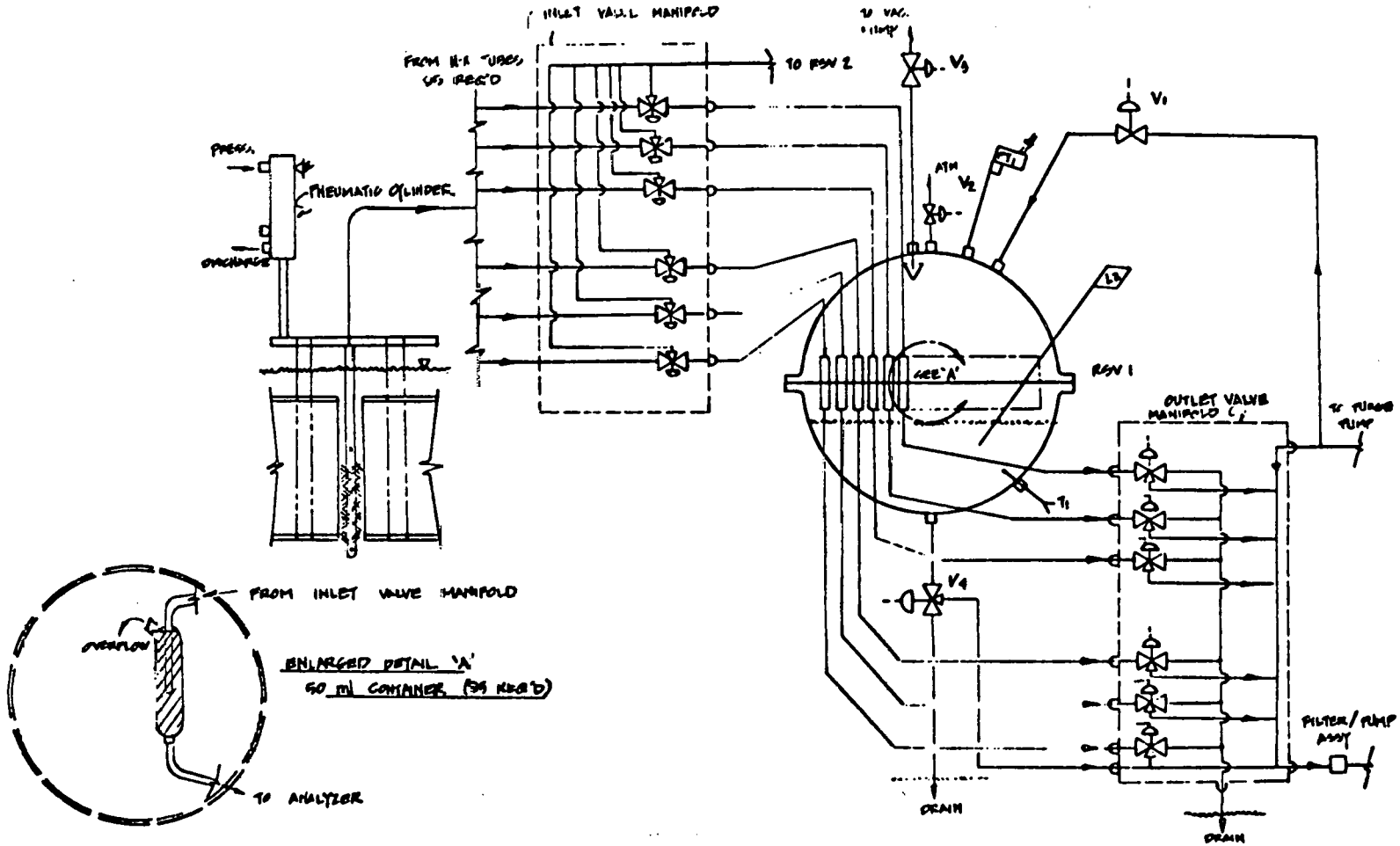

Figure 4-3. Individual Sampling Mode - Schematic

4.2 GENERAL REQUIREMENTS

A purge pump is provided to supply a background sample between effluent analyses or to wash down the process equipment into a deluge holding tank for subsequent discharge to the sea. Copious flushing is required to prevent cross-contamination from sample to sample.

A pump/filtering assembly is shown for filtering and back flushing. This assembly contains a positive displacement pump capable of 25 feet suction lift. The pump will also serve as a static pressure limiter since the reservoirs are expected to be located at an elevated level exceeding the 5 PSIG working pressure of the auto-analyzer.

4.3 TECHNICAL DISCUSSION

A cursory study was made to establish a feasible method of obtaining a sea water sample representative of a leak from the shell to tube sheet, tube to tube sheet and an individual H-X tube. The shell to tube sheet leak can probably be detected by the bulk system sample test. The tube/tube sheet interface and H-X tube leak is determined by the composite and individual tube sample testing of 95 tube groups. This requires development in certain areas as will be discussed in the design development section. A practical approach is to use the existing tube cleaning subsystem machinery for cost considerations.

Modifications to the existing design are necessary and may also require some development effort. The modification identified at this time requires a hollow (tube fabrication) brush rod for fluid passage to the sample storage reservoir. Also an interchangeable or modified brush head assembly will be required. This brush head will require a check valve, centering brushes and multi-hole entry ports. The concept of the reservoir location and brush assembly is shown by the sketch illustrated in Figure 4-4.

In order to prevent clogging of the sampling inlet lines, transfer lines and valving system, filter assemblies will be added at the inlet to the modified brush unit as shown in Figure 4.4. The major cause of

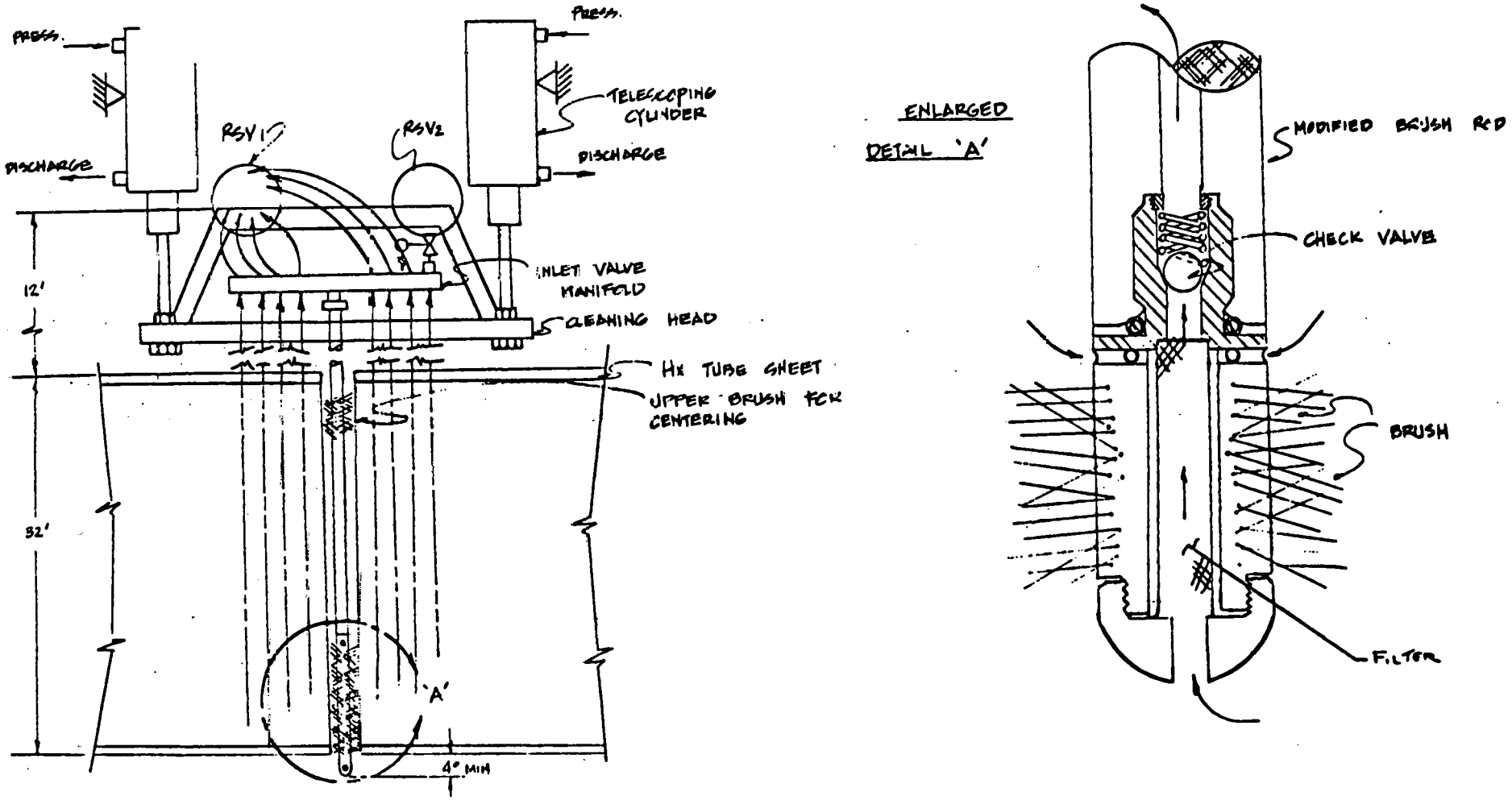

Figure 4-4. RESERVOIR LOCATION AND BRUSH ASSEMBLY

particulates would most likely be from the formation of $Mg(OH)_2$ caused by ammonia leakage into sea water containing relatively high concentrations of magnesium ions [1000 ppm or more].

A preliminary sizing for the hollow brush diameter and sample flow was conducted. Several available tube sizes were analyzed and are tabulated:

O.D.	WALL	ID	A_O-Ft^2	D_H-Ft.
1/2	.049	.402	8.814×10^{-4}	.0335
3/8	.065	.245	3.274×10^{-4}	.0204
1/4	.028	.194	2.053×10^{-4}	.0162

Figure 4-5 shows the pressure drop (PSI/Ft) characteristics for the above tube sizes for laminar flow and Figure 4-6 for turbulent flow. It is recommended that the sample reservoir be located on top of the brush unit and connected with short lines to minimize the static lift, entanglement, and dynamic pressure losses. Assuming the brush head can traverse one foot above the water box water level located another foot above the brush head, the maximum available ΔP would be 32 PSI with a minimum reservoir pressure of 1.66 PSIA limited by the saturation temperature of 120^{o}F to preclude boiling. The ΔP will vary from 32 PSI to 13.5 PSI when the brush tip immersion depth varies from 42 feet to 1 foot. The allowable pressure loss over this range would only vary from 12.15 PSI to 13.49 PSI because the pressure gradient is somewhat compensated by the elevation gradient. Therefore, nearly constant flow should exist for the steady state.

The system pressure drop was calculated assuming 100 feet of 1/4 inch ODX.028" wall tubing, four 90^{o} mitre turns, entrance/exit loss, and a static head of 44 feet. Figure 4-7 illustrated the expected steady state flow variation from 0.25 to 0.27 GPM. The sample reservoir volume is sized for approximately 1.77 cubic feet (13.2 gallons) and filling to half capacity would take 17 seconds for 95 tube samples. The reservoirs are spherical in shape with an ID of 18 inches which should contain 95 1 inch diameter 50 ml containers located at the center line.

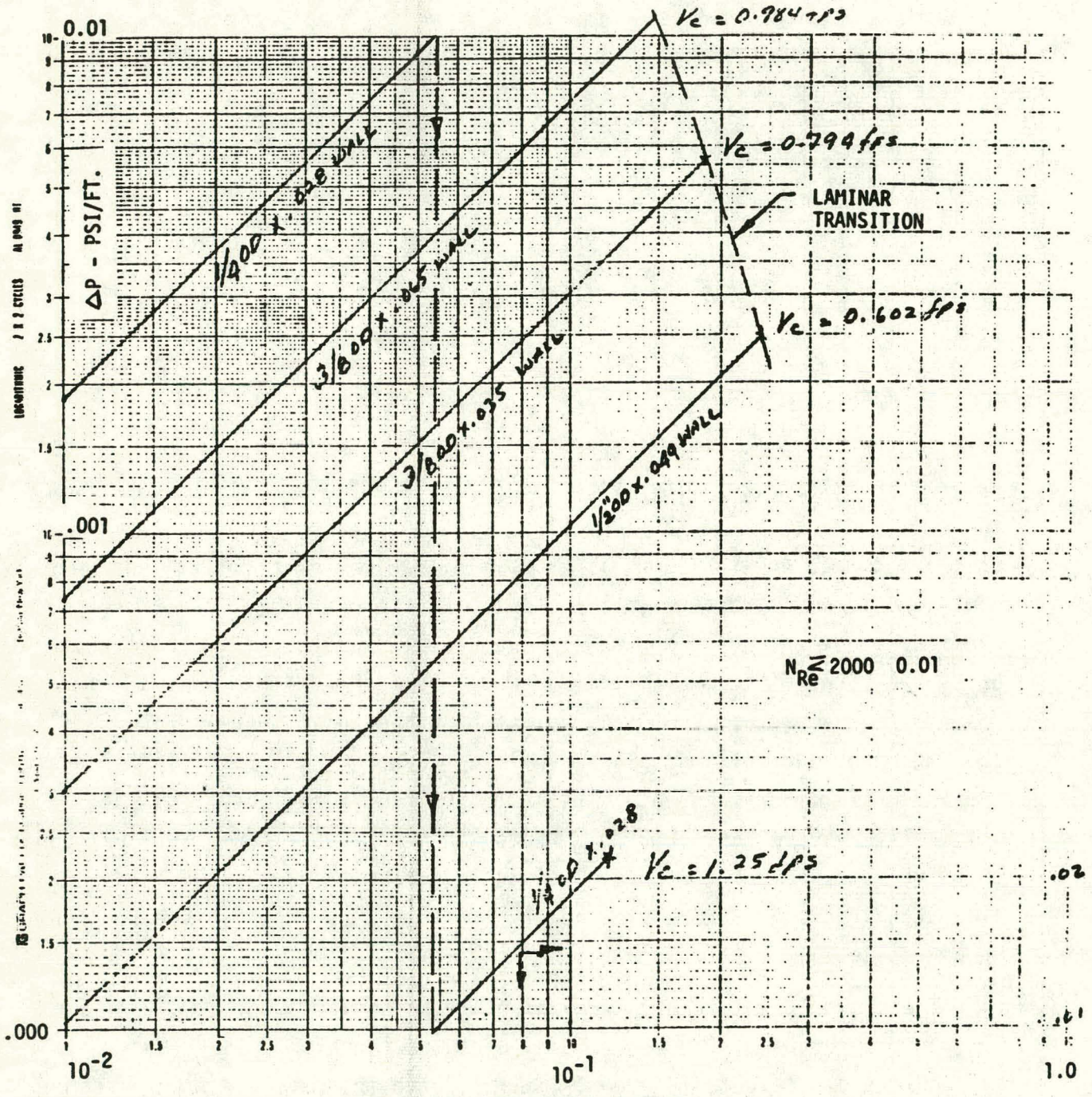

Figure 4-5. Brush Rod Pressure Drop vs Laminar Flow For Various Tube Sizes

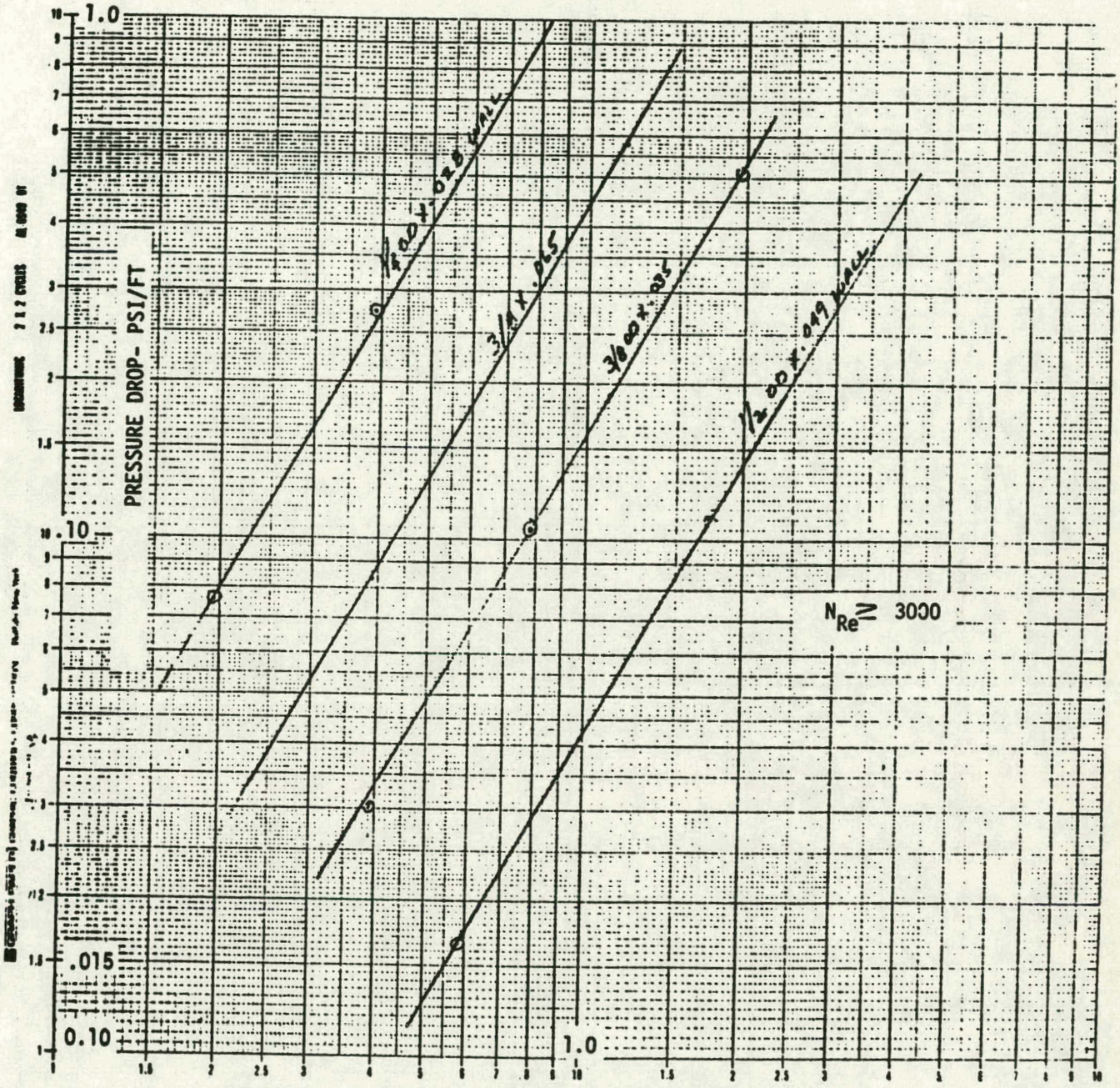

SEA WATER FLOW RATE, GPM/TUBE

Figure 4-6. Brush Rod Pressure Drop vs Turbulent Flow For Various Tube

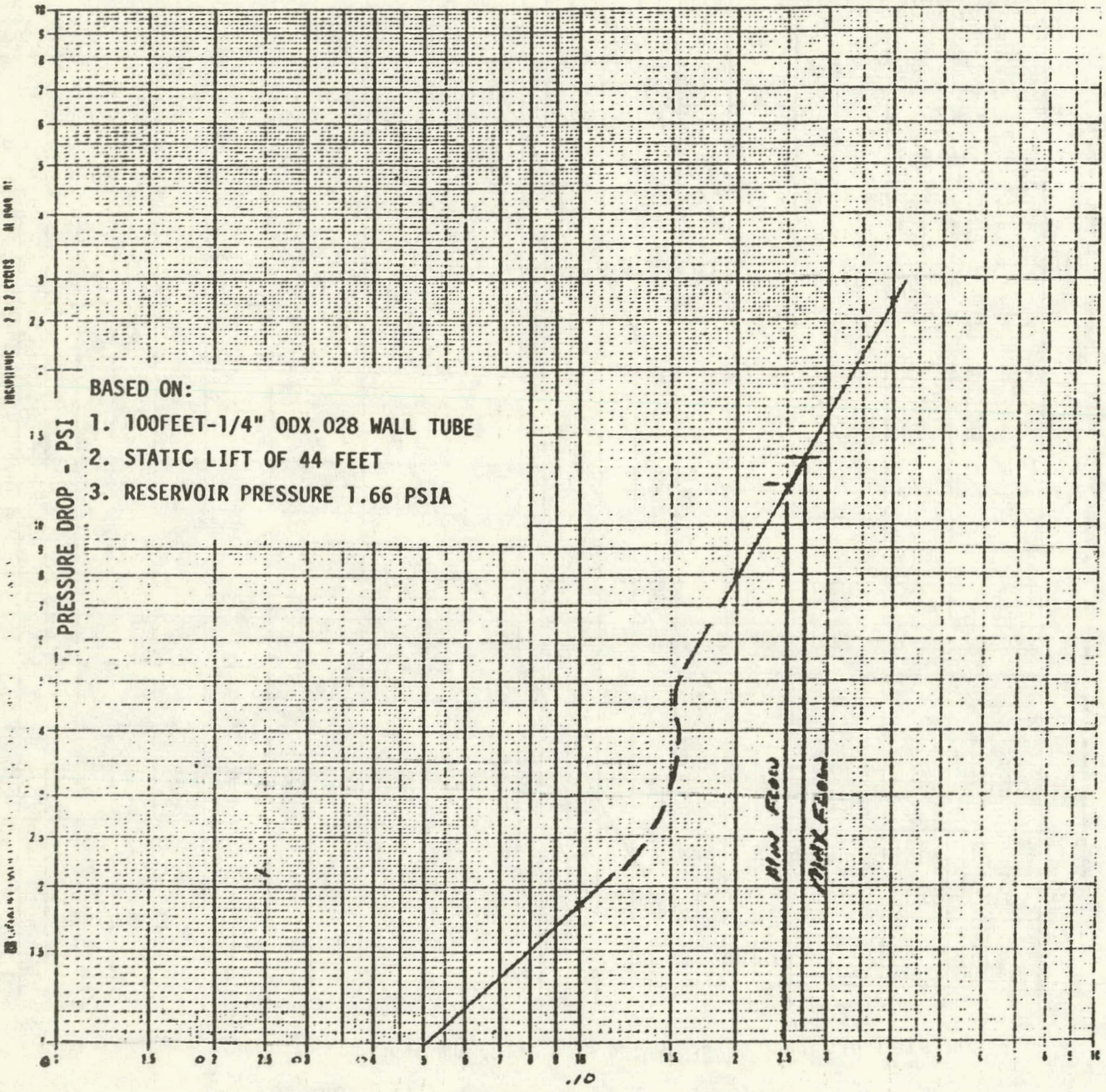

Figure 4-7. System Flow vs Pressure Drop

4.4 DESIGN DEVELOPMENT

This study revealed certain areas requiring design development. These areas are discussed briefly as design development tasks which are identified at this time.

4.4.1 Bulk Sampling Mode

The chief concern of this mode is the number, size and location of the sampling tubes within the flow stream of the H-X outlet. Presently there is no information describing an outlet shroud. The objective would be to determine the minimum number of sampling tubes necessary to provide a representative effluent sample and to narrow the location of a leak to a specific quadrant.

4.4.2 Composite Sampling Mode

Additional system studies are required for the feasibility of combining the composite sampling system with the biofouling control subsystem. Design development is required for the following modifications.

- Locating two reservoirs with an inlet and outlet valve manifold on a moving platform above the cleaning head.
- Modifying the brush rod for flow passage to reservoirs.
- Development or modifying the existing brush head with a check valve, brush and entry ports.
- Modify the brush actuators from 95 individual brush cylinders to two large brush head cylinders.

Additional effort is required for studying alternative concepts and detail analysis of the vacuum transport concept.

4.4.3 Individual Sample Mode

Hardware design is required for the multiplex valve/manifold and associated programmable micro processor. This valve/manifold shall have 95 inlet ports and 95 outlet ports for parallel thruput for one function. Another function is to bypass 95 inlet flows into a common manifold with a single outlet. In addition each of the 95 inlets may be sequenced in any predetermined combination. Each valve must have a low pressure drop (less than 0.20 psi at 0.25 GPM) and must also seal an internal vacuum. These functions are shown schematically by Figure 4-5.

The tentative selection for the analytical instrument is a "Technicon Monitor IV". This instrument may require re-packaging into a hermetic enclosure with temperature control for a continuous salt environment and to preclude electrical ignition of concentrated NH_3 atmosphere. Special shock mounts are also recommended.

EQUIPMENT ANALYSIS AND SAMPLING SYSTEM

4.5.1 INSTRUMENTATION AND CONTROLS

Suitable instrumentation and controls shall be provided for automatic operation. Air operated valves are suggested or explosion proof electric devices. Lists of measurement devices are tabulated in Tables 4-1 and 4-3.

4.5.2 EQUIPMENT AND COMPONENTS

Lists of the equipment and components are tabulated in Tables 4-3 and 4-4. Items specified for the sampling system are for one H-X system only.

The number of Monitor IV instruments required for bulk effluent analysis will depend on the final design of the OTEC PSD-1 module. If the evaporator and condenser are located close enough to each other, a single Monitor IV can be used to measure the ammonia level at the exit of each on a time-sharing-basis. Because the Monitor IV contains a heating bath to bring all sample and reagent solutions to a constant temperature, the difference in temperature of the condenser and evaporator effluents ($40^{o}F$ and $80^{o}F$) would not be a problem.

For leak location, a modified Monitor IV, which can accept samples at a rate faster than that needed for the bulk analysis, will be used in conjunction with each tube cleaner/sampling equipment set-up.

Table 4-1. Measurement List — Analysis System

A. For Evaporator

		Quantity	Range	Function
1.	NH_3 level at exit of evaporator (12 sample sites to locate leaking quadrant)	Continuous 1	0.00-0.30 ppm	Leak detection
2.	NH_3 level at entrance to evaporator	Continuous 1	0.00-0.30 ppm	Background NH_3 Estimation
3.	NH_3 level of 95 tube composite samples from tube cleaner and sampler as it traverses suspect quadrant(s)	110-440 as needed	0-1 ppm	Leak Location
4.	NH_3 level of each of 95 tubes	95, as needed	0-1 ppm	Leak Location
5.	Location of cleaner/sampler which corresponds to leaking bank of 95 tubes		TBD	Leak Location
6.	Location of leaking tube/tubes		TBD	Leak Location
7.	Reagent reservoir level	8	Full-empty	Monitor reagent supply
8.	Flow rate of sample lines into instruments	2	0-5 ml/min	Monitor inlet to instrument
9.	pH of complexing reagent stock solution	1/week	Determine pH=5.0	Preparation of reagent solution
10.	Weights of reagents in making stock solutions	4 solutions to be prepared once a week	0.00-500.00 g	Preparation of reagent solutions
11.	Pressure of air supply to continuous filter; regulator to 80 psig	2	TBD	Operations of continuous filter

Table 4-2. Equipment List — Analysis System

A. For Evaporator

I. Bulk Sampling

Part No.	Qty	Product Description
188-A003-01	1	Technicon Autoanalyzer Monitor IV System consisting of the following: One integral monitoring unit, incorporating a phototube calorimeter to provide linear readout and a 0-5 volt dc signal, proportional to concentration, for data handling or storage, a two speed proportional pump, 7 inch strip chart recorder, reagent containers and all necessary accessories.
		Monitor IV System for the determination of ammonia (2.8-140 µg-N/L) in water and seawater, complete with:
188-B028-01	1	A plattered manifold with heating bath
170-B070P27	1	Set/2, Interference Filters, 630 nm
ACC	1	Programmer Mechanism for automatic recalibration (Autocal)
Alarm	1	Hi-Level Alarm with Contact Closure
180-A001-01	1	Continuous Filter/Sampler (if ordered with Monitor IV System)
170-0144-01	4	Technicon In-Line reagent filter
	4	5-L reagent containers to provide larger reagent reservoirs for 1-week operation (1 container opaque)
	1	Simple acid scrubber bottle for air entering reagent bottle

Table 4-2. Equipment List — Analysis System (Continued)

A. For Evaporator (Continued)

II. Composite and Individual Sampling Mode

Part No.	Qty	Product Description
188-A003-01 188-B028-01 170-B070P27	1	Technicon Autoanalyzer system for NH_3 with the following modification: 15 x 1.5 mm short flow cell, type AA2, which will permit 60 samples/hour to be analyzed during leak search
180-A001-01	1	Continuous filter/sampler
170-0144-01	4	Technicon In-Line Reagent Filters
	4	5-L reagent containers, one of which opaque

B. For Condenser

I. Bulk Sampling

If the evaporator and condenser are located close enough to each other, a single Monitor IV can be used to measure the NH_3 level at the exit of each.

The following time-sharing option would allow both exit streams to be monitored on the same Monitor IV.

Part No.	Qty	Product Description
ACC	1	Automatic, Adjustable Programmer Control for two streams, including sequential valving system Otherwise duplicates of the equipment listed for the evaporator under "Bulk Sampling" must be purchased.

Table 4-2. Equipment List — Analysis System (Continued)

B. For Condenser (Continued)

II. Composite and Individual Sampling Mode

Duplicate requirements for evaporator "Composite and Individual Sampling Mode."

Separate equipment is recommended to minimize length of sample tubing required.

If there is a need to cut costs, and if the evaporator and condenser are close enough, there is a possibility that a single Technicon IV could be used for leak location in either (not simultaneously).

C. General

	Qty	Product Description
1.	1	Microprocessor to be used in monitoring the following: a. Condenser effluent NH_3, continuous b. Evaporator effluent NH_3, continuous c. 95-tube-composite NH_3 level (1-440 composites, as needed), condenser d. 95-tube-composite NH_3 level (1-440 composites, as needed), evaporator e. NH_3 level of individual tubes, as needed, condenser f. NH_3 levels of individual tubes, as needed, evaporator
2.		Housing for analytical equipment and reagent supplies Size depends on proximity of condenser and evaporator, which in turn determines the number of Technicon Monitor IV's to be purchased and the location of each.

Table 4-2. Equipment List — Analysis System (Continued)

C. General (Continued)

	Qty	Product Description
3.	1	Top-loading balance 0-1200 g (or TBD, depending on number of instruments and amount of reagent needed)
4.	1	Simple pH meter
5.		Reagent storage cabinet
6.	3	5-gal solution bottles — for solution batches. Heavy-duty polypropylene carbons
7.		Miscellaneous glassware
8.		Distilled water ~40 gal/week/instrument Solar-powered still on board?
9.		Compressed air
		Purchase by the tank or install air compressor, depending on amount needed
		(= function of No. of Technicon Monitor IV's)

TABLE 4.3 - MEASUREMENT LIST - SAMPLING SYSTEM

A. BULK SAMPLING MODE

	DESCRIPTION	REF. SYM	QTY.	RANGE	FUNCTION
1.	FLOW METER	FM1	1	0.10-1.00 GPM	CONTROL SAMPLE FLOW
2.	REAGENTS LEVEL	L3-L6	4	TBD	MONITOR REAGENT SUPPLY
3.	RESERVOIR LEVEL INDICATOR	L1, L2	2	TBD	MAINTAIN SAMPLE SUPPLY
4.	TEMPERATURE SENSOR	T1	1	32°F-150°F	MONITOR SAMPLE TEMERATURE

B. COMPOSITE AND INDIVIDUAL SAMPLING MODE (FIGURE 4.0 AND FIGURE 5.0)

1.	VAC. PRESS. TRANSDUCER	PT1-PT2	2	0-30"Hg	CONTROL RESERVOIR PRESS (FLOW)
2.	TEMPERATURE SENSOR	T1-T2	2	32°F-150°F	MONITOR SAMPLE TEMPERATURE
3.	VAC. PUMP PRESS GAUGE	P1	1	0-30"Hg	MONITOR VACUUM PUMP OPERATION
4.	PURGE PUMP PRESS GAUGE	P2	1	0-100 PSI	MOINTOR PURGE SYSTEM PRESSURE
5.	PURGE PUMP FLOW METER	FM2	1	0.2-2 GPM	MONITOR PURGE FLOW RATE
6.	HOLDING TANK LEVEL	L1	1	TBD	MOINTOR HOLDING TANK LEVEL
7.	SAMPLE RESERVOIR LEVEL	L2-L3	2	TBD	MONITOR SAMPLE RESERVOIR LEVEL
8.	REAGENT RESERVOIR LEVEL	L4	1	TBD	MOINTOR REAGENT SUPPLY
9.	CONTROL AIR PRESS GAUGE	P3	1	0-100 PSIG	MONITOR VALVE CONTROL AIR SUPPLY

TABLE 4.4 - EQUIPMENT LIST - SAMPLING SYSTEM

A. BULK SAMPLING MODE

	DESCRIPTION	REF SYM	QTY.	RANGE/SIZE	FUNCTION	MFG.*	P/N*
1.	PNEUMATIC VALVES	V1-V4, V7	5	0- .25 GPM	SAMPLE FLOW CONTROL	NUPRO	SS-8BK-91NO
2.	SUBMERSIBLE PUMP	PM1	1	0-1.0 GPM	BULK FLOW SOURCE	BYRON JACKSON	---
3.	SAMPLE RESERVOIR	RSV 2	1	TBD	SAMPLE STORAGE	TBD	TRW DCS
4.	HOLDING RESERVOIR	RSV 1	1	TBD	WASTE STORAGE	TBD	TRW DCS
5.	PUMP VALVES	V5-V6	2	0-1.0 GPM	PURGE FLOW CONTROL	WHITNEY	SS-5PDF8

* Suggested Source and Part Number

TABLE 4.4 - EQUIPMENT LIST - SAMPLING SYSTEM (CON'T)

B. COMPOSITE & INDIVIDUAL SAMPLING MODE

	DESCRIPTION	REF. SYM	QTY.	RANGE/SIZE	FUNCTION	MFG*	P/N*
1.	INDIVIDUAL RESERVOIR	RSV1	1	13 gal. (50 liters)	LABEL & STORAGE LOT #1	TBD	TRW DCS
2.	COMPOSITE RESERVOIR	RSV2	1	13 gal. (50 liters)	LABEL & STORAGE LOT #2	TBD	TRW DCS
3.	VACUUM PUMP	VP1	1	0-30"Hg, 30 CFM	RESERVOIR PUMP DOWN	KINNEY	TBD
4.	COLD TRAP	CT	1	0-30"Hg	CONDENSE MOISTURE	KINNEY	TBD
5.	VACUUM PRES. REG.	PR1	1	0-30"Hg	CONTROL RESERVOIR PRESS.	KINNEY	TBD
6.	RESERVOIR VENT VALVE	V2-V6	2	0-30"Hg	RELEASE RESERVOIR VAC.	NUPRO	SS-8BK-91NC
7.	VACUUM VALVES	V3-V7	2	0-30"Hg	FLOW CONTROL	NUPRO	SS-8BK-91NC
8.	RESERVOIR VALVES	V4-V8	2	0-0.01 GPM	SAMP. FLOW SHUTOFF&DRAIN (3-WAY)	TBD	TBD
9.	PURGE PUMP	PM1	1	0.2-2.0 GPM	PURGE SAMPLE SYSTEM "PRICE" H^{O}-175, 3/4 H^{O}	TBD	TBD
10.	PURGE CHECK VALVE	CV1	1	0.2-2.0 GPM	BACKFLOW CONTROL	NUPRO	SS-8C-10
11.	FLOW CONTROL VALVE	V12	1	0.2-2.0 GPM	PURGE FLOW CONTROL	WHITNEY	SS-5PDF8
12.	PURGE FILTER	F1	1	0.2-2.0 GPM	FILTER PURGE FLOW	NUPRO	SS-8TF-140S
13.	PURGE VALVES	V1-V9	2	0.2-2.0 GPM	PURGE SEQUENCING	NUPRO	SS-8BK-91NC
14.	HOLDING TANK	RSV3	1	TBD	PREVENT SEA WATER POLLUT.	TBD	TRW DCS
15.	HOLDING TANK VALVE	V11	1	TBD	DRAIN HOLDING TANK	NUPRO	SS-8BK-91NC
16.	REAGENT VALVES	SV11	1	0-0.016 GPM	CONTROL REAGENT FLOW	NUPRO	SS-4BK-91NC
17.	PUMP/FILTER ASSEMBLY	PF1	2	(TECHNICON)	FILTRATION OF SAMPLES	TECHNICON	TBD
18.	INLET MULTIPLEX VALVE	(ASSEMBLY)	95	0-.5 GPM	INDIVIDUAL SAMPLE CONTROL	NUPRO	SS-8BK-91NO
19.	OUTLET MULTIPLEX VALVE	(ASSEMBLY)	95	0-.5 GPM	INDIVIDUAL SAMPLE CONTROL	NUPRO	SS-8BK-91NO
20.	AIR PILOT SOLENOIDS VALVES		250	0-100 PSIG	PILOT VALVE FOR SYS. CTRL.	TBD	TBD
21.	TANK RELIEV VALVES		2	50-100 PSIG	TANK SAFETY VALVES	NUPRO	SS-4CPAZ-50
22.	INSTR. AIR COMPRESSOR		1	0-100 PSIG, 10 SCFM	SOURCE FOR AIR ACTUATED VLVS.	TBD	TBD

* SUGGESTED SOURCE

5. SUMMARY

A very feasible system has been devised for ascertaining the concentration of ammonia in sea water. A composite total sample will be analyzed and, in event of excessive leakage, individual composites of 95 tubes will be analyzed via use of a modified brush cleaning unit. Further, more limiting composites will be sequentially analyzed in order to narrow the leak to a small group of tubes or to the individual tube. Refer to Figure 5-1 showing a Logic Diagram used in Decision Criteria.

The detection system will use the standard Berthelot Reaction which is well documented and very reliable for measuring ammonia concentrations in sea water.

The sampling system concept has been finalized, and only localized design study will be needed. All transfer principles have been examined, including vacuum transfer, general line flushing, back-flushing, and final chemical analyses.

This system should prove very reliable and an asset to the program.

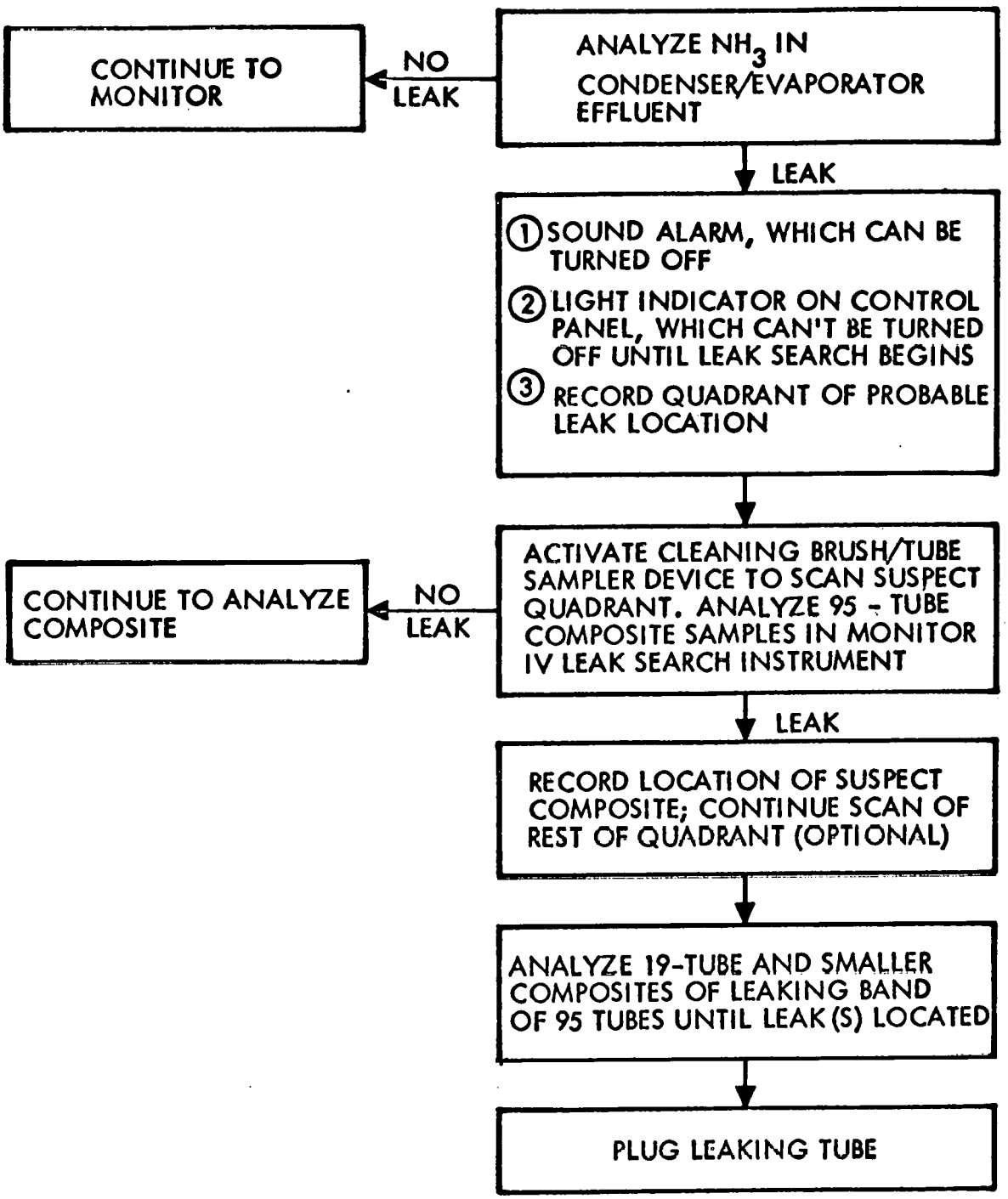

Figure 5-1. Logic Diagram for Sampling

ATTACHMENT 1

1. Methods for Chemical Analysis of Water and Wastes, 1971 Environmental Protection Agency, Water Quality Office, Cincinnati, Ohio.

2. Van Slyke, D.D. and Hillen, A.J., Bio Chem., 102, p. 499, 1933.

Kallman, S., Presentation at Div. I Meeting of ASTM Committee E-3, April 1967, San Diego, California.

Bolleter, W.T., Bushman, C.J. and Tidwell, P.N., Anal. Chem., 33, p. 592, 1961.

Tellow, J.A. and Wilson, A.L., Analyst, 89, p. 453, 1964.

Tarugi, A. and Lenci, F., Boll Chim. Farm., 50, p. 907, 1912.

FWPCA Methods of Chem. Anal. of Water and Wastewater, Nov., 1969, p. 137.

Gilbert, T.R. and Clay, A.M., Anal. Chem 45, p. 1757 (1973).

Zadorojny, C., Saxon, S., and Finger, R., Journal WPCF, 45, p. 905 (1973).

3. Riley, J.P. and Skirrow, G., "Chemical Oceanography, Vol. 1," Academic Press, London, 1965, p. 387.

ATTACHMENT 2

REFERENCES

IOC No. 4341.AC 78-161, J.S. Shapiro/J. Wilson to Lee Leventhal.

IOC No. 78.4725.3-126, W.F. Chew to L. Ryan.

APPENDIX H.2

OTEC PSD-1, EFFECTS OF SEAWATER LEAKAGE INTO AMMONIA SYSTEM

TRW
DEFENSE AND SPACE SYSTEMS GROUP
ONE SPACE PARK • REDONDO BEACH • CALIFORNIA 90278

INTEROFFICE CORRESPONDENCE

4341.AC.78-183

TO: Paul Edris CC: DATE: 14 September 1978

SUBJECT: OTEC PSD-1, Effects of Sea Water Leakage Into Ammonia System

FROM: J. S. Shapiro/J. Wilson
BLDG. 01 MAIL STA. 2030 EXT. 62451

Attached is the report on our study of the possibility of seawater flow into ammonia in the OTEC system. The chemistry of the ammonia-seawater system is discussed, and suggestions for minimizing harmful effects on the heat exchangers are presented.

Distribution
M. BIANCHI
W. CHEW
P. FUKUNAGA
G. GIBSON
A. GRANT
R. JONES
J. KAELLIS
L. KENT
D. REEVES
L. ROSALES
S. VINCENT

After reviewing the effects of ammonia leakage into water, the next logical step would be to review the effects of sea water leakage into ammonia, if any. One can look at this problem as being somewhat remote, but there still exists the possibility of incursion of sea water into the ammonia system.

POSSIBLE LEAKAGE

Since the lower pressure limit for the NH_3 system is about 90 psia and the water pressure at the bottom tube sheet will be only about 35 psia, the amount of sea water entering the ammonia is expected to be very small. Essentially back diffusion would be the main source of leakage. The other major source of leakage would be reduced pressure in the ammonia system. To prevent this, we recommend that make-up ammonia be added on a continuous basis so that any possible ammonia leak will not reduce the system pressure. This will minimize the back-diffusion of sea water into ammonia and deleterious effects on the efficiency of the power system.

The expected decrease in efficiency caused by water in ammonia used for the power loop has already been studied. [See attached addendum].

Any sea water entering the system would reduce thermal efficiency by lowering the pressure in the evaporator. However, blowdown pumps have already been designed into the system to permit removal of wet ammonia. This ammonia would be distilled and purified.

CHEMICAL EFFECTS

The salt content of the sea water presents the most serious threat to system efficiency. Magnesium ions present at a 1350 ppm level in sea water will precipitate as $Mg(OH)_2$ in the presence of the hydroxide ions formed in wet ammonia. The equations for this reaction are:

$$NH_3 + H_2O \rightleftharpoons NH_4^+ + OH^-$$

$$Mg^{+2} + 2\ OH^- \longrightarrow Mg(OH)_2 \qquad \text{(white flocculent precipitate)}$$

Accumulation of $Mg(OH)_2$ on the ammonia side of the heat exchanger tubes will provide a barrier or insulation of the tubes with the resultant decrease of heat transfer and the reduction of plant efficiency.

Calculations were made to estimate the magnitude of the problem for leaks of various sizes. The assumptions and data used in the calculations are:

- Magnesium hydroxide is very insoluble in water ($K_{sp} = 1.2 \times 10^{-11}$).
- The dielectric constant of ammonia is lower than that of water, making ammonia a poorer electrolytic solvent than water.
- Although no K_{sp} value was found for $Mg(OH)_2$ in ammonia, magnesium hydroxide would be expected to be less soluble in ammonia than in water.
- The aqueous solubility product constant for $Mg(OH)_2$ was used in the calculations, and for simplicity it was assumed that all Mg^{+2} present would precipitate if the K_{sp} were exceeded.

Table 1 summarizes the amounts of precipitate expected from different levels of sea water in a 200,000 pound ammonia system.

Formation of $Mg(OH)_2$ Precipitate from Sea Water Leak Into Ammonia System

Leak, ppm Sea Water in NH_3	Pounds of $Mg(OH)_2$ Which Would Precipitate in NH_3 System
50 ppm	No ppt
200	No ppt
1000	0.6
5000	3.0
200,000	12.0

While reviewing the data, other assumptions should be considered.

- Use of a K_{sp} value for $Mg(OH)_2$ in ammonia, which is expected to be smaller than that in water, would reduce the leak level at which precipitate begins forming but would not change the total amount of precipitate expected.

- The density of the $Mg(OH)_2$ is about four times greater than that of liquid ammonia, and the precipitate is expected to accumulate on the bottom tube sheet. It is impossible to estimate how much build-up on tube walls might occur at various leak sites in the system.

OTHER POSSIBLE CHEMICAL REACTIONS

Another problem anticipated is the precipitation of Calcium Carbonate, $CaCO_3$, caused by the increase in the sea water pH as it enters the ammonia system. Buildup of solid $CaCO_3$ would further reduce the thermal transfer efficiency of the system. Since only aqueous K_{sp} values are available, the magnitude of the problem must be determined experimentally.

The solubility of sodium chloride in ammonia is 3.02g NaCl/100g NH_3, compared with a solubility in water of 37g/100gH_2O. Even in leaks which result in sea water levels of 200,000 ppm, no NaCl is expected to precipitate.

POSSIBLE CORRECTIVE/PREVENTIVE ACTION

It may be possible to inhibit the formation of $Mg(OH)_2$ and Ca CO_3 by the addition of a sequestering agent, such as acid Versene, EDTA, which is available as a solid.

The compound is very soluble in water and is expected to be soluble in ammonia, but development work would be necessary to test the feasibility of this approach. Because the pH of the ammonia will be a function of the water present, it must also be verified that the magnesium-EDTA and the calcium-EDTA complexes will be stable at the expected pH levels.

An alternative approach for removal of these potential precipitates would be periodic cleaning of the system with an acid. This would necessitate removal of the ammonia, flushing with an acid which is compatible with titanium, and then flushing with appropriate solvent to remove said acid. It would be necessary to avoid nitric, sulfuric, or any halogenated acid.

MATERIALS COMPATIBILITY

Studies on the effect of sea water in ammonia on the materials of construction of the system have already been performed by Louis A. Rosales and

Maurice P. Bianchi of the Materials Engineering Department of the Manufacturing Division. In speaking with them, they stated that the details have all been documented and reported to the OTEC Program Office. As a consequence, we did not belabor this facet.

CONCLUSION

It is unlikely that sea water leakage into ammonia would occur to any extent, but in the event of some leakage, it would be imperative to have a method for removal of any solids formed. The primary chemical reactions would produce $Mg(OH)_2$ and $Ca\ CO_3$.

This potential leakage and resultant compounds underscore the necessity of a good NH_3 leak detection system on the water side of the heat exchangers. As soon as a leaking tube is located and plugged, the possibility of sea water's entering the NH_3 system at that point is eliminated.

Approved L E Ryan
L. E. Ryan, Section Head
Analytical Chemistry

ADDENDUM

AMMONIA SUPPORT SUBSYSTEMS

EFFECT OF AMMONIA PURITY Water in ammonia used for the power loop will concentrate in the evaporator because it is less volatile than ammonia. With a constant evaporator temperature, as set by the warm seawater, the presence of water will lower the pressure in the evaporator. The net result is a reduction in the efficiency of the power loop. More ammonia would have to be evaporated and equipment sizes and parasitic loads would increase.

The table that follows compares operation of the power loop with pure ammonia and with 98 weight percent ammonia in the evaporator. The following were fixed for both cases. Temperature in the evaporator. Pressure drop from evaporator to turbine inlet. Turbine exhaust pressure. Turbine efficiency. And gross power output. There would be about 20 ppm of water in the vapor leaving the evaporator in the 98 weight percent ammonia case.

BLOWDOWN As pointed out in the paragraph on ammonia purity, water in the evaporator will reduce the power system efficiency. To control the amount of water build up in the evaporators, blowdown pumps are provided so liquid from the evaporators can be blown down to the heel storage tank. From there, the blowdown is fed to the rectifying column.

If the water concentration in the evaporators is held at 1000 ppm, there will be a drop in evaporator pressure at constant temperature of about 0.1 psi and a system loss in efficiency of about 0.2 percent. This is based upon a straight line interpolation of the comparison given earlier between performance for pure ammonia and for 98 weight percent ammonia. It is assumed that 1000 ppm of water in the evaporator is a practical concentration to hold and that the 0.2 percent loss in system efficiency is tolerable.

TRW, OTEC, Project 5304-P, January 10, 1978

AMMONIA SUPPORT SUBSYSTEMS

EFFECT OF AMMONIA PURITY Continued

	PURE NH_3 IN EVAPORATOR	98 WEIGHT PERCENT NH_3 IN EVAPORATOR
Temperature in evaporator, °F	70	70
Pressure in evaporator, psia	128.8	126.7
Pressure drop to turbine, psi	1.5	1.5
Pressure at turbine, psia	127.3	125.2
Temperature at turbine, °F	69.53	69.49
Vapor enthalpy at turbine, Btu/lb	629.1	629.6
Vapor entropy at turbine, Btu/lb °F	1.2153	1.2179
Turbine outlet pressure, psia	89.2	89.2
Moisture at turbine outlet, wt %	2.90	2.65
Enthalpy at turbine outlet at constant entropy, Btu/lb	609.9	611.2
ΔH at constant entropy, Btu/lb	19.2	18.4
Ammonia flow for 34.77 MWe at 85% turbine efficiency, lb/hr	7,271,000	7,587,000
Ammonia flow increase, %	-	4.3
Increased heat to evaporator, %	-	4.6
Increased heat to condenser, %	-	4.7

The increases in heat to the evaporator and to the condenser are slightly greater than the increase in flow because the enthalpies leaving the evaporator and entering the condenser are also slightly higher for the 98 weight percent case than for the pure ammonia case. The increase in parasitic loads for a fixed net power output means even a greater disadvantage than shown.

TRW, OTEC, Project 5304-P, January 10, 1978

TABLE 4.4 - EQUIPMENT LIST - SAMPLING SYSTEM (CON'T)

B. COMPOSITE & INDIVIDUAL SAMPLING MODE

DESCRIPTION	REF. SYM	QTY.	RANGE/SIZE	FUNCTION	MFG*	P/N*
1. INDIVIDUAL RESERVOIR	RSV1	1	13 gal. (50 liters)	LABEL & STORAGE LOT #1	TBD	TRW DCS
2. COMPOSITE RESERVOIR	RSV2	1	13 gal. (50 liters)	LABEL & STORAGE LOT #2	TBD	TRW DCS
3. VACUUM PUMP	VP1	1	0-30"Hg, 30 CFM	RESERVOIR PUMP DOWN	KINNEY	TBD
4. COLD TRAP	CT	1	0-30"Hg	CONDENSE MOISTURE	KINNEY	TBD
5. VACUUM PRES. REG.	PR1	1	0-30"Hg	CONTROL RESERVOIR PRESS.	KINNEY	TBD
6. RESERVOIR VENT VALVE	V2-V6	2	0-30"Hg	RELEASE RESERVOIR VAC.	NUPRO	SS-8BK-91NC
7. VACUUM VALVES	V3-V7	2	0-30"Hg	FLOW CONTROL	NUPRO	SS-8BK-91NC
8. RESERVOIR VALVES	V4-V8	2	0-0.01 GPM	SAMP. FLOW SHUTOFF&DRAIN (3-WAY)	TBD	TBD
9. PURGE PUMP	PM1	1	0.2-2.0 GPM	PURGE SAMPLE SYSTEM "PRICE" H^O-175, 3/4 H^O	TBD	TBD
10. PURGE CHECK VALVE	CV1	1	0.2-2.0 GPM	BACKFLOW CONTROL	NUPRO	SS-8C-10
11. FLOW CONTROL VALVE	V12	1	0.2-2.0 GPM	PURGE FLOW CONTROL	WHITNEY	SS-5PDF8
12. PURGE FILTER	F1	1	0.2-2.0 GPM	FILTER PURGE FLOW	NUPRO	SS-8TF-140S
13. PURGE VALVES	V1-V9	2	0.2-2.0 GPM	PURGE SEQUENCING	NUPRO	SS-8BK-91NC
14. HOLDING TANK	RSV3	1	TBD	PREVENT SEA WATER POLLUT.	TBD	TRW DCS
15. HOLDING TANK VALVE	V11	1	TBD	DRAIN HOLDING TANK	NUPRO	SS-8BK-91NC
16. REAGENT VALVES	SV11	1	0-0.016 GPM	CONTROL REAGENT FLOW	NUPRO	SS-4BK-91NC
17. PUMP/FILTER ASSEMBLY	PF1	2	(TECHNICON)	FILTRATION OF SAMPLES	TECHNICON	TBD
18. INLET MULTIPLEX VALVE	(ASSEMBLY)	95	0-.5 GPM	INDIVIDUAL SAMPLE CONTROL	NUPRO	SS-8BK-91NO
19. OUTLET MULTIPLEX VALVE	(ASSEMBLY)	95	0-.5 GPM	INDIVIDUAL SAMPLE CONTROL	NUPRO	SS-8BK-91NO
20. AIR PILOT SOLENOIDS VALVES		250	0-100 PSIG	PILOT VALVE FOR SYS. CTRL.	TBD	TBD
21. TANK RELIEV VALVES		2	50-100 PSIG	TANK SAFETY VALVES	NUPRO	SS-4CPAZ-50
22. INSTR. AIR COMPRESSOR		1	0-100 PSIG, 10 SCFM	SOURCE FOR AIR ACTUATED VLVS.	TBD	TBD

* SUGGESTED SOURCE

APPENDIX I

HEAT EXCHANGER DESIGN SUPPORTING DATA

THIS PAGE

WAS INTENTIONALLY

LEFT BLANK

APPENDIX I.1

THERMAL/HYDRAULIC ANALYSIS

I.1. THERMAL/HYDRAULIC ANALYSIS

The tube side (sea water) heat transfer coefficients and the shell side heat transfer coefficients, both the ammonia condensing and the ammonia evaporating, were determined from equations developed from experimental data. The tube metal wall conductance was calculated on the basis of a "thermal thickness". All heat transfer coefficients were referred to an equivalent inside smooth tube; that is, a tube with an inside diameter which has the same flow area as the fluted tube. The overall heat transfer coefficient U was determined in the usual manner as the reciprocal of the sum of the reciprocals of the individual heat transfer coefficients plus the fouling factor.

I.1.1 Tube Side Equations - Heat Transfer and Pressure Drop

Seawater Heat Transfer. The seawater heat transfer coefficients were determined from equations developed from experimental data in the CMU thermal-hydraulic laboratories. These equations are based on the postulate that the seawater heat transfer coefficient for a fluted tube is greater than that of a smooth tube by the ratio of surface area of the fluted tube to that of an equivalent inside diameter smooth tube. This ratio is termed the area ratio.

The tube side equation developed at CMU is:

$$Nu = 0.027Re^{0.8}Pr^{1/3}AR$$

where Nu, Re, Pr are respectively the Nusselt, Reynolds and Prandtl numbers. The diameter used in both the Nusselt and Reynolds Numbers is the diameter of the equivalent smooth tube;

AR = the area, or surface, ratio.

It is the ratio of the surface of the fluted tube to that of the equivalent smooth tube.

$$Nu = \frac{hD}{k} \; ; \; h_{\substack{\text{tube} \\ \text{side}}} = Nu \frac{k}{D}, \; k = \text{thermal conductivity of seawater}$$

This equation is in the form originally proposed by Dittus-Boelter. Figures 1 thru 6 show plots of the same equation in the form proposed by Colburn, together with experimental points:

$$j_H = AR \times j_{H/S} = \frac{h}{C_p V \rho} Pr^{2/3}$$

V = velocity and ρ = density

j_H = Colburn j factor for heat transfer in a fluted tube

$j_{H/S}$ = Colburn j factor for the equivalent smooth tube

Figures 1 thru 6 also show the j_F factor for a fluted tube as determined from the Blasius Equation together with experimental points. For a smooth tube, the Blasius Equation is:

$$fs = \frac{0.316}{Re^{0.25}}$$

For a fluted tube this becomes

$$f = \frac{0.316 \times AR}{RE^{0.25}}$$

j_F for a fluted tube, thus is determinable as

$$j_F = \frac{f}{2} = \frac{0.316 \times AR}{2 \times Re^{0.25}} = \frac{fs}{2} \times AR$$

The equation actually used in design is:

$$fs = \exp[0.025\ (\ln Re)^2 - 0.7534\ (\ln R) + 1.1386]$$

which was developed by TRW. In the range $20{,}000 \leq Re \leq 60{,}000$. Both the Blasius and TRW equation give substantially the same values; however, for high Reynolds numbers the Blasius Equation extrapolates below all the published data for smooth drawn tubes whereas the TRW equation is consistent with published results.

I.1.2 Evaporation Heat Transfer Coefficient

Experimental data from CMU Heat Transfer Laboratories, for the composite evaporation heat transfer coefficient (a composite coefficient includes the metal wall) for the evaporation of Freon 11 on fluted 26 mill

tubes is shown in Figure 8. Experiments with 40 mill fluted tubes gave essentially the same results. This data on Freon 11 was converted to ammonia data by use of a correction factor. The ammonia evaporation composite heat transfer coefficient is 6.27 times the Freon 11 composite heat transfer coefficient. The validity of this correction factor was verified by further experiments with ammonia evaporating from 26 mill fluted tubes. Curve "B", shown on Figure 8, is then the starting relation between the expected local composite ammonia evaporation coefficient and the local Reynolds number. This curve was integrated between Re_B (Reynolds number at the bottom of the evaporator, always less than 3000) and Re_T (Reynolds number at the top of the evaporator, always greater than 3000). The Reynolds number is defined as:

$$Re = \frac{4\Gamma}{\mu}$$

μ = viscosity and Γ = tube loading

= (lb/hr)/(ft of "smooth tube peripheral length")

"smooth tube peripheral length" = πD where

D is the rill diameter.

The integrated equation, divided by $Re_T - Re_B$, is thus the mean value of the composite heat transfer coefficient.

$$h_{e/mean} = \frac{\left(2.939\ Re_T^{0.4151} - 63.217\right) 8 \times 10^5 - 5.633\ Re_B^{1.8452}}{\left(Re_T - Re_B\right)} \qquad \begin{matrix} Re_B \leq 3000 \\ Re_T \geq 3000 \end{matrix}$$

Re_T and Re_B must satisfy a material balance; that is the tube loading difference, and thus Reynolds number difference, between the top and bottom of the tube must reflect the quantity of ammonia evaporated. In addition, the maximum value of $h_{e/mean}$ is obtainable if Re_T and Re_B satisfy the relation:

$$Re_T = \frac{3.17508 \times 10^8}{Re_B^{1.44537}}$$

This equation and the material balance permit determining Re_T and Re_B for optimum (maximum $h_{e/mean}$) operation.

$h_{e/mean}$ thus determined, is corrected to a pure evaporation heat transfer coefficient by removing the metal resistance of the experimental evaporation tube and adding the metal resistance of the design tube.

The metal resistance of the experimental tube is 4.6695×10^{-5}.

$$h_{e,composite,design} = \frac{1}{\left(\frac{1}{h_{e/mean}} - 4.6695 \times 10^{-5} + r_m\right)}$$

r_m = metal wall resistance of the design tube.

I.1.3 Condensing Heat Transfer Coefficient

The experimental data for tube E in Oak Ridge Report ORNL-5356, Figure 7, was used as the basis for the condensing coefficient. This data was chosen because it most resembles the fluted tubing used for the TRW-OTEC design. The original Oak Ridge data was revised to an equivalent smooth tube surface basis in accordance with the TRW calculation procedure by use of the $A_{O.R./A_s}$ ratio. The ratio $A_{O.R./A_s}$ is the ratio of the total surface as used by Oak Ridge to the surface of a smooth tube having the same diameter as the rill diameter of Tube E. The heat transfer coefficient was divided by this ratio and the flux multiplied by this ratio. The experimental data was then fitted to an equation to give the following expression:

$$h_c = -3231.62 + \frac{3.684 \times 10^8}{\left(\frac{q}{A} + 20129.28\right)}$$

q = total flux BTU/hr

A = total smooth tube surface referred to rill diameter

The metal resistance of the experimental tube was then subtracted from this composite and the metal resistance of the actual tube reinserted in

a manner similar to that described for the evaporator composite coefficient. The resistance of tube E used in the Oak Ridge experiment is 2.245×10^{-5}

$$h_{c,composite,design} = \frac{1}{\left(\frac{1}{h_c} - 2.245 \times 10^{-5} + r_m\right)}$$

r_m = metal wall resistance

Both the evaporation and condensing coefficients have a rather small influence on the size of the final design since the attenuation factors, listed in Table 1 are 0.05 and 0.03 respectively for the evaporator and condenser.

I.1.4 Metal Resistance

Procedures for determining the metal wall resistance of tubes fluted both internally and externally are not generally available in the literature.

The metal resistance was determined as a thermal thickness divided by the tube thermal conductivity. The thermal thickness is the wall thickness of a smooth tube which has the same wall resistance as the fluted tube. Tube curvature, as encountered in a round tube, influences the results to such a small extent that it was ignored. Thermal thickness is determined in the following manner:

The one-dimensional Fourier Equation in finite difference form is:

$$q = -k\ PL\ \frac{\Delta T}{\Delta X} \qquad (1)$$

in which L is the length of the slab (visualize as corresponding to the length of the tube) and P is a distance perpendicular to the flux (visualize as the perimeter of the tube); ΔX is the thickness of the slab. The equation may be written:

$$\frac{\Delta X}{P} = \frac{-k\Delta T}{\frac{q}{L}} \qquad (2)$$

For several slabs in series we may add equation (2) for each of the slabs to obtain:

$$\Sigma\frac{\Delta X}{P} = \Sigma\frac{-k\Delta T}{\frac{q}{L}}$$

Since k and q/L are constant we may factor these outside of the Σ operator. The term $\Sigma\Delta T$, which remains, is simply the overall temperature difference, thus for a series of slabs

$$\Sigma\ \frac{\Delta X}{P} = \frac{-k\Delta T_{o.a.}}{\frac{q}{L}} \qquad (3)$$

Now, we consider a hypothetical single slab (corresponding to a smooth tube) which has the same heat rate per unit length and the same overall temperature difference, equation (2) becomes

$$\frac{\Delta X_s}{P_s} = \frac{-k\Delta T_{o.a.}}{\frac{q}{L}} \qquad (4)$$

Since we have postulated that the right hand side of equations (3) and (4) are equal, we may equate the left hand sides to obtain

$$\Delta X_s = \left(\Sigma\ \frac{\Delta X}{P}\right)P_s \qquad (5)$$

ΔX_s is the thickness of a smooth tube having a thermal thickness equivalent to a fluted tube and P_s may, essentially, be considered as the distance between lines of flute symmetry, i.e., about one-half the pitch, as shown in Figure 9 and Figure 10.

We now consider the method of determining $\Sigma\ \frac{\Delta X}{P}$. On the seawater side the purpose of the flutes is to enable the high thermal conductivity metal to protrude past the low conducting laminar sublayer into the turbulent core. In actuality the laminar sublayer in the rill of the flutes is much thicker than the laminar sublayer for a smooth tube, implying much poorer heat transfer, and significantly thinner on the crest, implying much improved heat transfer. We arbitrarily assume all surface

of the flute from the bottom of the rill to a distance 4.5 mills above the bottom of the rill to be an adiabatic and the remainder of the flute to be an isotherm.

For condensing on external flutes, condensate and essentially all of the heat, enters at the crest of the flute. Similarily, for evaporation, all of the heat leaves at the crest of the flute. We arbitrarily assume 50 percent of the flute surface close to the rill is an adiabatic. The lines of symmetry are, of course, adiabatics. The adiabatic lines are shown in Figure 9.

Once the adiabatics are established, the isotherms are lines between the adiabatics and perpendicular to the adiabatics, although in actual practice no attention was paid to the fact that the isotherms must be perpendicular to the adiabatics.

The lengths of each of the two adiabatics were measured and segmented into ten equally spaced distances. Lines were then drawn between the adiabatic connecting the terminus of each of the segments, these lines are considered isotherms; several isotherms are shown in Figure 9. Distances between isotherms measured at the midpoint, are considered to be the thicknesses (ΔX) of a stacking of slabs. The lengths of the isotherm is the distance (P) for use in equation 5.

Thermal thicknesses are now being determined by finite difference procedures using SINDA, a generally available library computer code, and are also being verified by testing specific evaporator and condenser tubes for use in the TRW OTEC design.

I.1.5 Shell Side Pressure Drop

The shell side pressure drop was determined by Carnegie-Mellon University using the Gunter-Shaw correlation (Gunter, A.Y. and Shaw, W.A., "A General Correlation of Friction Factors for Various Types of Surfaces in Crossflow", Trans. A.S.M.E., 67, 643 (1945)). These calculations are included elsewhere in the appendix. The Gunter-Shaw correlation was corrected using a correction factor determined experimentally at CMU. The equation was integrated across the tube bundle with due consideration for

the change in both flow and flow area across the bundle. The final equation obtained by CMU is, assuming no vapor lanes:

$$\Delta P = 6.36 \times 10^{-7} D^{2.855}$$

ΔP = pressure drop, $\#_{F/in.^2}$

D = Bundle dia., ft

This equation is applicable to a 1-1/2 inch tube on a 1.25 pitch to diameter ratio with 9.02 ft^3/(hr. ft. of tube) condensed on a one inch tube. The actual condensing rate in the TRW design is 7.44 ft^3/(hr. ft. of tube). Since pressure drop across the bundle varies as the cube of the tube diameter, and as the 1.855 power of the vapor generated, corrections are conveniently made for tube diameter and flow differences, and the corrected equation becomes:

$$\Delta P_c = 3.189 \times 10^{-6} D^{2.855}$$

In the evaporator, the evaporation rate is 5.94 ft^3/hr. ft. of tube). Pressure drop also varies with the 0.855 power of the density. The equation developed for the condenser, where flow is outward, is also applicable to the evaporator, where flow is inward. After correcting for diameter, flow differences and the higher density in the evaporator we obtain:

$$\Delta P_e = 2.805 \times 10^{-6} D^{2.855}$$

For the TRW design, assuming no vapor lanes, the pressure drop from bundle periphery to bundle center in the condenser is 0.031 psi and from center to periphery in the evaporator 0.027 psi. With these pressure drop values no flow distribution difficulties are expected.

Entrance and exit losses were calculated on the basis of K, or resistance coefficients, in the expression $\Delta P = KV^2\rho/2g$. ΔP,V,ρ and g are respectively the pressure drop, velocity, density and gravitational constant. K for an entrance was assumed to be 0.5 and an exit 1.

The total pressure drop in the evaporator is the sum of the entrance, distribution plenum crossing, orifice, bundle penetration and exit losses as diagrammed in Figure 11.

Total pressure drop in the condenser is the sum of the entrance and bundle penetration losses as diagrammed in Figure 11.

I.1.6 Evaporator and Condenser Dimentions

The tube bundle diameters for both the evaporator and condenser are determined by the required number of tubes.

The region between the condenser shell inlet and the condenser tube bundle, the vapor dome, was sized to have sufficient volume and flow areas to prevent the possibility of tube vibration due to high inlet velocities. The criterion for determining flow areas in this region was taken from the "Standards of Tubular Exchanger Manufacturers Association" (TEMA) which requires that at the inlet $\rho V^2 \leq 500$; ρ = density in lb/ft^3 and V is velocity in ft./sec. A shell diameter was then chosen which would accommodate this required flow area. Since vapor flow diminishes around the periphery of the tube bundle, a decreasing flow area, around the periphery, incorporating an eccentric shell was chosen. An impact baffle consisting of solid round bars was installed at the vapor inlet to disperse the inlet flow and prevent direct impingement on the tube.

A similar design procedure was followed for the evaporator except that a rod impact baffle is not required at the vapor outlet. A rod baffle was installed at the liquid inlet.

I.1.7 Non-Condensibles

I.1.7.1 Startup Removal

Initial non-condensible removal was determined by considering the system to resemble mixing tanks in series. W(lb/hr) of atmospheric ammonia enters the first tank. The tanks are initially full of nitrogen. The derivation was cognizant of density variation within the tanks due to the difference in molecular weight of ammonia and nitrogen. The expression for the concentration of non-condensibles in the effluent from the system

is given by the equations. The derivation of these equations is given later in the appendix.

$$\alpha = C_o \rho_o \left\{ 1 - e^{-PN} \sum_{i=1}^{N} \frac{(PN)^{N-i}}{(N-i)!} \right\}$$

$$C_{N.C.} = \frac{1 - \frac{\alpha}{\rho_o}}{1 + \alpha V_o \left(\frac{1}{M_{N_2}} - \frac{1}{M_{NH_3}} \right)}$$

$C_{N.C.}$ = conc. of non-condensibles, $lb_{N.C.}$/lb mix in effluent from last tank

ρ_o = density of ammonia entering = 0.04396 lb/ft^3

C_o = concentration of ammonia entering $\frac{lb_{NH3}}{lb\ mix} = 1$

V_o = mole volume at purging conditions = 386 ft^3

M_{N_2}, M_{NH_3} = molecular wt. of nitrogen and ammonia respectively, 28 and 17

P = number of purges

N = number of tanks in series

A plot of the exiting non-condensible concentration versus the number of purges is given in Figure 12, for several different "number of tanks" in series. The system is expected to operate as, or close to, three tanks in series. Approximately two to three purges should be sufficient to reduce the non-condensibles to a value which will permit pressurization of the system and further removal by the procedures for removing non-condensibles during normal operation. Figure 13 is a plot of non-condensible concentration in the exiting gas versus time if the system is being flushed at a rate of 1600 ft^3/min. of atmospheric ammonia.

I.1.7.2 Operational Removal of Non-Condensibles

Non-condensible purging during operation was considered in the following manner. A leak is presumed to occur which ultimately results in the inlet vapor to the condenser entering with a constant concentration of non-condensible. This process continues to build up non-condensibles in

the condenser until "discovery time." Discovery is initiated by some evidence of degraded system operation. Discovery time and normalized concentration are related by the expression:

$$t_D = \beta_{/D} \frac{\rho V}{W}$$

t_D = discovery time - hrs.

V = free condenser volume - ft^3

W = vapor inlet rate - lb/hr

ρ = vapor density

$\beta_{/D}$ = normalized concentration, ratio of concentration of non-condensibles in condenser to concentration of non-condensibles in inlet vapor at discovery time.

Purging begins at discovery time, while non-condensibles continue to enter, and the ratio of tank to inlet concentration is given by the expression:

$$\beta = \left(\frac{W}{\rho V} t_D - \frac{1}{F}\right) \exp\left[-\frac{FW}{\rho V}(t - t_D)\right] + \frac{1}{F}$$

F = fraction of the inlet flow removed by the purging system

t = total time from initial entry of non-condensibles - hr.

Both the above equations are derived elsewhere in the appendix. Figures 14 and 15 are plots of tank concentration for discovery times of 0.25 and 0.5 hrs respectively. The parameter is F x 100, the percent of the inlet flow purged. It is apparent that the shorter the discovery time (the greater the leak) the more difficult is recovery. Consideration of Figure 14 indicates that a 0.6 percent purge rate reduces condenser non-condensibles to about 37 percent of its discovery time value in 0.4 of an hour. Since the concentration after recovery is 37 percent of that value which made degraded system performance evident, it is presumed the system can continue to operate in a reasonable manner with purging until the leak is discovered and remedial steps taken.

The condenser purging system consists of an evacuation tube with holes, or orifices in the tube wall. The evacuation tube can remove considerably more than 0.6 percent of the inlet flow used in the above illustration. The evacuation is not limited by pressure drop since all the pressure within the condenser (approximately 75 psig) is available for flow. At a 0.6 percent withdrawal rate the velocity through the evacuation tube orifices is about 65 ft/sec. whereas the sonic velocity is about 1400 ft/sec. Pressure drop through the evacuation tube is at least two orders of magnitude less than pressure drop through the evacuation tube orifices, thus assuring uniform pick-up along its length. The evacuation tube has been positioned at the point where the non-condensibles have the greatest concentration, namely at the end of the vapor train (which is in the center of the condenser).

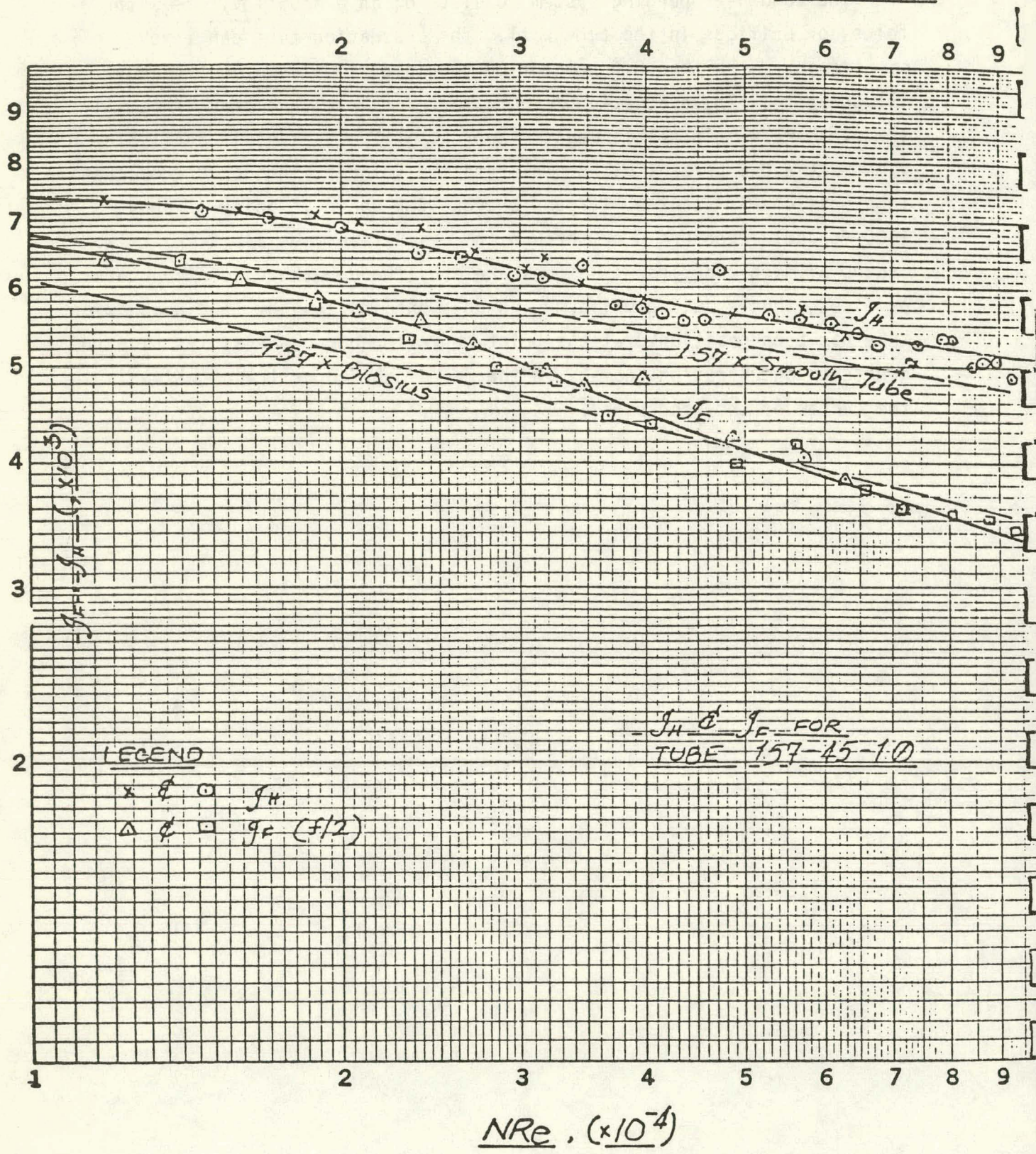
1.57-45-1.0
2 3 4 5 6 7 8 9
9 8 7 6 5 4 3 2 1
j_H & j_F (x10^{-3})
j_H
1.57 x Smooth Tube
j_F
1.57 x Olasius
j_H & j_F FOR TUBE 1.57-45-1.0
LEGEND
× & ○ j_H
△ & □ j_F (f/2)
NRe, (x10^{-4})

I-16

Figure 1.

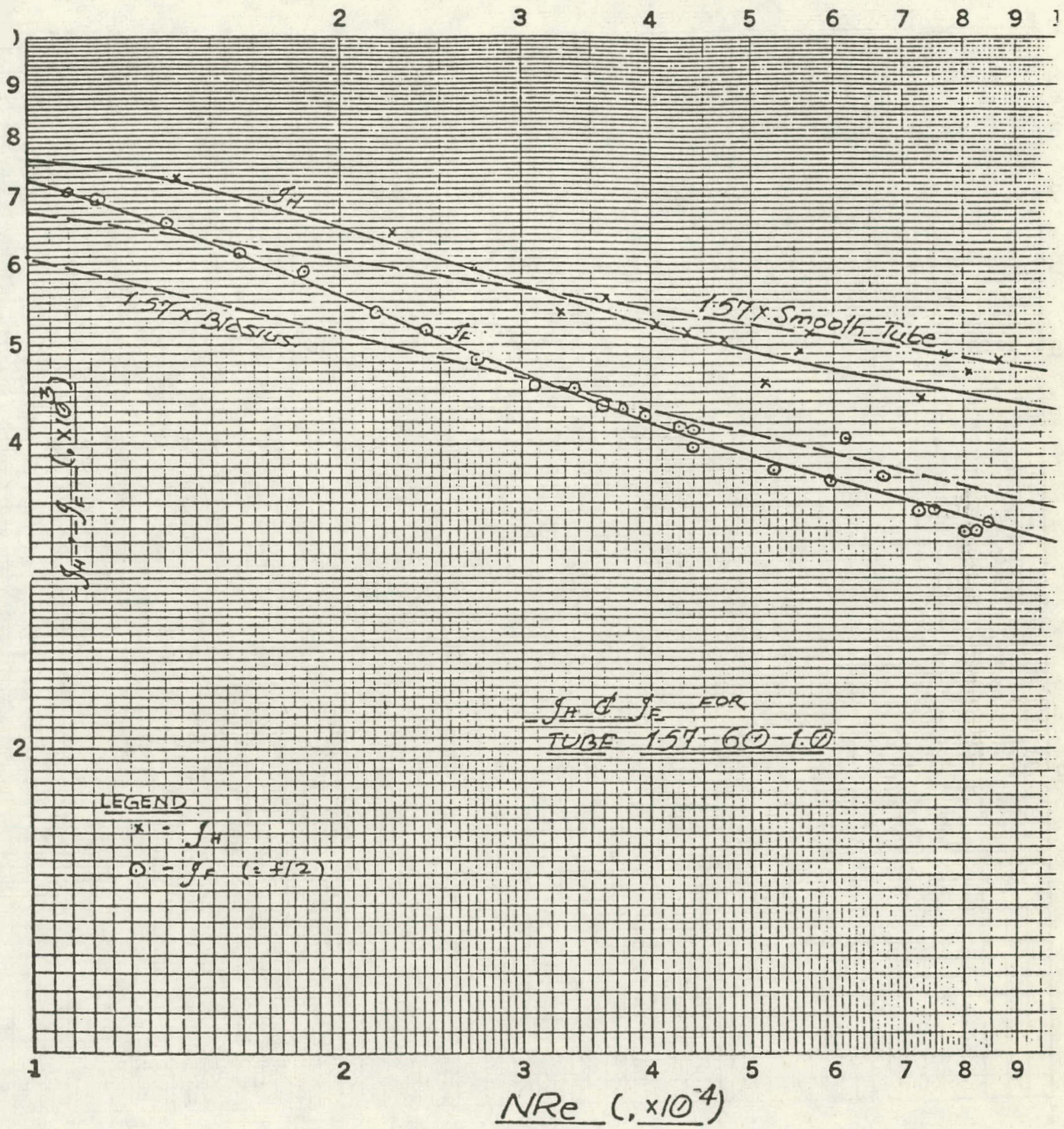
1.57 -60-1.0
2
3
4
5
6
7
8
9
9
8
7
6
5
4
2
1
j_H
j_F
1.57 x Blasius
1.57 x Smooth Tube
j_H & j_F FOR TUBE 1.57-60-1.0
LEGEND
x - j_H
⊙ - j_F (÷ f/2)
j_H or j_F (, x10^{-3})
NRe (, x10^{-4})

Figure 2.

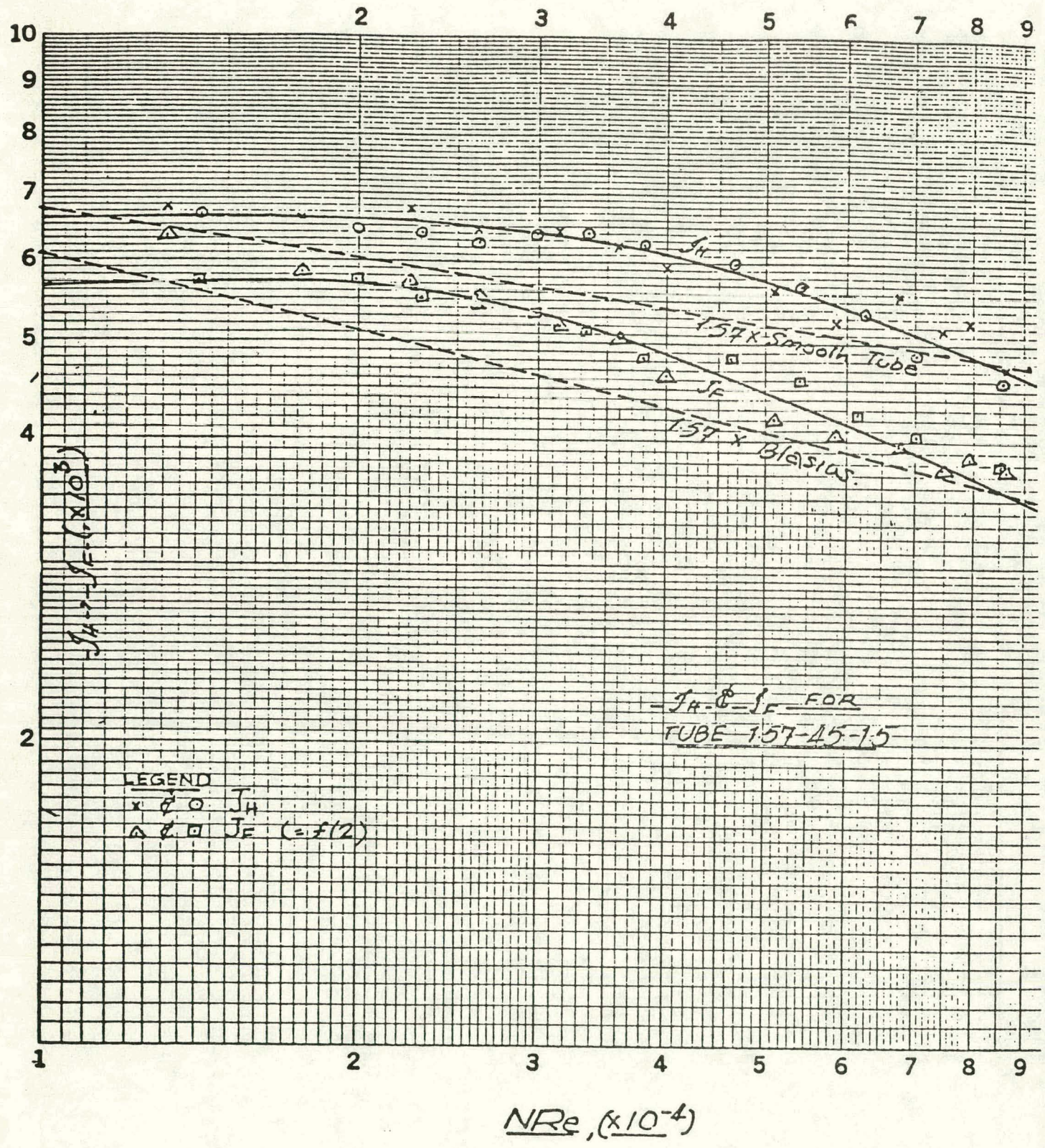
1.57-45-1.5
2
3
4
5
6
7
8
9
10
9
8
7
6
5
4
2
1
1
2
3
4
5
6
7
8
9
J_H
1.57 x Smooth Tube
J_F
1.57 x Blasius
J_H & J_F FOR
TUBE 1.57-45-1.5
LEGEND
x ¢ o J_H
△ ¢ □ J_F (=f/2)
J_H & J_F (x10^3)
NRe, (x10^{-4})

Figure 3.

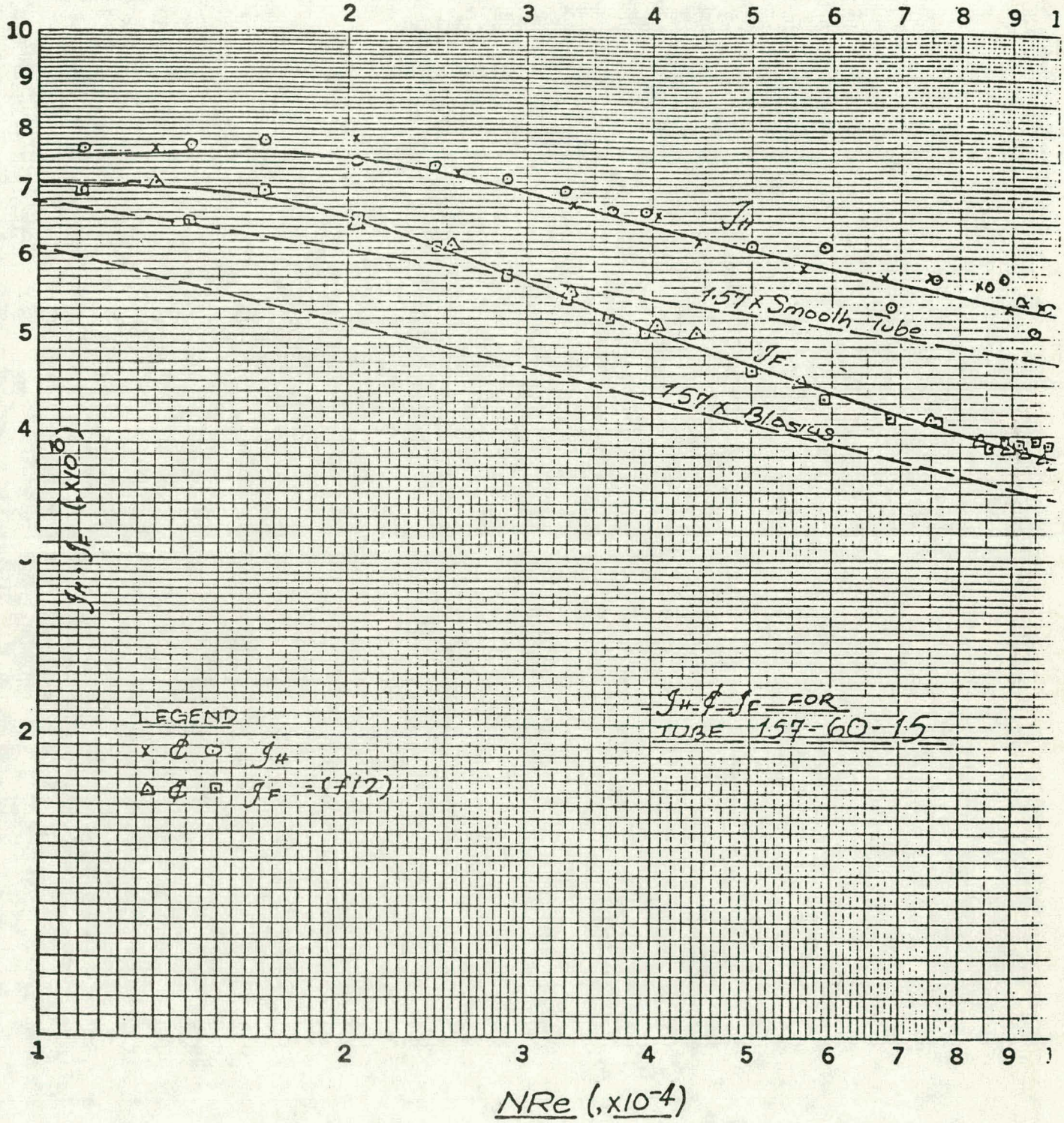
1.57-60-1.5
2
3
4
5
6
7
8
9
1
10
9
8
7
6
5
4
2
1
j_H, j_F (x10)
j_H
1.57 x Smooth Tube
j_F
1.57 x Blasius
LEGEND
x & ○ j_H
△ & □ j_F = (f/2)
j_H & j_F FOR
TUBE 1.57-60-1.5
NRe (, x10⁻⁴)

I-19

Figure 4.

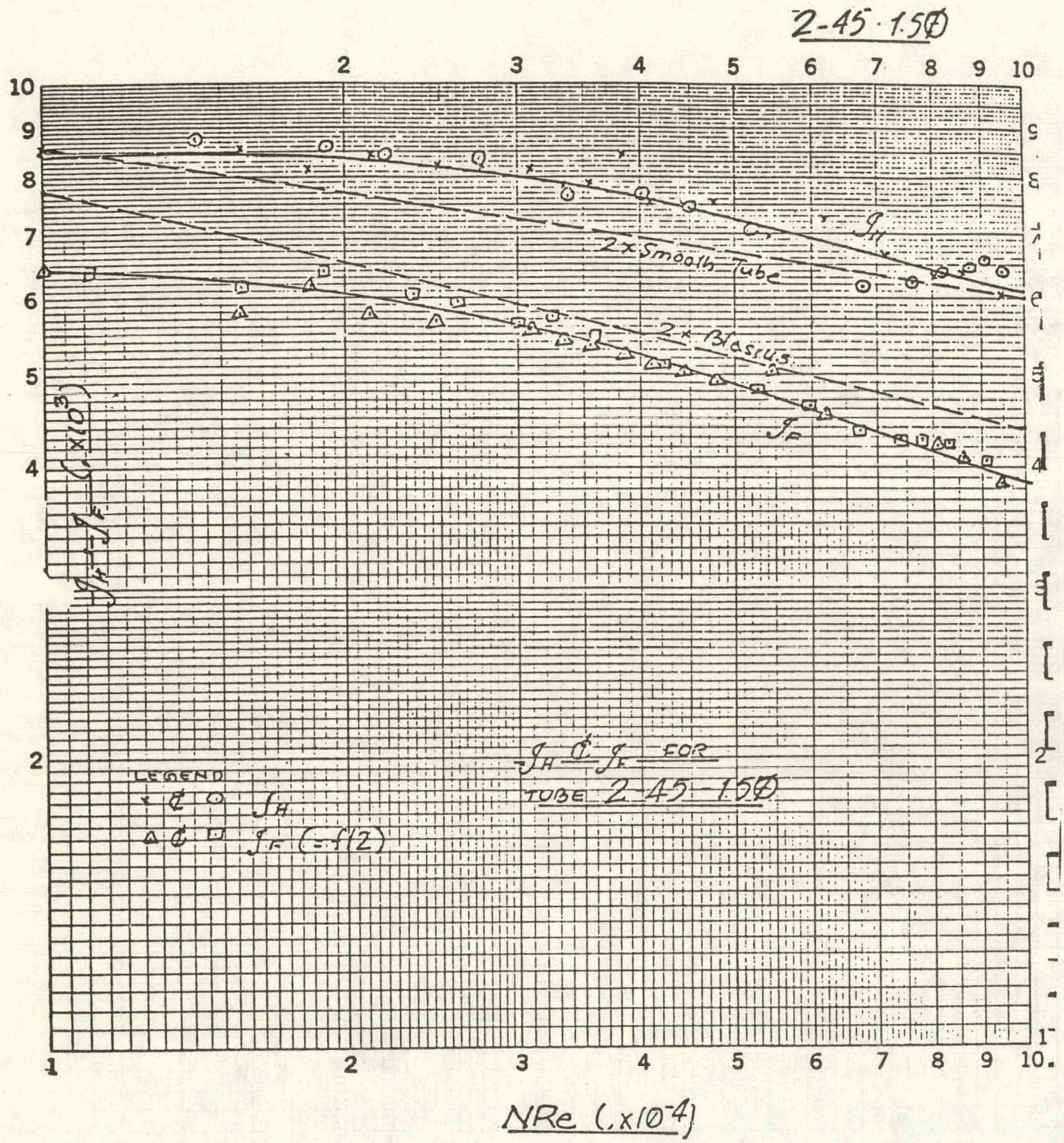
2-45·15Ø
2 3 4 5 6 7 8 9 10
10 9 8 7 6 5 4 2 1
2 3 4 5 6 7 8 9 10.
J_H
2 x Smooth Tube
2 x Brass
J_F
J_H & J_F FOR
TUBE 2-45-15Ø
LEGEND
× ¢ ○ J_H
△ ¢ □ J_F (=f/2)
J_H (x10³)
J_F (x10³)
NRe (x10⁻⁴)

I-20

Figure 5.

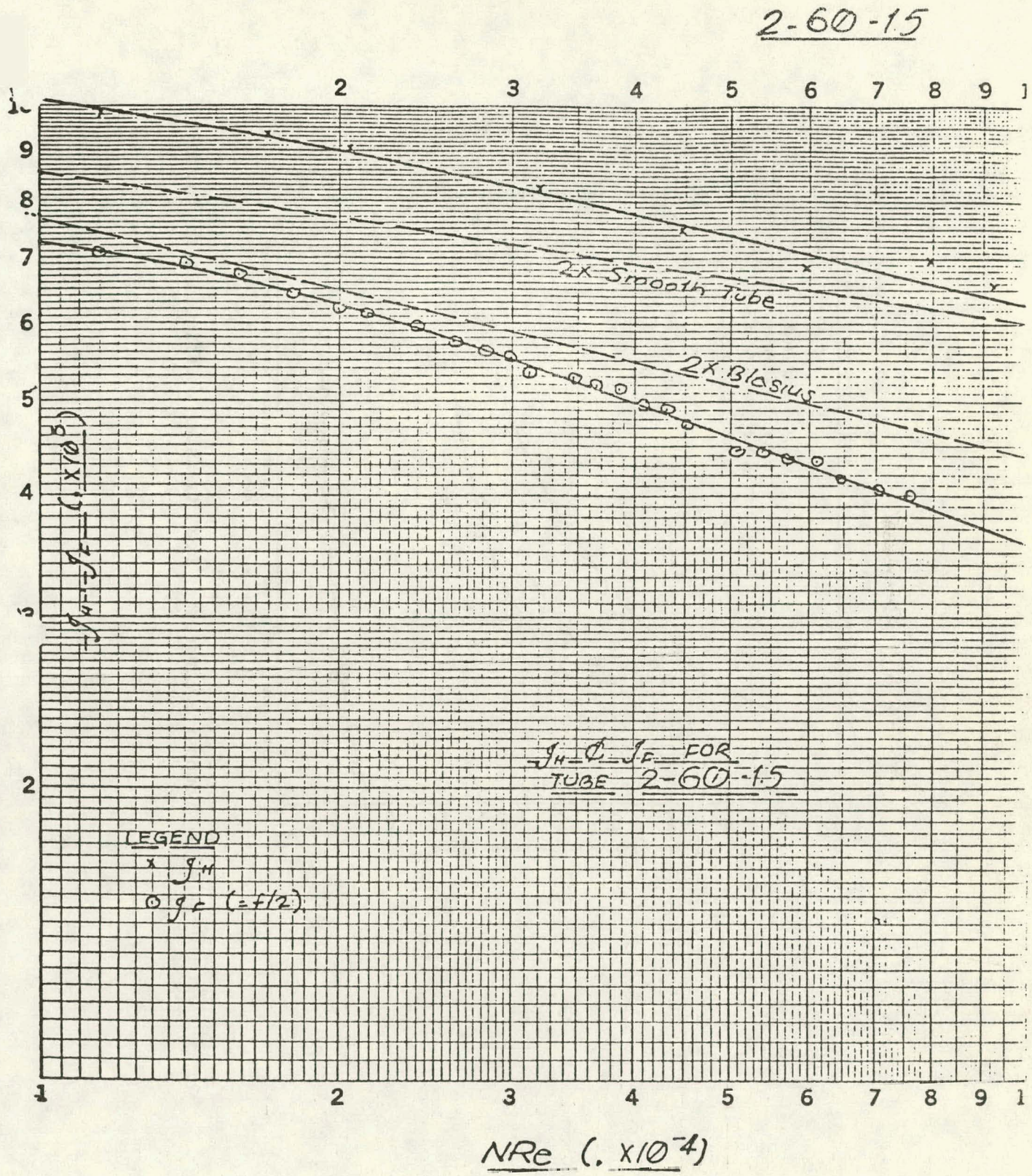
2-60-15
2X Smooth Tube
2X Blasius
$j_H = \phi = j_f = f/2$
TUBE 2-60-15
LEGEND
x j_H
⊙ j_f (=f/2)
$j_H = \phi = j_f = f/2$ (. X10⁵)
NRe (. X10⁻⁴)

I-21 Figure 6.

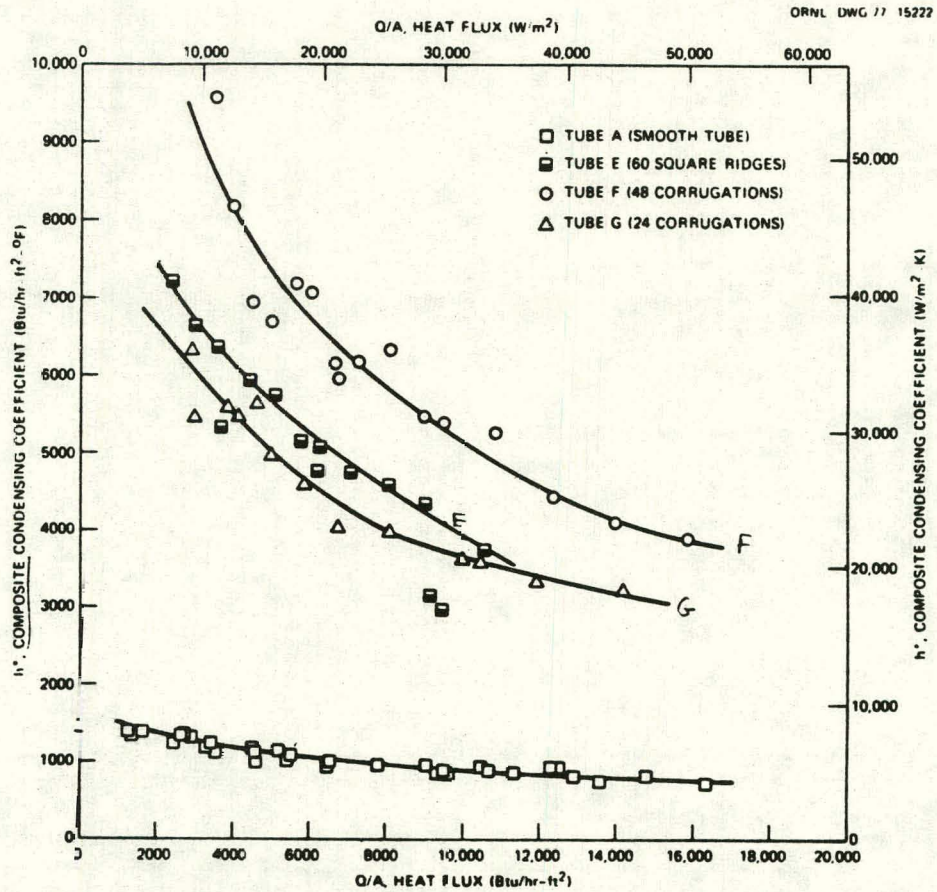

Figure 7. Composite condensing heat transfer coefficients for ammonia.

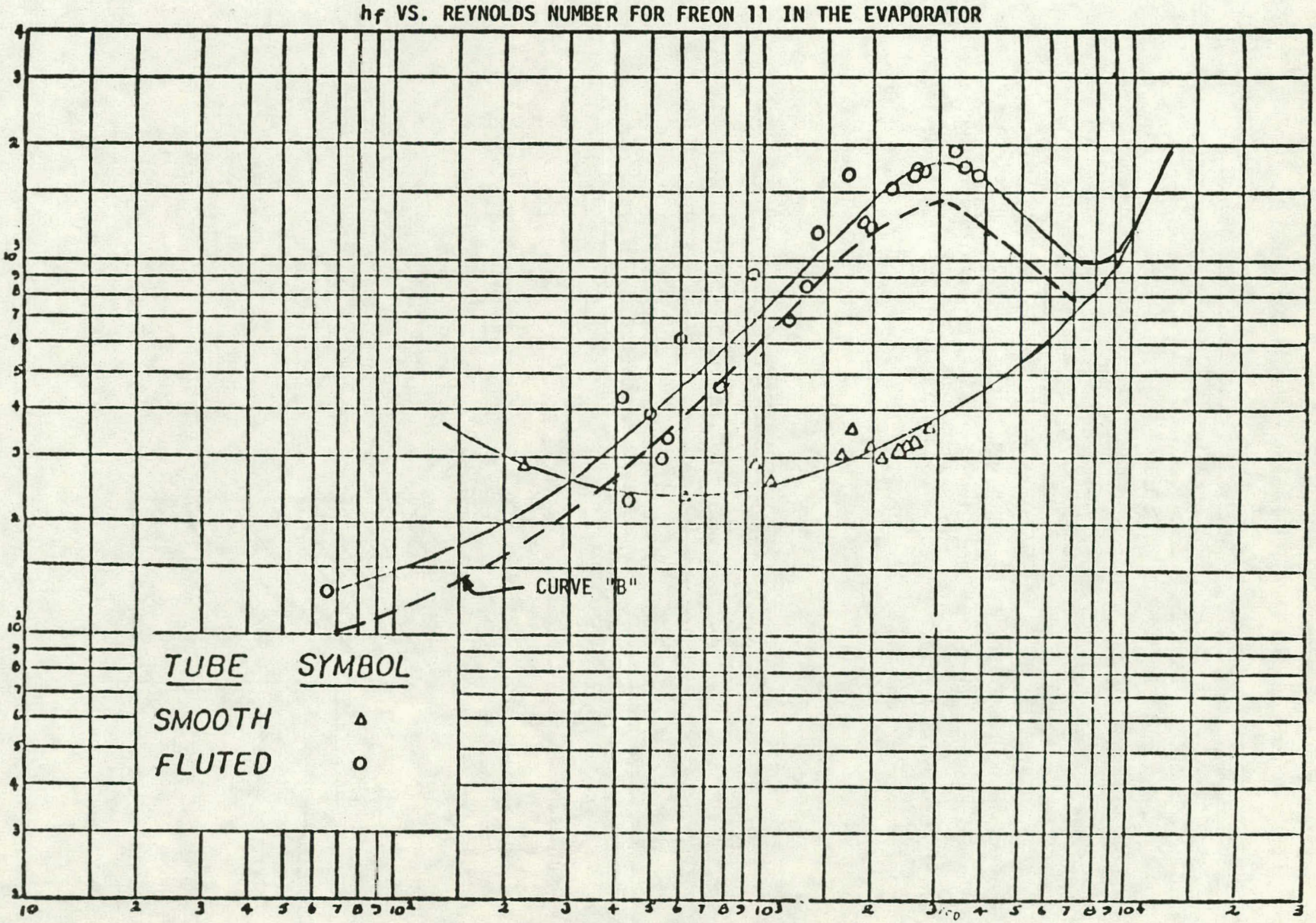
hf VS. REYNOLDS NUMBER FOR FREON 11 IN THE EVAPORATOR
hf (Btu/hr - ft²°F)
CURVE "B"
TUBE SYMBOL
SMOOTH Δ
FLUTED O
NRe (Reynolds Number)

Figure 8.

Table 1. ATTENUATION FACTORS ("CLEAN CONDITION")

	Evaporator	Condenser
Seawater, Convection	0.30	0.36
Metal Wall, Conduction	0.25	0.17
Ammonia, Convection	0.05	0.03

As an illustration, a 10% deviation of allthe heat transfer coefficients in the evaporator (all in the same direction), would give a performance deviation of (0.1 x 0.30) + (0.1 x 0.25) + (0.1 x 0.05) = 0.06, or a 6% deviation in performance.

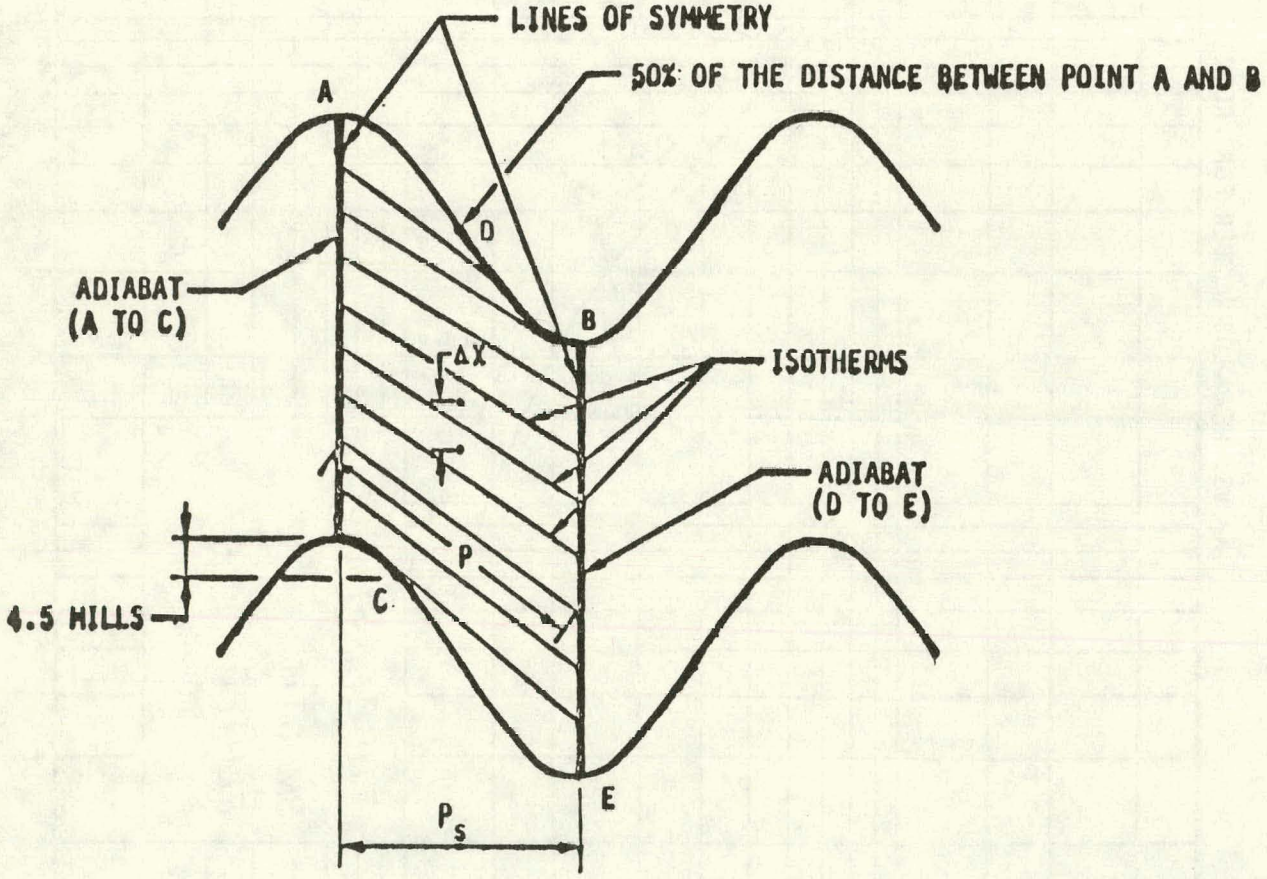

Figure 9.

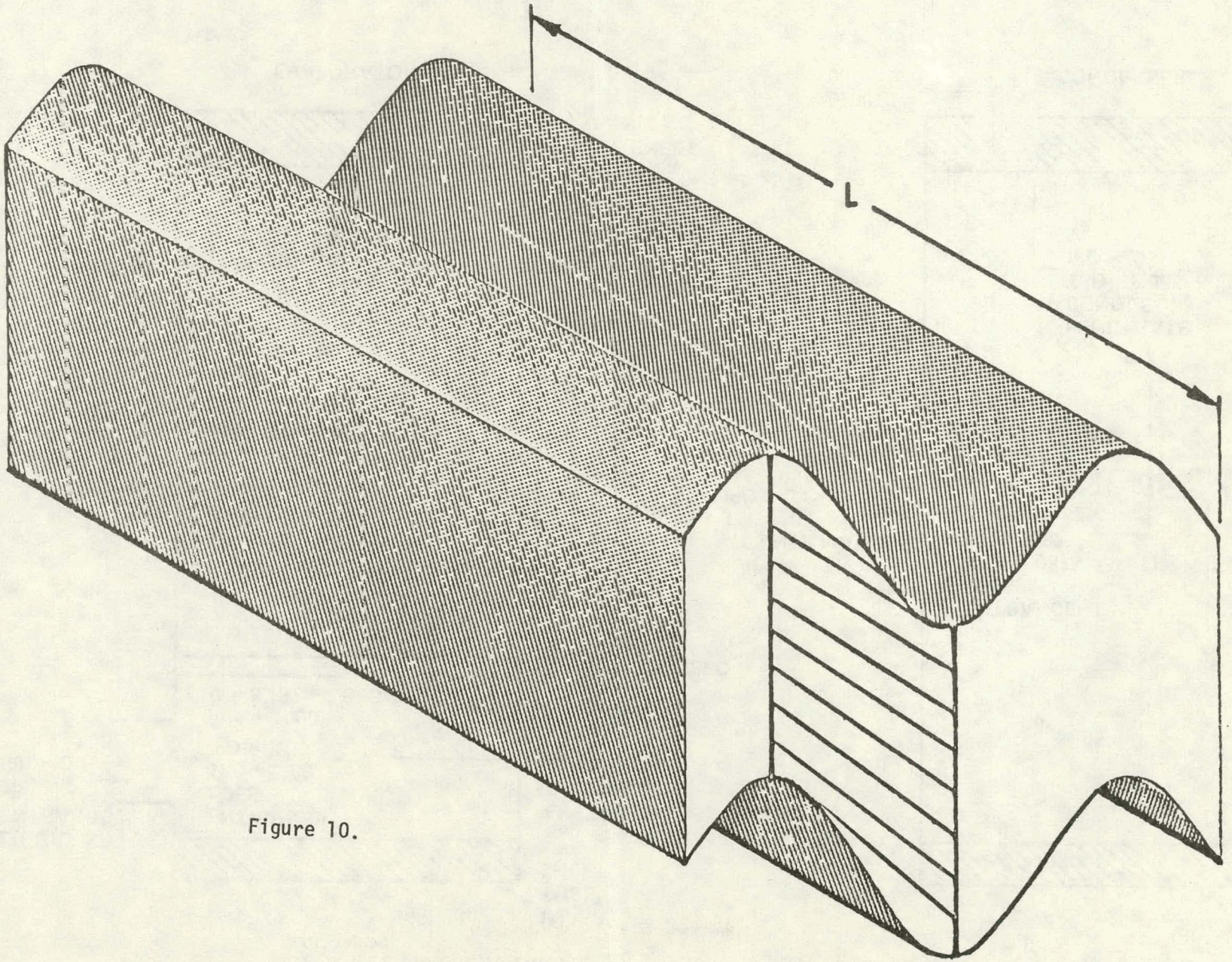

Figure 10.

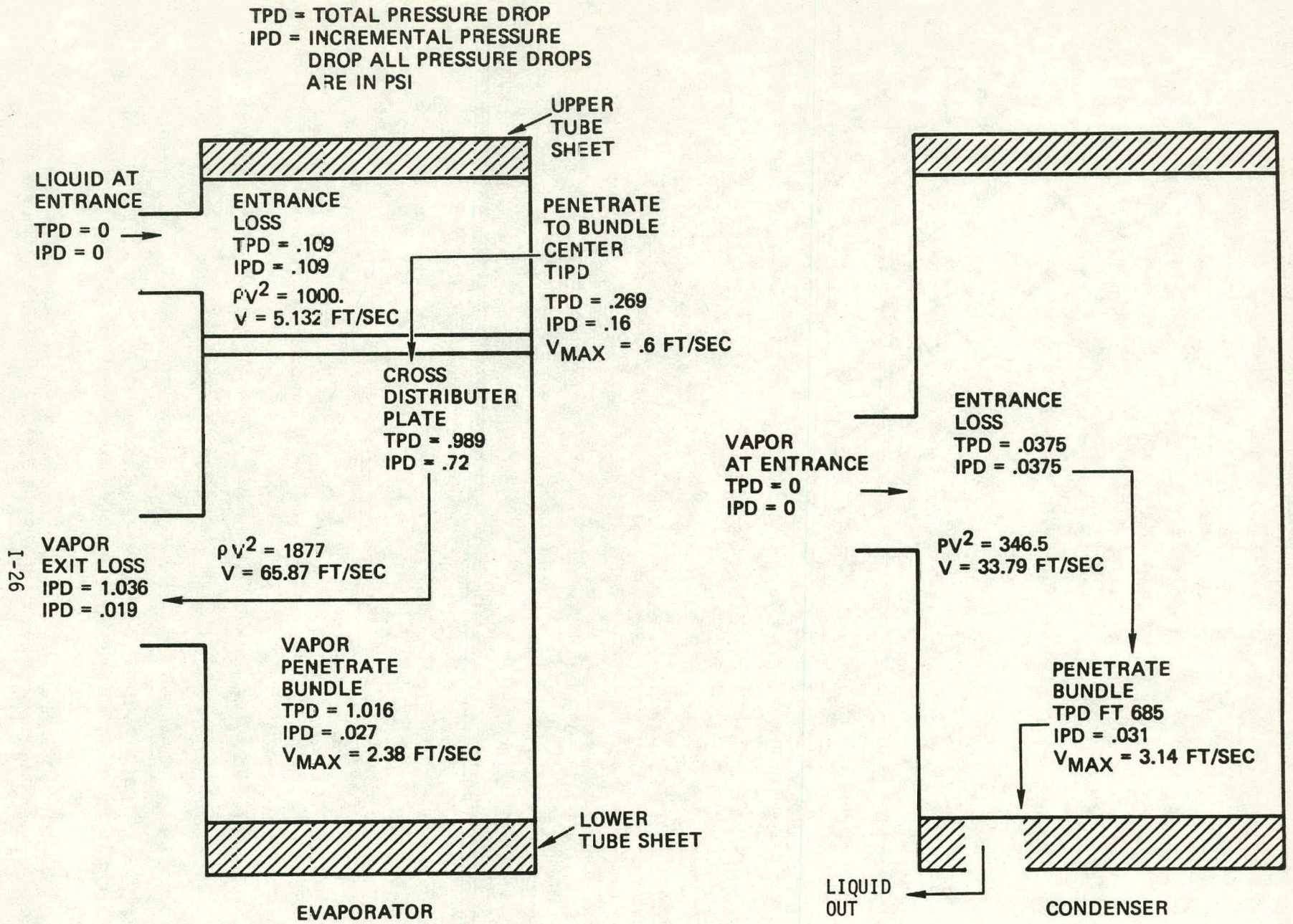
TPD = TOTAL PRESSURE DROP
IPD = INCREMENTAL PRESSURE DROP ALL PRESSURE DROPS ARE IN PSI
UPPER TUBE SHEET
LIQUID AT ENTRANCE
TPD = 0
IPD = 0
ENTRANCE LOSS
TPD = .109
IPD = .109
ρV2 = 1000.
V = 5.132 FT/SEC
PENETRATE TO BUNDLE CENTER TIPD
TPD = .269
IPD = .16
VMAX = .6 FT/SEC
CROSS DISTRIBUTER PLATE
TPD = .989
IPD = .72
VAPOR EXIT LOSS
IPD = 1.036
IPD = .019
ρV2 = 1877
V = 65.87 FT/SEC
VAPOR PENETRATE BUNDLE
TPD = 1.016
IPD = .027
VMAX = 2.38 FT/SEC
LOWER TUBE SHEET
EVAPORATOR
VAPOR AT ENTRANCE
TPD = 0
IPD = 0
ENTRANCE LOSS
TPD = .0375
IPD = .0375
PV2 = 346.5
V = 33.79 FT/SEC
PENETRATE BUNDLE
TPD FT 685
IPD = .031
VMAX = 3.14 FT/SEC
LIQUID OUT
CONDENSER

Figure 11.

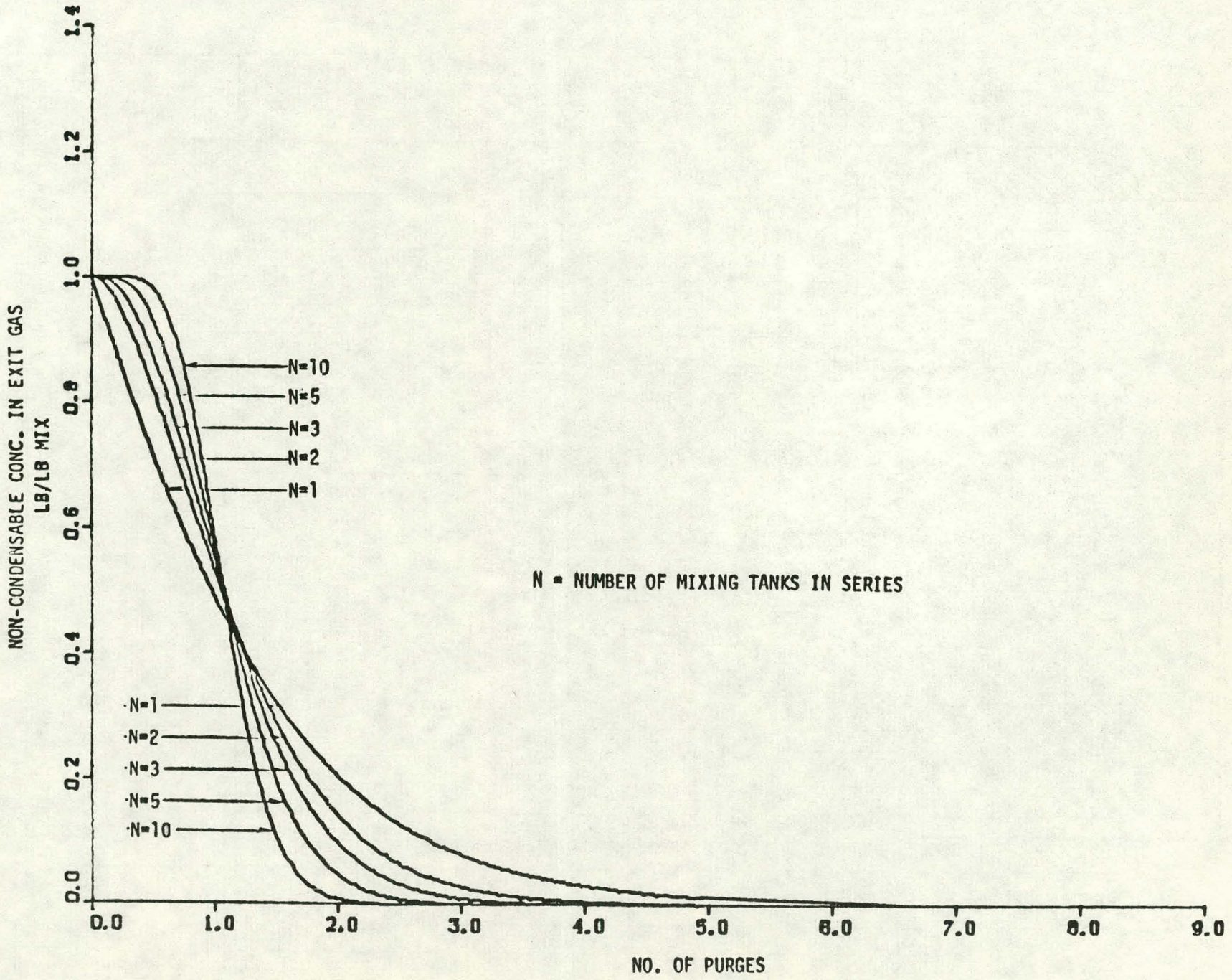
NON-CONDENSABLE CONC. IN EXIT GAS
LB/LB MIX
1.4
1.2
1.0
0.8
0.6
0.4
0.2
0.0
N=10
N=5
N=3
N=2
N=1
N=1
N=2
N=3
N=5
N=10
N = NUMBER OF MIXING TANKS IN SERIES
0.0
1.0
2.0
3.0
4.0
5.0
6.0
7.0
8.0
9.0
NO. OF PURGES

Figure 12

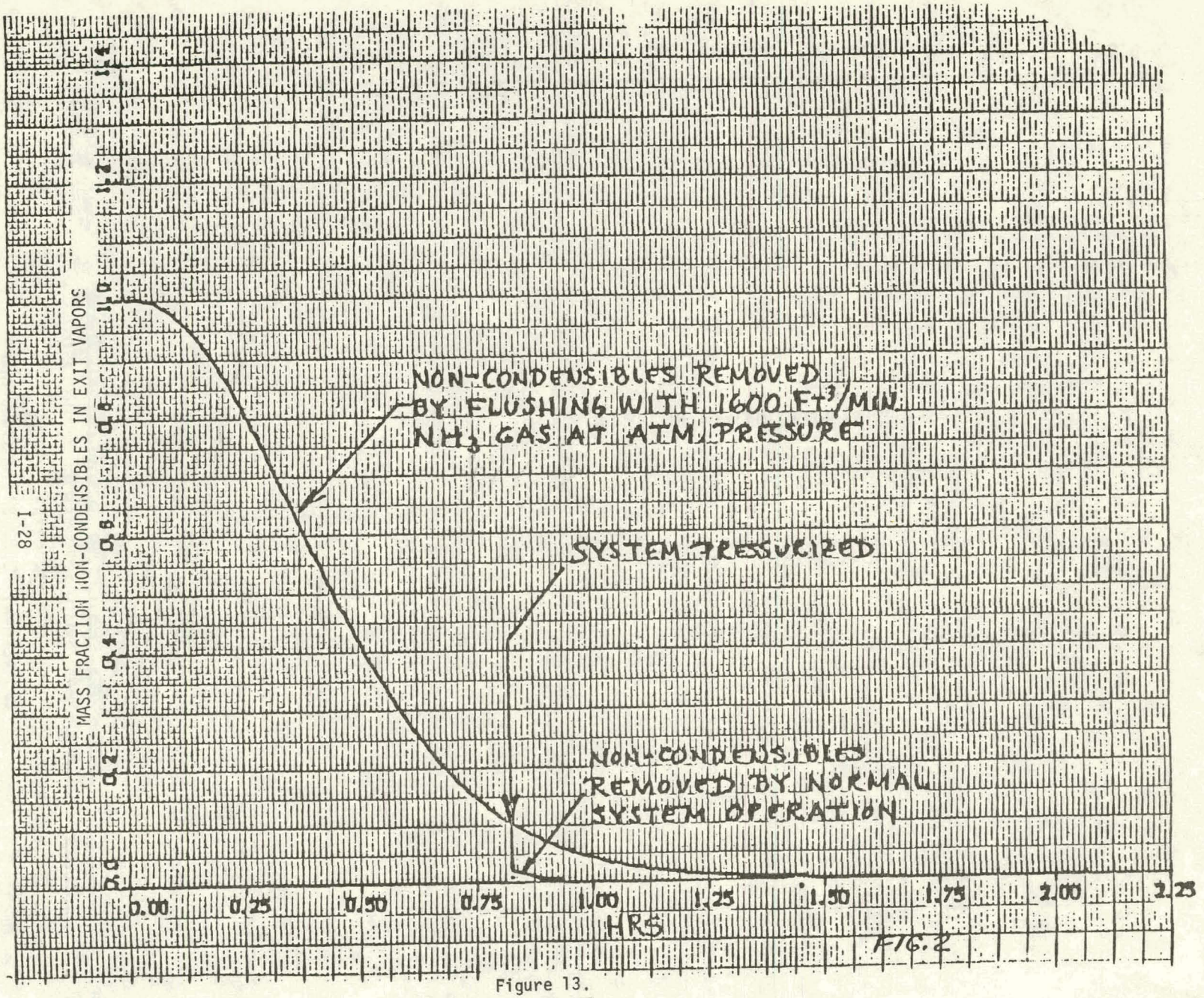
MASS FRACTION NON-CONDENSIBLES IN EXIT VAPORS
1.0
0.8
0.6
0.4
0.2
0.0
NON-CONDENSIBLES REMOVED BY FLUSHING WITH 1600 Ft³/MIN. NH₃ GAS AT ATM. PRESSURE
SYSTEM PRESSURIZED
NON-CONDENSIBLES REMOVED BY NORMAL SYSTEM OPERATION
0.00
0.25
0.50
0.75
1.00
1.25
1.50
1.75
2.00
2.25
HRS
FIG. 2

Figure 13.

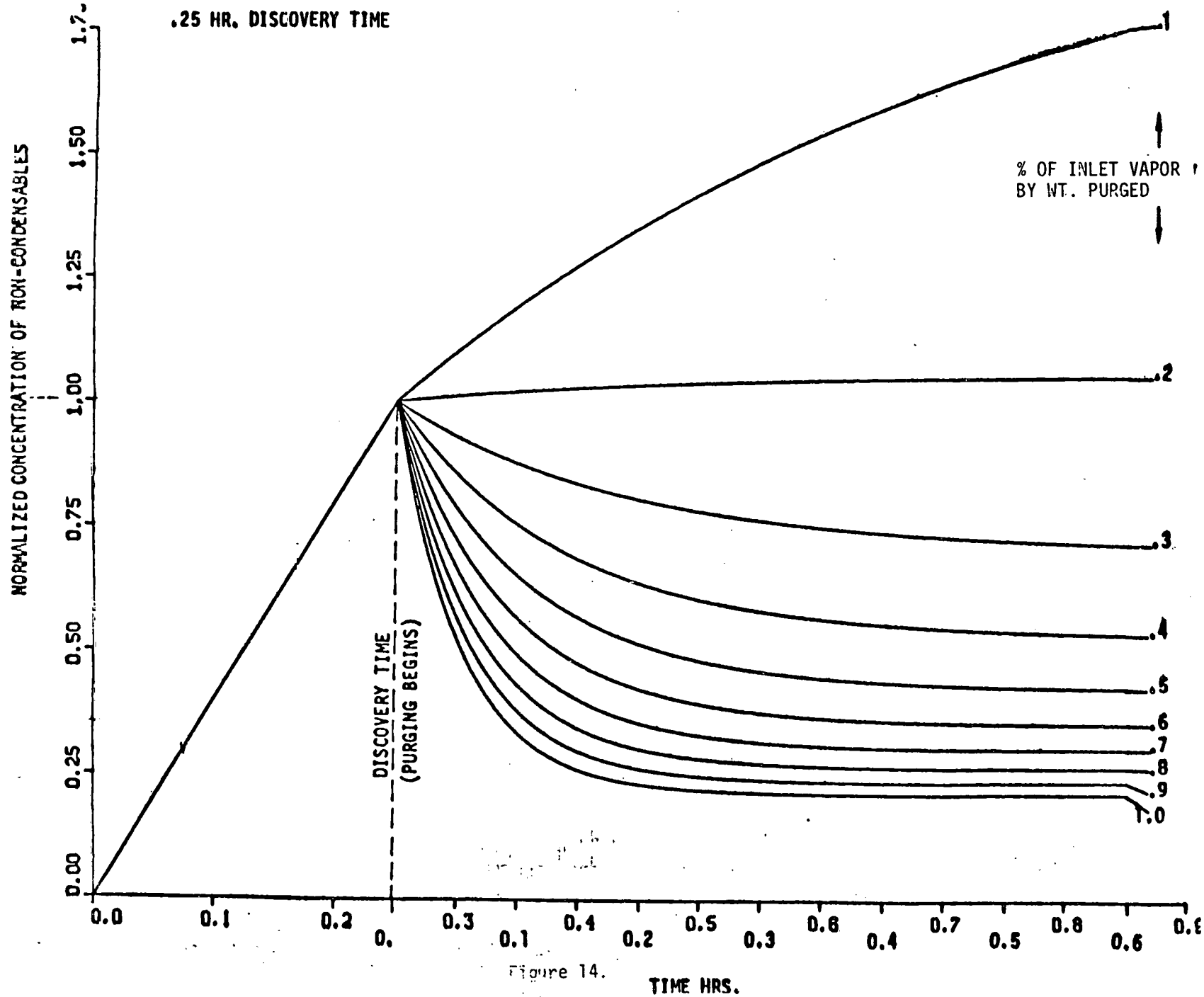
.25 HR. DISCOVERY TIME
NORMALIZED CONCENTRATION OF NON-CONDENSABLES
1.75
1.50
1.25
1.00
0.75
0.50
0.25
0.00
% OF INLET VAPOR
BY WT. PURGED
1
.2
.3
.4
.5
.6
.7
.8
.9
1.0
DISCOVERY TIME
(PURGING BEGINS)
0.0
0.1
0.2
0.
0.3
0.1
0.4
0.2
0.5
0.3
0.6
0.4
0.7
0.5
0.8
0.6
TIME HRS.

Figure 14.

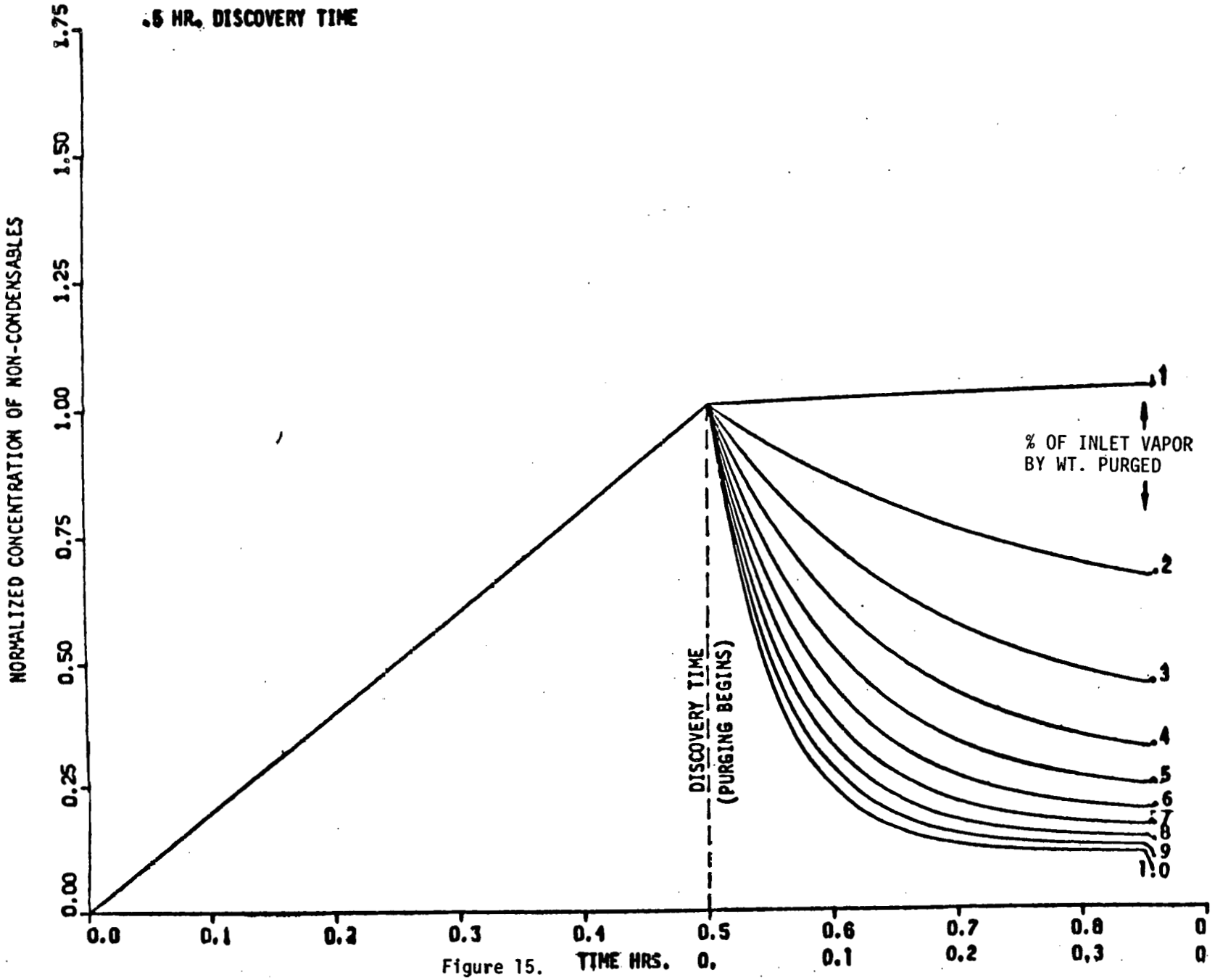
.6 HR. DISCOVERY TIME
NORMALIZED CONCENTRATION OF NON-CONDENSABLES
0.00
0.25
0.50
0.75
1.00
1.25
1.50
1.75
0.0
0.1
0.2
0.3
0.4
0.5
0.6
0.7
0.8
0
TIME HRS.
0.
0.1
0.2
0.3
0
DISCOVERY TIME
(PURGING BEGINS)
% OF INLET VAPOR
BY WT. PURGED
1
2
3
4
5
6
7
8
9
1.0

Figure 15.

ATTACHMENT 1

INTRODUCTION

TASK 3

Provide final analysis of expected heat exchanger thermal/hydraulic performance to verify satisfaction of system requirements.

CONCLUSIONS

Requested analysis is satisfied by attachment 1. Within the scope of the present state of the art, the calculated thermal/hydraulic performance will satisfy system requirements.

CHECK PSD-I
EVAPORATOR and CONDENSER RATING

This enclosed analysis;

1. Determines the individual heat transfer coefficients on the tube, metal wall and shell side and the overall U for the evaporator.
2. Checks the heat flow in the evaporator with the computer results.
3. Determines the individual heat transfer coefficients on the tube, metal wall and shell side and the overall U for the condenser.
4. Checks the heat flow in the condenser with the computer results.
5. Checks the evaporation heat transfer coefficient and condensation heat transfer coefficient as calculated from the equations against the plotted values in the original references.
6. Summarizes all heat transfer coefficients, tube velocities and heat rates calculated for the evaporator and condenser and compares the values with the optimization program computer results.
7. Determines the tube side pressure drops for both the evaporator and condenser.
8. Determines the thermal thickness for the evaporator and condenser.

A summary of the results and a comparison with the results of the Computer calculation is given on page 8.

Check PSD-I Evaporator & Condenser rating

Evaporator

Tube side resistance

$$Nu = .027\, Re^{.8}\, Pr^{1/3} \cdot AR$$

$w = 2.7348 \times 10^8$ lb/hr.

$$G = \frac{2.7348 \times 10^8}{42667 \times \frac{\pi}{4}\left(\frac{.87965}{12}\right)^2}$$

42667 tubes

$D_w = .87965$

$$\frac{lb/hr.}{ft^2}$$

$$1518749.8 \frac{lb}{hr.ft^2} \times \frac{ft^3}{63.8 lb} \times \frac{hr.}{3600 sec.} = 6.6125 \frac{ft}{sec.}$$

$G = 1518749.8$ lb/hr.ft^2

$\rho = 63.8$ lb/ft^3 @ 75°F

$$Re = \frac{\frac{.87965}{12} \times 1518749.8}{2.387}$$

Vis $= 2.387 \frac{lb}{ft.hr.}$ @ 75°F

$$\frac{ft. \cdot lb/hr.ft^2}{lb/ft.hr.}$$

$Re = 46640.425$

$$h = .027 \frac{k}{D} Re^{.8} Pr^{\frac{1}{3}} \cdot AR$$

$Pr = 6.5306$ @ 75°F

$$= .027 \times \frac{.3495}{\left(\frac{.87965}{12}\right)} (46640.425)^{.8} (6.5306)^{\frac{1}{3}} \times AR$$

$k = .3495$ BTU/(hr.ft°F) @ 75°F

$= 1307.2045 \times 1.46$

$AR = 1.46$

$h_{tube} = 1908.5185$

$r_{tube} = 5.23966 \times 10^{-4}$ ← Heat Transfer Coefficient and resistance Evaporator

Check PSD-I Evaporator & Condenser Rating

Evaporator metal heat transfer coefficient evaporator

$$h_{metal} = \frac{11.5}{.05623} \times 12 = 2454.2059$$

thermal thickness see page 11

$$\frac{\text{BTU/hr. ft}^{2\circ}\text{F/ft.}}{\text{in}} \times \frac{12\text{ in}}{\text{ft.}}$$

metal heat transfer resistance evaporator

$$r_{metal} = 4.07463 \times 10^{-4}$$

$$h_{composite} = \frac{(2.939 Re_T^{.4151} - 63.217).8 \times 10^5 - 5.633 Re_B^{1.8452}}{Re_T - Re_B}$$

(C.M.U. Tube A1)

From Attached computer sheet for Case NO. 17

$$Re_T = 5.2243 \times 10^3$$
$$Re_B = 2.0403 \times 10^3$$

$$= 7655.6751$$

$$r_{composite} = 1.30622 \times 10^{-4}$$

(C.M.U. Tube A1)

$$R_o = \frac{.065}{12(116)} = 4.66954 \times 10^{-5}$$

evaporation heat transfer coefficient and resistance evaporator

$$r_{evap} = 1.30622 \times 10^{-4} - 4.66954 \times 10^{-5}$$
$$= 8.39265 \times 10^{-5}$$
$$h_{evap} = 11916.173$$

$$= 8.39265 \times 10^{-5} + 4.07463 \times 10^{-4}$$

$r_{composite}$ (Ti tube) $= 4.91389 \times 10^{-4}$

$h_{composite}$ (Ti tube) $= 2035.0451$

$f_{oul} = .0001$ fouling factor

$$Re_T = \frac{3.17508 \times 10^8}{Re_B^{1.44537}} = \frac{3.17508 \times 10^8}{(2.0403 \times 10^3)^{1.44537}}$$

$= 5224.2332$ ✓ Check Reynolds Number top of tube

Check PSD-I Evaporator & Condenser Rating

Evaporator

$$R = \frac{D_w r_{composite} + r_{Tube} + f}{D}$$

$$= \frac{.87965 \times 4.9139 \times 10^{-4}}{.91} + 5.23966 \times 10^{-4} + .0001$$

$R = 1.09896 \times 10^{-3}$
$U = 909.945$

← Total resistance and overall heat transfer coefficient Evaporator

$$q = -(T-t)\, w\, C_p \left(1 - e^{-\frac{UA}{wC_p}}\right)$$

$T = 70$

$t = 80$

$w = 2.7348 \times 10^8$ lb/hr. ← from computer cal. sheet

$C_p = .9562$ @ 75°C

$U = 909.945$

$A = 26.5 \times \pi \left(\frac{.87965}{12}\right) \times 42667 = 260,385.33 \text{ ft}^2$

$$q = -(70-80) \times 2.7348 \times 10^8 \times .9562 \left(1 - e^{-\frac{909.945 \times 260,385.3}{2.7348 \times 10^8 \times .9562}}\right)$$

Heat rate in Evaporator

$q = 1.558225 \times 10^9 \cong 1.5431E+09$

Check PSD-I Evaporator & Condenser Rating

Condenser

Tube side resistance

$$N_u = .027 Re^{.8} Pr^{1/3} \cdot AR$$

$W = 2.5262 \times 10^8$ lb/hr.

$$G = \frac{2.5262 \times 10^8}{43678 \times \frac{\pi}{4}\left(\frac{.889}{12}\right)^2} = 1341757.6 \text{ lb/hr.ft}^2$$

43678 tubes
Dw = .889

$$Re = \frac{\frac{.889}{12} \times 1,341,757.6}{3.628}$$

$$\frac{ft. \frac{lb}{hr.ft^2}}{\frac{lb}{ft.hr}}$$

$$1,341,757.6 \frac{lb}{hr.ft^2} \times \frac{ft^3}{64.00 lb} \times \frac{hr}{3600 sec} = 5.8236 \frac{ft}{sec.}$$

$\rho = 64.00 \frac{lb}{ft^3}$ @ 45°F

$Vis = 3.628 \frac{lb}{ft.hr.}$ @ 45°F

$Re = 27398.533$

$$h = .027 \frac{k}{D} Re^{.8} Pr^{\frac{1}{3}} \cdot AR$$

$$= .027 \times \frac{.334}{\left(\frac{.889}{12}\right)} (27398.533)^{.8} \times (10.370214)^{\frac{1}{3}} \cdot 1.46$$

$k = .334$ BTU/(hr. ft °F) @ 45°F

$Pr = 10.370214$ @ 45°F

$h_{Tube} = 1375.6892$

$r_{Tube} = 7.26908 \times 10^{-4}$

heat transfer coefficient and resistance condenser

Check PSD-I Evaporator & Condenser Rating

Condenser

$h_{metal} = \frac{11.5}{.04716} \times 12 = 2926.2086$ — metal heat transfer coefficient and resistance Condenser

$r_{metal} = 3.41739 \times 10^{-4}$ — thermal thickness see page 13

$$h_{composite} = K_1 + \frac{K_2 \frac{P_{OR}}{P_{TRW}}}{\frac{Q}{A_{OR}} \frac{P_{OR}}{P_{TRW}} + K_3 \frac{P_{OR}}{P_{TRW}}}$$

(ORNL Tube A1)

$$h_{comp\ (ORNL\ Tube\ A1)} \times \frac{P_{OR}}{P_{TRW}} = K_1 \frac{P_{OR}}{P_{TRW}} + \frac{K_2 \left(\frac{P_{OR}}{P_{TRW}}\right)^2}{\frac{Q}{A_{OR}} \frac{P_{OR}}{P_{TRW}} + K_3 \frac{P_{OR}}{P_{TRW}}}$$

$$h_{comp\ (ORNL\ Tube\ A1\ -\ based\ on\ TRW\ system\ as\ smooth\ tube\ equivalent)} = C_1 + \frac{C_2}{\frac{Q}{A_{TRW}} + C_3}$$

$$h_{comp\ (ORNL\ Tube\ AL\ -\ based\ on\ TRW\ system\ -\ smooth\ tube\ equivalent)} = -3231.62 + \frac{3.684 \times 10^8}{\frac{Q}{A_{TRW}} + 20129.28}$$

$$\frac{Q}{A_{TRW}} = \frac{1.4950E09}{43678\ \pi \left(\frac{.99}{12}\right) \times 29} = 4553.928 \left[\frac{BTU}{hr.ft^2}\right]$$

$\frac{BTU}{hr.ft^2}$

$h_{comp\ (ORNL\ Tube\ AL\ -\ based\ on\ TRW\ system\ -\ smooth\ tube\ equivalent)}$

$r_{comp} = 8.55171 \times 10^{-5}$

Check PSD-I Evaporator & Condenser Rating

$r_{cond} = 8.55171 \times 10^{-5} - \frac{.03125}{12 \times 116} = 6.30673 \times 10^{-5}$

(.03125 = condenser thermal thickness; 2.24437×10^{-5} = Al conductivity; 6.30673×10^{-5} = condensing resistance)

$h_{cond} = 15856.053$ — condensing heat transfer coefficient

$r_{composit} = 6.30673 \times 10^{-5} + 3.47339 \times 10^{-4}$

$= 4.04806 \times 10^{-4}$

$h_{comp.} = 2470.3167$ — composite condensing coefficient for Ti tubes

$f_{oul} = .0001$ — fouling factor

$R = \frac{D_w}{D} r_{composite} + r_{cond} + f$

$R = \frac{.889}{.91} \times 4.04806 \times 10^{-4} + 22690 8 \times 10^{-4} + .0001$

$R = 1.22237 \times 10^{-3}$

$U = 818.08109$ — overall resistance and heat transfer coefficient condenser

$q = (T-t) w c_p \left(1 - e^{-\frac{UA}{wc_p}}\right)$

$T = 50$

$t = 40$

$w = 2.5262 E+08$

$c_p = .9547$ @ 46°

$U = 818.08109$

$A = 29 \times \pi \left(\frac{.889}{12}\right) \times 43678 = 294,802.47$

$q = (50-40) \times 2.5262 \times 10^8 \times .9547 \left(1 - e^{-\frac{818.08109 \times 294802.47}{2.5262 \times 10^8 \times .9547}}\right)$

$q = 1.5245 \times 10^9 \cong 1.495 \times 10^9$ ✓ — heat rate condenser

Check PSD-I Evaporator & Condenser Rating

- Check evaporator equation

$Re_T = 5.2243 \times 10^3$

$Re_B = 2.0403 \times 10^3$

$2 \overline{)\ 3632.3}$

Sally Ann Ward's Thesis

$h_{evap\ (composite)} \simeq 11{,}000 \times .8 = 8800.$

Cal. 7655.6751 accept

Check Condenser Equation

$q''_{TRW} = \frac{Q}{A_{TRW}} = 4553.824 \frac{BTU}{hr\ ft^2}$

$q''_{ORNL} = 4553.824 \times \frac{P_{TRW}}{P_{OR}} = 4553.824 \times \frac{.2454}{.41667} = 2682.001$

$h_{ORNL} \simeq 6500$

Composite

$h_{TRW\ composite} = 6500. \times \frac{P_{OR}}{P_{TRW}} = 6500. \times \frac{.41667}{.2454} = 11036.491 \simeq 11693.566$ cal.

Check PSD-I Evaporator & Condenser Ratings

Summary:

	Tube vel	h_{tube}	h_{total}	h_{evap}	U	q
Evap Cal.	6.6125	1908.5185	2456.2	11915.2	909.945	1.5582×10^9
Computer	6.614	193905	23026	11915.3	895.524	1.5431×10^9
Cond Cal.	5.8236	1375.69	2926.21	15856.05	818.08	1.5245×10^9
Computer	5.8229	1349.89	2774.56	15421.61	796.018	1.4950×10^9

P.D. tube side

Evaporator

$R_e = 46640.425$ say $\frac{\epsilon}{D} = .00016$

$f = .021 \times 1.46 = .03066$

$f_p = e^{\left[.025 \frac{(\ln R_e)^2}{2.6989117} - .7534(\ln R_e) + 1.386\right]}$

$f_p = .0218396 \times 1.46 = .0318659$

$h = f\left(\frac{L}{D}\right)\frac{V^2}{2g}$

$\Delta P = f\left(\frac{L}{D}\right)\frac{V^2\rho}{2g} = f\frac{L}{D}\frac{G^2}{2g\rho}$

$= .0319 \times \frac{30}{\frac{.37965}{12}} \times \frac{1519745.8^2}{64.4 \times 63.8} \times \frac{1}{144} \times \frac{1}{3600^2}$

$\frac{ft}{ft} \quad \frac{\frac{lb}{hr \cdot ft^2}}{\frac{ft}{sec^2} \frac{lb}{ft^3}} = \frac{lb}{hr^2 ft} \cdot \frac{sec^2}{ft} \times \frac{ft^2}{144 in^2} \times \frac{hr^2}{3600 sec^2}$

$= 3.927198$ psi

E.E. losses $= 1.5\frac{V^2}{2g} = 1.5\frac{V^2\rho^2}{2g\rho^2} = \frac{1.56^2}{2g\rho^2}$

$K = .5$ entr $K = 1.0$ exit $K_{Total} = 1.5$

Check PSD-I Evaporator & Condenser Rating

$h_L = 1.5 \frac{G^2}{2gf^2}$

$\Delta P = 1.5 \frac{G^2}{2gf} \times \frac{1}{3600^2 \times 144}$

$\frac{lb^2}{hr^2 ft^4} \times \frac{sec^2 ft^3}{ft \cdot lb} \times \frac{hr^2}{3600^2 sec^2} \times \frac{ft^2}{144 in^2}$

$\Delta P = 1.5 \times \frac{1518749.8^2}{64.4 \times 63.8} \times \frac{1}{3600^2} \times \frac{1}{144}$

$= .45122$ psi

$\Delta P_{Total} = 3927184.45122 =$ **4.37844 psi** compare 4.115

$4.37841 \frac{lb}{in^2} \times \frac{ft^3}{63.846} \times \frac{144 in^2}{ft^2} =$ **9.882 ft.**

tube side pressure drop including entrance & exit losses but not nozzle losses evaporator

---

F.D.
Condenser tubeside

$Re = 27398.533$ $\quad \frac{\epsilon}{D} = .00006$

$f = .024 \times 1.46 = .03504$

$f_p = e^{[.025 \times (\ln Re)^2 - .7534 (\ln Re) + 1.386]}$
2.6102902

$f_p = .02467 \times 1.46 = .0360205$

$\Delta P = f \frac{L}{D} \frac{G^2}{2gf} \times \frac{1}{144} \times \frac{1}{3600^2}$

$\Delta P = .036 \left(\frac{30}{\frac{35.5}{12}} \right) \times \frac{1,341,757.76^2}{64.4 \times 64.} \times \frac{1}{144} \times \frac{1}{3600^2}$

$\Delta P = 3.41211$ psi

Tube side pressure drop including entrance and exit losses but not nozzle losses condenser

$E.E.\ loss = 1.5 \frac{G^2}{2gf} \times \frac{1}{3600^2 \times 144} = 1.5 \frac{1,341,757.76^2}{64.4 \times 64} \times \frac{1}{3600^2} \times \frac{1}{144}$

$= .35108$

$\Delta P_{total} = 3.76319$ psi compare 3.6 $\quad 3.76318 \times \frac{1}{64.} \times 144 = 8.467155$ ft

Tube Geometric Properties

Diameter to center of circle = 0.86 + 2×0.037
= 0.934"

Area 1 = π (0.467)² = 0.68515 in²

area without semi-circle = 0.68515 − 18 × π × (0.037)²
= 0.60773 in²

$R_W^2 = \frac{0.60773}{\pi}$, $R_W = 0.4398$

$D_W = 0.87965$"

arc = 1.413722 × 0.037 + 1.535389 × 0.0025
= 0.0561547

$\frac{x}{11} = \frac{81}{180}$ arc based on $D_W = 0.038382$

$AR = \frac{0.056147}{0.038382} = 1.46$

Thermal Thickness

Δ T	
3/8	.375
3/16	.1875
1/4	.25
3/16	.1875
5/32	.15625
3/32	.09375
11/32	.34375
1/4	.25
3/16	.1875
7/32	.21875
9/16	.5625

P		Δ T	Δ T / P
1 3/8	1.375	.28125	.2045454
1 7/16	1.4375	.21875	.1521739
1 9/16	1.5625	.21875	.14
1 23/32	1.71875	.171875	.1
1 3/4	1.75	.125	.0714285
1 3/4	1.75	.21875	.125
2 3/16	2.1875	.296875	.1357142
2 1/4	2.25	.21875	.0972222
2 3/16	2.1875	.203125	.0928571
2 1/4	2.25	.390625	.1736111
			1.2925522

$$\Sigma \frac{\Delta T}{P} \times \frac{Pitch}{2} = 1.2925522 \times .0435 = .056226$$

SKOTEC-005 CHG LTR

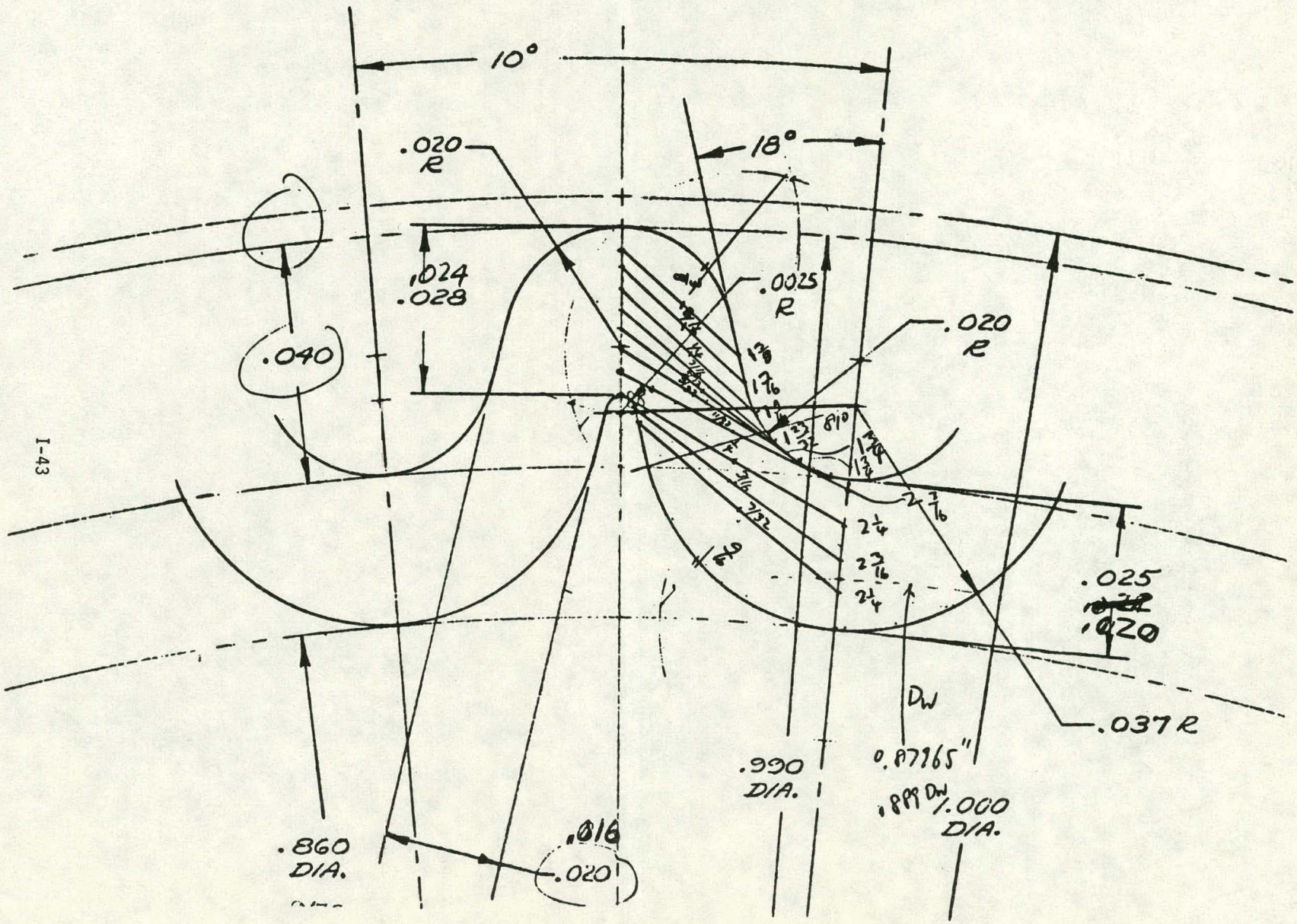

Thermal Thickness for Condenser

for 0.031" thickness

thermal thickness = 0.05623"

for 0.026" thickness

$$\frac{t_{wall_1}}{t_{wall_2}} = \frac{t_{th_1}}{t_{th_2}}$$

$$\text{the thermal thickness} = \frac{0.026}{0.031} \times 0.05623$$

$$= 0.04716"$$

MAY 18 1978

GREGORY S. GIBSON

CASE NO 17

	W WATER PIPE	C WATER PIPE
NGTH FEET	300	2900.0000
AMETER FT	15.8975	15.2525
NUMBER OF PIPES	1	1
H2O VEL FT/S	6.0000	6.0000
WATER FLOW LB/HR	2.7348E+08	2.5262E+08
PRESSURE DROP PSI	.5577	3.0504
	EVAPORATOR	CONDENSER
BOTTOM REYNOLDS NUM	2.0403E+03	2.7510E+03
TOP REYNOLDS NUM	5.2243E+03	0.0
HEAT TRAN LENGTH FT	26.5000	29.0000
TOTAL LENGTH FT	30.0000	30.0000
SHELL DIAM FT	24.9483	25.2422
TUBE DIAMETER IN	.9900	.9900
NUMBER TUBES	42667	43678
TUBE MAT COST $/FOOT	1.6500	1.3100
WATER TUBE VEL FT/SEC	6.6140	5.8228
NH3 ENT FLOW CFS		2.5943E+03
NH3 EXIT FLOW CFS	1.8666E+03	2.0691E+01
HEAT TRAN AREA SQ. FT.	2.6039E+05	2.9481E+05
HEAT TRANSFERED BTU/HR.	1.5431E+09	1.4950E+09
OVERALL BTU/HR/F/FT**2	- 895.5240	796.0179
NH3 HTC BTU/HR/F/FT**2	11915.3145	15421.6060
WALL HTC BTU/HR/F/FT**2	2302.5576	2774.5603
WATER HTC BTU/HR/F/FT**2	1939.0474	1349.8842
H2O AREA RATIO	1.4600	1.4600
FOULING (FT**2 HR F/BTU)	1.0000E-04	1.0000E-04
ENTRANCE TEMP F	80.0000	40.0000
CHANGE IN WATER TEMP	5.9000	6.2000
PRESSURE DROP PSID	4.1150	3.6098
NH3 OUTLET TEMP F	70.0000	50.0000
NH3 OUTLET PRES PSIA	128.7997	89.1924

Equivalent smooth tube area

CYCLE DATA

GROSS POWER MW	1.4032E+01	NET POWER MW	1.0500E+01
WW PUMPS MW	1.3514E+00	CW PUMPS MW	1.7731E+00
NH3 PUMPS MW	4.0766E-01	EVAPOR LB/HR	8.0715E+02
TUR ENTHAL BTU	1.6813E+01	TUR EX QUALITY	2.4553E-02
PLANT EFF	2.3217E-02		

LB/Sec

COST BREAKDOWN ($)

EVAP HE COST	4.8252E+06	CON HE COST	4.1391E+06
WW PUMP COST	4.5070E+05	CW PUMP COST	4.1885E+05
NH3 R PUMP	1.0394E+05	NH3 F PUMP	8.0886E+04
GEN COST	6.2274E+05	TURBINE COST	8.2473E+05
CW PIPE	1.4591E+06	MISCEL	1.5000E+06
TOTAL SYSTEM	1.4425E+07	TOTAL BOTH HE	8.9643E+06

	EVAPORATOR		CONDENSER	
PART	MATERIAL	LABOR	MATERIAL	LABOR
TUBES	2.1120E+06	1.1905E+06	1.7165E+06	1.2187E+06
CLAD	0.	0.	0.	0.
UNCLAD	7.7713E+04	3.0886E+05	8.0059E+04	3.2173E+05
PLATES	1.0071E+04	5.9842E+04	1.0437E+04	6.1685E+04
SHELL	7.0431E+04	2.2675E+05	7.2345E+04	2.3118E+05
BOXES	1.2459E+04	1.9359E+05	1.2769E+04	1.9661E+05
NOZZLES	9.9773E+03	7.7768E+04	1.0084E+04	7.8998E+04
[illegible]T	2.3415E+04	1.1471E+05	0.	0.
[illegible]TLE	1.7091E+04	1.9405E+05	0.	0.
INLETS	1.0886E+04	7.9390E+04	1.1050E+04	8.0580E+04
SUPPORT	3.5[illegible]7E+03	3.2076E+04	3.6663E+03	3.2579E+04
EACH TOTAL	[illegible]E+06	[illegible]776E+06	1.9170E+06	2.2221E+06

Method of calculating attenuation factors

Basic Equation

$$q = (T-t)\, w\, c_p \left(1 - e^{-\frac{UA}{wc_p}}\right)$$

$$\frac{dq}{dh_x} = \frac{dq}{dU}\,\frac{dU}{dh_x}$$

$$\frac{dq}{dU} = (T-t)\, wc_p (-)\, e^{-\frac{UA}{wc_p}}\, \frac{(-)A}{wc_p} = (T-t)\, e^{-\frac{UA}{wc_p}} A$$

$$U = \frac{1}{\frac{1}{h_{sw.}} + \frac{1}{h_{metal}} + \frac{1}{h_{NH_3}}}$$

$$\frac{dU}{dh_x} = (-)\, \frac{1}{\left(\frac{1}{h_{sw}} + \frac{1}{h_{metal}} + \frac{1}{h_{NH_3}}\right)^2}\, \frac{(-)}{h_x^2}$$

$$\frac{dU}{dh_x} = U^2\, \frac{1}{h_x^2}$$

$$\frac{dq}{dh_x} = (T-t)\, e^{-\frac{UA}{wc_p}}\, UA\, \frac{U}{h_x^2}$$

$$dq = (T-t)\, e^{-\frac{UA}{wc_p}}\, UA\, \frac{U}{h_x^2}\, dh_x$$

$$\frac{dq}{q} = (T-t)\, e^{-\frac{UA}{wc_p}}\, UA\, \frac{U}{h_x^2}\, \frac{h_x}{q}\, \frac{dh_x}{h_x}$$

$$= \frac{(T-t)\, e^{-\frac{UA}{wc_p}}\, UA\, \frac{U}{h_x}}{(T-t)\, wc_p \left(1 - e^{-\frac{UA}{wc_p}}\right)}\, \frac{dh_x}{h_x}$$

$$\frac{dq}{q} = \left(\frac{UA}{wc_p}\, \frac{e^{-\frac{UA}{wc_p}}}{\left(1 - e^{-\frac{UA}{wc_p}}\right)}\, \frac{U}{h_x}\right) \frac{dh_x}{h_x}$$

attenuation factor $\alpha_x = \frac{UA}{wc_p}\, \frac{e^{-\frac{UA}{wc_p}}}{\left(1 - e^{-\frac{UA}{wc_p}}\right)}\, \frac{U}{h_x}$

% variation in $q = \alpha_x \times$ (% variation in h_x)

Vapor
P.D. through tube bundle

1. Description

Determine the shell side pressuredrop in the evaporator and condenser

2. Assumptions made

Grinter – Shaw equation used by CMU
The equation was integrated across the tube bundle by CMV.

3. Input data used

Basic equation was derived by CMV – submitted by CMV on 17 October 1977

4. Strategy

CMV equation used

5. Equations

Pressure drop as a function of tube bundle diameter is given for the following conditions

Tube overall dia	1.5 inches
Tube length	25. ft.
Seawater vel.	6. ft/sec.
Seawater inlet temp	40°F
Ammonia saturation temp.	50°F
Triangular pitch dia.	1-7/8 inches (1.25 x 1.5 = 1 7/8)

Vapor P.D. through Tube bundle

Basis: No vapor lanes, feed passes from periphery to center

$$\frac{9.02\ ft^3}{hr.\ ft.\ of\ tube}$$ for a 1.5 inch tube

$$\Delta P = 6.36 \times 10^{-7} D^{2.855}$$

ΔP = press drop

D = tube bundle diameter in feet

The correction for a 1" tube bundle is

$$\frac{\Delta P_1}{\Delta P_2} = \left(\frac{O.D.\ tube1}{O.D.\ tube2}\right)^3$$

thus for a 1" tube bundle

$$\Delta P = 2.147 \times 10^{-6} D^{2.855}$$

$$9.02 \times \left(\frac{1}{1.5}\right) = 6.0133 \frac{ft^3}{hr.\ ft.\ of\ tube}$$ condensed

TRW Design Condenser

$$\frac{807.\ \frac{lb}{sec.}}{43678\ tubes \times 29\ ft.} \times 3600\ \frac{sec}{hr.} \times \frac{3.245\ ft^3\ @50°F}{lb} = 7.44269$$

Correcting for the increased vapor generation in the TRW Design

$$\Delta P = 2.147 \times 10^{-6} \left(\frac{7.44269}{6.0133}\right)^{1.855} \times D^{2.855}$$

$$\Delta P = 3.18867 \times 10^{-6} D^{2.855}$$ Condenser

$\Delta P \propto \rho \times \rho^{-.145} \sim \rho^{.855} \sim V^{-.855}$

TRW Design Evaporator

$$\frac{807 \frac{lb}{sec.}}{4.2667 \times 26.5} \times \frac{3600 sec}{hr.} \times \frac{2.312 ft^3}{lb} = 5.9405 \frac{ft^3}{hr\ ft.\ of\ tube}$$

$$\Delta P = 2.147 \times 10^{-6} \left(\frac{5.9405 V}{6.0133}\right)^{1.855} \left(\frac{2.312}{3.245}\right)^{-.855} D^{2.855}$$

$\Delta P = 2.8048 \times 10^{-6} D^{2.855}$ Evaporator

Say both a 25 ft. bundle

$\Delta P_{condenser} = 3.1887 \times 10^{-6} (25)^{2.855} = .03124$ psi

$\Delta P_{evaporator} = 2.8048 \times 10^{-6} (25)^{2.855} = .02748$ psi

(assuming no vapor lanes)

6. Results and Conclusions

Pressure drop of vapor penetrating the condenser bundle is less than .031 psi

Pressure drop of vapor penetrating the evaporator bundle is less than .027 psi

Vapor P.D. through Tube Bundle

Peripheral vel. in evap

$$\frac{807\ lb}{sec.} \times \frac{2.312\ ft^3}{lb} = 1865.784\ \frac{ft^3}{sec.}$$

Dia bundle $272\frac{1}{2}$ inches

$$\pi(272.5) \times \frac{.25}{1.25} = \text{minimum free inches} = 171.216 \text{ inches}$$

escape area around bundle

$$\frac{171.216}{12} \times 26.5\ ft. \text{ length} = 378.102\ ft^2$$

$$\text{peripheral vel} = \frac{1865.784}{378.102} = 4.934\ \frac{ft}{sec}$$

Too low for vapor to shear off liquid

P.D. in Evaporator Shell

1. Description / definition of issue

Determine the pressure drop in the distributing plenum of the evaporator for an assumed uniform flow distribution.

Determine the required pressure drop through the orifice to maintain this uniform distribution.

Determine the pressure drop to vapor formation and movement of this vapor to outside the tube bundle.

Determine total pressure drop from liquid entering the distribution plenum to vapor in the exit nozzle

2. Assumptions made — 3. Input source data used

Data used is that for pressure drop across the distributing plenum as determined by CMV using the Gunter, Shaw correlation and corrected for the TRW design

4. Method / strategy / logic applied

Method of Gunter, Shaw used and the pressure drop across the bundle was integrated

ΔP THROUGH EVAPORATOR DISTRIBUTING CHAMBER-

		ΔP AS FUNCTION OF BUNDLE DIA, FT. OF NH_3 LIQUID – FOR 1½" O.D.			
		BUNDLE DIA. FT.			
NR	D (FT.)	18	25	35	50
0	1	.626	~	~	~
	2	.173	.440	1.15	~
	3	.082	.207	.541	1.50
1	1	.756	~	~	~
	2	.209	.973	~	~
	3	.099	.459	2.23	~
3	1	.068	.278	~	~
	2	.019	.077	.349	1.82
	3	.008	.037	.164	.857
5	1	.029	.140	.377	~
	2	.015	.039	.104	.470
	3	.007	.018	.049	.222

NR = NUMBER OF TUBE ROWS REMOVED FROM EACH OF 6 RADIAL LANES

D = DEPTH OF DISTRIBUTION PLENUM

DATA IS FOR 1½" TUBES ON P/D RATIO OF 1.25

CORRECT FOR DIFFERENT P/D RATIO WITH THE FOLLOWING CORRECTION FACTOR

P/D	CORRECTION FACTOR
1.25	1.
1.375	.346
1.5	.168
1.625	.1029
1.75	.0648

CORRECT FOR DIFFERENT TUBE O.D.

$$\Delta P_{O.D.} = \Delta P_{1\frac{1}{2}} \left(\frac{1.5}{O.D.} \right)^{4.855}$$

P.D. in Evaporator shell

5. Equations and Calculations

Pressuredrops are tabulated on page 2 for the following conditions:

$1\frac{1}{2}$" tubes P/D 1.25

$\frac{424.5 \text{ lb}}{\text{hr. ft. of tube circumference}}$ $\frac{166.7 \text{ lb}}{\text{hr.}} \times \frac{1}{\pi(1.5)\text{ in}} \times \frac{12 \text{ in}}{\text{ft.}}$ (from enu)

$= 424.5$

Assume a $Re_{Top} = 5000. = \frac{4\Gamma}{\mu}$

$\mu = .359 \frac{\text{lb}}{\text{ft. hr.}}$ @ 70°F

$\Gamma = \frac{5000 \times .359}{4} = 448.75 \frac{\text{lb}}{\text{hr. ft. of tube circumference}}$

Correction factor to data on page 2

$\left(\frac{1.5}{1.}\right)^{4.855} \left(\frac{448.75}{424.5}\right)^{1.855} = 7.9374$

Choose a 2 ft. bundle height with 6 radial lanes 3 tube rows removed from each radial lane

$P_{Press\ Drop}$ on page 2 = .077 ft of NH_3 (for a 2.5 ft. Bundle)

$.077 \times 7.9374 = .61118$ ft. NH_3

P.D. in Evaporator Shell

$.61118\,\cancel{ft.} \times \frac{38.1b}{\cancel{ft}^3} \times \frac{\cancel{ft}^2}{144\,in^2} = .16128\ psi$

Pressure drop in crossing bundle for a uniform flow is .16128 psi

orifice pressure drop - say 4 to 5 times greater

$.16128 \times 4.5 = .72576$

say .72

Total Press. Drop to under orifice = .16128 + .72 = .88128

Total Press. Drop to outside bundle = 88128 + 027 = .90828

1. Previous cal.

P.D. vapor exiting

assume .5 vel heads

$h = .5\frac{V^2}{2g}$

$\Delta P = .5\frac{V^2\rho}{2g} = \frac{.5\,G^2}{2g\rho}$

110" outlet

$\frac{907\frac{lb}{sec.}}{\frac{\pi(110)^2_{in^2}}{4}} = .0849177\frac{lb}{sec.\,in^2} \times \frac{144\,in^2}{ft^2} = 12.22815$

$\Delta P = \frac{.5 \times 12.22815^2}{64.4} \times 2.312 \times \frac{1}{144} = .0186393$

$\frac{\frac{lb}{sec^2}\,\cancel{ft^4}}{\frac{\cancel{ft}}{sec^2}} \frac{\cancel{ft^3}}{lb} = \frac{lb}{ft^2} \times \frac{\cancel{ft^2}}{144\,in^2}$

P.D. in Evapor Shell

Total Press Drop to vapor outlet from liquid inlet = .908287.018853
= .9269193

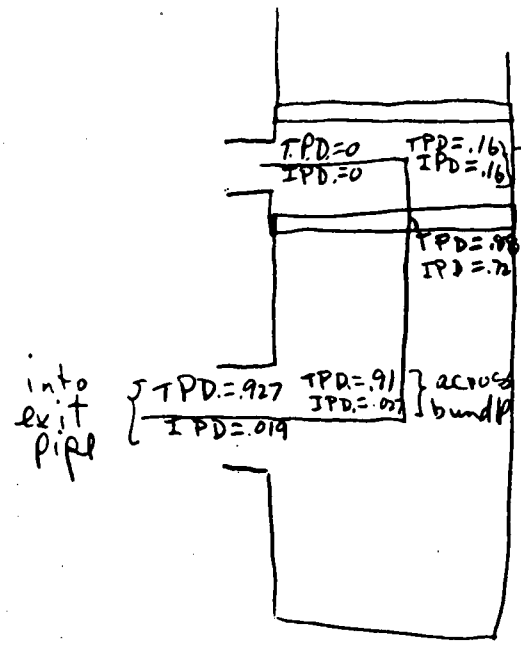

T.P.D. = total Pressure drop
I.P.D = incremental pressure drop

---

added 7/21/78

P.D. liquid entering

$h = K\frac{V^2}{2g}$ $K=1.$

$\Delta P = K\frac{v^2\rho}{2g} = \frac{KG^2}{2g\rho}$

$w = 111.71 \text{ lb/hr.tube} \times 42667 \text{ tubes} = 4.766 \times 10^6 \text{ lb/hr} = 1323.61 \text{ lb/sec}$

$G = \frac{1323.86 \text{ lb/sec}}{976 \text{ in}^2} \times \frac{144 \text{ in}^2}{\text{ft}^2} = 195.77 \frac{\text{lb}}{\text{sec.ft}^2}$

Tube Turns 36" std pipe

$\Delta P = 1. \times \frac{195.77^2}{64.4 \times 36} \times \frac{1}{144} \frac{\text{lb}^2}{\text{sec}^2 \text{ ft}^4} \times \frac{\text{sec}^2 \text{ ft}^3}{\text{ft.lb}} = \frac{\text{lb}}{\text{ft}^2} \times \frac{\text{ft}^2}{144 \text{ in}^2}$

$\Delta P = .109$

Total ΔP include entrance ΔP at = .927 + .109 = 1.036 psi
= 1.036 psi

TRW
DEFENSE AND SPACE SYSTEMS GROUP
ONE SPACE PARK • REDONDO BEACH, CALIFORNIA

PREPARED J. Kaellis
CHECKED
J/N 3442-82
REPORT NO.
PAGE

START-UP NON-CONDENSABLE Removal

STATEMENT OF PROBLEM

DETERMINE THE RATE AND QUANTITY OF AMMONIA REQUIRED TO PURGE THE SYSTEM OF NON-CONDENSABLES PRIOR TO START-UP

APPROACH

THE EQUATION GIVNG THE CONC. OF NON-CONDENSABLES IN THE EFFLUENT FROM "N" MIXING TANKS IN SERIES WAS DEVELOPED. FIGURE 1 GIVEV THE EFFLUENT CONCENTRATION VERSUS THE NUMBER OF PURGES FOR THE SPECIFIED NUMBER OF SERIES TANKS. PURGING PROCEDURE, PRESUMMING THREE SERIES TANKS AND 1600. CFM OF AMMONIA ENTERING, is DESCRIBED IN FIGURE 2.

CONCLUSION

APPROXIMATELY 3482. POUNDS OF AMMONIA IS REQUIRED TO REDUCE NON-CONDENSABLE CONCENTRATION TO LEVELS WHICH CAN BE REMOVED BY THE CONDENSER EVACUATION TUBE. THE OPERATION REQUIRES APPROXIMATELY .85 HRS.

Start-up Non-Condensable Removal

consider N mixing tanks in series

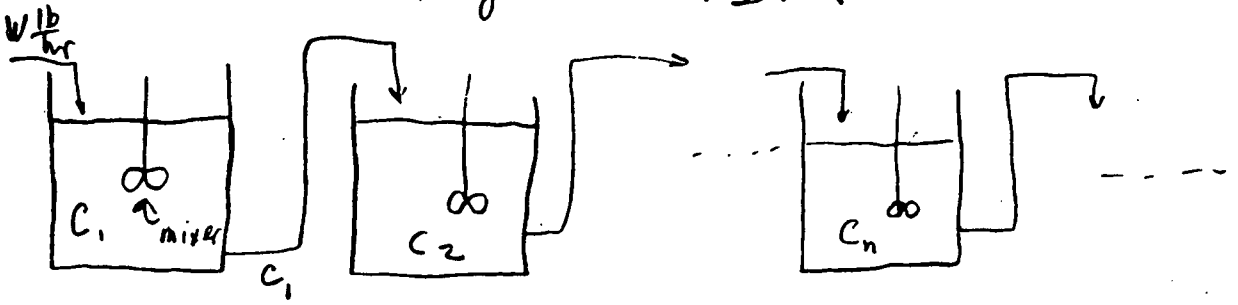

inlet − outlet = accumulation

$$C_{n-1} v \rho_{n-1} - C_n v \rho_n = \frac{d V \rho_n C_n}{dt}$$

$$\frac{lb_{NH_3}}{lb_{mix}} \frac{ft^3}{hr.} \times \frac{lb_{mix}}{ft^3} = \frac{ft^3}{hr.} \frac{lb_{NH_3}}{lb_{mix}}$$

v = flow rate $ft^3/hr.$ $\quad$ hr. $\quad$ V = tank volume = ft^3

molar volume $= 359 \times \frac{(460+70)}{492} \times \frac{14.7}{14.7} = 386.7264$

$$\rho_n = \frac{1}{386.7264 \left(\frac{1-C_n}{\text{m.w.}|_{N.C}} + \frac{C_n}{\text{m.w.}|_{NH_3}} \right)}$$

molecular weight

$$= \frac{1}{\frac{ft^3}{lb\,mole} \left(\frac{lb_{N.C.}/lb_{mix}}{lb_{mole\,N.C.}/lb_{mix}} + \frac{lb_{NH_3}/lb_{mix}}{lb_{mole\,NH_3}/lb_{mix}} \right)}$$

$$= \frac{1}{\frac{ft^3}{lb\,mole} \left(\frac{lb\,moles\,N.C.}{lb_{mix}} + \frac{lb\,mole\,NH_3}{lb_{mix}} \right)}$$

$$= \frac{lb_{mix}}{ft^3}$$

Start-up Non-Condensible Removal

$$\rho = \frac{1}{386.72764\left(\frac{1-C_N}{28} + \frac{C_N}{17}\right)}$$

Mo. wt. N.C. = 28

Mo. wt. NH_3 = 17

$$C_N \rho_N = \frac{C_N}{386.72764\left(\frac{1-C_N}{28} + \frac{C_N}{17}\right)}$$

$C_1 = C_2 = C_3 = \cdots C_n = \cdots = 0$ at time = 0

C_0 = inlet to first tank at all time = 1.

$$C_0 \rho_0 = \frac{1}{386.\left(\frac{1-1.}{28} + \frac{1}{17}\right)} = \frac{17}{386} = .0439585 = \alpha_0 \frac{lb_{NH_3}}{lb_{mix}}$$

$$\dot{w}\left(C_{N-1}\rho_{N-1} - C_N \rho_N\right) = V \frac{d C_N \rho_N}{dt}$$

$$\dot{w}\left(\alpha_{N-1} - \alpha_N\right) = V \frac{d\alpha_N}{dt}$$

For N tanks

$$(\alpha_0 - \alpha_1) = \frac{V}{\nu}\frac{d\alpha_1}{dt}$$

$$(\alpha_1 - \alpha_2) = \frac{V}{\nu}\frac{d\alpha_2}{dt}$$

$$(\alpha_{N-1} - \alpha_N) = \frac{V}{\nu}\frac{d\alpha_N}{dt}$$

Laplace transform

$$\frac{\alpha_0}{s} - \alpha_1 = \frac{V}{\nu}(s\alpha_1 - 0)$$

$$\alpha_1 - \alpha_2 = \frac{V}{\nu}(s\alpha_2 - 0)$$

$$\alpha_{N-1} - \alpha_N = \frac{V}{\nu}(s\alpha_N - 0)$$

$$\frac{\alpha_0}{s} = \left(\frac{V}{\nu}s + 1\right)\alpha_1$$

$$\alpha_1 = \left(\frac{V}{\nu}s + 1\right)\alpha_2$$

$$\alpha_{N-1} = \left(\frac{V}{\nu}s + 1\right)\alpha_N$$

$$\alpha_1 = \frac{\alpha_0}{s\left(\frac{V}{\nu}s + 1\right)}$$

$$\alpha_2 = \frac{\alpha_1}{\left(\frac{V}{\nu}s + 1\right)}$$

$$\alpha_N = \frac{\alpha_{N-1}}{\left(\frac{V}{\nu}s + 1\right)}$$

start-up Non-condensible Removal

$$\alpha_N = \frac{\alpha_0}{s}\frac{1}{\left(1+\frac{V}{\nu}s\right)^N}$$

$$= \frac{\alpha_0}{s\left(\frac{V}{\nu}\right)^n}\frac{1}{\left(\frac{\nu}{V}+s\right)^n}$$

Inverse Laplas transform

$$\alpha_N = \frac{\alpha_0}{\left(\frac{V}{\nu}\right)^n}\int_0^t L^{-1}\frac{d\tau}{\left(s+\frac{\nu}{V}\right)^n}$$

$$\alpha_N = \frac{\alpha_0}{\left(\frac{V}{\nu}\right)^n}\int_0^t e^{-\frac{\nu}{V}\tau}\left(L^{-1}\frac{1}{s^N}\right)d\tau$$

$$\alpha_N = \frac{\alpha_0}{\left(\frac{V}{\nu}\right)^n}\int_0^t e^{-\frac{\nu}{V}\tau}\frac{\tau^{N-1}}{(n-1)!}d\tau$$

$$\alpha_N = \frac{\alpha_0}{(n-1)!}\int_0^t e^{-\frac{\nu}{V}\tau}\left(\frac{\nu}{V}\tau\right)^{N-1}d\left(\frac{\nu}{V}\tau\right)$$

$$\frac{\nu}{V}\tau = \beta$$

$$\alpha_N = \frac{\alpha_0}{(n-1)!}\int_0^{\frac{\nu}{V}t} e^{-\beta}\beta^{N-1}d\beta$$

No. 403 Peirce

$$\int x^m e^{ax}dx = e^{ax}\left[\frac{x^m}{a} - \frac{m x^{m-1}}{a^2} + \sum_{i=3}^{m+1}(-1)^{i+1}\frac{m(m-1)\cdots(m+i)}{a^i}x^{m-i}\right.$$

Start-up non-condensable Removal

$$\alpha_N = \frac{\alpha_0}{(m-1)!} \int_0^{\left(\frac{\nu}{V}t\right)} e^{-\beta} \beta^{N-1} d\beta$$

$a = -1 \quad m = N-1$

$$\alpha_N = \frac{\alpha_0}{(n-1)!} \left\{ e^{-\beta} \sum_{i=1}^{N} (-1)^{i+1} \frac{(N-1)!}{(N-1-i+1)!} \frac{\beta^{N-1-i+1}}{(-1)^i} \right\}_0^{\frac{\nu}{V}t}$$

$$= \frac{\alpha_0}{(N-1)!} \left\{ -e^{-\beta} \sum_{i=1}^{N} \frac{(N-1)!}{(N-i)!} \beta^{N-i} \right\}_0^{\frac{\nu}{V}t}$$

$$\alpha_N = \frac{\alpha_0}{(N-1)!} \left\{ -e^{\frac{\nu}{V}t} \sum_{i=1}^{N} \frac{(N-1)!}{(N-i)!} \left(\frac{\nu}{V}t\right)^{N-i} + e^{0} \sum_{i=1}^{N} \frac{(N-1)!}{(N-i)!} (0)^{N-i} \right.$$

Now

$$\sum \frac{(N-1)!}{(N-i)!} (0)^{N-i} = \frac{(N-1)!}{(N-1)!} (0)^{N-1} + \frac{(N-1)!}{(N-2)!} (0)^{N-2} + \cdots + \frac{(N-1)!}{(N-(N-1))!} (0)^{N-(N-1)} + \frac{(N-1)!}{(N-N)!} (0)^{N-N}$$

$$= 0^{N-1} + (N-1)(0)^{N-2} + \cdots + \frac{(N-1)!}{1!} 0^1 + \frac{(N-1)!}{0!} (0)^0$$

Thus $\sum_{i=1}^{N} \frac{(N-1)!}{(N-i)!} (0)^{N-i} = \frac{(N-1)!}{1} (0)^0 \neq 0 = (N-1)!$

Start-up Non-Condensable Removal

$$\alpha_N = \frac{\alpha_0}{(N-1)!}\left\{-e^{\frac{\nu}{V}t}\sum_{i=1}^{N}\frac{(N-1)!}{(N-i)!}\left(\frac{\nu}{V}t\right)^{N-i}+(N-1)!\right\}$$

$$\boxed{\alpha_N = \alpha_0\left\{1-e^{\frac{\nu}{V}t}\sum_{i=1}^{N}\frac{\left(\frac{\nu}{V}t\right)^{N-i}}{(N-i)!}\right\}}$$

$$C_i\rho_i = \frac{C_i}{386.72764\left(\frac{1-C_i}{28}+\frac{C_i}{17}\right)} = \alpha_i$$

$$C_i = \frac{386}{28}(1-C_i)\alpha_i + \frac{386}{17}C_i\alpha_i$$

$$C_i = \frac{386}{28}\alpha_i - \frac{386}{28}C_i\alpha_i + \frac{386}{17}C_i\alpha_i$$

$$C_i = \frac{386}{28}\alpha_i + C_i\alpha_i\left(-\frac{386}{17}-\frac{386}{28}\right)$$

$$\boxed{C_i = \frac{\frac{386}{28}\alpha_i}{1+\alpha_i\left(\frac{386}{28}-\frac{386}{17}\right)} = \text{conc. } NH_3}$$

$C_{N.C.}$ = Conc. Non-condensables $= 1-C_N$

$$C_{N.C.} = \frac{1+\alpha_i\left(\frac{386}{28}-\frac{386}{17}\right)-\frac{386}{28}\alpha_i}{1+\alpha_i\left(\frac{386}{28}-\frac{386}{17}\right)}$$

$$= \frac{1-\frac{386}{17}\alpha_i}{1+\alpha_i 386\left(\frac{1}{28}-\frac{1}{17}\right)} = \frac{1-22.748611\alpha_i}{1-8.9369546\alpha_i}$$

$$\boxed{C_{N.C.} = \frac{1-22.748611\alpha_i}{1-8.9369546\alpha_i}}$$

$\alpha_0 = .0439585$

start-up Non-Condensable Removal

V_T = total volume of system

$\frac{V_T}{N}$ = volume of one tank = V

$\frac{V_T}{v} = \frac{ft^3}{\frac{ft^3}{hr.}} = hr$ = flush time (time for one flush) $= t_F$

$\frac{t}{t_F}$ = no. of flushes

Thus

$$\frac{v}{V} t = \frac{vNt}{V_T} = \frac{t}{t_F} N = FN$$

F = no. of system flushes

$$\alpha_i = .0439585 \left\{ 1 - e^{-FN} \sum_{i=1}^{N} \frac{(FN)^{N-i}}{(N-i)!} \right\}$$

$$C_{N.C.} = \frac{1 - 22.748611\,\alpha_i}{1 - 8.936954\,\alpha_i}$$

$C_{N.C.}$ = Conc. in exiting gas after "F" flushes – assume N tanks in series

PURGES

in exit gas

Figure 1 – Conc. in vs. No. of flushes (purges)

Figure 2 – Conc. in exit gas vs. time hrs. assume 1600 c.f.m of atm ammonia entering, 40,000 ft³ total system volume and a 3 series tank system.

$\rho_{NH_3} = \frac{17}{359} \times \frac{492}{530} = .0486$ $\quad 1600 \frac{ft^3}{min} \times .0439616 \frac{lb}{ft^3} \times .825 hr. \times \frac{60 min}{hr.} = 3481.5$ lbs required for initial purge

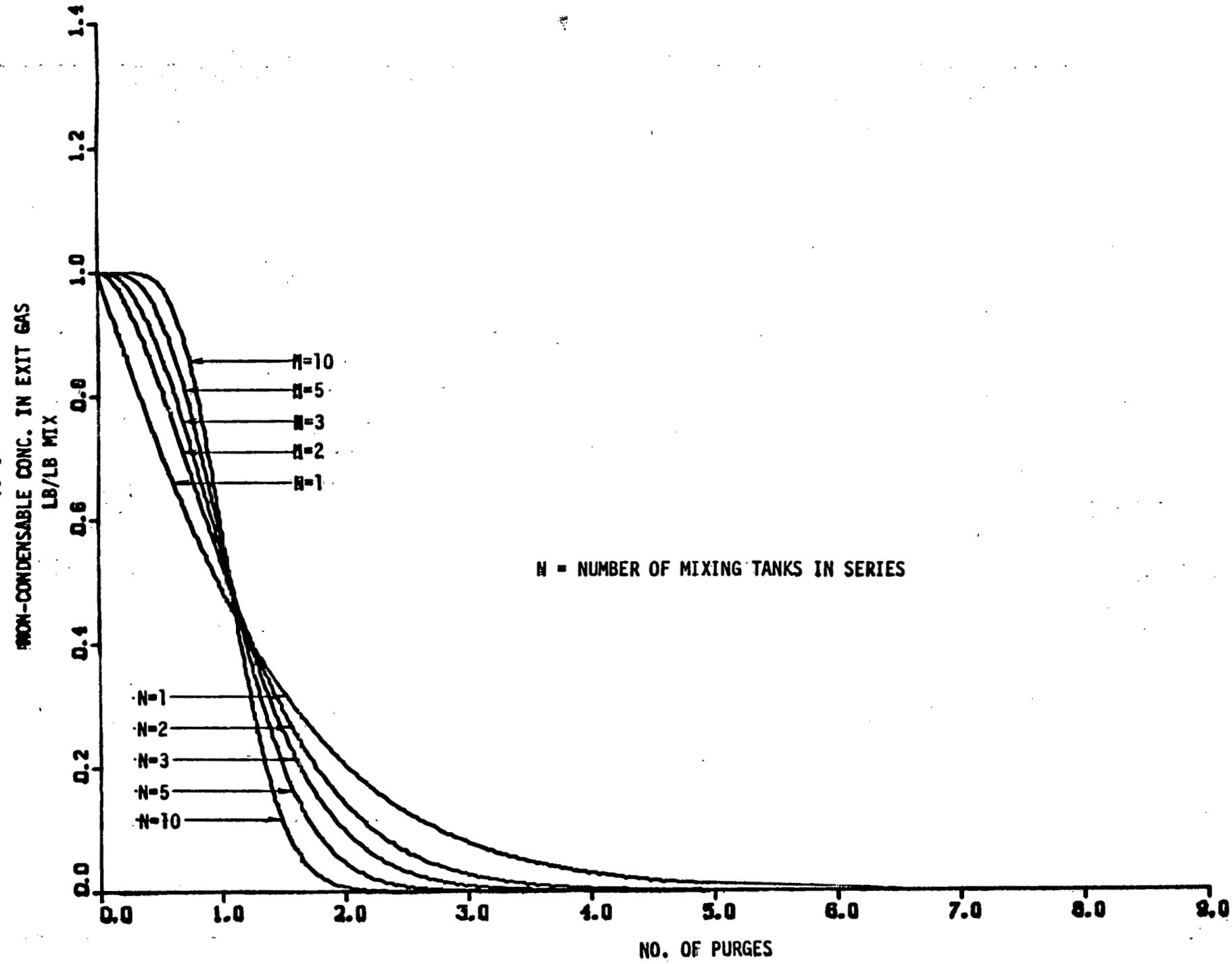
NON-CONDENSABLE CONC. IN EXIT GAS
LB/LB MIX
0.0
0.2
0.4
0.6
0.8
1.0
1.2
1.4
N=10
N=5
N=3
N=2
N=1
N=1
N=2
N=3
N=5
N=10
N = NUMBER OF MIXING TANKS IN SERIES
0.0
1.0
2.0
3.0
4.0
5.0
6.0
7.0
8.0
9.0
NO. OF PURGES

FIGURE 1

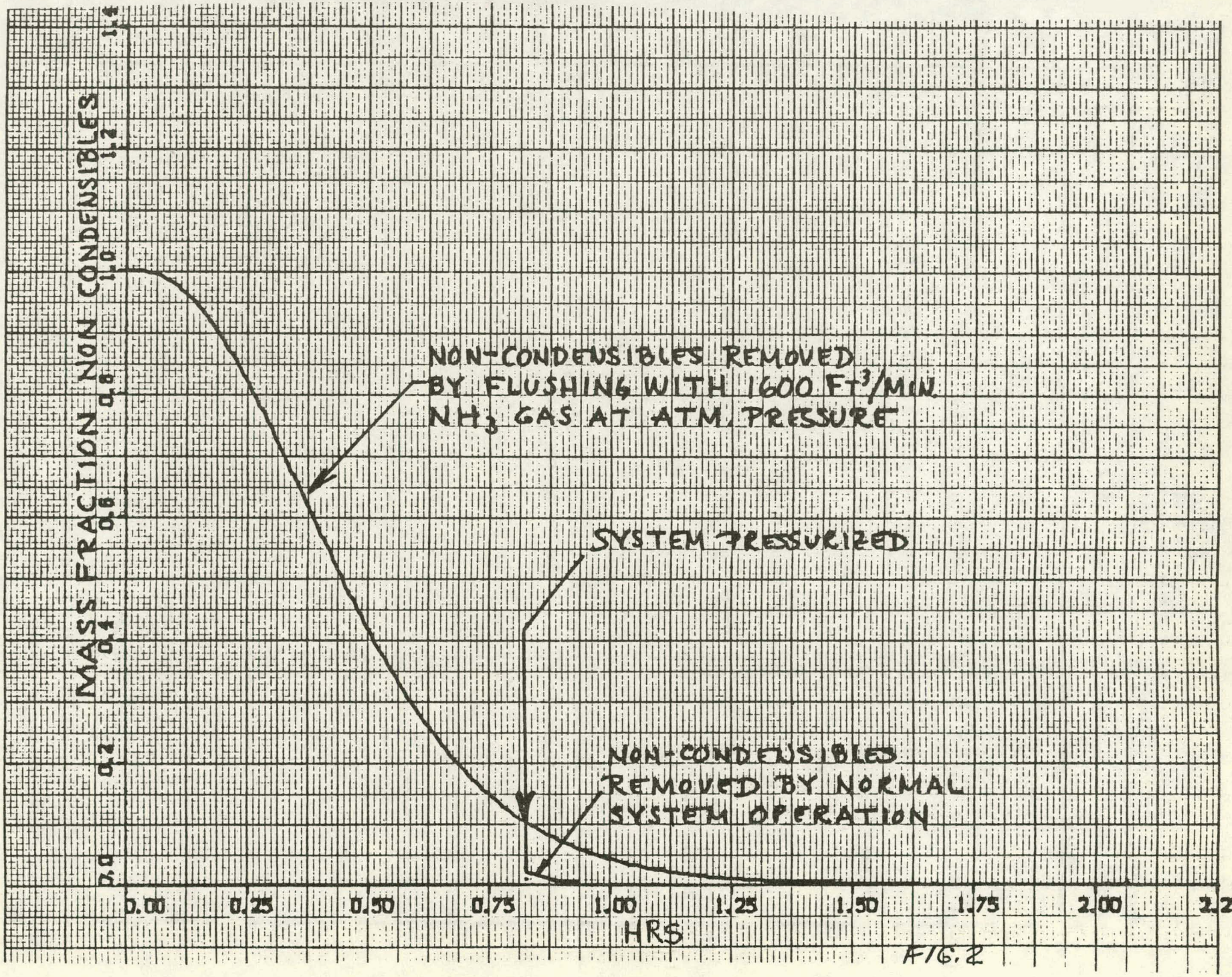
MASS FRACTION NON CONDENSIBLES
1.4
1.2
1.0
0.8
0.6
0.4
0.2
0.0
NON-CONDENSIBLES REMOVED
BY FLUSHING WITH 1600 FT³/MIN
NH₃ GAS AT ATM. PRESSURE
SYSTEM PRESSURIZED
NON-CONDENSIBLES
REMOVED BY NORMAL
SYSTEM OPERATION
0.00
0.25
0.50
0.75
1.00
1.25
1.50
1.75
2.00
2.25
HRS

FIG. 2

TRW
DEFENSE AND SPACE SYSTEMS GROUP
ONE SPACE PARK • REDONDO BEACH, CALIFORNIA

PREPARED J. Kallis
CHECKED
MODEL

REPORT NO.

PAGE

Non-Condensible Purging Durring Operation

LIST OF SYMBOLS

C_e, C_T = lb ratio entering, inside tank $\frac{\text{lb noncondensibles}}{\text{lb ammonia}}$

F = fraction of inlet flow bled off by noncondensible evacuation tube

t, t_o = time, discovery time hrs,

V = total free volume of condenser

W = lb/hr, ammonia and noncondensibles entering condenser

P = density $\frac{\text{lb}_{NH_3}}{ft^3}$

Non-Condensable Purging During Operation

Approach: Postulate a non-condensable leak into the system & time to discover this leak. Determine the time to reduce the non-condensable concentration at discovery time to a fraction (25 to 50. %) of its value at discovery time. We assume that a concentration of 25. to 50% of its value at discovery time is insufficient to create larg difficulties with system operation.

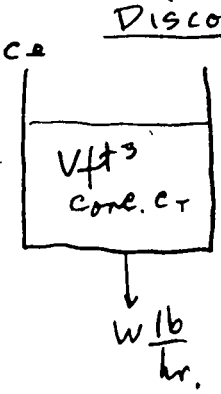

Density changes due to concentration changes are too small to be considered since concentration change span is very small.

inlet − outlet = rate of accumulation

$$Wc_e - 0 = \frac{d\,VPc_T}{dt}$$

$$\frac{lb_{NH_3}}{hr.} \cdot \frac{lb_{N.C.}}{lb_{NH_3}} = \frac{ft^3 \cdot \frac{lb_{NH_3}}{ft^3} \cdot \frac{lb_{N.C.}}{lb_{NH_3}}}{hr.}$$

$lb_{NH_3} \cong lb_{mix}$

$lb_{NH_3} \cong lb_{mix}$ } since conc. of non-condensable is small

Non-condensible Purging During Operation

$$W c_e = \frac{d V \rho c_T}{dt}$$

$$\frac{W c_e}{V \rho} = \frac{dc_T}{dt}$$

$$c_T \Big|_0^{c_T} = \frac{W c_e}{V \rho} t \Big|_0^t$$

$$\frac{c_T}{c_e} = \frac{W}{V \rho} t$$

$$\frac{c_T|_D}{c_e} = \frac{W}{V \rho} t_D$$

t_D = discovery time
$c_T|_D$ = conc. at discovery time

At discovery time conc. of non-condensables in condenser is $c_T|_D$.

Starting with a non-condensable conc. in condenser of $c_T|_D$ and an inlet conc. of c_e removal F fraction of inlet flow-determine conc. in condenser as a function of time

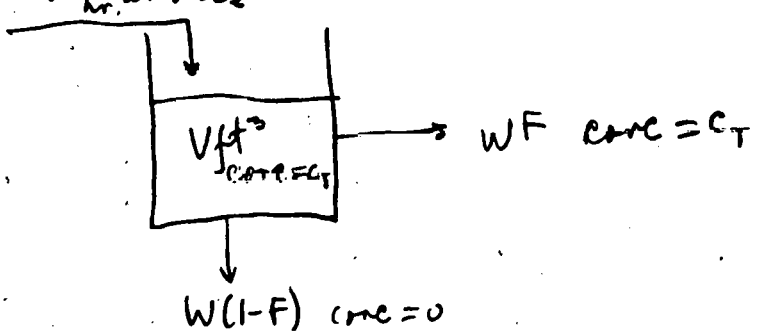

Non-Condensable Purging During Operation

inlet − outlet = rate of accumulation

$$WC_e - WFC_T = \frac{dVPC_T}{dt}$$

$$\frac{lb_{NH_3}}{hr.}\,\frac{lb_{N.C.}}{lb_{NH_3}} - \frac{lb_{NH_3}}{hr.} \times \frac{lb_{N.C.}}{lb_{NH_3}} = \frac{ft^3}{hr.} \times \frac{lb_{NH_3}}{ft^3} \times \frac{lb_{N.C.}}{lb_{NH_3}}$$

$lb_{NH_3} \cong lb_{mix}$ since $lb_{N.C.}$ is very small

$$VP\frac{dC_T}{dt} = WC_e - WFC_T$$

$$\frac{dC_T}{W(C_e - FC_T)} = \frac{dt}{VP}$$

$$\frac{dC_T}{FC_T - C_e} = -\frac{W}{VP}\,dt$$

$$\frac{1}{F}\ln(FC_T - C_e) = \Big|_{C_T|_0}^{C_T} = -\frac{W}{VP}t\Big|_{t_0}^{t}$$

$$\ln\frac{FC_T - C_e}{FC_T|_0 - C_e} = -\frac{FW}{VP}(t - t_0)$$

$$\frac{FC_T - C_e}{FC_T|_0 - C_e} = e^{-\frac{FW}{VP}(t-t_0)}$$

$$C_T = \frac{(FC_T|_0 - C_e)e^{-\frac{FW}{VP}(t-t_0)} + C_e}{F}$$

$$\frac{C_T}{C_e} = \left(\frac{C_T|_0}{C_e} - \frac{1}{F}\right)e^{-\frac{FW}{VP}(t-t_0)} + \frac{1}{F}$$

but $\frac{C_T|_0}{C_e} = \frac{W}{VP}t_0$

$$\frac{C_T}{C_e} = \left(\frac{Wt_0}{VP} - \frac{1}{F}\right)e^{-\frac{FW}{VP}(t-t_0)} + \frac{1}{F}$$

Non-condensable Purging During Operation

Build up time (time to discovery)

$$\frac{C_T}{Ce} = \frac{W}{PV} t$$

At discovery time

$$\frac{C_T|_D}{Ce} = \frac{W}{PV} t_D$$

After discovery time

$$\frac{C_T}{Ce} = \left(\frac{W}{PV} t_D - \frac{1}{F}\right) e^{-F\frac{W}{PV}(t-t_D)} + \frac{1}{F}$$

Volume of a 23.9 ft. Dia x 37 ft. long cylinder

$$\frac{\pi (23.9)^2}{4} \times 37 = 16,599.209 \text{ ft}^3$$

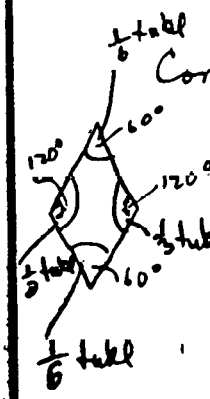

Consider a tube cell

tube area = $\frac{\pi D^2}{4}$ cell area $P^2 \sin 60$

Fraction of cell area occupied by the tube $= \frac{\frac{\pi D^2}{4}}{P^2 \sin 60} = \frac{\pi}{\left(\frac{P}{D}\right)^2 4 \sin 60}$

$\frac{1}{6} + \frac{1}{3} + \frac{1}{6} + \frac{1}{3} = 1.$

$$= \frac{.9069001}{\left(\frac{P}{D}\right)^2}$$

Fraction not occupied by the tube - free area

$$= 1 - \frac{.9069001}{\left(\frac{P}{D}\right)^2} = \frac{\left(\frac{P}{D}\right)^2 - .9069001}{\left(\frac{P}{D}\right)^2}$$

Non-Condensible Purging During Operation

Say $\frac{P}{D} = 1.25$

Free area $= \frac{(1.25)^2 - .9069001}{(1.25)^2}$

$= .4195839$

Free volume $= 16,599.209 \times .4195839 = 5230. ft^3$

$\frac{1}{\rho} = 3.294 \frac{ft^3}{lb}$ $\quad \rho = .3035822 \frac{lb}{ft^3}$

$W = 8.282 \times 10^2 \frac{lb}{sec.}$

$\frac{W}{\rho V} = \frac{8.282 \times 10^2}{.3035822 \times 5230.} \times 3600 = 1877.8/hr.$

$\frac{\frac{lb}{sec.}}{\frac{lb}{ft^3} ft^3} \times \frac{3600 sec.}{hr.}$

$\frac{C_T}{C_e} = 1877.8\,t$

$\frac{C_T|_D}{C_e} = 1877.8\,t_D$

$\frac{C_T}{C_e} = (1877.8\,t_D - \frac{1}{F})\,e^{-F\,1877.8\,(t-t_D)} + \frac{1}{F}$

Figure 1 is a plot of $\frac{C_T}{C_e}$ for a 15 minute (.25hr. discovery time)

Figure 2 is a plot of $\frac{C_T}{C_e}$ for a 30 minute (.5hr. discovery time)

Non-condensible Purging During Operation

Conclusion: The smaller the discovery time the more serious the non-condensable leak. A .6% purge rate (F=.006) will reduce the concentration of non-condensables in the condenser to 35% of its discovery time value in about .4 of an hr. (24 minutes)

Design purge system to accommodate a .006 fraction purge rate or $.006 \times 828.2 \frac{lb}{sec.} = 4.969 \frac{lb}{sec.}$

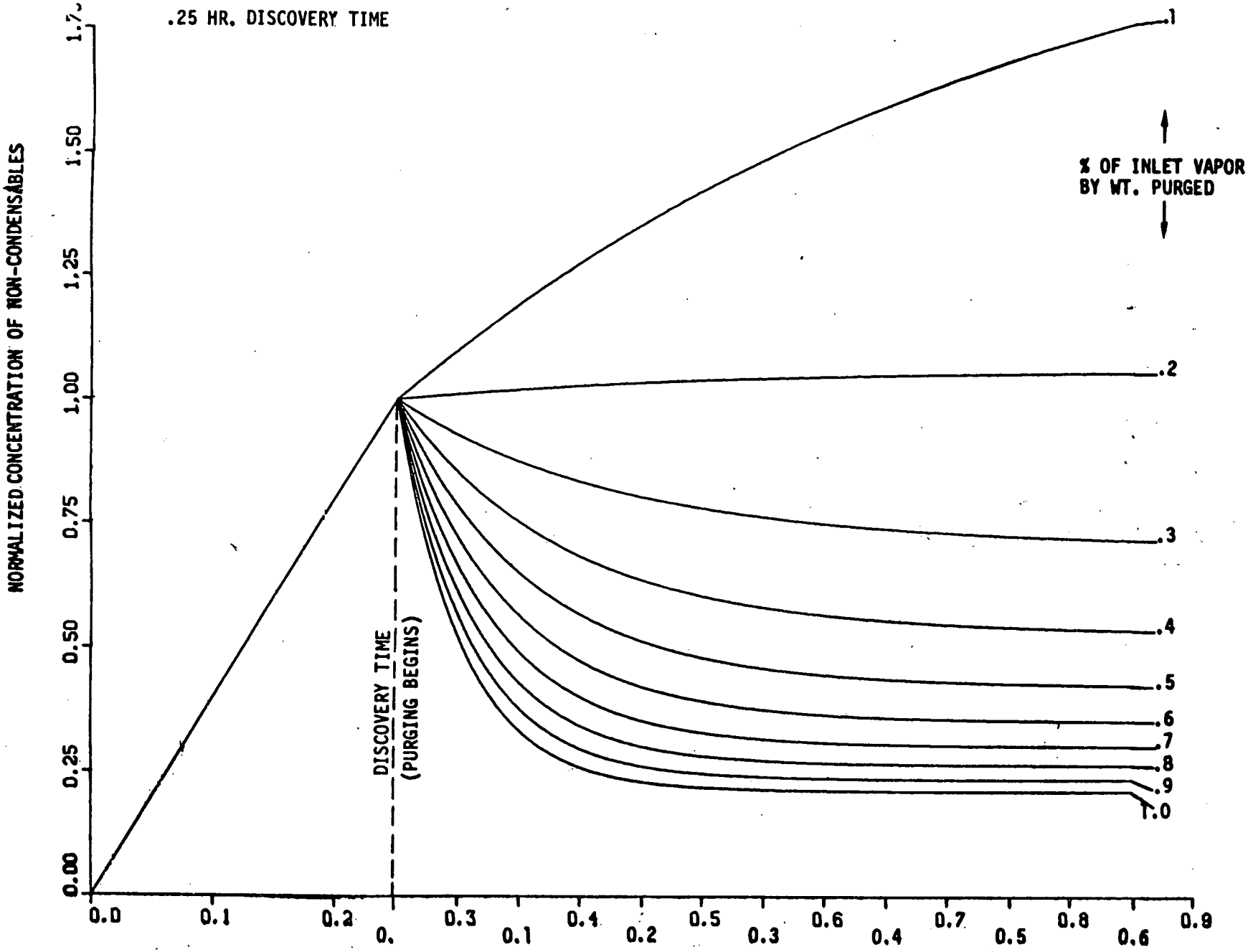
.25 HR. DISCOVERY TIME
NORMALIZED CONCENTRATION OF NON-CONDENSABLES
0.00
0.25
0.50
0.75
1.00
1.25
1.50
1.7
DISCOVERY TIME
(PURGING BEGINS)
% OF INLET VAPOR
BY WT. PURGED
.1
.2
.3
.4
.5
.6
.7
.8
.9
1.0
0.0
0.1
0.2
0.
0.3
0.1
0.4
0.2
0.5
0.3
0.6
0.4
0.7
0.5
0.8
0.6
0.9
TIME HRS.

FIGURE 1

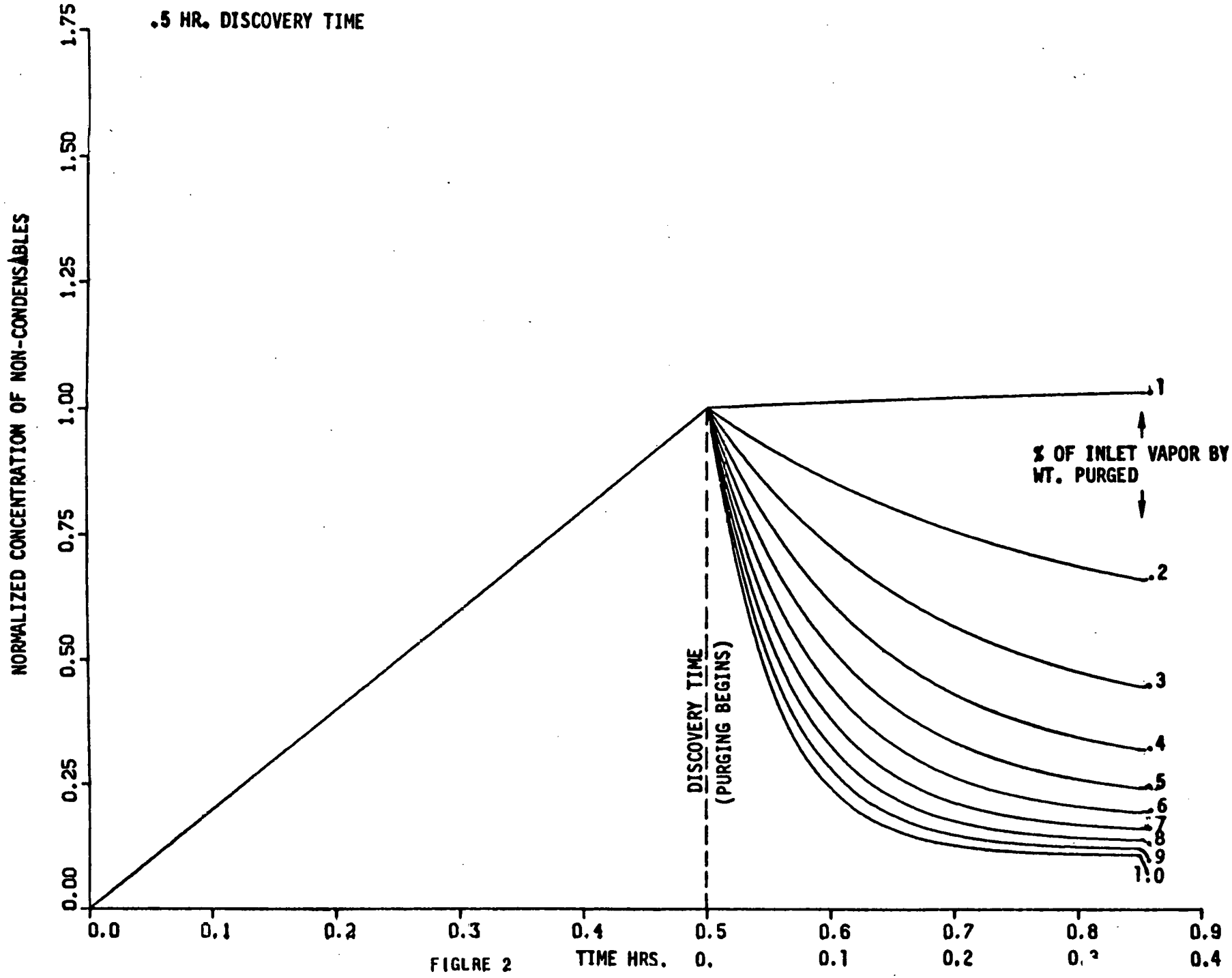
.5 HR. DISCOVERY TIME
NORMALIZED CONCENTRATION OF NON-CONDENSABLES
0.00
0.25
0.50
0.75
1.00
1.25
1.50
1.75
DISCOVERY TIME
(PURGING BEGINS)
% OF INLET VAPOR BY WT. PURGED
1
2
3
4
5
6
7
8
9
10
0.0
0.1
0.2
0.3
0.4
0.5
0.6
0.7
0.8
0.9
TIME HRS.
0.
0.1
0.2
0.4

FIGURE 2

Heat Losses Due To Immersion

Problem: To determine the heat gain to the condenser when submerged in 80°F water

Page 112 Brown & Marcet

eqn 7-7

$$\frac{1}{L} = \frac{1}{L_{horiz}} + \frac{1}{L_{vert}}$$

$$= \frac{1}{26.6667} + \frac{1}{30}$$

$$= .0708333$$

$$L = 14.1176$$

I.D. shell = 315"

say O.D. = 320" = L_{horiz}

L_{horiz} = 26.6667 ft.

L_{vert} = 30 ft.

a for pure* water at 80°F $= 3.0 \times 10^{8}$

$aL^3\theta = 3.\times 10^{8} \times 14.1176^3 \times (80-50)$ θ = temp. diff.

$= 2.53235 \times 10^{13}$

per page 113 $d = 1/3$

$C_1 = .12$ page 114.

$h = C_1 k (a\theta)^{\frac{1}{3}}$

$h = .12 \times .352 \times (3. \times 10^{8} \times 30)^{\frac{1}{3}}$ $k = .355$ pure water @ 80°F

$k = .352$ sea water @ 80°F

$h = 87.8626$

Considering wave motion say $h = 100$.

*sea water is 2½% lower 8/1/78

Heat Losses Due to Immersion

Metal conductance

$1\frac{1}{2}$" shell wall, after corrosion

$k_{carbon\ steel} = 30.$ BTU/(hr. ft² °F/ft.) TEMA

$h_m = \frac{30}{1.5/12} = 240.$

Condensing

$h_c = 1000.$ ORNL Report ORNL-5356 Fig. 6-1

$$U = \frac{1}{\frac{1}{100} + \frac{1}{240} + \frac{1}{1000}} = \frac{1}{.0151666} = 65.934$$

Surface of Condenser shell

$$\pi (26.6667) \times 30 = 2513.274\ ft^2$$

$$q = UA\Delta t = 65.934 \times 2513.27 \times 30$$
$$= 4,971,298.3\ BTU/hr.$$

$$4,971,298.3 \frac{BTU}{hr.} \times \frac{hr.}{60\,min} \times \frac{min\ KW}{56.87\ BTU} \times \frac{M.W.}{1000\ K.W.} = 1.456967\ M.W.$$

Total heat transferred in condenser $= 1.4950 \times 10^9$

Fraction of heat gained $= \frac{4971298.3}{1.4950 \times 10^9}$

$= .00332528$

$.33\%$

Added tubes required

$43678 \times .00332528 = 145.2417$

Heat ~~loss~~ gain

7.5×10^6 BTU/hr.

due to heat loss

$$\frac{\$}{yr} = \frac{7.5 \times 10^6 \text{ BTU/hr}}{3{,}413 \frac{\text{BTU}}{\text{Kw-hr}}} \times 8000 \frac{\text{hrs}}{\text{year}} \times (.025) \times .03 \frac{\$}{\text{Kw-hr}}$$

$$= \$13{,}185/yr$$

P.V. for 30 yr. annuity = 9.43

P.V. $= 13{,}185\,(9.43) = \$124{,}333$

---

ref Joe Kuellis 7/25/78

For. $Q = 5 \times 10^6$ BTU/hr.

P.V. $= \frac{2}{3}(124{,}333) = \$82{,}900$

Amount that can be spent for applying perfect insulation to Condenser for 30 yr life.

Per Forest Clemence of C. F. Braun
7/26/78 — insulation present value will be $100,000. which is greater than $82,900 — therefore do not insulate
G. M. Kukura 7/25/78
J. K.

TRW
DEFENSE AND SPACE SYSTEMS GROUP
ONE SPACE PARK • REDONDO BEACH, CALIFORNIA

PREPARED J. Kallis
CHECKED
J/N 3442-82
REPORT NO.
PAGE 0

Evaporator Bundle & shell dimensions
Condenser Bundle & shell dimensions
Non-Condensible pipe dimensions

This analysis calculates

① Evaporator and Condenser vapor nozzles

② Diameter of evaporator and Condenser tube bundles

③ Evaporator and Condenser shell diameters

④ Shell and tube bundle eccentricities in evaporator & Condenser

⑤ Size of non-condensable evacuation tube and number and size of tube holes required and the size of the discharge pipe

Evaporator Bundle & shell dimensions
Condenser Bundle & shell dimensions
No-Condensable pipe dimensions

Inlet Nozzle

Criterion for vapor nozzle sizes → $PV^2 = 500$, 807.15 lb/sec enters or leaves

Condenser

$P = .3036$

$V^2 = \frac{500}{.3036}$

$V = 40.582$ ft/sec (permissible vel.)

$807.15 \frac{lb}{sec} \times \frac{ft^3}{.3036\ lb} \times \frac{sec}{40.582\ ft}$

$807.15 \times \frac{1}{PV}$

$= 65.5117\ ft^2$

$= \frac{\pi D^2}{4}$

$D = 9.13302$ ft,

$\times 12$

$d = 109.596$ inches

$\times 1.1 = 120.555$

Say 120" ~~outlet~~ i.d.

Condenser inlet nozzle

Evaporator

$P = .43253$

$V^2 = \frac{500}{.43253}$

$V = 33.9998$ ft/sec

$807.15 \frac{lb}{sec} \times \frac{ft^3}{.43253\ lb} \times \frac{sec}{33.9998\ ft}$

$= 54.885\ ft^2$

$= \frac{\pi D^2}{4}$

$D = 8.355024$ ft

$d = 100.31522$ inches

$\times 1.1 = 110.343$

Say 110" ~~inlet~~ outlet

Evaporator * outlet nozzle

* later changed to a 72" I.D. since an outlet has less severe requirements

$V = 807.15 \frac{lb}{sec} \times \frac{ft^3}{.43253\ lb} \times \frac{1}{\frac{\pi}{4}\left(\frac{72}{12}\right)^2 ft^2}$

$= 65.87$

$PV^2 = .43253 \times 65.87^2 = 1877$

Dia. of tube bundles

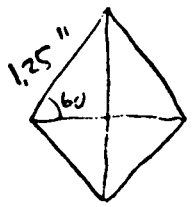

Area/tube

$4(\frac{1}{2}$ base × altitude)

$4(\frac{1}{2}\ \frac{1.25}{2} \times 1.25 \sin 60)$

$1.25^2 \sin 60 =$ **1.353164 in²/tube** ← area occupied by "1" tube

Cond

1.35 × 43678 tubes =

59103.497 in²

$= \frac{\pi D^2}{4}$

$D = 274.32264$ in

say **D = 275. in.** ← diameter of Condenser tube bundle

R = 137.5 in

Evap

1.353 × 42667. =

57735.451

$= \frac{\pi D^2}{4}$

D = 271.12923 in

say D = 272 in

R = 136 in

diameter of evaporator Tube bundle

Shell dia

1.25 Nozzle area = escape area

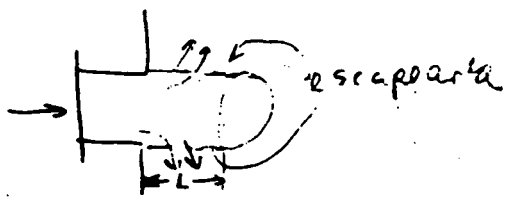

$1.25 \pi \frac{D^2}{4} = \pi D \times L$

Circumference × length

$\frac{1.25}{4} D = L$

Cond.

$\frac{1.25}{4} \times 120 = \boxed{37.5''} = L$

escape area Condenser

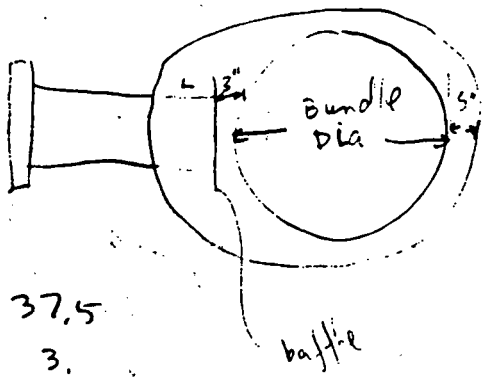

L	37.5
3"	3.
Bundle dia	275.0'
5"	5.0
	320.5 inches

say $\boxed{320.''}$ ← shell diameter condenser

Evap

$\frac{1.25 \times 1.10}{4} = \boxed{34.375} = L$

escape area evaporator

L =	34.375
	3.
	272.
	5.
	314.375

say $\boxed{315.''}$ ← shell diameter evaporator

PREPARED
CHECKED
MODEL

Excentricity

Cond.

distance to Bundle ℄

$\frac{275.0}{2}$ + 3" + $\frac{37.5}{3}$ = 137.5

178.0

distance to shell ℄

$\frac{320}{2} = 160$

excentricity = 178 − 160

= 14"

excentricity Condenser

Evap.

34.375 / 3 = 136

173.375

$\frac{315}{2} = 157.5$

173.375 − 157.5

= 15.875

say 15½

excentricity evaporator

Size of Evacuation tube in Condenser

$\frac{h_L}{\left(\frac{L}{D}\right)\frac{V^2}{2g}} = f$ from Crane

$h_L = f\frac{L}{D}\frac{V^2}{2g}$

$w \times \frac{1}{\rho} \times \frac{1}{\frac{\pi D^2}{4}} = V$

$\frac{lb}{hr.} \cdot \frac{ft^3}{lb} \cdot \frac{1}{ft^2} = \frac{ft}{hr.}$

$h_L = f\frac{L}{D}\frac{w^2}{\rho^2\left(\frac{\pi D^2}{4}\right)^2 2g}$

$\frac{ft}{ft.} \times \frac{hr.^2}{lb^2} \cdot \frac{lb^2}{ft^6} \cdot \frac{ft}{hr.^2} = ft. \times \frac{1}{ft^3}$

$\Delta P = f\frac{L}{D^5}\frac{w^2}{\left(\frac{\pi}{4}\right)^2\rho^2 2g}$

$\Delta P = \frac{1}{\left(\frac{\pi}{4}\right)^2 2g} f\frac{L}{d^5}\frac{w^2}{\rho}$

$L = ft.$ $d = inches$ $w = \frac{lb}{hr.}$ $\rho = \frac{lb}{ft^3}$

$\frac{1}{\frac{ft}{sec^2}} \cdot \frac{ft}{in^5} \cdot \frac{\frac{lb^2}{hr.^2}}{\frac{lb^2}{ft^6}} = \frac{lb\,ft^3\,sec^2}{hr^2\,in^5} \times \frac{hr.^2}{3600^2\,sec^2} \times \frac{12^5\,in^5}{ft^5}$

$= 1.33333 \times 10^{-4}$

$\Delta P = \frac{1.33333 \times 10^{-4}}{\left(\frac{\pi}{4}\right)^2 \times 64.4} f\frac{L}{d^5}\frac{w^2}{\rho}$

$\boxed{\Delta P = 3.35639 \times 10^{-6} f\frac{L}{d^5}\frac{w^2}{\rho}}$

Pressure drop equation $L = ft.$, $d = inches$, $w = lb/hr.$, $\rho = lb/ft^3$

PREPARED
CHECKED
MODEL

$$dP = 3.35639 \times 10^{-6} \frac{f}{d^5 \rho} w^2 \, dL$$

w varies with L

$w = 0 \quad L = 0$

$w = w_{exit} \quad L = \ell$ $\quad \ell$ = total length

$w = mL + b$

$0 = m(0) + b$

$b = 0$

$w_{exit} = m\ell$

$m = \frac{w_{exit}}{\ell}$

$$\boxed{w = \frac{w_{exit}}{\ell} L}$$

variation of w for of vapor uniform pick-up along evacuation tube from $L = 0$ to $L = \ell$

$$dP = 3.35639 \times 10^{-6} \frac{f}{d^5 \rho} \left(\frac{w_{exit}}{\ell}\right)^2 L^2 \, dL$$

$$\int_{P_1}^{P_2} dP = 3.35639 \times 10^{-6} \frac{f}{d^5 \rho} \left(\frac{w_{exit}}{\ell}\right)^2 \int_0^{\ell} L^2 \, dL$$

$$P_2 - P_1 = 3.35639 \times 10^{-6} \frac{f}{d^5 \rho} \left(\frac{w_{exit}}{\ell}\right)^2 \frac{\ell^3}{3}$$

$$\boxed{\Delta P = \frac{3.35639 \times 10^{-6}}{3} \frac{f}{d^5 \rho} w_{exit}^2 \, \ell}$$

P.D. in evacuation tube for uniform pick up of vapor from $L = 0$ to $L = \ell$

d inches $\quad w = \frac{lb}{hr.}$

ℓ ft.

ρ $\frac{lb}{ft^3}$

$$Re = \frac{D\,w}{\frac{\pi D^2}{4}\,\mu}$$

$$= \frac{4}{\pi}\,\frac{w}{D} \times \frac{1}{\mu}$$

.6% purge

$$w = 807\ \frac{lb}{sec.} \times \frac{3600\ sec.}{hr.} \times .006 = 17{,}431.2$$

$$Re = \frac{4}{\pi}\ \frac{17{,}431.2}{d\ in.} \times \frac{12\ in.}{ft.} \times \frac{1}{.0258}$$

$$\frac{lb}{hr.\ in.} \cdot \frac{\pi}{ft.\ lb/ft^3\ hr.}$$

$$Re = \frac{10{,}322{,}834.}{d} \text{ at ax.7}$$

d	Re at ax.T	f
1	10,322,834.	.0103
5	2,064,566.8	.0113
10	1,032,283.4	.0125
15	688,188.9	.0132

say $f = .015$

DETERMINE AVERAGE FRICTION FACTOR

$$\Delta P = \frac{3.35639 \times 10^{-6}}{3} \times \frac{.015}{.3036}\ \frac{(17{,}431.2)^2 \times 30}{d^5}$$

$$= \frac{503.86765}{d^5}$$

PREPARED
CHECKED
MODEL

$V = 807 \frac{lb}{sec.} \times .006 \times \frac{ft^3}{.3036 lb} \times \frac{1}{\frac{\pi d^2}{4} in^2} \times \frac{144 in^2}{ft^2}$

$V = \frac{2924.122}{d^2}$ ft/sec.

Sonic vel. = $\sqrt{\gamma RT}$

$\gamma = 1.3$

$R = 10.731 \frac{ft^3 \cdot lb}{in^2 \cdot lb \cdot R}$

$\times \frac{lb}{17 lb} \times \frac{32.17 ft \cdot lb}{sec^2 \cdot lb} \times \frac{144 in^2}{ft^2}$

$R = \frac{10.731 \times 32.17 \times 144}{17} = 2924.184 \frac{ft^2}{sec^2} \frac{460}{510} R$

$a = \sqrt{1.3 \times 2924 \times 510} = 1392.3$ ft/sec.

d	$\Delta P = \frac{503.86765}{d^5}$	$V = \frac{2924.122}{d^2}$ at exit
1	503.86765	2924.122
2	15.745864	731.0305
3	2.073529	324.902
4	.4920582	182.757
5	.1612376	116.965
6	.0647977	81.226 * choose
7	.0299796	59.6759
8	.0153768	45.689
9	8.53304×10^{-3}	36.100
10	5.03867×10^{-3}	29.24 + chosen

straight pipe

holes

say 1 hole every 2"

$$\frac{\text{hole}}{2\text{ inches}} \times 30 \times 12 \text{ inches} = 180 \text{ holes}$$

$$\frac{17{,}431.2 \frac{lb}{hr.}}{180 \text{ holes}} = 96.84 \frac{lb}{hr.\,hole} \times \frac{1 hr.}{3600 sec} = .0269 \frac{lb}{sec.\,hole}$$

$$V = .61\sqrt{2gh}$$

$$V^2 = .61^2\, 2gh$$

$$h = \frac{V^2}{.61^2 \times 2g}$$

$$\frac{ft^2}{sec^2} \times \frac{\rho\, lb}{ft^3} \times \frac{ft^2}{144 in^2}$$

$$\boxed{\Delta P = \frac{V^2}{.61^2 \times 2g} \frac{\rho}{144}}$$ ← P.D. through hole in evacuation tube

Choose hole size and numbers so that pressure drop through holes is an order of magnitude greater than pressure drop through evacuation pipe (an order of magnitude greater than .065) - thus ensuring good evacuation distribution

$$w \times \frac{1}{\rho} \times \frac{1}{\frac{\pi d^2}{4}} \times 144 = V$$

$$\frac{lb}{sec.} \frac{ft^3}{lb} \frac{1}{in^2} \times \frac{144 in^2}{ft^2}$$

$$\frac{4w}{\pi \rho d^2} \times 144 = V$$

$$\frac{4}{\pi} \times \frac{.0269}{\rho d^2} \times 144 = V$$

$$\boxed{\frac{4.9320207}{\rho d^2} = V}$$ ← Velocity through hole in evacuation tube

$$\Delta P = \frac{\frac{4.9320207^2 \not{\rho}}{\rho f d^4} \frac{\not{\rho}}{144}}{.61^2 \times 64.4} = \frac{4.9320207^2}{.3036 \times 144} \times \frac{1}{.61^2} \times \frac{1}{64.4} \times \frac{1}{d^4}$$

$\rho = .3036$

$$= \frac{.0232188}{d^4}$$

d_{in}		$\Delta P = \frac{.0232188}{d^4} = \frac{.0232188}{\left(\frac{n}{16}\right)^4} = .0232188 \times 16^4 = \frac{1521.6672}{n^4}$	$V = \frac{4158.7526}{n^2}$
$\frac{1}{16}$	1	1521.6672	4158.75
$\frac{2}{16}$	2	95.104	1039.69
	3	18.786	462.1
	4	5.9440	259.9
	5	2.43466	166.3
	6	1.174 1259	115.5
	7	.6337639	84.87 *
	8	.37	64.94 * Chosen

$$V = \frac{807. \times .006 \text{ lb}}{180 \text{ sec}} \times \frac{\text{ft}^3}{.3036 \text{ lb}} \times \frac{1}{\frac{\pi d^2}{4}} \times 144 \frac{\text{in}^2}{\text{ft}^2}$$

$$= \frac{16.245127}{d^2}$$

$$= \frac{16.245127}{\frac{n^2}{16^2}}$$

$$= \frac{4158.7526}{n^2}$$

$\frac{8}{16}$" (= ½") 10"

Choose #8 holes & 8" I.D. pipe

Discharge pipe

$$\Delta P = 3.35639 \times 10^{-6} f \frac{L}{d^5} \frac{W^2}{\rho}$$ from page 5

$f \cong .0125$

$L \cong \frac{137.5\,in}{12\,in/ft} = 11.458$

$W = 807 \frac{lb}{sq.} \times .006 \times 3600 \frac{sec.}{hr} = 17431.12$ $\rho = .3036$

$$\Delta P = \frac{3.35639 \times 10^{-6} \times .0125 \times 11.458 \times (17431.12)^2}{d^5 \times .3036}$$

$$= \frac{481.10963}{d^5}$$

$V = \frac{2924.122}{d^2}$ from page 8

d	$\Delta P = \frac{481.10963}{d^5}$	V	n	rows removed = n rounded to next integer
1	481.109	2924.	.6	1
2	15.0346	731.0305	1.4	2
3	1.9798	324.902	2.2	3
4	.4698	182.757	3.	4
5	.153955	116.965	3.8	4 * ← choose
6	.061871	81.226	4.6	5
8	.0146623		6.2	7

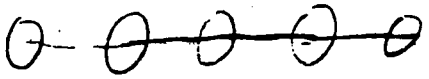

$1.25 \times (n-1) + 2(1.25) =$ distance avoided if removal takes place

$1.25 \times (n-1+2) - 1$

$1.25 \times (n+1) - 1 = d$

$n = \frac{d+1}{1.25} - 1$

discharge pipe

Conclusion

10 ~~6~~" center pipe

180 - $\frac{8}{16}$" holes

8" exiting pipe

ATTACHMENT 9

October 17, 1977

Pressure Losses in Condenser Tube Bundle (No Vapor Lanes)

The pressure loss from periphery to center of a cylindrical condenser tube bundle was calculated for various bundle radii, under the following conditions:

Tube overall diameter	1.5 inches
Tube length	25 ft
Sea water velocity	6 ft/sec
Sea water inlet temperature	40°F
Ammonia saturation temperature	50°F
Triangular pitch diameter	1-7/8 inches
No vapor lanes	
Feed, periphery to center	

For these conditions, pressure drop from periphery to center of bundles can be represented by the equation

$$\Delta P = 4.6 \times 10^{-6} r^{2.855} \quad \text{(psi)}$$

r = bundle radius, in feet

Calculated values of ΔP for various bundle radii are given in Table A.

TABLE A

Tube Bundle Radius, ft	Pressure Drop, psi
5	0.00045
10	0.003294
15	0.0105
20	0.0238
25	0.045

If tubes were reduced to 1 inch diameter, the losses would be roughly 3.38 times as high, which is still small except perhaps for bundles in excess of 20 ft radius.

It appears that vapor lanes will not be needed in condensers of the size contemplated. 50 feet will need (may be) vapor lanes ?

Support calculations follow.

Pressure Losses in Condenser Tube Bundle
(No Vapor Lanes)

Date

The pressure loss from periphery to center of a typical condenser tube bundle was calculated for various bundle radii, under the following conditions:

Tube outside diameter	1.5 inches
Tube length	25 ft
Sea water velocity	6 ft/sec
Sea water inlet temperature	40°F
Ammonia saturation temperature	50°F
Triangular pitch dia	1 7/8 inches
No vapor lanes.	
Feed, periphery to center	

For these conditions, pressure drop from periphery to center of bundle can be approximated by the equation

$$\Delta P = 4.6 \times 10^{-6} R^{2.855} \quad (psi)$$

R = bundle radius, in feet

Calculated values of ΔP for various bundle radii are given in Table A

Table A

Tube bundle radius, ft	Pressure drop, psi
5	0.00045
10	0.00329
15	0.0105
20	0.0238
25	0.045

If tubes were reduced to 1 inch diameter, the sizes would be approximately 3.38 times as high, which is still small except perhaps for bundles in excess of 20 ft radius.

It appears that pressure losses will not be reached in condensers of this size or smaller.

Support calculations follow.

I Geometric Calculations

Tube OD, D_o = 1.5 inches

External flutes, 0.040 −0.80 "

Wall thickness 0.109 −0.218 "

Internal root diameter 1.202 "

Water diameter D_w

= (1 − 0.065) · (Int. root diameter)

= 1.1239 inches

= 0.0936 ft.

Triangular pitch (specified)

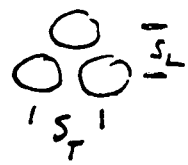

S_T = 1.5 × 1.25 = 1.875 inches

S_L = 1.875 × cos 30° = 1.624 inches

Area/tube

= $S_T \cdot S_L$ = 1.875² cos 30° = 3.045 sq in/tube

Tube area

= $\frac{\pi}{4} 1.5^2$ = 1.767 sq in

Packing ratio

= $\frac{3.045}{1.767}$ = 1.723

I Ammonia vapor generation per foot of tube

L	Tube length, assumed	25 ft
D_w	Water channels	0.0936 ft
ΔT_i	ΔT at water inlet	10°F
v	Sea water velocity, 6 ft/sec	21,600 ft/hr
ρ	Sea water density	64.02 lb/ft³
C_p	Sea water heat capacity	0.9543 BTU/lb-°F
U	Overall heat transfer coeff.	627 BTU/hr-ft²-°F

$$\theta = \Delta T_i \left(1 - e^{-\beta}\right) \qquad (1)$$

$$\beta = \frac{4 U L}{D_w v \rho C_p}$$

θ = sea water temperature rise

$$\beta = \frac{4 \times 627 \times 25}{0.0936 \times 21600 \times 64.02 \times 0.9543} = 0.5076$$

$$e^{-\beta} = 0.6019$$

$$\theta = 10\left(1 - 0.6019\right) = 3.981°F$$

$$q = \frac{\pi}{4} D_w^2 v \rho C_p \theta \qquad (2)$$

q = heat transferred per tube

$$q = \frac{\pi}{4}\left(0.0936\right)^2 (21600)(64.02)(0.9543)$$

$$= 3.615 \times 10^4 \text{ BTU/hr/tube}$$

Ammonia vapor, lb/hr

$$= \frac{q_r}{\Delta H}$$

ΔH = latent heat NH_3 @ 50°F = 527.3 BTU/lb

$$= \frac{3.615 \times 10^4}{527.3} = 68.55 \text{ lb/hr/ton}$$

$$= 68.55 \times 3.294 = 225.8 \text{ cu ft/hr/ton}$$

Vapor volume @ 50° = 3.294 cu ft/lb

$$\text{or } \frac{225.8}{25} = 9.02 \text{ cu ft/hr/foot of tube}$$

III Gunter-Shaw Calculations

← Gunter-Shaw, (uncorrected)

$$-\frac{\Delta P}{\rho \chi} = 1.92\, Re_v^{-0.145}\left(\frac{V^2}{2 g_c d_v}\right)\left(\frac{d_v}{S_T}\right)^{-0.4}\left(\frac{S_L}{S_T}\right)^{0.6}$$

where.

$$d_v = 4\left(\frac{S_L S_T - \frac{\pi D_o^2}{4}}{\pi D_o}\right) = \frac{4 S_T S_L}{\pi D_o} - D_o$$

V = velocity of vapor at constriction $= \frac{\Phi}{S_T - D_o}$

$$Re_v = \frac{d_v V \rho}{\mu}$$

Φ = transverse vapor flow through gap between tubes

χ = flow length

Rothfus correction for specified tube size = 0.81

Corrected Gunter Shaw

$$-\frac{\Delta P}{\rho \chi} = 0.81 \times 1.92 \left(\frac{d_v V \rho}{\mu}\right)^{-0.145}\left(\frac{V^2}{2 g_c d_v}\right)\left(\frac{d_v}{S_T}\right)^{0.4}\left(\frac{S_L}{S_T}\right)^{0.6}$$

$$= (0.81 \times 1.92)\left(\frac{d_v \rho}{\mu}\right)^{-0.145}\left(\frac{1}{2 g_c d_v}\right)\left(\frac{d_v}{S_T}\right)^{0.4}\left(\frac{S_L}{S_T}\right)^{0.6} V^{1.855}$$

$g_c = 32.17\ ft/sec^2$
$= 32.17 \times 3600^2\ ft/hr^2$

Substituting

$$D_v = \frac{4 \times 1.875^2 \times 30}{1.5\pi} - 1.5 = 1.084 \text{ inches}$$

$$= 0.09036 \text{ ft}$$

And

$$(0.81)(1.92)\left(\frac{0.0258 \times 3.294}{0.09036}\right)^{0.145}\left(\frac{1}{2 \times 32.17 \times 36.00^2 \times 0.09036}\right)\left(\frac{7.054}{1.875}\right)^{0.4}\left(\frac{1.624}{1.875}\right)$$

$$= 1.507 \times 10^{-8}$$

So

$$\frac{\Delta P}{\rho Z} = 1.507 \times 10^{-8} V^{1.855} \qquad (3)$$

IV Calculation of V & ΔP

Tubes per longitudinal ft = $\frac{12}{S_L} = \frac{12}{1.624} = 7.389$

Vapor released per longitudinal foot per column, per foot depth

= 7.389 tubes × 9.03 cu ft/hr = 66.74

$$V = \frac{\text{Vapor released}}{\text{width of T.T.}} = \frac{\text{CF/hr}}{S_T - D_O} = \frac{\text{CF/hr}}{0.875/12} = 32 \times \text{CF/hr}$$ [illegible]

In non-dimensional flow

$$V = 32 \times 66.74 X = 2135.6 X, \text{ ft/hr.}$$ (11

From 3, for a given X

$$\frac{\Delta P}{\rho dx} = 1.507 \times 10^{-8} (2135.6 X)^{1.855}$$

$$\frac{\Delta P}{\rho} = \left(\frac{1.507 \times 10^{-8} \times 2135.6^{1.855}}{2.855} \right) X^{2.855}$$

$$= 7.921 \times 10^{-3} X^{2.855}$$

X	ΔP/ρ	lb/in²
5	0.724	
10	8.673	0.012
15	28.05	
20	41.04	0.087
25	77.64	0.164

In cylindrical flow, V at any point is half that in two-dimensional flow, as.

$$V = \frac{2135.6\,R}{2} \quad ft/hr.$$

$$\frac{dP}{\rho dR} = 1.507\times10^{-8}\left(\frac{2135.6\,R}{2}\right)^{1.851}$$

$$\frac{\Delta P}{P} = \frac{1.507\times10^{-8}\times\left(\frac{2135.6}{2}\right)^{1.851}R^{2.851}}{-2.851}$$

which is $\left(\frac{1}{2}\right)^{1.851}$ times the value for two dimensional flow—

$$\left(\frac{1}{2}\right)^{1.851} = 0.276$$

So, for circular tube under water load for the static case, geometry, and operating conditions specified above

$$\Delta P = \frac{.276\times7.921\times10^{-3}R^{2.851}}{144\times32.174} = 4.6\times10^{-6}R^{2.55}\ (psi)$$

Pressure drops through bundles of various radii are given in Table A

V Pressure Loss in Tube Bundles – Scaling Equations

Relations will be developed to predict pressure losses in tube bundles geometrically similar but different in scale, i.e. using 1" tubes instead of 1½" tubes, but with all distances scaled down proportionately.

The Basic Center Shaw relation:

$$\frac{-\Delta P}{\rho L} = 0.61 \times 1.92\, Re_V^{-0.145} \left(\frac{V^2}{2 g_c d_v}\right) \left(\frac{d_v}{S_T}\right)^{0.4} \left(\frac{S_L}{S_T}\right)^{0.6}$$

Contains 2nd group unaffected by size, and other two are affected. Thus the factors:

$$0.61 \times 1.91 \left(\frac{d_v}{S_T}\right)^{0.4} \left(\frac{S_L}{S_T}\right)^{0.6}$$

are functions of geometric arrangement and not of scale. Designating them by F.

$$\frac{-\Delta P}{\rho L} = F\, Re_V^{-0.145} \left(\frac{V^2}{2 g_c d_v}\right)$$

The first term is identifiable as a Froude No.

$$Re_v = \frac{d_v V \rho}{\mu}$$

And in one dimensional flow (along a tube column)

$$V = \frac{\lambda m L}{w}$$

λ = gas conductivity of tube

m = no. of tubes/ft of column, $\sim d_v^{-1}$

w = width of aperture, $\sim d_v$

L = length of column flow origin

$$\frac{m}{w} \sim \frac{d_v^{-1}}{d_v} = d_v^{-2}$$

Also

$$\lambda \sim U D_w \Delta T$$

$$V \sim \frac{U D_w \Delta T L}{d_v^2}$$

So, at any L

$$\frac{-\Delta P}{\rho L} \sim \left(\frac{d_v V \rho}{\mu}\right)^{-0.145} \left(\frac{V^2}{d_v}\right) = \left(\frac{\mu}{\rho}\right)^{0.145} \frac{V^{1.855}}{d_v^{1.145}}$$

$$-\frac{dp}{\rho dx} \sim \left(\frac{\nu}{\rho}\right)^{0.14} \frac{(U D_w \Delta T z)^{1.85}}{d_v^{3.71} d_v^{1.14}}$$

Integrating

$$-\frac{\Delta P}{\rho} = \left(\frac{\nu}{\rho}\right)^{0.14} \frac{(U \Delta T D_w)^{1.85} L^{2.85}}{d_v^{4.85}}$$

To a close approximation, $D_w \sim d_v$. Assuming $\mu, \rho, \Delta T$, and V constants, for some L (in ft)

$$-\Delta P \sim d_v^{-3} \sim D_0^{-3} \quad \text{(approximately)}$$

So in 1" tubes, $\Delta P = 1.5^{-3} = .3375$ times ΔP in 1½" tube bundle.

Evaporator Plenum for Liquid Ammonia

Summary

The layout of tubes in a vertical OTEC evaporator must satisfy constraints on the pressure drop of the liquid ammonia flowing in the inlet-plenum. A plenum design has been determined for one case near the center of the projected range of design and operating variables. In this case,

Outside diameter of tubes = 1.5 in.
Pitch-to-diameter ratio = 1.25
Length of tubes = 25 ft.
Inlet water temperature = 80°F
Average water velocity = 6 ft/sec
Ammonia saturation temperature = 70°F
Inlet liquid ammonia temperature = 65°F
Ammonia applied per tube = 166.7 lb/hr

The tubes are doubly fluted with 60-mil, area ratio 2.0 flutes on the water side and 40-mil constant radius flutes on the ammonia side. Liquid from the plenum is applied through apertures formed by truncating the flutes to a height of 15 mils.

The pressure drop through the apertures from the plenum to the vapor space below is 4.4 ft. of liquid ammonia. Allowing for 0.4° tilt, pressure differences within the plenum can be kept within 10 per cent of the nominal value. The point-to-point variation affects the flow rate of liquid on individual tubes by no more than about 5 per cent, thus maintaining almost constant heat flux from tube to tube.

The layout of tubes is basically a circular bundle cut by six radial mains which separate the bundle into six identical pie-shaped segments. Entering liquid flows from the periphery of the bundle in a complex way. In the present calculations, however, pressure drops along three simple paths have been evaluated and the highest have been selected for conservative design.

Plenum heights and the widths of the radial mains that produce allowable pressure drops are associated with various shell diameters. For the illustrative case at hand, the plenum height L_T and the number of tube rows N_R removed to form a main are as follows:

$L = 25$ ft only

Shell Diam. (ft)	18	25	35	50
Assumed Bundle Diam. (ft)	17	23	32	46
L_T (ft)	2	2	2	3
N_R	0 *	3	3	5

* No radial mains are needed in this instance

These results are not optimized. They indicate, however, that radial mains alone are adequate to control the pressure distribution

Pressure drops in the vapor space are negligible, being in the order of 0.01 to 0.03 psi in the calculated case.

(1)

Evaporator Plenum for Liquid NH_3

Concept

The design is based on a cylindrical tube bank of radius R with the tubes in equilateral staggered array having pitch S. To reduce pressure drop, the bank is divided into six identical segments (pie-shaped) by radial mains, each of which is formed by removing N_R tubes.

Approach

The extent of maldistribution of liquid NH_3 is associated with the maximum pressure drop between the periphery of the tube bank and some point within the bank. To avoid time-consuming search for this particular point, the pressure drops along three paths have been studied. Figure 1 illustrates these paths:

- BD is the path of flow directly into the bank to the interior point D
- ACD and A'C'D are paths along the main for half the radius of the bank, then to point D by the direction normal to the main through the bank
- AE and A'E are paths of flow in the mains along the whole radius of the bank.

Figure 2 shows how the direction of flow influences the transverse and longitudinal pitches. These, in turn, affect the pressure drop.

Fig. 1. Geometry of Equilateral Tube-Bank Segment

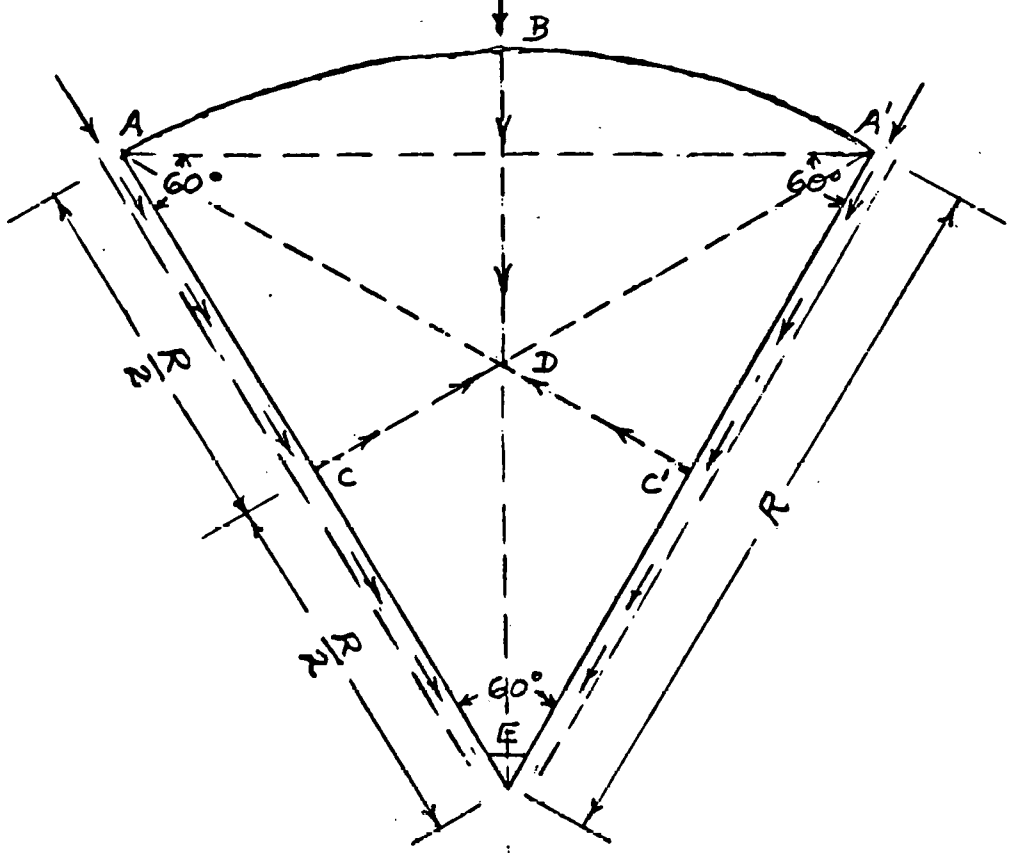

Tubes occupy total area ABA'E. Mains AE and A'E are formed by removing N_R tubes.

Pressure drops are evaluated along NH_3 paths BD, ACD (A'C'D) and AE (A'E) as shown by arrows.

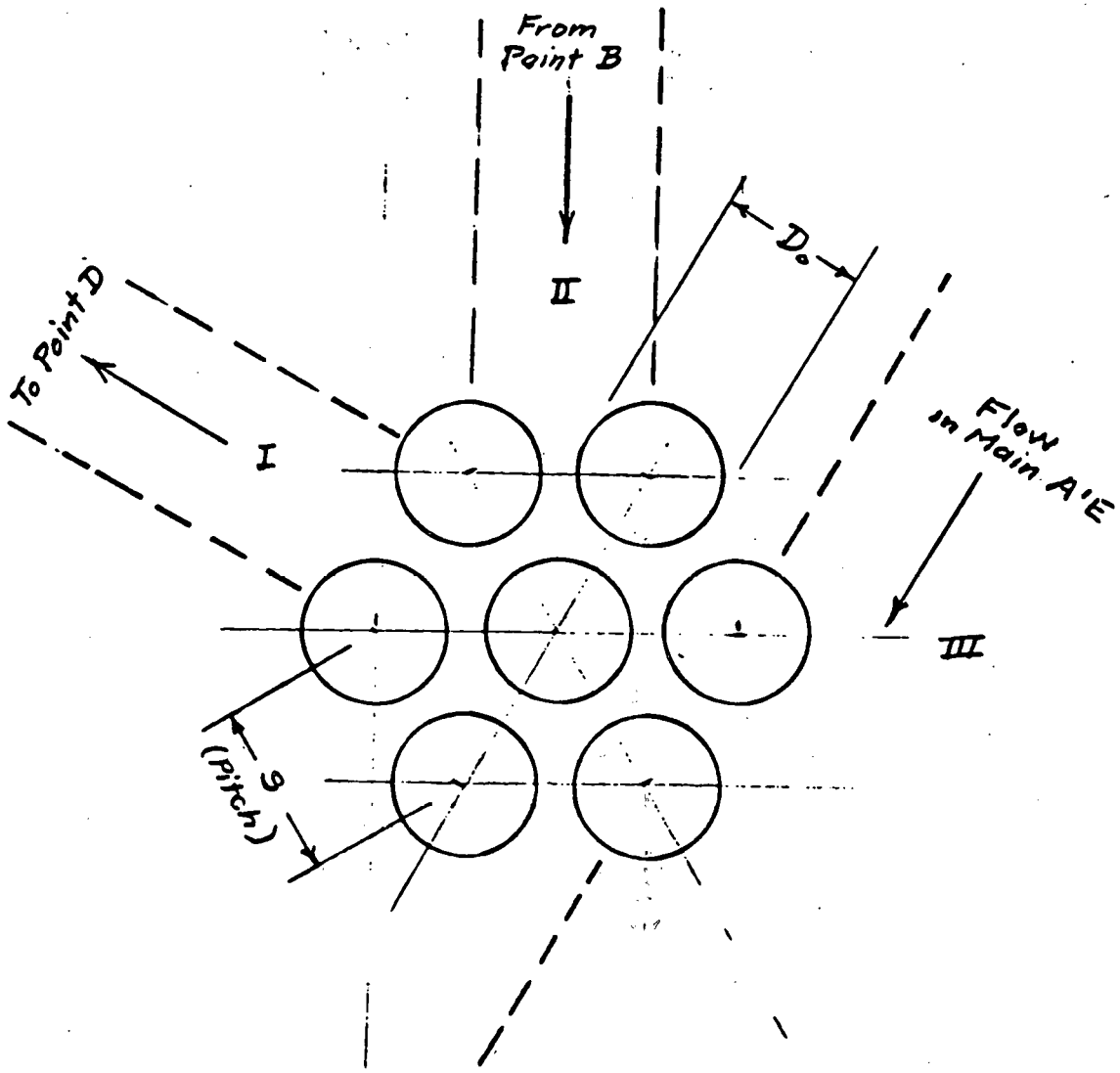

Fig 2. Geometry of Equilateral Tube Array

Path	Transverse Pitch	Longetudeinal Pitch
I	S	$\sqrt{3}S/2$
II	S	$\sqrt{3}S/2$
III	$(N_R+1)\sqrt{3}S/2$	S

Data Base for Pressure Drops

Pressure drops in both the uniform tube bundle and the mains are calculated by means of the equation of Gunter and Shaw (1) with appropriate adjustments. As shown by Boucher and Lapple (2), the Gunter - Shaw equation correlates data on in-line arrays better than those on staggered arrays. It is uncertain, however, how much of the fault lies with the correlation and how much with uncontrolled factors in the contributing experiments.

The convenient form of the Gunter - Shaw equation has been maintained and a simple multiplying factor has been used to bring the correlation into agreement with experimental data. The multiplying factor is shown in Figure 3 as a function of pitch-to-diameter ratio for various tube arrays.

The curve for equilateral, staggered array in Figure 3 corresponds closely to the data of Grimison (3). The curve for square, in-line array resembles Jakob's correlation (4) of Grimison's data, although older published data suggest that the Jakob correlation predicts too-high pressure drops at pitch-to-diameter ratios less than 1.5, data recently obtained in the OTEC laboratory at Carnegie-Mellon indicate that Jakob's correlation has the right trend.

Data obtained at Carnegie-Mellon also indicate that the adjusted Gunter-Shaw equations, applied locally, can be integrated without change to account for generation or loss of fluid at each tube position. This finding has been applied in the present case.

FIGURE 3

ADJUSTMENT OF THE GUNTER-SHAW EQUATION TO CONFORM TO PUBLISHED DATA

RRP 10/13/77

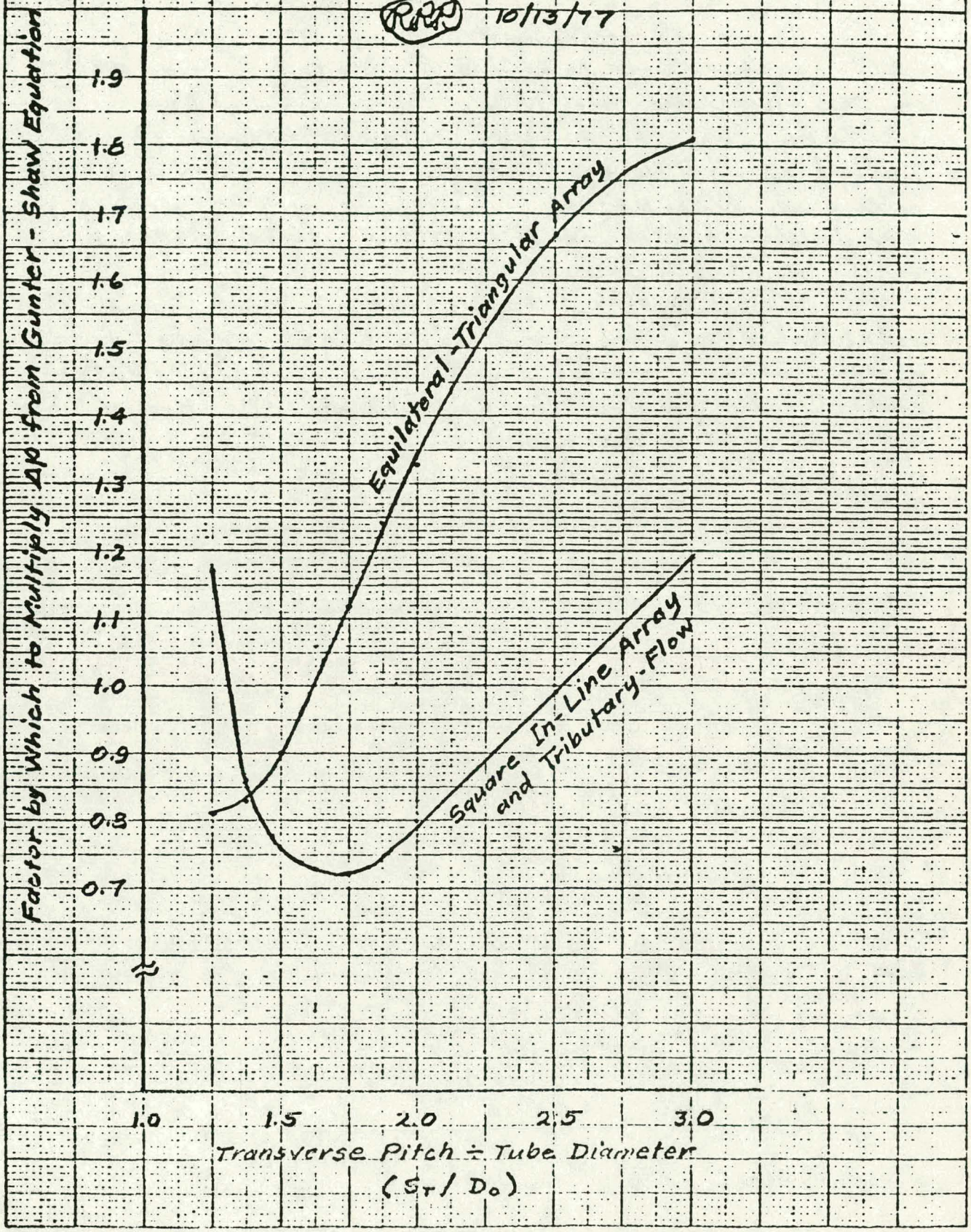

How much pressure drop in the plenum of the evaporator can be tolerated depends on the pressure difference between the plenum and the vapor space below it. The relationship of discharge rate and pressure difference depends on the design of the device for applying liquid NH_3 to the outer surface of the fluted tube.

Experiments at Carnegie-Mellon have established the head vs discharge characteristics of apertures formed by truncating the flutes and closely fitting them to holes in the bottom of the plenum. These data have been applied directly to the present case.

References Cited

1. Gunter, A.Y. and W.A. Shaw, "A General Correlation of Friction Factors for Various Types of Surfaces in Crossflow", Trans. A.S.M.E., 67, 643 (1945).

2. Boucher, D.F. and C.E. Lapple, "Pressure Drop Across Tube Banks: Critical Comparison of Available Data and of Proposed Methods of Correlation", Chem. Eng. Progress, 44, 117 (1948)

3. Grimison, E.D., "Correlation and Utilization of new Data on Flow Resistance and Heat Transfer for Cross Flow of Gases Over Tube Banks", Trans. A.S.M.E., 59, 583 (1937).

4. Jakob, M., Trans. A.S.M.E, 60, 384 (1938). Summarized in McAdams, W.H., "Heat Transmission", 3rd ed., McGraw-Hill Book Company, 1954, pp. 162-3.

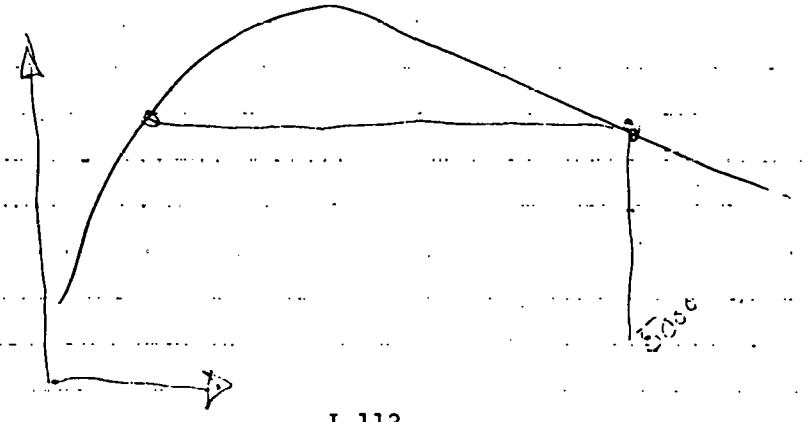

Gunter - Shaw Equation

Let (CF) = correction factor (Fig. 3)

Except at very low Reynolds numbers, not significant in the present case,

$$\frac{1}{(CF)}\frac{1}{\rho}\frac{dp}{dL} = 1.92\left(\frac{\mu}{D_v V_{max}\rho}\right)^{0.145}\left(\frac{1}{D_o}\right)\left(\frac{D_v}{S_T}\right)^{0.4}\left(\frac{S_L}{S_T}\right)^{0.6}\frac{V_{max}^2}{2g_c}$$

$$= 1.92\left(\frac{\mu}{\rho}\right)^{0.145} D_v^{-0.745} S_L^{0.6} S_T^{-1}\frac{V_{max}^{1.855}}{2g_c}$$

where V_{max} = velocity through minimum cross-section
S_T = transverse pitch
S_L = longitudinal pitch
g_c = conversion factor = $32.2 \frac{(lb\text{-}mass)(ft)}{(lb\text{-}force)(sec^2)}$
$= 4.18\times10^8 (lb\text{-}mass)(ft)/(lb\text{-}force)(hr^2)$
D_v = equivalent diameter
$= \frac{4(S_T S_L - \frac{\pi}{4}D_o^2)}{\pi D_o} = D_o\left[\frac{4}{\pi}\left(\frac{S_T}{D_o}\right)\left(\frac{S_L}{D_o}\right) - 1\right]$
D_o = outside diameter of tube
L = length of travel in direction of flow
p = static pressure
ρ = density of fluid
μ = viscosity of fluid

For an equilateral staggered array with pitch = S and flow such that $S_T = S$, by virtue of Fig. 2, $S_L = \sqrt{3}S/2$.

$$D_v = D_o\left[\frac{4}{\pi}\frac{\sqrt{3}}{2}\left(\frac{S}{D_o}\right)^2 - 1\right] = D_o\left[1.103\left(\frac{S}{D_o}\right)^2 - 1\right]$$

Integration of the Guater-Shaw Equation Within the Uniform Tube Bank

Let n = number of tubes in a row
$L = S_L n$ if n is more than a few
$dL = S_L\, dn$ (continuum model)

$$\frac{1}{(CF)}\frac{dp/\rho}{dn} = 1.92\left(\frac{\mu}{\rho}\right)^{0.145}\left(\frac{1}{D_v}\right)^{0.745}\frac{S_L^{1.6}}{S_T}\quad\frac{V_{max}^2}{2g_c}$$

But $V_{max} = \dot{V}/A_{min} = \dot{V}/(S_T - D_o)L_T$

where $\dot{V}$ = volumetric flow rate, cfs
L_T = height of plenum, ft.
V_{max} = velocity, ft/sec
g_c = 32.2 (lb-mass)(ft)/(lb-force)(sec^2)

If the velocity reaches zero n_o tubes from the inlet, the initial volumetric flow rate $\dot{V}_i$ must be

$$\dot{V}_i = \dot{V}_t\, n_o \quad \text{and} \quad d\dot{V} = \dot{V}_t\, dn$$

where $\dot{V}_t$ = volumetric rate of depletion per tube

$$dn = \frac{d\dot{V}}{\dot{V}_t} = \frac{(S_T - D_o)L_T}{\dot{V}_t}\, dV_{max}$$

$$\frac{1}{(CF)}\frac{dp}{\rho} = 1.92\left(\frac{\mu}{\rho}\right)^{0.145}\left(\frac{1}{D_v}\right)^{0.745}\left(\frac{S_L^{1.6}}{S_T}\right)\frac{(S_T - D_o)L_T}{\dot{V}_t}\quad\frac{V_{max}^2\, dV_{max}}{2g_c}$$

Integrating from $V_{max} = V_{maxi}$ to $V_{max} = 0$

$$\frac{1}{(CF)}\frac{\Delta p}{\rho} = \frac{1.92}{2.855}\left(\frac{\mu}{\rho}\right)^{0.145}\left(\frac{1}{D_v}\right)^{0.745}\left(\frac{S_L^{1.6}}{S_T}\right)\frac{(S_T-D_o)L_T}{\dot{V}_o}\quad\frac{V_{maxi}^{2.855}}{2g_c}$$

But $V_{maxi} = \dfrac{\dot{V}_i}{A_{min}} = \dfrac{\dot{V}_t n_o}{(S_T-D_o)L_T}$

$$\frac{1}{(CF)}\frac{\Delta p}{\rho} = 0.0104\left(\frac{\mu}{\rho}\right)^{0.145}\left(\frac{1}{D_v}\right)^{0.745}\left(\frac{S_L^{1.6}}{S_T}\right)\left(\frac{\dot{V}_t}{S_T-D_o}\right)^{1.855}\quad\frac{n_o^{2.855}}{L_T^{1.855}}$$

$$= 0.0104\left(\frac{\mu}{\rho}\right)^{0.145}\left(\frac{1}{D_v}\right)^{0.745}\left(\frac{1}{S_T}\right)\left(\frac{1}{S_L}\right)^{1.255}\left(\frac{\dot{V}_t}{S_T-D_o}\right)^{1.855}\frac{L^{2.855}}{L_T^{1.855}}$$

Solution of a Particular Case

Evaporator:

D_o = 1.5 inches = 0.125 ft.
S/D_o = 1.25
Length of tube = 25 ft.
Inlet water temperature = 80°F
Water velocity = 6 ft/sec.
NH_3 saturation temperature = 70°F
Inlet liquid NH_3 temperature = 65°F

NH_3 supplied / tube = 166.74 lb/hr

At 65°F, for liquid NH_3,
μ = 0.370 lb/(hr)(ft) = 1.028×10^{-4} lb/(sec)(ft)
ρ = 38.3 lb/ft³

$(\mu/\rho)^{0.145} = 0.1556$

$\dot{V}_t = 166.74/(38.3)(3600) = 0.001209$ cfs / tube

$\dot{V}_t^{1.855} = 3.8717 \times 10^{-6}$

$(S_T - D_o)^{1.855} = (0.375/12)^{1.855} = 0.001614$

$S_L^{1.6}/S_T = (0.135)^{1.6}/0.156 = 0.260$

$D_v = D_o \left[\frac{4}{\pi}\left(\frac{S_T}{D_o}\right)\left(\frac{S_L}{D_o}\right) - 1\right] = 0.0906$

$(1/D_v)^{0.745} = 5.983$ $\qquad L = n S_L$

$(CF) = 0.81$

$$\frac{1}{(CF)}\frac{\Delta p}{\rho} = (0.0104)(0.1556)(0.260)\left(\frac{3.8717 \times 10^{-6}}{0.001614}\right)(5.983)\frac{n_o^{2.855}}{L_T^{1.855}}$$

$$\frac{\Delta p}{\rho} = 4.89 \times 10^{-6}\, n_o^{2.855}/L_T^{1.855}$$

In alternative form,

$$\frac{\Delta p}{\rho} = \frac{4.89 \times 10^{-6}}{S_L^{2.855}} \frac{L^{2.855}}{L_T^{1.855}} = 0.00149 \frac{L^{2.855}}{L_T^{1.855}}$$

The effects of design parameters can be seen in the following forms of the local and integrated equations.

Local gradient:

$$\frac{dp/\rho}{dL} = 0.0273 \left(\frac{\mu}{\rho}\right)^{0.145} \left(\frac{1}{D_o}\right)^3 \frac{(CF) \quad (\dot{V}/L_T)^{1.855}}{\left(\frac{S}{D_o}\right)^{0.4} \left[1.103\left(\frac{S}{D_o}\right)^2 - 1\right]^{0.745} \left[\frac{S}{D_o} - 1\right]^{1.855}}$$

Integrated for depletion:

$$\frac{\Delta p}{\rho} = 0.0125 \left(\frac{\mu}{\rho}\right)^{0.145} \left(\frac{1}{D_o}\right)^{4.855} \dot{V}_t^{1.855} \frac{(CF) \quad L^{2.855}/L_T^{1.855}}{\left(\frac{S}{D_o}\right)^{2.255} \left[1.103\left(\frac{S}{D_o}\right)^2 - 1\right]^{0.745} \left[\frac{S}{D_o} - 1\right]^{1.855}}$$

The terms containing the pitch-to-diameter ratio are numerically evaluated in Table 1. S is the nominal pitch, in this case the transverse pitch S_T.

Table 1. Effect of Pitch-to-Diameter Ratio on Pressure Drop Within Equilateral, Staggered Arrays

Pitch / Diam. (S/D_o)	$\left[\frac{(CF)}{\left(\frac{S}{D_o}\right)^{0.4}\left[1.103\left(\frac{S}{D_o}\right)^2-1\right]^{0.745}\left[\frac{S}{D_o}-1\right]^{1.855}}\right]$
1.25	12.34
1.375	4.27
1.50	2.07
1.625	1.27
1.75	0.80

Pitch / Diam (S/D_o)	$\left[\frac{(CF)}{\left(\frac{S}{D_o}\right)^{2.255}\left[1.103\left(\frac{S}{D_o}\right)^2-1\right]^{0.745}\left[\frac{S}{D_o}-1\right]^{1.855}}\right]$
1.25	8.16
1.375	2.37
1.50	0.98
1.625	0.52
1.75	0.28

These results apply to the paths BD and CD (C'D) of Figure 1. The path lengths are

$$\overline{BD} = R - \frac{2}{\sqrt{3}}\left(\frac{R}{2}\right) = 0.423\,R$$

$$\overline{CD} = \overline{C'D} = \frac{1}{\sqrt{3}}\left(\frac{R}{2}\right) = 0.289\,R$$

Arbitrarily, set $R = 11.5$ ft for a shell diameter of 25 ft and maintain $R = (11.5/25) \times$ shell diameter for other shell sizes.

Shell diam. (ft)	18	25	35	50
R (ft)	8.3	11.5	16.1	23.0
L for path $\overline{BD}$ (ft)	3.5	4.9	6.8	9.7
L for path $\overline{CD}$ (ft)	2.4	3.3	4.7	6.7
$L^{2.855}$ for path $\overline{BD}$	35.8	93.4	238	657
$L^{2.855}$ for path $\overline{CD}$	12.2	30.2	83.0	228
$(\Delta p/p) L_T^{1.855}$ for path $\overline{BD}$	0.053	0.140	0.354	0.977
$(\Delta p/p) L_T^{1.855}$ for path $\overline{CD}$	0.018	0.045	0.123	0.339
$(\Delta p/p) L_T^{1.855}$ for whole R	0.626	1.590	4.156	11.51

Except for the smallest shell diameters it is therefore necessary to install radial mains to reduce the pressure drop, unless relatively large plenum heights are to be used.

Radial Mains

When six radial mains are used, the number (N_R) of tubes removed to form the main determines whether the tubes on the sides of the main are in-line or staggered in relation to the direction of flow. This is shown in Figure 2. If N_R is an odd number, an in-line array results. This is the case to be analyzed here.

For the arrangement shown in Figure 1, each main draws from two isoceles triangles having a base of R length and 30° base angles.

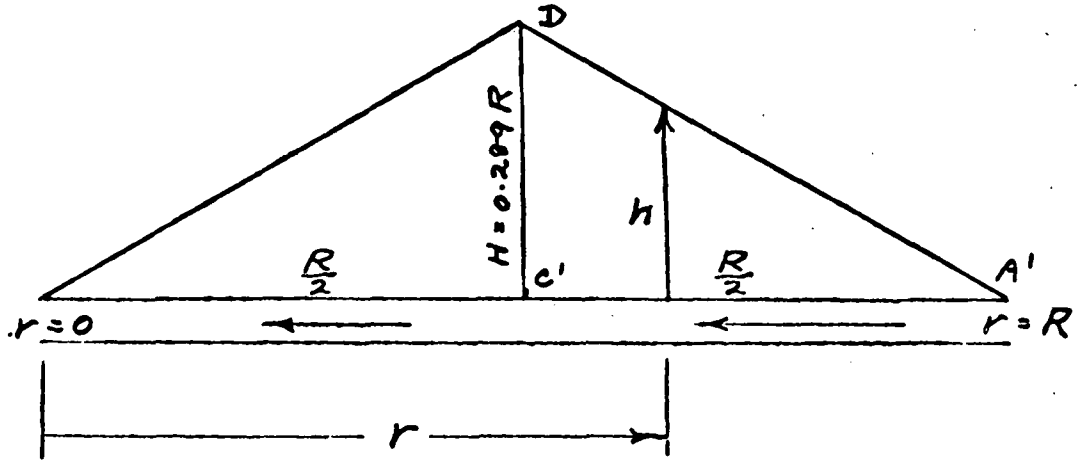

Let r = radial distance from center of exchanger
h = depth of triangular bank at r.
H = distance $\overline{C'D}$ or $\overline{CD}$ of Figure 1. = 0.289 R
R = radius of tube bundle

From $r = 0$ to $r = \frac{R}{2}$ $\quad h = \frac{2H}{R} r = 0.578\, r$

From $r = \frac{R}{2}$ to $r = R$ $\quad h = \frac{2H}{R}(R-r) = 0.578\,(R-r)$

Let n = number of tubes per row in the uniform bank

$$n = h/(0.866S) = h/(0.866\,D_o)(S/D_o)$$
$$= 1.155\,h/D_o(S/D_o)$$

Each row of tubes parallel to $\overline{C'D}$ carries the the volumetric flow rate $\dot{V}_r$ where

$$\dot{V}_r = 2\,\dot{V}_t\,n = 2.31\,\dot{V}_t\,h/D_o(S/D_o)$$

$\dot{V}_t$ is the volumetric depletion rate / tube and the factor of 2 accounts for the fact that each main is fed by two triangular sections.

The number of rows parallel to $\overline{C'D}$ that deplete the main is related to r:

$$dn_R = -dr/S$$

Let $\dot{V}$ = volumetric flow rate at r
$\dot{V}_i$ = volumetric flow rate in at $r = R$
$\dot{V}_{i/2}$ = volumetric flow rate at $r = R/2$

From $r = \frac{R}{2}$ to $r = 0$,

$$\dot{V} = \dot{V}_{i/2} - \int_{\dot{V}_{i/2}}^{\dot{V}} \dot{V}_r\,dn_R = \dot{V}_{i/2} - \frac{2.31\,\dot{V}_t}{S\,D_o(S/D_o)}\int_{R/2}^{r} -h\,dr$$

$$= \dot{V}_{i/2} - \frac{(2.31)(0.578)\,\dot{V}_t}{S\,D_o(S/D_o)}\int_{r}^{R/2} r\,dr$$

$$= \dot{V}_{i/2} - \frac{0.668\,\dot{V}_t}{D_o^2(S/D_o)^2}\left[\left(\frac{R}{2}\right)^2 - r^2\right]$$

at $r = 0$, $\dot{V} = 0$

$$\dot{V}_{1/2} = \frac{0.167\,\dot{V}_t R^2}{D_o^2 (S/D_o)^2}$$

From the geometry of Figure 1, $\dot{V}_i$ must equal the area $R \times 0.289\,R \times$ depletion rate per unit area.

$$\dot{V}_i = 0.289\,R^2\,\dot{V}_t / S_L S_T$$

$$= 0.289\,R^2\,\dot{V}_t / 0.866\,S^2$$

$$= 0.334\,R^2\,\dot{V}_t / D_o^2 (S/D_o)^2$$

From $r = R/2$ to $r = 0$,

$$\dot{V} = \frac{0.668\,\dot{V}_t R^2}{D_o^2 (S/D_o)^2} \left(\frac{r}{R}\right)^2$$

$$\dot{V} = 2\,\dot{V}_i (r/R)^2$$

From the geometry $\dot{V}_{1/2}$ would be expected to equal $0.5\,\dot{V}_i$ as shown.

From $r = R$ to $r = R/2$,

$$\dot{V} = \dot{V}_i - \frac{2.31\,\dot{V}_t}{D_o^2 (S/D_o)^2} \int_R^r -h\,dr$$

$$= \dot{V}_i - \frac{(2.31)(0.578\,\dot{V}_t}{D_o^2 (S/D_o)^2} \int_0^{R-r} (R-r)\,d(R-r)$$

$$= \dot{V}_i - \frac{0.668\,\dot{V}_t R^2}{D_o^2 (S/D_o)^2} \left[1 - \left(\frac{r}{R}\right)\right]^2$$

$$= \frac{0.668\,\dot{V}_t R^2}{D_o^2 (S/R_o)^2} \left[\frac{1}{2} - 1 + 2\left(\frac{r}{R}\right) - \left(\frac{r}{R}\right)^2\right]$$

$$\dot{V} = \frac{0.668\,\dot{V}_t R^2}{D_o^2 (S/D_o)^2} \left[2\left(\frac{r}{R}\right) - \left(\frac{r}{R}\right)^2 - \frac{1}{2}\right]$$

Gunter - Shaw Equation for Mains

$$\frac{1}{(CF)}\frac{dp/\rho}{dr} = 1.92\left(\frac{\mu}{\rho}\right)^{0.145}\left(\frac{1}{D_o}\right)^{0.745}\left(\frac{S_L^{0.6}}{S_T}\right)\frac{V_{max}^{1.855}}{2g_c}$$

$V_{max} = \dot{V}/(S_T - D_o)L_T$ as before

$$\frac{1}{(CF)}\frac{dp/\rho}{dr} = 1.92\left(\frac{\mu}{\rho}\right)^{0.145}\left(\frac{1}{D_o}\right)^{0.745}\left(\frac{S_L^{0.6}}{S_T}\right)\left[\frac{1}{(S_T-D_o)L_T}\right]^{1.855}\frac{\dot{V}^{1.855}}{2g_c}$$

$$\frac{1}{(CF)}dp/\rho = K_1\dot{V}^{1.855}dr$$

$$\frac{1}{(CF)}\frac{\Delta p}{\rho} = K_1\int \dot{V}^{1.855}dr = K_1R\int \dot{V}^{1.855}d\left(\frac{r}{R}\right)$$

From $r = R$ to $r = R/2$, $\dot{V} = K_2\left[2\left(\frac{r}{R}\right) - \left(\frac{r}{R}\right)^2 - \frac{1}{2}\right]$

$$\frac{1}{(CF)}\frac{\Delta p_1}{\rho} = K_1RK_2^{1.855}\int_{1/2}^{1}\left[2\left(\frac{r}{R}\right) - \left(\frac{r}{R}\right)^2 - \frac{1}{2}\right]^{1.855}d\left(\frac{r}{R}\right)$$

We can approximate the integral by numerical methods.

	r/R	$\Delta(r/R)$	$\left[2\left(\frac{r}{R}\right) - \left(\frac{r}{R}\right)^2 - \frac{1}{2}\right]^{1.855}$
0	1.000	0.125	0.276
1	0.875	"	0.260
2	0.750	"	0.216
3	0.625	"	0.150
4	0.500	"	0.076

By Simpson's Rule

Integral $= \frac{1}{3}(0.125)[0.352 + 1.640 + 0.432] = 0.101$

$$\frac{1}{(CF)}\frac{\Delta p_1}{\rho} = 0.101\,R\left[\frac{0.668\,\dot{V}_t R^2}{D_o^2(S/D_o)^2}\right]^{1.855} K_1$$

where $K_1 = \frac{1.92}{2g_c}\left(\frac{\mu}{\rho}\right)^{0.145}\left(\frac{1}{D_o}\right)^{0.745}\left(\frac{S_L^{0.6}}{S_T}\right)\left[\frac{1}{(S_T-D_o)L_T}\right]^{1.855}$

From $r = R/2$ to $r = 0$, $\quad \dot{V} = K_2\left(\frac{r}{R}\right)^2$

$$\frac{1}{(CF)}\frac{\Delta p_2}{\rho} = K_1 R K_2^{1.855}\int_0^{1/2}\left(\frac{r}{R}\right)^{3.71} d\left(\frac{r}{R}\right)$$

$$= \frac{K_1 R K_2^{1.855}}{4.71}\left(\frac{1}{2}\right)^{4.71} = 0.00811\,K_1 R K_2^{1.855}$$

$$\frac{1}{(CF)}\frac{\Delta p_2}{\rho} = 0.00811\,R\left[\frac{0.668\,\dot{V}_t R^2}{D_o^2(S/D_o)^2}\right]^{1.855} K_1$$

The total pressure drop in the main is the sum

$$\frac{\Delta p}{\rho} = 0.1091\,(CF)\,R\left[\frac{0.668\,\dot{V}_t R^2}{D_o^2(S/D_o)^2}\right]^{1.855} K_1$$

$$D_v = D_o\left[\frac{4}{\pi}\left(\frac{S_T}{D_o}\right)\left(\frac{S_L}{D_o}\right) - 1\right]$$

$$= D_o\left[\frac{4}{\pi}\frac{\sqrt{3}}{2}\left(\frac{S}{D_o}\right)^2(N_R+1) - 1\right]$$

$$= D_o\left[1.103\left(\frac{S}{D_o}\right)^2(N_R+1) - 1\right]$$

$$S_L^{0.6}/S_T = S^{0.6}/\frac{\sqrt{3}}{2}(N_R+1)S = 1.163/(N_R+1)\,S^{0.4}$$

$$= \frac{1.163/D_o^{0.4}}{(N_R+1)(S/D_o)^{0.4}}$$

$$(S_T - D_o) = \frac{\sqrt{3}}{2}(N_R-1)\left(\frac{S}{D_o}\right)D_o - D_o$$

$$= D_o\left[0.866(N_R+1)(S/D_o)\right]$$

Solution of the Particular Case Previously Stated

$$D_v = D_o\left[1.723(N_R+1) - 1\right] = 0.125\left[1.723(N_R+1) - 1\right]$$

$$S_L^{0.6}/S_T = \frac{1.163/0.435}{1.093(N_R+1)} = \frac{2.446}{N_R+1}$$

$$(S_T - D_o) = 0.125\left[0.866(N_R+1)(1.25)\right] = 0.1353(N_R+1)$$

$(\mu/\rho)^{0.145} = 0.1556$ as before

N_R	1	3	5
N_R+1	2	4	6
D_v	0.306	0.736	1.167
$D_v^{0.745}$ →	0.414	0.796	1.122
$S_L^{0.6}/S_T$ →	1.223	0.612	0.408
$S_T - D_o$	0.2706	0.5412	0.8118
$(S_T - D_o)^{1.855}$ →	0.0885	0.320	0.679

$$K_1 = \frac{1.92}{64.4}(0.1556)\frac{1}{D_v^{0.745}}\left(\frac{S_L^{0.6}}{S_T}\right)\left(\frac{1}{S_T - D_o}\right)^{1.885}\left(\frac{1}{L_T}\right)^{0.855}$$

$$K_1 L_T^{1.855} = 0.00464\ \frac{1}{D_v^{0.745}}\left(\frac{S_L^{0.6}}{S_T}\right)\left(\frac{1}{S_T - D_o}\right)^{1.855}$$

N_R	→	1	3	5
$K_1 L_T^{1.855}$	→	0.155	0.0111	0.00248

$$\left[\frac{0.668\,\dot{V}_t R^2}{D_o^2 (S/D_o)^2}\right]^{1.855} = \left[\frac{(0.668)(0.001209)R^2}{(0.125)^2(1.25)^2}\right]^{1.855}$$

$$= (0.03308 R^2)^{1.855}$$

$$= 0.001794\, R^{3.71}$$

$$\frac{\Delta p}{\rho} = (0.1091)(1.17)(0.001794)\, K_1 R^{4.71} \quad (CF)$$

$$= 0.000229\, K_1 R^{4.71}$$

N_R	→	1	3	5
$\left[\frac{(\Delta p/\rho) L_T^{1.855}}{R^{4.71}}\right]$	→	3.55×10^{-5}	2.54×10^{-6}	5.68×10^{-7}

Shell Diam. (ft) →	18	25	35	50
R (ft) →	8.3	11.5	16.1	23.0
$R^{4.71}$	2.13×10^4	9.91×10^4	4.83×10^5	2.59×10^6

$(\Delta p/p)\, L_T^{1.855}$ →

$N_R = 1$	0.756	3.52	17.1	91.9
$N_R = 3$	0.054	0.252	1.23	6.58
$N_R = 5$	0.012	0.056	0.274	1.47

$\Delta p/p$ in main

N_R	L_T (ft)				
1	1	0.756	3.52	17.1	91.9
	2	0.209	0.973	4.73	25.4
	3	0.099	0.459	2.23	12.0
3	1	0.054	0.252	1.23	6.58
	2	0.015	0.070	0.340	1.82
	3	0.007	0.033	0.160	0.857
5	1	0.012	0.056	0.274	1.47
	2	0.003	0.015	0.076	0.406
	3	0.002	0.007	0.036	0.192

Add the following pressure drop through $\overline{CD}$

Shell diam. (ft)	18	25	35	50
	$\Delta p/p$ in $\overline{CD}$			
L_T = 1 ft	0.018	0.045	0.123	0.339
2	0.005	0.012	0.034	0.094
3	0.002	0.006	0.016	0.044

92.6 % of the pressure drop through the main occurs between $r = R$ and $r = R/2$. For the shell diameters above, this is as follows:

Shell Diam (ft)		18	25	35	50
N_R	L_T (ft)		$\Delta p/p$ in 1/2 main		
1	1	0.700	3.26	15.8	85.1
	2	0.194	0.901	4.38	23.5
	3	0.092	0.425	2.06	11.1
3	1	0.050	0.233	1.14	6.09
	2	0.014	0.065	0.315	1.68
	3	0.006	0.031	0.148	0.794
5	1	0.011	0.052	0.254	1.36
	2	0.003	0.014	0.070	0.376
	3	0.002	0.006	0.033	0.178

(25)

Total $\Delta p/\rho$ Through Outer Half of Main and Path $\overline{CD}$

Shell Diam. (ft)		18	25	35	50
N_R	L_T (ft)	$\Delta p/\rho$ (ft. of liquid NH_3)			
1	1	0.718	–	–	–
	2	0.199	0.913	–	–
	3	0.094	0.431	2.08	–
3	1	0.068	0.278	–	–
	2	0.019	0.077	0.349	1.72
	3	0.008	0.037	0.164	0.838
5	1	0.029	0.097	0.377	–
	2	0.008	0.026	0.104	0.470
	3	0.004	0.012	0.049	0.222

Pressure Drop Through Path $\overline{BD}$

Shell Diam. (ft)	18	25	35	50
	$\Delta p/\rho$ through $\overline{BD}$			
L_T = 1 ft	0.053	0.140	0.354	0.977
2	0.015	0.039	0.098	0.270
3	0.007	0.018	0.046	0.127

Pressure Drop Through Tube Bank Having No Mains

Shell Diam, (ft)	18	25	35	50
	$\Delta p/p$ in Solid Bank			
L_T = 1 ft	0.626	–	–	–
2	0.173	0.440	1.15	–
3	0.082	0.207	0.541	1.50

APPENDIX I.2

STRESS ANALYSIS

I.2. STRESS ANALYSIS

Mechanical design calculations for the 10 MWe OTEC evaporator and condenser attempt to determine the basic metal thickness requirements with no more than 20 percent error in weight requirements for elements of the pressure envelopes. Because the design is preliminary, little detailed consideration is made for local reinforcement requirements at nozzles, tubesheet to shell joints, or similar points of high localized stress where further design effort in the final design stage is indicated.

Calculations for the 0.2 MWe exchangers are less rigorous than those for the 10 MWe exchangers due to the less severe environment and to the more straightforward construction.

The first approximation for the wall thickness in the evaporator and condenser shells is based on the ASME Boiler and Pressure Vessel Code, Section VIII, Division 1, using a 136 psig shell pressure in the evaporator with an inside diameter of 315 inches and a minimum wall thickness of 2 inches including 1/2 inch allowance for corrosion. Similarly the 325 inch diameter condenser shell requires 1-1/2 inch thickness for a design pressure of 86.3 psig. However, the 1-1/2 inch thick condenser shell requires stiffening rings in order to withstand a specified external pressure of 13.5 psig.

In both the evaporator and the condenser, the tubesheets are stayed by the 1 inch tubes spaced on a 1-1/4 inch spacing. Since the 274-1/4 inch diameter evaporator tube bundle is eccentric to the shell by 14 inches, the maximum unsupported span in the tubesheet is 34-3/8 inches. A stayed flat head with 34-3/8 inch pitch and 20 percent ligament efficiency would seem to imply a 4-5/16 inch thickness according to the code, although no Section 8, Division 1, rules exist to combine considerations of ligament efficiency and stay rod pitch for a flat head. The above deduction is conservative, and tubesheet thicknesses of 4-13/16 inches for the evaporator and of 4-5/16 inches for the condenser are therefore selected for further investigation.

In both the evaporator and the condenser, deformed titanium tubes are to be used. Thirty-six ridges are to be rolled or pressed into the wall of 1 inch diameter tubing, 0.031 inch thick in the case of the evaporator and 0.026 inch thick in the case of the condenser. The deformation will occur for the entire length of each tube except at the tube ends, where the tube joints the tubesheet. Since the tube stiffness is reduced by compressing the tube wall material inward toward the tube axis, subsequent mechanical analysis requires that the deformed tubes be assigned a combination of wall thickness and diameter such that the "equivalent tube" has the same cross-sectional area and moment of inertia as the deformed tube.

The remainder of the preliminary calculations consider a shellside pressure containment envelope to consist of six elements. There is the tube bundle, the upper and lower tubesheets which have the same outside diameter as the tube bundle, the upper and lower annular rings which bridge the span between the tubesheet and the shell, and finally the shell itself. Stresses within the elements of the shellside pressure envelope are investigated by approximating the system with an axisymmetric system. Since high shell stresses at the annular ring are anticipated, the maximum ring width is assumed. The tubesheet diameter is reduced accordingly. Dimensions of the shell and tubes are assumed unchanged from the earlier shell and "equivalent tubes". A computer program is used to investigate system stresses resulting from axial loads caused by weight, shellside and tubeside fluid pre-sures, and temperature changes.

A design life of 30 years is desired. This period is defined as 1000 shellside pressure cycles as well as an undefined number of specified accelerations representing loading cycles due to motion of the ocean surface. Additional undetermined loads will result from motion of the vessel upon which the apparatus is mounted and from impact of ocean waves upon the apparatus. The specified accelerations due to motion of the ocean surface are so low as to make resulting stress ranges trivial, and they are therefore ignored. Motion of the vessel and impact of ocean waves is beyond the scope of preliminary design, and these effects are therefore undefined.

The computer program used to evaluate the effects of system loading yields stress values based upon elastic deformation only. High secondary stresses therefore indicate that local yielding can be expected to occur. This shakedown plastic deformation occurs typically during hydrostatic testing. Final design should explore the possible need for reinforcement in areas where high secondary stress is indicated.

Only the shell stresses are expected to undergo significant stress variations resulting from shellside pressure cycling. Other loading cycles however may cause the final design to incorporate reinforcement for the shell.

APPENDIX I.2.1

10 MWe HEAT EXCHANGER

Customer	TRW	Pages	Page 5
Subject	Evaporator & Condenser Tubes	By	DRM
Project	5304-100	Date	9-18-75

Tube moment of inertia (Evaporator)

Undeformed tube 1" OD × .031 wall

$$I = \frac{\pi}{64}(D^4 - d^4) = .0110873$$

$$J = .0221746$$

$$A = \frac{\pi}{4}(D^2 - d^2) = .0943703$$

polar radius of gyration

$$\rho = [J/A]^{1/2} = 0.4847414$$

mean radius of wall

$$\bar{r} = \frac{1}{4}(D^2 + d^2) = 0.469961$$

$$A\bar{r}^2 = 0.0208429$$

$$J - A\bar{r}^2 = 0.0013317$$

Deformed tube

Note: It is obviously inaccurate but of relatively small error to hold $(J - A\bar{r}^2)$ constant

$$J - A\bar{r}^2 = 0.0013317$$

$$\bar{r} \approx \frac{1}{4}(.99 + .81) = 0.4725$$

$$J = 0.021511$$

$$I = 0.010759$$

Customer	TRW	Pages	Page 6
Subject	Evaporator & Condenser Tubes	By	
Project	5304-100	Date	

Equivalent evaporator tube dimensions.

$A = .0943703 = \frac{\pi}{4}(D_E^2 - d_E^2)$

$I = .010759 = \frac{\pi}{64}(D_E^4 - d_E^4)$

PRELIMINARY FOR DESIGN

$D_E^4 - d_E^4 = .2191805$

$D_E^2 - d_E^2 = .1201559$

$D_E^2 = .1201559 + d_E^2$

$D_E^4 = .0144374 + .2403118\, d_E^2 + d_E^4$

$.0144374 + .2403118\, d_E^2 = .2191805$

$.2403118\, d_E^2 = .2047431$

$d_E = .9233126$

$D_E = .9859741$

Customer	TRW	Pages	Page 7
Subject	Evaporator & Condenser Tubes	By	
Project	5304-100	Date	

(Condenser)

Undeformed tube 1" OD x .026 wt

$I = \frac{\pi}{64}(D^4 - d^4) = .0090441$

$J = .018582$

$A = \frac{\pi}{4}(D^2 - d^2) = .0795576$

$\rho = [J/A]^{1/2} = .4871728$

$\bar{r} = \frac{1}{4}(D^2 + d^2) = .474376$

$A\bar{r}^2 = 0.0179257$

$J - A\bar{r}^2 = 0.0009563$

PRELIMINARY FOR DESIGN

Deformed tube

$\bar{r}_c \cong \frac{1}{4}(.9948) = .465$

$J \cong 0.0181586$

$I = 0.0090793 = \frac{\pi}{64}(D_c^4 - d_c^4)$

$A = 0.0795576 = \frac{\pi}{4}(D_c^2 - d_c^2)$

$D_c^4 - d_c^4 = .1849619$

$D_c^2 - d_c^2 = .1012958$

$D_c^4 = .0102669 + .2025916\, d_c^2 + d_c^4$

$.2025916\, d_c^2 = .1849619 - .0102669 = .1746950$

$d_c = 0.928618$

$D_c = 0.931645$

Customer	TRW	Pages	Page 8
Subject	Evaporator / Condenser	By	NRM
Project	5304-100-117-1	Date	8/25/78

Furnish Section VIII div 1 design for Item 100

I Evaporator

Shell side

for NH_3 sat @ 70°F

P_{sat} = 129.8 psia = 114.1 psig

v_g = 2.312 ft³/lbm

ρ_g = .4325259 lbm/ft³

= .0002503043 lbm/in³

θ_{s_1} = 57.8° F θ_{s_2} = 70 °F

ρ_s = .0002503 sat'd lbm/in³ (vapor)

T_s = 150°F

P_s = 136 psig

d_s = 315" ID

PRELIMINARY FOR DESIGN

Tubesheet

D_t = 274.25" OD tube bundle

D_{pt} = 1" OD tube in TS

t_{pt} = .031" thk tube in TS

Tubeside

θ_{t_1} = 80° F θ_{t_2} = (74.1 °F)

equivalent tube properties for stiffness:

D'_p = 1.3542698

t'_p = 0.0225566

for flow

d'_p = 0.960"

depth of groove = 0.025"

n_p = 42667 tubes

ρ_{t_1} = 63.77 lbm/ft³ = .0369c39 lbm/in³ @ 80° F

ρ_{t_2} = 63.8072 lbm/ft³ = .0369254 lbm/in³ @ 74.1°F

$\dot{m}_t$ = 273,500,000 lbm/hr = 75 972.222 lbm/sec

Customer	Pages	Page 7
Subject	By	
Project	Date	

MAX HEAD LOSS

assumed flow area

$a'_f = \frac{\pi}{4}(.860)^2 = .580884$ in^2 per

$A_f = 24784.424$ in^2

$\rho_{avg} = .0369146$ lbm/in^3

$\dot{m} = \bar{\rho} A V_{avg}$: $V_{avg} = \frac{\dot{m}}{\bar{\rho} A_f}$

$= 83.038181$ in/sec

(6.9 ft/sec)

$\mu_{avg} = \frac{\mu_1 + \mu_2}{2}$

$= \frac{2.24 + 2.5756}{2}$

$= 2.3778 \frac{\text{lbm}}{\text{ft-hr}}$

$= 55.041666 \times 10^{-6} \frac{\text{lbm}}{\text{in-sec}}$

$N_{RE} = \frac{\bar{\rho} V_{avg} d'_p}{\mu}$

$= .0478941 \times 10^6$

Customer	Pages	Page 10
Subject	By	
Project	Date	

Re: Binder: Fluid Mechanics 3rd

assume e/D = .012 (very rough)

V_{orig} = 83.03 8181 in/sec

V	83.04	106.7	106.2 ←
N_{RE}	4.79×10^4	6.16×10^4	6.13×10^4
$\left(\frac{V}{V_{orig}}\right)$	.778	.782	.782

PRELIMINARY FOR DESIGN

flow is turbulent

$f = 0.04$

$$\text{head loss} = f \cdot \frac{1}{d_i} \cdot \frac{V^2}{2 g_c}$$

$$= .04 \cdot \frac{12}{.186} \cdot \frac{83.04^2}{144 \times 2 \times 32.2}$$

$$= 0.415 \text{ ft/ft}$$

in a 29' long tube

head loss = 12.035' plus entrance and exit losses

This is close enough to TRW's guess to accept their value of 3'-6"

Customer	TRW	Pages	Page 11
Subject	10 MWe EVAPORATOR	By	TWC
Project	5304-103-111-1	Date	7/2[illegible]-78

PRELIMINARY FOR DESIGN

1. INTERNAL PRESSURE PER UG 27

P = 136 PSIG, CA = 1/2 OUTSIDE & INSIDE

MTL - SA-516-60

T = UNDER 650 F

$$t = \frac{PR}{SE-6P} + C = \frac{136 \times 157.5}{15000 \times 1 - .6 \times 136} + \frac{1}{2} = 1.436 + \frac{1}{2} = 1.936$$

USE 2" TR

100% X-R & PWHT REQUIRED

2. EXTERNAL PRESSURE PER UG 28

P = 13.5 PSIG CA 1/2 OUTSIDE, 0 INSIDE

MTL - SA 516-60

T - < 300 F A = .0004

$L/D_o = \frac{348}{318} = 1.09$ B = 5900

$D_o/t = \frac{318}{1.5} = 212$

$$P_a = \frac{4}{3}\frac{B}{(D_o/t)} = \frac{4}{3} \cdot \frac{5900}{212} = 37.1 \text{ PSIG} > 13.5 \quad \text{OK}$$

NO RINGS NEEDED W/ 1 1/2 TR (+ 1/2 CA).

BUT USE RINGS AS FINAL DESIGN, INCORPORATING WAVE EFFECTS, WILL CERTAINLY REQUIRE STIFFENING.

Customer	TRW	Pages	Page 12
Subject	10 MWe CONDENSER	By	FWC
Project	5304 - 100 - 117-1	Date	7-26-78

3. INTERNAL PRESSURE PER UG 27

P = 86 PSIG CA ½ OUTSIDE 0 INSIDE

MTL - SA 516-60

T - UNDER 650F

$$t = \frac{PR}{SE - .6P} + C = \frac{86 \times 162.5}{15000 \times 1 - .6 \times 86} + \frac{1}{2} = .935 + \frac{1}{2} = 1.434$$

USE 1½ TR

100% X-R IS REQUIRED

PRELIMINARY FOR DESIGN

4. EXTERNAL PRESSURE PER UG 28

P = 13.5 PSIG CA ½" OUTSIDE, 0 INSIDE

MTL - SA 516-60

T < 300F

A = .00038

$$L/D_o = \frac{174}{326.875} = .532$$

B = 5500

$$D_o/t = \frac{326.875}{.9375} = 349$$

$$P_a = \frac{4}{3}\frac{B}{(D_o/t)} = \frac{4}{3} \times \frac{5500}{349} = 21.0 \text{ PSIG} > 13.5 \quad \text{OK}$$

ONE RING REQUIRED BUT USE 2 RINGS TO STRADDLE VAPOR INLET

5. SIZE THE STIFFENING RINGS PER UG-29

RING { NEW 11" .2½
CORR 10.5" x 1½ $A_1 = A_s$

$A_1 = 10.5 \times 1\frac{1}{2} = 15.75 \text{ IN}^2$

$A_2 = .937 \times [1.1\sqrt{D_o t}]$

$A_2 = .937 \times [1.1\sqrt{326.875 \times .937}]$

$A_2 = 18.1$

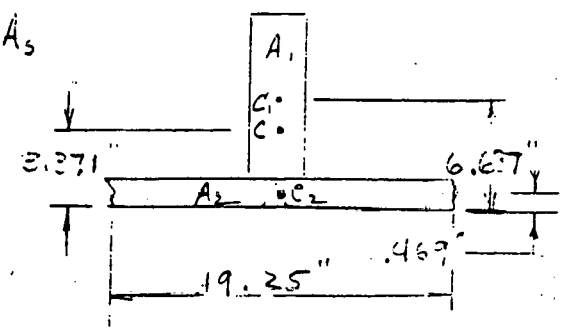

Customer	TRW	Pages	Page 13
Subject	10 MWe CONDENSER	By	FWC
Project	5304-1000-117-1	Date	7-26-78

PRELIMINARY FOR DESIGN

SIZING STIFFENER RING (CONT)

$I_1 = \frac{1.5 \times 10.5^3}{12} = 144.7 \text{ IN}^4$

$I_2 = \frac{19.25 \times .937^3}{12} = 1.320 \text{ IN}^4$

COMPOSITE CG

$C = \frac{C_1 A_1 + C_2 A_2}{A_1 + A_2} = \frac{6.687 \times 15.75 + .469 \times 18}{15.75 + 18} = 3.371$

COMPOSITE I'

$I' = I_1 + A_1 d_1^2 = 144.7 + 15.75 \times 3.316^2 = 317.9$

$I'' = I_2 + A_2 d_2^2 = 1.32 + 18 \times 2.902^2 = 152.7$

TOTAL I 470.8 IN^4 AVAILABLE.

$B = \frac{3}{4}\left[\frac{P D_o}{t + A_s/L_s}\right] = \frac{4}{3}\left[\frac{13.5 \times 326.875}{.937 + \left(\frac{15.75}{12}\right)}\right] = 5485$

$A = .00038$

I_s' REQUIRED

$I_s' = \frac{\left[D_o^2 L_s \left(t + \frac{A_s}{L_s}\right) A\right]}{10.9}$

$I_s' = \frac{\left[326.875^2 \times 116 \left(.937 - \frac{15.75}{116}\right) .00038\right]}{10.9}$

I_s' 463 IN^4 REQUIRED

2 — 11" x 2½" RINGS REQUIRED

Customer	Pages	Page 14
Subject	By	
Project	Date	

PRELIMINARY FOR DESIGN

Tubesheet

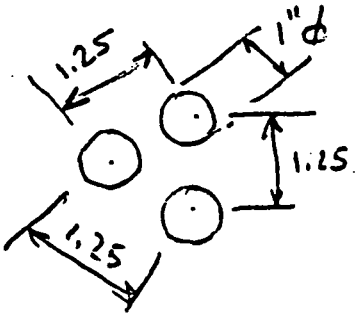

$$p = \frac{1.25\sqrt{3}}{2} = 1.0825317$$

$P = 136$ psi

$S = 15000$

$C = 2.2$

$$t = 1.0825317\sqrt{\frac{136}{2.2 \times 15000}}$$

$t_R = 0.06$" req'd.

However, the dist. of tube bundle to shell is 34.375" max

ligament efficiency $= \eta = \frac{1.25 - 1.0}{1.25} = 0.2$

$$p' = \frac{34.375\sqrt{3}}{2} = 29.769623$$

$P = 136$

$\eta S = 3000$

$C = 2.2$

$$\therefore t = 29.8\sqrt{\frac{136}{2.2 \times 3000}} = 4.273$$"

$4\frac{13}{16}$" Thickness suffices

Customer	Pages	Page 15
Subject	By URM	
Project	Date 9/18/8	

Item 101 Evaporator

Shell Side (subscript "s")

$\theta_{s\,in} = 57.8^{\circ}F$

$\theta_{s\,out} = 70^{\circ}F$

P_{sat} @ 70°F = 129.8 psia = 114.1 psig

$P_{design} = P_s = 136$ psig

$\rho_s = .0002503043$ lbm/in³ (vapor)

$d_s = 315"$ ID

$D_s = 319"$ OD

Tubesheet

actual tubesheet 274.25" OD w/ 42667 ea 1"ϕ holes

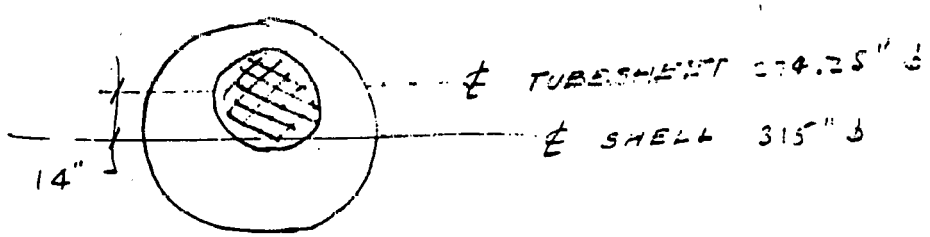

equivalent tube sheet 274.25" avg, 246.25 min, 302.25 max

Tube Side

$\theta_{t\,in} = 80^{\circ}F$

$\theta_{t\,out} = 74.1^{\circ}F$

$\rho_{t_1} = .0369039$ lbm/in³ @ 80°F

$\rho_{t_2} = .0369259$

Customer	Pages	Page 16
Subject	By	
Project	Date	

Input to FTS program

$A_p = .0943763 \times 42667 = 4026.4975$ in²

$A_f = \frac{\pi}{4}\left[1 - (.025 + .04)\right]^2 \times 42667 = 25364.57$

$A_t = \frac{\pi}{4}(274.15)^2 - A_p - A_f = 29681.543$ in²

59072.197 in²

l_p = tube length = 348"

Tube bundle volume

$l_p (A_p + A_t) = 11\,730\,397$ in³

wt of sea water displaced = 432 897.39 lb_m

$P_{t_1} = 9.5' \times 64/144 = 4.222$ psi

$P_{t_2} = 348 \times 64/1728 = 12.888$ psi

wt of tubes =	227 130.38 lb
tubesheets	71 047.018
baffles	51 175.22
tube bundle wt	349 353.03 lb
tube bundle ΔP force	249 415.34
total downward force	598 768.37 lb
less displacement	432 897.39
apparent wt, opn	165 871.38 lb

Customer	Pages	Page 17
Subject	By	
Project	Date	

PRELIMINARY FOR DESIGN

In the computer runs,

Horizontal run neglects gravity effects

In operation, effective $\Delta P = (4.222 - 12.885)$ [illegible]

$\Delta P = -10.749611$

Vertical run includes gravity effects

In operation, effective weight = 165871.58 lbf

CH15

PROJECT 5304-100 FIXED TUBESHEET EXCHANGERS 9-16-76
PROBLEM NO 21 ENGLISH UNITS

INPUT

EVAPORATOR ITEM 101 315 IN ID 348 IN LG 274-1/4 IN TB
HORIZONTAL W/SMALL TUBE BUNDLE & THIN WALLS

UNITS	
LENGTH	INCH
TEMPERATURE	DEGREE F
PRESSURE	PSI
STRESS	PSI
MASS	LB
DENSITY	LB/CUIN
OPTIONS	
TUBESHEETS	SYMMETRIC
EXCHANGER	HORIZONTAL
TEMA	REQUESTED
TUBES	ROLLED
EXPANSION JOINT	NO
WT OR PRES	PRESSURE DROP

CH15

PROJECT 5304-100 FIXED TUBESHEET EXCHANGERS 9-16-78
PROBLEM NO 21 ENGLISH UNITS

TUBE DATA

OD	0.98597
THICKNESS	0.03147
LENGTH	348.00000
UNSUPPORTED LENGTH	
BAFFLE TO BAFFLE	58.00000
TUBESHEET TO BAFFLE	58.00000
LAYOUT ANGLE	60.00000
PITCH	1.25000
NUMBER OF TUBES	42667
OPERATING PRESSURE	4.22220
HYDROSTATIC TEST PRESSURE	25.88900
MAXIMUM TEMPERATURE	77.05000
AVERAGE TEMPERATURE	70.47500
YIELD STRENGTH AT	
MAX TUBE TEMPERATURE	40000.00000
SHELL TEMPERATURE	40000.00000
ATMOSPHERIC	40000.00000
INSIDE CORROSION ALLOWANCE	0.00000
OUTSIDE CORROSION ALLOWANCE	0.00000
POISSONS RATIO	0.34000
ELASTIC MODULUS AT	
MAX TUBE TEMPERATURE	1.62837E+07
AVERAGE TEMPERATURE	1.62834E+07
SHELL TEMPERATURE	1.63982E+07
ATMOSPHERIC	1.64000E+07
ALLOWABLE STRESS AT	
MAX TUBE TEMPERATURE	12500.00000
SHELL TEMPERATURE	12500.00000
ATMOSPHERIC	12500.00000
EXPANSION COEFFICIENT	4.80000E-06
BUNDLE WEIGHT OR PRESSURE DROP	-10.75000

CH15

PROJECT 5304-100 FIXED TUBESHEET EXCHANGERS 9-16-78
PROBLEM NO 21 ENGLISH UNITS

SHELL DATA	
ID	315.00000
THICKNESS	2.00000
OPERATING PRESSURE	136.00000
HYDROSTATIC TEST PRESSURE	204.00000
AVERAGE METAL TEMPERATURE	71.95000
YIELD STRENGTH AT OPERATING	32000.00000
YIELD STRENGTH AT ATMOSPHERIC	32000.00000
ALLOWABLE STRESS AT OPERATING	15000.00000
ALLOWABLE STRESS AT ATMOSPHERIC	15000.00000
ELASTIC MODULUS AT OPERATING	2.90000E+07
ELASTIC MODULUS AT ATMOSPHERIC	2.90000E+07
CORROSION ALLOWANCE	0.50000
EXPANSION COEFFICIENT	6.13000E-06
DENSITY OF FLUID	0.00025
POISSONS RATIO	0.30000
AMBIENT TEMPERATURE	70.00000

TUBESHEETS	1	2
THICKNESS	4.81250	4.81250
FLEXURAL EFFICIENCY	0.00000	0.00000
EXPANSION COEFFICIENT	6.13000E-06	6.13000E-06
TEMPERATURE DROP	22.20000	22.20000
TUBE IN TUBESHEET OD	1.00000	1.00000
TUBE IN TUBESHEET THICKNESS	0.03100	0.03100
CORROSION ALLOWANCE TUBESIDE	0.00000	0.00000
CORROSION ALLOWANCE SHELLSIDE	0.00000	0.00000
TUBE BUNDLE OD	246.25000	
ELASTIC MODULUS AT OPERATING	2.90000E+07	2.90000E+07
ELASTIC MODULUS AT ATMOSPHERIC	2.90000E+07	2.90000E+07
TEMPERATURE		
TUBESIDE	80.00000	80.00000
SHELLSIDE	57.80000	57.80000
AVERAGE	68.90000	68.90000
YIELD STRENGTH AT MAX TEMP	32000.00000	32000.00000
YIELD STRENGTH AT ATMOSPHERIC	32000.00000	32000.00000
ALLOWABLE STRESS AT MAX TEMP	15000.00000	15000.00000
ALLOWABLE STRESS AT ATMOSPHERIC	15000.00000	15000.00000
POISSONS RATIO	0.30000	0.30000
ANNULUS RING		
EXPANSION COEFFICIENT	6.13000E-06	6.13000E-06
AVERAGE TEMPERATURE	79.60000	79.60000
TEMPERATURE DROP	22.20000	22.20000
ELASTIC MODULUS	2.90000E+07	2.90000E+07

* REQUIRES LOCAL REINFORCEMENT. LOCAL REINFORCEMENT WILL BE PROVIDED IN THE DETAILED DESIGN.

CH15

PROJECT 5304-100 FIXED TUBESHEET EXCHANGERS 9-16-78
PROBLEM NO 21 ENGLISH UNITS

OUTPUT

		H-1 NORMAL OPERATING	H-2 HYDROSTATIC TEST SHELL	H-3 HYDROSTATIC TEST TUBES
PRESSURE	PSI			
TUBESIDE		4.222	0.000	25.889
SHELLSIDE		136.000	204.000	0.000
METAL TEMPERATURE	DEGREE F			
TUBE		70.475	70.000	70.000
SHELL		71.950	70.000	70.000
UNSTAYED THICKNESS	INCH			
TUBESHEET 1		18.806	18.746	6.678
TUBESHEET 2		18.806	18.746	6.678
SECONDARY STRESSES	PSI			
TUBES				
CALCULATED		1364.404	1644.492	-462.229
ALLOWABLE		18750.000	28125.000	-4813.922
TUBESHEETS				
1 BENDING CALCULATED		8384.180	10573.885	2689.474
ALLOWABLE		32000.000	48000.000	48000.000
SHEAR CALCULATED		787.848	304.648	-273.293
ALLOWABLE		16000.000	24000.000	24000.000
2 BENDING CALCULATED		8384.180	10573.885	2689.474
ALLOWABLE		32000.000	48000.000	48000.000
SHEAR CALCULATED		787.848	304.648	-273.293
ALLOWABLE		16000.000	24000.000	24000.000
RINGS				
1 BENDING CALCULATED		9287.214	21922.555	531.411
ALLOWABLE		32000.000	48000.000	48000.000
2 BENDING CALCULATED		9287.214	21922.555	531.411
ALLOWABLE		32000.000	48000.000	48000.000
SHELL				
CALCULATED		95404.114*	127438.999*	-3035.160
ALLOWABLE		64000.000	96000.000	96000.000
PRIMARY STRESSES	PSI			
TUBES				
CALCULATED		2887.677	4470.298	567.312
ALLOWABLE		12500.000	18750.000	18750.000
SHELL				
CALCULATED		14325.333	16065.000	0.000
ALLOWABLE		15000.000	22500.000	22500.000

* REQUIRES LOCAL REINFORCEMENT. LOCAL REINFORCEMENT WILL BE
CH15 PROVIDED IN THE DETAILED DESIGN.

PROJECT 5304-100 FIXED TUBESHEET EXCHANGERS 9-16-78
PROBLEM NO 21 ENGLISH UNITS

OUTPUT

		H-4 LOSS OF TUBESIDE POWER	H-5 LOSS OF SHELLSIDE POWER	H-6 BUNDLE AND FLUID WEIGHT
PRESSURE	PSI			
TUBESIDE		0.000	4.222	0.000
SHELLSIDE		136.000	0.000	0.000
METAL TEMPERATURE	DEGREE F			
TUBE		70.475	70.475	70.000
SHELL		71.950	71.950	70.000
UNSTAYED THICKNESS	INCH			
TUBESHEET 1		18.806	3.314	0.000
TUBESHEET 2		18.806	3.314	0.000
SECONDARY STRESSES	PSI			
TUBES				
CALCULATED		1442.800	-66.206	0.000
ALLOWABLE		18750.000	-3208.972	18750.000
TUBESHEETS				
1 BENDING CALCULATED		8799.091	1301.764	0.000
ALLOWABLE		32000.000	32000.000	22500.000
SHEAR CALCULATED		835.684	-42.148	0.000
ALLOWABLE		16000.000	16000.000	11250.000
2 BENDING CALCULATED		8799.091	1301.764	0.000
ALLOWABLE		32000.000	32000.000	22500.000
SHEAR CALCULATED		835.684	-42.148	0.000
ALLOWABLE		16000.000	16000.000	11250.000
RINGS				
1 BENDING CALCULATED		9336.767	-109.212	0.000
ALLOWABLE		32000.000	32000.000	22500.000
2 BENDING CALCULATED		9336.767	-109.212	0.000
ALLOWABLE		32000.000	32000.000	22500.000
SHELL				
CALCULATED		96053.418*	-915.099	0.000
ALLOWABLE		64000.000	64000.000	64000.000
PRIMARY STRESSES	PSI			
TUBES				
CALCULATED		2980.199	61.920	0.000
ALLOWABLE		12500.000	12500.000	12500.000
SHELL				
CALCULATED		14325.333	0.000	0.000
ALLOWABLE		15000.000	15000.000	15000.000

CH15

PROJECT 5304-100 FIXED TUBESHEET EXCHANGERS 9-16-78
PROBLEM NO 22 ENGLISH UNITS

INPUT

EVAPORATOR ITEM 101 315 IN ID 348 IN LG 274-1/4 IN TB
VERTICAL W/SMALL TUBE BUNDLE & THIN WALLS

UNITS

LENGTH	INCH
TEMPERATURE	DEGREE F
PRESSURE	PSI
STRESS	PSI
MASS	LB
DENSITY	LB/CUIN

OPTIONS

TUBESHEETS	SYMMETRIC
EXCHANGER	VERTICAL
TEMA	REQUESTED
TUBES	ROLLED
EXPANSION JOINT	NO
WT OR PRES	BUNDLE WEIGHT

CH15

PROJECT 5304-100 FIXED TUBESHEET EXCHANGERS 9-16-78
PROBLEM NO 22 ENGLISH UNITS

TUBE DATA

OD	0.98597
THICKNESS	0.03147
LENGTH	348.00000
UNSUPPORTED LENGTH	
BAFFLE TO BAFFLE	58.00000
TUBESHEET TO BAFFLE	58.00000
LAYOUT ANGLE	60.00000
PITCH	1.25000
NUMBER OF TUBES	42667
OPERATING PRESSURE	4.21800
HYDROSTATIC TEST PRESSURE	25.88900
MAXIMUM TEMPERATURE	76.30000
AVERAGE TEMPERATURE	70.90000
YIELD STRENGTH AT	
MAX TUBE TEMPERATURE	40000.00000
SHELL TEMPERATURE	40000.00000
ATMOSPHERIC	40000.00000
INSIDE CORROSION ALLOWANCE	0.00000
OUTSIDE CORROSION ALLOWANCE	0.00000
POISSONS RATIO	0.34000
ELASTIC MODULUS AT	
MAX TUBE TEMPERATURE	1.62837E+07
AVERAGE TEMPERATURE	1.63834E+07
SHELL TEMPERATURE	1.63982E+07
ATMOSPHERIC	1.64000E+07
ALLOWABLE STRESS AT	
MAX TUBE TEMPERATURE	12500.00000
SHELL TEMPERATURE	12500.00000
ATMOSPHERIC	12500.00000
EXPANSION COEFFICIENT	4.80000E-06
BUNDLE WEIGHT OR PRESSURE DROP	165872.00000

CH15

PROJECT 5304-100 FIXED TUBESHEET EXCHANGERS 9-16-78
PROBLEM NO 22 ENGLISH UNITS

SHELL DATA	
ID	315.00000
THICKNESS	2.00000
OPERATING PRESSURE	136.00000
HYDROSTATIC TEST PRESSURE	204.00000
AVERAGE METAL TEMPERATURE	71.95000
YIELD STRENGTH AT OPERATING	32000.00000
YIELD STRENGTH AT ATMOSPHERIC	32000.00000
ALLOWABLE STRESS AT OPERATING	15000.00000
ALLOWABLE STRESS AT ATMOSPHERIC	15000.00000
ELASTIC MODULUS AT OPERATING	2.90000E+07
ELASTIC MODULUS AT ATMOSPHERIC	2.90000E+07
CORROSION ALLOWANCE	0.50000
EXPANSION COEFFICIENT	6.13000E-06
DENSITY OF FLUID	0.00025
POISSONS RATIO	0.30000
AMBIENT TEMPERATURE	70.00000

TUBESHEETS	1	2
THICKNESS	4.81250	4.81250
FLEXURAL EFFICIENCY	0.00000	0.00000
EXPANSION COEFFICIENT	6.13000E-06	6.13000E-06
TEMPERATURE DROP	22.20000	22.20000
TUBE IN TUBESHEET OD	1.00000	1.00000
TUBE IN TUBESHEET THICKNESS	0.03100	0.03100
CORROSION ALLOWANCE TUBESIDE	0.00000	0.00000
CORROSION ALLOWANCE SHELLSIDE	0.00000	0.00000
TUBE BUNDLE OD	246.25000	
ELASTIC MODULUS AT OPERATING	2.90000E+07	2.90000E+07
ELASTIC MODULUS AT ATMOSPHERIC	2.90000E+07	2.90000E+07
TEMPERATURE		
TUBESIDE	80.00000	80.00000
SHELLSIDE	57.80000	57.80000
AVERAGE	68.90000	68.90000
YIELD STRENGTH AT MAX TEMP	32000.00000	32000.00000
YIELD STRENGTH AT ATMOSPHERIC	32000.00000	32000.00000
ALLOWABLE STRESS AT MAX TEMP	15000.00000	15000.00000
ALLOWABLE STRESS AT ATMOSPHERIC	15000.00000	15000.00000
POISSONS RATIO	0.30000	0.30000
ANNULUS RING		
EXPANSION COEFFICIENT	6.13000E-06	6.13000E-06
AVERAGE TEMPERATURE	79.60000	79.60000
TEMPERATURE DROP	22.20000	22.20000
ELASTIC MODULUS	2.90000E+07	2.90000E+07

* REQUIRES LOCAL REINFORCEMENT. LOCAL REINFORCEMENT WILL BE PROVIDED IN THE DETAILED DESIGN.

CH15

PROJECT 5304-100 FIXED TUBESHEET EXCHANGERS 9-16-78
PROBLEM NO 22 ENGLISH UNITS

OUTPUT

		NORMAL OPERATING	HYDROSTATIC TEST SHELL	HYDROSTATIC TEST TUBES
PRESSURE	PSI			
TUBESIDE		4.218	0.000	25.88[illegible]
SHELLSIDE		136.000	204.000	0.[illegible]00
METAL TEMPERATURE	DEGREE F			
TUBE		70.900	70.000	70.000
SHELL		71.950	70.000	70.000
UNSTAYED THICKNESS	INCH			
TUBESHEET 1		18.806	18.746	6.678
TUBESHEET 2		18.806	18.746	6.678
SECONDARY STRESSES	PSI			
TUBES				
CALCULATED		1352.264	1643.172	-487.830
ALLOWABLE		18750.000	28125.000	-4813.922
TUBESHEETS				
1 BENDING CALCULATED		10933.219	22984.372	12832.831
ALLOWABLE		32000.000	48000.000	48000.000
SHEAR CALCULATED		876.049	652.794	327.765
ALLOWABLE		16000.000	24000.000	24000.000
2 BENDING CALCULATED		5876.980	13676.722	15067.399
ALLOWABLE		32000.000	48000.000	48000.000
SHEAR CALCULATED		693.308	-281.928	-682.208
ALLOWABLE		16000.000	24000.000	24000.000
RINGS				
1 BENDING CALCULATED		8179.166	16519.751	5934.214
ALLOWABLE		32000.000	48000.000	48000.000
2 BENDING CALCULATED		10440.409	27528.486	5181.540
ALLOWABLE		32000.000	48000.000	48000.000
SHELL				
CALCULATED		107219.540*	159717.212*	-34497.951
ALLOWABLE		64000.000	96000.000	96000.000
PRIMARY STRESSES	PSI			
TUBES				
CALCULATED		2887.769	4470.290	567.312
ALLOWABLE		12500.000	18750.000	18750.000
SHELL				
CALCULATED		14325.333	16065.000	0.000
ALLOWABLE		15000.000	22500.000	22500.000

* REQUIRES LOCAL REINFORCEMENT. LOCAL REINFORCEMENT WILL BE PROVIDED IN THE DETAILED DESIGN.

CH15

PRELIMINARY DESIGN

PROJECT 5304-100 FIXED TUBESHEET EXCHANGERS 9-16-78
PROBLEM NO 22 ENGLISH UNITS

OUTPUT

		V-4 LOSS OF TUBESIDE POWER	V-5 LOSS OF SHELLSIDE POWER	V-6 BUNDLE AND FLUID WEIGHT
PRESSURE	PSI			
TUBESIDE		0.000	4.218	0.000
SHELLSIDE		136.000	0.000	0.000
METAL TEMPERATURE	DEGREE F			
TUBE		70.900	70.900	70.000
SHELL		71.950	71.950	70.000
UNSTAYED THICKNESS	INCH			
TUBESHEET 1		18.806	3.312	0.000
TUBESHEET 2		18.806	3.312	0.000
SECONDARY STRESSES	PSI			
TUBES				
CALCULATED		1430.725	-72.200	-7.967
ALLOWABLE		18750.000	-3208.972	-3209.281
TUBESHEETS				
1 BENDING CALCULATED		11347.032	4030.989	3257.594
ALLOWABLE		32000.000	32000.000	22500.000
SHEAR CALCULATED		923.866	73.439	88.810
ALLOWABLE		16000.000	16000.000	11250.000
2 BENDING CALCULATED		6290.794	4031.206	-3257.580
ALLOWABLE		32000.000	32000.000	22500.000
SHEAR CALCULATED		741.125	-137.238	-93.931
ALLOWABLE		16000.000	16000.000	11250.000
RINGS				
1 BENDING CALCULATED		8228.575	-1215.188	1111.420
ALLOWABLE		32000.000	32000.000	22500.000
2 BENDING CALCULATED		10489.818	-1098.550	-1149.823
ALLOWABLE		32000.000	32000.000	22500.000
SHELL				
CALCULATED		107867.207*	-12353.882	-11891.008
ALLOWABLE		64000.000	64000.000	64000.000
PRIMARY STRESSES	PSI			
TUBES				
CALCULATED		2980.199	61.858	0.000
ALLOWABLE		12500.000	12500.000	12500.000
SHELL				
CALCULATED		14325.333	0.000	0.000
ALLOWABLE		15000.000	15000.000	15000.000

Customer	
Subject	Pages Page 28
Project	By [illegible]
	Date 5/18/8

PRELIMINARY FOR DESIGN

Analysis of FTS Computer Run [illegible]
(RESOLUTION INTO FORCES AND MOMENTS

Tubesheet Shears

TS dia = 246.25"

TS thk = 4.8125"

TS shear area = 3692.7948 in²

		TS 1	TS 2
1. Consider bundle & shell fluid wt submerged in sea water (column V6)	stress	+ 88.10	- 93.931
	load	325335.22 lb ↓	346867.9 lb ↓
2.* Consider wt of seawater displaced		(+ 55.614)	(- 59.614)
		216448.69 lb ↓	216448.69 ↑
* NOT ON COMPUTER RUN			
3. Consider shellside pressure @ 136 psi (column H4)	stress	+ 835.684	+ 835.684
	load	3086009.5 ↑	3086009.5 ↓
4. Consider tubeside pressure @ 4,222 psi (column H5)		- 42.148	- 42.148
	load	155643.91 ↓	155643.91 ↑
5. Consider wt of shellside fluid [columns (V4 - V6 - H4)]	stress	+ 0.082	- 0.625
	load	302.80317 ↓	2319.0751 ↑
6. Consider wt & ΔP of tubeside fluid [columns (V5 - H5 - V6)]	stress	+ 27.427	- 1.159
	load	101503.55 ↓	4279.9731 ↑
7 Consider thermal effects (V1 + V6 - V4 - V5)	Stress	- 32.446	- 4.510
	load	119816.42 ↑	16654.50 ↓

PRELIMINARY FOR DESIGN

Evaporator

I Tubesheet 1

opn shear force : $F_t = 876.049 \times 4.9125 \times 246.25\pi$
$= +3\ 261\ 558.8\ lb_f$

submerged

(from FTS output) $\sigma_{p\ max} \cong \frac{6 M_b}{t^2}$

$= 10933.219$ psi

$\sigma_{t\ max} = 136$ psi

$\sigma_{\lambda\ max} = -136$ psi

$\therefore \sigma_p - \sigma_\lambda = 11069.219$ psi

II Tubesheet 2

opn shear force $= 693.308 \times 4.8125 \times 246.25\pi$
$= +2\ 581\ 208.7\ lb_f$

$\sigma_{p\ max} = 5876.980$ psi

$\sigma_t = 136$ psi

$\sigma_\lambda = -136$ psi

$\therefore \sigma_p - \sigma_\lambda = 6012.98$ psi

III Shell

$\sigma_t = 14325.333$ psi

$A_s = 1496.1532\ in^2$

$Z_s = 118215.95\ in^3$

(fm FTS output) $\sigma'_\lambda = 107219.54$ psi

Customer	Pages	Page 30
Subject	By	
Project	Date	

add effects of buoyancy σ_λ'' = 422.8909 psi

add effects of eccentricity $\sigma_\lambda''' = \frac{14\ F_t}{\Sigma}$ = 3[illegible]6856 psi

σ_λ = 107948.11 psi

σ_ρ = -136 psi

$\sigma_\lambda - \sigma_\rho$ = 107741.79 psi

PRELIMINARY FOR DESIGN

IV Tubesheet 1

de-pressurized submerged

shear force = F_t = 5417[illegible]

$\sigma_{\rho\ max}$ = 3257.594 psi

σ_θ = 0

σ_λ = 0

$\therefore \sigma_\rho - \sigma_\lambda$ = 3257.594 psi

V Tubesheet 2

F_t = 563 316.59 lb

de-pressurized submerged

$\sigma_{\rho\ max}$ = 3257.580 psi

σ_θ = -12.88 psi

σ_λ = -12.88 psi

$\therefore \sigma_\rho - \sigma_\lambda$ = 3270.46 psi

VI Shell

de-pressurized submerged

σ_θ = -1370.5[illegible] psi

σ_λ' = -11991.00[illegible] psi

(due to buoyancy) σ_λ'' = - 422.8909 psi

(due to eccentricity) σ_λ''' = ± 64.162024 psi

σ_λ = 12378.060 psi

$\sigma_\lambda - \sigma_\phi$ = 13748.5 [illegible] psi

	TS1	TS2	shell
Stress Differences	11069.219	6012.98	107948.11
	3257.594	3270.46	12378.06
Range	7811.625	2742.52	95570.05
Alt. Stress Intensity	3905.8 < 10,000psi	1371.26 < 10,000psi	47785.03

Note: Alt. Stress intensity only exceeds 10000psi in the shell at the tubesheets.

N = 10,600 cycles

PRELIMINARY FOR DESIGN

Customer	Pages	Page 32
Subject	By	
Project	Date	

Investigate axial shell stress attributed to tube bundle weight

EVAPORATOR

1. Submerged in Sea Water (v-6)	stress	-11 891.008
2. Sea Water $\frac{58.614}{88.100} \times -11891.008 =$		-7911.2315
1. Total axial shell stress due to tube bundle weight		-19802.239
4 Stress Range (±.05g)		1980.224

$S < 10{,}000$ psi

$N \longrightarrow \infty$

∴ Alternating stress intensity due to vertical sea state & water surface acceleration is trivial.

Customer	Pages	Page 33
Subject	By	
Project	Date	

PRELIMINARY FOR DESIGN

Item 102 Condenser

Shell side (subscript "s")

$\theta_{s\,in}$ = 50°F

$\theta_{s\,out}$ = 50°F

P_{sat} @ 50°F = 89.19 psia = 74.5 psig

P_{design} = 101 psia = 86.3 psig

ρ_s = .0001603739 lbm · in^{-3}

d_s = 325"OD

D_s = 328"OD

Tubesheet

actual TS 278.25"ID w/43883 tubes @ 1"ϕ hole

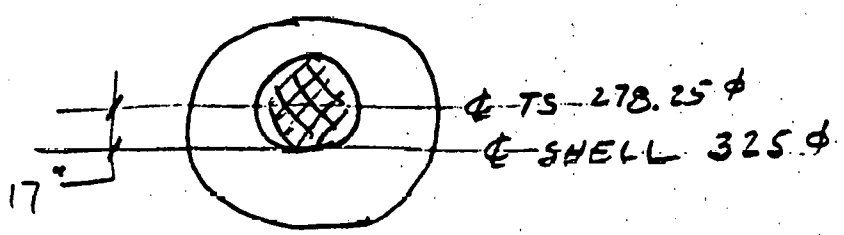

Equivalent TS 278.25" avg; 244.25" min; 312.25" max

Tubeside

$\theta_{p\,in}$ = 40°F (45° avg metal temp)

$\theta_{p\,out}$ = 46.2°F (48.1° avg metal temp)

46.55 avg tube temp

$P_{p\,in}$ = (8'-4" head) = 3.7037036 psig

$P_{p\,out}$ = 12.8888 psig

ΔP = − 9.185185

PRELIMINARY FOR DESIGN

A_p = 3491.2261 in^2
A_f = 26087.03 in^2
A_t = 31229.671 in^2
60807.927 in^2

l_p = tube length = 348"

Tube bundle volume = 12 082 961 in^3
wt of sea water displaced = 447 517.06 lb
p_{t_1} = 8.333 × 64/144 = 3.7037036 psig
p_{t_2} = 348 × 64/1728 = 12.888 psig

wt tubes	196 936.65 lb
tubesheets	78 910.04
baffles	51 175.22
tube bundle	327 021.91 lb
ΔP	225 214.53
total downward force	552 236.44 lb
less displacement	447 517.06
apparent wt, gm	104 719.38

Customer | Pages | Page 35

Subject | By

Project | Date

PRELIMINARY FOR DESIGN

In the computer run, tube bundle is assumed to correct shell stress for eccentricity.

In the Horizontal run, neglecting gravity forces on the steel

effective $\Delta P = (12.8888 - 3.7037)\left(\frac{278.25}{276.25}\right)^2$

$= -11.727398$ psi

In the vertical run, including gravity forces on the steel

effective wt = 10719.38 lb

PROJECT 5304-100 FIXED TUBESHEET EXCHANGERS 9-19-78
PROBLEM NO 23 ENGLISH UNITS

PRELIMINARY FOR DESIGN

INPUT

CONDENSER ITEM 102 325 IN ID 348 IN LG 278-1/4 IN TH
HORIZONTAL W/SMALL TUBE BUNDLE & THIN WALLS

UNITS	
LENGTH	INCH
TEMPERATURE	DEGREE F
PRESSURE	PSI
STRESS	PSI
MASS	LB
DENSITY	LB/CUIN
OPTIONS	
TUBESHEETS	SYMMETRIC
EXCHANGER	HORIZONTAL
TEMA	REQUESTED
TUBES	ROLLED
EXPANSION JOINT	NO
MT OR PRES	PRESSURE DROP

PROJECT 5304-100 FIXED TUBESHEET EXCHANGER 9-19-78
PROBLEM NO. 25 ENGLISH UNITS

PRELIMINARY FOR DESIGN

TUBE DATA	
OD	0.98165
THICKNESS	0.02652
LENGTH	348.00000
UNSUPPORTED LENGTH	
BAFFLE TO BAFFLE	58.00000
TUBESHEET TO BAFFLE	58.00000
LAYOUT ANGLE	60.00000
PITCH	1.25000
NUMBER OF TUBES	43883
OPERATING PRESSURE	4.21800
HYDROSTATIC TEST PRESSURE	25.88900
MAXIMUM TEMPERATURE	76.30000
AVERAGE TEMPERATURE	70.90000
YIELD STRENGTH AT	
MAX TUBE TEMPERATURE	40000.00000
SHELL TEMPERATURE	40000.00000
ATMOSPHERIC	40000.00000
INSIDE CORROSION ALLOWANCE	0.00000
OUTSIDE CORROSION ALLOWANCE	0.00000
POISSONS RATIO	0.34000
ELASTIC MODULUS AT	
MAX TUBE TEMPERATURE	1.62837E+07
AVERAGE TEMPERATURE	1.63834E+07
SHELL TEMPERATURE	1.63982E+07
ATMOSPHERIC	1.64000E+07
ALLOWABLE STRESS AT	
MAX TUBE TEMPERATURE	12500.00000
SHELL TEMPERATURE	12500.00000
ATMOSPHERIC	12500.00000
EXPANSION COEFFICIENT	4.80000E-06
BUNDLE WEIGHT OR PRESSURE DROP	-11.73000

PRELIMINARY FOR DESIGN

PROJECT 5304-100 FIXED TUBESHEET EXCHANGERS 9-19-78
PROBLEM NO 23 ENGLISH UNITS

SHELL DATA		
ID	325.00000	
THICKNESS	1.50000	
OPERATING PRESSURE	86.30000	
HYDROSTATIC TEST PRESSURE	129.50000	
AVERAGE METAL TEMPERATURE	65.00000	
YIELD STRENGTH AT OPERATING	32000.00000	
YIELD STRENGTH AT ATMOSPHERIC	32000.00000	
ALLOWABLE STRESS AT OPERATING	15000.00000	
ALLOWABLE STRESS AT ATMOSPHERIC	15000.00000	
ELASTIC MODULUS AT OPERATING	2.90000E+07	
ELASTIC MODULUS AT ATMOSPHERIC	2.90000E+07	
CORROSION ALLOWANCE	0.50000	
EXPANSION COEFFICIENT	6.13000E-06	
DENSITY OF FLUID	0.00030	
POISSONS RATIO	0.30000	
AMBIENT TEMPERATURE	70.00000	
TUBESHEETS	1	2
THICKNESS	4.31250	4.31250
FLEXURAL EFFICIENCY	0.00000	0.00000
EXPANSION COEFFICIENT	6.13000E-06	6.13000E-06
TEMPERATURE DROP	22.20000	22.20000
TUBE IN TUBESHEET OD	1.00000	1.00000
TUBE IN TUBESHEET THICKNESS	0.02600	0.02600
CORROSION ALLOWANCE TUBESIDE	0.00000	0.00000
CORROSION ALLOWANCE SHELLSIDE	0.00000	0.00000
TUBE BUNDLE OD	244.25000	
ELASTIC MODULUS AT OPERATING	2.90000E+07	2.90000E+07
ELASTIC MODULUS AT ATMOSPHERIC	2.90000E+07	2.90000E+07
TEMPERATURE		
TUBESIDE	40.00000	40.00000
SHELLSIDE	50.00000	50.00000
AVERAGE	45.00000	45.00000
YIELD STRENGTH AT MAX TEMP	32000.00000	32000.00000
YIELD STRENGTH AT ATMOSPHERIC	32000.00000	32000.00000
ALLOWABLE STRESS AT MAX TEMP	15000.00000	15000.00000
ALLOWABLE STRESS AT ATMOSPHERIC	15000.00000	15000.00000
POISSONS RATIO	0.30000	0.30000
ANNULUS RING		
EXPANSION COEFFICIENT	6.13000E-06	6.13000E-06
AVERAGE TEMPERATURE	45.00000	45.00000
TEMPERATURE DROP	10.00000	10.00000
ELASTIC MODULUS	2.90000E+07	2.90000E+07

PRELIMINARY FOR DESIGN

PROJECT 5304-100 FIXED TUBESHEET EXCHANGERS 9-19-78
PROBLEM NO 23 ENGLISH UNITS

OUTPUT

		NORMAL OPERATING	HYDROSTATIC TEST SHELL	HYDROSTATIC TEST TUBES
PRESSURE	PSI			
TUBESIDE		4,218	0.000	25,888
SHELLSIDE		86,300	129,500	0.000
METAL TEMPERATURE	DEGREE F			
TUBE		70,900	70,000	70,000
SHELL		65,000	70,000	70,000
UNSTAYED THICKNESS	INCH			
TUBESHEET 1		15,455	15,410	6,890
TUBESHEET 2		15,455	15,410	6,890
SECONDARY STRESSES	PSI			
TUBES				
CALCULATED		1698,155	1484,822	-704,567
ALLOWABLE		18750,000	28125,000	-4818,175
TUBESHEETS				
1 BENDING CALCULATED		9852,821	14445,168	3849,170
ALLOWABLE		32000,000	48000,000	48000,000
SHEAR CALCULATED		1107,062	1051,970	-420,256
ALLOWABLE		16000,000	24000,000	24000,000
2 BENDING CALCULATED		9852,821	14445,168	3849,170
ALLOWABLE		32000,000	48000,000	48000,000
SHEAR CALCULATED		1107,062	1051,970	-420,256
ALLOWABLE		16000,000	24000,000	24000,000
RINGS				
1 BENDING CALCULATED		4590,054	13923,787	554,114
ALLOWABLE		32000,000	48000,000	48000,000
2 BENDING CALCULATED		4590,054	13923,787	554,114
ALLOWABLE		32000,000	48000,000	48000,000
SHELL				
CALCULATED		82426,586*	115262,271*	-4516,135
ALLOWABLE		64000,000	96000,000	96000,000
PRIMARY STRESSES	PSI			
TUBES				
CALCULATED		2134,208	3367,119	673,138
ALLOWABLE		12500,000	18750,000	18750,000
SHELL				
CALCULATED		14066,900	14029,167	0,000
ALLOWABLE		15000,000	22500,000	22500,000

* REQUIRES LOCAL REINFORCEMENT. LOCAL REINFORCEMENT WILL BE PROVIDED IN THE DETAILED DESIGN.

PROJECT 5304-100 FIXED TUBESHEET EXCHANGERS 9-19-78
PROBLEM NO 23 ENGLISH UNITS

OUTPUT

		LOSS OF TUBESIDE POWER	LOSS OF SHELLSIDE POWER	BUNDLE AND SOLID WEIGHT
PRESSURE	PSI			
TUBESIDE		0.000	4.218	0.000
SHELLSIDE		86.300	0.000	0.000
METAL TEMPERATURE	DEGREE F			
TUBE		70.900	76.300	70.000
SHELL		70.900	65.000	70.000
UNSTAYED THICKNESS	INCH			
TUBESHEET 1		15.455	3.417	0.000
TUBESHEET 2		15.455	3.417	0.000
SECONDARY STRESSES	PSI			
TUBES				
CALCULATED		1722.529	-82.378	0.000
ALLOWABLE		18750.000	-3192.064	18750.000
TUBESHEETS				
1 BENDING CALCULATED		12259.500	2377.864	0.000
ALLOWABLE		32000.000	32000.000	22500.000
SHEAR CALCULATED		1142.973	-43.851	0.000
ALLOWABLE		16000.000	16000.000	11250.000
2 BENDING CALCULATED		12259.500	2377.864	0.000
ALLOWABLE		32000.000	32000.000	22500.000
SHEAR CALCULATED		1142.973	-43.851	0.000
ALLOWABLE		16000.000	16000.000	11250.000
RINGS				
1 BENDING CALCULATED		4486.235	254.216	0.000
ALLOWABLE		32000.000	32000.000	22500.000
2 BENDING CALCULATED		4486.235	254.216	0.000
ALLOWABLE		32000.000	32000.000	22500.000
SHELL				
CALCULATED		80308.960*	-2617.892	0.000
ALLOWABLE		64000.000	64000.000	64000.000
PRIMARY STRESSES	PSI			
TUBES				
CALCULATED		2283.979	73.848	0.000
ALLOWABLE		12500.000	12500.000	12500.000
SHELL				
CALCULATED		14066.900	0.000	0.000
ALLOWABLE		15000.000	15000.000	15000.000

* REQUIRES LOCAL REINFORCEMENT. LOCAL REINFORCEMENT WILL BE PROVIDED IN THE DETAILED DESIGN.

CH15

PROJECT 5304-100 FIXED TUBESHEET EXCHANGERS 9-16-78
PROBLEM NO 24 ENGLISH UNITS

PRELIMINARY FOR DESIGN

INPUT

CONDENSER ITEM 102 325 IN ID 348 IN LG 278-1/4 IN TB
VERTICALAL W/SMALL TUBE BUNDLE & THIN WALLS

UNITS	
LENGTH	INCH
TEMPERATURE	DEGREE F
PRESSURE	PSI
STRESS	PSI
MASS	LB
DENSITY	LB/CUIN
OPTIONS	
TUBESHEETS	SYMMETRIC
EXCHANGER	VERTICAL
TEMA	REQUESTED
TUBES	ROLLED
EXPANSION JOINT	NO
WT OR PRES	BUNDLE WEIGHT

PRELIMINARY FOR DESIGN

PROJECT 5304-100 FIXED TUBESHEET EXCHANGERS 9-16-78
PROBLEM NO 24 ENGLISH UNITS

TUBE DATA	
OD	0.98165
THICKNESS	0.02652
LENGTH	348.00000
UNSUPPORTED LENGTH	
BAFFLE TO BAFFLE	58.00000
TUBESHEET TO BAFFLE	58.00000
LAYOUT ANGLE	60.00000
PITCH	1.25000
NUMBER OF TUBES	43883
OPERATING PRESSURE	4.21800
HYDROSTATIC TEST PRESSURE	25.88900
MAXIMUM TEMPERATURE	76.30000
AVERAGE TEMPERATURE	70.90000
YIELD STRENGTH AT	
MAX TUBE TEMPERATURE	40000.00000
SHELL TEMPERATURE	40000.00000
ATMOSPHERIC	40000.00000
INSIDE CORROSION ALLOWANCE	0.00000
OUTSIDE CORROSION ALLOWANCE	0.00000
POISSONS RATIO	0.34000
ELASTIC MODULUS AT	
MAX TUBE TEMPERATURE	1.62837E+07
AVERAGE TEMPERATURE	1.63834E+07
SHELL TEMPERATURE	1.63982E+07
ATMOSPHERIC	1.64000E+07
ALLOWABLE STRESS AT	
MAX TUBE TEMPERATURE	12500.00000
SHELL TEMPERATURE	12500.00000
ATMOSPHERIC	12500.00000
EXPANSION COEFFICIENT	4.80000E-06
BUNDLE WEIGHT OR PRESSURE DROP	104719.00000

PRELIMINARY FOR DESIGN

PROJECT 5304-100 FIXED TUBESHEET EXCHANGERS 9-16-76
PROBLEM NO 24 ENGLISH UNITS

SHELL DATA		
ID	325.00000	
THICKNESS	1.50000	
OPERATING PRESSURE	86.30000	
HYDROSTATIC TEST PRESSURE	129.50000	
AVERAGE METAL TEMPERATURE	65.00000	
YIELD STRENGTH AT OPERATING	32000.00000	
YIELD STRENGTH AT ATMOSPHERIC	32000.00000	
ALLOWABLE STRESS AT OPERATING	15000.00000	
ALLOWABLE STRESS AT ATMOSPHERIC	15000.00000	
ELASTIC MODULUS AT OPERATING	2.90000E+07	
ELASTIC MODULUS AT ATMOSPHERIC	2.90000E+07	
CORROSION ALLOWANCE	0.50000	
EXPANSION COEFFICIENT	6.13000E-06	
DENSITY OF FLUID	0.00030	
POISSONS RATIO	0.30000	
AMBIENT TEMPERATURE	70.00000	
TUBESHEETS	1	2
THICKNESS	4.31250	4.31250
FLEXURAL EFFICIENCY	0.00000	0.00000
EXPANSION COEFFICIENT	6.13000E-06	6.13000E-06
TEMPERATURE DROP	22.20000	22.20000
TUBE IN TUBESHEET OD	1.00000	1.00000
TUBE IN TUBESHEET THICKNESS	0.02600	0.02600
CORROSION ALLOWANCE TUBESIDE	0.00000	0.00000
CORROSION ALLOWANCE SHELLSIDE	0.00000	0.00000
TUBE BUNDLE OD	244.25000	
ELASTIC MODULUS AT OPERATING	2.90000E+07	2.90000E+07
ELASTIC MODULUS AT ATMOSPHERIC	2.90000E+07	2.90000E+07
TEMPERATURE		
TUBESIDE	40.00000	40.00000
SHELLSIDE	50.00000	50.00000
AVERAGE	45.00000	45.00000
YIELD STRENGTH AT MAX TEMP	32000.00000	32000.00000
YIELD STRENGTH AT ATMOSPHERIC	32000.00000	32000.00000
ALLOWABLE STRESS AT MAX TEMP	15000.00000	15000.00000
ALLOWABLE STRESS AT ATMOSPHERIC	15000.00000	15000.00000
POISSONS RATIO	0.30000	0.30000
ANNULUS RING		
EXPANSION COEFFICIENT	6.13000E-06	6.13000E-06
AVERAGE TEMPERATURE	45.00000	45.00000
TEMPERATURE DROP	10.00000	10.00000
ELASTIC MODULUS	2.90000E+07	2.90000E+07

PRELIMINARY FOR DESIGN

PROJECT 5304-100 FIXED TUBESHEET EXCHANGERS 9-16-78
PROBLEM NO 24 ENGLISH UNITS

OUTPUT

		NORMAL OPERATING	HYDROSTATIC TEST SHELL	HYDROSTATIC TEST TUBE
PRESSURE	PSI			
TUBESIDE		4.218	0.000	25.889
SHELLSIDE		86.300	129.500	0.000
METAL TEMPERATURE	DEGREE F			
TUBE		70.900	70.000	70.000
SHELL		65.000	70.000	70.000
UNSTAYED THICKNESS	INCH			
TUBESHEET 1		15.455	15.410	6.890
TUBESHEET 2		15.455	15.410	6.890
SECONDARY STRESSES	PSI			
TUBES				
CALCULATED		1692.765	1453.060	-732.324
ALLOWABLE		18750.000	28125.000	-4818.175
TUBESHEETS				
1 BENDING CALCULATED		11507.925	28960.966	17698.533
ALLOWABLE		32000.000	48000.000	48000.000
SHEAR CALCULATED		1174.531	1499.362	386.323
ALLOWABLE		16000.000	24000.000	24000.000
2 BENDING CALCULATED		8227.209	18195.381	18269.274
ALLOWABLE		32000.000	48000.000	48000.000
SHEAR CALCULATED		1037.056	584.935	-887.291
ALLOWABLE		16000.000	24000.000	24000.000
RINGS				
1 BENDING CALCULATED		3831.995	7342.895	7135.006
ALLOWABLE		32000.000	48000.000	48000.000
2 BENDING CALCULATED		5368.043	20688.291	6320.450
ALLOWABLE		32000.000	48000.000	48000.000
SHELL				
CALCULATED		96842.695*	170941.580*	-59144.872
ALLOWABLE		64000.000	96000.000	96000.000
PRIMARY STRESSES	PSI			
TUBES				
CALCULATED		2134.208	3367.119	673.138
ALLOWABLE		12500.000	18750.000	18750.000
SHELL				
CALCULATED		14066.900	14029.167	0.000
ALLOWABLE		15000.000	22500.000	22500.000

* REQUIRES LOCAL REINFORCEMENT. LOCAL REINFORCEMENT WILL BE PROVIDED IN THE DETAILED DESIGN.

PRELIMINARY FOR DESIGN

PROJECT 5304-100 FIXED TUBESHEET EXCHANGERS 9-16-78
PROBLEM NO. 24 ENGLISH UNITS

OUTPUT

		V_4 LOSS OF TUBESIDE POWER	V_5 LOSS OF SHELLSIDE POWER	V_6 HANDLE FLUID WEIGHT
PRESSURE	PSI			
TUBESIDE		0.000	4.218	0.000
SHELLSIDE		86.300	0.000	0.000
METAL TEMPERATURE	DEGREE F			
TUBE		70.900	76.300	70.000
SHELL		70.900	65.000	70.000
UNSTAYED THICKNESS	INCH			
TUBESHEET 1		15.455	3.417	0.000
TUBESHEET 2		15.455	3.417	0.000
SECONDARY STRESSES	PSI			
TUBES				
CALCULATED		1717.139	-86.487	-5.393
ALLOWABLE		18750.000	-3192.064	-3212.116
TUBESHEETS				
1 BENDING CALCULATED		13914.604	5128.956	3177.412
ALLOWABLE		32000.000	32000.000	22500.000
SHEAR CALCULATED		1210.443	57.592	67.469
ALLOWABLE		16000.000	16000.000	11250.000
2 BENDING CALCULATED		10633.889	4003.524	-3177.000
ALLOWABLE		32000.000	32000.000	22500.000
SHEAR CALCULATED		1072.967	-113.856	-70.006
ALLOWABLE		16000.000	16000.000	11250.000
RINGS				
1 BENDING CALCULATED		3728.176	721.774	758.059
ALLOWABLE		32000.000	32000.000	22500.000
2 BENDING CALCULATED		5264.224	1032.204	-777.989
ALLOWABLE		32000.000	32000.000	22500.000
SHELL				
CALCULATED		94785.069*	-17339.316	-14521.449
ALLOWABLE		64000.000	64000.000	64000.000
PRIMARY STRESSES	PSI			
TUBES				
CALCULATED		2243.079	73.848	0.000
ALLOWABLE		12500.000	12500.000	12500.000
SHELL				
CALCULATED		14066.900	0.000	0.000
ALLOWABLE		15000.000	15000.000	15000.000

* REQUIRES LOCAL REINFORCEMENT. LOCAL REINFORCEMENT WILL BE PROVIDED IN THE DETAILED DESIGN.

Customer	Pages	Page 46
Subject	By VRM	
Project	Date 9/18/8	

PRELIMINARY FOR DESIGN

Condenser

Analysis of FTS Computer run Results
(Resolution into FORCES)

TUBESHEETS

TS dia = 244.25"

TS thk = 4.3125"

TS shear area = 3309.1273 in²

		[TS 1]	[TS2]
1. Consider bundle & shell fluid submerged in sea water (column V6)	stress	+67.469	-70.006
	load	223263.54 ↓	231658.8 ↓
2. Consider wt of seawater displaced (not on computer run)	stress	(+67.618592)	(-67.618592)
	load	223758.53 ↓	223758.53 ↓
3. Consider shellside pressure @ 86.3psi (column H4)	stress	+1142.973	+1142.973
	load	3782243.7 ↓	3782243.7 ↑
4. Consider tubeside pr. @ 4.218psi (column H5)	stress	-43.851	-43.851
	load	145108.56 ↑	145108.56 ↓
5. Consider wt of shellside fluid columns (V4-V6-H4)	stress	+.001	0
	load	3.309 ↓	0
6. Consider wt & ΔP of tubeside fluid columns (V5-V6+H5)	stress	+33.974	+.001
	load	112424.3 ↓	3.309 ↑
7. Consider thermal effects columns (V1+V6-V4-V5)	stress	-26.035	+7.333
	load	86153.142 ↑	26271.165 ↑

PRELIMINARY FOR DESIGN

Condenser

I Tubesheet 1 — Shear force F_t = 3,88[illegible]73.1 lb_f

operating
submerged

σ_p max = 11507.925 psi
σ_t = 86.3 psi
σ_λ max = −86.3 psi
$\therefore \sigma_p - \sigma_\lambda$ = 11594.225 psi

II Tubesheet 2 — F_t = 3 431 750.8

open
submerged

σ_p max = 8227.209 psi
σ_t = 86.3
σ_λ max = −86.3
$\sigma_p - \sigma_\lambda$ = 8313.509

III Shell — σ_θ = +14000.9 psi

A_s = 1027.3007 in^2
Z_s = 83726.575 in^3

(from computer approx) σ_λ' = ±96 842.695
(add effects of buoyancy) σ_λ'' = −214.22817
(add effects of eccentr.) σ_λ''' = ± 696.78907

σ_λ = ±97 325.256
$\sigma_\lambda - \sigma_\theta$ = 111392.15 psi

IV Tubesheet 1 — F_t = 447 022.07 lb_f

depressurized
submerged

σ_p max = 3177.412 psi
σ_t = 0
σ_λ = 0
$\therefore \sigma_p - \sigma_\lambda$ = 3177.412 psi

PRELIMINARY FOR DESIGN

V Tubesheet 2

F_t = 455[illegible]07.[illegible] lb$_f$

$\sigma_{\rho\ max}$ = -3190.[illegible]

$\sigma_\theta \cong 0$

$\sigma_{\lambda\ max}$ = -12.993 psi

$\sigma_\rho - \sigma_\lambda$ = 3177.4 psi

VI Shell

σ_θ = -2113.7776 psi

σ'_λ = -14521.449

(due to buoyancy) σ''_λ = -214.22817

(due to eccentr.) σ'''_λ = ± 92.468781

σ_λ = -14643.208 psi

$\sigma_\theta - \sigma_\lambda$ = 12529.431 psi

	TS 1	TS 2	Shell
Stress Differences	11594.225	8313.589	111392.15
	3177.412	3177.412	12529.4
Range	8416.813	5136.097	98862.75
Alt. Stress Intensity	4208.4	2568.5	49431.4

Note: only shell is significant

N = 3000 cycles

Customer | Pages | Page 49

Subject | By

Project | Date

PRELIMINARY FOR DESIGN

Investigate axial shell stress attributed to tube bundle weight

CONDENSER

1. Submerged in sea water (v-6) stress -14521.449

2. Sea Water

$$\frac{67.6185}{67.469} \times -14521.449 = -14553.625$$

3. Total axial shell stress due to tube bundle wt -29075.074

4. Stress Range ($\pm .05g$) 2907.507

$S < 10\,000$ psi

$N \longrightarrow \infty$

∴ Alternating stress intensity due to sea state 6 vertical water surface acceleration is trivial.

Tubesheet Thickness

Bending (TEMA R-7.122)

where G = 316 mch

$$\frac{t_t}{ID_s} = \frac{4.8125}{316.000} = .01522$$

$$F = 1.00$$

$$T = \frac{FG}{2}\sqrt{\frac{P}{S}}$$

where P is the effective shellside, tubeside or differential design pressure

In order to establish tubesheet thickness requirements, actual tube bundle dimensions should be used with varying shell diameter accounting for tubesheet eccentricity

orig prob	problem	A R Width	Shell dia
22	31	6.375	287
22	32	34.375	343.00
24	41	6.375	291
24	42	40.375	359

PRELIMINARY FOR DESIGN

PROJECT 5304-100 FIXED TUBESHEET EXCHANGERS 9-22-78
PROBLEM NO 31 ENGLISH UNITS

INPUT

EVAPORATOR ITEM 101 315 IN ID 348 IN LG 274-1/4 IN TD
VERTICAL W/ACT TUBE BUNDLE & THIN SM DIA WALLS

UNITS	
LENGTH	INCH
TEMPERATURE	DEGREE F
PRESSURE	PSI
STRESS	PSI
MASS	LB
DENSITY	LB/CUIN
OPTIONS	
TUBESHEETS	SYMMETRIC
EXCHANGER	VERTICAL
TEMA	REQUESTED
TUBES	ROLLED
EXPANSION JOINT	NO
WT OR PRES	BUNDLE WEIGHT

PROJECT 5304-100 FIXED TUBESHEET EXCHANGERS 9-22-78
PROBLEM NO 31 ENGLISH UNITS

PRELIMINARY FOR DESIGN

TUBE DATA	
OD	0.98597
THICKNESS	0.05147
LENGTH	348.00000
UNSUPPORTED LENGTH	
BAFFLE TO BAFFLE	58.00000
TUBESHEET TO BAFFLE	58.00000
LAYOUT ANGLE	60.00000
PITCH	1.25000
NUMBER OF TUBES	42667
OPERATING PRESSURE	4.21800
HYDROSTATIC TEST PRESSURE	25.88900
MAXIMUM TEMPERATURE	76.30000
AVERAGE TEMPERATURE	70.90000
YIELD STRENGTH AT	
MAX TUBE TEMPERATURE	40000.00000
SHELL TEMPERATURE	40000.00000
ATMOSPHERIC	40000.00000
INSIDE CORROSION ALLOWANCE	0.00000
OUTSIDE CORROSION ALLOWANCE	0.00000
POISSONS RATIO	0.34000
ELASTIC MODULUS AT	
MAX TUBE TEMPERATURE	1.62837E+07
AVERAGE TEMPERATURE	1.63834E+07
SHELL TEMPERATURE	1.63982E+07
ATMOSPHERIC	1.64000E+07
ALLOWABLE STRESS AT	
MAX TUBE TEMPERATURE	12500.00000
SHELL TEMPERATURE	12500.00000
ATMOSPHERIC	12500.00000
EXPANSION COEFFICIENT	8.80000E-06
BUNDLE WEIGHT OR PRESSURE DROP	165872.00000

PRELIMINARY FOR DESIGN

PROJECT 5300-100 FIXED TUBESHEET EXCHANGERS 9-22-78
PROBLEM NO 31 ENGLISH UNITS

SHELL DATA		
ID	287.00000	
THICKNESS	2.00000	
OPERATING PRESSURE	136.00000	
HYDROSTATIC TEST PRESSURE	204.00000	
AVERAGE METAL TEMPERATURE	71.95000	
YIELD STRENGTH AT OPERATING	32000.00000	
YIELD STRENGTH AT ATMOSPHERIC	32000.00000	
ALLOWABLE STRESS AT OPERATING	15000.00000	
ALLOWABLE STRESS AT ATMOSPHERIC	15000.00000	
ELASTIC MODULUS AT OPERATING	2.90000E+07	
ELASTIC MODULUS AT ATMOSPHERIC	2.90000E+07	
CORROSION ALLOWANCE	0.50000	
EXPANSION COEFFICIENT	6.13000E-06	
DENSITY OF FLUID	0.00025	
POISSONS ...TIO	0.30000	
AMBIENT TEMPERATURE	70.00000	
TUBESHEETS	1	2
THICKNESS	4.81250	4.81250
FLEXURAL EFFICIENCY	0.00000	0.00000
EXPANSION COEFFICIENT	6.13000E-06	6.13000E-06
TEMPERATURE DROP	22.20000	22.20000
TUBE IN TUBESHEET OD	1.00000	1.00000
TUBE IN TUBESHEET THICKNESS	0.03100	0.03100
CORROSION ALLOWANCE TUBESIDE	0.00000	0.00000
CORROSION ALLOWANCE SHELLSIDE	0.00000	0.00000
TUBE BUNDLE OD	245.25000	
ELASTIC MODULUS AT OPERATING	2.90000E+07	2.90000E+07
ELASTIC MODULUS AT ATMOSPHERIC	2.90000E+07	2.90000E+07
TEMPERATURE		
TUBESIDE	80.00000	80.00000
SHELLSIDE	57.80000	57.80000
AVERAGE	68.90000	68.90000
YIELD STRENGTH AT MAX TEMP	32000.00000	32000.00000
YIELD STRENGTH AT ATMOSPHERIC	32000.00000	32000.00000
ALLOWABLE STRESS AT MAX TEMP	15000.00000	15000.00000
ALLOWABLE STRESS AT ATMOSPHERIC	15000.00000	15000.00000
POISSONS RATIO	0.30000	0.30000
ANNULUS RING		
EXPANSION COEFFICIENT	6.13000E-06	6.13000E-06
AVERAGE TEMPERATURE	79.60000	79.60000
TEMPERATURE DROP	22.20000	22.20000
ELASTIC MODULUS	2.90000E+07	2.90000E+07

PROJECT 5304-100 FIXED TUBESHEET EXCHANGERS 9-22-78
PROBLEM NO - 31 - ENGLISH UNITS

THICKNESSES OF TUBESHEETS REQUIRED BY TEMA (CORRODED) WITH

	FROM BENDING	FROM SHEAR
RESULT 1	4.9715	0.9860 **
RESULT 2	4.9715	0.9860 **

RESULT 1 THICKNESSES ARE REQUIRED FOR BOTH TUBESHEETS OF THE EXCHANGER CONSIDERING THAT THEY BOTH HAVE THE SAME MATERIAL PROPERTIES AND TEMPERATURES AS THOSE SPECIFIED ON INPUT FOR TUBESHEET 1

RESULT 2 THICKNESSES ARE REQUIRED FOR BOTH TUBESHEETS OF THE EXCHANGER CONSIDERING THAT THEY BOTH HAVE THE SAME MATERIAL PROPERTIES AND TEMPERATURES AS THOSE SPECIFIED ON INPUT FOR TUBESHEET 2

** THICKNESS REQUIRED BY TEMA G=7.121

NOTE: NOT CONTROLLING SEE PROB 32.

PRELIMINARY FOR DESIGN

PROJECT 5304-100 FIXED TUBESHEET EXCHANGERS 9-22-78
PROBLEM NO 52 ENGLISH UNITS

INPUT

EVAPORATOR ITEM 101 315 IN ID 348 IN LG 274-1/4 IN TO
VERTICAL W/ACT TUBE BUNDLE & THIN LG DIA WALLS

UNITS	
LENGTH	INCH
TEMPERATURE	DEGREE F
PRESSURE	PSI
STRESS	PSI
MASS	LB
DENSITY	LB/CUIN
OPTIONS	
TUBESHEETS	SYMMETRIC
EXCHANGER	VERTICAL
TEMA	REQUESTED
TUBES	ROLLED
EXPANSION JOINT	NO
WT OR PRES	BUNDLE WEIGHT

PROJECT 5304-100 FIXED TUBESHEET EXCHANGERS 9-22-78
PROBLEM NO 32 ENGLISH UNITS

PRELIMINARY FOR DESIGN

TUBE DATA	
OD	0.98597
THICKNESS	0.03147
LENGTH	348.00000
UNSUPPORTED LENGTH	
BAFFLE TO BAFFLE	58.00000
TUBESHEET TO BAFFLE	58.00000
LAYOUT ANGLE	60.00000
PITCH	1.25000
NUMBER OF TUBES	42667
OPERATING PRESSURE	4.21800
HYDROSTATIC TEST PRESSURE	25.88900
MAXIMUM TEMPERATURE	76.30000
AVERAGE TEMPERATURE	70.90000
YIELD STRENGTH AT	
MAX TUBE TEMPERATURE	40000.00000
SHELL TEMPERATURE	40000.00000
ATMOSPHERIC	40000.00000
INSIDE CORROSION ALLOWANCE	0.00000
OUTSIDE CORROSION ALLOWANCE	0.00000
POISSONS RATIO	0.34000
ELASTIC MODULUS AT	
MAX TUBE TEMPERATURE	1.62837E+07
AVERAGE TEMPERATURE	1.63834E+07
SHELL TEMPERATURE	1.63982E+07
ATMOSPHERIC	1.64000E+07
ALLOWABLE STRESS AT	
MAX TUBE TEMPERATURE	12500.00000
SHELL TEMPERATURE	12500.00000
ATMOSPHERIC	12500.00000
EXPANSION COEFFICIENT	4.80000E-06
BUNDLE WEIGHT OR PRESSURE DROP	165872.00000

PRELIMINARY FOR DESIGN

PROJECT 5304-100 FIXED TUBESHEET EXCHANGERS 9-22-78
PROBLEM NO 32 ENGLISH UNITS

SHELL DATA		
ID	343.00000	
THICKNESS	2.00000	
OPERATING PRESSURE	136.00000	
HYDROSTATIC TEST PRESSURE	204.00000	
AVERAGE METAL TEMPERATURE	71.95000	
YIELD STRENGTH AT OPERATING	32000.00000	
YIELD STRENGTH AT ATMOSPHERIC	32000.00000	
ALLOWABLE STRESS AT OPERATING	15000.00000	
ALLOWABLE STRESS AT ATMOSPHERIC	15000.00000	
ELASTIC MODULUS AT OPERATING	2.90000E+07	
ELASTIC MODULUS AT ATMOSPHERIC	2.90000E+07	
CORROSION ALLOWANCE	0.50000	
EXPANSION COEFFICIENT	6.13000E-06	
DENSITY OF FLUID	0.00025	
POISSONS RATIO	0.30000	
AMBIENT TEMPERATURE	70.00000	
TUBESHEETS	1	2
THICKNESS	4.81250	4.81250
FLEXURAL EFFICIENCY	0.00000	0.00000
EXPANSION COEFFICIENT	6.13000E-06	6.13000E-06
TEMPERATURE DROP	22.20000	22.20000
TUBE IN TUBESHEET OD	1.00000	1.00000
TUBE IN TUBESHEET THICKNESS	0.03100	0.03100
CORROSION ALLOWANCE TUBESIDE	0.00000	0.00000
CORROSION ALLOWANCE SHELLSIDE	0.00000	0.00000
TUBE BUNDLE OD	246.25000	
ELASTIC MODULUS AT OPERATING	2.90000E+07	2.90000E+07
ELASTIC MODULUS AT ATMOSPHERIC	2.90000E+07	2.90000E+07
TEMPERATURE		
TUBESIDE	80.00000	80.00000
SHELLSIDE	57.80000	57.80000
AVERAGE	68.90000	68.90000
YIELD STRENGTH AT MAX TEMP	32000.00000	32000.00000
YIELD STRENGTH AT ATMOSPHERIC	32000.00000	32000.00000
ALLOWABLE STRESS AT MAX TEMP	15000.00000	15000.00000
ALLOWABLE STRESS AT ATMOSPHERIC	15000.00000	15000.00000
POISSONS RATIO	0.30000	0.30000
ANNULUS RING		
EXPANSION COEFFICIENT	6.13000E-06	6.13000E-06
AVERAGE TEMPERATURE	79.60000	79.60000
TEMPERATURE DROP	22.20000	22.20000
ELASTIC MODULUS	2.90000E+07	2.90000E+07

PRELIMINARY FOR DESIGN

PROJECT 5304-100 FIXED TUBESHEET EXCHANGERS 9-22-78
PROBLEM NO 32 ENGLISH UNITS

THICKNESSES OF TUBESHEETS REQUIRED BY TEMA (CORRODED) INCH

	FROM BENDING	FROM SHEAR
RESULT 1	6.0084	0.9860 **
RESULT 2	6.0084	0.9860 **

RESULT 1 THICKNESSES ARE REQUIRED FOR BOTH TUBESHEETS OF THE EXCHANGER CONSIDERING THAT THEY BOTH HAVE THE SAME MATERIAL PROPERTIES AND TEMPERATURES AS THOSE SPECIFIED ON INPUT FOR TUBESHEET 1

RESULT 2 THICKNESSES ARE REQUIRED FOR BOTH TUBESHEETS OF THE EXCHANGER CONSIDERING THAT THEY BOTH HAVE THE SAME MATERIAL PROPERTIES AND TEMPERATURES AS THOSE SPECIFIED ON INPUT FOR TUBESHEET 2

** THICKNESS REQUIRED BY TEMA R-7.121

NOTE: CONTROLLING FOR THE EVAPORATOR. ANTICIPATED TUBESHEET THICKNESS REQUIREMENT FOR FINAL DESIGN IS LESS THAN 4.8125 IN. A VENDORS QUOTATION BASED ON TEMA R TUBESHEET THICKNESS IS THEREFORE CONSERVATIVE.

PRELIMINARY FOR DESIGN

PROJECT 5304-100 FIXED-TUBESHEET EXCHANGERS 9-22-78
PROBLEM NO 41 ENGLISH UNITS

INPUT

CONDENSER ITEM 102 325 IN ID 348 IN LG 278-1/4 IN TH
VERTICAL W ACT TUBE BUNDLE & THIN SM DIA WALLS

UNITS	
LENGTH	INCH
TEMPERATURE	DEGREE F
PRESSURE	PSI
STRESS	PSI
MASS	LB
DENSITY	LB/CUIN
OPTIONS	
TUBESHEETS	SYMMETRIC
EXCHANGER	VERTICAL
TEMA	REQUESTED
TUBES	ROLLED
EXPANSION JOINT	NO
AT OR PRES	BUNDLE WEIGHT

PRELIMINARY FOR DESIGN

PROJECT 5304-100 FIXED TUBESHEET EXCHANGERS 9-22-78
PROBLEM NO 41 ENGLISH UNITS

TUBE DATA	
OD	0.98165
THICKNESS	0.02652
LENGTH	348.00000
UNSUPPORTED LENGTH	
BAFFLE TO BAFFLE	58.00000
TUBESHEET TO BAFFLE	58.00000
LAYOUT ANGLE	60.00000
PITCH	1.25000
NUMBER OF TUBES	43883
OPERATING PRESSURE	4.21800
HYDROSTATIC TEST PRESSURE	25.88900
MAXIMUM TEMPERATURE	76.30000
AVERAGE TEMPERATURE	70.90000
YIELD STRENGTH AT	
MAX TUBE TEMPERATURE	40000.00000
SHELL TEMPERATURE	40000.00000
ATMOSPHERIC	40000.00000
INSIDE CORROSION ALLOWANCE	0.00000
OUTSIDE CORROSION ALLOWANCE	0.00000
POISSONS RATIO	0.34000
ELASTIC MODULUS AT	
MAX TUBE TEMPERATURE	1.62837E+07
AVERAGE TEMPERATURE	1.63834E+07
SHELL TEMPERATURE	1.63962E+07
ATMOSPHERIC	1.64000E+07
ALLOWABLE STRESS AT	
MAX TUBE TEMPERATURE	12500.00000
SHELL TEMPERATURE	12500.00000
ATMOSPHERIC	12500.00000
EXPANSION COEFFICIENT	4.80000E-06
BUNDLE WEIGHT OR PRESSURE DROP	104719.00000

PRELIMINARY FOR DESIGN

PROJECT 5304-100 FIXED TUBESHEET EXCHANGERS 9-22-78
PROBLEM NO 41 ENGLISH UNITS

SHELL DATA		
ID	291.00000	
THICKNESS	1.50000	
OPERATING PRESSURE	86.30000	
HYDROSTATIC TEST PRESSURE	129.50000	
AVERAGE METAL TEMPERATURE	65.00000	
YIELD STRENGTH AT OPERATING	32000.00000	
YIELD STRENGTH AT ATMOSPHERIC	32000.00000	
ALLOWABLE STRESS AT OPERATING	15000.00000	
ALLOWABLE STRESS AT ATMOSPHERIC	15000.00000	
ELASTIC MODULUS AT OPERATING	2.90000E+07	
ELASTIC MODULUS AT ATMOSPHERIC	2.90000E+07	
CORROSION ALLOWANCE	0.50000	
EXPANSION COEFFICIENT	6.13000E-06	
DENSITY OF FLUID	0.00030	
POISSONS RATIO	0.30000	
AMBIENT TEMPERATURE	70.00000	
TUBESHEETS	1	2
THICKNESS	4.31250	4.31250
FLEXURAL EFFICIENCY	0.00000	0.00000
EXPANSION COEFFICIENT	6.13000E-06	6.13000E-06
TEMPERATURE DROP	22.20000	22.20000
TUBE IN TUBESHEET OD	1.00000	1.00000
TUBE IN TUBESHEET THICKNESS	0.02600	0.02600
CORROSION ALLOWANCE TUBESIDE	0.00000	0.00000
CORROSION ALLOWANCE SHELLSIDE	0.00000	0.00000
TUBE BUNDLE OD	244.25000	
ELASTIC MODULUS AT OPERATING	2.90000E+07	2.90000E+07
ELASTIC MODULUS AT ATMOSPHERIC	2.90000E+07	2.90000E+07
TEMPERATURE		
TUBESIDE	40.00000	40.00000
SHELLSIDE	50.00000	50.00000
AVERAGE	45.00000	45.00000
YIELD STRENGTH AT MAX TEMP	32000.00000	32000.00000
YIELD STRENGTH AT ATMOSPHERIC	32000.00000	32000.00000
ALLOWABLE STRESS AT MAX TEMP	15000.00000	15000.00000
ALLOWABLE STRESS AT ATMOSPHERIC	15000.00000	15000.00000
POISSONS RATIO	0.30000	0.30000
ANNULUS RING		
EXPANSION COEFFICIENT	6.13000E-06	6.13000E-06
AVERAGE TEMPERATURE	45.00000	45.00000
TEMPERATURE DROP	10.00000	10.00000
ELASTIC MODULUS	2.90000E+07	2.90000E+07

PRELIMINARY FOR DESIGN

PROJECT 5304-100 FIXED TUBESHEET EXCHANGERS 9-22-78
PROBLEM NO 41 ENGLISH UNITS

THICKNESSES OF TUBESHEETS REQUIRED BY TEMA (CORRODED) IN.

	FROM BENDING	FROM SHEAR
RESULT 1	3.8347	0.9817 **
RESULT 2	3.8347	0.9817 **

RESULT 1 THICKNESSES ARE REQUIRED FOR BOTH TUBESHEETS OF THE EXCHANGER CONSIDERING THAT THEY BOTH HAVE THE SAME MATERIAL PROPERTIES AND TEMPERATURES AS THOSE SPECIFIED ON INPUT FOR TUBESHEET 1

RESULT 2 THICKNESSES ARE REQUIRED FOR BOTH TUBESHEETS OF THE EXCHANGER CONSIDERING THAT THEY BOTH HAVE THE SAME MATERIAL PROPERTIES AND TEMPERATURES AS THOSE SPECIFIED ON INPUT FOR TUBESHEET 2

**THICKNESS REQUIRED BY TEMA R=7.121

NOTE: NOT CONTROLLING. SEE PROB. 42.

PRELIMINARY FOR DESIGN

PROJECT 5304-100 FIXED TUBESHEET EXCHANGERS 9-22-78
PROBLEM NO 42 ENGLISH UNITS

INPUT

CONDENSER ITEM 102 325 IN ID 348 IN LG 278-1/4 IN TB
VERTICAL w ACT TUBE BUNDLE & THIN LG DIA WALLS

UNITS	
LENGTH	INCH
TEMPERATURE	DEGREE F
PRESSURE	PSI
STRESS	PSI
MASS	LB
DENSITY	LB/CUIN
OPTIONS	
TUBESHEETS	SYMMETRIC
EXCHANGER	VERTICAL
TEMA	REQUESTED
TUBES	ROLLED
EXPANSION JOINT	NO
WT OR PRES	BUNDLE WEIGHT

PRELIMINARY FOR DESIGN

PROJECT 5304-100 FIXED TUBESHEET EXCHANGERS 9-22-78
PROBLEM NO 42 ENGLISH UNITS

TUBE DATA	
OD	0.98165
THICKNESS	0.02652
LENGTH	348.00000
UNSUPPORTED LENGTH	
BAFFLE TO BAFFLE	58.00000
TUBESHEET TO BAFFLE	58.00000
LAYOUT ANGLE	60.00000
PITCH	1.25000
NUMBER OF TUBES	43883
OPERATING PRESSURE	4.21800
HYDROSTATIC TEST PRESSURE	25.88900
MAXIMUM TEMPERATURE	76.30000
AVERAGE TEMPERATURE	70.90000
YIELD STRENGTH AT	
MAX TUBE TEMPERATURE	40000.00000
SHELL TEMPERATURE	40000.00000
ATMOSPHERIC	40000.00000
INSIDE CORROSION ALLOWANCE	0.00000
OUTSIDE CORROSION ALLOWANCE	0.00000
POISSONS RATIO	0.34000
ELASTIC MODULUS AT	
MAX TUBE TEMPERATURE	1.62837E+07
AVERAGE TEMPERATURE	1.63834E+07
SHELL TEMPERATURE	1.63982E+07
ATMOSPHERIC	1.64000E+07
ALLOWABLE STRESS AT	
MAX TUBE TEMPERATURE	12500.00000
SHELL TEMPERATURE	12500.00000
ATMOSPHERIC	12500.00000
EXPANSION COEFFICIENT	4.80000E-06
BUNDLE WEIGHT OR PRESSURE DROP	104719.00000

PRELIMINARY FOR DESIGN

PROJECT 5304-100 FIXED TUBESHEET EXCHANGERS 9-22-78
PROBLEM NO 42 ENGLISH UNITS

SHELL DATA		
ID	359.00000	
THICKNESS	1.50000	
OPERATING PRESSURE	86.30000	
HYDROSTATIC TEST PRESSURE	129.50000	
AVERAGE METAL TEMPERATURE	65.00000	
YIELD STRENGTH AT OPERATING	32000.00000	
YIELD STRENGTH AT ATMOSPHERIC	32000.00000	
ALLOWABLE STRESS AT OPERATING	15000.00000	
ALLOWABLE STRESS AT ATMOSPHERIC	15000.00000	
ELASTIC MODULUS AT OPERATING	2.90000E+07	
ELASTIC MODULUS AT ATMOSPHERIC	2.90000E+07	
CORROSION ALLOWANCE	0.50000	
EXPANSION COEFFICIENT	6.13000E-06	
DENSITY OF FLUID	0.00030	
POISSONS RATIO	0.30000	
AMBIENT TEMPERATURE	70.00000	
TUBESHEETS	1	2
THICKNESS	4.31250	4.31250
FLEXURAL EFFICIENCY	0.00000	0.00000
EXPANSION COEFFICIENT	6.13000E-06	6.13000E-06
TEMPERATURE DROP	22.20000	22.20000
TUBE IN TUBESHEET OD	1.00000	1.00000
TUBE ID TUBESHEET THICKNESS	0.02600	0.02600
CORROSION ALLOWANCE TUBESIDE	0.00000	0.00000
CORROSION ALLOWANCE SHELLSIDE	0.00000	0.00000
TUBE BUNDLE OD	244.25000	
ELASTIC MODULUS AT OPERATING	2.90000E+07	2.90000E+07
ELASTIC MODULUS AT ATMOSPHERIC	2.90000E+07	2.90000E+07
TEMPERATURE		
TUBESIDE	40.00000	40.00000
SHELLSIDE	50.00000	50.00000
AVERAGE	45.00000	45.00000
YIELD STRENGTH AT MAX TEMP	32000.00000	32000.00000
YIELD STRENGTH AT ATMOSPHERIC	32000.00000	32000.00000
ALLOWABLE STRESS AT MAX TEMP	15000.00000	15000.00000
ALLOWABLE STRESS AT ATMOSPHERIC	15000.00000	15000.00000
POISSONS RATIO	0.30000	0.30000
ANNULUS RING		
EXPANSION COEFFICIENT	6.13000E-06	6.13000E-06
AVERAGE TEMPERATURE	45.00000	45.00000
TEMPERATURE DROP	10.00000	10.00000
ELASTIC MODULUS	2.90000E+07	2.90000E+07

PRELIMINARY FOR DESIGN

PROJECT 5304-100 FIXED TUBESHEET EXCHANGERS 9-22-76
PROBLEM NO 42 ENGLISH UNITS

THICKNESSES OF TUBESHEETS REQUIRED BY TEMA (CORRODED) INCH

	FROM BENDING	FROM SHEAR
RESULT 1	4.7576	0.9817 **
RESULT 2	4.7576	0.9817 **

RESULT 1 THICKNESSES ARE REQUIRED FOR BOTH TUBESHEETS OF THE EXCHANGER CONSIDERING THAT THEY BOTH HAVE THE SAME MATERIAL PROPERTIES AND TEMPERATURES AS THOSE SPECIFIED ON INPUT FOR TUBESHEET 1

RESULT 2 THICKNESSES ARE REQUIRED FOR BOTH TUBESHEETS OF THE EXCHANGER CONSIDERING THAT THEY BOTH HAVE THE SAME MATERIAL PROPERTIES AND TEMPERATURES AS THOSE SPECIFIED ON INPUT FOR TUBESHEET 2

** THICKNESS REQUIRED BY TEMA R-7.121

NOTE : CONTROLLING FOR THE CONDENSER. ANTICIPATED TUBESHEET THICKNESS FOR FINAL DESIGN IS LESS THAN 4.3125 INCH. A VENDOR'S QUOTATION BASED ON TEMA-R TUBESHEET THICKNESS IS THEREFORE CONSERVATIVE.

THIS PAGE

WAS INTENTIONALLY

LEFT BLANK

APPENDIX I.2.2

0.2 MWe TEST ARTICLES

Customer	TRW	Pages	Page 67
Subject	2 MW TEST FACILITY	By	TJG
Project	5304-100	Date	8.10.78

PRELIMINARY FOR DESIGN

CODE - UG-27

CIRCUMFERENTIAL STRESS -

$t = \frac{PR}{SE - .6P}$ WHERE E = .85 S_{allow} = 15,000 R = 49 1/8" PER ASME CH. VIII

$t = \frac{136(49.125)}{15000(.85) - .6(136)} + .125 = .374 + .125 = .652$ IN

$S_{circ} = \frac{136(49.125)}{t_{corroded}} + .6(136) = 10,256$ PSI

LONGITUDINAL STRESS -

$t = \frac{136(49.125)}{2(15000)(.85) + .4(136)} + .125 = .2614 + .125 = .3864$ IN

$S_{long} = \frac{136(49.125)}{2(.527)} - .4(136) = 6,284$ PSI

USING E516-60 @ 28X10⁶

UNIT - STRAIN -

$\frac{6284}{28 \times 10^6} = .00022$

TOTAL STRAIN -

$.00022 \times 352 = 0.077$" (EXPANSION)

TUBE LENGTH 30'-0" END TO END -

SHELL - 29'-4" BACK TO BACK OF TUBE SHEETS - (352")

LONGITUDINAL STRAIN ABOVE ASSUMES ALL END LOADING ON THE SHELL. IN ACTUAL PRACTICE THE LOAD SHOULD ALSO DISTRIBUTE TO THE VAPOR BARRIERS AND SOME TO THE TUBES. TUBESHEET CONSTRAINT IS PRIMARILY ACCOMPLISHED WITH THE VAPOR BARRIERS AND THE STIFFENERS AS SHOWN, PIPE UNDER LOW STRESS.

SINCE THE TUBESHEET IS STRESSED AS A SEMICIRCULAR FLAT PLATE WITH EDGE

PRELIMINARY FOR DESIGN

Customer TVA

Subject 2 MW TEST ARTICLE

Project 5304 - 100

Pages Page 68

By RGC

Date 8-10-77

FIXED, AND SINCE THE VAPOR [illegible] ACT AS TUBESHEET STAYS AND FIX EACH SEMICIRCULAR TUBESHEET SECTION, ANY LOADING OF THE TUBES IS INCONSEQUENTIAL WITH ONLY A Δ temp of 2°F BETWEEN THE TUBES AND THE STEEL SHELL (OR JACKET) THERE IS NO TEMPERATURE EXPANSION STRESS ON THE TUBES.

ACCOMPANYING CALCULATIONS SHOW THAT THE VAPOR BARRIERS ALONE ARE CAPABLE OF CARRYING 1,091,000 # of END FORCE.

TOTAL END FORCE = 920,000 POUNDS.

THEREFORE, THE TUBES ARE NOT REQUIRED TO SUSTAIN ANY END FORCES.

ASSUMING THE TUBES ARE BEING PULLED BY THE ELONGATION OF THE SHELL AND VAPOR BARRIERS - THE MAXIMUM STRESS IN THE TUBES IS 3,924 PSI

THE TUBES HAVE AN ALLOWABLE STRESS OF AT LEAST 10,600 PSI FOR G.R II [illegible] THEREFORE, THE TUBES ARE ONLY STRESSED TO 37% of THEIR ALLOWABLE

Customer	TRW	Pages	Page 69
Subject	.2 MWe TEST ARTICLE EVAPORATOR	By	JWC
Project	5304-100-117-2	Date	8-2-78

PRELIMINARY FOR DESIGN

INTERNAL PRESSURE PER UG 27

P = 136 PSIG , CA 1/8

T - UNDER 650 F

MTL SA 516-60

$$t = \frac{PR}{SE - .6P} + C = \frac{136 \times 49.125}{15000 \times .85 - .6 \times 136} + \frac{1}{8} = .527 + \frac{1}{8} = .652$$

SHELL USE $\frac{11}{16}$" ID.

WATER BOX - USE $\frac{3}{8}$" TK.

BOTTOM CONE PER UG 32 (g)

PRESSURE 18.6 PSI.

$$t = \frac{PD}{2\cos\alpha(SE - .6P)} + C$$

$$= \frac{18.6 \times 90.25}{2\cos 30^\circ(15000 \times .85 - .6 \times 18.6)} + \frac{1}{8}$$

$t = .076" + \frac{1}{8} = .201"$ USE $\frac{1}{4}$" TK MIN

NOZZLE REINFORCEMENT (PER UG 37)

MANWAY 20" WITH 20" SCH 80 PIPE NECK.

AREA REQ'D

$A = d \times t_r \times F$ WHERE $F = 1$

$A = (17.938 + .25)(.448)$

$A = 8.145 \text{ in}^2$

$A_1 = (E t - F t_r) \frac{1}{2} = (.563 - .448) 18.188 = 2.092 \text{ in}^2$

or

$A_1 = (E_1 t - F t_r)(t_n + t) 2 = (.563 - .448)(.906 + .563) 2 = .338 \text{ in}^2$

PRELIMINARY FOR DESIGN

Customer	TRW
Subject	.2 MWe TEST ARTICLE EVAPORATOR
Project	
Pages	Page 70
By	
Date	

$A_2 = (t_n - t_{rn}) 5t = (.906 - .083) 5 \times .563 = 2.317 \text{ in}^2$

OR

$A_2 = (t_n - t_{rn}) 5t_n = (.906 - .083) 5 \times .906 = 3.728 \text{ in}^2$

$A_3 = 0$

$A_4 = 2 \times .5 \times .25 = .25$

TOTAL AVAILABLE 4.659

REINF PAD REQ'D = 8.145 − 4.659 = 3.486 in^2

USE PAD $\frac{1}{2}$" x 27" Ø PAD

NOZZLE N2 18" SCHD 80 PIPE NECK.

AREA REQ'D, $A = d\, t_r F = 16.376 \times .448 \times 1 = 7.336 \text{ in}^2$

$A_1 = (E_1 t - F t_r) d = (.563 - .448) 16.376 = 1.883$

OR

$A_1 = (E_1 t - F t_r)(t_n + t) 2 = (.563 - .448)(.812 + .563) 2 = .316$

$A_2 = (t_n - t_{rn}) 5t = (.812 - .075) 5 \times .563 = 2.070$

$A_3 = 0$

$A_4 = 2 \times .5 \times .25 = .25$

AVAILABLE 4.209 in^2

NET ADD = 7.336 − 4.209 = 3.127 in^2

USE $\frac{1}{2}$ x 25 Ø PAD

PRELIMINARY FOR DESIGN

Customer	T R W	Pages	Page 71
Subject	.2 MWe TEST ARTICLE EVAPORATOR	By	JWC
Project	5304-100-117-2	Date	6-3-75

NOZZLE N1 5" X-STR PIPE 5.563" OD x .375" wall

AREA REQ'D, $A = d \times t_r + F = 5.063 \times .563 \times 1 =$ 2.850 in²

$A_1 = (E_1 t - F t_r) d = (.563 - .448)\, 5.063 =$ .644

$A_1 = (E_1 t - F t_r)(t_n \overset{OR}{+} t) 2 = (.563 - .448)(.25 + .563) 2 =$ ~~.187~~

$A_2 = (t_n - t_{rn})\, 5t = (.25 - .0023) 5 \times .563 =$ .639

$A_3 =$ 0

$A_4 = 2 \times .5 \times .25$ .25

TOTAL AVAIL 1.533 in²

REQ'D IN PAD = 2.850 − 1.533 = 1.317 in²

USE 1/2" x 9½ ϕ PAD. 2" WIDE MIN PAD.

Customer	TRW	Pages	Page 72
Subject	.2 MWe TEST ARTICLE EVAPORATOR	By	TWC
Project		Date	8-3-78

PRELIMINARY FOR DESIGN

FIXED TS DESIGN.

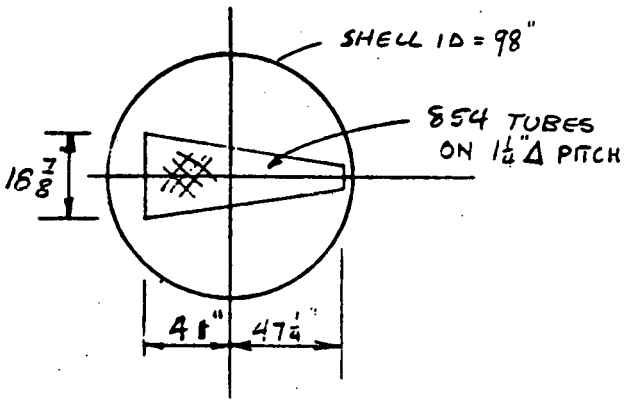

LOOK AT UNSTAYED PORTION OF TS. ASSUME FULL SEMICIRCLE.

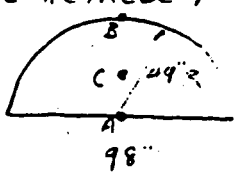

$$\sigma_A = -.42 \frac{q a^2}{t^2}$$

$$t^2 = -42 \frac{q a^2}{\sigma_A} \qquad \text{WHERE } \sigma_A = 15000 \text{ PSI}$$

$$t_A = \sqrt{.42 \frac{136.5 \times 49^2}{15000}} = 3.029" + \tfrac{1}{8}" = 3.15"$$

$$t_B = \sqrt{\frac{.36 \times 136.5 \times 49^2}{15000}} = 2.805" + \tfrac{1}{8}" = 2.93"$$

$$t_C = \sqrt{\frac{.21 \times 136.5 \times 49^2}{15000}} = 2.14 + \tfrac{1}{8}" = 2.267"$$

3.15" MIN TS THICKNES REQD FOR THE UNSTAYED PORTION. METHOD FROM ROARK & YOUNG FIFTH EDITION, CASE 30 pp371

3⅜" ID (FULL CIRCLE) IS STRESSED TO 14030 PSI

Customer	TRW	Pages	Page 73
Subject	.2 MWe TEST ARTICLE EVAPORATOR	By	JWC
Project	5304-100-117-2	Date	8-3-78

FIXED TS DESIGN. RUFF CALCS.

(TEMPERATURE DIFFERENCES ARE OF LITTLE CONSEQUENCE)

TOTAL TUBE CROSS SECTION

$A_1 = (1 - .938^2).7854 \times 8^2 = 102.6 \text{ in}^2$

$P_T = SA_1 = 12500 \times 102.6 = 1.2825 \times 10^6$ lbs. ALLOWABLE

END LOAD ON TS. 9.38×10^5 lbs.

$E_{TS} = 29 \times 10^6$

$E_{TUBE} = 16.4 \times 10^6$

$9.38 \times 10^6 \times \frac{16.4}{20} = 530,532$ on TS

$938 \times 10^6 - 530532 = 407633^{\#}$ on TUBES

TS. $t^2 = \frac{3W}{8\pi m s}(3m+1)$

$t^2 = \frac{3 \times 530532}{8\pi \times 3.333 \times 15000}(3 \times 3.333 + 1)$

$t^2 = 13,932$

$t = 3.733 + \frac{1}{8} = 3.85$ SAY 4" THICK.

TUBES

$S = \frac{P}{A} = \frac{407633}{102.6} = 3973^{\#}/\text{in}^2$

THIS DOES NOT TAKE INTO ACCOUNT THE VAPOR BARRIERS WELDED TO BOTH TUBESHEETS.

Customer TRW
Subject .2 MW TEST ARTICLE
Project 5304-100

Pages Page 74
By EEC
Date 7-10-78

PRELIMINARY FOR DESIGN

TOTAL END LOADING - EVAPORATOR -

USING 136 PSI DESIGN -

ID = 98 1/4" ϕ

TUBES = 854 1" ϕ AREA = 854 X .7854 IN = 670.73 IN²

TOTAL AREA = $\frac{98.25^2 \pi}{4}$ = 7581.5

PRESSURE AREA (NOT SUBTRACTING THE SHELL)
= 6911 IN²

ASSUME BAFFLES @ 3/4" THICK X 96" LONG = 144 IN²

NET AREA FOR PRESSURE = 6767 IN²

TOTAL END PRESSURE = 6767 X 136 = 920,312 POUNDS

TOTAL PERIMETER TO HOLD END LOAD
98.25 π + 2(96) = 500.66 INCHES -

LOAD REQUIRED / INCH = 1838 POUNDS

REVISE FOR 3/8" BAFFLE - ADD - 72 IN² to END LOADING
OR 6839 IN²

TOTAL END PRESSURE 6839 X 136 = 930,104 #
OR 1,857 = PER LIN INCH

STRESS ON 3/8" THK BAFFLE = 4,954 PSI ↑ 9903 PSI ↑

STRESS ON 9/16" (NET) SHELL = 3,301 PSI ↑ 6602 PSI ↑

Customer	TRW	Pages	Page 75
Subject	.2 MW3 TEST RATTLE	By	RGC
Project	5304-100	Date	8-10-76

TUBES — 1" OD X .938 ID $L = 352"$

$\Delta l = .077"$

$l\varepsilon = \Delta l$ - (INCHES)

$\varepsilon = \frac{\Delta l}{l} = \frac{.077}{352} = .000218$

$\varepsilon = \frac{S}{E}$

$E = 18 \times 10^6$ PSI.

$S = E\varepsilon$

$S = 18 \times 10^6 \times .000218 = 3,924$ PSI.

PRELIMINARY FOR DESIGN

Customer	TRW	Pages	Page 76
Subject	.2 MW₀ TEST ARTICLE	By	FWC
Project	5304-100-117-2	Date	8-3-78

PRELIMINARY FOR DESIGN

VAPOR BARRIER.

$A = 2 \times 3/8 \times 97 = 72.75\ in^2$

ASSUME WELD SIZED TO CARRY SAME LOAD.

WHAT CAN THE BARRIER CARRY?

$P = SA = 72.75 \times 15000 = 1091250\ \#$

THIS IS MORE THAN THE HYDROSTATIC END LOAD.

THIS PAGE

WAS INTENTIONALLY

LEFT BLANK

APPENDIX I.2.3

HEAT EXCHANGERS SUPPORT

PREPARED L R MORTALONI 29 AUG 1978 REPORT NO. PAGE 1

CHECKED

MODEL PSD-I, 10 MWe, PDR

HEAT EXCHANGERS SUPPORT STRESS ANALYSIS

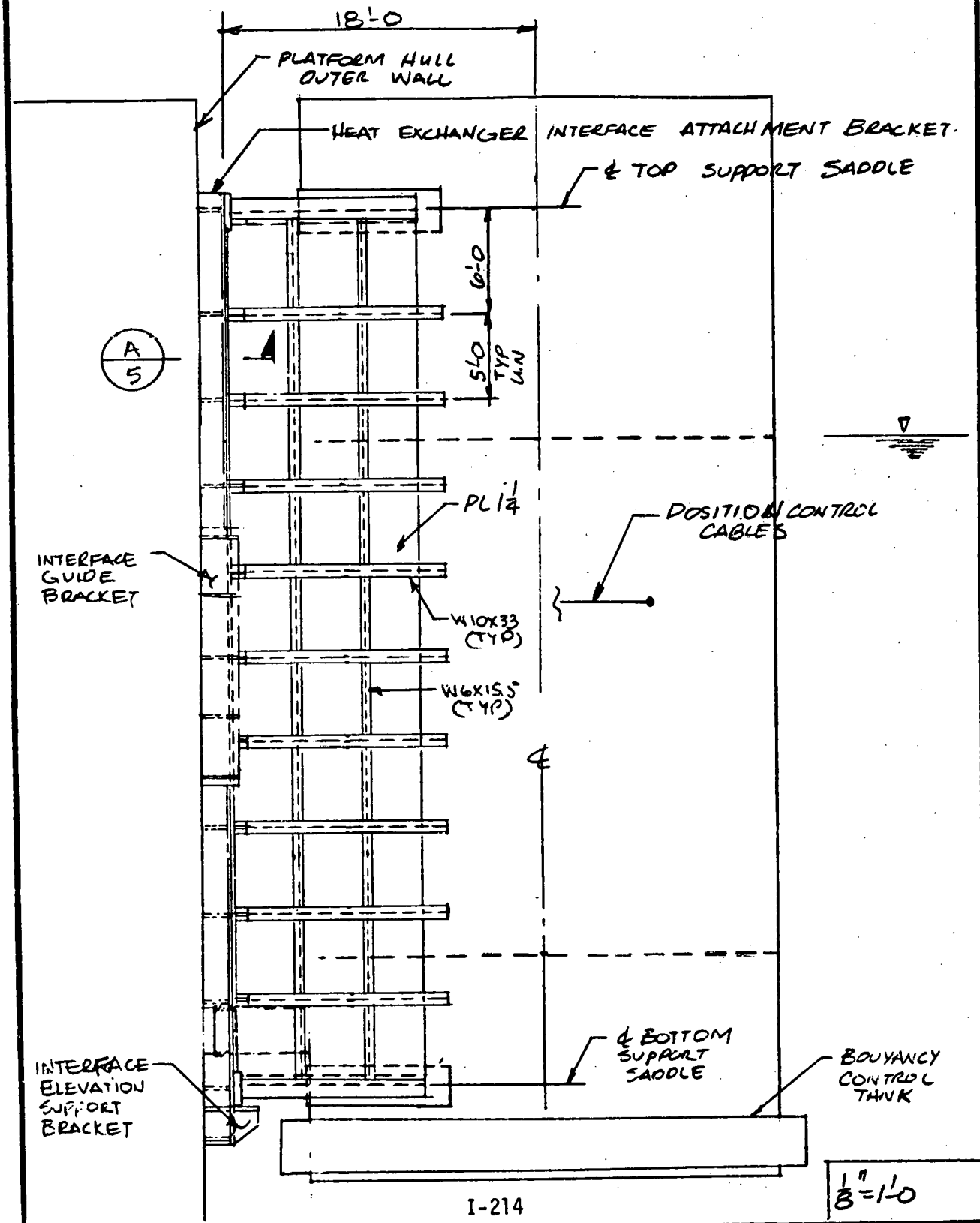

TOP SUPPORT SADDLE

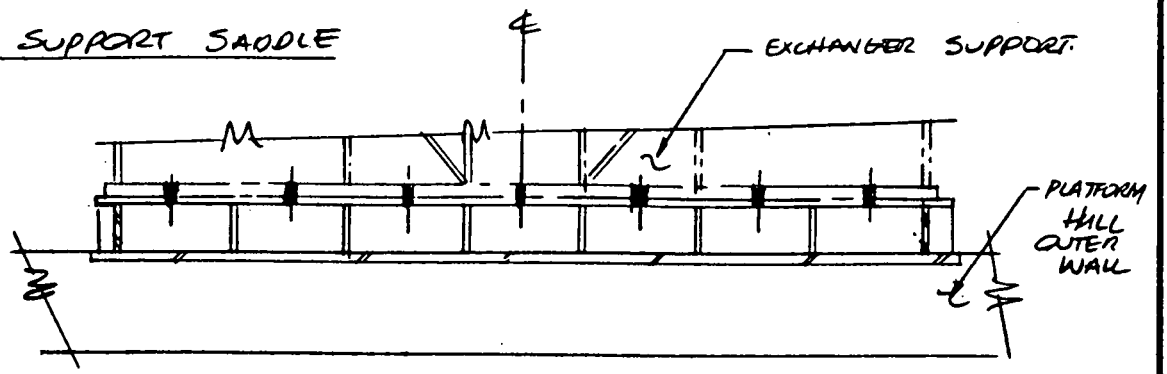

HEAT EXCHANGER TOP SUPPORT INTERFACE ATTACHMENT BRACKET

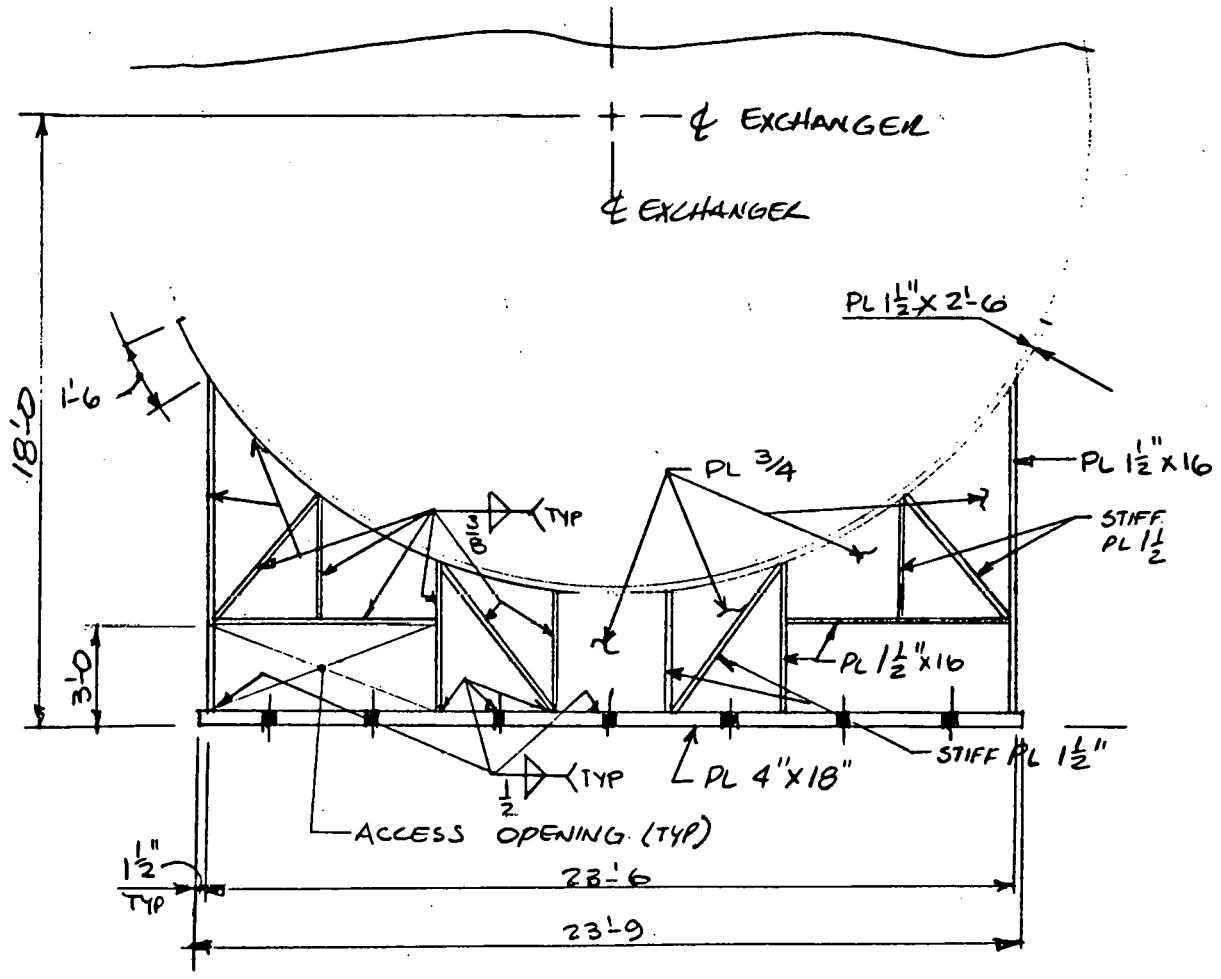

HEAT EXCHANGER TOP SUPPORT SADDLE

3/16" = 1'-0

CONDENSER SUPPORTS.

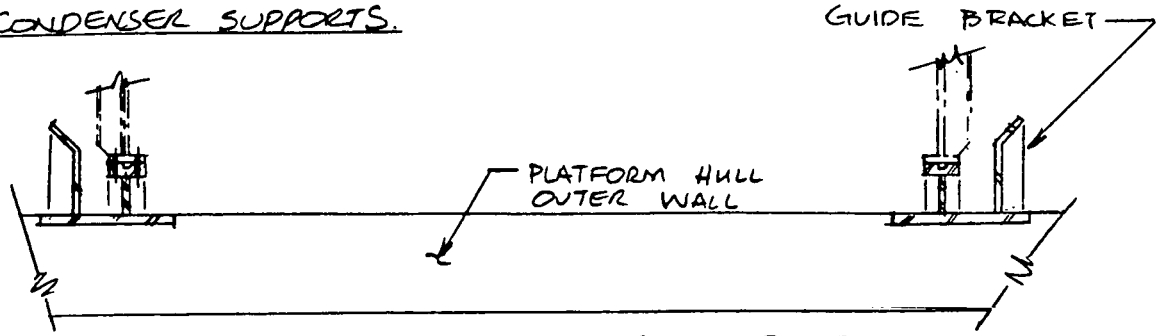

HEAT EXCHANGER COFFERDAM SIDE PLATE ATTACHMENT AND GUIDE BRACKET

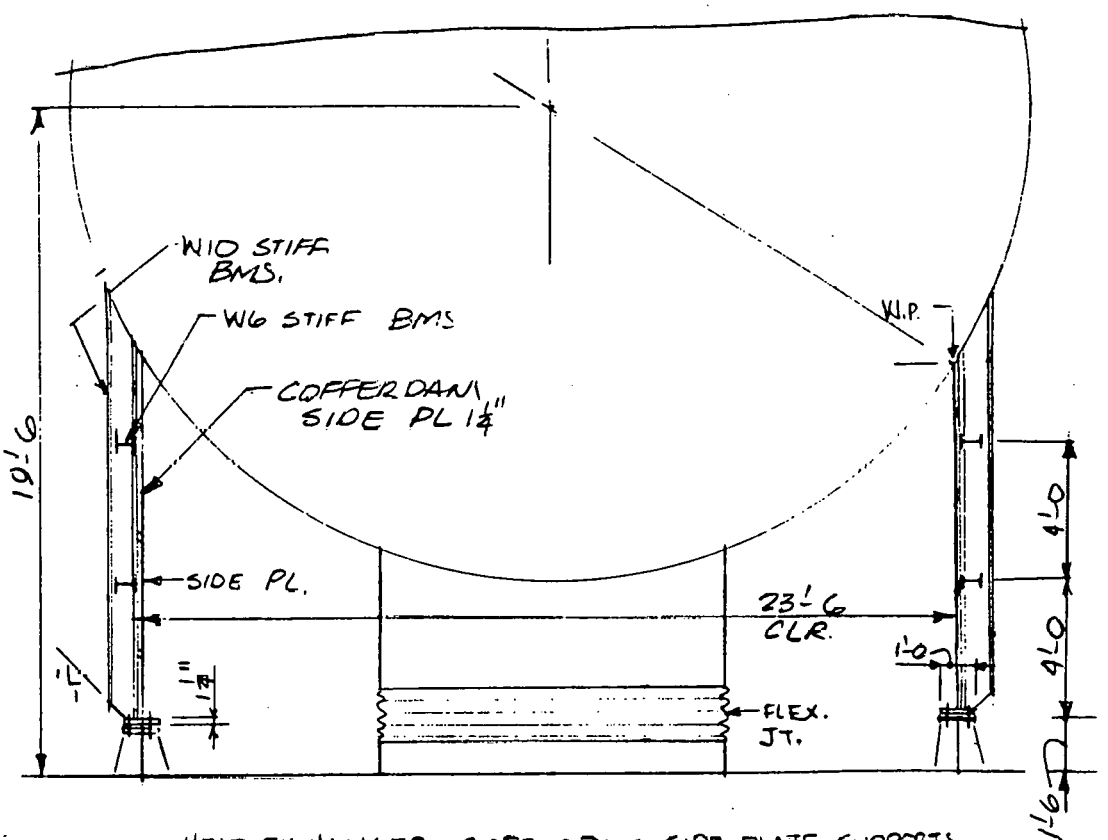

HEAT EXCHANGER COFFERDAM SIDE PLATE SUPPORTS

3/16" = 1'-0"

PREPARED L R MORTALONI 30 AUG 1978 REPORT NO. PAGE 4

CHECKED

MODEL

BOTTOM SUPPORT SADDLE

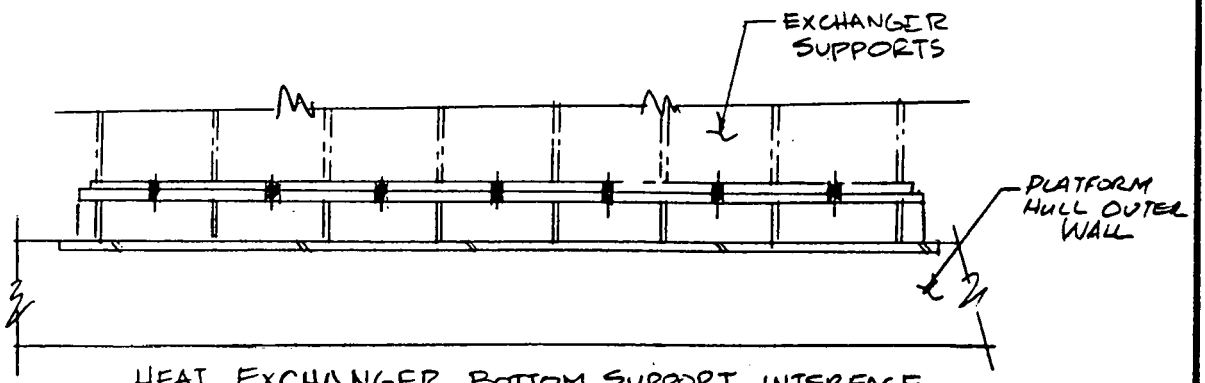

HEAT EXCHANGER BOTTOM SUPPORT INTERFACE ATTACHMENT BRACKET.

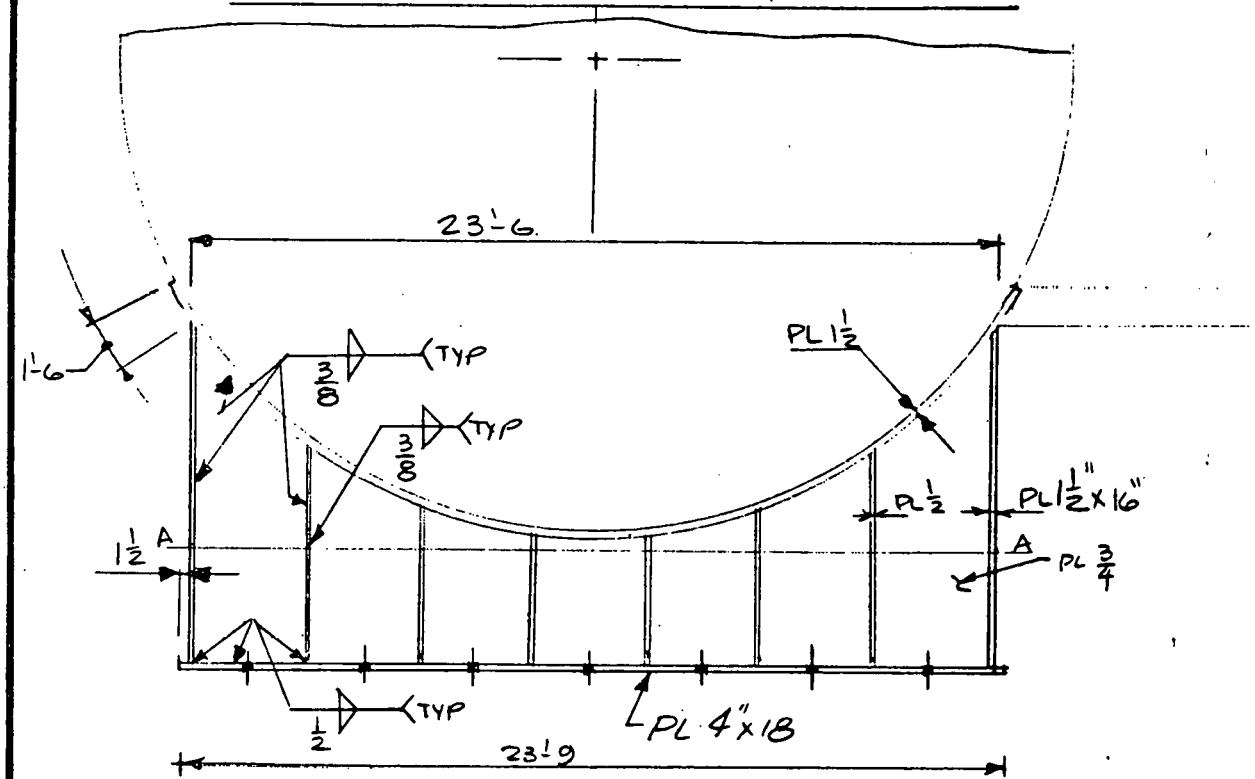

HEAT EXCHANGER BOTTOM SUPPORT SADDLE

$A_{\text{TOTAL LINE A}} = 23.25*12*0.75" + 2*16"*1.5 + 6*(16-0.75)*1.5 = 394.5^{0"}$ PER SUPPORT

$I_{\text{LINE A}} = 2.961 \times 10^6 \text{ in}^4$

3/16" = 1'-0

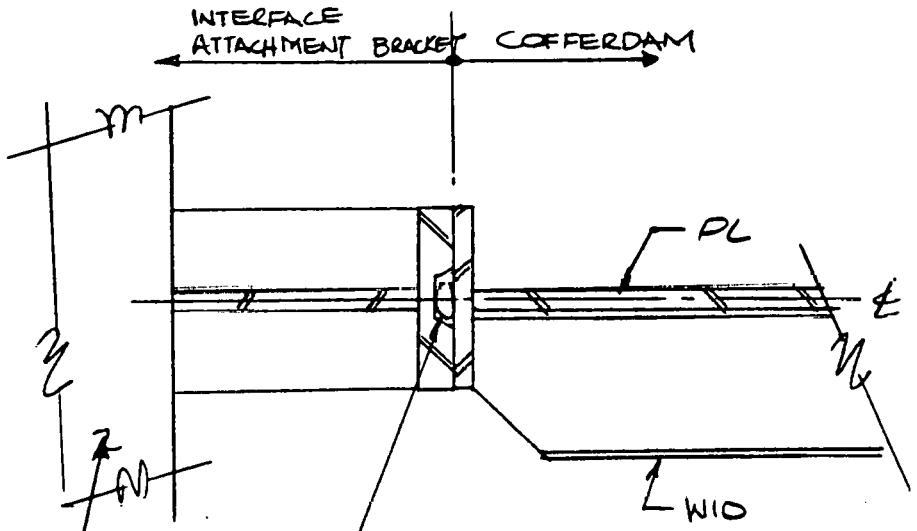

INFLATABLE O RING GASKET — COLLAPSED DURING DOCKING AND INFLATED DURING ATTACHMENT OF PIPES.

PLATFORM HULL OUTER WALL

A REF. SHEET 1

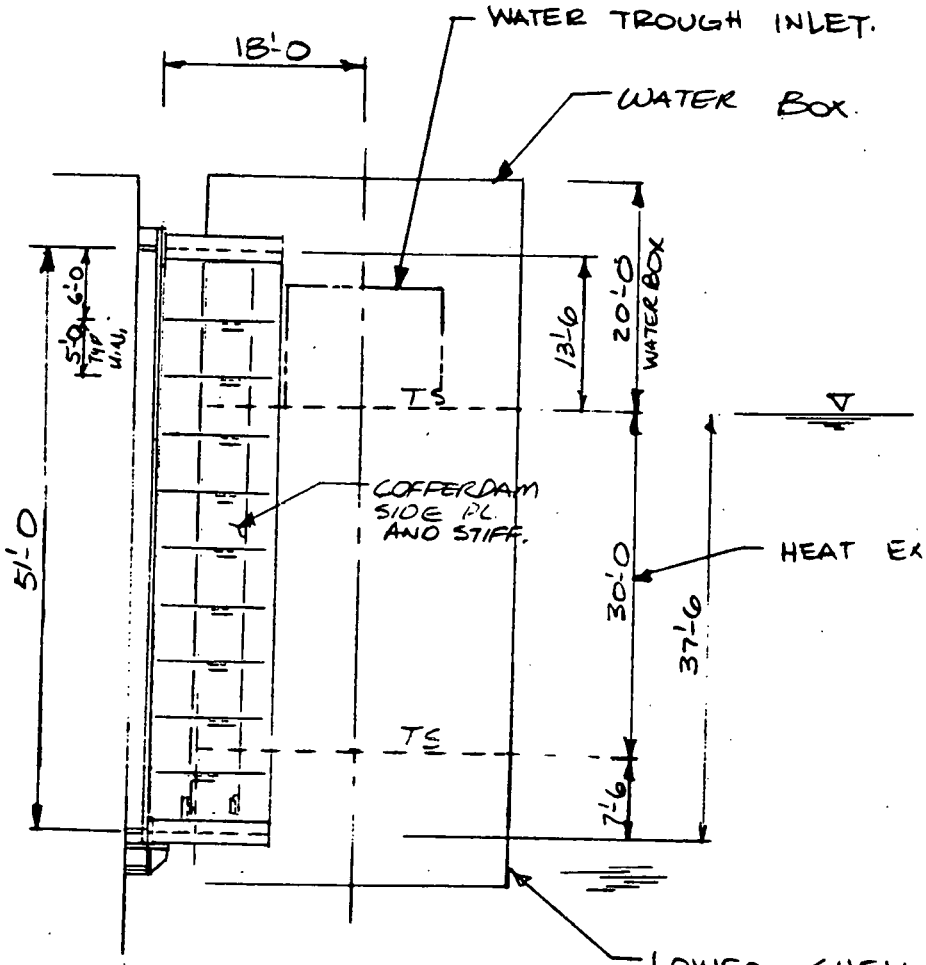
WATER TROUGH INLET.
18'-0
WATER BOX.
5'-0 6'-0 TYP. U.N.O.
5'-0
13'-6
20'-0 WATER BOX
TS
COFFERDAM SIDE PL. AND STIFF.
HEAT EXCHANGER
30'-0
37'-6
TS
7'-6
LOWER SHELL (ESTIMATED)
315" ID X 15'-0 X 1" THICK.
WT = 50,671# (DRY)
WT = 44,053# (WET)
6618# DELTA.
DISPLACED WATER
1/16"=1'-0

COFFERDAM

PLATE THICKNESS

MAX. PRESSURE = 37.5* 64 = 2400 #/□' = 16.67 #/□"

$$M_{MAX} = \frac{wL^2}{8} = \frac{16.67 * 60^2}{8} = 7500\ ''\text{-K/IN}.$$

$$t_{MIN} = \sqrt{\frac{6M}{F_y}} + 0.5 = 1.618'' \Rightarrow \text{TRY } 1\tfrac{5}{8}''\ PL$$

NOTE: LET $F_y = 36^K/\square''$ ← CORROSION ALLOWANCE SINCE THIS LOADING CONDITION IS ONLY TEMPORARY

STIFFENER BEAMS

SECTION PROPERTIES

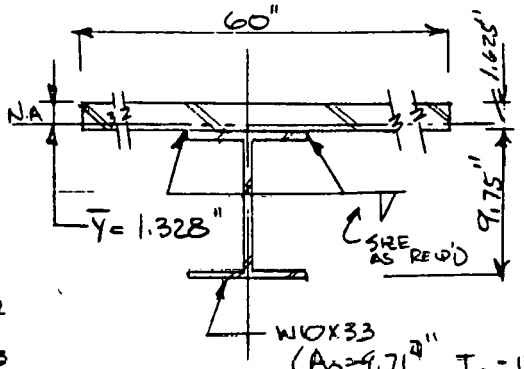

FOR COMPOSITE SECTION

$A_T = 107.21\ \square''$

$I_T = 478.1\ IN^4$

$S_{MAX} = 360.1\ IN^3$ — TENSION SIDE

$S_{MIN} = 47.6\ IN^3$

CHECK BENDING

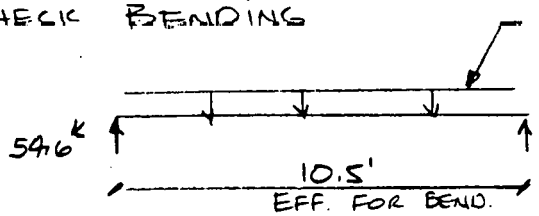

$M_{MAX} = 143.33\ ^{1\text{-K}}$

$$f_{b\,MAX} = \frac{M}{S_{MIN}} = 36.1\ ^K/\square'' \leftarrow$$

O.K.; DUE TO TEMP. LOAD.

COFFERDAM - CONTi

TRY REDUCE BEAM SPACING TO 4'-3 = 51"

$w = 16.67^{\#}/_{IN}$ $M_{max} = 5418.75^{IN-K}/_{IN}$

$t_{min} = 0.95 + 0.5 = 1.45" \Rightarrow$ TRY $1\frac{1}{2}"$

STIFFENER BEAMS. $w = 33.25 * 4.25 * 64 = 9044^{\#}/_{FT.}$

$M_{MAX} = 124.64^{1-K} \Rightarrow S_{MIN} = \frac{124.64 * 12}{36} = 41.5^{IN^3}$

N.T.G.A.S.

TRY VERTICAL STIFFENER BEAMS (WILL PROBABLE BE REQ'D FOR SHEAR)

PLATE THICKNESS - TWO WAY PLATE BENDING

$w = 16.67^{\#}/_{IN}$ $A = 48"$ $B = 60"$ $\frac{B}{A} = 1.25$

REF. "THEORY OF PLATES AND SHELLS", BY TIMOSHENKO

$M_{max} = 0.06661 w A^2 = 2536.3^{IN-K}/_{IN}$

$t_{min} = \sqrt{\frac{6M}{F_y}} + 0.5 = 1.15^{IN} \Rightarrow$ USE PL $1\frac{1}{4}"$

STIFFENER BEAMS.

SHORT BEAMS.

$M_{max} = \frac{16.67 * 60^2}{8} * 48 = 360072^{IN-\#} = 360.07^{IN-K}$

$S_{min} = \frac{360.07}{36} = 10.0 \Rightarrow$ USE W6X15.5

LONG BEAMS.

$M_{max} = 143.33^{IN-K} \Rightarrow$ USE W10X33

$A_T = 84.71^{IN^2}$

$I_T = 440.82^{IN^4}$

$S_{min} = 45.2^{IN^3}$

$S_{MAX} = 351.1^{IN^3}$

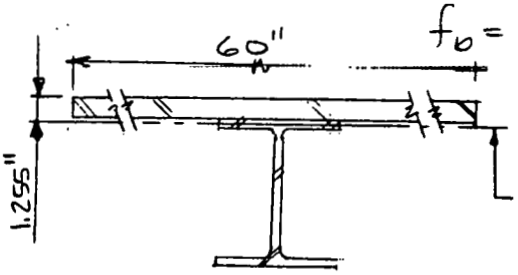

$f_b = \frac{143.33 * 12}{45.2} = 38^{K}/_{IN^2}$

O.K. DUE TO CONSERVATIVE NATURE OF CALCULATIONS

COEFFERDAM -CONTI

EST WEIGHT

SIDE PL.

$2*((51'-0)*(11'-0)*\frac{1.25}{12})*490 = 57269^{\#}$

STIFFENERS.

W10X 33.

2-9 BMS @ 11'-0

$2*(9*11*33) = 6534^{\#}$

W6 X 15.5.

2- 2 BMS @ 51'

$2*(2*51*15.5) = 3162^{\#}$

FLANGES (ESTIMATE THICKNESS).

PL 1/4 X 8" X 102'

$102*\frac{1.25*8}{12}*490 = 41650^{\#}$

SUBTOTAL $= 108615^{\#}$

SUPPORT SADDLES

2 @ 15,000# $= 30,000^{\#}$

$138,615^{\#}$

OR

VOL = 282.8 FT³ - FOR BOUYANCE CALC.

EQUIVALENT UNIT AREAS.

No. OF BMS. →

$\bar{A} = \frac{9*9.7/+1.25*51*12}{51*12} = 1.39\ 0''/IN$

$A_{TOTAL} = 852.39\ 0''$ PER SIDE

CONDENSER WEIGHTS - FROM INTEGRAL HULL AND 40MWE SHIP DATA

TUBES.		
TUBE	241495#	
WATER		380,163#
SHELL	247094	
WATERBOX.		
SHELL	59093	
WATER		346360
TUBESHEET	130909	
NH_3		12503
BAFFLES & TIERODS	96592	
COEFFERDAM	138615	
LOWER SHELL	50671	
	964469#	+ 739026# = 1,703495# = 852 Tons

BY MISTAKE I USE EVAPORATOR WEIGHTS. USE THESE VALUES FOR THE SUPPORT DESIGN SINCE THEY ARE GREATER THAN THAT OF THE CONDENSER.

DRY WT. USE 980,000# (490T) FOR SUPPORT DESIGN

OPERATING FLUID WT.

TOTAL OPERATING WT.

BOUYANY WEIGHT

CONDENSER

$$O.D. = 325 + 2\times 2\tfrac{3}{8} + 2\times\tfrac{1}{2} = 330.75'' = 27.5625'$$

$$\nabla_{COND} = 30' \times \tfrac{\pi}{4}\times 27.5625^2 + 282.8 = 18{,}182.6\ FT^3$$

OR

$$\Delta = 18182.6 \times 64 + 6618 = 1{,}170{,}305\# = 1170\ KIPS$$

NET REACTION - $R_{COND} = 1703 - 1170 = 533^K$ - USE 600^K FOR DESIGN

NOTE: FROM OTEC-PSD-1, HEAT EXCHANGER DESIGN CRITERIA THE FOLLOWING ACCELERATIONS ARE IMPOSED

SEA STATE	VERTICAL ACCELERATION	HORIZONTAL ACCELERATION
SS6	0.05g	0.01g
SS9	0.15g	0.07g

SUPPORT CALCULATIONS

EXCHANGER IN HORIZ POSITION — OCCURS DURING TRANSPORATION

GRAVITY LOADS

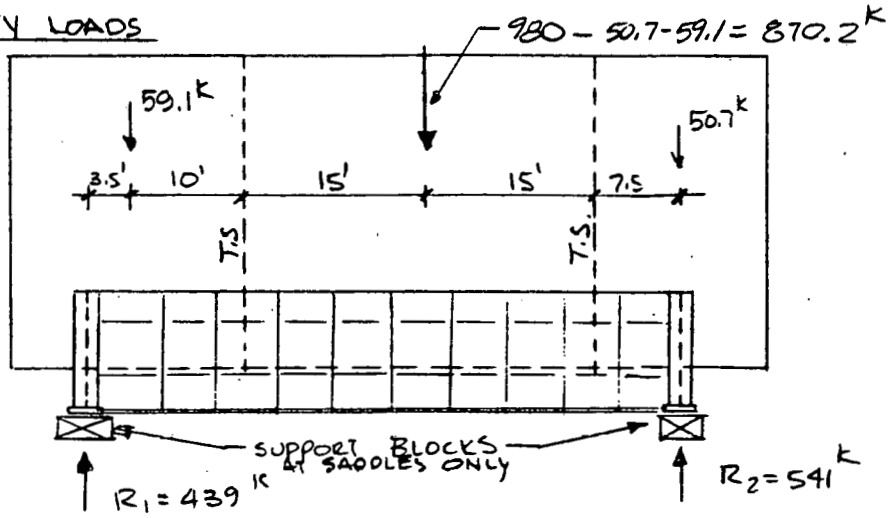

HORIZONTAL LOADS - DUE TO BARGE TRANSPORTATION LOADS

SURGE LOADING:

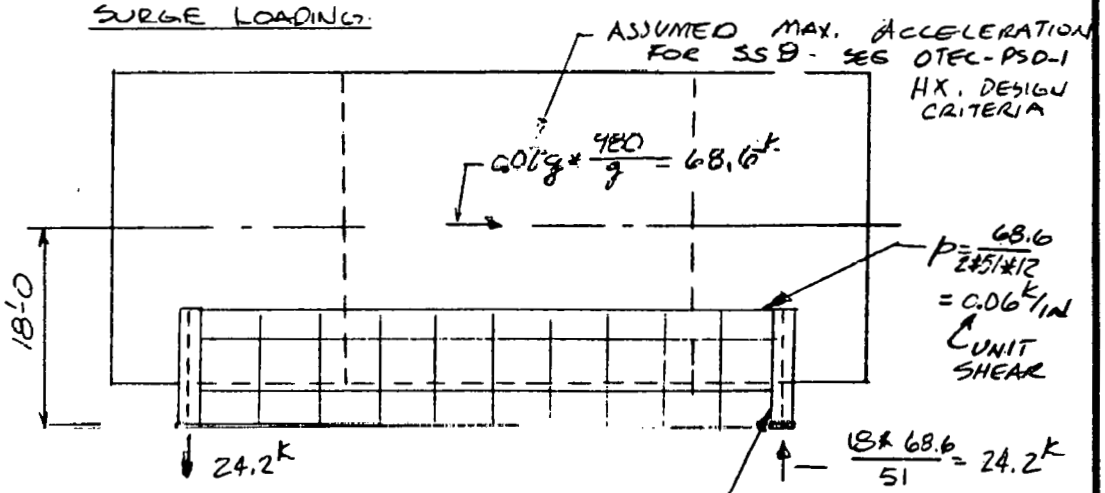

ASSUMING E70XX ELECTRODES

$q_{ALL} = 0.928\ ^{K}/_{IN}/\ ^{1}/_{16}$" WELD SIZE

∴ WELD STRESSES WOULD NOT BE EXCESSIVE

UNIT SHEAR = $\frac{24.2}{2*1*12} = 0.09\ ^{K}/_{IN}$

SUPPORT CALCULATIONS - CONTI

EXCH. HORIZ'B - CONT

HORIZONTAL LOADS - CONTI

SWAY LOADING

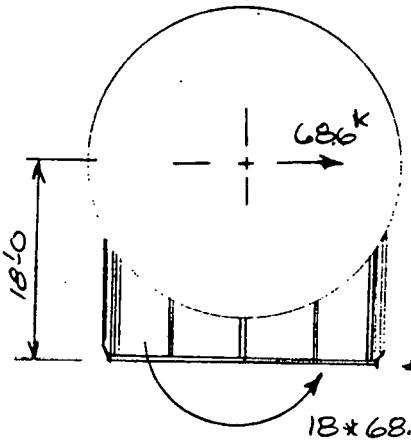

68.6K OR 34.3K/SUPPORT.

18 * 68.6 = 1234.8 '-K OR 617.4 '-K/SUPPORT

VERTICAL LOAD - HEAVE ACCELERATIONS (+ OR -)

SEE GRAVITY LOADS.

$R_1 = 0.15 * 439 = 65.9^K$

$R_2 = 0.15 * 541 = 81.2^K$

SUMMARY FOR SUPPORT LOADS

MAX. REACTIONS

$R_1 = 541 + 24.2 + 81.2 = 646.4^K$ - USE 700^K FOR DESIGN

$R_2 = 439 + 24.2 + 65.2 = 528.4^K$ - USE 550^K FOR DESIGN

MIN. REACTIONS

$R_2 = 439 - 24.2 - 65.9 = 348.9^K$

BOTTOM SUPPORT PLATE THICKNESS

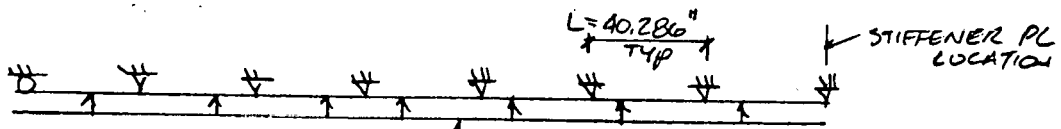

$\omega = \frac{700}{18 * 282''} = 0.138^{K/\square''}$ O.K.

ASSUME 18" WIDTH

$M_{MAX} = \frac{15}{142} \omega L^2 = \frac{15}{142} * 0.155 * 40.286^2 = 23.6^{''-K/IN}$

$t_{min} = \sqrt{\frac{6M}{F_y}} = \sqrt{\frac{6 * 26.6}{27}} = 2.29''$ → SEE TOP SUPPORT FOR THICKNESS REQ'D.

TOP SUPPORT – ACCESS REQUIRED

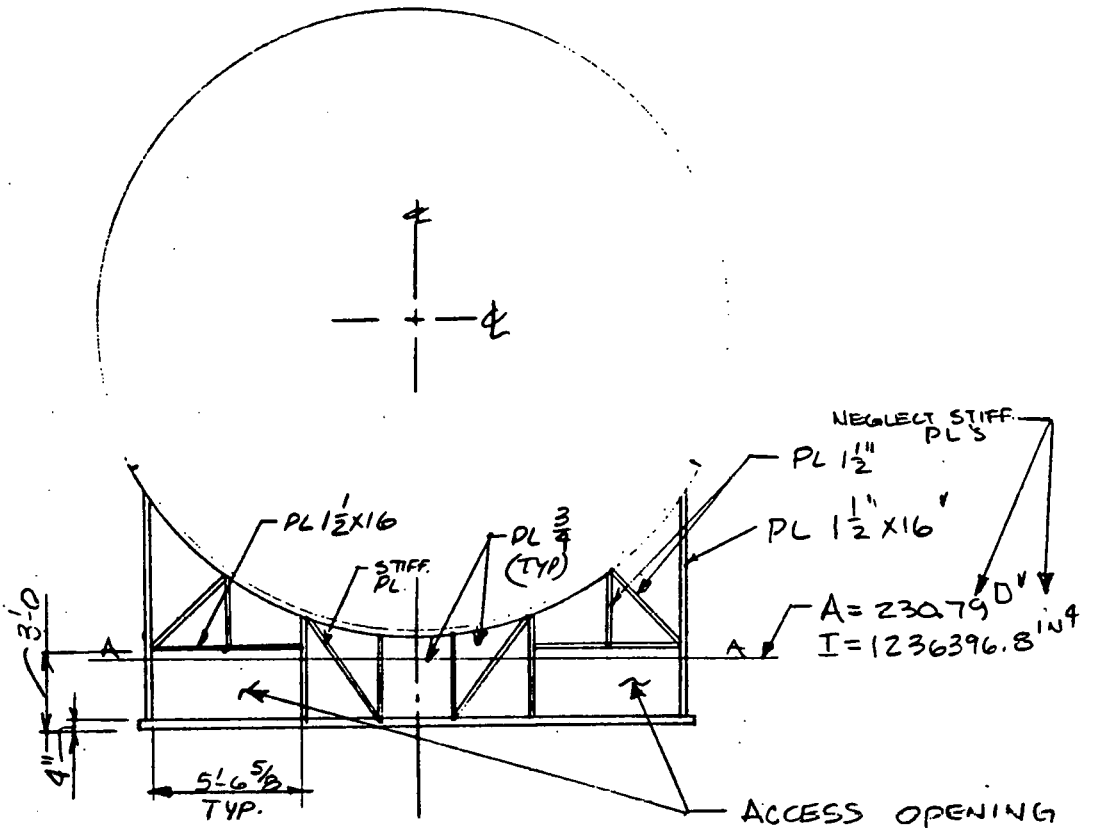

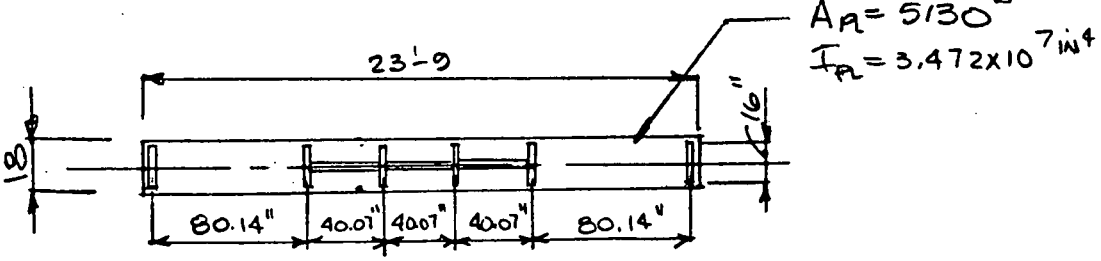

CHECK STRESSES IN THE STEEL

$$f = \frac{P}{A} \pm \frac{Mc}{I} = \frac{550}{230.79} \pm \frac{617.4 * 12 * 141}{1.24 \times 10^6}$$

$$= 2.383 \pm 0.845 = \begin{cases} 3.23^{K}/_{\square"} \text{ OK} & \text{COMPR} \\ 1.54^{K}/_{\square"} \text{ OK} \end{cases}$$

CHECK IF TENSION EXISTS FOR MIN. REACTIONS.

$$f = \frac{348.9}{230.79} - \frac{617.4 * 12 * 141}{1.24 \times 10^6} = 0.67^{K}/_{\square"} \text{ OK}$$

COMPR.

1/8" = 1'-0

TRW
DEFENSE AND SPACE SYSTEMS GROUP
ONE SPACE PARK • REDONDO BEACH, CALIFORNIA

PREPARED L R MORTALONI 31 AUG 1978 REPORT NO. PAGE 14

CHECKED

MODEL

TOP SUPPORT - CONTI

BASE PL. THICKNESS

$$f_b = \frac{P}{A_{PL}} \pm \frac{Mc}{I_{PL}} = \frac{550}{5130} \pm \frac{7408.8 * 142.5}{3.472 \times 10^7} = 0.107 \pm 0.03$$

↳ SMALL NEGLECT

$$w = \frac{550 * 18}{23.5 * 12 * 18} = 0.108^{K}/_{0}" * 18 = 1.944^{K}/_{IN}$$

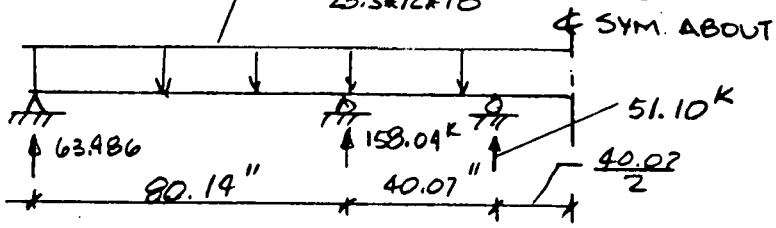

NOTE: BEAM BENDING SOLVED BY MOMENT DISTRIBUTION

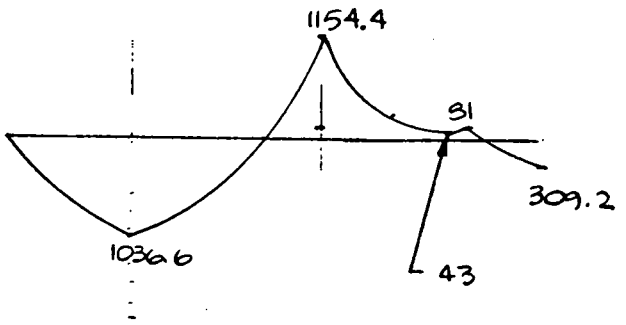

$$t = \sqrt{\frac{6M}{bF_y}} = \sqrt{\frac{6 * 1154.4}{18 * 27}} = 3.78"$$

USE PL 4"

STIFFENER PL

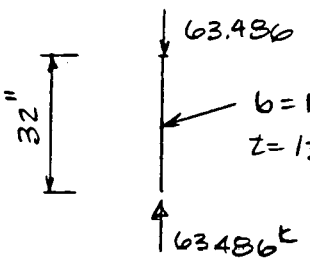

$A = 24.0"$ $I = 4.5$ $r = 0.433"$ $K = 1.0$

$$\frac{KL}{r} = 73.9 \Rightarrow F_a = 16.01^{K}/_{0}"$$

$$f_a = \frac{63.49}{24} = 2.65^{K}/_{0}" \quad \text{O.K.}$$

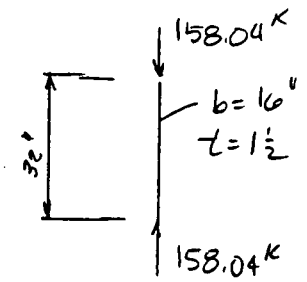

$$f_a = \frac{158.04}{24} = 6.59^{K}/_{0}" \quad \text{O.K.}$$

SUPPORT CALCULATIONS

EXCHANGERS IN

EXCESS EXCHANGER WEIGHT

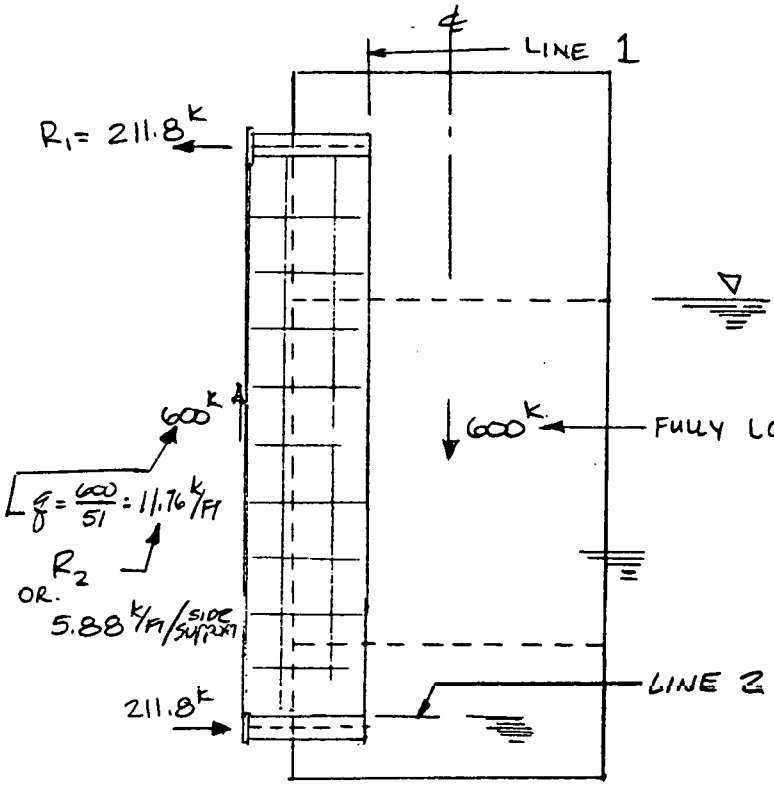

NOTE: FOR VERTICAL ACCELERATION

P = 0.15 * 1703 = 255.45 K

R_1 = 90.2 K

R_2 = 5.01 K/FT.

OR 2.50 K/FT/SUPPORT.

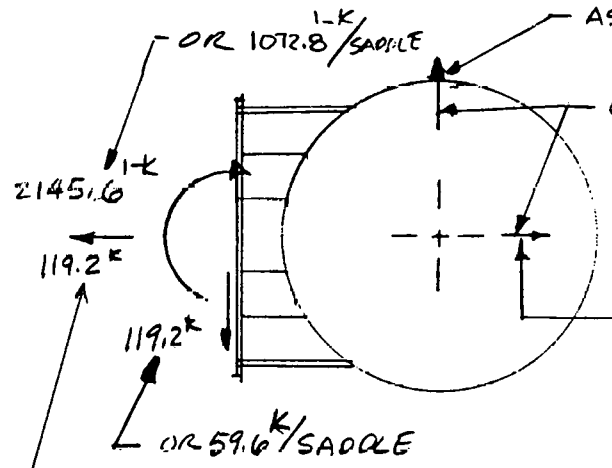

$A_{TOTAL\ SUPPORTS}$ = 2 * 852.39 + 394.5 * 2

= 2493.78 □"

$Q_{SADDLE} = \frac{394.5}{2493.78} * 119.2 = 18.9$ K/SUPPORT

$Q_{PLATE} = \frac{852.39}{2493.78} * 119.2 = 40.7$ K/SIDE SUPPORT

OR $f_{WELD\ PLATE_2} = \frac{40.7}{51 * 12} = 0.067$ K/IN

SUPPORT CALCULATIONS - CONTI

CHECK WELD STRESS ON COFFERDAM SIDE PLATE

LINE 1

$$q_{w1\,VERTICAL} = \frac{600+255.45}{2*51*12} = 0.699\ ^K/_{IN}$$

SEE CALC. BELOW FOR W10 REACTION

$$q_{w1\,HORIZ_1} = \frac{40.7}{51*12} = 0.067\ ^K/_{IN}$$

$$q_{w1\,HORIZ_2} = \frac{54.6}{5*12} < 0.91\ ^K/_{IN}$$

$$q_R = \sqrt{q_{w1_V}^2 + q_{w1H_1}^2 + q_{w1H_2}^2} = 1.15\ ^K/_{IN}$$

1 1/4" FW OK.

LIN 2

$$q_{w2} = \frac{211.8+90.2}{2*11*12} = 1.14\ ^K/_{IN}$$ 1/4" F.W. OK

COFFERDAM SIDE PL FLANGES'

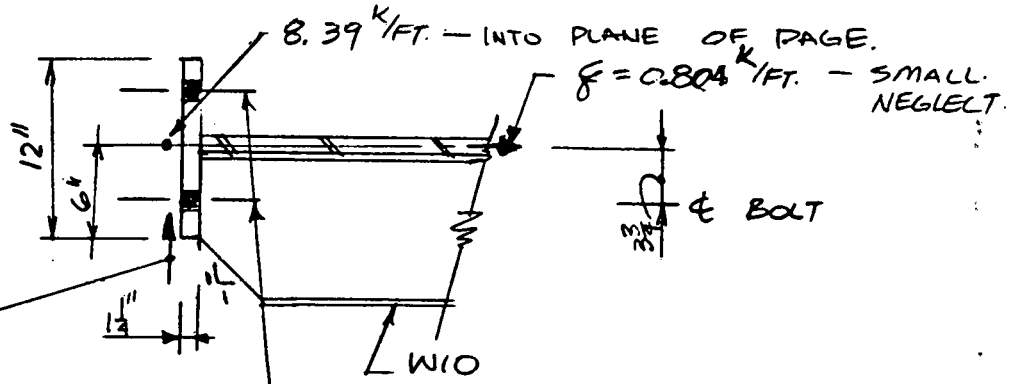

1 1/4" Φ BOLTS @ 12" O.C. — DUE TO CORROSION ASSUME BOLT EFF. = 3/4" Φ

$$q = \frac{54.6}{5^{FT}} = 10.92\ ^K/_{BOLT}$$ ← REACTION FROM HYDROSTATIC PRESSURE ON W10X33

SPACING OF W10

TOTAL SHEAR PER BOLT = $\frac{1}{2}\sqrt{8.39^2 + 10.92^2} = 6.88\ ^K/_{BOLT}$ (CONSERVATIVE).

O.K. FOR 1 1/4" Φ BOLT.

REACTION FROM W10X33 - SEE COFFERDAM PLATE DESIGN

OTHER LOADS DO NOT GOVER SADDLE DESIGN.

THIS PAGE

WAS INTENTIONALLY

LEFT BLANK

APPENDIX I.3

TUBE SELECTION/DESIGN DATA

TRW
SYSTEMS GROUP
ONE SPACE PARK • REDONDO BEACH • CALIFORNIA 90278

INTEROFFICE CORRESPONDENCE

78.6853.6-005

TO: R. Pearson CC: see Distribution DATE: 18 April 1978

SUBJECT: Fluted Tube Design Studies

FROM: C. E. Williamson
BLDG 81 MAIL STA. 1513 EXT. 62635

A study of fluted tube configurations manufactured by the GROB, INC process has been performed to establish candidate flute shapes with large (approx 1.5) area enhancement on configurations considered producible. The study included the following considerations:

1. Prediction of the GROB flute shape for a 2" dia tube scaled from GROB's 1" dia specimen.
2. Maintenance of an 0.040 deep convolute, regardless of tube diameter.
3. Constant thickness walls.
4. Wall thinning based on the GROB, INC/Union Carbide tube samples.
5. Wall thinning based on the GROB, INC/TRW first samples.

GROB, INC provided TRW with a drawing (Attachment 1) of the tubes they proposed to deliver to us. When received, the specimens matched the drawing precisely. These are the samples currently being tested for collapse pressure.

Our first design efforts were directed by the Project Office to address 2" dia tubes. Hence, the GROB 1" dia concept was scaled to a 2" dia based on maintaining the same level of material thinning. Attachment 2 was prepared and used as the basis for initial buckling analyses. Note: both the 1" and 2" tubes have low (approx 1.3) area enhancement.

Design layouts of 1", 1-1/2" and 2" dia fluted tubes based on maintaining the requested 0.040 flute depth were made. Tube wall thicknesses were based on preliminary predictions of thicknesses required for a corrugated/spiraled tube. Constant thickness was assumed. These concepts are illustrated in Attachment 3. Note that maintaining the 0.040 flute depth results in degraded

area enhancement at the larger diameters. Also note that equal 0.020 radii are not practical, when appropriate wall thicknesses are accounted for.

The next design iteration (Attachment 4, pages 1, 2, and 3) was based on constant wall thicknesses with tangent radii of the inner surfaces and ignoring the 0.040 flute depth constraint. The number of teeth was reduced until some tool tip radii was attained in the rills. These concepts are academic, since material thinning will occur during forming. Note that internal area enhancement is over 1.5.

Next, the degree of thinning experienced for the GROB, INC/Union Carbide tube was applied to the concepts of Attachment 4. These concepts are illustrated in Attachment 5, pages 1, 2, and 3 for the three diameters. Note that improved tool tip radii and tool wedge angles resulted. The inner profile, which is governed by the die remained unchanged. Area enhancement greater than 1.5 is realized.

The final design iteration is illustrated in Attachment 6, pages 1, 2, and 3. This concept accounts for wall thinning consistent with the first GROB/TRW specimens. Further improvement in tool tip radii and wedge angle was achieved. Note that these configurations, especially page 1, closely resembles the CMU configuration.

Status

No further design studies are planned unless requested by the Project Management, since these studies were considered out of scope with our PWA.

Recommendations

Depending on the results of the collapse pressure tests, we offer the following recommendations:

1. Review the designs of Attachment 6 for thermal characteristics.
2. Submit page 1 of Attachment 6 to GROB, INC for their review and request samples for pressure tests, if they concur.
3. Perform finite element analyses of these concepts to refine wall thicknesses.
4. Perform cost analyses to establish tube diameter for titanium in fluted configuration vs extruded aluminum.

Other Considerations

From a material volume standpoint, the titanium tubes in a CMU configuration are not competitive with fluted tubes unless the fins contribute to resistance to collapse pressures. Further studies are required to establish their contribution.

Tube cleaning considerations favor larger tubes.

Mike Nee and Dr. Hausrath favor consideration of smooth interior walled tubes in composite (0.020 inner liner of titanium in carbon steel or aluminum outer tubes). Several candidate fabrication methods require investigation, such as shrink fit, explosive forming or hydroforming. This concept may permit the use of larger diameter tubes. Thermal characteristics require analyses.

CEW:bai

DISTRIBUTION

T. Baumann
J. Denton
T. Dvorak
P. Edis
P. Fukunaga
A. Hausrath
J. Kaellis
L. Rosales
W. Tallon

attachments

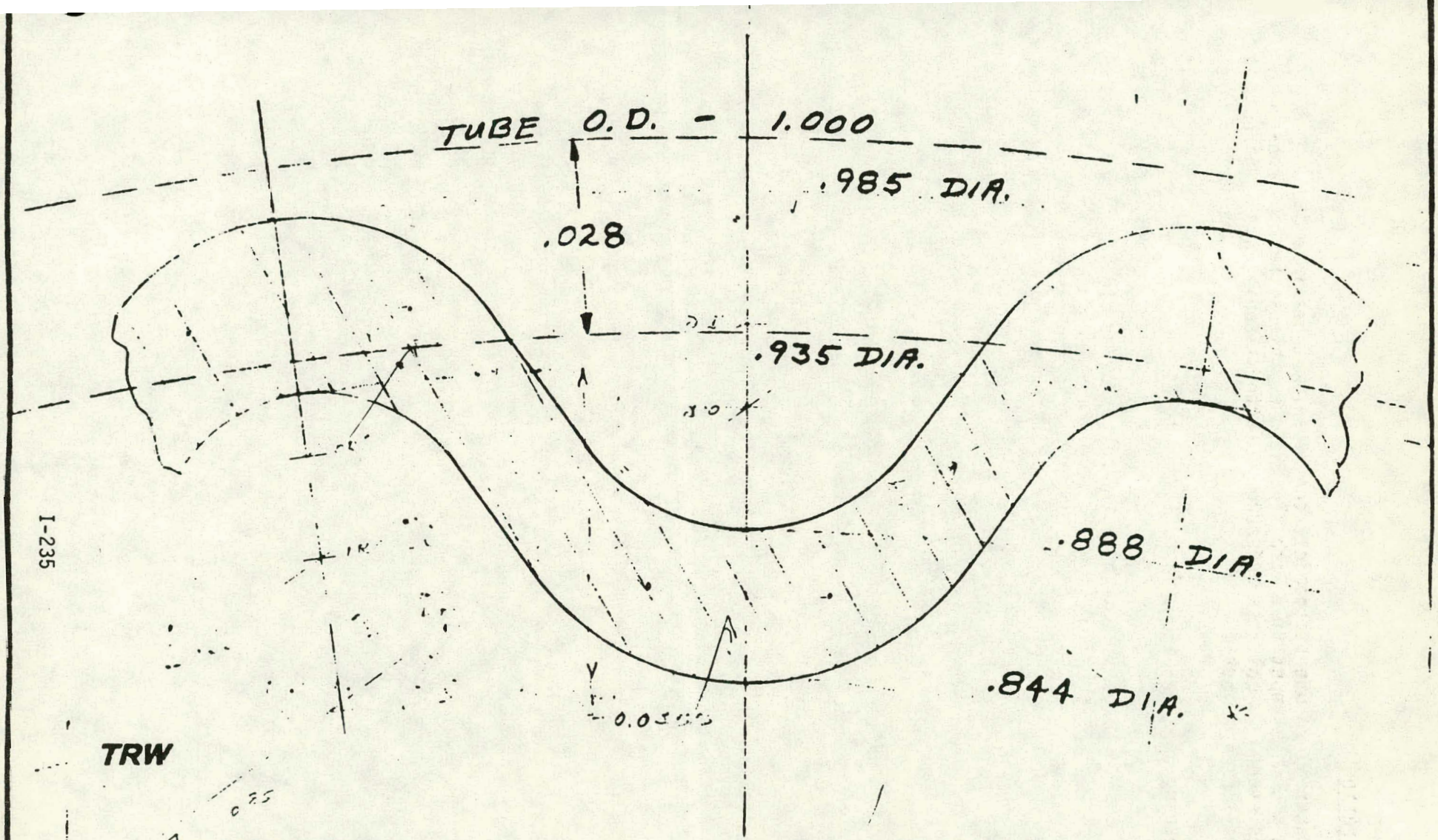

THOMAS C. DVORAK
Member of Technical Staff
Applied Materials Department

SYSTEMS GROUP OF TRW INC.
One Space Park, Redondo Beach, California 90278 (213) 679-8711

GROB INC. GRAFTON, WIS.

PROPOSED TOOTH SHAPE FOR TRW
22 TEETH 1" O.D x .028 WALL TITANIUM

NO. REQ'D	PART NO.	MATERIAL	HEAT TREATMENT	DRN. MFV	TR.	CH.
				DATE 5-2-70	SCALE 50 X	O. K.

TRW

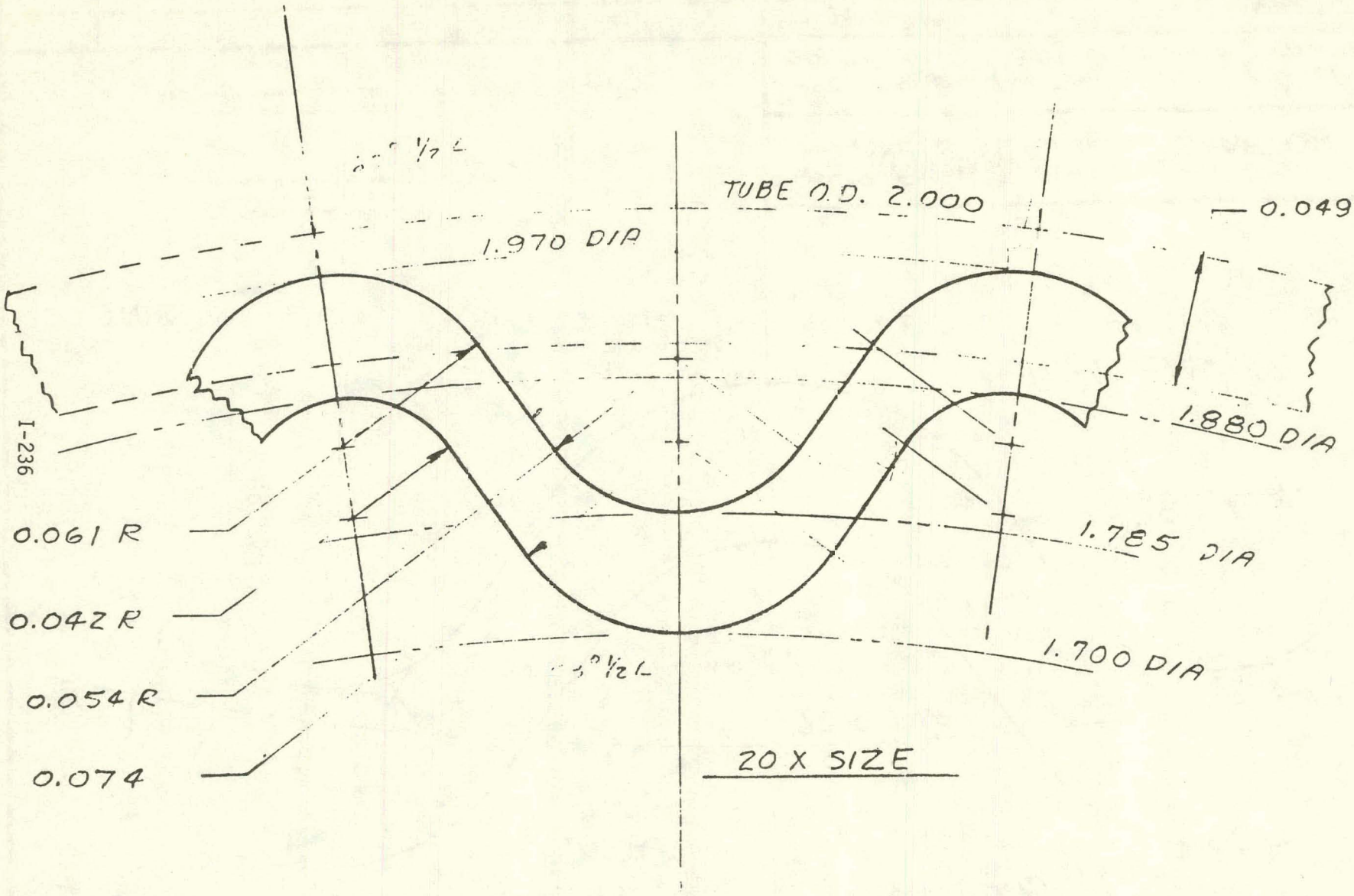

NOTE : ESTIMATED PROPORTIONS BASED ON [illegible] INC FORMING TECHNIQUE.

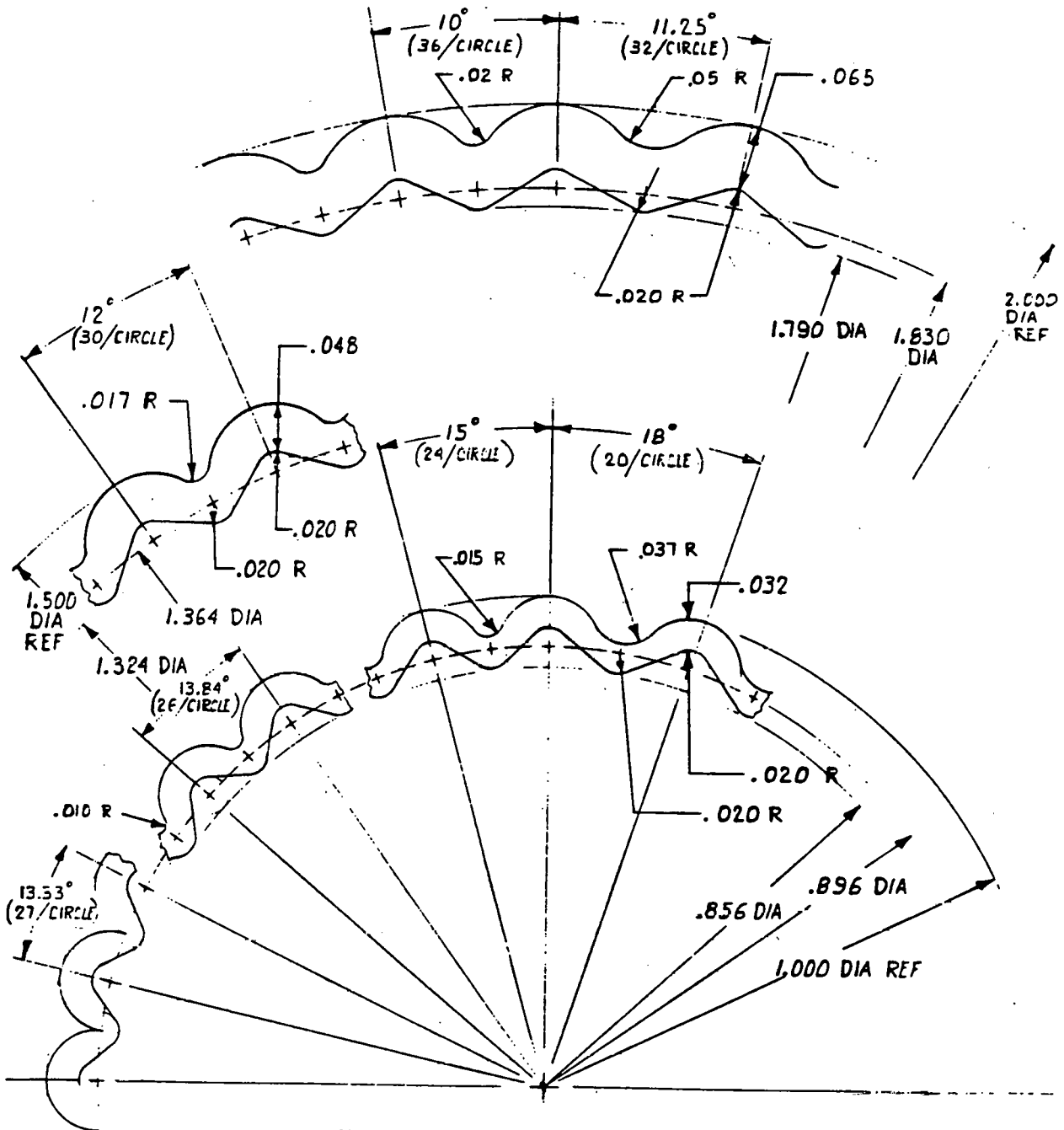

CONSTANT WALL THICKNESS CORRUGATED TUBES W/0.040
DEEP INNER SURFACE CONVOLUTES

CONSTANT THICKNESS DESIGN FOR 1" DIA FINISHED O.D.

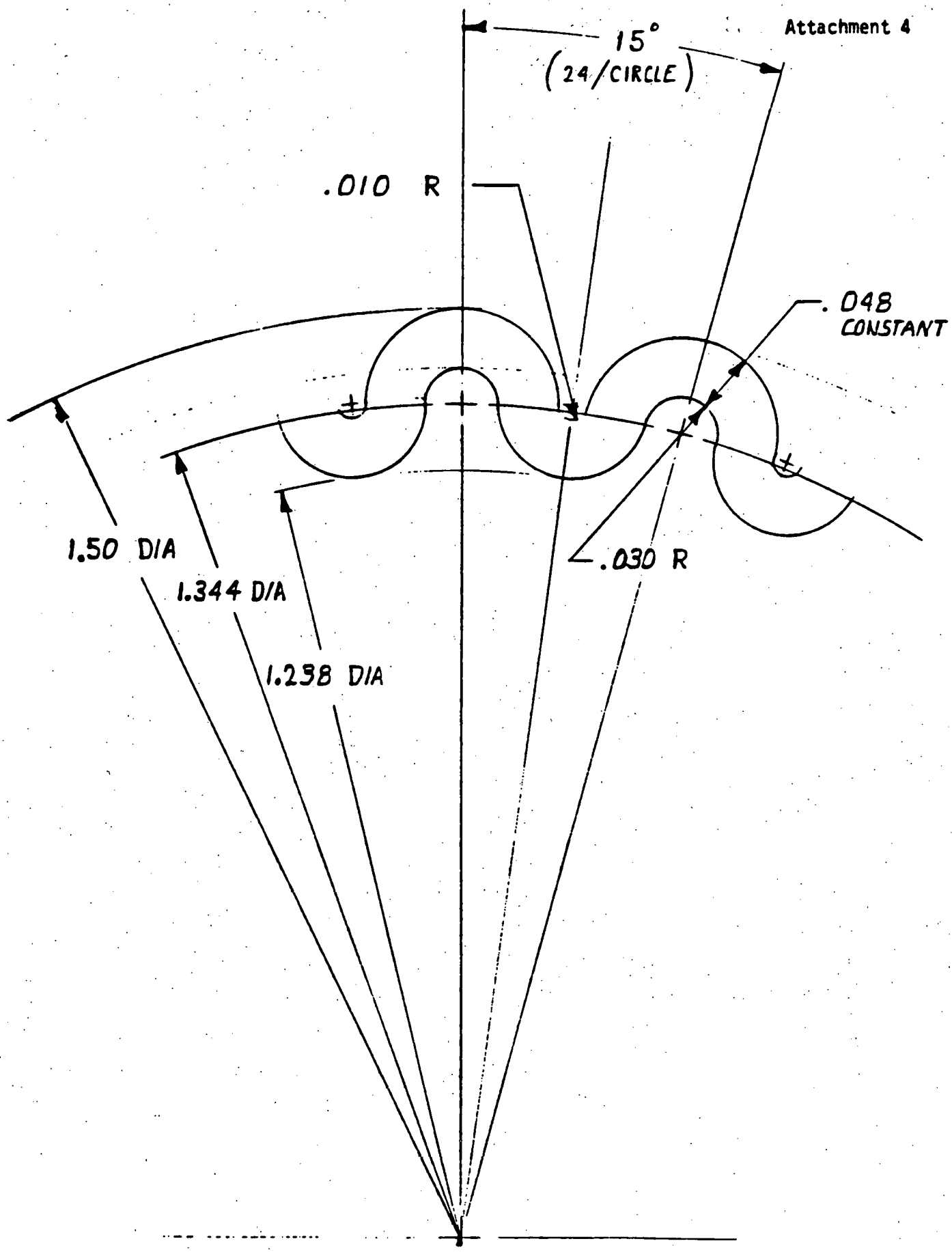

CONSTANT THICKNESS DESIGN FOR 1-1/2" DIA FINISHED O.D.

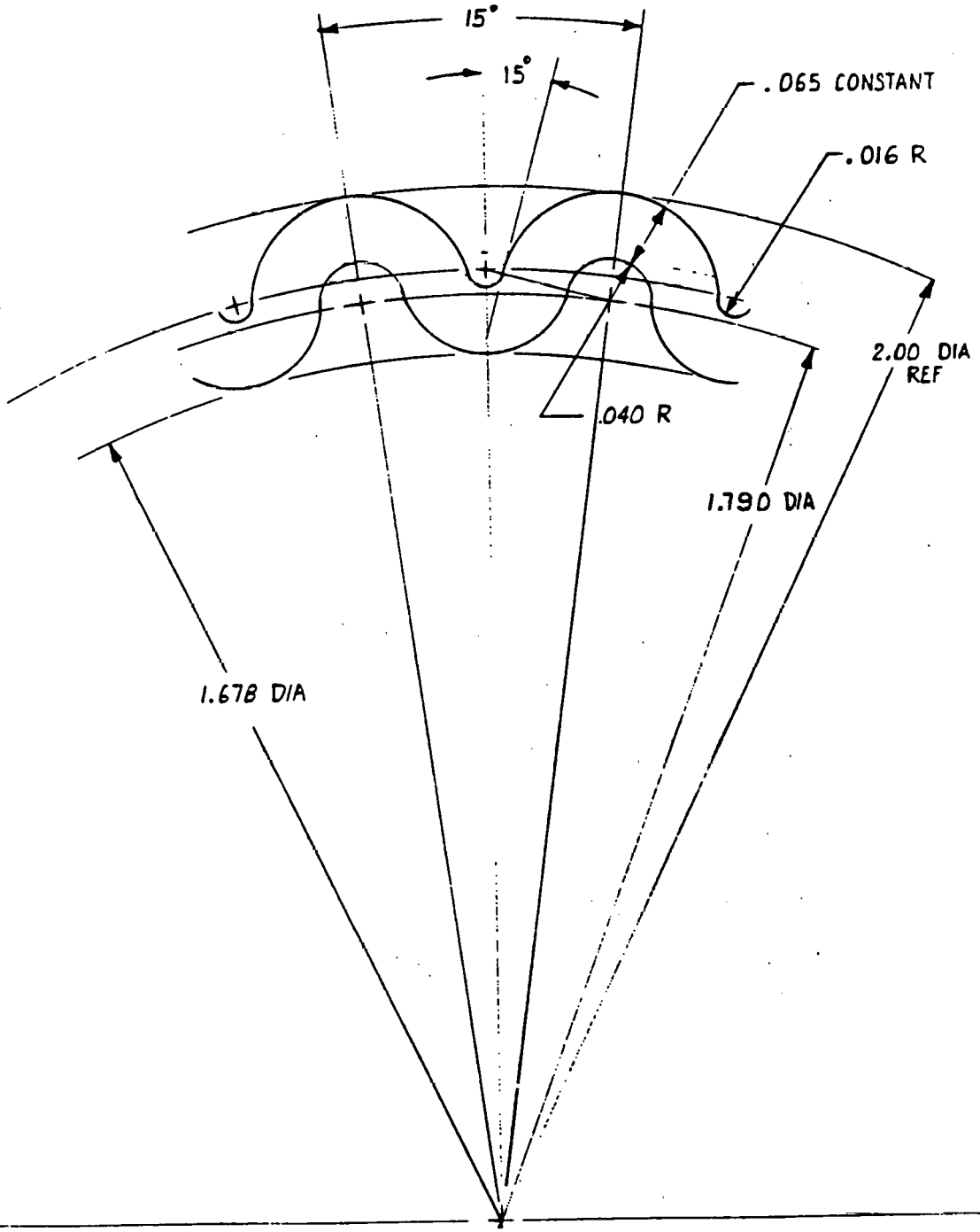

CONSTANT THICKNESS DESIGN FOR 2" DIA FINISHED O.D.

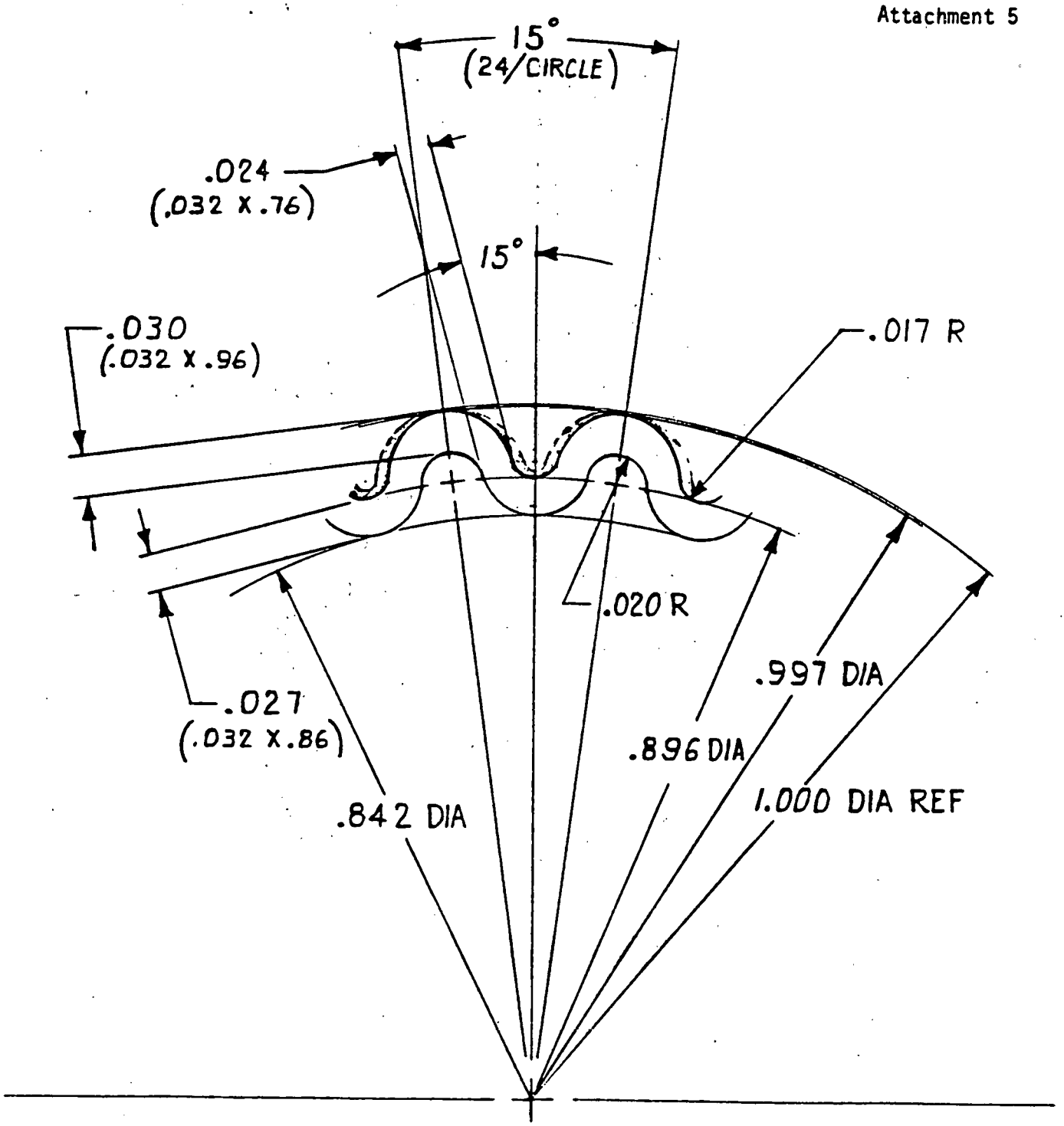

CONSTANT THICKNESS, 1" DIA FINISHED O.D. ADJUSTED
FOR THINNING BASED ON GROB/UNION CARBIDE RESULTS

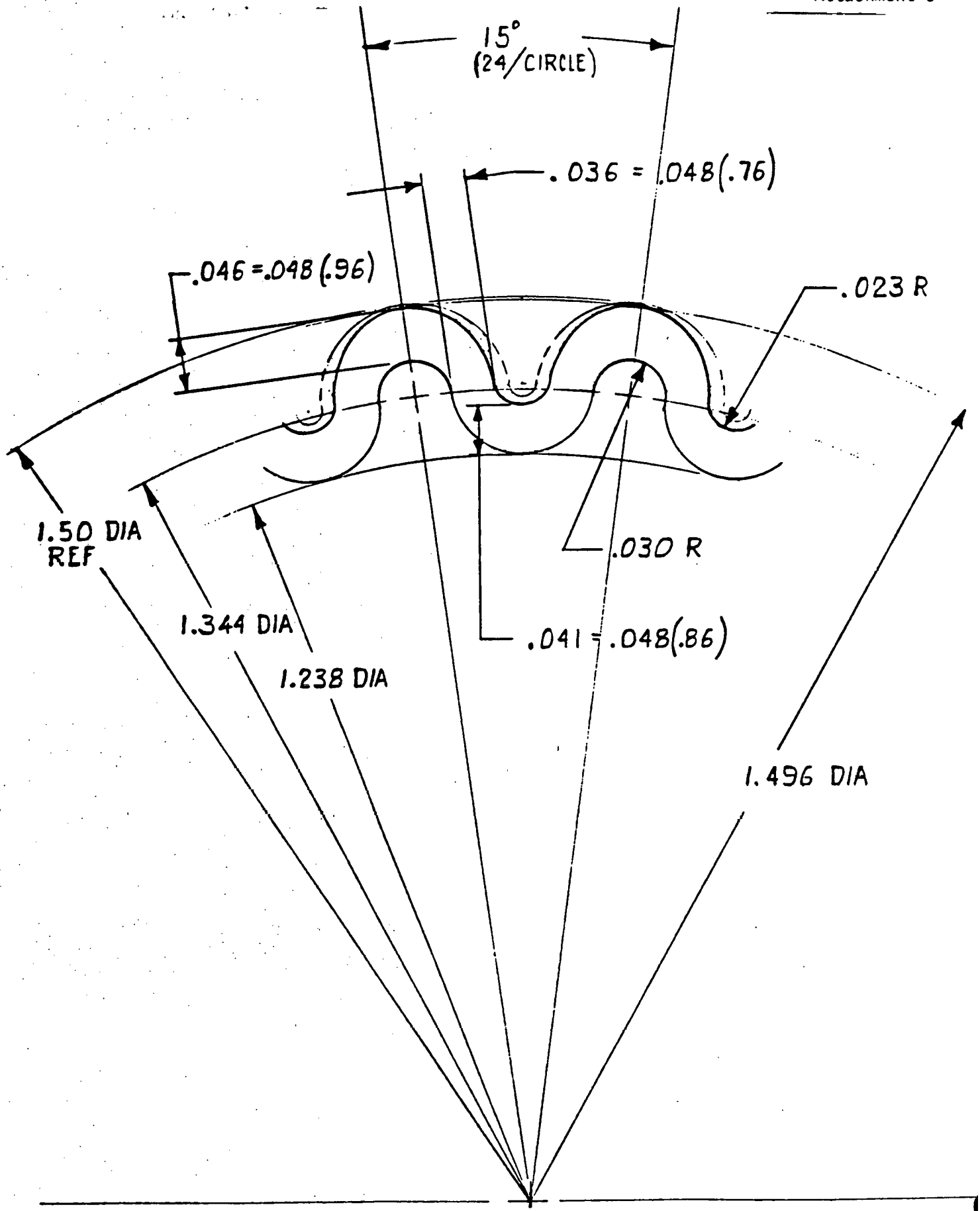

CONSTANT THICKNESS, 1-1/2" DIA FINISHED O.D. ADJUSTED
FOR THINNING BASED ON GROB/UNION CARBIDE RESULTS

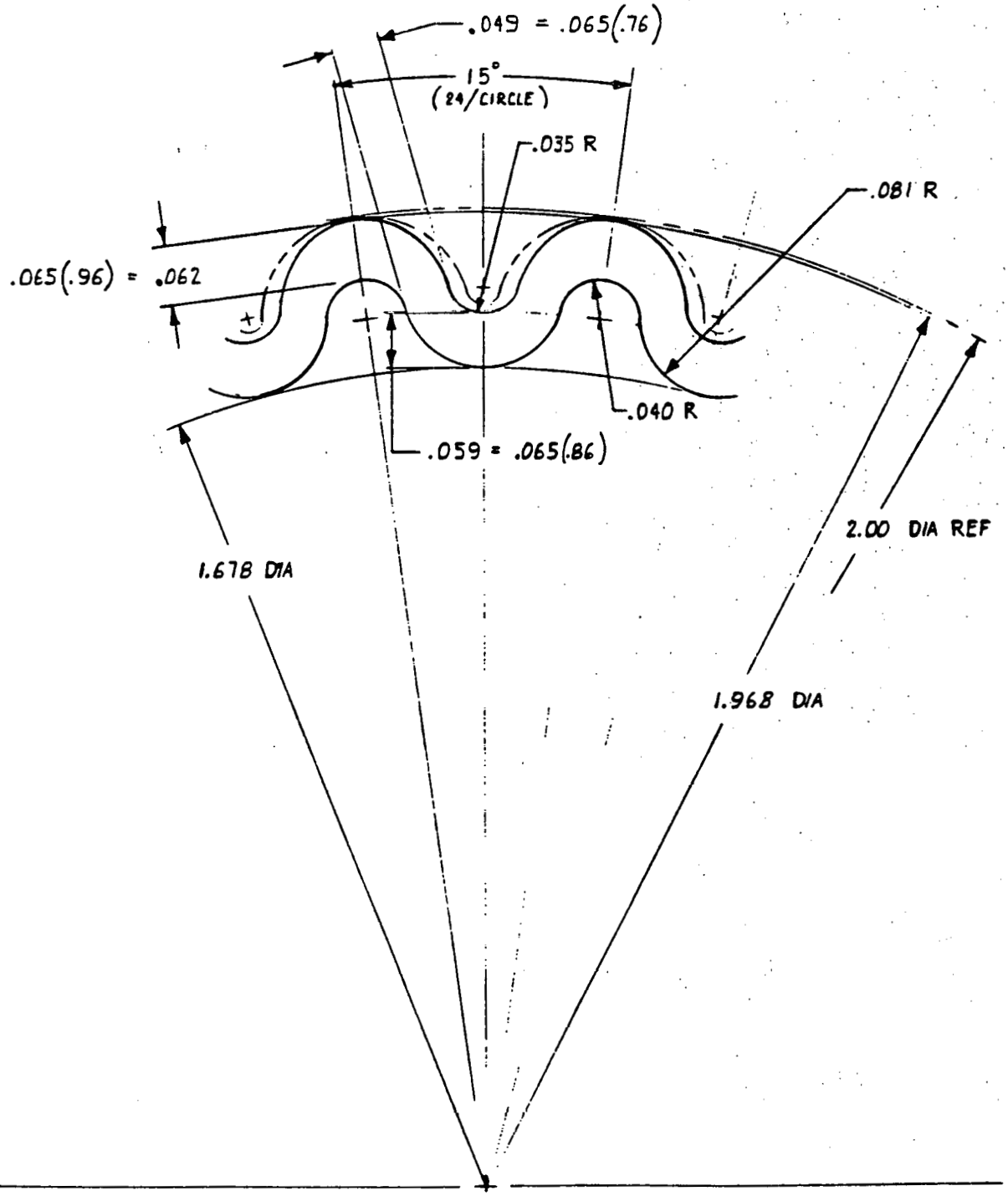

CONSTANT THICKNESS, 2" DIA FINISHED O.D. ADJUSTED
FOR THINNING BASED ON GROB/UNION CARBIDE RESULTS

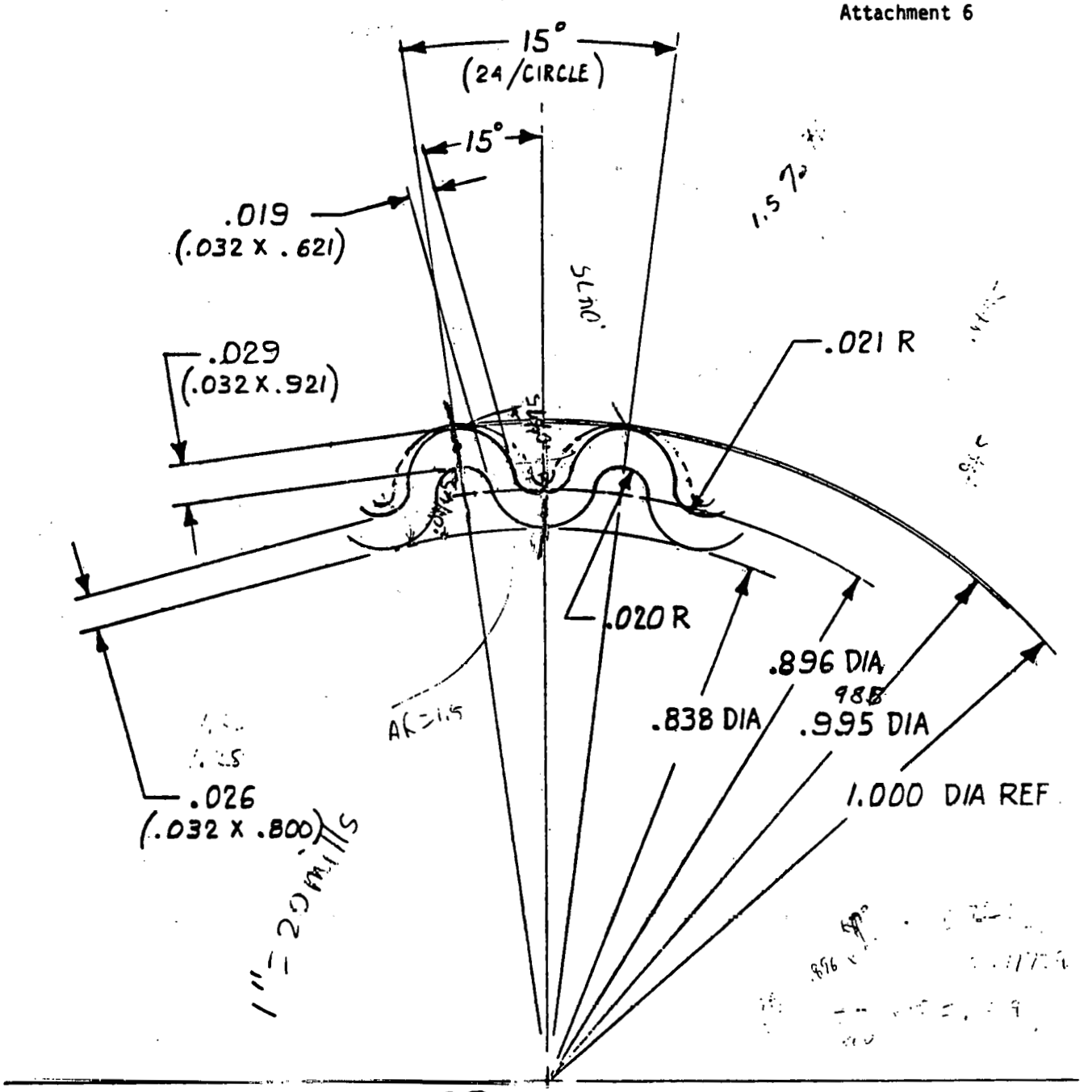

CONSTANT THICKNESS, 1" DIA FINISHED O.D. ADJUSTED
FOR THINNING BASED ON FIRST SAMPLES OF GROB/TRW DESIGN

.000

.021R X 50 = 1.05R

.995 DIA

.015 on DIA

= .0075 on R X 50 = .375

1.000

.031

.162 on DIA

.081 on rad x 50

= 4.05

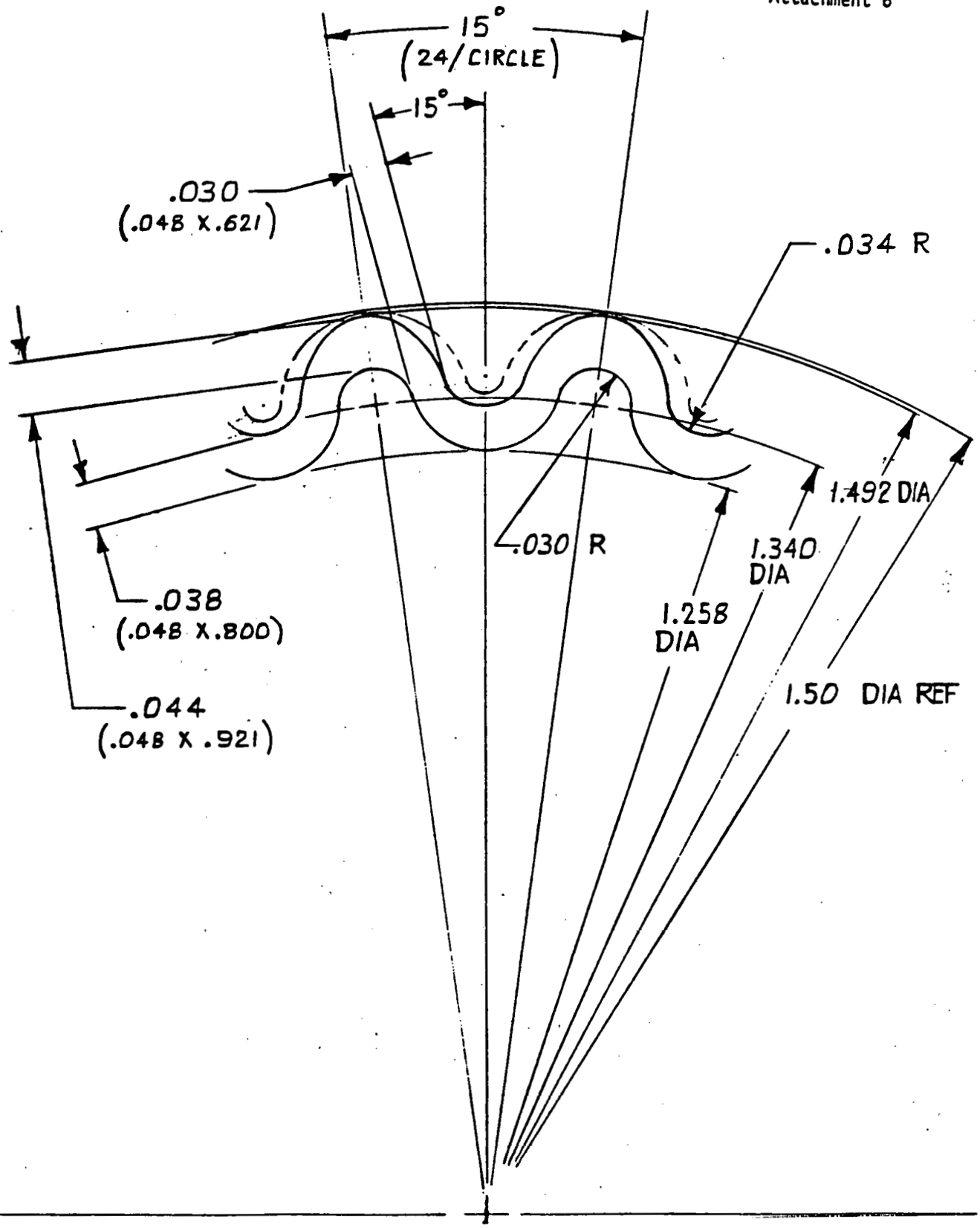

CONSTANT THICKNESS, 1-1/2" DIA FINISHED O.D. ADJUSTED
FOR THINNING BASED ON FIRST SAMPLES OF GROB/TRW DESIGN

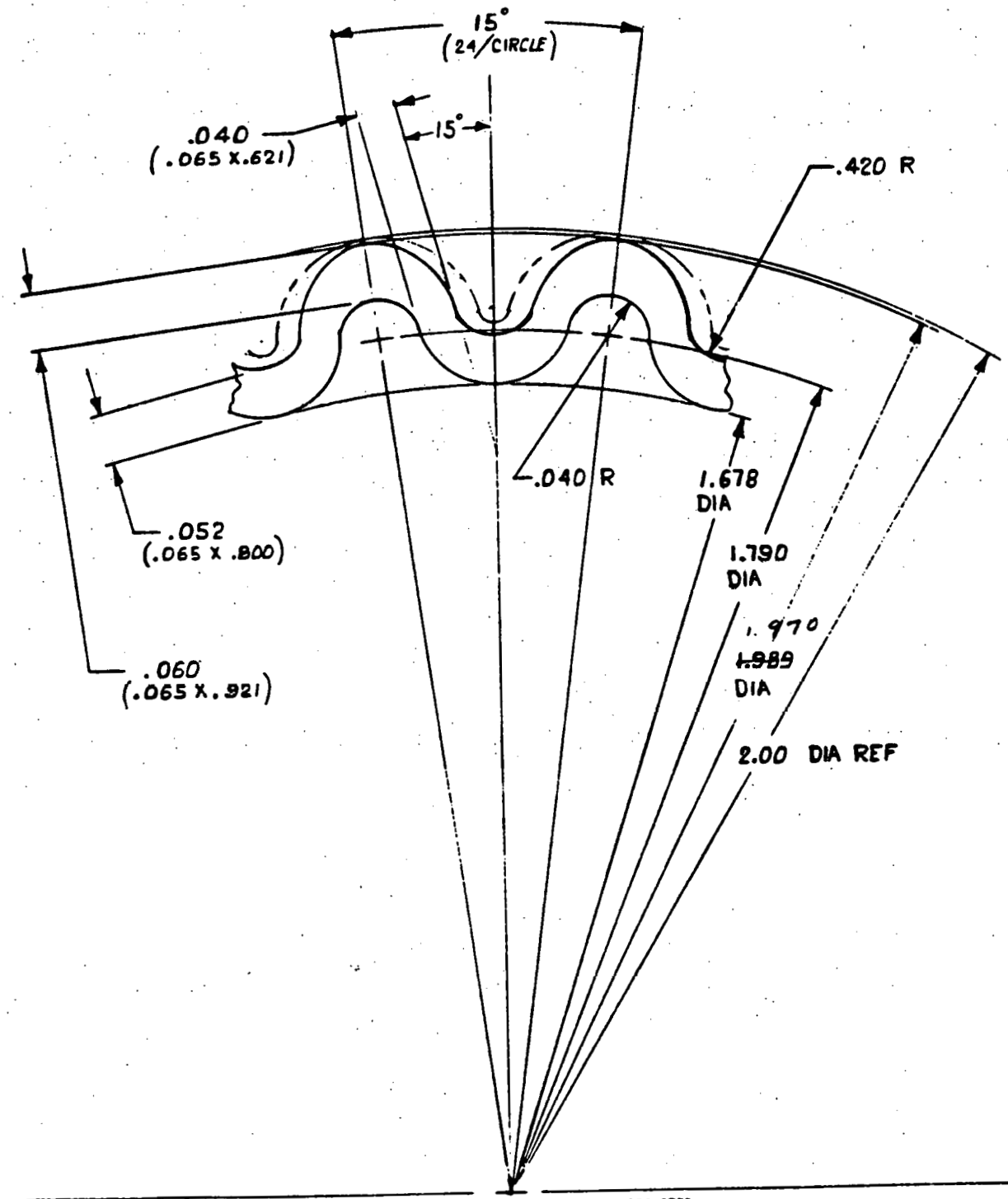

CONSTANT THICKNESS, 2" DIA FINISHED O.D. ADJUSTED
FOR THINNING BASED ON FIRST SAMPLES OF GROB/TRW DESIGN

TRW
DEFENSE AND SPACE SYSTEMS GROUP
ONE SPACE PARK • REDONDO BEACH • CALIFORNIA 90278

INTEROFFICE CORRESPONDENCE

TO: P. Edris CC: DATE: 19 May 1978

SUBJECT: Producibility Considerations for Tube Configuration Selection

FROM: L. A. Rosales

BLDG.	MAIL STA.	EXT.
01	2220	52630

Reference: "Tube Selection Meeting Minutes", P. Edris to Distribution, 17 May 1978

For convenience, the backup tube producibility data used for the selection (see reference) is included. The formability limits are given in graph form with best engineering judgement used to assess these limits. The first tubes attempted by Teledyne will be a 1.00 inch O.D. x .028 inch wall, C.P. Titanium (ASME SB338 GR2) formed to the CMU shape with a .040 inch amplitude (flute to rill). A total of 36 flutes will be attempted (pitch approximately .087 inch).

It is expected that the results of this run will be available about June 15, 1978.

LAR:dj

Distribution

T. Baumann
J. Denton
R. Douglass
T. Dvorak
P. Fukunaga
A. Hausrath
J. Hsu
J. Kaellis
G. Kikin
R. Pearson
W. Rogers
W. Tallon
C. Williamson

TUBE CONFIGURATION SELECTION

CRITERIA:

1. CMU Shape on O.D.
2. Maximum Possible Enhancement on I.D.
3. Maximum Nº of Flutes Possible
4. Titanium Tubing
5. Lowest Cost Forming Process

SELECTION

1. 1.00 INCH OD TUBE, 36 FLUTES, .040 INCH FLUTE HEIGHT, CORRUGATED CROSS SECTION.
   RATIONALE: THIS TUBE CONFIGURATION HAS A POSSIBILITY OF BEING ACCOMPLISHED BY AVAILABLE PROCESSES.

BACKUP POSITION

1. INVESTIGATE EFFECT ON HX COST/PERFORMANCE IF WE MUST USE:
   a) 28 FLUTES
   b) 32 FLUTES
   c) MODIFIED CMU PROFILE W/36 FLUTES
2. INVESTIGATE ALTERNATE MATERIAL (ALLEGHENY 6X).
   RATIONALE: IF 36 FLUTE PROFILE CAN NOT BE ACCOMPLISHED IN THICKNESSES REQUIRED FOR OTEC, EITHER THE PITCH MUST BE MODIFIED AND/OR THE SHAPE MUST BE CHANGED.
   : IF DOE DATA SHOWS THAT THE CORROSION ALLOWANCE REQUIRED FOR ALLEGHENY 6X IS VERY LOW (< .002), THEN THIS MATERIAL CAN BE USED SINCE $E = 30 \times 10^6$, $F_{ty} = 90$KSI (INITIAL WALL CAN BE THINNER).

TLIBE PRODUCIBILITY DATA

"CORRUGATED" APPROACH

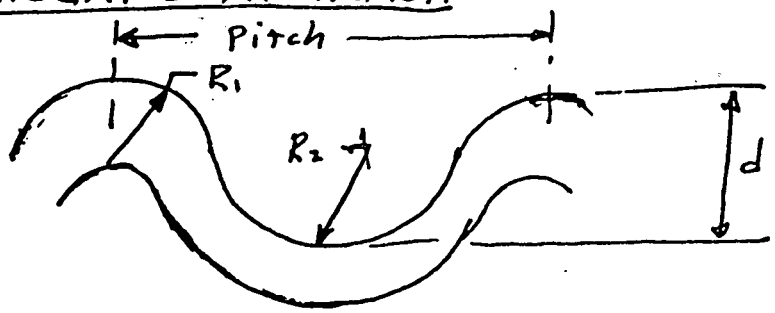

Mat'l: C.P. Titanium ASME SB 338 GR 2. Tubing of Equivalent

Key:

PRODUCIBLE	▭	BEST ENGINEERING JUDGEMENT AS OF 18 MAY 1978
POSSIBLY PRODUCIBLE	▨	
NOT PRODUCIBLE	▩	

O.D. / $\overset{\text{nominal}}{\text{thick.}}$ / d / R_1 / R_2 / shape = Identification Code

Identification Code	Number of Flutes (Pitch)									
	0 → 22	24	26	28	30	32	34	36	38	40
	(0 - .143)	(.131)	(.121)	(1.12)	(1.05)	(.098)	(.092)	(.087)	(083)	(.079)

1/.028/.040/.020/.020/ CMU

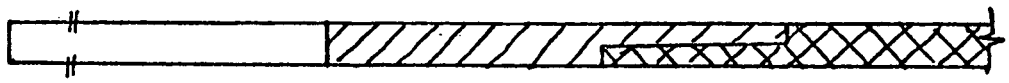

1/.038/.040/.020/.020/ CMU

1/.031/.040/$\overset{R_1}{+\Delta}$/$\overset{R_2}{-\Delta}$/ Modified CMU

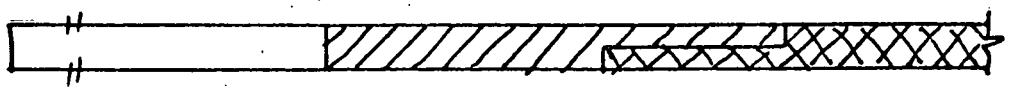

Candidate Forming Processes / Fabricators

1. Form / Roll — Teledyne - Aero Cal, San Marcos, Calif
2. Drawing — Valley Metals, El Cajon, Calif (or) La Fiell Tube, Santa Fe Spr., Calif.
3. Pneumatic (Hot) — Rockwell, Los Angeles, Calif
4. Roll / Upset — Grob Inc, Grafton, Wis. (or) Yorkshire - Imperial, Leeds, England.
5. Hydraulic — TRW - Materials Engineering Dept.

TUBE PRODUCIBILITY DATA

"RIBBED" APPROACH

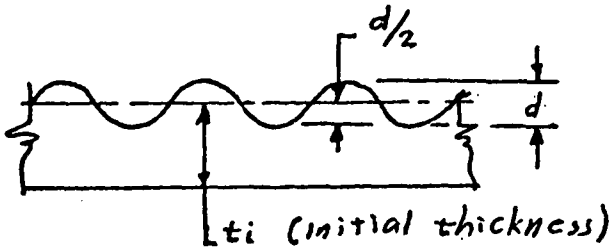

Mat'l: C.P. Titanium
ASME SB 338 GR 2
Tubing or Equivalent

Key:

PRODUCIBLE
POSSIBLY PRODUCIBLE
NOT PRODUCIBLE

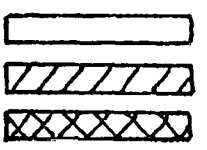

} BEST ENGINEERING JUDGEMENT AS OF 18 MAY 1978

d (inches) Initial Thickness (inches)

d (inches)	0-.040	.044	.048	.052	.056	.060	.064
~~.025 to .040~~ .025 to .040							

Candidate Processes / Fabricators

1. Roll / Upset — Grob, Grafton, Wis. (Info reflected in graph)
2. Coining — Nardon, Alhambra, Calif (Info incomplete)
3. Roll — (No vendor ~~with~~ located)
4. Extrusion — Nuclear Metals, Concord, Mass. (Very expensive)
5. Embossing — Rigidized Metal, Buffalo, N.Y. (Refused to quote).

TRW
DEFENSE AND SPACE SYSTEMS GROUP
ONE SPACE PARK - REDONDO BEACH - CALIFORNIA 90278

INTEROFFICE CORRESPONDENCE

TO: J. W. Denton CC: Distribution DATE: 30 May 1978

SUBJECT: OTEC Heat Exchanger Tube Structural Trade-off and Analysis

FROM: T. R. Baumann TRB
BLDG. 81 MAIL STA. 1513 EXT. 62635

INTRODUCTION

This memorandum summarizes the results of the structural tradeoff studies of five selected titanium tube candidates for the OTEC Heat Exchanger tubes. It also summarizes the structural design criteria used in the analysis.

SUMMARY

Five selected candidate configurations for OTEC Heat Exchanger tubes were analyzed. The results of the analysis are summarized in Table 1. All candidates were titanium corrugated tubes having diameters of 1, 1 1/2 and 2 inches. The thickness requirements for each of these candidates were established from ASME pressure vessel code requirements for round tubes. Each candidate was analyzed by a finite element computer analysis to derive a "corrugation factor" which accounts for the effect of the difference between the actual tube shape and a round tube. Some of the candidate configurations showed a substantial reduction in external pressure capability due to corrugation.

DISCUSSION

Five titanium tube candidates were selected for analysis. Thickness requirements were established for each candidate for an evaporator pressure of 136 psi and a condenser pressure of 86 psi in tube diameters of 1, 1 1/2 and 2 inches.

Each candidate configuration was first analyzed by a finite element computer analysis to derive its corrugation factor. The "corrugation factor" is the ratio of the buckling pressure of the corrugated tube to that of an equivalent round tube of the same diameter and reference thickness. The SAP - IV finite element computer program was used for this analysis. Previous studies of a similar corrugated tube configuration have shown excellent comparison of SAP IV results with static analysis using the Nastran computer program. An attempt was made to derive a corrugation factor with the Nastran shell buckling procedure, this was however unsuccessfull due to problems encountered in the Nastran software by the program vendor.

Tests conducted on a limited number of corrugated and round tubes samples have shown that the static analysis for derivation of the corrugation factor is adequate for use in tube design.

The corrugation factors for each candidate were used to compute an effective pressure of an equivalent round tube of the same diameter and reference thickness. The effective pressure was then applied to round tube design curves derived from the ASME pressure vessel code to select the required thickness of the corrugated tube. The results of this analysis are shown in Table 1 and Figure 1. The use of the ASME code data rather than a less conservative procedure is discussed in the following paragraphs.

DESIGN CRITERIA OPTIONS

Three structural design criteria options were evaluated in the tube structural requirements study. The effect of these options is shown in Figure 2 for the selected tube design candidate (1 inch tube/36 corrugations). Option 3 results in a decrease in required wall thickness of .005 inches in the evaporator and .004 inches in the condenser. This option was however not selected due to its extremely high risk. Option 2 results in a decrease of .001 inches in the evaporator and .0015 inches in the condenser. Since these savings are small and the option involves both additional risk and potential test problems Option 2 was not selected. Option 1, which was the baseline option in the study, was selected as the appropriate structural design criteria for sizing OTEC Heat Exchanger tubes. This option uses the ASME pressure vessel code for round tubes and compensates for loss of external pressure capability based upon finite element deflection analysis of the corrugated tube.

OPTION 1

This procedure is based upon the ASME pressure vessel code. Corrugated tubes are evaluated based upon an equivalent round thin walled cylinder shape. The degradation of buckling pressure due to corrugation is accounted for by an analytical corrugation factor which is derived by finite element analysis of both the corrugated tube and equivalent round tube. The corrugation factor is the ratio of the buckling pressure of the corrugated shape to the buckling pressure of the equivalent round tube. The round tube allowable buckling pressures are computed using the procedure for determining the thickness of shells and tubes under external pressure, according to the ASME boiler and pressure vessel code (Section VIII, Division 1, UG - 28). Tubes designed to this procedure should present no problems when tested to a pressure of 1.5 times the maximum allowable pressure required by the ASME code for hydrostatic testing. They also should present no problems under operating conditions when subjected to additional loading conditions such as sea state dynamics. This option is a conservative low risk approach which will require a minimum of effort to satisfy safety and environment requirements. Qualification and acceptance testing will also be minimized.

OPTION 2

This analytical procedure is similar to that in Option 1 with the following exception. The allowable buckling pressure is computed based upon the theory of elastic stability for round cylinderical tubes having an initial out of roundness of one percent. Corrugated tube requirements are obtained by use of the same analytical corrugation factor derived for Option 1. This procedure increases the allowable buckling pressure. Since it also removes most of the ASME code safety margin a factor of safety of 1.25 must be added to assure that the tubes will not fail. This is considered the minimum acceptable factor and will lower the allowable pressure accordingly. Tubes designed to this procedure should be able to withstand a pressure of 1.25 times the maximum allowable pressure required by the ASME code for pneumatic testing but may not be able to withstand the pressure required for hydrostatic testing of the Heat Exchanger structure according to ASME code and may require either pneumatic testing or an exemption from testing to the ASME code. This option may also present problems when combined loading conditions due to sea state dynamics are analyzed. It will require a substantial effort to show that it satisfies safety and environmental requirements and will require a more extensive effort for tube qualification and acceptance testing. This procedure is a moderate risk approach.

OPTION 3

The analytical procedure for Option 3 is almost the same as Option 2, However, instead of using elastic stability theory, a curve based upon the mean of actual test results is used. Past testing of steel tubes shows that the actual buckling pressure is somewhat higher than predicted by use of an initial one percent out of roundness assumption in elastic stability theory. The steel tube test data is converted to equivalent titanium data and utilized to predict the buckling pressure of round thin walled cylindrical tubes. Corrugated tube data is again obtained by use of the analytical corrugation factor. The risk in this procedure is high since the test data curve is based upon the average of a great many commerical tubes taken at random from stock. In several individual tests buckling pressures comperable to perfectly round tubes were achieved while other tests had failures at lower pressures than the test data curve. As in the case of Option 2 this procedure requires use of a minimum factor of safety of 1.25. Tubes designed to this procedure might be able to withstand a pressure required by the ASME code for pneumatic testing but there is a high degree of risk of tube failure. Hydrostatic testing according to the ASME code should not even be considered for this option unless the tubes are pressurized internally. This option also involves a high degree of risk for combined loading conditions. The procedure would require a large analytical and test effort to show that it satisfies safety and environmental requirements.

REFERENCE LIST

1) ASME — "ASME Boil and Pressure Vessel Code Section VIII Division 1", 1 July 1977, Amer. Soc. of Mechanical Engineers

2) KING — " Pipeing Handbook" , Fifth Edition 1967, Mc Graw Hill Co.

3) ASME — "Pressure Vessel and Piping Design Collected Papers 1927-1959" 1960, American Soc of Mechanical Engineers

4) MEGYESY — "Pressure Vessel Handbook", Oct, 1977, Pressure Vessel Handbook Publishing Co.

5) EER 73-11 — "SAP IV Structural Analysis Program for Static and Dynamic Response of Linear System", April, 1974 Univ. of Calif. Berkeley, CA.

TABLE 1
TITANIUM TUBE THICKNESS REQUIREMENTS
FOR OTEC HEAT EXCHANGER TUBES
(1, 1 1/2 AND 2 INCH TUBE DIAMETERS)

CANDIDATE TUBE CONFIGURATIONS	CORRUGATION FACTOR	EFFECTIVE PRESSURE (PSI)		TUBE THICKNESS (INCHES)					
				EVAPORATOR TUBE DIAMETER (INCHES)			CONDENSER TUBE DIAMETER (INCHES)		
		EVAP.	COND.	1"	1-1/2"	2"	1"	1-1/2"	2"
SINGLE FLUTE TUBE SMOOTH INSIDE (64 CORRUGATIONS)*	1.000	136	86	.023	.035	.047	.020	.030	.040
DOUBLE FLUTE TUBE .026 AMP. (64 CORRUGATIONS)**	.840	162	102	.024	.036	.049	.021	.032	.043
DOUBLE FLUTE TUBE .040 AMP. (64 CORRUGATIONS)**	.660	207	130	.026	.039	.053	.023	.034	.046
GROB CONFIGURATION TUBE (24 CORRUGATIONS)***	.375	363	229	.033	.049	.065	.027	.041	.055
CMU EXTERNAL CONFIGURATIONS TUBE (36 CORRUGATIONS)***	.416	327	207	.031	.047	.063	.026	.040	.053

1) ALL THICKNESSES ARE IN INCHES

2) ALL THICKNESS REQUIREMENTS ARE BASED UPON ASME CODE AND SAP IV COMPUTER ANALYSIS.

3) THICKNESS ARE MINIMUM AND SHOULD BE INCREASED BY 10% FOR MANUFACTURING TOLERANCES TO OBTAIN NOMINAL THICKNESSES.

* BASED UPON INSIDE DIAMETER. THICKNESS DOES NOT INCLUDE FLUTE MATERIAL.

** BASED UPON AVERAGE INSIDE DIAMETER. THICKNESS IS MINIMUM THICKNESS OF TUBE.

*** BASED UPON EXTERNAL DIAMETER. THICKNESS IS ORRIGINAL ROUND TUBE THICKNESS PRIOR TO CORRUGATION PROCESS. MINIMUM THICKNESS IS 60% OF ORRIGINAL THICKNESS.

FIGURE 1
TITANIUM HEAT EXCHANGER TUBE
CANDIDATE COMPARISON

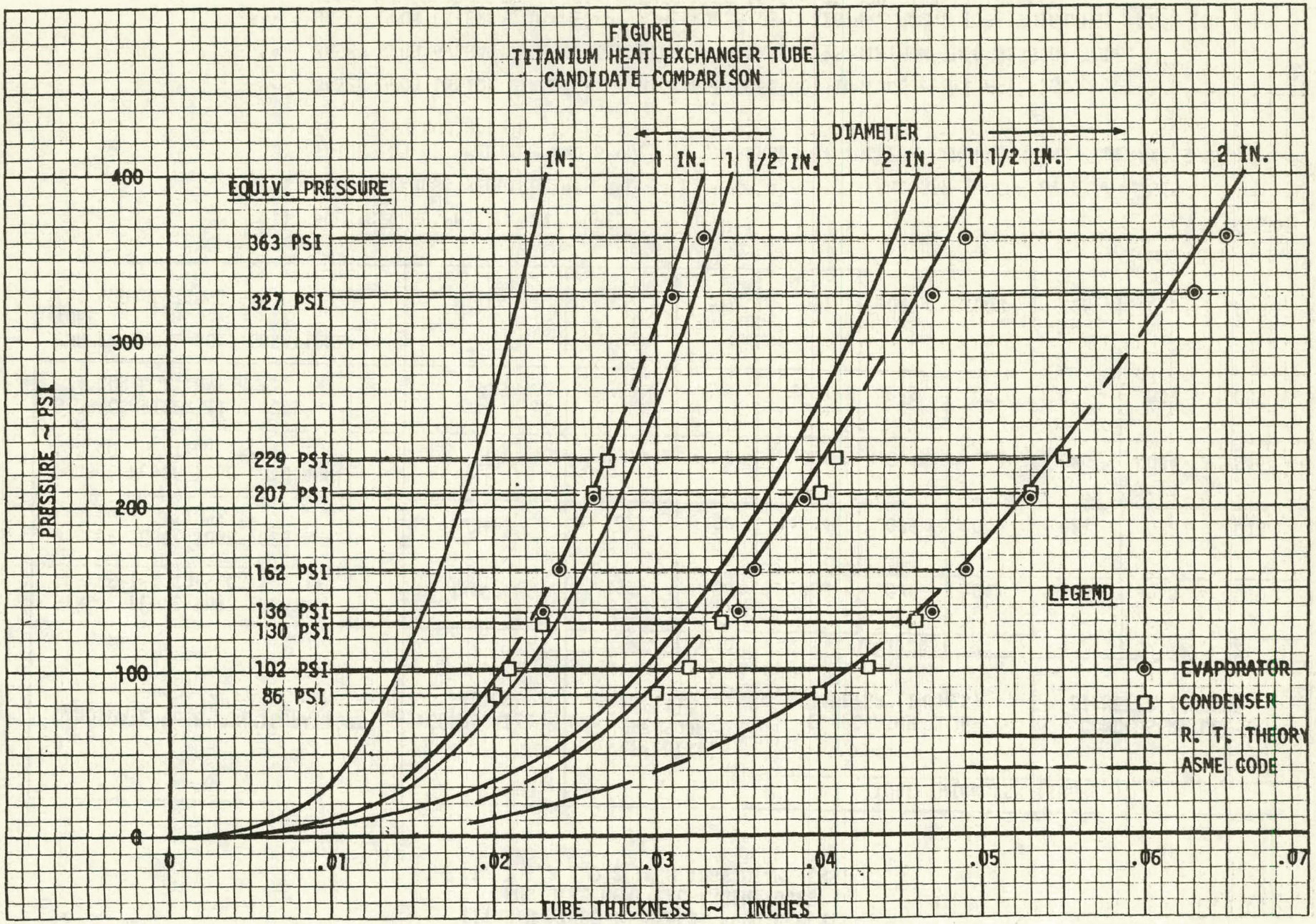

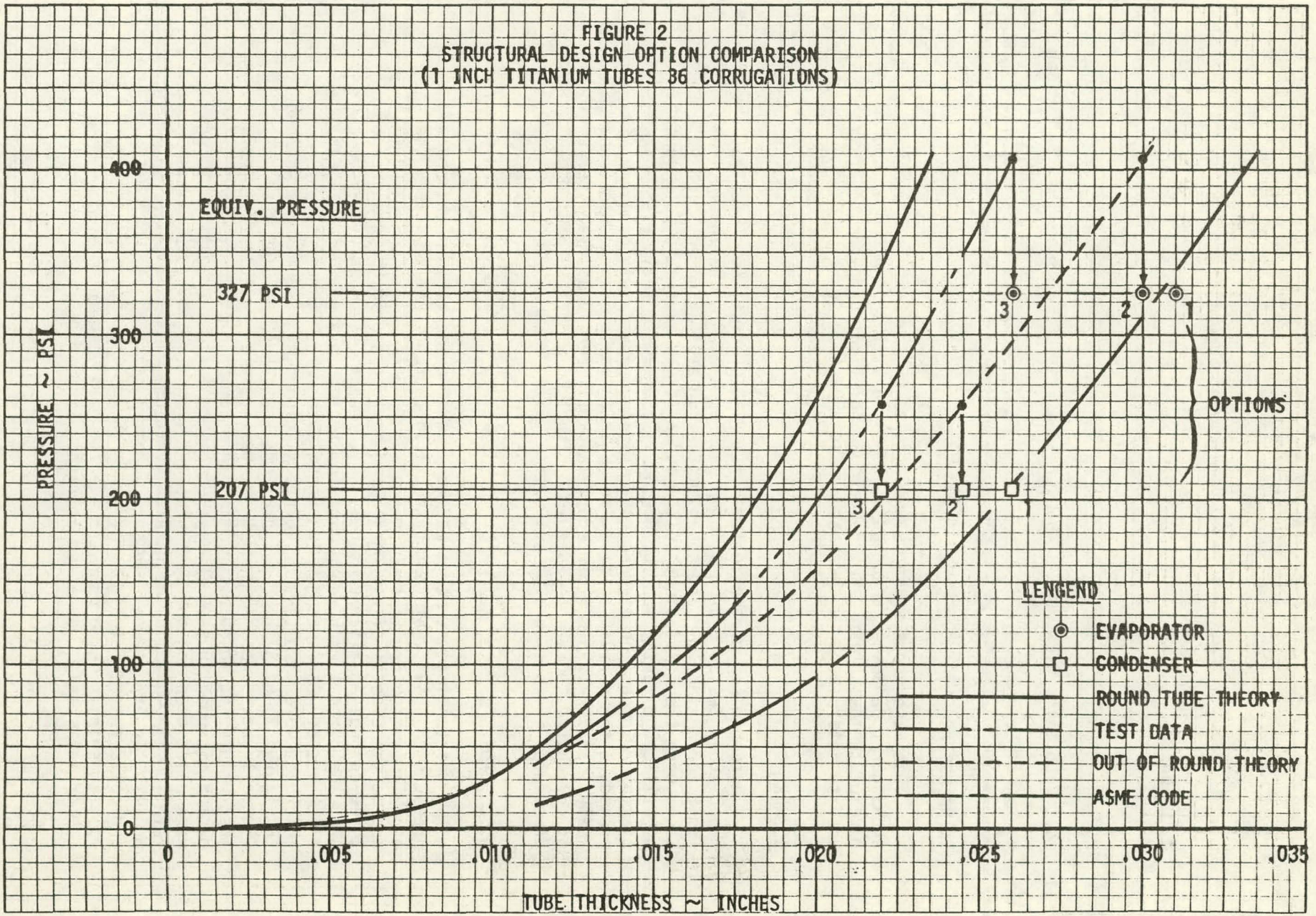
FIGURE 2
STRUCTURAL DESIGN OPTION COMPARISON
(1 INCH TITANIUM TUBES 36 CORRUGATIONS)
PRESSURE ~ PSI
400
300
200
100
0
EQUIV. PRESSURE
327 PSI
207 PSI
3
2
1
OPTIONS
LENGEND
EVAPORATOR
CONDENSER
ROUND TUBE THEORY
TEST DATA
OUT OF ROUND THEORY
ASME CODE
0
.005
.010
.015
.020
.025
.030
.035
TUBE THICKNESS ~ INCHES

TRW
SYSTEMS GROUP
ONE SPACE PARK • REDONDO BEACH • CALIFORNIA 90278

INTEROFFICE CORRESPONDENCE

TO: J. W. Denton CC: Distribution DATE: 1 June 1978

SUBJECT: Test Report for OTEC Heat Exchanger Tube Tests

FROM: T. R. Baumann TRB
BLDG 81 MAIL STA. 1513 EXT. 62635

INTRODUCTION

This memorandum presents the results of the OTEC Titanium heat exchanger tube tests conducted on 18-19 April 1978. A comparison is made of the test results with various analytical computer studies used to determine tube external pressure capability.

SUMMARY

A comparison of the test results with predictions shows that the round tubes tested had buckling pressures close to the theoretical limit for perfectly round tubes, which is better than anticipated. Based upon the limitations in the number of samples this data cannot be utilized directly in tube design without additional test substantiation. Comparison of test data with the results of the analytical procedure for derivation of a "corrugation factor" showed that the analytical SAP-IV 3 DOF procedure was sufficiently accurate for design of corrugated tubes when used in conjunction with the ASME code procedures for pressure vessel design.

DISCUSSION

Tube testing was performed to determine the maximum external pressure capability of corrugated titanium tubes and to verify the analytical procedure for computing the reduction in pressure capability due to the effects of corrugation. The test specimens consisted of three corrugated titanium tubes (22 corrugations) manufactured by GROB Inc. from 1 inch round titanium tubing having a norminal wall thickness of .028 inches. Two round tubes of .028 nominal wall thickness were also tested. Cross sections to these tubes are shown in Figures 2 and 3. Table 1 presents the results of the five tests. Figure 1 shows a comparison of the test results to the predicted test values and to buckling strength relationships commonly used for design of round tubes. Tube strength predictions prior to testing were based upon the one percent out of round elastic stability relationship which is the generally accepted lower limit for round tube buckling under external pressure. Past testing on steel tubes indicates a somewhat higher pressure capability, however, the test relationship is based upon the average of a large number of commerical steel tubes taken at random from stock.

Individual failures during past testing ranged all the way from round tube theory for perfectly round tubes to values near the one percent out of round relationship. The round titanium samples of this test achieved pressures of 710 and 720 PSI in test which is slightly above the theoretical limit for perfectly round tubes. Some of the factors which account for the test pressure being above the theoretical limit are the tube thickness (average thickness was slightly above .026 used in predictions) and modulus of elasticity (15.5 x 10^6 PSI lower limit for titanium was used in computations). Taking these factors in account it is concluded that the particular samples tested achieved buckling pressures close to those predicted by round tube theory rather than one percent out of round theory even though these tubes had an initial out of roundness of approximately one percent prior to testing. Since the two sections of round tube tested were cut from the same tube this observation is limited to the particular tube tested and cannot be used as a design point for design of OTEC heat exchanger tubes without additional test substatiation.

A comparison of the buckling strength of corrugated tubes to round tubes resulted in good correlation with analytical predictions using the SAP-IV and Nastran computer codes (see table 2). Although the test samples were limited, the three corrugated tubes failed at approximately the same pressure and the corrugation factor determined by test (.32) was close to that previously predicted (.44). After the pre test prediction was made the SAP-IV computer program model was increased from a two degree of freedom node model to three degrees of freedom. This resulted in even better comparison with test data (.40). A check using the Nastran computer code verified the SAP-IV analysis and derived a corrugation factor of (.37). It is concluded that the analytical SAP-IV procedure is sufficiently accurate to be used in tube design in conjunction with the ASME code procedures for pressure vessel design.

TEST SPECIMENS

The test specimens consisted of three corrugated tubes, having 22 corrugations each, manufactured by Grob Inc, and two round tubes. All tubes were titanium and were manufactured based upon a nominal wall thickness of .028 inches. Measurement of actual wall thickness prior to testing showed an average wall thickness which was closer to .026 inches. This was true for both the round tubes and undeformed ends of the corrugated tubes. The test specimens prior to testing are shown in Figures A-1 through A-4. Pictures of the deformed specimens are shown in Figures C-1 through C-4. Sketches of the round tube, Grob tube corrugation and computer corrugation model are shown in Figures 2 and 3.

TEST FACILITY AND DATE

Tests were conducted in facilities of the Applied Technology Division of TRW on 18 & 19 April 1978. The test conductor was Ed Burchman and the responsible engineer was T. R. Baumann.

TEST SETUP AND INSTRUMENTATION

Pictures of the test fixture, test setup and instrumentation are shown in Figures B-1 through B-4. The test fixture consisted of aluminum tube sections welded to end flanges. Two end plates were used to hold the test specimens. The end plates utilized "O-Ring" seals to provide a pressure seal having minimum restraining effects at the ends of the specimens. Details and dimensions of the test fixture are given in Figure 4. Water was used as the pressurizing fluid between the test fixture and external walls of the test specimens. The test specimens were open at both ends to allow internal tube measurements, during the tests. Two pressure gages were used for the tests. The smaller gage had a maximum capability of 150 PSI and was used to measure pressures up to its maximum capability and to verify the calibration of the larger gage up to 150 PSI.

TEST PROCEDURE

The test procedure was similar for all specimens. After installation in the test fixture the test specimen was measured internally with an inter-mike or bore gage to determine the approximate location and orientation of its minimum internal diameter. During testing this point was monitored periodically to determine deflection under pressure. The fluid pressure was increased in initial increments up to 150 PSI. At 150 PSI the small pressure gage was disconnected and the pressure was increased incrementally using the larger gage. In the vicinity of the failure point all corrugated tubes were measured at 5 PSI increments and all round tubes at 10 PSI increments.

TEST RESULTS

All test specimens behaved similarly during testing. Deformations were not measureable during the early stages of testing. During the higher test pressures slight deformations were encountered but these were barely measurable. Within 10-20 PSI of failure the deformations started to become significant. Deformations increased very rapidly near the failure pressure. At failure there was a rapid decrease in gage pressure. Despite attempts to pump up and increase the pressure the deformation of the tubes increased correspondingly and would not support higher pressure. Two of the corrugated tubes eventually cracked as the deformations became large. The other corrugated tube was not deformed to the point of cracking but probably would have cracked had pumping continued. The round tubes deformed much more than the corrugated tubes without cracking but they might have also experienced cracks if pumping had continued. In all tests the tube collapse occurred near the point of minimum internal diameter.

The test results are given in Table 1. The buckling pressure is the maximum pressure shown on the pressure gage prior to tube collapse. The mean buckling pressure was 715 PSI for the two round tube specimens and 231.3 PSI for the three corrugated specimens.

TRB:dp

TABLE 1

TEST RESULTS

SPECIMEN NUMBER	BUCKLING PRESSURE
SPECIMEN #1 CORRUGATED	232 PSI
SPECIMEN #2 CORRUGATED	232 PSI
SPECIMEN #3 CORRUGATED	230 PSI
SPECIMEN #4 ROUND TUBE	710 PSI
SPECIMEN #5 ROUND TUBE	720 PSI

TABLE 2

CORRUGATION FACTOR COMPARISON

TYPE OF ANALYSIS OR TEST	CORRUGATION FACTOR
SAP IV PREDICTED TEST VALUE (TWO DEGREE OF FREEDOM NODES)	.44
TEST RESULTS (ROUND TUBE VRS CORRUGATED TUBES)	.32
SAP IV ANALYSIS (THREE DEGREE OF FREEDOM NODES)	.40
NASTRAN STATIC ANALYSIS THREE DEGREE OF FREEDOM NODES	.37

CORRUGATION FACTOR IS THE RATIO OF THE BUCKLING PRESSURE OF THE CORRUGATED TUBE TO THAT OF AN EQUIVALENT ROUND TUBE HAVING THE SAME REFERENCE DIAMETER AND THICKNESS.

FIGURE 1
TITANIUM TUBE TESTS
PREDICTIONS AND TEST RESULTS

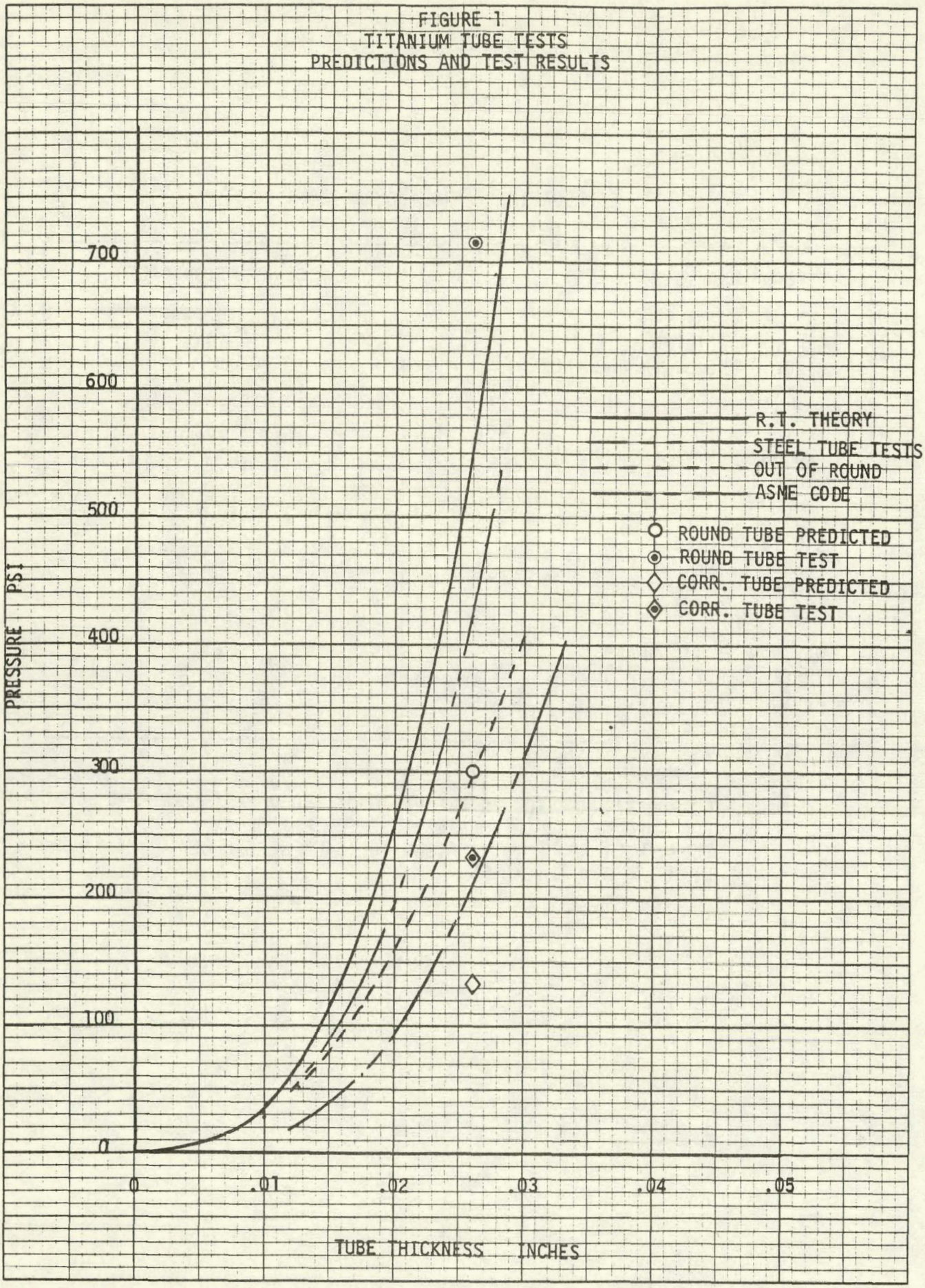

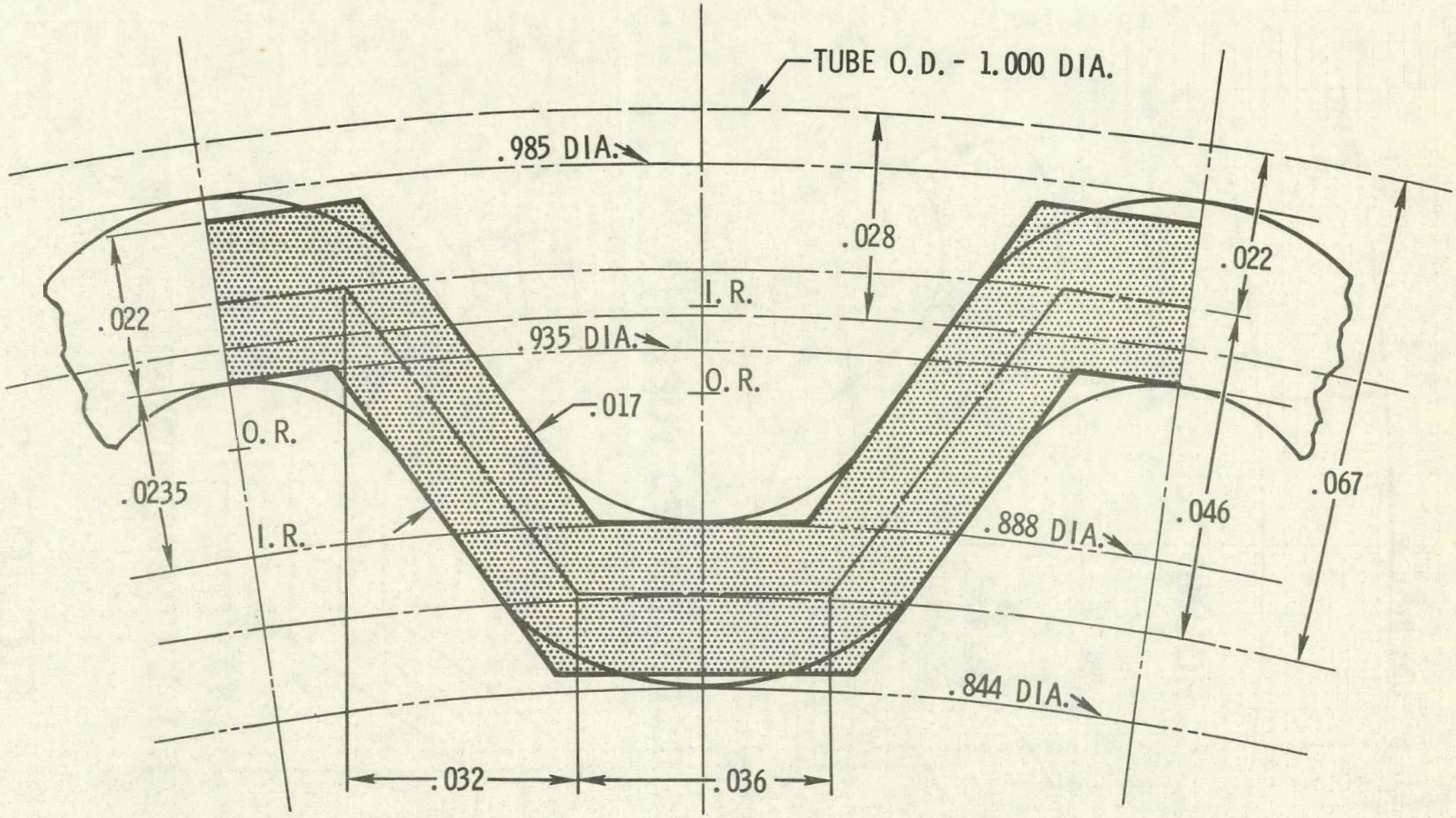

NOTE:

1. ALL DIMENSIONS ARE IN INCHES.
2. ▩ ANALYTICAL MODEL

FIGURE 2 . GROB TUBE CONFIGURATION (CORRUGATION DEFINITION)

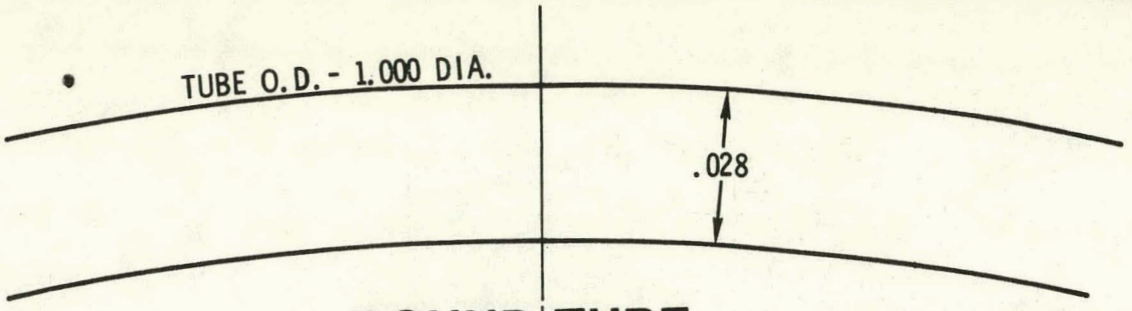

ROUND TUBE

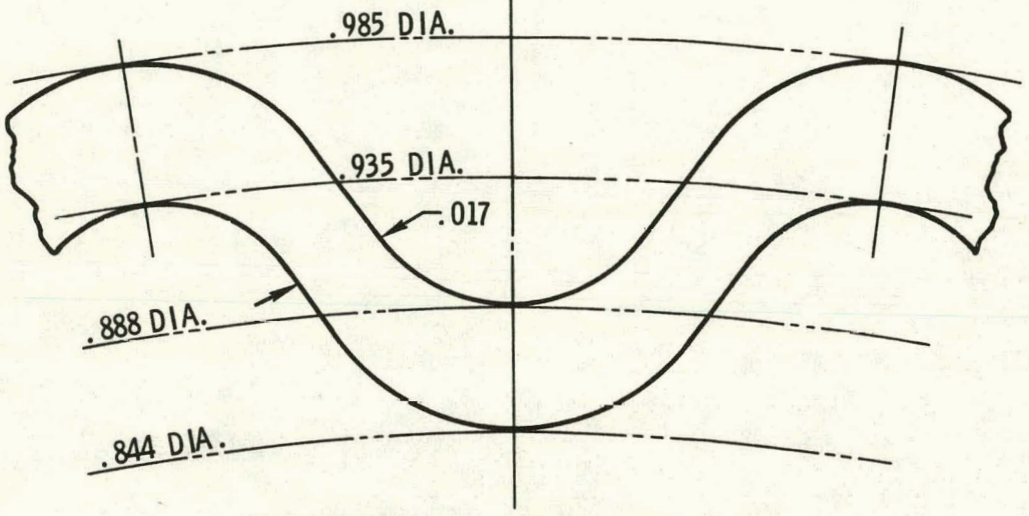

CORRUGATED TUBE

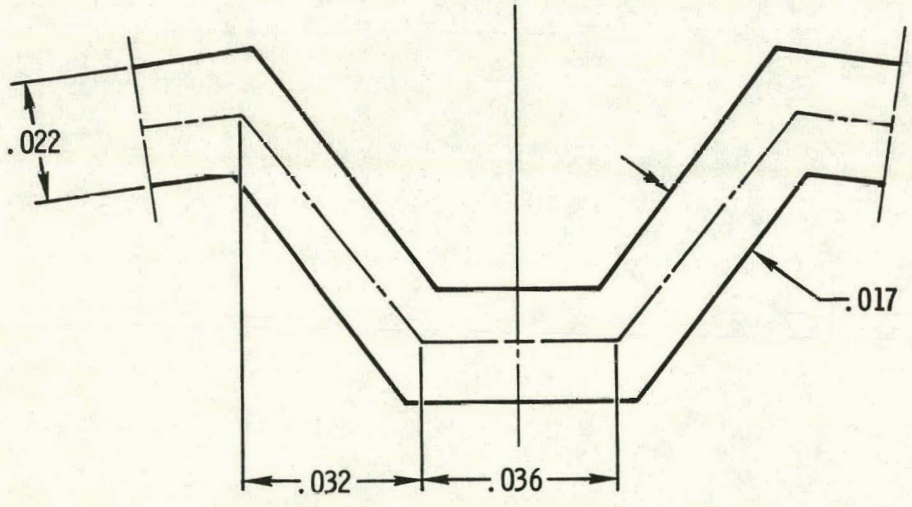

ANALYTICAL MODEL

FIGURE 3.
GROB TUBE COMPARISON

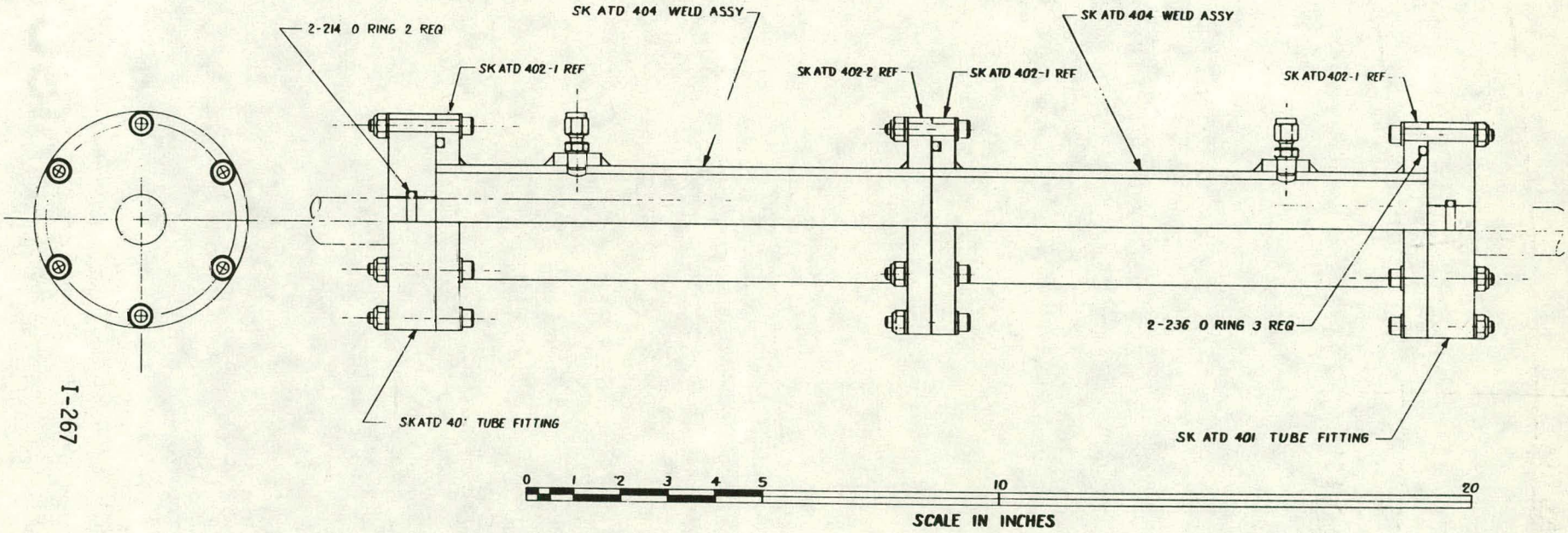
2-214 O RING 2 REQ
SK ATD 404 WELD ASSY
SK ATD 402-1 REF
SK ATD 402-2 REF
SK ATD 402-1 REF
SK ATD 404 WELD ASSY
SK ATD 402-1 REF
2-236 O RING 3 REQ
SKATD 40' TUBE FITTING
SK ATD 401 TUBE FITTING
0 1 2 3 4 5 10 20
SCALE IN INCHES

FIGURE 4

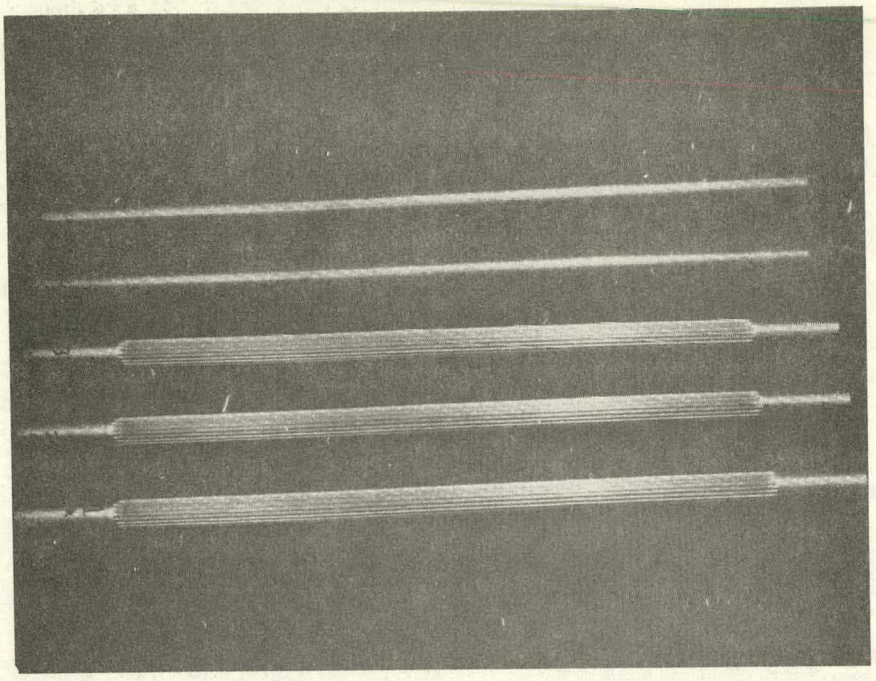

FIGURE A-1
TEST SPECIMENS FULL LENGTH

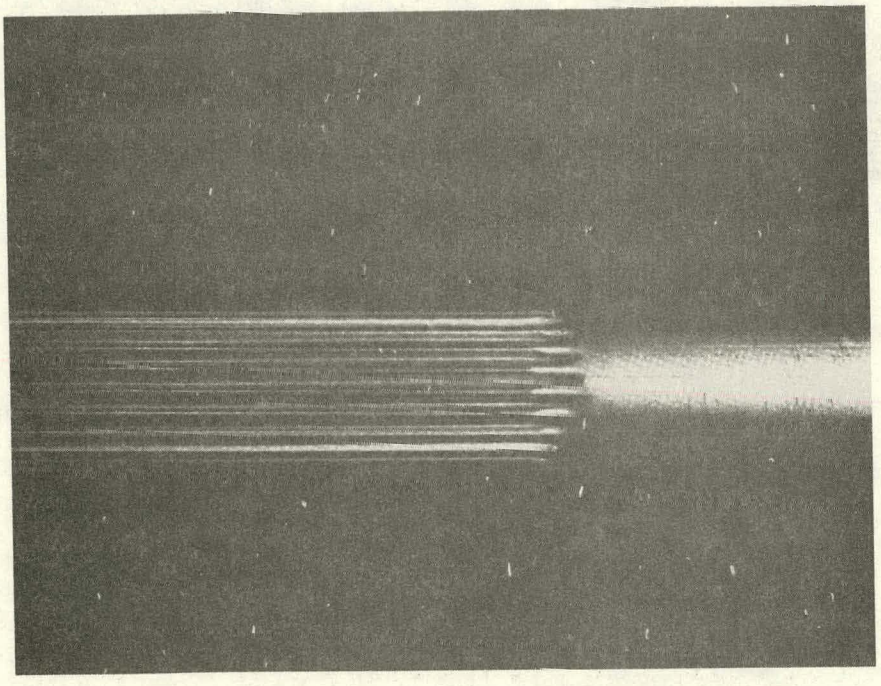

FIGURE A-2
CORRUGATED TUBE CLOSEUP
I-268

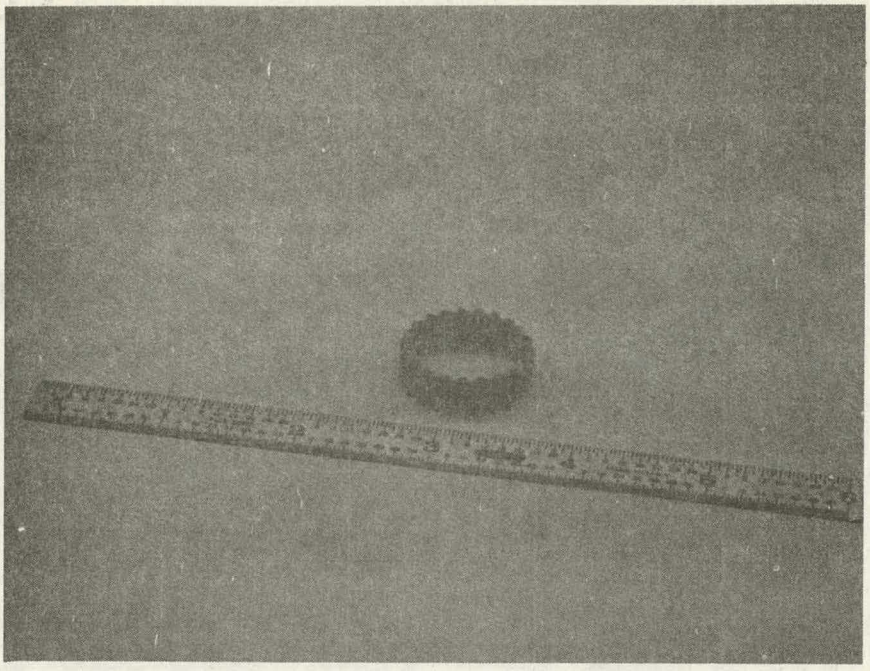

FIGURE A-3
CORRUGATED TUBE CROSS SECTION

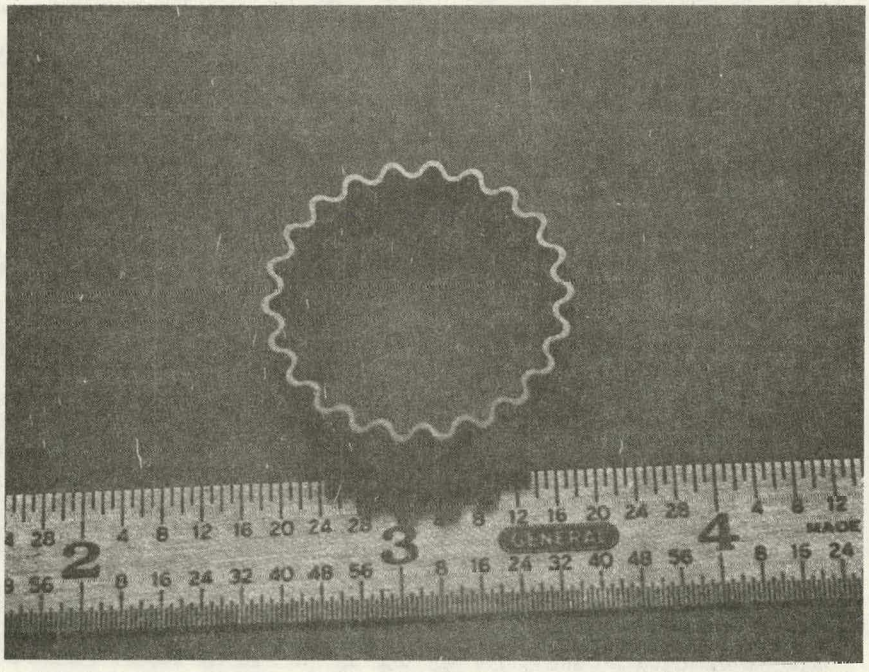

FIGURE A-4
CORRUGATED CROSS SECTION CLOSEUP

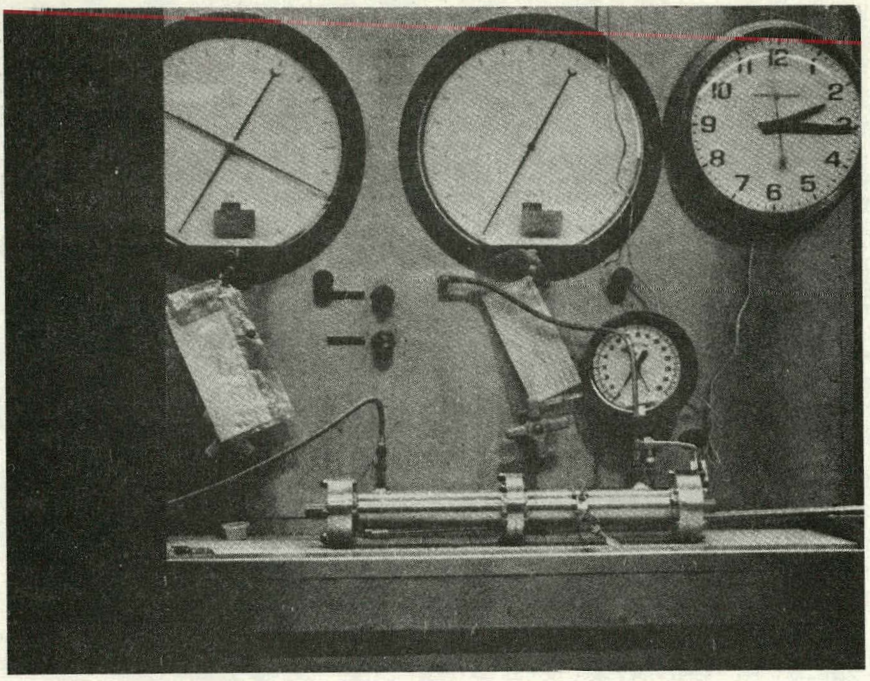

FIGURE B-1
TEST SETUP & INSTRUMENTATION

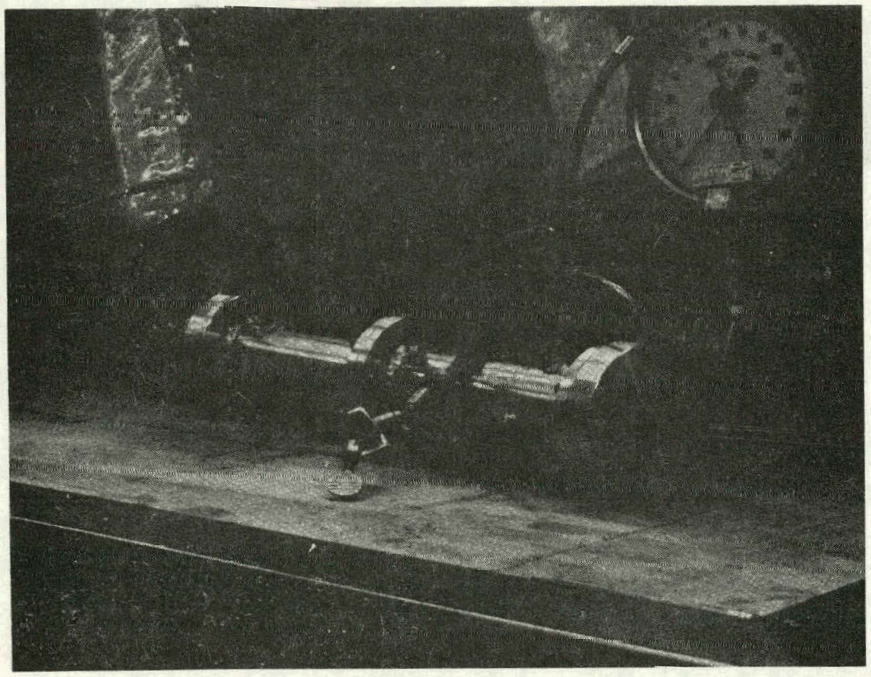

FIGURE B-2
TEST FIXTURE INCLINED VIEW

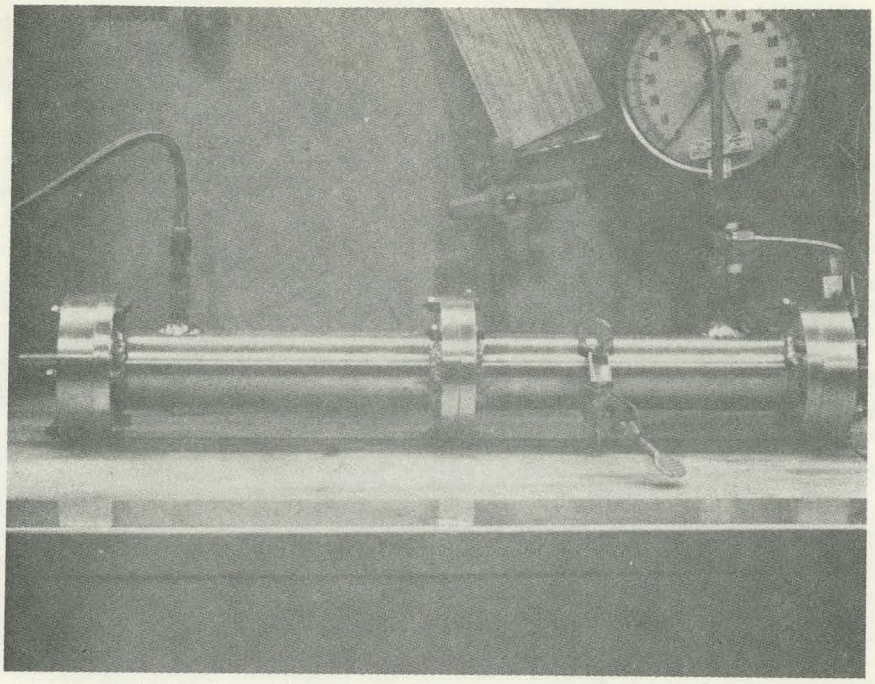

FIGURE B-3
TEST FIXTURE FRONT VIEW

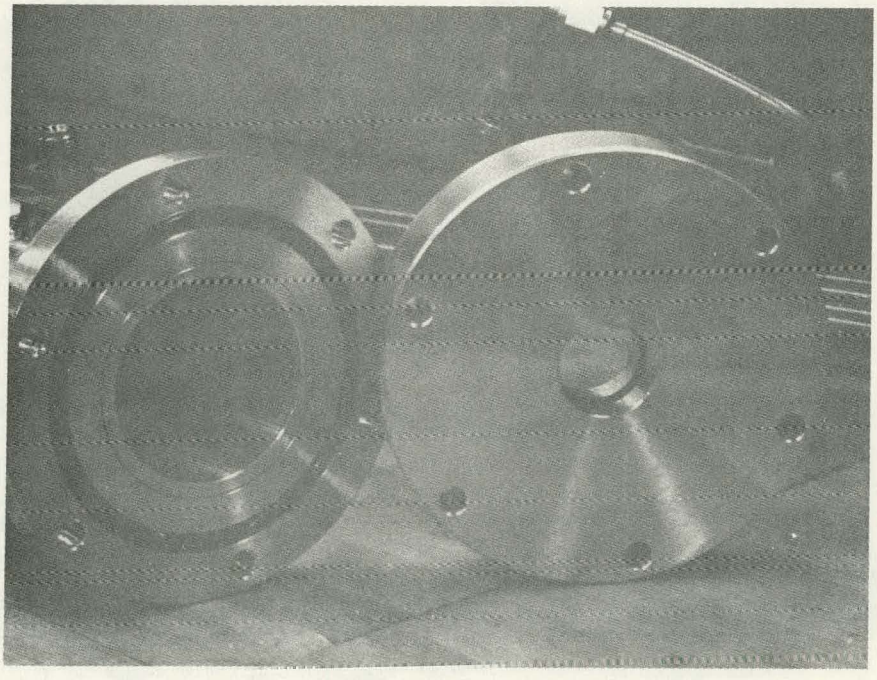

FIGURE B-4
TEST FIXTURE DETAILS

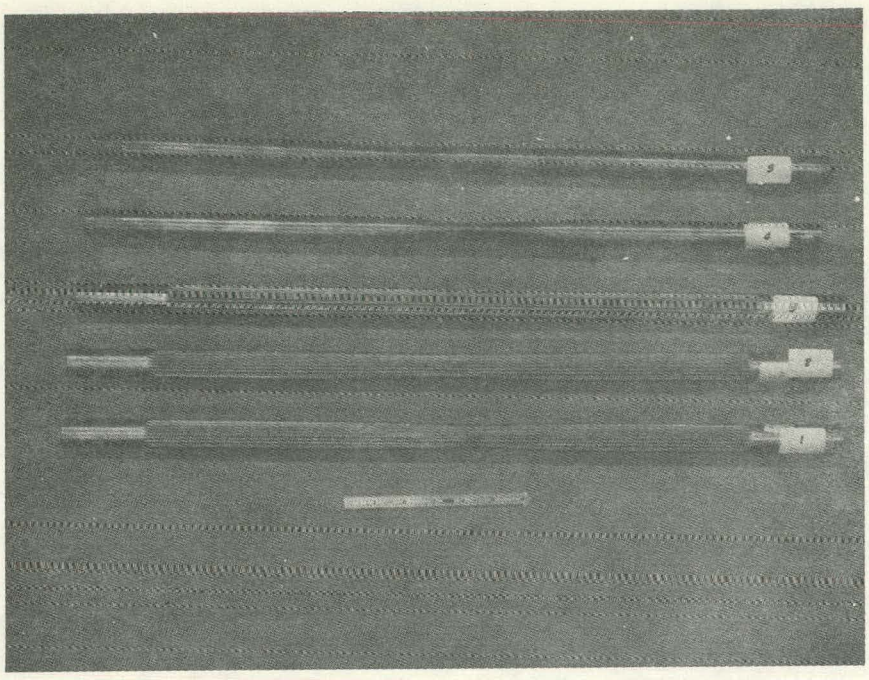

FIGURE C-1
FAILED SPECIMENS NARROW SIDE

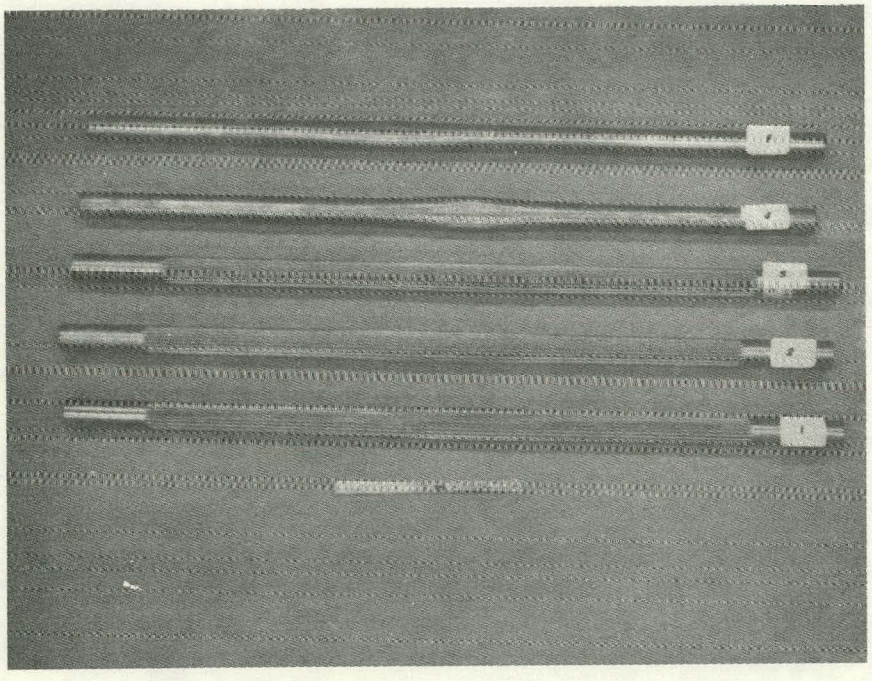

FIGURE C-2
FAILED SPECIMENS FLAT SIDE

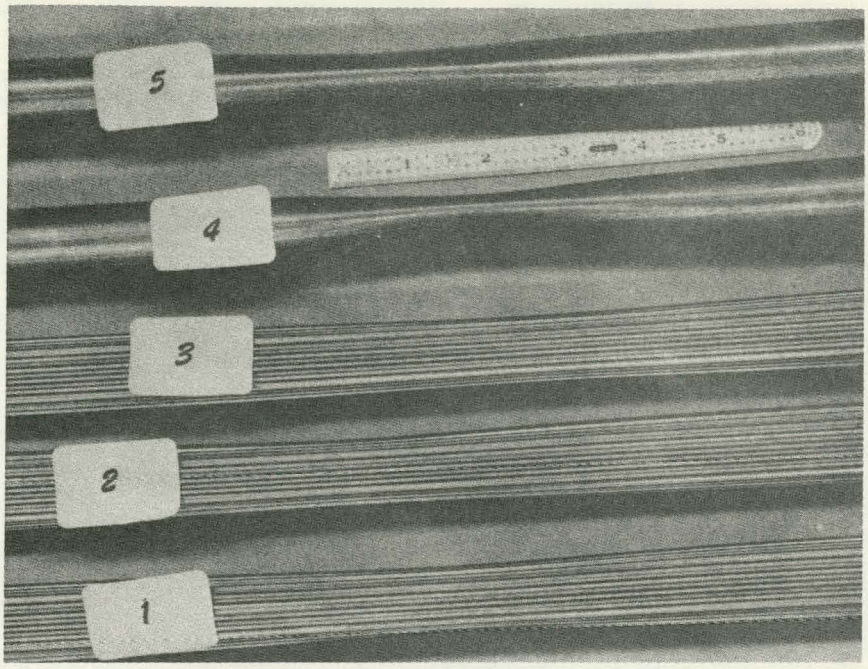

FIGURE C-3
FAILURE DETAILS NARROW SIDE

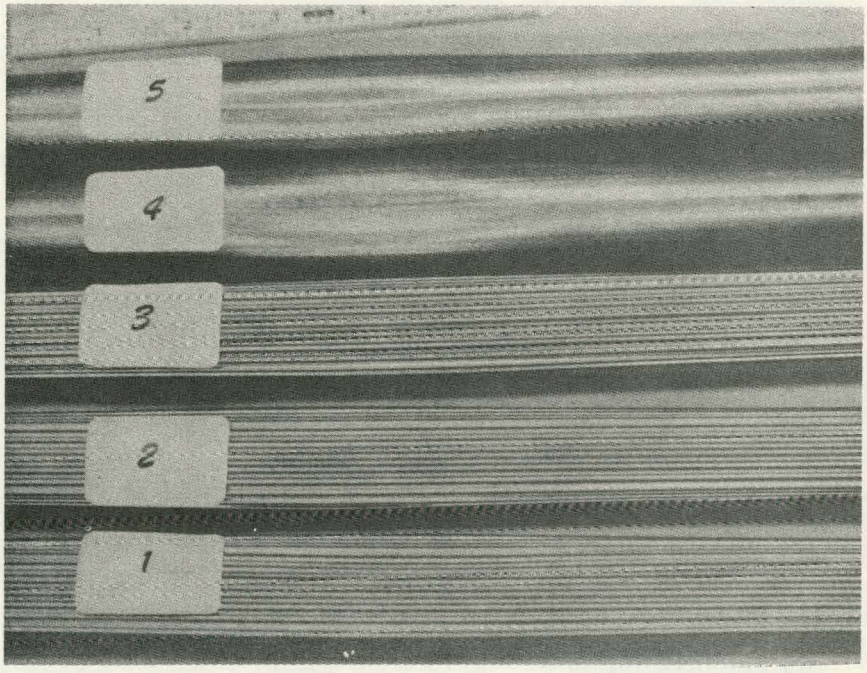

FIGURE C-4
FAILURE DETAILS FLAT SIDE

THIS PAGE

WAS INTENTIONALLY

LEFT BLANK

APPENDIX I.4

0.2 MWe TEST ARTICLE LOOP

APPENDIX I.4

0.2 MWe TEST ARTICLE LOOP

This appendix provides additional details of the design and equipment for 0.2 MWe test article loop.

It includes sketches on the proposed layout, plan views, equipment details and the piping and instrumentation diagram.

PREPARED P. L. TRUBEY 8-24-78 REPORT NO. PAGE 1

CHECKED

MODEL

OTEC 0.2 MWe TEST ARTICLE PROPOSED LAYOUT

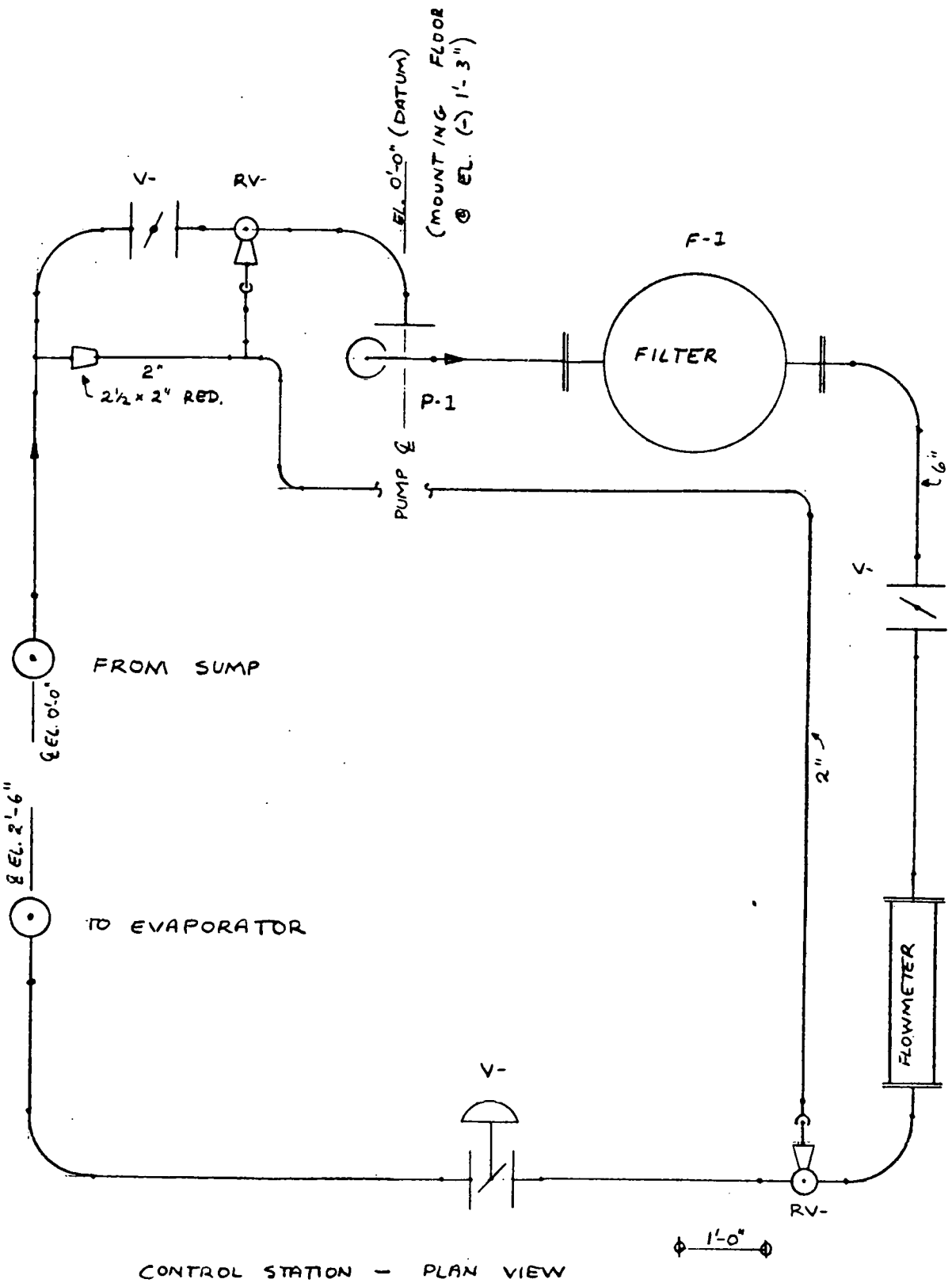

CONTROL STATION — PLAN VIEW

PREPARED P.L. TRUBEY 6-29-78 REPORT NO. PAGE 2

CHECKED

MODEL

OTEC 0.2 MW$_e$ TEST ARTICLE
PROPOSED LAYOUT

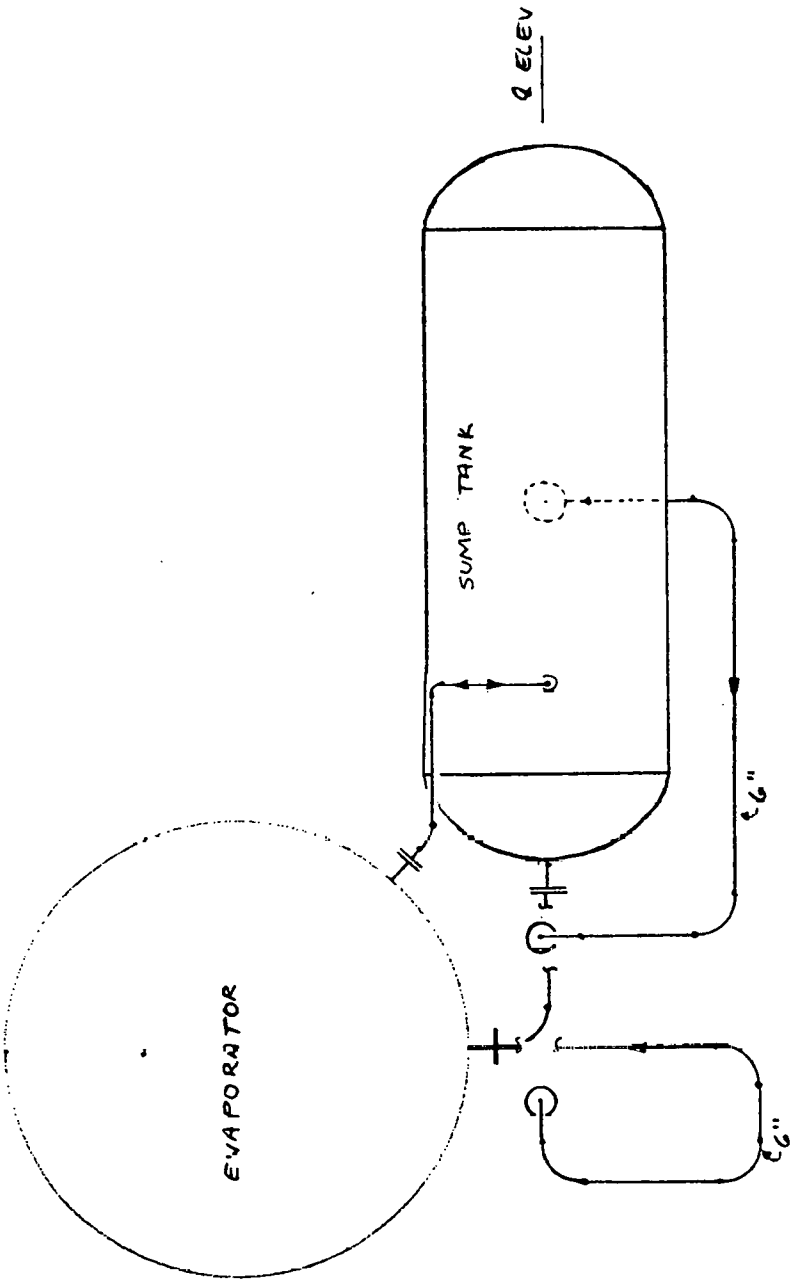

PREPARED P. L. TRUBEY
CHECKED
MODEL

REPORT NO.

PAGE 3

OTEC 0.2 MW_e TEST ARTICLE
PROPOSED LAYOUT

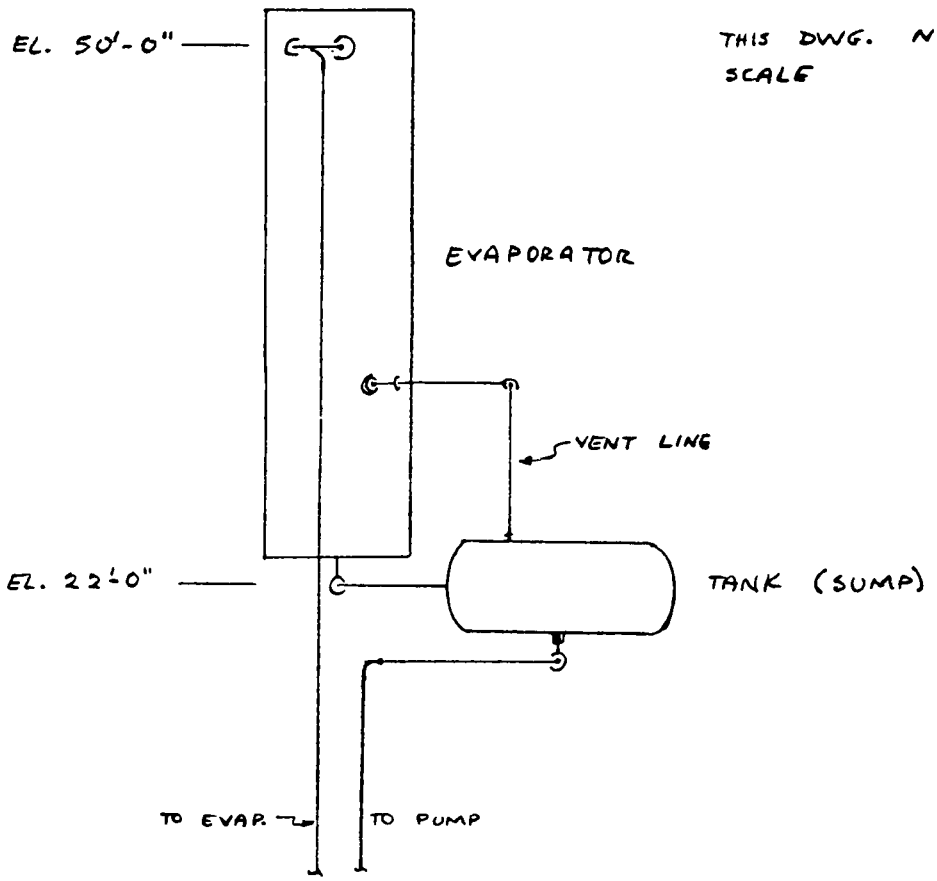

THIS DWG. NOT TO SCALE

FOR ALL DWGS:

1) All elbows 1½-D (LONG RADIUS)
2) CRITICAL DIMENSIONS GIVEN
3) SCALE (MEASURED) DIMENSIONS APPROXIMATE

EQUIPMENT DETAILS

1) FILTER

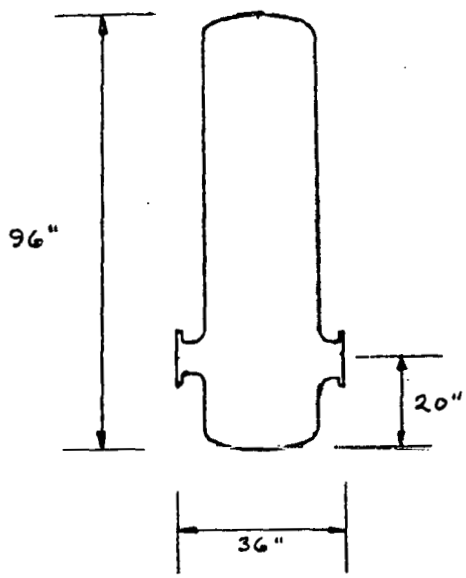

2) PUMP

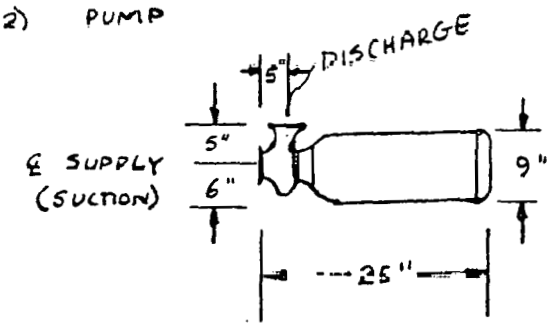

3)

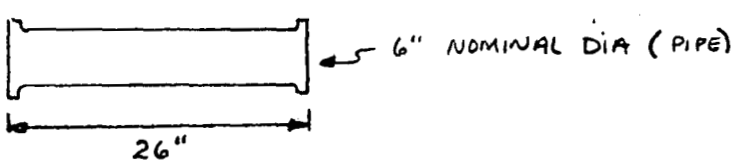

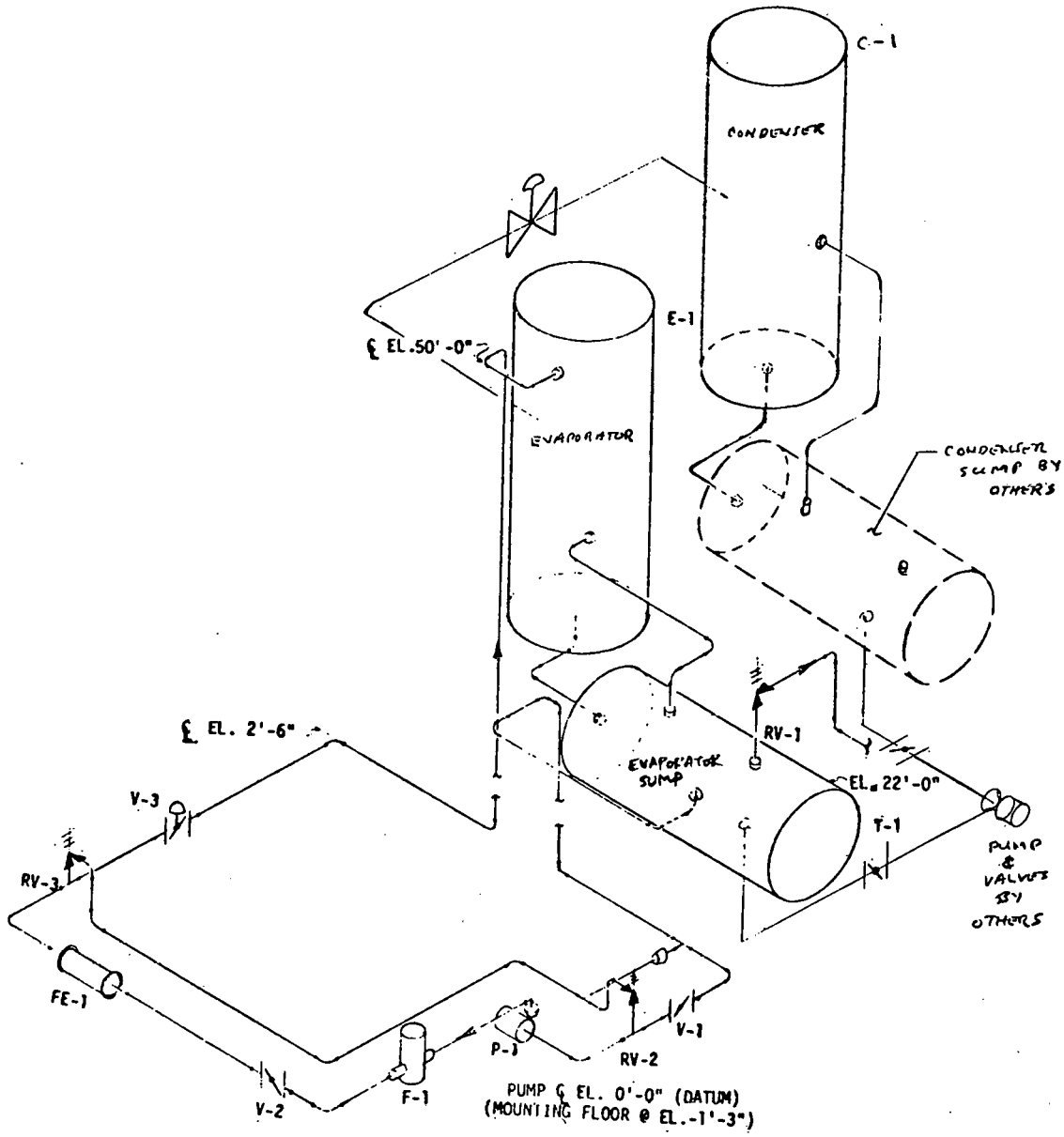

DESIGNED P. TRUDEY DRAWN H. HUDSON CHECKED APPROVALS FACILITIES OFFICE	OTEC 0.2 MWe TEST ARTICLE PROPOSED LAYOUT	LTR DATE REVISION BY APPD TRW	FACILITIES, MECHANICAL AND POWER INTEGRATION LABORATORY	DRAWING NUMBER 6850.78-71 ISSUE DATE / DWG LTR

THIS PAGE

WAS INTENTIONALLY

LEFT BLANK

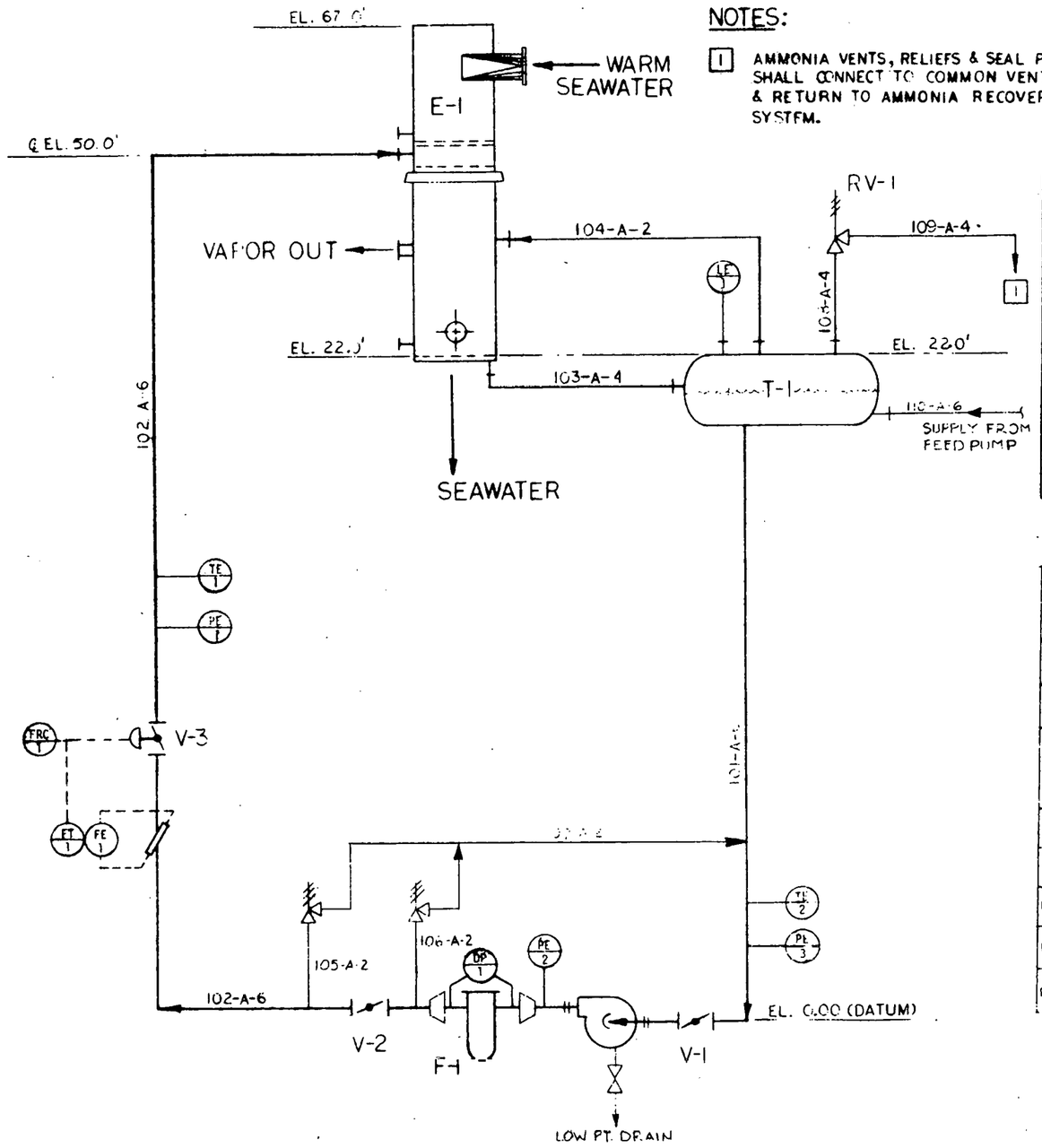

NOTES:

1. AMMONIA VENTS, RELIEFS & SEAL PURGES SHALL CONNECT TO COMMON VENT LINE & RETURN TO AMMONIA RECOVERY SYSTEM.

T-1 EVAPORATOR SUMP
CAPACITY 1,000 GAL
DESIGN PRESS 150 PSIG
DESIGN TEMP -28F TO 120F

E-1 EVAPORATOR
HX RATING .2 MWe
10,694 GPM WATER 84F
325 GPM AMMONIA 135 PSIA

F-1 FILTER
5 MICRON
1 PSI ΔP
325 GPM

P-1 NH_3 RECIRCULATION PUMP
325 GPM 58 FT TDH 3 BHP

INSTRUMENT LIST

NO.	SENSOR NAME	PURPOSE	RANGE	ACCU.	SET POINT	COMMENTS
DP-1	DIFFERENTIAL PRESSURE	PRESSURE DROP ACROSS FILTER UNIT F-1	0-10 PSI	± 0.10 PSI	NA	LOCAL AND REMOTE READING
FE-1	FLOW ELEMENT	MEASURE NH_3 FLOW RATE	0-350 GPM			SONIC FLOW MEASUREMENT SYSTEM WITH REMOTE READ AND STRIP RECORDER, INPUT SIGNAL TO FLOW CONTROL VALVE V-3
FT-1	FLOW TRANSMITTER	TRANSMITS FE-1 OUTPUT				
FRC-1	FLOW RECORDING CONTROLLER	DISPLAYS AND RECORDS FE-1 OUTPUT			325	
LE-1	LEVEL ELEMENT	INDICATE NH_3 FLUID LEVEL IN TANK T-1	0-4 FT	±1"	2 FT	CONTROLS FEED RATE
PE-1	PRESSURE ELEMENT	INDICATE E-1 NH_3 FLUID INLET PRESSURE	0-150 PSI	0.5% OF F.S.	NA	TO RECORDER
PE-2	PRESSURE ELEMENT	INDICATE PUMP P-1 DISCHARGE PRESSURE	0-150 PSI		NA	TO RECORDER
PE-3	PRESSURE ELEMENT	INDICATE PUMP P-1 SUCTION PRESSURE	0-150 PSI		NA	TO RECORDER
TE-1	TEMPERATURE ELEMENT	INDICATE E-1 NH_3 FLUID INLET TEMPERATURE	(-)30 TO +120°F	0.25% OF F.S.	NA	TO RECORDER
TE-2	TEMPERATURE ELEMENT	INDICATE PUMP P-1 SUCTION TEMPERATURE			NA	TO RECORDER

EQUIPMENT LIST

ITEM NO.	ITEM FUNCTION	MANUFACTURER	PART NUMBER	SIZE & TYPE CONNECTION	DESIGN PRESSURE (PSIG)	TYPE OPERATOR	SERVICE	WEIGHT (POUNDS)	COST (DOLLARS)	LONG LEAD	MISCELLANEOUS DATA
T-1	EVAPORATOR SUMP TANK	SEE SPECIFICATION		4' IDx10' TEF TANGENTS	150	NA	NH_3			L	ASME FLANGED & DISHED HEADS 18" MANWAY
P-1	AMMONIA RECIRCULATION PUMP	SEE SPECIFICATION		6" 300# R.F. SUCT. 4" 300# R.F. DISCH.	150	ELEC. MOTOR DRIVE	NH_3	205	2K	L	SPECIFY LOW NPSH AMMONIA SERVICE
F-1	AMMONIA FULL FLOW FILTER UNIT	SEE SPECIFICATION		8" BW	150	NA	NH_3			L	ΔP(DIRTY)=1.0 PSI 325 GPM MULTIPLE UNITS 40MICRON ABSOLUTE
V-1	PUMP SHUTOFF	POSI-SEAL		6" 300# BUTTERFLY	150	MANUAL	NH_3	37	432 (M)		ETHYLENE PROPYLENE O-RINGS, STEEL SEAT
V-2	PUMP SHUTOFF	POSI-SEAL		6" 300# BUTTERFLY	150	MANUAL	NH_3	37	432 (M)		SAME AS V-1
V-3	FLOW CONTROL MODULATING	POSI-SEAL		6" 300# BUTTERFLY	150	PNEUMATIC	NH_3	70	1522 (M)	L	SAME AS V-1 AND PNEUMATIC OPERATOR
RV-1	TANK T-1 PRESSURE RELIEF	COMMERCIAL		4" 300#	150	NA	NH_3				SET 150 PSI C/S
RV-2	LINE RELIEF	COMMERCIAL		2" 300#	150	NA	NH_3				SET 150 PSI C/S
RV-3	LINE RELIEF	COMMERCIAL		2" 300#	150	NA	NH_3				SET 150 PSI C/S

INSTRUMENT SYMBOLS

- DP — DIFFERENTIAL PRESSURE
- FE — FLOW ELEMENT
- FT — FLOW TRANSMITTER
- FRC — FLOW RECORDING CONTROLLER
- LE — LEVEL ELEMENT
- PE — PRESSURE ELEMENT
- TE — TEMPERATURE ELEMENT
- LOCAL READOUT
- SIGNAL TRANSMITTED TO CONTROL ROOM PANEL
- RELIEF VALVE
- BUTTERFLY VALVE
- DIAPHRAGM OPERATED VALVE
- FLOW METER
- REDUCER

DESIGNED E. DI CAMILLO	.2 MWe EVAPORATOR TEST LOOP P & I.D.	TRW — FACILITIES, MECHANICAL AND POWER INTEGRATION LABORATORY
DRAWN R. WELTHER		DRAWING NUMBER 6550.78-70
CHECKED [illegible]		ISSUE DATE
APPROVALS		CHG LTR
PROG OFFICE		

☆U.S. GOVERNMENT PRINTING OFFICE: 1980-640-258/370